



UNIL | Université de Lausanne

FACULTÉ DES SCIENCES SOCIALES ET POLITIQUES

INSTITUT DES SCIENCES DU SPORT

**Classification of spontaneous running patterns using
biomechanics: from the laboratory towards the field**

THÈSE DE DOCTORAT

présentée à la

Faculté des sciences sociales et politiques
de l'Université de Lausanne

pour l'obtention du grade de

Docteur ès Sciences en sciences du mouvement et du sport de l'Université de Lausanne

par

Aurélien Patoz

Directeur de thèse

MER Davide Malatesta

Jury

Prof. Fabienne Crettaz von Roten – Université de Lausanne

Prof. Jean-Benoît Morin – Université Jean Monnet de Saint-Etienne

Prof. Arthur Dewolf – Université Catholique de Louvain

LAUSANNE

2023



UNIL | Université de Lausanne

Faculté des sciences
sociales et politiques

IMPRIMATUR

Le Décanat de la Faculté des sciences sociales et politiques de l'Université de Lausanne, au nom du Conseil et sur proposition d'un jury formé des professeurs

- Monsieur Davide MALATESTA, directeur de thèse, Maître d'Enseignement et de Recherche à l'Université de Lausanne
- Madame Fabienne CRETZAZ VON ROTEN, Professeure à l'Université de Lausanne
- Monsieur Arthur DEWOLF, Professeur à l'Université Catholique de Louvain
- Monsieur Jean-Benoît MORIN, Professeur à l'Université Jean Monnet à Saint Priest en Jarez

autorise, sans se prononcer sur les opinions du candidat, l'impression de la thèse de Monsieur Aurélien PATOZ, intitulée :

« **Classification of spontaneous running patterns using biomechanics : from the laboratory towards the field** »

Nicky LE FEUVRE
Doyenne

Lausanne, le 2 décembre 2022

Résumé

Chaque personne adopte un pattern de course unique et spontané qui est un système global et dynamique avec plusieurs paramètres biomécaniques interconnectés. Ainsi, il est d'intérêt majeur d'utiliser des méthodes multi-composantes pour comprendre les différences individuelles dans la biomécanique de course à pied. De ce fait, cette thèse a investigué l'évaluation objective du pattern de course spontané et sa relation en termes de classification des coureurs au laboratoire et en perspective sur le terrain. Pour cela, cette thèse contient deux sous-but. Premièrement, cette thèse a étendu les connaissances sur le duty factor (DF ; la proportion du temps passé au contact avec le sol pendant une foulée) et la fréquence de foulée (SF), deux variables globales et objectives qui permettent d'évaluer le pattern de course spontané. Cette thèse a montré que la variable locale qui définit le type de pose de pied et le DF ne représentent pas la même information du pattern du course spontané quand ces variables sont investiguées au niveau individuel et que le DF doit être préféré au type de pose de pied quand on souhaite évaluer le pattern de course global du coureur. De plus, cette thèse a apporté des preuves supplémentaires et renforcé les déclarations précédentes selon lesquelles les coureurs à faible DF reposent davantage sur l'optimisation du modèle masse-ressort (stockage et restitution de l'énergie élastique) que les coureurs à haut DF. Deuxièmement, cette thèse a développé des algorithmes permettant de mesurer précisément le temps de contact (t_c), le temps de vol (t_f), le DF, la SF et le pic de force de réaction au sol vertical ($F_{z,max}$) en l'absence de la méthode de référence (basée sur la mesure des forces de réaction au sol) mais en utilisant une centrale inertielle (IMU) attachée au sacrum. Cela permettrait ensuite d'effectuer des mesures sur le terrain. Cette thèse supporte l'utilisation des algorithmes basés sur l'accélération verticale enregistrée par l'IMU attaché au sacrum pour estimer $F_{z,max}$, t_c , t_f , DF et SF pour des courses sur tapis roulant à des vitesses faibles. De plus, cette thèse a montré que l'application de l'intelligence artificielle (des modèles de régression linéaire dans ce cas spécifique) a permis d'améliorer la précision des estimations de t_c , t_f et DF. En conclusion, avoir des estimations précises de $F_{z,max}$, t_c , t_f , DF et SF obtenues à l'aide d'une IMU peuvent être très pratique pour les entraîneurs et les professionnels de la santé car une IMU a l'avantage d'être très peu couteuse et portable. Ces estimations précises peuvent être bénéfique lors de la surveillance des facteurs de risque de blessures liés à la course à pied sur le terrain.

Mots-clés : analyse du pattern ; analyse du mouvement ; appareil portable ; senseur ; centrale inertielle ; accéléromètre ; plateforme de force.

Abstract

Everyone adopts a unique spontaneous running pattern, which is a global and dynamic system with several interconnected biomechanical parameters. It is therefore of major interest to use multicomponent methods to understand individual differences in running biomechanics. Hence, this thesis investigated the objective evaluation of the spontaneous running pattern and its relationship in terms of runners' classification in the laboratory and towards the field. To do so, the thesis contains two sub-goals. First, this thesis extended about the knowledge of duty factor (DF; the proportion of time spent in contact with the ground during a running stride) and step frequency (SF) as global objective variables to assess spontaneous running patterns. This thesis showed that "local" foot-strike pattern and DF do not represent similar running pattern information when investigated at the individual level and DF should be preferred to foot-strike pattern when evaluating the global running pattern of a runner. Moreover, this thesis brought further evidence and reinforce previous statements that low DF runners rely more on the optimization of the spring-mass model (better storage and re-use of elastic energy) than high DF runners. Second, this thesis developed algorithms allowing to accurately measure ground contact time (t_c), flight time (t_f), DF, SF, and peak vertical ground reaction force ($F_{z,max}$) in absence of the gold standard method (ground reaction force data) but using an inertial measurement unit (IMU) attached to the sacrum. This would latter allow to perform these measurements in the field. This thesis supports the use of algorithms based on the vertical acceleration recorded by a sacral-mounted IMU to estimate $F_{z,max}$, t_c , t_f , DF, and SF for level treadmill runs at endurance running speeds. In addition, this thesis showed that further applying machine learning (linear regression models in this specific case) allowed us to improve the accuracy of the estimations of t_c , t_f , and DF. To conclude, having accurate IMU-based estimations of $F_{z,max}$, t_c , t_f , DF, and SF might be very practical for coaches and healthcare professionals, especially because an IMU has the advantage to be low-cost and portable and therefore those accurate estimations might be beneficial when monitoring running-related injury risk factors in real-word settings.

Keywords: gait analysis; motion analysis; wearable; sensor; inertial measurement unit; accelerometer; force plate.

*I never lose.
I either win or learn.
— Nelson Mandela —*

Acknowledgements

This thesis became a reality with the help and kind support of many people. I would like to express my deep sense of gratitude to all of them.

Foremost, I am grateful to my advisor, Davide, for all the scientific discussions and the generous guidance, all along the past three years. Your patience, enthusiasm, and genuine caring attitude have undoubtedly helped me to reach the finish line. It was a pleasure working with you and on this very interesting topic.

I am hugely indebted to Cyrille, Thibault, and Bastiaan from the Volodalen Swiss Sport Lab (Aigle, CH) for sharing their scientific knowledge and technical know-how.

I would like to express my gratitude to Fabio for the intense discussions during coffee breaks.

Many thanks and appreciations to Prof. Fabienne Crettaz von Roten, Prof. Jean-Benoît Morin, and Dr. Arthur Dewolf for kindly agreeing to evaluate this work.

A special mention to the vast number of people who participated in my experiments for generously offering their own precious time. This research could never have happened without you. I extend my thanks to the master's students who helped me with the data collection.

Finally, to my family and friends, thanks for all the good moments we had together.

Lausanne, February 2023

A. P.

List of abbreviations

3D	three-dimensional
AER	aerial runner
BW	body weight
COM	center of mass
COM-M	center of mass method
DF	duty factor
DF _{high}	high duty factor group
DF _{low}	low duty factor group
DF _{mid}	mid duty factor group
eFS	effective foot-strike
eTO	effective toe-off
FFS	forefoot striker
FS	foot-strike
FSA	foot-strike angle
FSP	foot-strike pattern
$F_{z,max}$	peak vertical ground reaction force
g	gravitational constant
GSM	gold standard method
IMU	inertial measurement unit
IMUM	inertial measurement unit method
I_z	vertical impulse
KA	kinematic algorithm
k_{leg}	leg stiffness
L_0	leg length
LCS	local coordinate system
lloa	lower limit of agreement
LR	linear regression
MAPE	mean absolute percentage error
MFS	midfoot striker
ML	machine learning
NN	neural network

NN2	two-layers neural network
r	Pearson's correlation coefficient
R^2	coefficient of determination
R_{comp}^2	coefficient of determination during leg compression
R_{decomp}^2	coefficient of determination during leg decompression
RFS	rearfoot striker
RMSE	root mean square error
SACR-M	sacral marker method
SF	step frequency
SPM	statistical parametric mapping
SVR	support vector regression
t_c	ground contact time
t_{ce}	effective contact time
t_f	flight time
t_{fe}	effective flight time
t_s	swing time
t_{step}	step time
TER	terrestrial runner
TO	toe-off
uloa	upper limit of agreement
$V^{\text{®}}_{\text{score}}$	Volodalen [®] subjective score

Table of contents

Résumé	i
Abstract	i
Acknowledgements	v
List of abbreviations	vii
1 Preamble	1
2 Introduction	5
2.1 From local to global assessment of spontaneous running patterns.....	7
2.1.1 <i>The local assessment of spontaneous running patterns</i>	7
2.1.2 <i>The global subjective assessment of spontaneous running patterns</i>	9
2.1.3 <i>The duty factor as a global objective assessment of spontaneous running patterns</i>	9
2.1.4 <i>Combining the duty factor and step frequency to globally assess spontaneous running patterns</i>	10
2.1.5 <i>Using topological methodology to investigate the association of duty factor and step frequency on running biomechanics</i>	13
2.2 From the laboratory towards field measurement of spontaneous running patterns.....	14
2.2.1 <i>The accurate measurement of contact and flight times without a force plate: using a motion capture system</i>	14
2.2.2 <i>The accurate measurement of peak vertical ground reaction force without a force plate: using a motion capture system</i>	15
2.2.3 <i>The accurate measurement of contact and flight times and peak vertical ground reaction force without a force plate: using an inertial measurement unit</i>	17
2.2.4 <i>The accurate measurement of effective contact and flight times without a force plate: using an inertial measurement unit</i>	19
2.2.5 <i>Enhancing sacral acceleration-based estimations of running stride temporal variables and peak vertical ground reaction force using machine learning</i>	19
3 Aim of the thesis	21
4 General methodology	25
4.1 Participant characteristics	27
4.2 Experimental procedure.....	28

4.3 Data collection	28
4.4 Event detection	32
4.4.1 Gold standard method	32
4.4.2 Kinematic algorithm	32
4.4.3 Inertial measurement unit method	33
4.5 Biomechanical variables	34
4.5.1 Temporal variables	34
4.5.2 Peak vertical ground reaction force variable	34
4.5.3 Stiffness related variables	34
4.5.4 Predicted variables obtained using machine learning models	35
4.5.5 Runners' classification	37
4.6 Data analysis and statistical analysis	37
5 Main results and discussion	39
5.1 Duty factor and foot-strike pattern do not represent similar running pattern at the individual level (study 1)	42
5.1.1 Results	42
5.1.2 Discussion	44
5.2 Examination of running pattern consistency across speeds (study 2)	47
5.2.1 Results	47
5.2.2 Discussion	50
5.3 Using statistical parametric mapping to assess the association of duty factor and step frequency on running kinetic (study 3)	54
5.3.1 Results	54
5.3.2 Discussion	59
5.4 A novel kinematic detection of foot-strike and toe-off events during non-instrumented treadmill running to estimate contact time (study 4)	62
5.4.1 Results	62
5.4.2 Discussion	63
5.5 Both a single sacral marker and the whole-body center of mass accurately estimate peak vertical ground reaction force in running (study 5)	66
5.5.1 Results	66
5.5.2 Discussion	68

5.6 A single sacral-mounted inertial measurement unit to estimate peak vertical ground reaction force, contact time, flight time, effective contact time, and effective flight time in running (studies 6 and 7)	72
5.6.1 Results	72
5.6.2 Discussion	75
5.7 Comparison of different machine learning models to enhance sacral acceleration-based estimations of running stride temporal variables and peak vertical ground reaction force (study 8).....	80
5.7.1 Results	80
5.7.2 Discussion	83
6 Conclusion	87
7 References	93
8 List of publications	109
8.1 Duty factor and foot-strike pattern do not represent similar running pattern at the individual level	115
8.2 Examination of running pattern consistency across speeds.....	133
8.3 Using statistical parametric mapping to assess the association of duty factor and step frequency on running kinetic	151
8.4 A novel kinematic detection of foot-strike and toe-off events during non-instrumented treadmill running to estimate contact time	169
8.5 Both a single sacral marker and the whole-body center of mass accurately estimate peak vertical ground reaction force in running.....	179
8.6 A single sacral-mounted inertial measurement unit to estimate peak vertical ground reaction force, contact time, and flight time in running	191
8.7 Estimating effective contact and flight times using a sacral-mounted inertial measurement unit.....	205
8.8 Comparison of different machine learning models to enhance sacral acceleration-based estimations of running stride temporal variables and peak vertical ground reaction force.....	213
9 Annexes.....	247

9.1 Critical speed estimated by statistically appropriate fitting procedures	249
9.2 Effect of mathematical modeling and fitting procedures on the assessment of critical speed and its relationship with aerobic fitness parameters.....	263
9.3 The oxygen uptake at critical speed and power in running: perspectives and practical applications.....	277
9.4 A multivariate polynomial regression to reconstruct ground contact and flight times based on a sine-wave model for vertical ground reaction force and measured effective timings	287
9.5 There is no global running pattern more economic than another at endurance running speeds.....	299
9.6 Different plantar flexors neuromuscular and mechanical characteristics depending on the preferred running form	305
9.7 Does characterizing global running pattern help to prescribe individualized strength training in recreational runners?	315
9.8 PIMP Your Stride: Preferred Running Form to Guide Individualized Injury Rehabilitation.....	327
9.9 Non-South East Asians have a better running economy and different anthropometrics and biomechanics than South East Asians.	335
9.10 The Nike Vaporfly 4%: a game changer to improve performance without biomechanical explanation yet	353
9.11 Accurate estimation of peak vertical ground reaction force using the duty factor in level treadmill running.....	359

1. Preamble

Amongst all endurance sports, running is probably the most popular one with the most adherents. In the United States, around 36 million people (~10% of the population) are yearly practicing this activity [1]. In Switzerland, 27% of the population is running and 10% considers running as their main physical activity [2].

While running offers many health benefits, 19 to 79% of recreational runners are yearly contracting a running related injury [3, 4]. Therefore, the incidence of these injuries is high. One of the main reasons of the occurrence of these injuries is that the loading of the musculoskeletal system exceeds the load bearing capacities [5]. For instance, as every running step is associated with an impact shock, in the order of 1.5 to 2.5 body weights (BW) at moderate endurance running speed (11-13 km/h) for the active peak [6], approximately one million of active peaks have to be absorbed by the human body for an average weekly mileage of 20 km during a one year period [7].

To develop a safe and economical running gait, each runner spontaneously and subconsciously adopts a self-optimized running pattern [8-11]. Therefore, the understanding of the individual running patterns might be important for preventing running-related injuries, improving performance, and optimizing training.

This individually unique running pattern is challenging to describe using a single variable [12]. It is therefore of major interest to use multicomponent methods to understand individual differences in running biomechanics. As early as 1985, the running pattern was viewed as a global system with several interconnected variables such as foot placement, arm swing, body angle, rear leg lift, and stride length [13]. More recently, the synthetic review of van Oeveren et al. [14] proposed that the full spectrum of running patterns could be described objectively by combining two temporal variables: step frequency (SF) and duty factor (DF), where DF reflects the relative contribution of the ground contact time (t_c) to the stride duration [12, 15]. According to van Oeveren et al. [14], knowing DF and SF allows to categorize each running pattern in one of five distinct categories, namely “stick”, “bounce”, “push”, “hop”, and “sit”, but still reminding that there is a continuum of running patterns (see Fig. 1 in subsection 2.1.4).

Although a force plate is the gold standard method (GSM) to measure DF and SF, it could not always be available and used [16, 17]. In such case, alternatives would be to use a motion capture system [18, 19] or a light-based optical technology [20]. Nevertheless, even though

these systems can be used outside the laboratory [21-23], they suffer from a lack of portability and are restricted to a specific and small capture volume. To overcome such limitation, techniques were developed to estimate DF and SF using portable tools such as inertial measurement units (IMUs), which are low-cost and practical to use in a coaching environment [24].

Hence, the main purpose of this thesis was to investigate the objective evaluation of the spontaneous running pattern and its relationship in terms of runners' classification in the laboratory and towards the field. To do so, the thesis contains two sub-goals. First, this thesis extended about the knowledge of DF and SF as global objective variables to assess spontaneous running patterns. Second, this thesis developed algorithms allowing to accurately measure t_c , flight time (t_f), DF, SF, and peak vertical ground reaction force ($F_{z,max}$) in absence of GSM but using a sacral-mounted IMU. This would later allow performing these measurements in the field.

This thesis was written following a project performed in collaboration with the Volodalen Swiss Sportlab company. This project entitled "V3: a personalized and adapted 'inertial' package to identify origin of running injuries and treat them" was supported by Innosuisse (grant no. 35793.1 IP-LS). The goal of this project was to establish standards of validity in laboratory conditions of key stride variables using a sacral-mounted IMU to latter consider field monitoring. The target customers being potentially injured recreational runners, the developed algorithms based on IMU data were expected to accurately assess their spontaneous running pattern on a treadmill and at their preferred running speed, i.e., around 10-12 km/h.

2. Introduction

2.1 From local to global assessment of spontaneous running patterns

2.1.1 *The local assessment of spontaneous running patterns*

The spring–mass model represents running as a “bouncing” gait modeled using a mass connected to a massless spring [25]. In this model, the supporting leg behaves like a spring during stance and each stance is separated by a t_f , i.e., a period where the limbs are not in contact with the ground. The presence of this flight phase constitutes one criterion to distinguish running from walking [26]. The other criteria are 1) a vertical ground reaction force pattern showing a maximum situated around mid-stance, 2) a maximal bent knee around mid-stance, and 3) in-phase fluctuations of kinetic and gravitational potential energy [26]. These four criteria in general coincide.

Even though each runner adopts a unique spontaneous running pattern, runners are typically classified in one of three discrete categories depending on their preferred foot-strike pattern (FSP). A runner is either categorized as a: (1) rearfoot striker (RFS) when the initial contact of the foot with the ground is made on the heel or rear third part of the sole; (2) midfoot striker (MFS) when the heel and toes contact the ground simultaneously; or (3) forefoot striker (FFS) when the initial contact of the foot with the ground is made on the forefoot or front half of the sole [27]. This classification can be obtained using the foot-strike angle (FSA) following the procedure proposed by Altman and Davis [28].

These FSPs involve different neuromuscular activation patterns [29] and impact attenuation strategies [30-33]. The latter pattern has been shown to induce different loads on the lower limb and different three-dimensional (3D) stress patterns in the ankle, knee, and hip joints [34-37], as well as different sagittal plane joint angles during stance [36, 38]. However, Knorz et al. [34] showed that there are no global advantages of one FSP over another in terms of joint stresses. Indeed, no statistically significant difference in the injury rate between RFS, MFS, and FFS has been reported in a large-scale epidemiological study [39]. The likelihood of certain type of running-related injuries was shown to depend on FSP [40-42], with hip and knee injuries more common in RFS, and ankle and foot injuries more common in MFS and FFS. The change in the relative risk of running-related injuries can be associated to the redistribution of loads based on FSP [43-46]. Besides, no differences in running economy have been reported

among different FSAs [47] or FSPs [48-50], and changing FSPs is no longer recommended for RFS [36, 49, 51].

FSP, though important, only represents a single specific event of the overall running pattern and is given by a single segment (the foot) of the overall human body. Therefore, the spontaneous running pattern should not be reduced to its FSP but should be considered as a whole, i.e., as a global and dynamic system with several interconnected biomechanical parameters [52]. As typical extreme examples, Arendse et al. [53] and Dreyer and Dreyer [54] investigated “Pose” and “Chi” running, respectively, characterized by mid- to forefoot striking, short t_c and step length, and less knee flexion during stance. On the other hand, McMahon et al. [55] tested the “Groucho” running, a running pattern with excessive knee flexion and associated with increased t_c and step length together with decreased t_f and vertical oscillation of the body. A similar running pattern is given by the “Grounded” running, which is used at slow running speed and has the particularity to alternate single and double stance with no flight phase [56, 57]. A flight phase is sometimes lacking when people run slowly [58]. According to the first mentioned distinction, this grounded locomotion pattern should be classified as walking but not as running. However, running without a flight phase seems to behave as a spring-mass model, i.e., very different from the typical walking inverted pendulum motion [58]. Similar observations were reported for quails, ostriches, and gibbons [59-61]. On this basis, Vereecke et al. [59] suggested that the presence of a flight phase should not be used to distinguish between walking and running. Hence, the term grounded running was employed in animal literature for such locomotion, but this term is also valid for human locomotion. Therefore, these examples show that it is of major interest to use multi-component methods instead of single-parameter analyses.

This consideration should lead to a better understanding of the global running pattern, which is nowadays an emergent area of research. For example, Hoerzer et al. [62] applied a machine learning (ML) algorithm on global biomechanical parameters obtained from a cohort of 88 runners and identified eight functional groups with distinct running patterns that differed mostly in age or gender. Similarly, two different functional groups were deciphered when using hierarchical cluster analysis on 121 runners, with the main differences being observed on the frontal and sagittal plane knee angles [63]. Both studies reported different running gait

strategies within a large population of runners, due to different anthropometric characteristics in the first study and different intrinsic ways to run in the second study.

2.1.2 The global subjective assessment of spontaneous running patterns

Instead of using an automatic pattern recognition approach, other researchers categorized runners in two groups termed terrestrial (TER) and aerial (AER) runners, based on a subjective evaluation of their spontaneous running pattern [64]. Runners were scored by running coaches with several years of experience using the Volodalen[®] method. Coaches paid attention to five key elements: vertical oscillation of the head, antero-posterior motion of the elbows, pelvis position at ground contact, foot position at ground contact, and FSP. Each element was scored from one to five, leading to a global subjective score ($V^{\text{®}}$ score) that represents the global running pattern of participants. This score ultimately allows the classification of runners into the two different categories (i.e., AER if $V^{\text{®}}$ score greater than 15 and TER otherwise). The $V^{\text{®}}$ score was shown to be a reliable method to assess running pattern [65]. This categorization revealed kinematic differences but a similar running economy [22, 64, 66, 67]. To minimize the metabolic cost, AER runners favor a long t_f together with a more fore-FSP and a larger leg stiffness (k_{leg}) than TER runners for whom a long t_c associated with a more rear-FSP was favored [67]. These findings demonstrate the presence of a holistic running system which seems to be subconsciously driven, reinforcing the theory of self-optimization, which is central in the development of an economical running gait [8, 10, 11, 68, 69].

2.1.3 The duty factor as a global objective assessment of spontaneous running patterns

This previous classification of runners requires a coach to be familiar with the usage of the subjective evaluation of the running pattern, which might sometimes prove to be inconvenient. Moreover, outcomes might also be biased because of the experimenter.

Another way to categorize runners is based on DF [18, 19], i.e., the ratio of t_c to stride time [t_c + swing time (t_s)], with a higher DF reflecting a greater relative contribution of t_c to the running step [12, 15]. Considering both t_c and t_s simultaneously provides a better understanding of the global running pattern compared with when these temporal variables are considered separately [18, 19]. The authors observed that the 20 subjects with highest DF

values and 20 subjects with lowest DF values (among a cohort of 54 participants) used different running strategies but had a similar running economy, showing that these two strategies are energetically equivalent at endurance running speeds [18]. A more symmetrical running pattern between braking and propulsion phases in terms of time and vertical center of mass (COM) displacement, anterior FSP (MFS and FFS), and extended lower limb during t_c at the hip, knee, and ankle joints were observed for low than for high DF runners [18, 19]. On the contrary, high DF runners exhibited greater lower limb flexion during t_c at the hip, knee, and ankle joints, a more RFS, and less vertical oscillation of the whole-body COM to promote forward propulsion than low DF runners [18, 19]. This would suggest that the two DF groups may optimize differently the elastic property of the linear lower limb spring (i.e., the leg stiffness: k_{leg} , defined as the ratio of the peak ground reaction force over the change in leg length during stance [70]) for reducing the metabolic cost of running. Hence, high and low DF runners reflected different FSPs [18, 19], most likely because t_c is related to FSP [27, 71]. Nonetheless, DF was thought to not only be directly related to the angle at the initial ground contact (via t_c) as is FSP but to also be functionally representative of a more global running behavior because it takes both the duration of force production (t_c) and the cycle frequency of running into account [18, 19, 72]. For this reason, although FSA and DF values should be different among DF (high, mid, and low DF runners) and FSP (RFS, MFS, FFS) groups, respectively, FSP and DF groups should not necessarily be constituted by the same runners. This would confirm that DF should be preferred to FSP/FSA when evaluating the global running pattern of a runner. Nonetheless, to the best of our knowledge, the relationship between the groups created using FSA and DF values has not yet been considered.

Hence, this thesis (**study 1**) compared these two different classification methods in analyzing running gait at several running speeds. We hypothesized that i) FSP groups should have significantly different DF values, ii) DF groups should have significantly different FSA values, and iii) weak correlations should be obtained between FSA and DF values.

2.1.4 Combining the duty factor and step frequency to globally assess spontaneous running patterns

Recently, the synthetic review of van Oeveren et al. [14] proposed that the full spectrum of running patterns could be described combining two temporal variables: SF and DF. According

to these authors [14], knowing DF and SF allows to categorize running patterns in one of five distinct categories, namely “stick”, “bounce”, “push”, “hop”, and “sit”, but keeping in mind that running patterns operate along a continuum (Fig. 1). Individuals spontaneously and subconsciously adopt their own running pattern, a choice shown to be self-optimized and central in the development of an economical and safe running gait [8-11]. The understanding of the individual running patterns might be important for improving performance, optimizing training, and preventing running-related injuries.

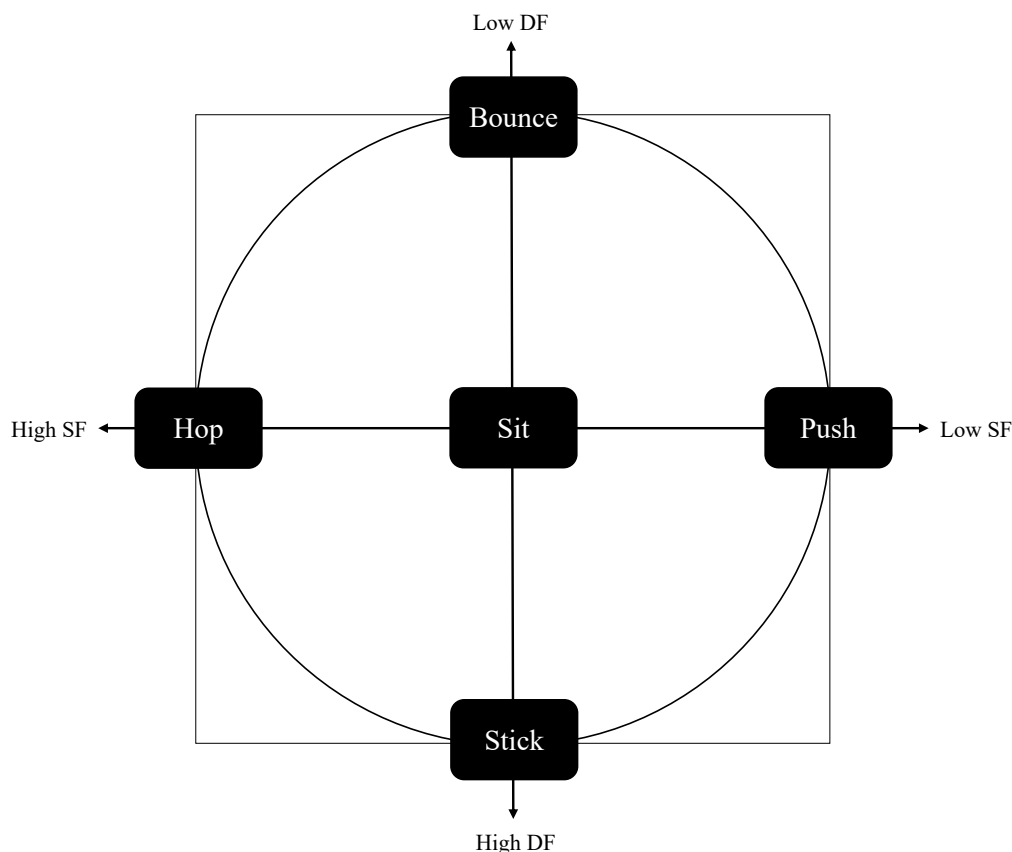


Figure 1. Visualization of the duty factor (DF) and step frequency (SF) axes that describe a continuous spectrum of running patterns with on the extremes “Stick”, “Bounce”, “Hop”, and “Push”, as well as “Sit” in the center. Adapted from van Oeveren et al. [14].

The importance of DF and SF in determining running patterns [14] corroborates previous findings. On the one hand, DF has been used to categorize runners with distinct running patterns [18, 19]. On the other hand, SF can reveal individual muscle recruitment patterns of runners and strategies to increase running speed [73] or achieve top-end running speeds [74]. Even in subgroups of individuals with similar sprint velocities, a range of SF and step length combinations are present [75].

Running speed affects DF and SF, with an increase in running speed decreasing DF [14, 15, 18] and increasing SF [14, 73, 76]. These changes are likely related to changes in their subcomponent variables t_c and t_f . Indeed, t_c decreases with an increase in running speed, whereas t_f increases [14, 18, 76, 77]. Given the speed-dependency of these variables, van Oeveren et al. [14] suggested using an absolute speed to define running patterns as stick, bounce, push, hop, and sit.

Worth noting is the large interindividual variations in temporal variables (DF, t_c , t_f , and SF) reported at absolute running speeds [18, 76] and the large interindividual variations in the individual strategies adopted to adapt to changes in running speeds [21, 47, 74]. For instance, a curve-clustering approach on the FSA of runners across speeds revealed three subgroups: those that maintained a rear-FSP, those that maintained a fore- or mid-FSP, and those that transitioned from a rear-FSP to a less rear-RFS with increasing speed [47]. Therefore, the running pattern of an individual could also change with speed if the relationship between or changes in the underlying temporal variables are inconsistent across running speeds. Such understanding would then allow us assessing if the evaluation of running patterns could be generalized across speeds and studies.

Hence, this thesis (**study 2 – aim 1**) assessed if running patterns are consistent across running speeds by examining the consistency in four temporal variables (DF, SF, t_c , and t_f). For instance, we investigated whether a runner with a high DF (with respect to the group median) at a slow running speed also exhibits a high DF at a faster running speed. We hypothesized that consistency would be greater when differences in running speeds were smaller, as previously observed for FSA [47].

Besides, this thesis (**study 2 – aim 2**) assessed the consistency across the four temporal variables at an absolute running speed. Given that DF and SF are proposed to be two independent key running pattern determinants [14], the association between these two variables should be low. Hence, we hypothesized that consistency would be low between DF and SF. On the other hand, we anticipated greater consistency between DF and its subcomponent variables (t_c and t_f) as well as between SF and t_c and t_f .

2.1.5 Using topological methodology to investigate the association of duty factor and step frequency on running biomechanics

The previous studies that investigated the association of DF or SF on running biomechanics used summary metrics, i.e., specific temporal focus like foot-strike (FS) or toe-off (TO) events, of signals such as the whole-body COM trajectory or the lower limb angles during t_c [18, 19]. This reduction to summary-metric space is not strictly necessary because statistical hypothesis testing can also be conducted in a continuous manner [78]. Indeed, one-dimensional biomechanical curves such as the ground reaction force signals are registrable and their fluctuations can be described and then, compared expressing them as a function of the normalized stance phase duration [79, 80]. In this case, statistical analysis can be conducted on the original registered curves using the state-of-the-art topological methodology called statistical parametric mapping (SPM) [81], which was recently applied to the field of biomechanics [82]. SPM has the advantages to consider the signal as a whole and presents the results directly in the original sampling space. For this reason, the spatiotemporal biomechanical context is immediately apparent, and allows direct visualization of where do significant differences occur during t_c [78].

Therefore, this thesis (**study 3 – aim 1**) investigated the association of DF and SF on the vertical and fore-aft ground reaction force signals for treadmill runs at several endurance running speeds (9, 11 and 13 km/h) using SPM. In addition, this thesis (**study 3 – aim 2**) investigated the association of DF and SF on the spring-mass characteristics of the lower limb.

We hypothesized that i) a lower DF should be associated to higher vertical and fore-aft ground reaction force fluctuations, and that a lower SF should be associated to higher vertical and fore-aft ground reaction force fluctuations but to a lower extent than for DF [83]. Besides, as higher DF runners demonstrated a more rear-FSP [18, 19] but should show lower vertical force than lower DF runners, we hypothesized that ii) the linearity of the force-length relationship should decrease with increasing DF, due to the higher chance to observe an impact peak when increasing DF (high DF runners are more RFS than low DF runners). Furthermore, we hypothesized that iii) a higher SF should correspond to a smaller leg compression, as previously observed [70, 84, 85].

2.2 From the laboratory towards field measurement of spontaneous running patterns

2.2.1 The accurate measurement of contact and flight times without a force plate: using a motion capture system

As previously mentioned, DF depends on both t_c and t_f , which are usually obtained from FS and TO events. Therefore, t_c and t_f rely on the accuracy of these event detections, for which the use of a force plate is considered as the GSM. However, force plates could not always be available and used [16, 17]. In these cases, using kinematic algorithms (KA), which are for instance based on the outcome of a motion capture system [18, 19], may be a useful and alternative solution. Nevertheless, these FS and TO detection must be sufficiently accurate.

The first algorithms detecting gait events were developed for walking [86-89]. However, their direct application to running can be problematic due to kinematic differences between walking and running [90]. Therefore, several algorithms were developed specifically for running and compared to GSM [16, 90-95] or to a footswitch device [96], but they did not all offer the same accuracy. Moreover, previous datasets were limited to less than 30 runners [92, 96], which may be too small to allow generalizing the algorithm to every runner. In addition, not only the gait type but also FSP might impact the accuracy of the algorithm. Indeed, Smith et al. [93] reported relatively different errors (up to 30 ms) for both FS and TO between RFS, MFS, and FFS for five KA. Similarly, Leitch et al. [92] depicted that the most accurate algorithm detecting FS was dependent on FSP but not the one detecting TO. These previous algorithms were based on heel kinematics, which differ based on FSPs. Indeed, Milner and Paquette [95] and Smith et al. [93] reported larger errors for non-RFS than for RFS when using these heel-based algorithms.

It also seems necessary to compare t_c computed from FS and TO based on GSM and KA, due to its biomechanical importance [68]. For instance, a larger error in t_c was observed for an algorithm that was more precise in FS and TO detection than for those that were less precise [93], due to accumulation of errors in FS and TO detection.

Hence, this thesis (**study 4**) proposed a novel KA to detect FS and TO and compared it to GSM at several treadmill endurance running speeds (9, 11, and 13 km/h) and across FSAs. In addition, FS and TO were used to estimate t_c which was then compared to that based on GSM. This algorithm uses a combination of heel and toe kinematics to detect FS. We hypothesized that i) no systematic bias would be reported between GSM and KA for FS and TO at any of the speeds examined and ii) no systematic bias, significant difference between t_c derived from GSM and KA, or effect of FSA would be obtained.

2.2.2 The accurate measurement of peak vertical ground reaction force without a force plate: using a motion capture system

In addition to t_c and t_f , $F_{z,\max}$ is also an important biomechanical parameter. Indeed, even though running can offer many health benefits, the incidence of running related injuries remains high [5]. These injuries often occur when the loading of the musculoskeletal system exceeds its load bearing capacities. This loading corresponds to the repetitive shocks associated with every step that the human body must absorb by adopting a specific running biomechanics. Although the magnitude of these shocks are relatively insubstantial, their quantity can be significant [6].

The internal forces contribute most to the experienced loading [97, 98]. However, the external forces are often used as substitute measures to estimate the loading of the musculoskeletal system [98-101]. For instance, moderate correlation was observed between the active peak force and peak axial tibial compressive force [99]. It was also suggested that the peak tibial bone loading occurs during mid-stance at $F_{z,\max}$ [98, 101] and that $F_{z,\max}$ is representative of the magnitude of external bone loading during the stance running phase [98]. For these reasons, $F_{z,\max}$ proved to be one important biomechanical parameter to accurately measure, though this variable alone should not be used to assess running related injuries [102].

The measurement of $F_{z,\max}$ is usually performed using force plates, i.e., the GSM. However, an instrumented treadmill would be required to conduct such measurement in the laboratory, which could not always be affordable or at hand [16, 17]. In such case, alternatives would be to use a sacral-mounted IMU [103-106] or a motion capture system [18, 19]. The former is low-cost and practical to use in a coaching environment [24] while the latter, though more

expensive, allows an in-depth assessment of running kinematics and is the alternative employed herein.

Using Newton's second law, which states that the sum of the forces applied to the human body is given by the body mass multiplied by the acceleration of its COM, vertical ground reaction force can easily be recovered when assuming no air resistance. The acceleration of the COM can be provided by the outcome of the motion capture system. Indeed, based on the 3D kinematics of the entire body, the COM trajectory is computed as a weighted sum of the COM of each body segments (segmental analysis) [107], which ultimately allows obtaining the whole-body COM acceleration by computing the second derivative of the COM trajectory.

Although the segmental analysis is quite widespread, it is not a perfect estimation. For instance, it is subject to soft tissue artefact [108] and relies on accurate markers placement [109]. Moreover, this method is time-consuming due to the large number of markers required to approximate each segment as a rigid body, where the choice of each rigid body, i.e., the schematic model of each body segment, is essential to correctly estimate the whole-body COM [110]. Furthermore, body segments need to be assigned inertial properties and COM locations based on their shape [111], and attributed relative mass based on standard regression equations [112], which add extra approximations. For these reasons, Napier et al. [113] approximated the whole-body COM trajectory by the trajectory of a single marker placed on the sacrum at the midpoint of the posterior superior iliac spines. These authors demonstrated that this very simple alternative was a valid proxy for the COM trajectory in vertical and fore-aft directions at specific events of the running cycle [113]. However, to the best of our knowledge, using the vertical acceleration of a single sacral marker to estimate $F_{v,\max}$ has never been investigated while using the whole-body vertical COM acceleration has already been attempted but using a single participant [114].

Alternatively, sacral acceleration directly recorded using sacral-mounted IMU were used to estimate $F_{z,\max}$ [103-106]. For instance, Alcantara et al. [104] predicted $F_{z,\max}$ using ML and reported a root mean square error (RMSE) of 0.15 BW. Moreover, weak to moderate correlations were obtained between $F_{z,\max}$ measured using GSM and estimated using IMU data [103]. These authors observed an effect of the low-pass cut-off frequency used for the IMU data, where a better correlation was depicted for a 10 than a 5 or 30 Hz cut-off frequency.

The previous findings suggest that the choice of the cut-off frequency proved to be important. Indeed, a substantial filtering method is required to avoid unrealistic peaks in the acceleration signal [107]. However, the effect of the cut-off frequency was not investigated when estimating $F_{z,\max}$ from whole-body COM [114]. Hence, this thesis (**study 5 – aim 1**) estimated $F_{z,\max}$ based on whole-body COM (COM method; COM-M) and sacral marker (sacral marker method: SACR-M) accelerations filtered using several cut-off frequencies (between 2 and 20 Hz). In addition, this thesis (**study 5 – aim 2**) compared these estimations against GSM at several treadmill endurance running speeds (9, 11, and 13 km/h). We hypothesized that i) a single cut-off frequency should minimize RMSE and that this cut-off frequency should be different for each method and ii) a similar RMSE than in Alcantara et al. [104] should be obtained, i.e., ~ 0.15 BW.

2.2.3 The accurate measurement of contact and flight times and peak vertical ground reaction force without a force plate: using an inertial measurement unit

Using a motion capture system [18, 19] or a light-based optical technology [20] were shown to provide useful alternatives to force plates. Nevertheless, even though these systems can be used outside the laboratory [21-23], they suffer from a lack of portability and are restricted to a specific and small capture volume. To overcome such limitation, techniques to identify gait events were developed using portable tools such as IMUs, which are low-cost and practical to use in a coaching environment [24].

$F_{z,\max}$ was previously estimated using the vertical acceleration signal recorded by a sacral-mounted IMU [103, 104]. For instance, an RMSE of 0.15 BW was reported when using a ML algorithm that used data filtered using a 10 Hz 8th order low-pass Butterworth filter [104]. Another method calculated the COM and sacral marker vertical accelerations from their corresponding 3D kinematic trajectories and reported an RMSE smaller than or equal to 0.17 BW when estimating $F_{z,\max}$ from these acceleration signals [115]. The whole-body COM acceleration calculated from the kinematic trajectories was also used by Pavei et al. [114] to estimate $F_{z,\max}$ but for a single participant and by Verheul et al. [116] to estimate the resultant ground reaction force impact peak (within the first 30% of the stance). Pavei et al. [114] reported an RMSE ~ 0.15 BW for running speeds ranging from 7 to 20 km/h while an error of ~ 0.20 BW was reported by Verheul et al. [116] for speeds between 7 and 18 km/h.

t_c and t_f , calculated from FS and TO, can themselves be identified using different available techniques that used IMU data [103, 104, 117-127]. When using a sacral-mounted IMU, which is a natural choice as it approximates the location of the COM [113], either the forward [119] or the vertical acceleration [103, 104] were used to estimate t_c and t_f . On the one hand, Lee et al. [119] detected specific spikes in their unfiltered forward acceleration signals sampled at 100 Hz to identify FS and TO. On the other hand, the vertical ground reaction force was estimated from the vertical acceleration signal recorded by the IMU (using Newton's second law), which allowed detecting FS and TO using a 0 N threshold [103, 104]. A 5 Hz low-pass Butterworth filter (8th order) was shown to result in the best correlation between t_c obtained from GSM and IMU data (sampled at 500 Hz) [103] while a ML algorithm that used data filtered using a 10 Hz 8th order low-pass Butterworth filter resulted in a RMSE of 11 ms for t_c [104]. The vertical acceleration (sampled at 208 Hz) was also used to estimate the effective contact (t_{ce}) and flight (t_{fe}) times [127], two variables that allow deciphering the on-off ground asymmetry of running [128, 129]. The authors estimated these effective timings by using a BW threshold instead of a 0 N threshold, which allowed detecting effective FS (eFS) and effective TO (eTO) events and thus estimating t_{ce} and t_{fe} . Moreover, the vertical acceleration was filtered using a Fourier series truncated to 5 Hz instead of the usual low-pass Butterworth filter. The authors reported an RMSE smaller than or equal to 22 ms for both t_{ce} and t_{fe} .

As previously stated, more research investigating the effect of different filtering methods are needed when estimating biomechanical variables such as $F_{z,max}$ and t_c [103], especially because the low-pass cut-off frequency could affect the estimation of biomechanical variables [130, 131]. For this reason, this thesis (**study 6 – aim 1**) estimated $F_{z,max}$ using a Fourier series truncated to 5 Hz to filter the acceleration signal recorded by a sacral-mounted IMU (IMU method: IMUM). Moreover, this thesis (**study 6 – aim 2**) estimated t_c and t_f using the same filtered acceleration signal. This filter was previously used by Patoz et al. [127] to estimate both t_{ce} and t_{fe} but has never been used, to the best of the authors knowledge, to estimate $F_{z,max}$, t_c , and t_f . Herein, t_c and t_f were estimated from FS and TO, themselves detected by modifying the BW threshold previously used by Patoz et al. [127]. We hypothesized that i) an RMSE smaller than or equal to the 0.15 BW reported in Alcantara et al. [104] should be obtained for $F_{z,max}$, even if the IMUM is a simple method which does not rely on ML, as was the 3D kinematic method [115], and ii) t_c and t_f should have an RMSE smaller than or equal to that reported in Patoz et al. [127] (i.e., 0.22 ms).

2.2.4 The accurate measurement of effective contact and flight times without a force plate: using an inertial measurement unit

Back in 1988, Cavagna et al. [132] defined two key running parameters denoted as t_{ce} and t_{fe} . They differ from the usual t_c and t_f by the fact that t_{ce} and t_{fe} correspond to the amount of time where the vertical ground reaction force is above and below BW, respectively, rather than where the foot is in contact with the ground or not [133]. These effective timings were proven to be appropriate to decipher the on-off ground (a)symmetry of running [128, 129].

These two variables are usually obtained from eFS and eTO. To obtain these effective timings outside the laboratory, the previously mentioned IMUM could be slightly modified. For this reason, this thesis (**study 7**) estimated t_{ce} and t_{fe} using the Fourier series truncated to 5 Hz to filter the sacral-mounted IMU data (IMUM) and compared these estimations to those from GSM.

2.2.5 Enhancing sacral acceleration-based estimations of running stride temporal variables and peak vertical ground reaction force using machine learning

$F_{z,max}$, t_c , and DF were shown to play a role in running-related injury development [98-101, 134-136]. t_f might also play a role as it takes both the vertical ground reaction force and its time of production into account.

t_c , t_f , and $F_{z,max}$ were previously estimated using a single sacral-mounted IMU [137]. Compared to gold standard values (force plate), RMSEs of 20 ms were obtained for t_c and t_f and 0.15 BW for $F_{z,max}$. Applying advanced analysis methods such as ML on top of these estimations may provide more accurate predictions. ML was used to explain the differences of gait patterns between high and low-mileage runners [138] as well as to estimate biomechanical variables based on IMU data [104, 139-141]. ML has the advantage to provide an analytical model which is trained and tested using different subsets of the dataset [142] and built from physics-based variables, i.e., variables that demonstrated to provide changes in running biomechanics [104]. The modeling of the relationships between clinical outcomes and biomechanical measures was attempted using ML models like linear regressions (LRs), support vector machines, and artificial neural networks (NNs) [142, 143]. Though limited to linear

relationships, LRs are widely used because the regression coefficients are useful for model interpretability [144]. On the other hand, support vector machines and NNs are used to model non-linear relationships. Although they usually provide better accuracies than LRs, their coefficients are difficult to interpret because of their large numbers [142]. Therefore, using both basic and complex ML models might illustrate the tradeoff between interpretability and accuracy and give the option to prioritize between the former and the latter.

Hence, this thesis (**study 8**) applied ML to predict t_c , t_f , DF, and $F_{z,\max}$ from their respective IMU-based estimations. We hypothesized that further applying ML to these IMU-based estimations should provide predictions with higher accuracies than those previously reported for the estimations [137]. The comparison among the predictions of several ML models would allow defining which model has the best tradeoff between interpretability and accuracy.

3. Aim of the thesis

The main purpose of this thesis was to investigate the objective evaluation of the spontaneous running pattern and its relationship in terms of runners' classification in the laboratory and towards the field. To do so, the thesis contains two sub-goals.

First, this thesis extended about the knowledge of DF and SF as global objective variables to assess spontaneous running patterns (**first 3 studies**).

The first of these three studies (**study 1**) aimed to compare FSP and DF classification methods in analyzing running gait at several endurance running speeds (9, 11, and 13 km/h). The second study (**study 2**) aimed to assess the consistency of running patterns across running speeds (10, 12, 14, 16, and 18 km/h) by examining the consistency in four temporal variables (DF, SF, t_c , and t_f) as well as the consistency across the four temporal variables at an absolute running speed. The third study (**study 3**) aimed to investigate the association of DF and SF on the vertical and fore-aft ground reaction force signals using SPM as well as on the spring-mass characteristics of the lower limb for treadmill runs at several endurance running speeds (9, 11, and 13 km/h).

We hypothesized that:

- Study 1 – 1. FSP groups should have significantly different DF values.
- Study 1 – 2. DF groups should have significantly different FSA values.
- Study 1 – 3. Weak correlations should be obtained between FSA and DF values.
- Study 2 – 1. Consistency should be greater when differences in running speeds were smaller.
- Study 2 – 2. Consistency should be low between DF and SF and we anticipated greater consistency between DF and its subcomponent variables (t_c and t_f) as well as between SF and t_c and t_f .
- Study 3 – 1. A lower DF should be associated to higher vertical and fore-aft ground reaction force fluctuations, and a lower SF should be associated to higher vertical and fore-aft ground reaction force fluctuations but to a lower extent than for DF.
- Study 3 – 2. The linearity of the force-length relationship should decrease with increasing DF.
- Study 3 – 3. A higher SF should correspond to a smaller leg compression.

Second, this thesis developed algorithms allowing to accurately measure t_c , t_f , DF, SF, and $F_{z,\max}$ in absence of the GSM but using a sacral marker and a motion capture system or a sacral-mounted IMU. This would later allow performing these measurements in the field (**next 5 studies**).

The first of these five studies (**study 4**) aimed to develop a novel KA to detect FS and TO and to compare it to GSM at several treadmill endurance running speeds (9, 11, and 13 km/h) and across FSAs. In addition, FS and TO were used to estimate t_c which was then compared to that based on GSM. The second study (**study 5**) aimed to estimate $F_{z,\max}$ based on whole-body COM and sacral marker accelerations filtered using several cut-off frequencies, and to compare these estimations against GSM at several treadmill endurance running speeds (9, 11, and 13 km/h). The third study (**study 6**) aimed to estimate $F_{z,\max}$ as well as t_c and t_f using a Fourier series truncated to 5 Hz to filter the acceleration signal recorded by a sacral-mounted IMU. The fourth study (**study 7**) aimed to estimate t_{ce} and t_{fe} using the same Fourier series to filter the sacral-mounted IMU data. The fifth study (**study 8**) aimed to apply ML to predict t_c , t_f , DF, and $F_{z,\max}$ from their respective IMU-based estimations.

We hypothesized that:

- Study 4 – 1. No systematic bias should be reported between GSM and KA for FS and TO at any of the speeds examined
- Study 4 – 2. No systematic bias, significant difference between t_c derived from GSM and KA, or effect of FSA should be obtained.
- Study 5 – 1. A single cut-off frequency should minimize RMSE and that this cut-off frequency should be different for each method
- Study 5 – 2. A similar RMSE than in Alcantara et al. [104] should be obtained, i.e., ~ 0.15 BW.
- Study 6 – 1. An RMSE smaller than or equal to the 0.15 BW reported in Alcantara et al. [104] should be obtained for $F_{z,\max}$.
- Study 6 – 2. t_c and t_f should have an RMSE smaller than or equal to that reported in Patoz et al. [127] (i.e., 0.22 ms).
- Study 7 – 1. Exploratory study.
- Study 8 – 1. Further applying ML to the IMU-based estimations should provide predictions with higher accuracies than those previously reported for the estimations.

4. General methodology

4.1 Participant characteristics

For all except the second study, the experimentation, consisting of a single visit to the laboratory, was conducted over two months between September and October 2020. This permitted to recruit and test 115 recreational runners including 87 males (age: 30 ± 8 yr, height: 180 ± 6 cm, leg length: 86 ± 4 cm, body mass: 70 ± 7 kg, weekly running distance: 38 ± 24 km, and running experience: 10 ± 8 yr) and 28 females (age: 30 ± 7 yr, height: 169 ± 5 cm, leg length: 82 ± 4 cm, body mass: 61 ± 6 kg, weekly running distance: 22 ± 16 km, and running experience: 11 ± 8 yr). These data were collected to conduct the Innosuisse project (grant no. 35793.1 IP-LS) for which the goal was to establish standards of validity in laboratory conditions of key stride variables using a sacral-mounted IMU to later consider field monitoring. This thesis is constituted of a series of secondary analyses of these data (studies 1 and 3-8). The third and fifth studies considered the entire dataset, while studies 1 and 4, 6 and 8, and 7 considered different subsets of 100 participants who were randomly selected from the entire dataset. The different datasets employed in the studies allow us to have heterogeneity in the data. For study inclusion, participants were required to be in good self-reported general health, to not have current or recent lower-extremity injury (≤ 1 month), to run at least once a week, and to have an estimated maximal aerobic speed greater than or equal to 14 km/h. The study protocol was approved by the Ethics Committee (CER-VD 2020-00334) and adhered to the latest Declaration of Helsinki of the World Medical Association.

As for the second study, 52 runners out of an existing database of 54 participants were considered [18], which included 32 men (age: 32 ± 9 yr, mass: 66 ± 11 kg, height: 175 ± 7 cm, running distance: 53 ± 21 km/week, running experience: 8 ± 8 yr, and best half-marathon time: 92 ± 10 min) and 20 women (age: 32 ± 9 yr, mass: 52 ± 6 kg, height: 162 ± 4 cm, running distance: 50 ± 22 km/week, running experience: 7 ± 4 yr, and best half-marathon time: 102 ± 12 min). Two runners were removed from the database because they had no data at the 18 km/h running condition (see Section 4.2 for further information about the experimental procedure) and we did not want to deal with missing data. These data were collected in Malaysia to study running biomechanics between high and low DF runners. The hypotheses were that 1) high DF runners should have a larger forward COM displacement during t_c and a smaller vertical COM displacement during t_f compared to low DF runners for a given running speed and 2) low DF runners should have a greater symmetry within t_c and t_f compared to high DF runners. This thesis is constituted of a secondary analysis of these data (study 2). For study inclusion,

participants were required to be in good self-reported general health with no current or recent (< 3 months) musculoskeletal injuries and to meet a certain level of running performance. More specifically, in the last year, runners were required to have competed in a road race with finishing times smaller than or equal to 50 min for 10 km or smaller than or equal to 2 h for 21.1 km. Each participant completed one experimental laboratory session. The ethical committee of the National Sports Institute of Malaysia approved the study protocol prior to participant recruitment (ISNRP: 26/2015), which adhered to the latest version of the Declaration of Helsinki of the World Medical Association.

4.2 Experimental procedure

After providing written informed consent, retroreflective markers were positioned on participants (see below). As for all but study 2, an IMU (Movesense sensor, Suunto, Vantaa, Finland) was attached to the sacrum at the midpoint between the posterior superior iliac spinae using an elastic strap belt (Movesense Belt, Suunto, Vantaa, Finland). As for each participant, first, a standing static trial using a standard anatomical position was recorded on an instrumented treadmill (Arsalis T150 – FMT-MED, Louvain-la-Neuve, Belgium; **studies 1 and 3-8**) or on a regular treadmill (h/p/cosmos mercury[®], h/p/cosmos sports & medical gmbh, Nussdorf-Traunstein, Germany; **study 2**) for calibration purposes. Then, a warm-up run was performed on the same treadmill to ensure stabilization of shoe stiffness properties [145] and to promote treadmill familiarization [146, 147]. This was followed, after a short break (< 5 min), by three 1-min runs (9, 11, and 13km/h) performed in a randomized order (**studies 1 and 3-8**) or by 5x 30-s runs at 10, 12, 14, 16, and 18km/h (**study 2**), with 1-min recovery periods between each run, to collect 3D data during the first 10 strides following the 30-s mark of running trials (**studies 1 and 3-8**) or during the last 10-s segment of the runs, resulting in at least 20 steps being analyzed [148]. All participants were familiar with running on a treadmill as part of their usual training program and wore their habitual running shoes during testing.

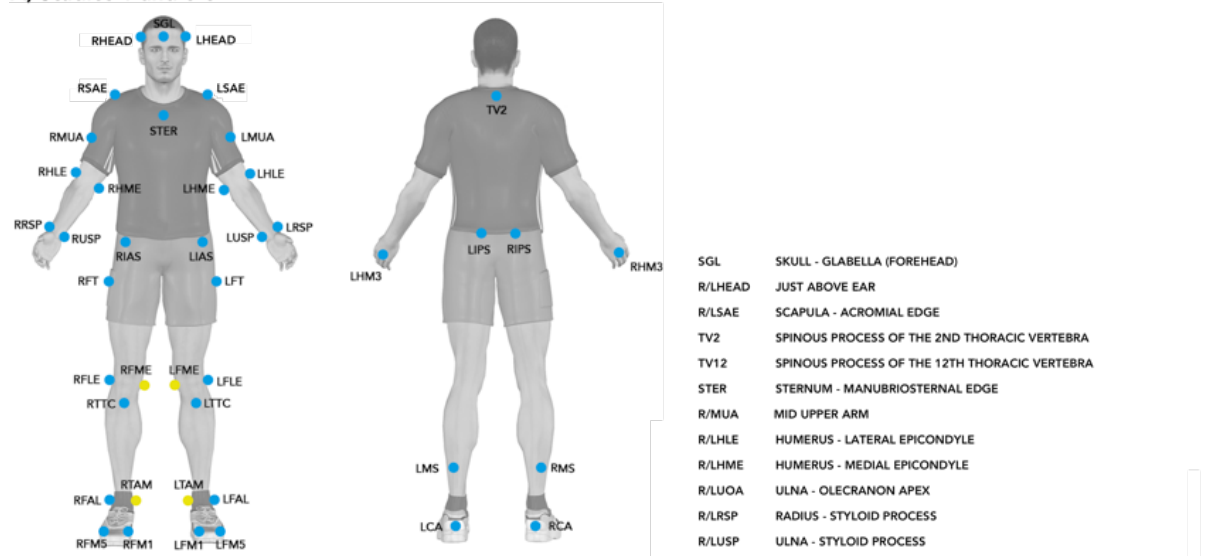
4.3 Data collection

Whole-body 3D kinematic data were collected at 200 Hz using motion capture and Vicon Nexus software v2.9.3 (Vicon, Oxford, UK; studies 1 and 3-8) or Qualisys Track Manager software version 2.1.1 build 2902 together with the Project Automation Framework Running

package version 4.4 (Qualisys AB, Göteborg, Sweden; study 2). The laboratory coordinate system was oriented such that x -, y -, and z -axis denoted medio-lateral (pointing towards the right side of the body), posterior-anterior, and inferior-superior axis, respectively. **Studies 1 and 3-8** used forty-three and 39 retro-reflective markers of 12.5 mm diameter for static calibration and running trials, respectively, while **study 2** used 35 retro-reflective markers of 12 mm in diameter for both static calibration and running trials (Fig. 2). They were affixed to skin and shoes of individuals over anatomical landmarks using double-sided tape following standard guidelines [149]. Synchronized 3D kinetic data (1000 Hz) were collected using the force plate embedded into the treadmill (**studies 1 and 3-8**). IMU data were collected at 208 Hz (saturation range: ± 8 g) using an iPhone SE (Apple, Cupertino, CA, USA) and a home-made iOS application that communicated with the IMU via Bluetooth.

The 3D marker and ground reaction force (analog signal) data were exported in .c3d format and processed in Visual3D Professional software v6.01.12 (C-Motion Inc., Germantown, MD, USA). 3D marker data were interpolated using a third-order polynomial least-square fit algorithm (using three frames of data before and after the “gap” to calculate the coefficients of the polynomial), allowing a maximum of 20 frames for gap filling, and subsequently low-pass filtered at 20 Hz using a fourth-order Butterworth filter. 3D ground reaction force signal was filtered using the same filter and downsampled to 200 Hz to match the sampling frequency of marker data.

A) Studies 1 and 3-8



B) Study 2

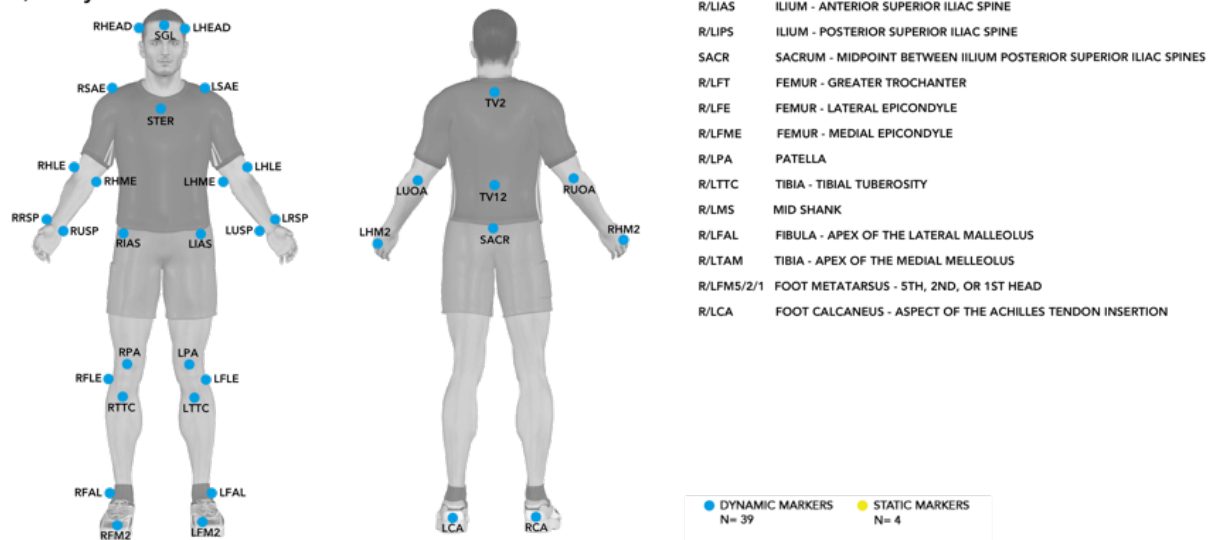


Figure 2. Retro-reflective markers placed on anatomical landmarks of participants for biomechanical data collection for A) studies 1 and 3-8 ($N = 43$) and B) study 2 ($N = 35$). R and L at the start of the acronyms denote right and left, respectively.

A full-body biomechanical model with six degrees of freedom and 15 rigid segments was constructed from the marker set (Fig. 3). The segments included the head, upper arms, lower arms, hands, thorax, pelvis, thighs, shanks, and feet. In Visual3D, the segments were treated as geometric objects, assigned inertial properties and COM locations based on their shape [111], and attributed relative masses based on standard regression equations [112].

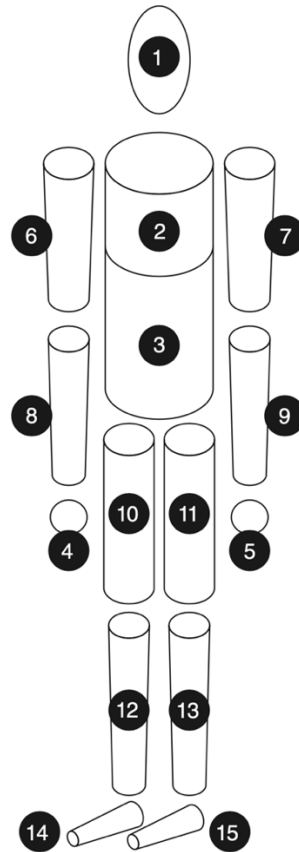


Figure 3. Geometric model of the human body consisting of 15 rigid segments.

The foot segment was obtained using five markers which were placed at the apex of both the lateral and medial malleolus, foot calcaneus (aspect of the Achilles tendon insertion), and head of the first and fifth metatarsals. The foot segment angle was defined as the angle of the foot segment relative to the laboratory coordinate system and computed using an x - y - z Cardan sequence. The x -component of the foot segment angle (the angle in the sagittal plan) at FS was used to determine FSP following the procedure proposed by Altman and Davis [28]. In brief, the average foot segment angle of the standing static trial was subtracted from that of running trials such that 0° corresponded to a foot parallel to the ground. Then, the angle at FS, i.e., FSA, was computed using the x -component of the rescaled foot segment angle (negative and positive angle values represented plantar flexion and dorsiflexion, respectively).

The whole-body COM location was calculated from the parameters of all 15 segments (the whole-body COM was directly provided by Visual3D). A sacral marker was reconstructed (virtual marker) at the midpoint between the two markers affixed to the posterior superior iliac spines [113]. Noteworthy, similar results would have been obtained by using a real marker at

this same location because marker placement error and soft tissue movement artefact are expected to be low in this region (prominence of bony landmarks and lack of soft tissue) [113]. The acceleration of the COM and sacral marker trajectories were calculated by computing their second derivative and were subsequently low-pass filtered using a fourth-order Butterworth filter. Several cut-off frequencies have been tested: 20, 10, 5, 4, 3, and 2 Hz. This choice of cut-off frequencies follows from the fact that any frequency above 20 Hz should arise due to vibration [7] while 3 Hz spike is considered to be reflective of step frequencies (vertical sinusoidal pelvic motion) [150]. For each low-pass filtered acceleration of both COM and sacral marker, the vertical ground reaction force was reconstructed using Newton's second law.

For all biomechanical measures, the values extracted from the data collection for each participant, including both right and left steps, were averaged for subsequent statistical analyses.

4.4 Event detection

4.4.1 Gold standard method

For each running trial, FS and TO as well as eFS and eTO (Fig. 5) were identified within Visual3D. These events were detected by applying a 20 N [93] and BW [132] threshold to the previously filtered and down sampled vertical ground reaction force, respectively.

4.4.2 Kinematic algorithm

The KA was implemented within Visual3D to detect FS and TO from kinematic data. A mid-toe landmark was created midway between markers placed at the head of the first and fifth metatarsals. The mid-toe landmark position was rescaled by subtracting its respective global minimum (within the 10 strides) to overcome bias due to shoe height. Heel and mid-toe accelerations were calculated as the second derivative (second order central method) of the heel marker (foot calcaneus: aspect of the Achilles tendon insertion) and rescaled mid-toe landmark positions, respectively. Following visual observations of heel and mid-toe z -acceleration curves, an approach similar to that of Hreljac and Stergiou [91], was followed. The KA was constructed such that FS was detected within a time window of 120 ms centered

around the instant when the mid-toe z -position reached 3.5 cm on descent. FS was defined as the first occurring maximum between the maxima of the heel marker and mid-toe landmark on z -acceleration curves within this time window. TO was detected at the instance when the mid-toe z -position reached 3.5cm on ascent after the preceding FS, following a similar approach to that of Alvim et al. [96]. If such a threshold did not exist, 4 and 4.5 cm thresholds were used instead. The distance between the mid-toe landmark and the end part of the shoe (on the toe-side) being close to 5.5 cm, the global minimum of the mid-toe landmark being close to 2 cm, and the foot angle at TO being close to 90° justified the 3.5 cm threshold. The KA requires three markers per foot to detect FS and TO but whole-body motion capture was used because a whole-body biomechanical model was needed to construct foot segment angles to obtain FSA, which permitted to validate the KA across FSAs.

4.4.3 Inertial measurement unit method

A home-made c++ code [151] was used to process IMU data. First, the z -axis of IMU was aligned with z -axis of the local coordinate system (LCS) using a truncated Fourier series to 0.5 Hz in each dimension, allowing to remove any acceleration due to movement of the IMU (vibrations and body motion) [103]. Indeed, a truncated Fourier series allows removing any frequency component within the original signal that are above the requested cut-off. Noteworthy, the number of terms to include in the truncated Fourier series is given by $N = n F / f$, where n is the number of IMU data points, F is the requested truncation frequency, and f is the IMU sampling frequency. Then, the median of each component of the filtered 3D signal was computed. Knowing that the average acceleration should be equal to g in the z -axis of LCS and 0 in the other two axes, the average angle between the z -axis of IMU and LCS could be calculated based on the previously computed medians. This average angle corresponds to the average tilt of the IMU with respect to the z -axis of LCS. Therefore, the IMU can be reoriented using this average angle so that its z -axis is, in average, aligned with the one of LCS. However, it was assumed that the rotational motion of the sensor around any of the three axes was negligible so that no complicated reorientation of the IMU had to be performed at each timestamp, which would anyway require several approximations (see for instance Falbriard et al. [123] for foot-worn IMU). This reorientation process is usually not considered when using sacral-mounted IMU and signals from sacral-mounted IMU are usually analyzed along the IMU's coordinate system and compared to ground reaction forces analyzed in LCS [103, 104,

119]. Then, aligned raw acceleration data were filtered using a truncated Fourier series to 5 Hz. This cut-off frequency was chosen because it led to the best estimation of t_c in Day et al. [103]. The vertical ground reaction force was approximated by the filtered vertical acceleration signal multiplied by body mass and used to detect FS and TO using a 20 N threshold and eFS and eTO using a BW threshold.

4.5 Biomechanical variables

4.5.1 Temporal variables

t_c , t_f , and t_s were defined as the time from FS to TO of the same foot (Fig. 4), from TO of one foot to FS of the contralateral foot, and from TO to FS of the same foot, respectively, while t_{ce} was given by the time between eFS and eTO (Fig. 4), and t_{fe} by the time between eTO and eFS. DF was calculated as $DF = t_c / (t_c + t_s)$ [15] while SF was defined as the inverse of the sum of t_c and t_f , i.e., $SF = 1 / (t_c + t_f)$. Furthermore, as for the third study, SF was normalized by $\sqrt{g/L_0}$ [14, 152], where g is the gravitational constant and L_0 the leg length, calculated as the distance between hip and ankle joint center using the static calibration.

4.5.2 Peak vertical ground reaction force variable

$F_{z,\max}$ was defined by the maximum of the vertical ground reaction force between FS and TO (Fig. 4) [153]. $F_{z,\max}$ was normalized by BW.

4.5.3 Stiffness related variables

The spring-mass characteristics of the lower limb were assessed by computing the force-length relationship [154], i.e., the force vector projected along the leg as function of the leg compression/decompression during stance (Fig. 5). Following the definition of the spring-mass model, i.e., a massless spring attached to a point mass located at the whole-body COM [25], the leg length was represented by the magnitude of a 3D leg vector defined from the whole-body COM to the center of pressure of the foot. The center of pressure being subject to large fluctuations for low vertical force values, a 200 N vertical threshold was used for FS and TO in this specific case.

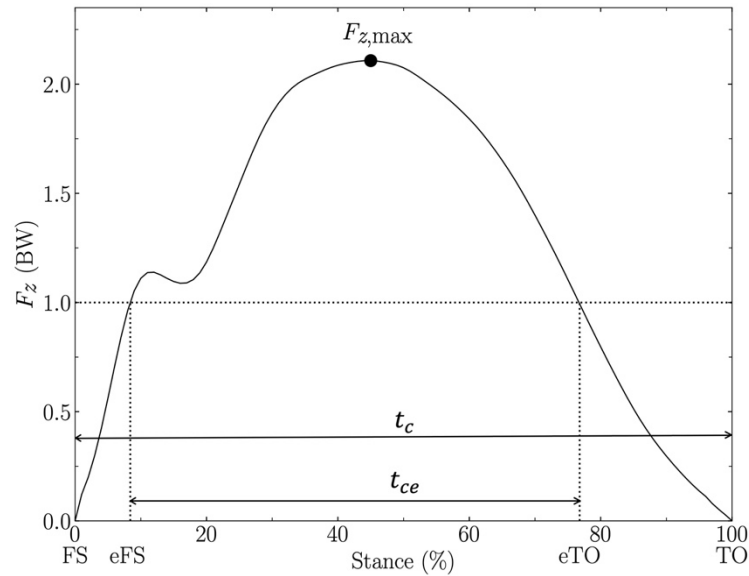


Figure 4. Example of a vertical ground reaction force signal (F_z) in body weights (BW) during stance, for a representative participant and at 11 km/h. The maximum between foot-strike (FS) and toe-off (TO) events defines the peak vertical ground reaction force ($F_{z,max}$). Effective FS and effective TO events are denoted by eFS and eTO, respectively. These events allow deciphering the on-off ground asymmetry of running. Ground contact time (t_c) is defined by the time from FS to TO while effective ground contact time (t_{ce}) is given by the time between eFS and eTO.

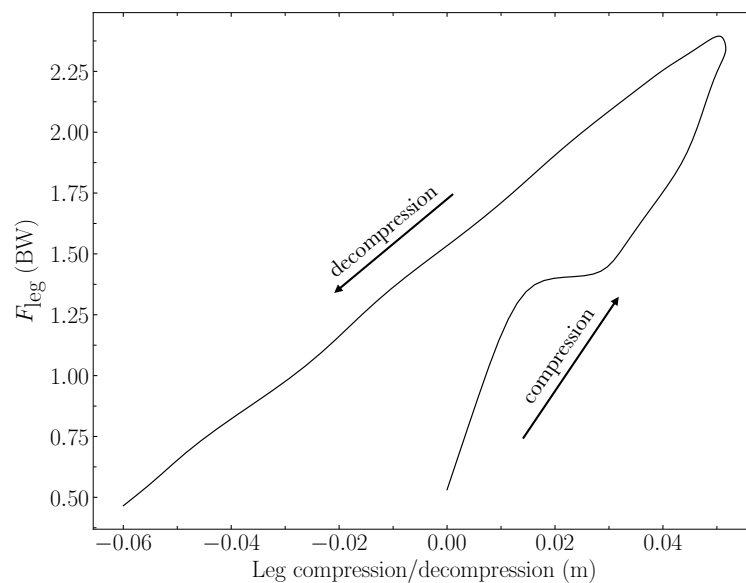


Figure 5. Example of a force-length relationship, i.e., ground reaction force projected along the leg (F_{leg}) in body weights (BW) as function of the leg compression/decompression during stance, for a representative participant and at 11 km/h.

4.5.4 Predicted variables obtained using machine learning models

As for **study 7**, three ML models: LR, support vector regression (SVR) – the regression analog of support vector machine – with the radial basis function kernel, and two-layers NN (NN2),

were constructed to predict t_c , t_f , DF, and $F_{z,\max}$ using a train/test method (80%–20% split; 80% and 20% runners in the training and testing set, respectively). All the running trials from one subject were included in only one set to prevent overfitting and to ensure that the models generalize well to new data. Additionally, a similar distribution of male (72.5%) and female (27.5%) was maintained in both subsets to avoid introducing bias in the model during training [142]. For each variable predicted by the three models, four features were used as predictors: running speed, runner's body mass, SF, and corresponding IMU-based estimation. This choice follows from their relationship with changes in running biomechanics [104, 155, 156] and to keep the models relatively simple. The SF included in the features was the IMU-based estimation. The training features were standardized by removing the mean and by scaling to unit variance. The different models were trained using a 5-fold cross validation approach for hyperparameter optimization. Hyperparameters are given in Table 1. The trained models were used to make predictions on the testing set. The testing data were previously standardized based on the mean and standard deviation of the training data.

Table 1. Hyperparameters optimized during the 5-fold cross validation for the three machine learning models employed.

Machine learning model	Hyperparameter	Values
Linear regression	Intercept in the model	True and False
	C (inversely proportional to the strength of the regularization)	20 points (logarithmic scale between 0.001 and 10000)
Support vector regression	Epsilon (specifies the epsilon-tube within which no penalty is associated in the training loss function with points predicted within a distance epsilon from the actual value)	20 points (logarithmic scale between 0.001 and 100)
	Activation function of the first layer	relu, tanh, sigmoid, and softmax
Two-layers neural network	Dimensionality of the inner layer	8, 16, 32, and 64
	Batch size	2, 4, 8, and 16
	Loss function	mean absolute error and mean squared error

4.5.5 Runners' classification

As for **study 1**, high (DF_{high}), mid (DF_{mid}), and low (DF_{low}) DF groups were created at each speed using the terciles of the main group. Runners were also classified as RFS, MFS, and FFS at each speed if FSA values were greater than or equal to 8° , smaller than 8° but greater than or equal to -1.6° , and smaller than -1.6° , respectively [28], which was also used in **study 4**.

4.6 Data analysis and statistical analysis

A more detailed version of both the data analysis and statistical analysis of each study is presented in its respective article given in the *List of publications* section because each study has its own analysis. Briefly, linear mixed models were used in studies 1, 3, and 4 while repeated measures ANOVA were used in studies 5-8. Additionally, Pearson's correlation coefficients (r) were computed in studies 1-3, SPM was used in study 4 and Bland-Altman plots [157, 158] were constructed to examine the presence of systematic bias in studies 4-8. The choice of the statistical analyses used in the different studies was dependent on when the manuscript was sent to review in each scientific journal and on feedbacks received from the reviewers. As for a repeated measures ANOVA based on two groups and three repeated measures, which is a common statistical analysis used in the present thesis, the sample size calculation led to the requirement of 82 participants when assuming a small effect size of 0.2 [159], an α error of 0.05, a statistical power of 0.8, and no correlation among the repeated measures. As for Pearson's correlations, still assuming an α error of 0.05 and a statistical power of 0.8, as well as an expected correlation coefficient of at least 0.3, the sample size calculation led to the requirement of 84 participants. These sample sizes are smaller than the 100 or 115 participants used in the different studies presented in this thesis, which allowed to increase the statistical power [160]. Sample size calculations were performed using G*Power (v3.1.9, available at <https://www.psychologie.hhu.de/arbeitsgruppen/allgemeine-psychologie-und-arbeitspsychologie/gpower>). Data analysis was performed using Python (v3.7.4, available at <http://www.python.org>). Statistical analysis was performed using Jamovi (v1.6.23, available at <https://www.jamovi.org>) with a level of significance set at $P \leq 0.05$.

5. Main results and discussion

The main purpose of this thesis was to investigate the objective evaluation of the spontaneous running pattern and its relationship in terms of runners' classification in the laboratory and towards the field. To do so, first, this thesis extended about the knowledge of DF and SF as global objective variables to assess spontaneous running patterns (studies 1-3). Second, this thesis developed algorithms allowing to accurately measure t_c , t_f , DF, SF, as well as $F_{z,\max}$ in absence of the GSM but using a sacral marker and a motion capture system or a sacral-mounted IMU (studies 4-8). This would later allow performing these measurements in the field.

The main findings and discussion of the studies included in this thesis are presented in this section. A more detailed version of the results and discussion of each study is presented in its respective article given in the *List of publications* section.

5.1 Duty factor and foot-strike pattern do not represent similar running pattern at the individual level (study 1)

5.1.1 Results

The linear mixed model revealed a significant FSP group effect on DF ($P < 0.001$). The Holm post hoc tests indicated a significantly higher DF for RFS than for MFS and FFS ($P \leq 0.005$), and for MFS than for FFS ($P = 0.001$). A significant effect of speed was reported on DF ($P < 0.001$). A significantly smaller DF was obtained at a faster speed, as shown by the Holm post hoc tests ($P < 0.001$). There was no FSP group x speed interaction ($P < 0.66$). Data are represented in Fig. 6A.

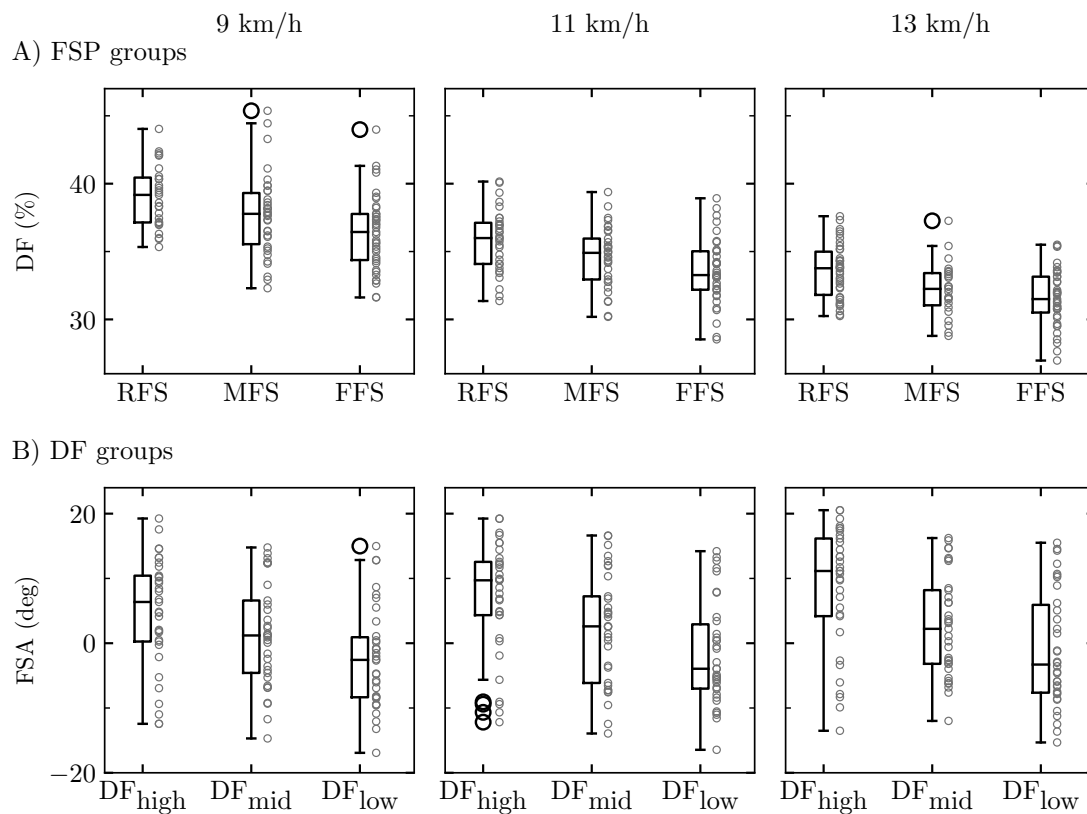


Figure 6. Boxplots of (A) the duty factor (DF) for the different foot-strike pattern (FSP) groups, i.e., rearfoot (RFS), midfoot (MFS), and forefoot (FFS) strikers, and (B) the foot-strike angle (FSA) for the different DF groups, i.e., high (DF_{high}), mid (DF_{mid}), and low (DF_{low}) DF runners, at 9, 11, and 13 km/h (see paragraph “4.5.5 Runners’ classification” for more methodological details about the constitution of DF and FSA groups). The box extends from the lower to upper quartile values of the data, with a line at the median. The whiskers extend from the box to show the range of the data while flier points (black empty circles) are those past the end of the whiskers. The upper whisker extends to the last data less than $Q3 + 1.5(Q3 - Q1)$, where $Q1$ and $Q3$ are the first and third quartile. Similarly, the lower whisker extends to the first data greater than $Q1 - 1.5(Q3 - Q1)$. The small gray empty circles denote the data of each participant.

The linear mixed model revealed a significant DF group effect on FSA ($P < 0.001$). The Holm post hoc tests indicated a significantly higher FSA for DF_{high} than for DF_{mid} and DF_{low} ($P < 0.001$), and for DF_{mid} than for DF_{low} ($P = 0.005$). A significant effect of speed was reported on FSA ($P < 0.001$). A significantly higher FSA was obtained at a faster speed, as reported by the Holm post hoc tests ($P \leq 0.01$). There was no DF group x speed interaction ($P < 0.42$). Data are represented in Fig. 6B.

When considering all groups together, a significant group x running speed interaction effect was reported by the linear mixed models for both DF and FSA values ($P \leq 0.01$). Pairwise post hoc comparisons between the three group pairs (RFS and DF_{high}, MFS and DF_{mid}, FFS and DF_{low}) at each running speed revealed no significant differences for DF and FSA values ($P \geq 0.16$).

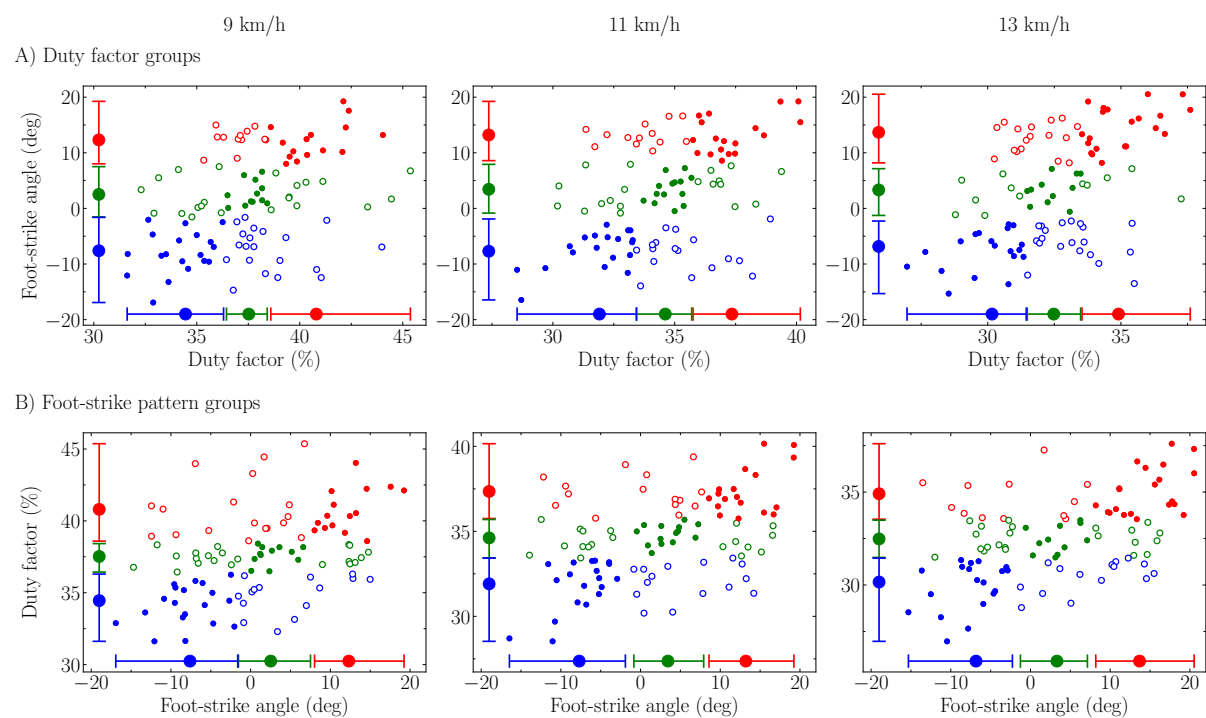


Figure 7. Duty factor (DF) and foot-strike angle (FSA) values of runners attributed to (A) a DF group but not being classified in the supposedly corresponding foot-strike pattern (FSP) group and (B) a FSP group but not being classified in the supposedly corresponding DF group at each tested running speed (see paragraph “4.5.5 Runners’ classification” for more methodological details about the constitution of DF and FSA groups). Mean DF and FSA value (filled circle) and range of values (whiskers) for each DF and FSP group, i.e., high DF runners and rearfoot strikers (RFS; red), mid DF runners and midfoot strikers (MFS; green), and low DF runners and forefoot strikers (FFS; blue). The upper whisker extends to the maximum while the lower whisker extends to the minimum value. Empty circles denote the runners attributed to a DF or FSP group but not being classified in the supposedly corresponding FSP or DF group, respectively, e.g., high DF runners but classified as MFS or FFS (green and blue empty circles within the red whiskers of the high DF runners) in (A) and RFS but classified as mid or low DF runners (green and blue empty circles within the red whiskers of RFS) in (B).

The DF and FSA values of runners attributed to a DF group but not being classified in the supposedly corresponding FSP group, for instance DF_{high} runners but classified as MFS and FFS, are given in Fig. 7A. Similarly, Fig. 7B depicts FSA and DF values of runners attributed to a FSP group but not being classified in the supposedly corresponding DF group, for instance RFS but classified as DF_{mid} or DF_{low}.

The correlations between FSA and DF, t_c , and SF, together with their 95% confidence intervals, are given in Table 2. For DF and t_c , the correlation was weak (low) but statistically significant ($r \leq 0.50$; $P < 0.001$) for all speeds, while the correlation between DF and SF was negligible and not statistically significant ($|r| \leq 0.14$; $P \geq 0.18$).

Table 2. Pearson's correlation coefficients (r) and the corresponding 95% confidence intervals (lower, upper) and P -values for the relationships between the foot-strike angle and duty factor (DF), contact time (t_c), and stride frequency (SF) for three tested speeds.

Variable	Running speed (km/h)	r	P
DF	9	0.39 (0.21, 0.55)	<0.001
	11	0.42 (0.24, 0.57)	<0.001
	13	0.48 (0.31, 0.62)	<0.001
t_c	9	0.43 (0.26, 0.58)	<0.001
	11	0.47 (0.30, 0.61)	<0.001
	13	0.50 (0.34, 0.63)	<0.001
SF	9	-0.13 (-0.32, 0.06)	0.18
	11	-0.14 (-0.28, 0.11)	0.36
	13	-0.11 (-0.30, 0.09)	0.29

Note. Statistically significant correlations ($P \leq 0.05$) are in bold font.

5.1.2 Discussion

A significantly higher DF was obtained for RFS than for MFS and FFS and for MFS than for FFS, supporting the first hypothesis. Moreover, a significantly higher FSA was reported for DF_{high} than for DF_{mid} and DF_{low} and for DF_{mid} than for DF_{low}, supporting the second hypothesis. Although the three group pairs (RFS and DF_{high}, MFS and DF_{mid}, FFS and DF_{low}) did not report

any significant difference in DF and FSA values at each tested speed, weak correlations were obtained between FSA and DF values, supporting the third hypothesis.

DF was significantly lower for FFS than for RFS and MFS and for MFS than for RFS (Fig. 6A). These results confirm previous observations that there should be a trend towards a more fore-FSP with a decreasing DF value [18, 19]. Similarly, FSA was significantly lower for DF_{low} than for DF_{high} and DF_{mid} and for DF_{mid} than for DF_{high} (Fig. 6B). Besides, the DF values of runners attributed to a DF group but not being classified in the supposedly corresponding FSP group mostly span the entire range of DF values of this DF group (Fig. 7A). A similar observation is made for FSA values of runners attributed to a FSP group but not being classified in the supposedly corresponding DF group (Fig. 7B). Thereby, these results suggest that “local” FSP/FSA and DF do not represent similar running pattern information when investigated at the individual level.

Weak but significant correlations were observed between DF and FSA at all speeds ($r \leq 0.48$ and $P < 0.001$; Table 2). Nonetheless, FSA was only able to explain ~20% of the variance of DF. The angle of the lower limb at initial ground contact relative to the vertical axis [161] can be estimated using t_c and therefore DF (indirectly). In addition, according to the observations of Breine et al. [162] which showed that RFS have a less vertical leg at the point of contact than do runners landing further forward on their foot (MFS and FFS), FSP is indirectly related to the lower limb angle at initial contact. As RFS position their foot to be much more forward than their pelvis to strike the ground with their heel, these runners have a higher lower limb angle at initial contact than do FFS. Therefore, the lower limb angle at initial contact may be indirectly related to FSA. Hence, there is an indirect relationship between FSA and DF which is supported by the indirect relationship between the lower limb angle at initial contact and both DF and FSA. Besides, DF is computed from t_c and SF, which makes it to be functionally representative of a more global biomechanical behavior [18, 19, 72]. For instance, DF has been shown to represent the trade-off between muscle contractile mechanics and energetics in running as a valid estimate of the muscle force-length-velocity related to mechanical work, total active muscle volume, and energy expenditure in running [72].

Correlation coefficients between DF and FSA increased with increasing running speed (+20% from 9 to 13 km/h; Table 2), depicting that FSA was more strongly correlated with DF with increasing speed. These results suggest that FSA and DF should be more similar at faster

speeds. This might partly be attributed to the smaller ranges of DF and FSA values with increasing speed. Nevertheless, the relation between FSP and DF groups as well as FSA and DF values at faster running speeds should be further investigated.

The correlations between t_c and FSA were weak but statistically significant and slightly stronger than those between DF and FSA (+4%; Table 2). Nonetheless, FSA was only able to explain up to 25% of the variance of t_c , confirming that t_c (as DF) does not only represent what happens at initial contact with the ground as does FSP. The weaker correlation between DF and FSA than that between t_c and FSA can be explained by the negligible correlations between SF and FSA ($|r| \leq 0.14$; Table 2) coupled to the fact that DF is given by the product between t_c and SF.

An unexpected high proportion of runners were classified as FFS, indicating that the study population may not be representative of the general population. Moreover, participants wore their own running shoes during testing, which could be confounding our results. Given that differences in footwear characteristics can underpin differences in running biomechanics [163], using a standardized shoe might have led to different study outcomes in terms of FSA and DF. However, recreational runners are more comfortable wearing their own shoes [164], and show individual responses to novel footwear [164, 165] and cushioning properties [166]. Furthermore, the speeds were limited to endurance speeds, and running trials were only performed on a treadmill. As very few studies on DF exist, it is therefore difficult to determine how DF may be affected by confounding variables such as footwear or the running surface. Therefore, future studies should focus on the relation between DF and FSP under additional conditions (i.e., faster speeds, different types of ground, and different shoes). Nonetheless, the presented results suggest that at an individual level, “local” FSP/FSA and DF do not represent similar running pattern and DF should be preferred to FSP/FSA when evaluating the global running pattern of a runner.

5.2 Examination of running pattern consistency across speeds (study 2)

5.2.1 Results

Correlations for each one of the four relative temporal variables were *high* to *very high* for each pair of running speeds when changes were 2-4 km/h ($P < 0.001$, Table 3), except for the correlation between 10-14 km/h for t_c being *moderate*. Correlations were *moderate* to *high* for each pair of running speeds when changes were 6-8 km/h for the four relative temporal variables ($P < 0.001$; Table 3).

Table 3. Pearson's correlation coefficients (r) and corresponding 95% confidence intervals [lower, upper] and P -values for the relationships of the relative values for pair of running speeds among five different speeds (10, 12, 14, 16, and 18 km/h) and for four temporal variables (duty factor, contact time, flight time, and step frequency).

Running speed pair (km/h)	Statistics	Duty factor	Contact time	Flight time	Step frequency
10 - 12	r	0.86 [0.76, 0.92]	0.83 [0.73, 0.90]	0.89 [0.81, 0.93]	0.98 [0.96, 0.99]
	P	<0.001	<0.001	<0.001	<0.001
10 - 14	r	0.72 [0.56, 0.83]	0.69 [0.51, 0.81]	0.78 [0.64, 0.87]	0.93 [0.88, 0.96]
	P	<0.001	<0.001	<0.001	<0.001
10 - 16	r	0.64 [0.45, 0.78]	0.63 [0.44, 0.77]	0.73 [0.56, 0.83]	0.86 [0.77, 0.92]
	P	<0.001	<0.001	<0.001	<0.001
10 - 18	r	0.58 [0.37, 0.74]	0.54 [0.32, 0.71]	0.66 [0.47, 0.79]	0.77 [0.63, 0.86]
	P	<0.001	<0.001	<0.001	<0.001
12 - 14	r	0.91 [0.84, 0.95]	0.90 [0.83, 0.94]	0.93 [0.88, 0.96]	0.97 [0.94, 0.98]
	P	<0.001	<0.001	<0.001	<0.001
12 - 16	r	0.79 [0.66, 0.88]	0.83 [0.72, 0.90]	0.83 [0.73, 0.90]	0.92 [0.87, 0.96]
	P	<0.001	<0.001	<0.001	<0.001
12 - 18	r	0.68 [0.51, 0.81]	0.71 [0.54, 0.82]	0.73 [0.57, 0.84]	0.83 [0.71, 0.90]
	P	<0.001	<0.001	<0.001	<0.001
14 - 16	r	0.86 [0.77, 0.92]	0.90 [0.83, 0.94]	0.90 [0.83, 0.94]	0.97 [0.95, 0.98]
	P	<0.001	<0.001	<0.001	<0.001
14 - 18	r	0.73 [0.57, 0.83]	0.82 [0.70, 0.89]	0.77 [0.63, 0.86]	0.88 [0.80, 0.93]
	P	<0.001	<0.001	<0.001	<0.001
16 - 18	r	0.86 [0.77, 0.92]	0.91 [0.85, 0.95]	0.90 [0.83, 0.94]	0.93 [0.88, 0.96]
	P	<0.001	<0.001	<0.001	<0.001

Note. Statistically significant correlations ($P \leq 0.05$) are in bold font. Correlations were considered very high, high, moderate, low, and negligible when absolute r values were between 0.90-1.00, 0.70-0.89, 0.50-0.69, 0.30-0.49, and 0.00-0.29, respectively [167]. Cells were colored according to the intensity of the correlations, i.e., the larger the correlation, the darker the shaded area.

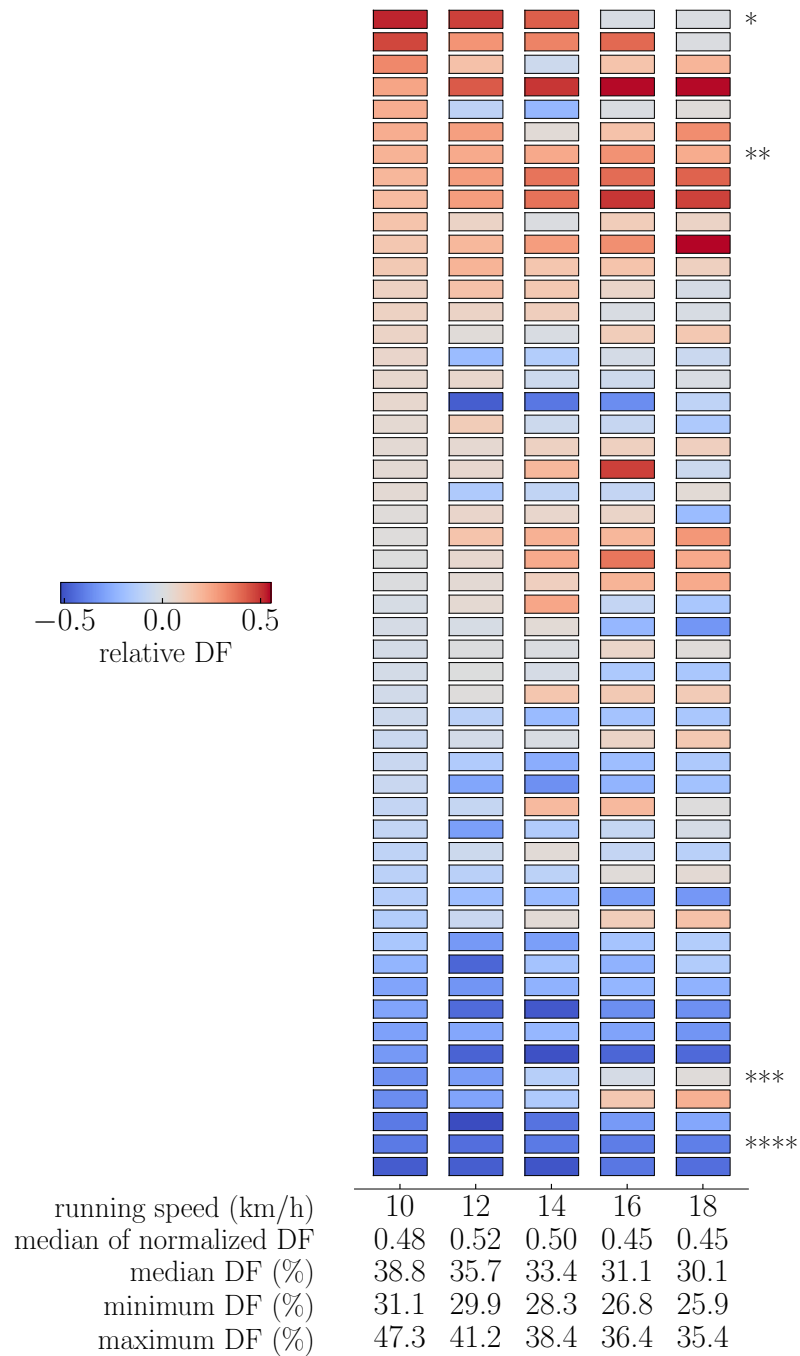


Figure 8. Relative (deviations from the median) duty factor (DF) values for all participants and five running speeds. Runners were relatively positioned according to their relative DF values at 10 km/h. The star symbols depict four participants with distinct behaviors. * participant with a DF much higher than the median at 10 km/h, but a decreasing DF with increasing speed resulting in a DF closer to the median at 18 km/h. ** participant with a DF higher than the median at all tested speeds. *** participant with a DF lower than the median at 10 km/h, but an increasing DF with increasing speed resulting in a DF closer to the median at 18 km/h. **** participant with a DF much lower than the median at all tested speeds.

The relative DF values for all participants and each running speed are depicted in Fig. 8. According to the correlations reported in Table 3, similar figures and corresponding interpretations would result using the three other variables (t_c , t_f , and SF).

Correlations were *low* between relative DF and SF at all tested speeds ($P \leq 0.02$; Table 4). Correlations were *very high* between relative DF and t_f at all tested speeds ($P < 0.001$); and *high* between relative DF and t_c at 10 and 12 km/h ($P < 0.001$), but *moderate* at 14, 16, and 18 km/h ($P < 0.001$; Table 4). Correlations between relative SF and t_f were *moderate* at all speeds ($P < 0.001$), except for being *high* at 18 km/h ($P < 0.001$). Correlations were *low* between relative SF and t_c at 10, 12, and 14 km/h ($P \leq 0.03$), and *moderate* at 16 and 18 km/h ($P < 0.001$; Table 4). Correlations between relative t_c and t_f were *moderate* at 10 km/h ($P < 0.001$), *low* at 12, 14, and 16 km/h ($P \leq 0.04$), and *negligible* at 18 km/h ($P = 0.21$; Table 4)

Table 4. Pearson's correlation coefficients (r) and corresponding 95% confidence intervals [lower, upper] and P -values for the relationships of the relative values for pair of temporal variables among duty factor (DF), contact time (t_c), flight time (t_f), and step frequency (SF), for five running speeds.

Variable pair	Statistics	10 km/h	12 km/h	14 km/h	16 km/h	18 km/h
DF - SF	r	0.38 [0.11, 0.59]	0.38 [0.13, 0.60]	0.34 [0.07, 0.56]	0.32 [0.05, 0.55]	0.41 [0.16, 0.62]
	P	0.006	0.005	0.01	0.02	0.002
DF - t_f	r	-0.98 [-0.99, -0.97]	-0.96 [-0.98, -0.93]	-0.94 [-0.96, -0.89]	-0.91 [-0.95, -0.85]	-0.91 [-0.95, -0.85]
	P	<0.001	<0.001	<0.001	<0.001	<0.001
DF - t_c	r	0.77 [0.63, 0.86]	0.71 [0.54, 0.82]	0.67 [0.48, 0.80]	0.65 [0.46, 0.79]	0.57 [0.35, 0.73]
	P	<0.001	<0.001	<0.001	<0.001	<0.001
SF - t_f	r	-0.53 [-0.70, -0.30]	-0.62 [-0.76, -0.41]	-0.64 [-0.78, -0.44]	-0.67 [-0.80, -0.49]	-0.74 [-0.85, -0.59]
	P	<0.001	<0.001	<0.001	<0.001	<0.001
SF - t_c	r	-0.30 [-0.53, -0.03]	-0.38 [-0.59, -0.12]	-0.47 [-0.66, -0.23]	-0.50 [-0.68, -0.27]	-0.51 [-0.69, -0.28]
	P	0.03	0.006	<0.001	<0.001	<0.001
t_c - t_f	r	-0.65 [-0.79, -0.46]	-0.49 [-0.67, -0.25]	-0.37 [-0.58, -0.11]	-0.29 [-0.52, -0.02]	-0.18 [-0.43, 0.10]
	P	<0.001	<0.001	0.007	0.04	0.21

Note. Statistically significant correlations ($P \leq 0.05$) are in bold font. Correlations were considered very high, high, moderate, low, and negligible when absolute r values were between 0.90-1.00, 0.70-0.89, 0.50-0.69, 0.30-0.49, and 0.00-0.29, respectively [167]. Cells were colored according to the intensity of the correlations, i.e., the closer to one the correlation, the darker the red shaded area and the closer to minus one the correlation, the darker the blue shaded area.

The relative temporal variables are depicted in Fig. 9 for all participants running at 10 km/h. According to the correlations reported in Table 4, similar figures and corresponding interpretations would result using the four other running speeds (12, 14, 16, and 18 km/h).

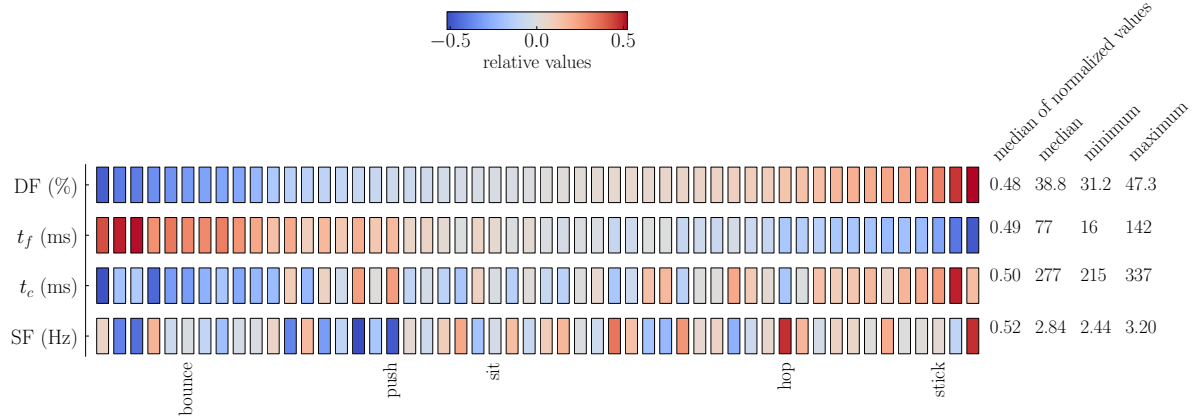


Figure 9. Relative (deviations from the median) duty factor (DF), contact time (t_c), flight time (t_f), and step frequency (SF) values for all participants at 10 km/h. Runners were relatively positioned according to their relative DF values at 10 km/h. The relative t_f values are almost the exact opposite to the relative DF values (Pearson correlation coefficient: -0.98). One participant representing each of the five running pattern categories proposed by van Oeveren et al. [14] based on the combination of DF and SF (Fig. 1) is identified, namely bounce (low DF and median SF), push (low SF and median DF), sit (median DF and SF), hop (high SF and median DF), and stick (high DF and median SF).

5.2.2 Discussion

In agreement with the first hypothesis, smaller differences between two running speeds were associated with greater consistency in running patterns, i.e., greater consistency in the four temporal variables examined (DF, SF, t_c , and t_f). Correlations of the relative values were *high* to *very high* for 2-4 km/h speed differences, whereas *moderate* to *high* for 6-8 km/h differences. In agreement with the second hypothesis, the consistency between DF and SF variables was low at each tested speed, and greater between DF and both its subcomponents as well as between SF and both its subcomponents than between DF and SF variables. Across speeds, correlations were *low* between relative DF and SF, *very high* between relative DF and t_f , and *low* to *high* between relative DF and t_c , SF and t_c , and SF and t_f .

The stronger correlations of the relative temporal variables (DF, SF, t_c , and t_f) for 2-4 km/h than 6-8 km/h speed differences (Table 3) indicate greater consistency in variables when changes in running speeds are smaller. In other words, the running pattern is less consistent when measured over a larger speed range (Fig. 8). This result supports that the running pattern should be defined at a given speed [14]. Moreover, large interindividual variations in the consistency in running patterns across running speeds was observed (Fig. 8). For instance, there were runners with a DF higher than the median at 10 km/h, but a decreasing DF with increasing speed resulting in a DF closer to the median at 18 km/h; runners with a DF higher than the

median at all tested speeds; runners with a DF lower than the median at 10 km/h, but an increasing DF with increasing speed resulting in a DF closer to the median at 18 km/h; and runners with a DF much lower than the median at all tested speeds. This agrees with previous observations that individuals adapt to running speeds differently [21, 47, 74], which might be linked to differences in anthropometric characteristics, age, and running training [168]. Performing a more detailed analysis that incorporates clustering approaches might reveal subgroups that respond similarly to changes in running speeds. As absolute running speeds were used rather than relative speeds (based on the level of participants), it would not be possible to identify whether sudden changes in DF and/or SF take place at given relative intensities. Overall, coaches should evaluate the running pattern of their athletes using a range of speeds or at a specific speed.

As indicates the *low* correlations between relative DF and SF values at all tested speeds (Table 4), the consistency between these two variables was low. Similarly, Fig. 9 depicts how runners with a low/high DF can present with either a low/high SF. These results again reflect previous ones wherein SF does not necessarily encapsulate the same running pattern information than DF, and that combining DF and SF information should allow to describe the full running pattern spectrum [14]. As depicted in Fig. 9, each of the five categories proposed by van Oeveren et al. [14] were represented herein. Specifically, there were stick (high DF and median SF), bounce (low DF and median SF), hop (high SF and median DF), push (low SF and median DF), and sit (median DF and SF) runners. Moreover, there were runners in between these categories, which also confirms that running patterns operate along a spectrum (Fig. 9) [14].

Given that the risk of injury was shown greater in runners using softer shoes and with a lower DF [136], quantifying DF might be informative for lower-limb injury prevention. The present study found *very high* correlations between relative DF and t_f values at all tested speed (Table 4 and Fig. 9), suggesting that the relative t_f is equivalent to the relative DF. In other words, individual variations in t_f are equivalent to variations in DF. The interrelatedness of DF and t_f and their importance in running are further highlighted by their established correlations to ground reaction force metrics. Indeed, DF and t_f are related to the average vertical ground reaction force during t_c [72] and effective vertical impulse during t_c [73], respectively. Both the average vertical ground reaction force during t_c and effective vertical impulse during t_c are proportional to the peak vertical ground reaction force, as supports the sine wave model of the

vertical ground reaction force [169] and experimental data [83]. The present study reported lower association between relative t_c and DF values (correlations were *moderate* to *high*; Table 4 and Fig. 9) than relative t_f to DF values. This result is primarily driven by the midrange DF runners (Fig. 9). Altogether, these observations indicate that runners with a relatively long t_f (or short t_c) are runners with a relatively low DF within a group of runners, i.e., DF is mainly controlled by t_f and less by t_c . Overall, the kinematic differences previously observed between high and low DF runners [18, 19] should generalize well to runners with short and long t_f , but might not generalize as well to runners with long and short t_c . Among these three variables (DF, t_f , and t_c), one might be easier to evaluate subjectively, which would be ideal for track and field running coaches, athletes, and practitioners seeking to describe running patterns along a spectrum. Indeed, running coaches could then subjectively evaluate their runners and identify the low DF runners using either DF, t_f , or t_c . Nevertheless, further studies comparing subjective and objective evaluations of runners using DF, t_f , and t_c would be needed to assess if one of these variables is easier to subjectively evaluate than the others.

The *moderate* to *high* correlations between relative SF and t_f values and *low* to *moderate* correlations between relative SF and t_c values (Table 4 and Fig. 9) follow the same trend than those between relative DF and t_f or t_c , i.e., correlations were larger with t_f than with t_c . Hence, t_f also determines more of the variation of SF than t_c . To better understand the correlations reported among relative DF, t_f , t_c , and SF for each running speed, further analyses concerning the relationships within these variables might be needed.

From a practical perspective, the lower consistency in running patterns observed as speed differences increased suggests that running patterns should be assessed at a range of speeds or at a specific speed. In other words, the generalization of running patterns across speeds may not be valid. Noteworthy is the considerable interindividual differences observed in terms of the evolution of the relative variables with changes in speed, with some runners demonstrating similar running patterns across speeds and others changing running patterns. The low consistency between DF and SF at a given running speed corroborates previous findings that SF does not necessarily encapsulate the same running pattern information than DF. As proposed by van Oeveren et al. [14], the full spectrum of running patterns can be described using both DF and SF (Fig. 1). Individuals spontaneously and subconsciously adopt their own running pattern. This spontaneous choice was shown to be self-optimized, which is a central

element in the development of an economical and safe running gait [8-11]. Hence, being able to analyze the full spectrum of running patterns may be important to interpret measurements, to design and test specific coaching interventions, and to conduct research to answer questions regarding performance, running economy, and injury risk.

5.3 Using statistical parametric mapping to assess the association of duty factor and step frequency on running kinetic (study 3)

5.3.1 Results

The vertical ground reaction force signal was significantly negatively related to DF at all tested speeds (stance range: 0 and 15-100% at 9 and 11 km/h, and 0 and 14-100% at 13 km/h; Fig. 10). Similar findings were obtained for SF but to a lower extent (stance range: 60-99% at 9 km/h, 59-99% at 11 km/h, and 67-83% at 13 km/h; Fig. 11).

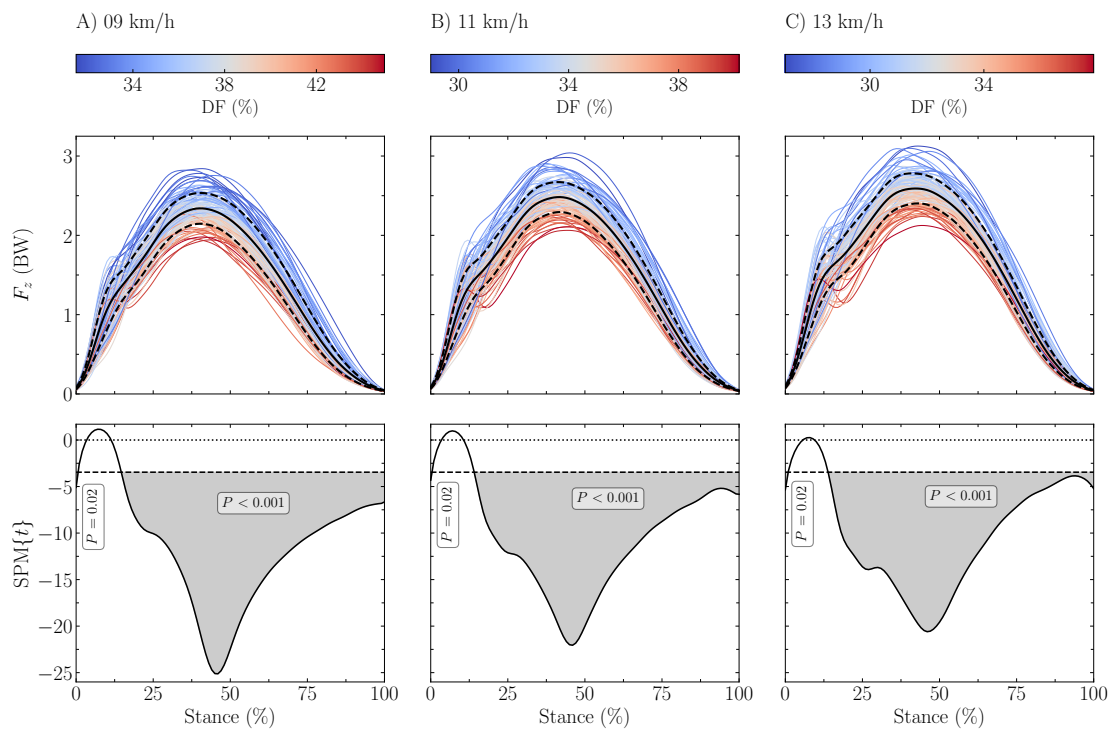


Figure 10. Statistical parametric mapping (SPM) analysis, i.e., t-statistics ($SPM\{t\}$), of the linear relationship between the vertical ground reaction force (F_z) and the duty factor (DF) along the running stance phase at (A) 9 km/h, (B) 11 km/h, and (C) 13 km/h. In the upper panels, F_z , expressed in body weight (BW), is depicted for each participant (the color depends on the DF value) and for the mean (black line) \pm standard deviation (dashed black line) over all participants. In the lower panels, the black dashed horizontal lines represent the critical (parametric) threshold while the portion of the running stance phase which is statistically significant ($P \leq 0.017$; Bonferroni correction was applied to take into the three tested speeds) is given by the gray shaded area.

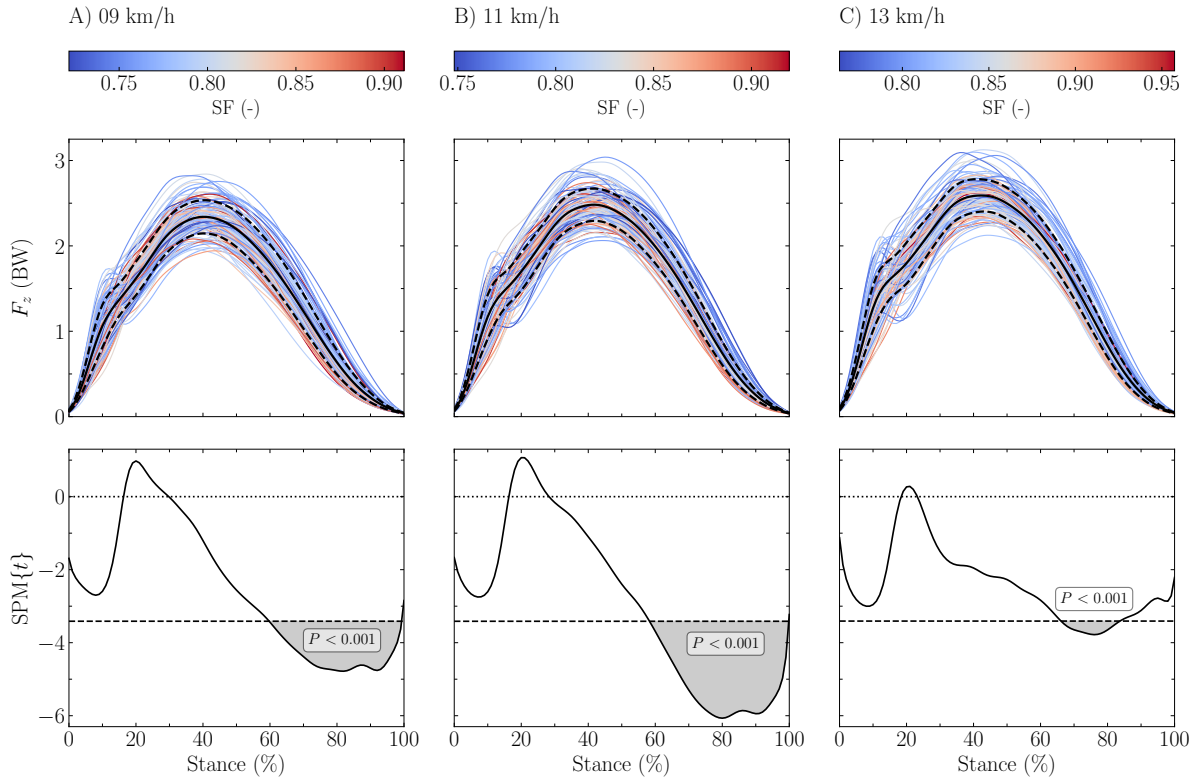


Figure 11. Statistical parametric mapping (SPM) analysis, i.e., t-statistics ($SPM\{t\}$), of the linear relationship between the vertical ground reaction force (F_z) and the step frequency (SF) normalized by $\sqrt{g/L_0}$, where g is the gravitational constant and L_0 the leg length, along the running stance phase at (A) 9 km/h, (B) 11 km/h, and (C) 13 km/h. In the upper panels, F_z , expressed in body weight (BW), is depicted for each participant (the color depends on the DF value) and for the mean (black line) \pm standard deviation (dashed black line) over all participants. In the lower panels, the black dashed horizontal lines represent the critical (parametric) threshold while the portion of the running stance phase which is statistically significant ($P \leq 0.017$; Bonferroni correction was applied to take into the three tested speeds) is given by the gray shaded area.

The fore-aft ground reaction force signal was significantly positively related to both DF and SF in the first 50% of the stance (negative fore-aft force) and negatively related to both DF and SF in the last 50% of the stance at all tested speeds (stance range for DF: 5-11, 27-34, and 69-100% at 9 km/h, 7-12, 29-35, and 71-100% at 11 km/h, and 6-13 and 68-100% at 13 km/h; Fig. 12; stance range for SF: 15-33 and 68-95% at 9 km/h, 14, 19-35, 47-52, and 70-98% at 11 km/h, and 14-28 and 71-89% at 13 km/h; Fig. 13).

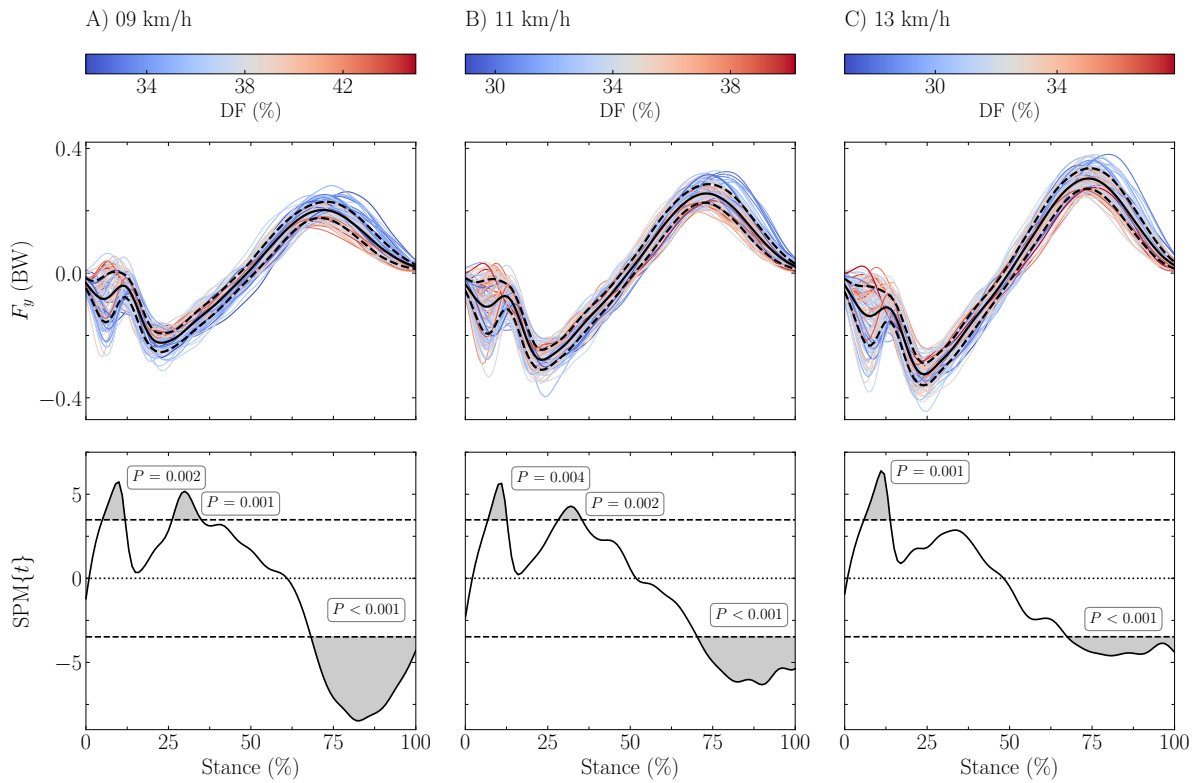


Figure 12. Statistical parametric mapping (SPM) analysis, i.e., t-statistics ($SPM\{t\}$), of the linear relationship between the fore-aft ground reaction force (F_y) and the duty factor (DF) along the running stance phase at (A) 9 km/h, (B) 11 km/h, and (C) 13 km/h. In the upper panels, F_y , expressed in body weight (BW), is depicted for each participant (the color depends on the DF value) and for the mean (black line) \pm standard deviation (dashed black line) over all participants. In the lower panels, the black dashed horizontal lines represent the critical (parametric) threshold while the portion of the running stance phase which is statistically significant ($P \leq 0.017$; Bonferroni correction was applied to take into the three tested speeds) is given by the gray shaded area.

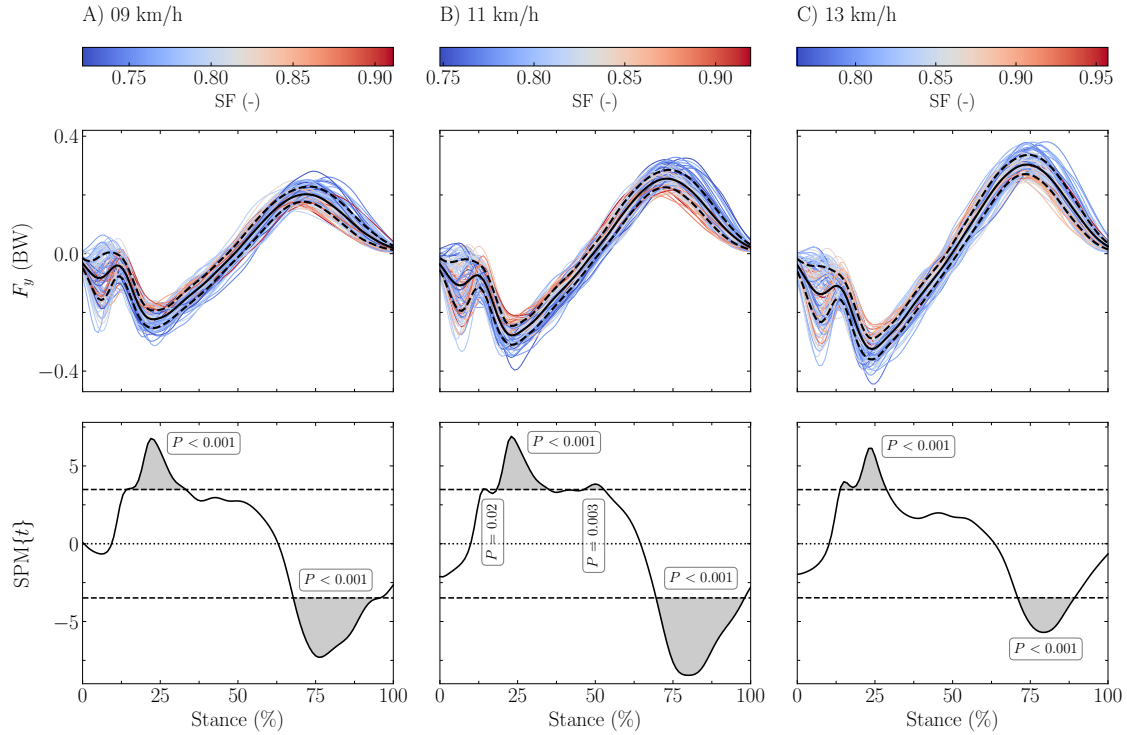


Figure 13. Statistical parametric mapping (SPM) analysis, i.e., t-statistics (SPM $\{t\}$), of the linear relationship between the fore-aft ground reaction force (F_y) and the step frequency (SF) normalized by $\sqrt{g/L_0}$, where g is the gravitational constant and L_0 the leg length, along the running stance phase at (A) 9 km/h, (B) 11 km/h, and (C) 13 km/h. In the upper panels, F_y , expressed in body weight (BW), is depicted for each participant (the color depends on the DF value) and for the mean (black line) \pm standard deviation (dashed black line) over all participants. In the lower panels, the black dashed horizontal lines represent the critical (parametric) threshold while the portion of the running stance phase which is statistically significant ($P \leq 0.017$; Bonferroni correction was applied to take into the three tested speeds) is given by the gray shaded area.

The force-length relationships of all participants, colored according to their DF and SF, are depicted in Figs. 14 and 15, respectively, for each tested speeds and separately for the compression and decompression phases. The coefficient of determination during leg compression (R_{comp}^2) significantly decreased with increasing DF or running speed and increased with increasing SF ($P \leq 0.007$; Table 5), while the coefficient of determination during leg decompression (R_{decomp}^2) did not change with DF, SF, and running speed.

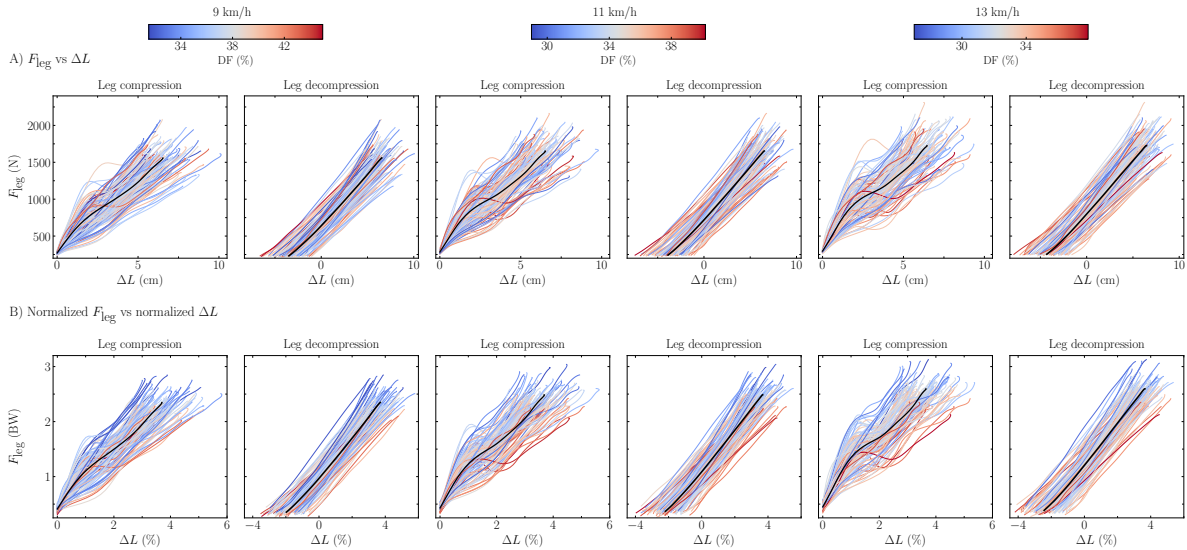


Figure 14. Force-length relationship, i.e., ground reaction force projected along the leg (F_{leg}) as function of the leg compression/decompression, for each participant [the color depends on the duty factor (DF) value] and for the mean (black line) over all participants during the running stance phase, at three running speeds, and expressed using (A) SI units and (B) normalized units, i.e., body weight (BW) for F_{leg} and percentage of runners' height for leg compression. As ΔL was set to zero at foot-strike (the beginning of the leg compression), ΔL was smaller than zero at toe-off (the end of the leg decompression), leading to a non-zero force for a null ΔL during the leg decompression.

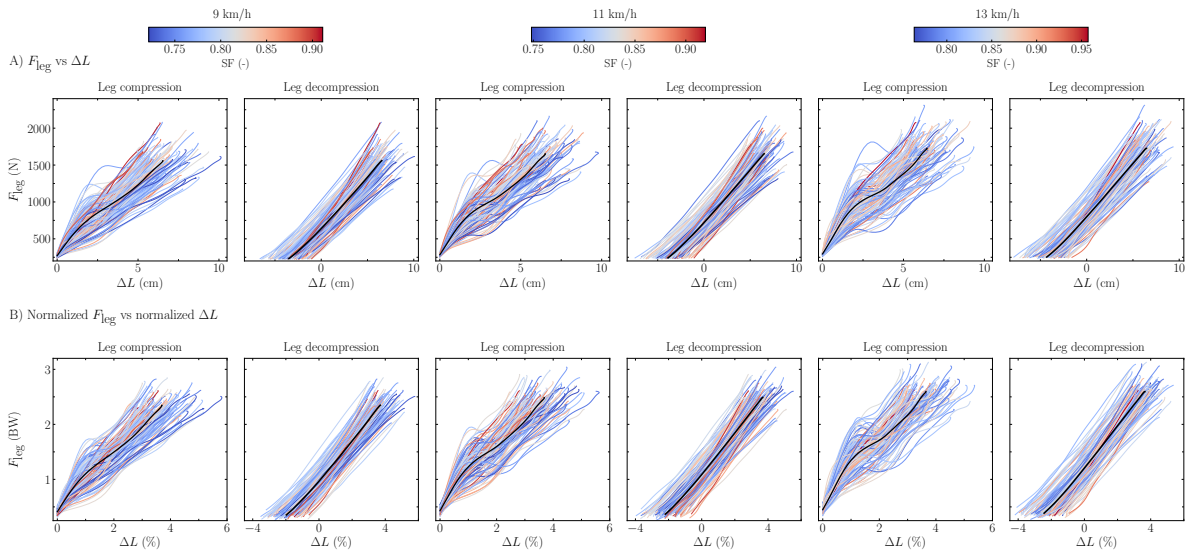


Figure 15. Force-length relationship, i.e., ground reaction force projected along the leg (F_{leg}) as function of the leg compression/decompression, for each participant [the color depends on the step frequency (SF) value; SF was normalized by $\sqrt{g/L_0}$, where g is the gravitational constant and L_0 the leg length] and for the mean (black line) over all participants during the running stance phase, at three running speeds, and expressed using (A) SI units and (B) normalized units, i.e., body weight (BW) for F_{leg} and percentage of runners' height for leg compression. As ΔL was set to zero at foot-strike (the beginning of the leg compression), ΔL was smaller than zero at toe-off (the end of the leg decompression), leading to a non-zero force for a null ΔL during the leg decompression.

Table 5. Linearity of the force-length relationship during leg compression (R_{comp}^2) and decompression (R_{decomp}^2). Significant differences ($P \leq 0.05$) identified by linear mixed effects modeling are indicated in bold.

Running speed (km/h)	R_{comp}^2	R_{decomp}^2
9	$0.95 \pm 0.06^{*,\dagger}$	0.99 ± 0.02
11	$0.93 \pm 0.08^{\ddagger}$	0.99 ± 0.01
13	0.90 ± 0.10	0.99 ± 0.01
Running speed effect (P)	< 0.001	0.14
DF covariate effect (P)	↓ < 0.001	0.06
SF covariate effect (P)	↑ 0.007	0.85

Note. Values are presented as mean \pm standard deviation. DF: duty factor, SF: step frequency, SF covariate was normalized by $\sqrt{g/L_0}$, where g is the gravitational constant and L_0 the leg length. Up (\uparrow) and down (\downarrow) arrows indicate positive and negative effects of the covariate, respectively. * Significantly different from the value at 11 km/h. \dagger and \ddagger Significantly different from the value at 13 km/h.

5.3.2 Discussion

According to the first hypothesis, lower DF and lower SF were associated to higher vertical and fore-aft ground reaction force fluctuations, but SF to a lower extent than DF. The linearity of the force-length relationship during the leg compression decreased with increasing DF but did not change during the leg decompression, partly refuting the second hypothesis. According to the third hypothesis, a higher SF was associated to a smaller leg compression.

DF was previously analytically shown to be inversely proportional to the maximum of an estimated vertical ground reaction force signal [169] via a sine-wave model [72]. The present study extends to the fact that a lower DF results in a larger vertical ground reaction force during most of the stance but after the 15% temporal window representative of the “impact” phase [170] (~15-100%; Fig. 10). Therefore, the SPM analysis additionally revealed that the association between DF and the vertical ground reaction force signal is not only given at $F_{z,\text{max}}$ but through almost the entire stance (after the impact phase; $\geq 15\%$). Moreover, the shape of the vertical ground reaction force during the impact phase is not affected by the DF. This result might be attributed to the fact that the vertical ground reaction force signal is given by the force contributions of two discrete body mass components, i.e., a distal mass composed of the foot and shank and the remaining mass [171, 172]. Hence, the impact phase, represented by the distal mass in this model, might not be affected by the DF.

Similarly, a lower SF resulted in a larger vertical ground reaction force, but only at the end of the stance (~65-95%; Fig. 11). This was likely related to the longer step length for running at the same speed. In fact, it has previously been shown that a larger vertical ground reaction force (i.e., support force) produces a larger step length [73, 173]. Our SPM analysis demonstrated that this larger support force was located only at the end of the stance. Nonetheless, the reason why this larger support force was located at the end of the stance could not readily be explained.

The fore-aft ground reaction force signal was positively related to DF around ~5-10% of the stance and to both DF and SF around ~25-35% (positively) and ~70-90% (negatively; Figs. 12 and 13). The positive association of DF on the fore-aft ground reaction force signal reported by the SPM analysis around ~5-10% of the stance can be explained by the FSP. Indeed, forefoot strikers were shown to have a negative spike on the fore-aft ground reaction force signal around ~5-10% of the stance [174] and DF was related to the FSP [18, 19]. However, the association of DF on the fore-aft force signal around ~5-10% of the stance in the fore-aft force signal was not accompanied by an association of DF on the vertical force signal at the same percentage of the stance. This suggests that the effect of DF during the impact phase was more important in the fore-aft than vertical force signal. The other two significant regions are around the braking and propulsive peaks. These results partly corroborate previous observations, which showed that the peak braking force was correlated to DF but not to SF [83]. Moreover, they confirm that larger ground reaction forces during propulsion are needed to lift and accelerate the body during stance to generate longer step lengths [175]. As previously suggested [14], combining vertical and horizontal ground reaction forces into a single vector could be useful to properly characterize their orientations and actions and carefully describe the relationship of this single vector with DF and SF, especially at the end of the stance. The present results corroborate that DF and SF can be viewed as two variables that complement each other and that should be used together to describe the full spectrum of running patterns [14].

The linearity of the force-length relationship was higher for lower DF and SF than for higher DF and SF runners during the leg compression but there was no difference during the leg decompression (Table 5). This means that higher DF and SF values were associated to more variations of the instantaneous compressive stiffness, i.e., the slope for each pair of point during the leg compression. However, the decompressive stiffness during the leg decompression was independent of DF and SF (Table 5). This result corroborates the choice made by several

authors to use the decompression phase instead of the compression one to calculate the vertical stiffness [132, 176].

The deviation from linearity of the force-length relationship among individuals was also reported by Gill et al. [154]. Indeed, these authors reported that the linearity of the force-length curve was foot-strike index dependent and thus FSP dependent and that this curve should be investigated before using the spring-mass model. Furthermore, these authors suggested that for $R^2 < 0.95$, it may be more appropriate to segment the stance phase and to individually investigate the different subphases. Hence, the deviation from linearity observed herein during the leg compression for higher than lower DF and SF runners suggests that the stiffness should be split into several phases during the leg compression and thus invalidate the usage of the compressive leg stiffness for these runners.

The higher linearity of the force-length relationship for low than high DF runners during the compression phase was accompanied with a larger vertical force and smaller t_c . These results suggest a more vertical compression for low than high DF runners and that high DF runners could be characterized by a slow stretch-shortening cycle (runners with t_c longer than 250 ms) while low DF runners by a fast one [177]. These findings bring further evidence and reinforce previous statements that low DF runners rely more on the optimization of the spring-mass model (better storage and re-use of elastic energy) than high DF runners [18, 19].

5.4 A novel kinematic detection of foot-strike and toe-off events during non-instrumented treadmill running to estimate contact time (study 4)

5.4.1 Results

Systematic biases were obtained for both FS and TO at all speeds (Table 6) and were ≤ 5 ms (≤ 1 frame), except for TO at 11 km/h (no bias; the zero line is between the 95% confidence interval).

Table 6. Systematic bias, lower limit of agreement (lloa), and upper limit of agreement (uloa) for foot-strike and toe-off detected using ground reaction force and the kinematic algorithm at three running speeds. 95% confidence intervals are given in square brackets [lower, upper].

Event	9 km/h			11 km/h			13 km/h		
	bias (ms)	lloa (ms)	uloa (ms)	bias (ms)	lloa (ms)	uloa (ms)	bias (ms)	lloa (ms)	uloa (ms)
Foot-strike	-4.4 [-4.8, -4.0]	-20.8 [-21.4, -20.2]	12.0 [11.3, 12.6]	-4.8 [-5.2, -4.5]	-20.1 [-20.7, -19.6]	10.5 [9.9, 11.0]	-4.6 [-5.0, -4.3]	-19.1 [-19.7, -18.6]	9.9 [9.3, 10.4]
Toe-off	3.5 [3.1, 3.9]	-13.9 [-14.6, -13.2]	20.9 [20.2, 21.6]	0.2 [-0.1, 0.5]	-13.6 [-14.1, -13.1]	14.1 [13.5, 14.6]	-1.8 [-2.1, -1.5]	-15.9 [-16.4, -15.4]	12.3 [11.7, 12.8]

Note. For systematic bias, positive and negative values indicate that the kinematic algorithm overestimated and underestimated gait events, respectively.

Systematic biases were reported for t_c at all speeds (< 8 ms), and the corresponding RMSE was ≤ 14 ms ($\leq 5\%$; Table 7). FFS, MFS, and RFS had RMSEs for t_c (averaged over speed) of 8.6 ± 3.6 ms ($3.5 \pm 1.4\%$), 13.0 ± 6.2 ms ($5.1 \pm 2.3\%$), and 13.9 ± 5.3 ms ($5.4 \pm 1.9\%$), respectively.

The linear mixed model depicted significant effects of method, speed, FSA, and method x speed interaction ($P \leq 0.004$). t_c was significantly overestimated by the KA, decreased with increasing speed, and increased with increasing FSA. Holm post hoc tests yielded significantly higher t_c when calculated by the KA than by the GSM at all speeds ($P \leq 0.01$; Table 7).

Table 7. Contact time (t_c) calculated based on foot-strike and toe-off detected using ground reaction force (gold standard method - GSM) and the kinematic algorithm together with systematic bias, 95% confidence intervals (in square brackets [lower, upper]), and root mean square error [RMSE; both in absolute (ms) and relative (%) units]. Data are presented for three running speeds. The linear mixed model revealed a significant method (kinematic algorithm vs. GSM) x speed interaction effect ($P = 0.004$). * Significant difference ($P \leq 0.01$) between t_c calculated based on GSM and that calculated based on the kinematic algorithm, as determined by Holm post hoc tests.

Variable	9 km/h	11 km/h	13 km/h
t_c (ms)	286.6 ± 27.5*	255.4 ± 23.7*	230.7 ± 20.5*
t_c GSM (ms)	278.6 ± 24.9	250.3 ± 20.7	227.9 ± 18.4
bias (ms)	7.9 [7.3, 8.5]	5.1 [4.6, 5.6]	2.8 [2.4, 3.3]
RMSE (ms)	13.7 ± 7.0	11.2 ± 4.8	9.9 ± 3.9
RMSE (%)	4.9 ± 2.5	4.5 ± 1.9	4.4 ± 1.7

Note. Values are presented as mean ± standard deviation. For systematic bias, positive and negative values indicate that the kinematic algorithm overestimated and underestimated t_c , respectively.

5.4.2 Discussion

Systematic biases were reported for FS and TO at all speeds, refuting the first hypothesis. Systematic biases, as well as significant differences, were reported for t_c at all speeds and the RMSE for t_c increased with increasing FSA, thus refuting the second hypothesis. Nonetheless, smaller errors than those obtained by existing methods were obtained for FS, TO, and t_c . Therefore, this novel KA can be applied to accurately estimate FS, TO, and t_c from kinematic data obtained during non-instrumented treadmill running, independently of FSA.

The biases for FS were smaller than or equal to 5 ms at all speeds (Table 6). These errors were smaller than those obtained with existing algorithms [90, 92, 93, 95, 96]. Milner and Paquette [95] showed that algorithms based solely on heel kinematics (position, velocity, or acceleration) were less accurate in FS detection for MFS or FFS than for RFS because heel kinematics around FS differ according to FSP, i.e., a non-RFS does not initiate contact with the ground using the heel. In addition, the heel-based algorithm reported in Smith et al. [93] had poorer FS detection abilities in non-RFS than in RFS (RMSE: 22 to 6 ms). Their results are opposed to those of this study, most likely because Smith et al. [93] used a heel-based algorithm. Leitch et al. [92] demonstrated that heel-based and mid-foot-based algorithms were best suited for RFS and FFS, respectively. Therefore, the novel KA proposed here, which

accounts for this recommendation and combines heel and toe kinematic data to detect FS, proved to be useful and showed a smaller error than existing methods.

The algorithm proposed by Milner and Paquette [95] was based on the velocity of the COM of the pelvis and had a 15 ms offset for FS. Similarly, the algorithm of Dingwell et al. [89], originally designed for walking gait and based on knee extension spikes and used by Smith et al. [93], depicted a 28 ms RMSE for FS. These algorithms performed worse than the KA proposed herein for FS detection ($\text{RMSE} \leq 8$ ms or $|\text{bias}| \leq 5$ ms). One reason could be that these algorithms used more proximal segments, which might be temporally shifted compared to what is happening directly at the foot.

TO necessarily occurs based on the toes moving away from the ground, suggesting that a toe-based algorithm should accurately detect TO. The error for TO was similar to the error of RFS given by the algorithm proposed by Smith et al. [93] but slightly higher than the modified version of the algorithm of Alton et al. [87]. However, the error obtained herein was smaller than that obtained for FFS (17 [93] or 12 ms [87]). Therefore, TO detection with the novel KA showed similar or better accuracy than existing methods.

Small systematic biases, as well as significant differences, were reported for t_c at all speeds (Table 7). Even though the novel KA yielded smaller errors for FS than the algorithm of Smith et al. [93], those authors did not report significant differences in t_c between methods. This discrepancy might be due to a combination of under- and over-estimations in FS and TO. Moreover, a high speed (20 km/h) was used in Smith et al. [93], which makes t_c smaller than that observed in this study, implicitly reducing observed differences and affecting the outcomes of statistical tests. In this study, the RMSE decreased with increasing speed [13.7–9.9 ms (5–4.5%) for 9–13 km/h] and was smaller than that in Smith et al. [93] [18.4 ms (11%) at 20 km/h]. Hence, this previous algorithm [93] could be less effective at slower speeds because the time scale of kinematic trajectories might be slower, thus resulting in larger errors (i.e., greater differences in the number of frames) than in this study at similar speeds.

This study proposed a novel KA that uses a combination of heel and toe kinematics (three markers per foot) to detect FS and TO. In conclusion, our findings showed that our novel KA

can be applied to accurately estimate FS, TO, and t_c from kinematic data obtained during non-instrumented treadmill running, independently of FSA.

5.5 Both a single sacral marker and the whole-body center of mass accurately estimate peak vertical ground reaction force in running (study 5)

5.5.1 Results

RMSE of the estimation of $F_{z,\max}$ with respect to GSM using either COM-M or SACR-M as function of the cut-off frequency of the fourth-order Butterworth filter is depicted in Fig. 16 for three running speeds. The filter frequencies which minimized RMSE were 5 and 4 Hz for COM-M and SACR-M, respectively, for the three speeds. RMSE for COM-M with a 5 Hz cut-off frequency at 9, 11, and 13 km/h were 0.06, 0.07, and 0.08 BW, respectively, while RMSE for SACR-M with a 4 Hz cut-off frequency at 9, 11, and 13 km/h were 0.14, 0.13, and 0.17 BW, respectively. $F_{z,\max}$ estimated by COM-M and SACR-M using these best frequencies were kept for the following analyses.

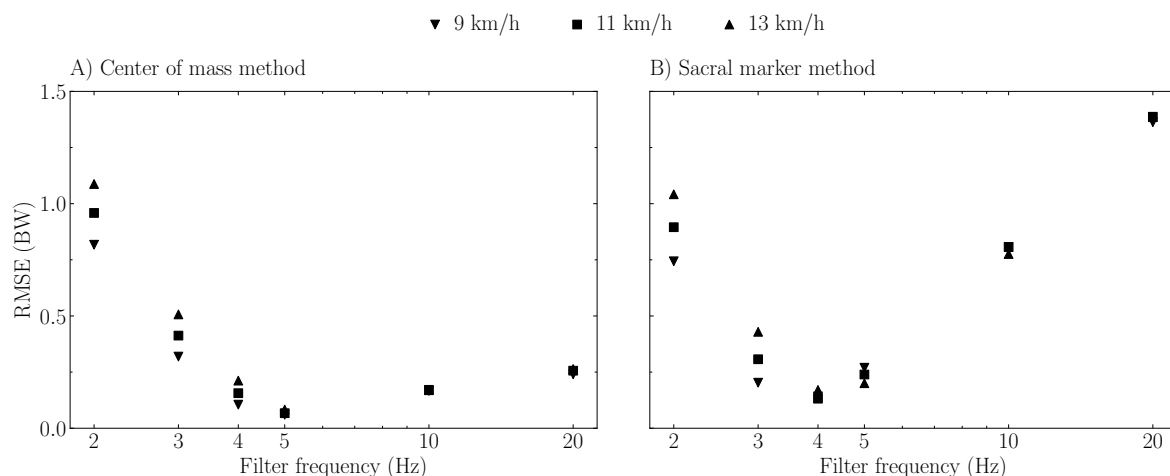


Figure 16. Root mean square error [RMSE; in body weight (BW)] of the estimation of the peak vertical ground reaction force with respect to the gold standard method using (A) the center of mass method (COM-M) and (B) the sacral marker method (SACR-M), as function of the cut-off frequency of the fourth-order Butterworth low-pass filter and for three running speeds. Noteworthy, a log-scale was used on the x -axis to improve readability and vertical force was filtered at 20 Hz.

No systematic bias was reported for $F_{z,\max}$ at 11 km/h for both COM-M and SACR-M compared to GSM (the bias lied within the 95% CI) while small biases were obtained at 9 and 13 km/h [≤ 0.09 BW (≤ 61.8 N for a 70 kg person); Table 8]. RMSE was smaller than or equal to 0.06 BW ($\leq 2.6\%$) and 0.17 BW ($\leq 6.5\%$) for the comparison between GSM and COM-M and between GSM and SACR-M, respectively (Table 8).

Table 8. Systematic bias, lower limit of agreement (lloa), upper limit of agreement (uloa), and root mean square error [RMSE; both in absolute (body weight; BW) and relative (%) units] between peak vertical ground reaction force ($F_{z,max}$) obtained using center of mass (COM-M) and gold standard (GSM) method as well as using sacral marker method (SACR-M) and GSM at three running speeds. 95% confidence intervals are given in square brackets.

Method pair	Running speed (km/h)	Systematic bias (BW)	Lloa (BW)	Uloa (BW)	RMSE (BW)
COM-M vs. GSM	9	0.02 [0.01, 0.03]	-0.09 [-0.11, -0.07]	0.13 [0.11, 0.15]	0.06 (2.6%)
	11	-0.01 [-0.02, 0.01]	-0.14 [-0.16, -0.12]	0.12 [0.10, 0.15]	0.07 (2.7%)
	13	-0.04 [-0.05, -0.03]	-0.18 [-0.21, -0.16]	0.10 [0.08, 0.13]	0.08 (3.2%)
SACR-M vs. GSM	9	0.08 [0.06, 0.10]	-0.14 [-0.18, -0.11]	0.31 [0.27, 0.34]	0.14 (6.0%)
	11	0.01 [-0.01, 0.03]	-0.25 [-0.29, -0.21]	0.27 [0.23, 0.31]	0.13 (5.3%)
	13	-0.09 [-0.11, -0.06]	-0.37 [-0.42, -0.33]	0.20 [0.15, 0.24]	0.17 (6.5%)

Note. For systematic bias, positive and negative values indicate the COM-M and SACR-M methods overestimated and underestimated $F_{z,max}$, respectively. COM and sacral marker data were filtered at 5 and 4 Hz, respectively, while vertical force was filtered at 20 Hz.

Repeated measures ANOVA depicted significant effects for both running speed and method of calculation x running speed interaction ($P < 0.001$; Table 9) but there was no effect of the method of calculation ($P = 0.41$; Table 9). Holm post hoc tests yielded significant differences between $F_{z,max}$ obtained using pair of methods at 9 and 13 km/h ($P \leq 0.003$) but not at 11 km/h ($P \geq 0.23$). The other pairwise post hoc comparisons were all statistically significant ($P \leq 0.03$) except the pair GSM at 11 km/h and SACR-M at 13 km/h ($P = 0.23$).

Table 9. Peak vertical ground reaction force [$F_{z,\max}$; in body weight (BW)] obtained using gold standard (GSM), center of mass (COM-M), and sacral marker (SACR-M) methods for three running speeds. Significant ($P \leq 0.05$) method of calculation, running speed, and interaction effect, as determined by repeated measures ANOVA, are reported in bold font. *, †, and ‡ depict significant differences between $F_{z,\max}$ obtained using GSM and COM-M, GSM and SACR-M, and COM-M and SACR-M, respectively, at a given running speed and as determined by Holm post hoc tests. Noteworthy, the other pairwise post hoc comparisons were all statistically significant ($P \leq 0.03$) except the pair GSM at 11 km/h and SACR-M at 13 km/h ($P = 0.23$) but not represented by a symbol in the table.

Variable	Running Speed (km/h)	GSM	COM-M	SACR-M
$F_{z,\max}$ (BW)	9	2.25 ± 0.28 ^{*,†}	2.27 ± 0.28 [‡]	2.33 ± 0.29
	11	2.39 ± 0.30	2.38 ± 0.29	2.40 ± 0.30
	13	2.50 ± 0.31 ^{*,†}	2.46 ± 0.30 [‡]	2.41 ± 0.30
Method of calculation effect		$P = 0.41$		
Running speed effect		$P < \mathbf{0.001}$		
Interaction effect		$P < \mathbf{0.001}$		

Note. Values are presented as mean ± standard deviation. COM and sacral marker data were filtered at 5 and 4 Hz, respectively, while vertical force was filtered at 20Hz.

5.5.2 Discussion

According to the first hypothesis, a single cut-off frequency minimized RMSE and was different for each method. Indeed, the most accurate estimations of $F_{z,\max}$ were obtained using a 5 and 4 Hz cut-off frequency for the fourth order Butterworth low-pass filtering of COM and sacral marker accelerations, respectively. Besides, according to the second hypothesis, RMSE close to 0.15 BW were obtained for both COM-M and SACR-M at each tested speed (RMSE ≤ 0.17 BW). Conventional statistical approaches demonstrated no systematic bias and no significant difference of $F_{z,\max}$ between GSM, COM-M, and SACR-M at 11 km/h. However, systematic biases and significant differences were obtained at 9 and 13 km/h, though COM-M gave systematic biases three times smaller than SACR-M as well as two times smaller RMSE. Nonetheless, systematic biases at 9 and 13 km/h were small (≤ 0.09 BW) and accompanied with an RMSE $\leq 6.5\%$.

COM-M and SACR-M depicted the smallest RMSE for a cut-off frequency of 5 and 4 Hz, respectively (Fig. 16). As the body segments were not considered in the sacral acceleration, this might not attenuate and “smooth” the signal compared to COM acceleration (the whole-body COM trajectory being a weighted sum of all body segments, its overall shape should be

smoother than the sacral marker trajectory). This suggests that the vertical peaks in the unfiltered sacral acceleration signal were slightly higher than in COM acceleration. Therefore, a smaller cut-off frequency was required to filter the sacral than COM acceleration to decrease the magnitude of the vertical peaks and to make them match with the ones of GSM. Nonetheless, as the sacral marker should be close to COM location [113], the corresponding acceleration signals should be similar, i.e., the noise in the sacral acceleration was not drastically larger than in the COM one, justifying the small difference of 1 Hz in optimal cut-off frequencies.

Different RMSE between speeds were reported at lower than optimal cut-off frequencies while similar RMSE were obtained at larger than optimal cut-off frequencies (Fig. 16). In other words, the effect of speed on RMSE increased as cut-off frequency decreased. This might be explained by the fact that the 2-4 Hz cut-off frequencies were close to the oscillatory behavior of COM or sacral marker. Indeed, 3 Hz is considered as the frequency corresponding to the vertical sinusoidal pelvic motion, reflective of step frequencies [150]. Besides, the higher the speed, the higher the step rate, and thus the even more likely to be close to the oscillatory behavior of the COM or sacral marker, further explaining the higher RMSE reported at 13 km/h than at 11 and 9 km/h at lower than optimal cut-off frequencies.

A previous study evaluating the effect of the cut-off frequency to filter sacral-mounted IMU data to estimate $F_{z,\max}$ reported that the smallest RMSE was obtained using a 10 Hz cut-off [103]. The present study reported optimal cut-off frequencies that were two times smaller (4 and 5 Hz). The discrepancy might be explained by the fact that the authors were directly measuring the sacral acceleration, which might be more prone to high frequency noise [103]. Furthermore, ground reaction force was filtered at 30 Hz whereas a 20 Hz cut-off was used in this study. In addition, the authors recorded treadmill runs from 13.7 to 19.4 km/h, which is faster than the endurance speeds used in the present study. Therefore, as the present study slightly overestimated and underestimated $F_{z,\max}$ at 9 and 13 km/h, respectively, this suggests that a larger cut-off frequency should be used at a faster speed and a smaller one at a slower speed, which goes in the direction of the previous findings [103]. Indeed, increasing/decreasing the cut-off frequency increases/decreases the magnitude of the filtered signal [103]. Moreover, a significant effect of running speed was observed (Table 9). Therefore, a speed-dependent cut-off frequency would probably provide better results. However, future studies should focus on

testing several slower and faster running speeds to further decipher the running speed effect. Besides, a more complicated model could be constructed to better estimate $F_{z,max}$, for instance following recent research [104, 178, 179], which uses artificial intelligence to estimate the vertical ground reaction force. Then, in practice, a systematic addition of the bias corresponding to the given speed could be applied when estimating $F_{z,max}$.

The differences between GSM and COM-M or SACR-M obtained in this study reported the same level of accuracy than in the study based on a single participant [114] [≤ 100 N (≤ 0.15 BW for a 70 kg person) at 7-20 km/h]. Moreover, $F_{z,max}$ estimated using sacral-mounted inertial sensors reported similar differences [103] [≤ 20 N (≤ 0.03 BW for a 70 kg person) at 14-19 km/h] and RMSE [104] (0.15 BW at 13.5-19.5 km/h) with respect to GSM than COM-M and SACR-M used in the present study. In addition, a 6% error on $F_{z,max}$ (6-21 km/h) was reported using an inertial sensor placed on the leg along the tibial axis [180] while a 3% error (10-14 km/h) was achieved using three IMUs (two on lower legs and one on pelvis) and two artificial neural networks [141]. Thus, estimated $F_{z,max}$ depicted a similar error ($\sim 5\%$) to previous estimations which used whole-body COM trajectory or inertial sensors. Nonetheless, the present study only tested running speeds ranging between 9 and 13 km/h, thus not permitting to generalize on the accuracy of COM-M and SACR-M at faster running speeds, especially because a significant effect of running speed was observed (Table 9).

No systematic bias or significant differences were reported for both COM-M and SACR-M at 11 km/h (Tables 8 and 9). However, systematic but small biases were reported at 9 and 13 km/h (Table 8), which were accompanied by significant differences (Table 9). The systematic bias of SACR-M was almost three times larger than the one of COM-M at 9 and 13 km/h while RMSE was two times larger (Table 8). Besides, a less important linear increase in $F_{z,max}$ with increasing speed was reported for SACR-M than for GSM and COM-M (Table 9). These results could be explained by the fact that the speed-dependence of the cut-off frequency might be more important for SACR-M than COM-M, which is depicted by the larger range of RMSE over the three running speeds at a given cut-off frequency for SACR-M than COM-M (Fig. 16). Therefore, SACR-M might require a more pronounced variation of the cut-off frequency with running speed than COM-M, i.e., the cut-off frequency for SACR-M might need to vary (even if < 1 Hz) when speed changes by 2 km/h while the one of COM-M might not. This might allow obtaining a similar linear increase of $F_{z,max}$ with increasing speed for SACR-M

than for GSM and COM-M. Nonetheless, further studies should be conducted to validate this assumption.

No significant difference was reported between COM-M and SACR-M at 11 km/h but were at 9 and 13 km/h (Table 9), which follows the differences between GSM and both COM-M and SACR-M. However, SACR-M depicted larger deviations around the mean than COM-M, as reported by the larger lower and upper limit of agreements and 95% CI (Table 8). These larger deviations could be explained by the fact that the whole-body COM trajectory is a weighted sum of all body segments while the sacral marker trajectory is not (see above). These findings showed that COM-M is more consistent amongst participants than SACR-M and might be a preferred choice but is not reflected by the statistical analysis. Therefore, we suggest researchers with access to a motion capture system but not to a force plate to use COM-M or SACR-M with data filtered at 5 and 4 Hz, respectively, to estimate $F_{z,max}$. Furthermore, similar methods but employing a sacral-mounted IMU might be used to estimate $F_{z,max}$ overground, as long as an optimal cut-off frequency has been determined [103].

To conclude, there were no systematic bias and no significant difference between each pair of methods that estimated $F_{z,max}$ at 11 km/h but there were systematic but small biases and significant differences at 9 and 13 km/h. Nonetheless, estimated $F_{z,max}$ showed similar error (~5%) to previous estimations which used whole-body COM trajectory or inertial sensors. Hence, the findings of this study support the use of either COM-M or SACR-M to estimate $F_{z,max}$ during level treadmill runs, and especially at 11 km/h.

5.6 A single sacral-mounted inertial measurement unit to estimate peak vertical ground reaction force, contact time, flight time, effective contact time, and effective flight time in running (studies 6 and 7)

5.6.1 Results

Systematic biases (average over running speeds) were obtained for $F_{z,\max}$ (0.07 BW) and t_c and t_f (13 ms), and 11 km/h gave the smallest absolute bias, followed by 9 km/h and 13 km/h (Table 10). The three variables reported a significant negative proportional bias at all speeds and the proportional bias of t_f was larger than that of t_c (Table 10).

Table 10. Systematic bias, lower limit of agreement (lloa), upper limit of agreement (uloa), and proportional bias \pm residual random error together with its corresponding P -value between peak vertical ground reaction force ($F_{z,\max}$), contact time (t_c), and flight time (t_f) obtained using inertial measurement unit method and gold standard method at three running speeds. Confidence intervals of 95% are given in square brackets [lower, upper]. Significant ($P \leq 0.05$) proportional biases are reported in bold font.

Variable	Speed (km/h)	Systematic bias	lloa	uloa	Proportional bias (P)
$F_{z,\max}$ (BW)	9	0.05 [0.04, 0.05]	-0.21 [-0.22, -0.20]	0.30 [0.29, 0.31]	-0.28 \pm 0.02 (< 0.001)
	11	-0.04 [-0.04, -0.03]	-0.31 [-0.32, -0.30]	0.23 [0.22, 0.24]	-0.41 \pm 0.02 (< 0.001)
	13	-0.13 [-0.13, -0.12]	-0.45 [-0.46, -0.43]	0.19 [0.18, 0.20]	-0.51 \pm 0.02 (< 0.001)
t_c (ms)	9	-9.9 [-10.6, -9.1]	-43.7 [-45.0, -42.4]	23.9 [22.6, 25.2]	-0.38 \pm 0.02 (< 0.001)
	11	7.3 [6.5, 8.0]	-24.6 [-25.8, -23.4]	39.1 [37.9, 40.3]	-0.37 \pm 0.02 (< 0.001)
	13	20.2 [19.5, 20.9]	-10.1 [-11.3, -9.0]	50.6 [49.4, 51.7]	-0.29 \pm 0.02 (< 0.001)
t_f (ms)	9	9.9 [9.1, 10.7]	-23.8 [-25.0, -22.5]	43.5 [42.3, 44.8]	-0.79 \pm 0.02 (< 0.001)
	11	-7.4 [-8.1, -6.6]	-39.2 [-40.5, -38.0]	24.5 [23.3, 25.8]	-0.86 \pm 0.02 (< 0.001)
	13	-20.4 [-21.1, -19.7]	-50.8 [-52.0, -49.7]	10.0 [8.9, 11.2]	-0.91 \pm 0.02 (< 0.001)

Note. For systematic biases, positive and negative values indicate the inertial measurement unit method overestimated and underestimated $F_{z,\max}$, t_c , and t_f , respectively.

t_{ce} and t_{fe} depicted small systematic biases (≤ 20 ms) at all speeds. The smallest absolute bias was given for 9 km/h, followed by 11 km/h and 13 km/h (Table 11). Both effective timings reported a significant negative proportional bias at all speeds but were accompanied with small coefficients of determination (R^2 ; Table 11).

Table 11. Systematic bias, lower limit of agreement (lloa), upper limit of agreement (uloa), proportional bias \pm residual random error together with its corresponding P -value, and coefficient of determination (R^2) between effective contact (t_{ce}) and flight (t_{fe}) times obtained using inertial measurement unit method and gold standard method at three running speeds. 95% confidence intervals are given in square brackets. Significant ($P \leq 0.05$) proportional bias are reported in bold font.

Variable	Speed (km/h)	Systematic bias	lloa	uloa	Proportional bias (P)	R^2
t_{ce} (ms)	9	9.0 [8.4, 9.5]	-15.8 [-16.7, -14.9]	33.7 [32.8, 34.7]	-0.64 \pm 0.02 (< 0.001)	0.30
	11	14.5 [13.9, 15.0]	-10.0 [-10.9, -9.0]	38.9 [38.0, 39.8]	-0.60 \pm 0.02 (< 0.001)	0.25
	13	18.8 [18.3, 19.3]	-4.1 [-5.0, -3.2]	41.7 [40.8, 42.5]	-0.50 \pm 0.03 (< 0.001)	0.15
t_{fe} (ms)	9	-8.9 [-9.4, -8.3]	-34.6 [-35.6, -33.6]	16.9 [15.9, 17.9]	-0.35 \pm 0.02 (< 0.001)	0.10
	11	-14.5 [-15.0, -13.9]	-39.9 [-40.9, -39.0]	11.0 [10.0, 12.0]	-0.51 \pm 0.02 (< 0.001)	0.18
	13	-18.9 [-19.4, -18.3]	-43.0 [-43.9, -42.1]	5.3 [4.3, 6.2]	-0.50 \pm 0.02 (< 0.001)	0.19

Note. For systematic bias, positive and negative values indicate the inertial measurement unit method overestimated and underestimated t_{ce} and t_{fe} , respectively.

Repeated measures ANOVA depicted significant effects for both methods and running speed, as well as an interaction effect for $F_{z,max}$, t_c , and t_f ($P \leq 0.002$; Table 12). Holm post hoc tests yielded significant differences between $F_{z,max}$, t_c , and t_f obtained using the GSM and IMUM at all speeds ($P \leq 0.006$). The average RMSE over running speed was 0.15 BW for $F_{z,max}$ (6%), while it was 20 ms for t_c and t_f , corresponding to 8% and 18%, respectively (Table 12).

Significant effects for both method of calculation and running speed as well as an interaction effect were depicted by repeated measures ANOVA for t_{ce} and t_{fe} ($P < 0.001$; Table 13). Significant differences between GSM and IMUM for t_{ce} and t_{fe} at all speeds ($P < 0.001$) were reported by Holm post hoc tests. RMSE was ≤ 22 ms ($\leq 14\%$) for t_{ce} and t_{fe} (Table 13).

Table 12. Peak vertical ground reaction force ($F_{z,max}$), contact time (t_c), and flight time (t_f) obtained using the gold standard method (GSM) and inertial measurement unit method (IMUM) together with the root mean square error [RMSE; both in absolute (ms or BW) and relative (%) units] for three running speeds. Significant ($P \leq 0.05$) method of calculation, running speed, and interaction effect, as determined by repeated measures ANOVA, are reported in bold font. * Significant difference between $F_{z,max}$, t_c , and t_f obtained using the GSM and IMUM at a given running speed, as determined by Holm post hoc tests.

Running speed (km/h)	Variable	$F_{z,max}$ (BW)	t_c (ms)	t_f (ms)
9	GSM	$2.37 \pm 0.19^*$	$278.3 \pm 22.2^*$	$92.8 \pm 22.4^*$
	IMUM	2.42 ± 0.14	268.4 ± 15.5	102.7 ± 10.8
	RMSE (absolute)	0.13	18.5	18.6
	RMSE (%)	5.3	6.7	20.1
11	GSM	$2.51 \pm 0.19^*$	$249.7 \pm 19.2^*$	$111.5 \pm 19.7^*$
	IMUM	2.47 ± 0.13	256.9 ± 13.9	104.1 ± 9.1
	RMSE (absolute)	0.13	16.4	16.5
	RMSE (%)	5.1	6.6	14.8
13	GSM	$2.62 \pm 0.20^*$	$227.6 \pm 16.5^*$	$122.8 \pm 17.5^*$
	IMUM	2.49 ± 0.11	247.8 ± 12.8	102.4 ± 8.0
	RMSE (absolute)	0.19	24.4	24.5
	RMSE (%)	7.4	10.7	20.0
Method of calculation effect		$P = 0.002$	$P < 0.001$	$P < 0.001$
Running speed effect		$P < 0.001$	$P < 0.001$	$P < 0.001$
Interaction effect		$P < 0.001$	$P < 0.001$	$P < 0.001$

Note. Values are presented as mean \pm standard deviation.

Table 13. Effective contact (t_{ce}) and flight (t_{fe}) times obtained using gold standard method (GSM) and inertial measurement unit method (IMUM) together with root mean square error [RMSE; both in absolute (ms or N) and relative (%) units] for three running speeds. Significant ($P \leq 0.05$) method of calculation, running speed, and interaction effect, as determined by repeated measures ANOVA, are reported in bold font. *Significant difference between t_{ce} and t_{fe} obtained using GSM and IMUM, as determined by Holm post hoc tests.

Running speed (km/h)	Variable	t_{ce} (ms)	t_{fe} (ms)
9	GSM	172.2 ± 14.4*	198.6 ± 14.3*
	IMUM	181.2 ± 8.0	189.8 ± 10.3
	RMSE (ms)	14.7	14.8
	RMSE (%)	8.5	7.4
11	GMS	162.5 ± 13.6*	198.7 ± 13.8*
	IMUM	177.0 ± 8.1	184.2 ± 8.4
	RMSE (ms)	18.5	18.6
	RMSE (%)	11.4	9.4
13	GSM	152.7 ± 12.0*	197.3 ± 13.3*
	IMUM	171.5 ± 7.9	178.4 ± 8.0
	RMSE (ms)	21.6	21.7
	RMSE (%)	14.2	11.0
Method of calculation effect		$P < 0.001$	$P < 0.001$
Running speed effect		$P < 0.001$	$P < 0.001$
Interaction effect		$P < 0.001$	$P < 0.001$

Note. Values are presented as mean ± standard deviation.

5.6.2 Discussion

According to the first hypothesis, an RMSE equal to 0.15 BW was reported for $F_{z,max}$. Moreover, according to the second hypothesis, an RMSE equal to 20 ms was obtained for t_c and t_f . Our findings demonstrated systematic and proportional biases, as well as significant differences between gold standard and estimated $F_{z,max}$, t_c , t_f , t_{ce} , and t_{fe} at each speed employed. Nonetheless, systematic biases averaged over running speeds were small (0.07 BW and 20 ms) suggesting the use of IMUM to estimate $F_{z,max}$, t_c , t_f , t_{ce} , and t_{fe} for level treadmill runs at endurance running speeds.

A systematic bias of 0.07 BW and an RMSE of 0.15 BW (6%) were reported for $F_{z,max}$ (Tables 10 and 12). These errors seemed to be comparable to those obtained using a 10 Hz low-pass

cut-off frequency [103], though the bias and RMSE were not explicitly reported [~ 0.15 BW by visual inspection of their Fig. 4 (14-19 km/h)]. In addition, the RMSE found for $F_{z,\max}$ in the present study was equal to the RMSE obtained using two different ML algorithms (LR and quantile regression forest) [104]. This result suggests that combining IMU data with ML algorithms seems to not necessarily be advantageous to estimate $F_{z,\max}$. Using inertial sensors placed on the legs along the tibial axis, Charry et al. [180] obtained a 6% error on $F_{z,\max}$ (6-21km/h) while Wouda et al. [141] achieved a 3% error (10-14 km/h), but using three IMUs (two on lower legs and one on pelvis) and two artificial NNs. Besides, an RMSE smaller than or equal to 0.17 BW was reported when estimating $F_{z,\max}$ using 3D kinematic data of the COM or sacral marker trajectory [115]. An RMSE ~ 0.15 BW was reported by Pavei et al. [114] when the whole-body COM acceleration, obtained using kinematic data to estimate $F_{z,\max}$ for running speeds ranging from 7 to 20 km/h, was used for a single participant. Thus, the errors reported for $F_{z,\max}$ in the present study were comparable to those obtained using previously published methods [103, 104, 114, 115, 141, 180].

The IMUM reported a systematic bias of 13 ms and an RMSE of 20 ms (8%) for t_c (Tables 10 and 12). These errors seemed to be smaller than those obtained using a 5 Hz low-pass cut-off frequency [103], though the bias and RMSE were not explicitly reported [~ 30 ms by visual inspection of their Fig. 5 (14-19 km/h)]. The IMUM employed in the present study might be advantageous compared to that previously used [103] because the present IMUM utilized a single low-pass cut-off frequency (5Hz) to estimate both $F_{z,\max}$ and t_c while the previous method required two different cut-off frequencies (10 Hz for $F_{z,\max}$ and 5 Hz for t_c). However, the present errors were much higher than those reported by Lee et al. [119] (0 ms). These authors used specific spikes in an unfiltered forward acceleration signal recorded by a sacral-mounted IMU sampled at 100 Hz to detect FS and TO events which were not present in most of the data recorded in the present study. One possible explanation could be that the 10 national level runners recruited by these authors shared a very similar running pattern with specific acceleration spikes that were not always observed in the present study. As a side note, the anterior-posterior acceleration signal recorded by the IMU was quite different from that depicted in Lee et al. [119] and both anterior-posterior IMU signals were different from that assessed using the gold standard anterior-posterior ground reaction force signal [181]. This was also previously observed when reconstructing the anterior-posterior acceleration signal using 3D kinematic trajectories [114]. Besides, the 20 ms RMSE obtained in our study is almost two

times larger than the 10 ms RMSE reported by Alcantara et al. [104]. Such difference might be explained by the fact that these authors predicted t_c using two different ML algorithms (LR and quantile regression forest) while the present study estimates t_c directly from the post-processing of the vertical acceleration signal recorded by the sacral-mounted IMU. Moreover, such difference suggests that combining IMU data with a ML algorithm may improve the estimations of t_c and t_f compared to those obtained using IMU data alone. However, the robustness of the ML algorithms employed by these authors might be questioned as these algorithms were trained on 28 runners and tested on 9 runners, which is below the median value of 40 participants used for this kind of research question [142]. Nonetheless, further studies would be required to evaluate if applying a ML algorithm on our IMU data, which contains 100 participants, would be more accurate in estimating t_c and t_f . As for foot-worn inertial sensors, a systematic bias on t_c of ~ 10 ms (10-20 km/h) [121] and RMSE of ~ 10 ms (11 km/h) [126] were reported, which placed IMUM at a similar level of accuracy. In addition, Falbriard et al. [121] depicted a proportional bias for t_c , as in this study for both t_c and t_{ce} .

IMUM reported systematic biases smaller than or equal to 20 ms and RMSE smaller than or equal to 22 ms ($\leq 14\%$) for t_{ce} (Tables 11 and 13). Errors in t_{ce} and t_{fe} could not directly be compared to the actual literature because, to the best of our knowledge, no study comparing several methods to calculate these effective timings was conducted so far. Indeed, we are only aware of the comparison between t_{ce} and t_{fe} obtained using Myotest[®] and t_c and t_f obtained from photocell- and optical-based systems [118], which makes this comparison useless as different outcomes (t_{ce} vs. t_c and t_{fe} vs. t_f) were actually being compared. Nevertheless, the authors were aware of this limitation and clearly stated this limitation [118]. Comparing t_{ce} and t_{fe} to t_c and t_f led to the fact that, similarly to t_c , the error in t_{ce} reported in this study seemed to be smaller than or similar to the ones previously reported for t_c [103, 104, 121, 126]. The error reported for the IMUM when estimating t_c was comparable to the error obtained using an optoelectronic system [93], but was much larger than the error obtained using a photoelectric system [182]. However, even though these two systems can be used outside the laboratory [21, 22], they suffer from a lack of portability and do not allow continuous data collection. For this reason, using a single IMU was advantageous by its portability, and was shown to be quite accurate to estimate t_c , and therefore t_f and similarly for t_{ce} and t_{fe} . Indeed, when the error is calculated for many running steps, as t_c and t_f (t_{ce} and t_{fe}) are based on the

same TO (eTO) events, the bias of t_f (t_{fe}) is the negative of the bias of t_c (t_{ce}) and the RMSEs for t_c and t_f (t_{ce} and t_{fe}) are mostly the same in absolute (ms) units.

A significant effect of running speed was observed for $F_{z,\max}$, t_c , and t_f , t_{ce} , and t_{fe} (Tables 10 and 12). Moreover, the most accurate estimation was given at 11 km/h for $F_{z,\max}$, t_c , and t_f (Tables 10 and 12) and at 9 km/h for t_{ce} , and t_{fe} (Tables 11 and 13). These findings could not readily be explained. However, further studies should focus on testing several slower and faster running speeds to further decipher the running speed effect. Then, future studies could focus on constructing a more sophisticated model considering the running speed to try to improve the estimations of $F_{z,\max}$, t_c , and t_f .

Due to the inexact synchronization between kinetic and IMU data, FS, TO, eFS, and eTO could not be compared between GSM and IMUM. However, we suspect that even under perfect synchronization, FS, TO, eFS, and eTO from GSM and IMUM would not exactly coincide as vertical force used in IMUM approximates ground truth vertical force recorded by the force plate. Nonetheless, further studies involving synchronized kinetic and IMU data would prove useful, especially if one is interested in assessing metrics at specific FS, TO, eFS, and eTO, for instance using additional IMUs [183] themselves synchronized with the sacral-mounted one which would provide FS, TO, eFS, and eTO.

A single cut-off frequency was used to filter the vertical ground reaction force, i.e., 20 Hz. Though this choice of cut-off frequency is quite widespread [130, 184], other cut-off frequencies (e.g., 30 or 80 Hz) are also used in the literature [104, 162]. In this case, the error of IMUM might increase because the cut-off frequency affects the magnitude of the vertical ground reaction force and thus the time at which FS, TO, eFS, and eTO occur. Hence, it would also be useful to explore the effect of the cut-off frequency of the truncated Fourier series on the accuracy of IMUM, as already explored by Day et al. [103] for a low-pass filter. Additionally, the effect of the filter itself (e.g., truncated Fourier series, 4th order low-pass Butterworth filter, 8th order low-pass Butterworth filter, etc.) might also be worth exploring. Therefore, further studies investigating the effect of the cut-off frequency of both the gold standard and IMU signals as well as the kind of filter should be conducted. Furthermore, the significant effect of running speed suggests that the cut-off frequency that estimates best $F_{z,\max}$,

t_c , t_f , t_{ce} , and t_{fe} might be speed dependent and reinforce the need to further explore the effect of the cut-off frequency of both GSM and IMUM, and to explore slower and faster speeds.

To conclude, the comparison between the GSM and IMUM showed an RMSE of 0.15 BW for $F_{z,max}$, and ≤ 22 ms for t_c , t_f , t_{ce} , and t_{fe} together with systematic but small biases (0.07 BW for $F_{z,max}$ and ≤ 20 ms for t_c , t_f , t_{ce} , and t_{fe}). These errors were comparable to those obtained using previously published methods. Therefore, the findings of this study support the use of the IMUM to estimate $F_{z,max}$, t_c , t_f , t_{ce} , and t_{fe} for level treadmill runs at endurance running speeds (9-13 km/h), especially because an IMU has the advantage to be low-cost and portable, and therefore seems very practical for coaches and healthcare professionals.

5.7 Comparison of different machine learning models to enhance sacral acceleration-based estimations of running stride temporal variables and peak vertical ground reaction force (study 8)

5.7.1 Results

The SF obtained from the IMU-based estimation (included in the features) was almost identical to the gold standard SF (Fig. 17).

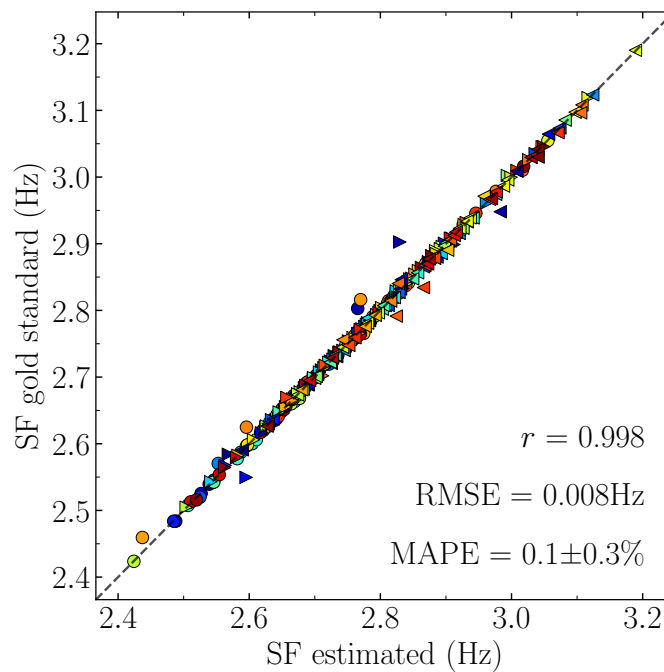


Figure 17. Gold standard (obtained using force plate data) step frequency (SF) as function of estimated SF (obtained using inertial measurement unit data, no machine learning) for the entire set of data and corresponding Pearson correlation coefficient (r), root mean square error (RMSE), and mean absolute percentage error (MAPE). Each point represents the value for a given combination of participant and running speed. Colors represent different participants while the three symbols represent different running speeds (o: 9 km/h, ▷: 11 km/h, ◁: 13 km/h).

The ML models predicted t_c with an r of 0.89 ± 0.01 , RMSE of 12.2 ± 0.2 ms, and mean absolute percentage error (MAPE) of $3.6 \pm 0.1\%$ (mean \pm standard deviation for the three models). As for t_f , the r , RMSE, and MAPE were 0.86 ± 0.01 , 11.7 ± 0.4 ms, and $9.3 \pm 0.4\%$. DF was predicted with an r of 0.84 ± 0.03 , RMSE of $1.7 \pm 0.1\%$, and MAPE of $3.6 \pm 0.2\%$. As for $F_{z,\max}$, the r , RMSE, and MAPE were 0.77 ± 0.01 , 0.13 ± 0.01 BW, and $3.8 \pm 0.1\%$ (Fig. 18).

A significant model effect was reported for the MAPE of t_c , t_f , and DF ($P \leq 0.001$) but not of $F_{z,\max}$ ($P = 0.37$). Post hoc tests revealed that the MAPEs obtained using the three ML models were significantly smaller than the MAPE obtained without ML for t_c , t_f , and DF ($P \leq 0.003$; Fig. 18). However, there was no significant difference among the MAPEs obtained using the three ML models for these three variables ($P \geq 0.80$).

Using ML allowed increasing r by $28 \pm 1\%$, $59 \pm 2\%$, $65 \pm 5\%$, and $15 \pm 1\%$, for t_c , t_f , DF, and $F_{z,\max}$, respectively, compared to those obtained from IMU-based estimations. As for the RMSEs, they decreased by $37 \pm 1\%$, $39 \pm 2\%$, $37 \pm 4\%$, and $16 \pm 4\%$ for t_c , t_f , DF, and $F_{z,\max}$, respectively, while the MAPEs decreased by $40 \pm 1\%$, $40 \pm 3\%$, $41 \pm 3\%$, and $9 \pm 1\%$ (Table 14).

Table 14. Percentage difference of the Pearson correlation coefficients (r), root mean square error (RMSE), and mean absolute percentage error (MAPE) between those obtained using estimations based on inertial-measurement unit data and those obtained using a machine learning model among linear regression, support vector regression with the radial basis function kernel, and two-layers neural network, for four predicted variables, i.e., contact time, flight time, duty factor, and peak vertical ground reaction force.

Variable	Statistics	Linear regression (%)	Support vector regression (%)	Two-layers neural network (%)
Contact time	r	29	27	27
	RMSE	-38	-36	-36
	MAPE	-40	-42	-40
Flight time	r	59	61	57
	RMSE	-39	-41	-37
	MAPE	-38	-43	-38
Duty factor	r	67	59	69
	RMSE	-40	-32	-40
	MAPE	-42	-37	-43
Peak vertical ground reaction force	r	16	15	13
	RMSE	-20	-13	-13
	MAPE	-11	-9	-8

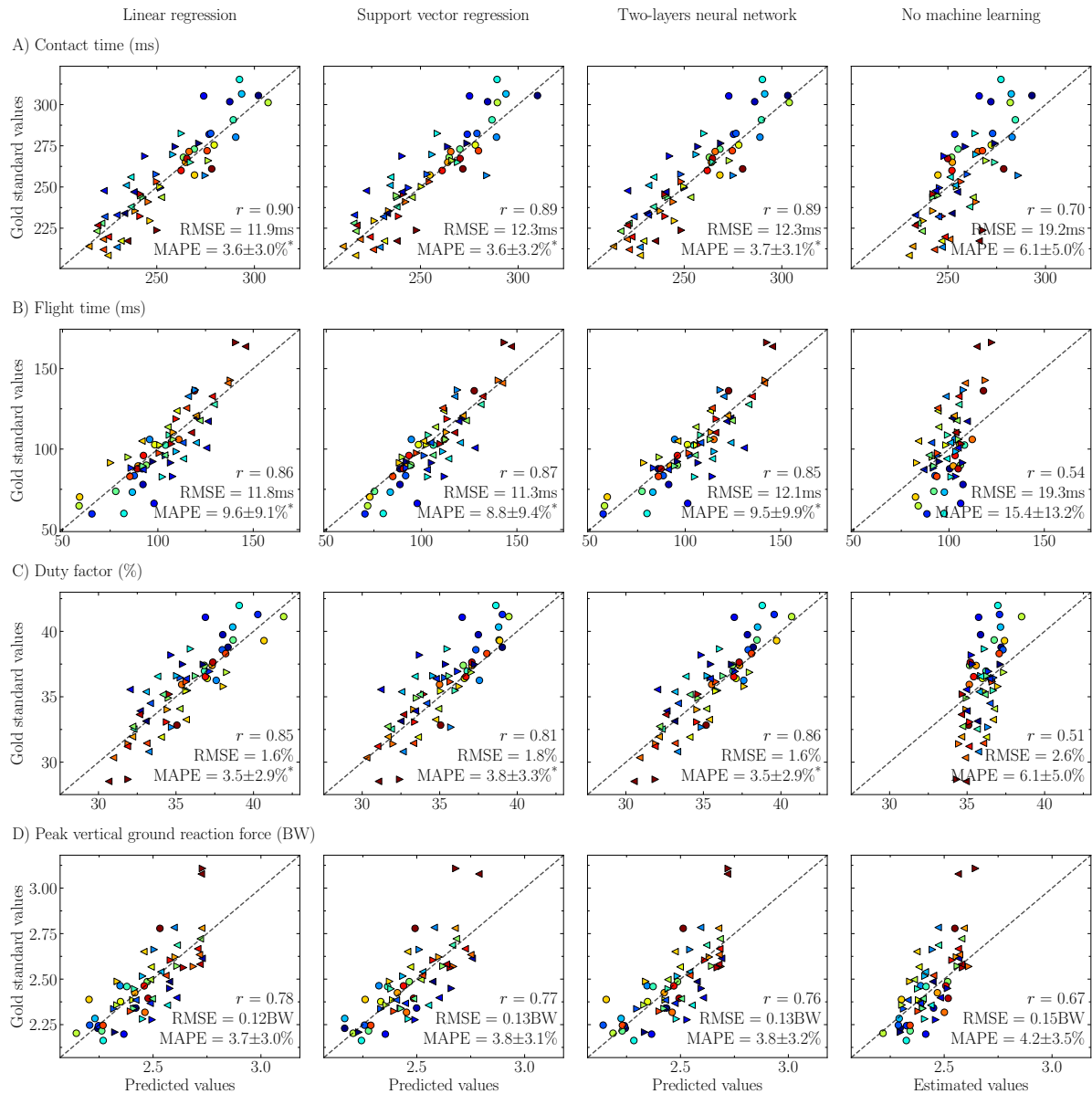


Figure 18. Gold standard (obtained using force plate data) as function of predicted (obtained using three different machine learning models) and estimated (obtained using inertial measurement unit data, no machine learning) (A) contact time, (B) flight time, (C) duty factor, and (D) peak vertical ground reaction force for the testing set and corresponding Pearson correlation coefficient (r), root mean square error (RMSE), and mean absolute percentage error (MAPE). The one-way repeated measures ANOVA revealed a significant model effect (no model vs linear regression vs support vector regression with the radial basis function kernel vs two-layers neural network) for contact time, flight time, and duty factor when comparing the MAPE among the models. *Significant difference ($P \leq 0.003$) between the MAPE of the predictions obtained using a given machine learning model and the MAPE of the estimations obtained using inertial measurement unit data, as determined by Holm post hoc tests. Each point represents the value for a given participant-running speed combination (60 points: three running speeds \times 20 runners). Colors represent different participants while the three symbols represent different running speeds (\circ : 9km/h, \triangleright : 11km/h, \triangleleft : 13km/h).

5.7.2 Discussion

According to the hypothesis, further applying ML to IMU-based estimations of t_c , t_f , DF, and $F_{z,max}$ increased the accuracy of their predictions. However, the enhancement was not significant for $F_{z,max}$. The simplest ML model (LR) was characterized by a similar prediction accuracy than more complicated models (SVR and NN2). Therefore, LR should be used to improve the accuracy of the estimations of t_c , t_f , and DF obtained using a sacral-mounted IMU across a range of running speeds. These improvements may be beneficial when monitoring running-related injury risk factors in real-world settings.

ML was able to improve the prediction accuracy, as reported by the higher r and lower RMSE and MAPE compared to those of the IMU-based estimations (Fig. 18 and Table 14). Nonetheless, the enhancement reported for $F_{z,max}$ was not significant. Using more complicated ML models (SVR and NN2) did not further improve the prediction accuracy compared to the simple LR (Fig. 18 and Table 14). These results corroborate previous findings which observed similar errors for LR and quantile regression forest when predicting t_c , $F_{z,max}$, and vertical impulse with an accelerometer [104]. Moreover, the present RMSE and MAPE of t_c and $F_{z,max}$ were similar to those previously obtained (t_c : ~ 10 ms and $\sim 4\%$ and $F_{z,max}$: ~ 0.14 BW and $\sim 4\%$) using a different algorithm to estimate t_c and $F_{z,max}$ from IMU data [104]. Nonetheless, these previous results might suffer from generalization due to the small sample size ($N=37$). Using three inertial sensors placed on the lower limb (two on lower leg and one on pelvis), Wouda et al. [141] achieved a 3% error with a NN (10-14 km/h), which is similar to the present accuracy (MAPE $\sim 4\%$, Fig. 18). Despite their low prediction error, their results were harder to interpret because of the experimental setup (three IMUs instead of one) and more complicated ML model than the model employed herein. Practically, the improvements reported for our study may be beneficial for practitioners seeking to monitor running-related injury risk factors in real-world settings, though keeping in mind that there exists only limited evidence for most running-related injury-specific risk factors [185].

Previously, ML was also used to predict the vertical impulse from its IMU-based estimation as well as body mass, running speed, and SF [104]. The authors reported an almost perfect correlation between gold standard and predicted vertical impulse values ($r = 0.995$) and obtained that the intercept and SF of the LR were the only significant predictors of the vertical

impulse. However, this was not necessarily needed. Indeed, as the integral of the vertical external forces during a running step is null (Eq. 1):

$$\int_0^{t_c} F_z(t) dt - mg(t_c + t_f) = 0, \quad (1)$$

we get

$$t_{\text{step}} = \frac{\int_0^{t_c} F_z(t) dt}{mg} = \frac{I_z}{mg}, \quad (2)$$

where $t_{\text{step}} = t_c + t_f$ and I_z represent the step time and vertical impulse, respectively. Therefore, according to Eq. 2, SF, i.e., the inverse of t_{step} , is given by the inverse of the vertical impulse expressed in BW units. Hence, the model created by Alcantara et al. [104] to predict the vertical impulse was redundant and not necessarily needed. First, the vertical impulse is directly given by t_{step} and thus by the inverse of SF (Eq. 2). Second, they assumed that SF estimated using IMU data is a valid surrogate to its gold standard counterpart (they used SF estimated using IMU data as a predictor for the vertical impulse, t_c , and $F_{z,\text{max}}$). Thus, they already indirectly assumed that the estimated vertical impulse, i.e., t_{step} (the inverse of SF), is equivalent to its gold standard counterpart. In the present study, gold standard and estimated SF were shown to be equivalent ($r = 0.998$; Fig. 17), which corroborates what has been explained above. Indeed, t_{step} could be approximated by half of the stride time because small symmetry indices smaller than or equal to 4% were previously reported for t_{step} of competitive, recreational, and novice runners at running speeds ranging from 8 to 12 km/h [186].

As expected, as gold standard and estimated SF were equivalent ($r = 0.998$; Fig. 17), similar MAPEs were reported between t_c and DF ($\sim 4\%$; Fig. 18). Thus, the DF prediction is almost only dependent on the t_c prediction.

The “large” dataset employed ($N = 100$) might allow better generalization of the results than those previously obtained with the smaller cohorts of 37 runners [104], though the generalization might not apply to populations not represented in the training data. Hence, further studies should include a broader population, i.e., further increase N , to make the trained ML models more and more generalizable. Furthermore, running trials were performed only at level, endurance speeds, and on a treadmill. However, predictions obtained using ML might also perform well overground because spatiotemporal parameters between treadmill and overground running are largely comparable [187]. Nonetheless, further studies should focus on

improving the predictions by using additional conditions (i.e., faster speeds, positive and negative slopes, and different types of ground) when training the ML models. Finally, the simple ML model, i.e., the LR, was calculated using three different running speeds for each participant. This omits the intra-individual component, which might be problematic because the observations made on a given participant might not be independent and the slope of the LR might be different at the different running speeds.

6. Conclusion

The main aim of this thesis was to investigate the objective evaluation of the spontaneous running pattern and its relationship in terms of runners' classification in the laboratory and towards the field.

First, this thesis aimed to extend the knowledge of DF and SF as global objective variables to assess spontaneous running patterns. This thesis revealed that “local” FSP/FSA and DF do not represent similar running pattern information when investigated at an individual level. DF should be preferred to FSP/FSA when evaluating the global running pattern of a runner because DF is functionally representative of a more global biomechanical behavior than FSA. Moreover, this thesis revealed that the consistency in running patterns decreased as speed differences increased. Therefore, running patterns should be assessed using a range of speeds or at a specific speed. Moreover, there were large interindividual differences across the relative temporal variables examined (DF, SF, t_c , and t_f), highlighting individualized strategies to adapt in running speed changes. Finally, this thesis brought further evidence and reinforce previous statements that low DF runners rely more on the optimization of the spring-mass model (better storage and re-use of elastic energy) than high DF runners. These results corroborate that DF and SF encapsulate different information on running patterns.

Second, this thesis aimed to develop algorithms allowing to accurately measure t_c , t_f , DF, SF, and $F_{z,max}$ in absence of the GSM but using a sacral marker and a motion capture system or a sacral-mounted IMU. This would later allow performing these measurements in the field. This thesis proposed a novel KA that uses a combination of heel and toe kinematics (three markers per foot) to detect FS and TO and to estimate t_c . Small systematic biases were reported for FS, TO, and t_c at all speeds, and this novel KA yielded smaller errors than existing methods for FS, TO, and t_c . Therefore, it can be applied to accurately estimate FS, TO, and t_c from kinematic data obtained during treadmill running, independent of FSA. This thesis also proposed to estimate $F_{z,max}$ by reconstructing the vertical ground reaction force from either the whole-body COM or sacral marker accelerations, themselves obtained by double differentiations of their respective trajectories (motion capture) and further low-pass filtered using a fourth-order Butterworth filter. The most accurate estimations of $F_{z,max}$ were obtained using a 5 and 4 Hz cut-off frequency for the filtering of COM and sacral marker accelerations, respectively. The findings of this thesis support the use of either COM-M or SACR-M using data filtered at 5 and 4 Hz, respectively, to estimate $F_{z,max}$ during level treadmill runs at

endurance speeds. Additionally, this thesis estimated $F_{z,\max}$, t_c , t_f , t_{ce} , t_{fe} , DF, and SF using the vertical acceleration signal recorded by a single sacral-mounted IMU, which was filtered using a truncated Fourier series to 5 Hz. The comparison between the GSM and IMUM showed errors comparable to those obtained using previously published methods [103, 104, 121, 126]. Therefore, the findings of this thesis support the use of the IMUM to estimate $F_{z,\max}$, t_c , t_f , t_{ce} , t_{fe} , DF, and SF for level treadmill runs at endurance running speeds. Further applying ML to IMU-based estimations of t_c , t_f , DF, and $F_{z,\max}$ increased the accuracy of their predictions, though the enhancement was not significant for $F_{z,\max}$. The simplest ML model (LR) was characterized by a similar prediction accuracy to more complicated models (SVR and NN2). Therefore, LR should be used to improve the accuracy of the estimations of t_c , t_f , and DF obtained using a sacral-mounted IMU across a range of running speeds. To conclude, having accurate IMU-based estimations of $F_{z,\max}$, t_c , t_f , t_{ce} , t_{fe} , DF, and SF might be very practical for coaches and healthcare professionals, especially because an IMU has the advantage to be low-cost and portable. Therefore, those accurate estimations might be beneficial when monitoring running-related injury risk factors in real-world settings.

A few limitations to the present thesis exist. Seven out of 8 studies are based on the same dataset. Although heterogeneity was increased in studies 1, 4, and 6-8 by randomly selecting 100 participants from the entire dataset composed of 115 participants, an important weight is given in this thesis to the quality of these data and to the characteristics of the participants. Hence, further studies should be conducted to confirm the present results. Furthermore, no sex distinction was considered in the present thesis. Although the large sample size might have allowed us to separate out men and women, we preferred to not do such separation to increase the statistical power. Additionally, in all except the second study, the running speeds were limited to endurance speeds (9-13 km/h) representative of the running speeds employed by recreational runners during endurance running training [188]. Moreover, the experimental trials were performed on a treadmill. Similar results might also be obtained using overground running trials because spatiotemporal parameters between motorized treadmill and overground running are largely comparable [187]. However, it was also concluded that participants behaved differently when attempting to achieve faster speeds overground than on a treadmill [189]. Therefore, further studies should investigate the objective evaluation of the spontaneous running pattern and its relationship in terms of runners' classification in the laboratory and

towards the field using additional conditions (i.e., faster speeds, positive and negative slopes, and different types of ground) and considering the sex differences.

7. References

1. Messier, S.P., C. Legault, C.R. Schoenlank, et al., *Risk factors and mechanisms of knee injury in runners*. *Medicine and Science in Sports and Exercise*, 2008. **40**(11): p. 1873-9.
2. Lamprecht, M., R. Bürgi, and H. Stamm, *Sport Suisse 2020: activité et consommation sportives de la population suisse*. 2020: Observatoire Suisse du Sport c & o Lamprecht & Stamm Sozialforschung und Beratung AG.
3. van der Worp, M.P., D.S.M. ten Haaf, R. van Cingel, et al., *Injuries in runners; a systematic review on risk factors and sex differences*. *PloS one*, 2015. **10**(2): p. e0114937-e0114937.
4. van Gent, R.N., D. Siem, M. van Middelkoop, et al., *Incidence and determinants of lower extremity running injuries in long distance runners: a systematic review*. *British Journal of Sports Medicine*, 2007. **41**(8): p. 469-80.
5. Bertelsen, M.L., A. Hulme, J. Petersen, et al., *A framework for the etiology of running-related injuries*. *Scandinavian Journal of Medicine & Science in Sports*, 2017. **27**(11): p. 1170-1180.
6. Miller, D.I., *Ground reaction forces in distance running*, in *Biomechanics of Distance Running*, P.R. Cavanagh, Editor. 1990, Human Kinetics: Champaign, IL. p. 203-224.
7. Derrick, T.R., D. Dereu, and S.P. McLean, *Impacts and kinematic adjustments during an exhaustive run*. *Medicine and Science in Sports and Exercise*, 2002. **34**(6): p. 998-1002.
8. Moore, I.S., *Is there an economical running technique? A review of modifiable biomechanical factors affecting running economy*. *Sports Medicine*, 2016. **46**(6): p. 793-807.
9. Moore, I.S., A.M. Jones, and S.J. Dixon, *Reduced oxygen cost of running is related to alignment of the resultant GRF and leg axis vector: A pilot study*. *Scandinavian Journal of Medicine & Science in Sports*, 2016. **26**(7): p. 809-815.
10. Williams, K.R. and P.R. Cavanagh, *Relationship between distance running mechanics, running economy, and performance*. *Journal of Applied Physiology*, 1987. **63**(3): p. 1236-1245.
11. Cavanagh, P.R. and K.R. Williams, *The effect of stride length variation on oxygen uptake during distance running*. *Medicine and Science in Sports and Exercise*, 1982. **14**(1): p. 30-35.
12. Folland, J.P., S.J. Allen, M.I. Black, et al., *Running Technique is an Important Component of Running Economy and Performance*. *Medicine & Science in Sports & Exercise*, 2017. **49**(7): p. 1412-1423.
13. Subotnick, S.I., *The biomechanics of running. Implications for the prevention of foot injuries*. *Sports Medicine*, 1985. **2**(2): p. 144-53.
14. van Oeveren, B.T., C.J. de Ruyter, P.J. Beek, et al., *The biomechanics of running and running styles: a synthesis*. *Sports Biomechanics*, 2021(ahead of print): p. 1-39.

15. Minetti, A.E., *A model equation for the prediction of mechanical internal work of terrestrial locomotion*. Journal of Biomechanics, 1998. **31**(5): p. 463-468.
16. Maiwald, C., T. Sterzing, T.A. Mayer, et al., *Detecting foot-to-ground contact from kinematic data in running*. Footwear Science, 2009. **1**(2): p. 111-118.
17. Abendroth-Smith, J., *Stride adjustments during a running approach toward a force plate*. Research Quarterly for Exercise and Sport, 1996. **67**(1): p. 97-101.
18. Lussiana, T., A. Patoz, C. Gindre, et al., *The implications of time on the ground on running economy: less is not always better*. Journal of Experimental Biology, 2019. **222**(6): p. jeb192047.
19. Patoz, A., T. Lussiana, A. Thouvenot, et al., *Duty Factor Reflects Lower Limb Kinematics of Running*. Applied Sciences, 2020. **10**(24): p. 8818.
20. Debaere, S., I. Jonkers, and C. Delecluse, *The Contribution of Step Characteristics to Sprint Running Performance in High-Level Male and Female Athletes*. The Journal of Strength & Conditioning Research, 2013. **27**(1): p. 116-124.
21. Hébert-Losier, K., L. Mourot, and H.C. Holmberg, *Elite and amateur orienteers' running biomechanics on three surfaces at three speeds*. Medicine & Science in Sports & Exercise, 2015. **47**(2): p. 381-9.
22. Lussiana, T. and C. Gindre, *Feel your stride and find your preferred running speed*. Biology Open, 2016. **5**(1): p. 45-48.
23. Logan, S., I. Hunter, J.T. J Ty Hopkins, et al., *Ground reaction force differences between running shoes, racing flats, and distance spikes in runners*. Journal of sports science & medicine, 2010. **9**(1): p. 147-153.
24. Camomilla, V., E. Bergamini, S. Fantozzi, et al., *Trends Supporting the In-Field Use of Wearable Inertial Sensors for Sport Performance Evaluation: A Systematic Review*. Sensors, 2018. **18**(3): p. 873.
25. Blickhan, R., *The spring-mass model for running and hopping*. Journal of Biomechanics, 1989. **22**(11): p. 1217-1227.
26. Novacheck, T.F., *The biomechanics of running*. Gait & Posture, 1998. **7**(1): p. 77-95.
27. Hasegawa, H., T. Yamauchi, and W.J. Kraemer, *Foot strike patterns of runners at the 15-km point during an elite-level half marathon*. Journal of Strength and Conditioning Research, 2007. **21**(3): p. 888-893.
28. Altman, A.R. and I.S. Davis, *A kinematic method for footstrike pattern detection in barefoot and shod runners*. Gait & posture, 2012. **35**(2): p. 298-300.
29. Ahn, A.N., C. Brayton, T. Bhatia, et al., *Muscle activity and kinematics of forefoot and rearfoot strike runners*. Journal of Sport and Health Science, 2014. **3**(2): p. 102-112.
30. Wei, Z., Z. Zhang, J. Jiang, et al., *Comparison of plantar loads among runners with different strike patterns*. Journal of Sports Sciences, 2019. **37**(18): p. 2152-2158.

31. Ruder, M., S.T. Jamison, A. Tenforde, et al., *Relationship of Foot Strike Pattern and Landing Impacts during a Marathon*. *Medicine & Science in Sports & Exercise*, 2019. **51**(10): p. 2073-2079.
32. Gruber, A.H., K.A. Boyer, T.R. Derrick, et al., *Impact shock frequency components and attenuation in rearfoot and forefoot running*. *Journal of Sport and Health Science*, 2014. **3**(2): p. 113-121.
33. Breine, B., P. Malcolm, E.C. Frederick, et al., *Relationship between running speed and initial foot contact patterns*. *Medicine and Science in Sports and Exercise*, 2014. **46**(8): p. 1595-603.
34. Knorz, S., F. Kluge, K. Gelse, et al., *Three-dimensional biomechanical analysis of rearfoot and forefoot running*. *Orthopaedic Journal of Sports Medicine*, 2017. **5**(7): p. 2325967117719065.
35. Sun, X., Y. Yang, L. Wang, et al., *Do strike patterns or shoe conditions have a predominant influence on foot loading?* *Journal of Human Kinetics*, 2018. **64**: p. 13-23.
36. Anderson, L.M., D.R. Bonanno, H.F. Hart, et al., *What are the benefits and risks associated with changing foot strike pattern during running? A systematic review and meta-analysis of injury, running economy, and biomechanics*. *Sports Medicine*, 2019. **50**(5): p. 885-917.
37. Kulmala, J.-P., J. Avela, K. Pasanen, et al., *Forefoot strikers exhibit lower running-induced knee loading than rearfoot strikers*. *Medicine and Science in Sports and Exercise*, 2013. **45**(12): p. 2306-2313.
38. Almeida, M.O., I.S. Davis, and A.D. Lopes, *Biomechanical differences of foot-strike patterns during running: A systematic review with meta-analysis*. *The Journal of Orthopaedic and Sports Physical Therapy*, 2015. **45**(10): p. 738-755.
39. Goss, D.L. and M.T. Gross, *A review of mechanics and injury trends among various running styles*. *US Army Medical Department journal*, 2012: p. 62-71.
40. Daoud, A.I., G.J. Geissler, F. Wang, et al., *Foot strike and injury rates in endurance runners: a retrospective study*. *Medicine and Science in Sports and Exercise*, 2012. **44**(7): p. 1325-34.
41. Walther, M., I. Reuter, T. Leonhard, et al., *Injuries and response to overload stress in running as a sport*. *Orthopade*, 2005. **34**(5): p. 399-404.
42. Altman, A.R. and I.S. Davis, *Prospective comparison of running injuries between shod and barefoot runners*. *British Journal of Sports Medicine*, 2016. **50**(8): p. 476-80.
43. Rooney, B.D. and T.R. Derrick, *Joint contact loading in forefoot and rearfoot strike patterns during running*. *Journal of Biomechanics*, 2013. **46**(13): p. 2201-2206.
44. Almonroeder, T., J.D. Willson, and T.W. Kernozek, *The effect of foot strike pattern on achilles tendon load during running*. *Annals of Biomedical Engineering*, 2013. **41**(8): p. 1758-66.

45. Dos Santos, A.F., T.H. Nakagawa, F.V. Serrão, et al., *Patellofemoral joint stress measured across three different running techniques*. *Gait & Posture*, 2019. **68**: p. 37-43.
46. Vannatta, C.N. and T.W. Kernozek, *Patellofemoral joint stress during running with alterations in foot strike pattern*. *Medicine and Science in Sports and Exercise*, 2015. **47**(5): p. 1001-8.
47. Forrester, S.E. and J. Townend, *The effect of running velocity on footstrike angle--a curve-clustering approach*. *Gait & Posture*, 2015. **41**(1): p. 26-32.
48. Craighead, D.H., N. Lehecka, and D.L. King, *A novel running mechanic's class changes kinematics but not running economy*. *Journal of Strength and Conditioning Research*, 2014. **28**(11): p. 3137-3145.
49. Hamill, J. and A.H. Gruber, *Is changing footstrike pattern beneficial to runners?* *Journal of Sport and Health Science*, 2017. **6**(2): p. 146-153.
50. Ekizos, A., A. Santuz, and A. Arampatzis, *Short- and long-term effects of altered point of ground reaction force application on human running energetics*. *Journal of Experimental Biology*, 2018. **221**: p. 1-15.
51. Alexander, J.L.N., R.W. Willy, C. Napier, et al., *Infographic. Running myth: switching to a non-rearfoot strike reduces injury risk and improves running economy*. *British Journal of Sports Medicine*, 2021. **55**(3): p. 175-176.
52. Dickinson, M.H., C.T. Farley, R.J. Full, et al., *How animals move: an integrative view*. *Science*, 2000. **288**(5463): p. 100.
53. Arendse, R.E., T.D. Noakes, L.B. Azevedo, et al., *Reduced eccentric loading of the knee with the pose running method*. *Medicine and Science in Sports and Exercise*, 2004. **36**(2): p. 272-277.
54. Dreyer, D. and K. Dreyer, *ChiRunning: A Revolutionary Approach to Effortless, Injury-Free Running. Revised and Fully Updated ed.* 2009, New York, USA: Simon & Schuster.
55. McMahon, T.A., G. Valiant, and E.C. Frederick, *Groucho running*. *Journal of Applied Physiology (Bethesda, Md.: 1985)*, 1987. **62**(6): p. 2326-2337.
56. Bonnaerens, S., P. Fiers, S. Galle, et al., *Grounded Running Reduces Musculoskeletal Loading*. *Medicine and Science in Sports and Exercise*, 2019. **51**(4): p. 708-715.
57. Davis, S., A. Fox, J. Bonacci, et al., *Mechanics, energetics and implementation of grounded running technique: a narrative review*. *BMJ Open Sport & Exercise Medicine*, 2020. **6**(1): p. e000963.
58. Shorten, M. and E. Pisciotta. *Running biomechanics: what did we miss?* in *Proceedings of the 35th Conference of the International Society of Biomechanics in Sport*. 2017.

-
59. Vereecke, E.E., K. D'Août, and P. Aerts, *The dynamics of hylobatid bipedalism: evidence for an energy-saving mechanism?* *Journal of Experimental Biology*, 2006. **209**(15): p. 2829-2838.
 60. Andrada, E., C. Rode, and R. Blickhan, *Grounded running in quails: Simulations indicate benefits of observed fixed aperture angle between legs before touch-down.* *Journal of Theoretical Biology*, 2013. **335**: p. 97-107.
 61. Rubenson, J., D.B. Heliam, D.G. Lloyd, et al., *Gait selection in the ostrich: mechanical and metabolic characteristics of walking and running with and without an aerial phase.* *Proceedings of the Royal Society of London. Series B: Biological Sciences*, 2004. **271**(1543): p. 1091-1099.
 62. Hoerzer, S., V. von Tscherner, C. Jacob, et al., *Defining functional groups based on running kinematics using Self-Organizing Maps and Support Vector Machines.* *Journal of Biomechanics*, 2015. **48**(10): p. 2072-2079.
 63. Phinyomark, A., S. Osis, B.A. Hettinga, et al., *Kinematic gait patterns in healthy runners: A hierarchical cluster analysis.* *Journal of Biomechanics*, 2015. **48**(14): p. 3897-3904.
 64. Gindre, C., T. Lussiana, K. Hébert-Losier, et al., *Aerial and Terrestrial Patterns: A Novel Approach to Analyzing Human Running.* *International Journal of Sports Medicine*, 2016. **37**(01): p. 25-29.
 65. Patoz, A., C. Gindre, L. Mourot, et al., *Intra and Inter-rater Reliability of the Volodalen® Scale to Assess Aerial and Terrestrial Running Forms.* *Journal of Athletic Enhancement*, 2019. **8**(3): p. 1-6.
 66. Lussiana, T., C. Gindre, L. Mourot, et al., *Do subjective assessments of running patterns reflect objective parameters?* *European Journal of Sport Science*, 2017. **17**(7): p. 847-857.
 67. Lussiana, T., C. Gindre, K. Hébert-Losier, et al., *Similar Running Economy With Different Running Patterns Along the Aerial-Terrestrial Continuum.* *International journal of sports physiology and performance*, 2017. **12**(4): p. 481.
 68. Moore, I.S., K.J. Ashford, C. Cross, et al., *Humans Optimize Ground Contact Time and Leg Stiffness to Minimize the Metabolic Cost of Running.* *Frontiers in Sports and Active Living*, 2019. **1**(53).
 69. Moore, I.S., A.M. Jones, and S.J. Dixon, *Mechanisms for improved running economy in beginner runners.* *Medicine and Science in Sports and Exercise*, 2012. **44**(9): p. 1756-63.
 70. Coleman, D.R., D. Cannavan, S. Horne, et al., *Leg stiffness in human running: Comparison of estimates derived from previously published models to direct kinematic-kinetic measures.* *Journal of Biomechanics*, 2012. **45**(11): p. 1987-1991.
 71. Hayes, P. and N. Caplan, *Foot strike patterns and ground contact times during high-calibre middle-distance races.* *Journal of Sports Science*, 2012. **30**(12): p. 1275-83.

-
72. Beck, O.N., J. Gosyne, J.R. Franz, et al., *Cyclically producing the same average muscle-tendon force with a smaller duty increases metabolic rate*. Proceedings of the Royal Society B: Biological Sciences, 2020. **287**(1933): p. 20200431.
 73. Dorn, T.W., A.G. Schache, and M.G. Pandy, *Muscular strategy shift in human running: dependence of running speed on hip and ankle muscle performance*. Journal of Experimental Biology, 2012. **215**(11): p. 1944-1956.
 74. Salo, A.I.T., I.N. Bezodis, A.M. Batterham, et al., *Elite Sprinting: Are Athletes Individually Step-Frequency or Step-Length Reliant?* Medicine & Science in Sports & Exercise, 2011. **43**(6): p. 1055-62.
 75. Hunter, J.P., R.N. Marshall, and P.J. McNair, *Interaction of step length and step rate during sprint running*. Medicine and Science in Sports and Exercise, 2004. **36**(2): p. 261-71.
 76. Ogueta-Alday, A.N.A., J.A. Rodriguez-Marroyo, and J. Garcia-Lopez, *Rearfoot striking runners are more economical than midfoot strikers*. Medicine & Science in Sports & Exercise, 2014. **46**(3): p. 580-5.
 77. da Rosa, R.G., H.B. Oliveira, N.A. Gomeñuka, et al., *Landing-Takeoff Asymmetries Applied to Running Mechanics: A New Perspective for Performance*. Frontiers in Physiology, 2019. **10**(415).
 78. Pataky, T.C., *One-dimensional statistical parametric mapping in Python*. Computer Methods in Biomechanics and Biomedical Engineering, 2012. **15**(3): p. 295-301.
 79. Sadeghi, H., P.A. Mathieu, S. Sadeghi, et al., *Continuous curve registration as an intertrial gait variability reduction technique*. IEEE Transactions on Neural Systems and Rehabilitation Engineering, 2003. **11**(1): p. 24-30.
 80. Cavanagh, P.R. and M.A. LaFortune, *Ground reaction forces in distance running*. Journal of Biomechanics, 1980. **13**(5): p. 397-406.
 81. Friston, K.J., J.T. Ashburner, S.J. Kiebel, et al., *Statistical parametric mapping: the analysis of functional brain images*. 2007, Amsterdam: Elsevier Academic Press.
 82. Pataky, T.C., *Generalized n-dimensional biomechanical field analysis using statistical parametric mapping*. Journal of biomechanics, 2010. **43**(10): p. 1976-82.
 83. Bonnaerens, S., P. Fiers, S. Galle, et al., *Relationship between duty factor and external forces in slow recreational runners*. BMJ Open Sport & Exercise Medicine, 2021. **7**(1): p. e000996.
 84. Hobara, H., H. Sakata, Y. Namiki, et al., *Effect of step frequency on leg stiffness during running in unilateral transfemoral amputees*. Scientific Reports, 2020. **10**(1): p. 5965.
 85. Morin, J.B., P. Samozino, K. Zameziati, et al., *Effects of altered stride frequency and contact time on leg-spring behavior in human running*. Journal of Biomechanics, 2007. **40**(15): p. 3341-3348.

-
86. Zeni, J.A., J.G. Richards, and J.S. Higginson, *Two simple methods for determining gait events during treadmill and overground walking using kinematic data*. *Gait & Posture*, 2008. **27**(4): p. 710-714.
 87. Alton, F., L. Baldey, S. Caplan, et al., *A kinematic comparison of overground and treadmill walking*. *Clinical Biomechanics*, 1998. **13**(6): p. 434-440.
 88. O'Connor, C.M., S.K. Thorpe, M.J. O'Malley, et al., *Automatic detection of gait events using kinematic data*. *Gait & Posture*, 2007. **25**(3): p. 469-74.
 89. Dingwell, J.B., J.P. Cusumano, P.R. Cavanagh, et al., *Local dynamic stability versus kinematic variability of continuous overground and treadmill walking*. *Journal of Biomechanical Engineering*, 2001. **123**(1): p. 27-32.
 90. Fellin, R.E., W.C. Rose, T.D. Royer, et al., *Comparison of methods for kinematic identification of footstrike and toe-off during overground and treadmill running*. *Journal of Science and Medicine in Sport*, 2010. **13**(6): p. 646-650.
 91. Hreljac, A. and N. Stergiou, *Phase determination during normal running using kinematic data*. *Medical and Biological Engineering and Computing*, 2000. **38**(5): p. 503-6.
 92. Leitch, J., J. Stebbins, G. Paolini, et al., *Identifying gait events without a force plate during running: A comparison of methods*. *Gait & Posture*, 2011. **33**(1): p. 130-132.
 93. Smith, L., S. Preece, D. Mason, et al., *A comparison of kinematic algorithms to estimate gait events during overground running*. *Gait & Posture*, 2015. **41**(1): p. 39-43.
 94. De Witt, J.K., *Determination of toe-off event time during treadmill locomotion using kinematic data*. *Journal of Biomechanics*, 2010. **43**(15): p. 3067-3069.
 95. Milner, C.E. and M.R. Paquette, *A kinematic method to detect foot contact during running for all foot strike patterns*. *Journal of Biomechanics*, 2015. **48**(12): p. 3502-5.
 96. Alvim, F., L. Cerqueira, A.D. Netto, et al., *Comparison of Five Kinematic-Based Identification Methods of Foot Contact Events During Treadmill Walking and Running at Different Speeds*. *Journal of Applied Biomechanics*, 2015. **31**(5): p. 383-8.
 97. Edwards, W.B., J.C. Gillette, J.M. Thomas, et al., *Internal femoral forces and moments during running: Implications for stress fracture development*. *Clinical Biomechanics*, 2008. **23**(10): p. 1269-1278.
 98. Scott, S.H. and D.A. Winter, *Internal forces of chronic running injury sites*. *Medicine and Science in Sports and Exercise*, 1990. **22**(3): p. 357-69.
 99. Matijevich, E.S., L.M. Branscombe, L.R. Scott, et al., *Ground reaction force metrics are not strongly correlated with tibial bone load when running across speeds and slopes: Implications for science, sport and wearable tech*. *PLoS One*, 2019. **14**(1): p. e0210000.

100. Lenhart, R.L., D.G. Thelen, C.M. Wille, et al., *Increasing running step rate reduces patellofemoral joint forces*. *Medicine and Science in Sports and Exercise*, 2014. **46**(3): p. 557-64.
101. Sasimontongkul, S., B.K. Bay, and M.J. Pavol, *Bone contact forces on the distal tibia during the stance phase of running*. *Journal of Biomechanics*, 2007. **40**(15): p. 3503-3509.
102. van der Worp, H., J.W. Vrielink, and S.W. Bredeweg, *Do runners who suffer injuries have higher vertical ground reaction forces than those who remain injury-free? A systematic review and meta-analysis*. *British Journal of Sports Medicine*, 2016. **50**(8): p. 450.
103. Day, E.M., R.S. Alcantara, M.A. McGeehan, et al., *Low-pass filter cutoff frequency affects sacral-mounted inertial measurement unit estimations of peak vertical ground reaction force and contact time during treadmill running*. *Journal of Biomechanics*, 2021. **119**: p. 110323.
104. Alcantara, R.S., E.M. Day, M.E. Hahn, et al., *Sacral acceleration can predict whole-body kinetics and stride kinematics across running speeds*. *PeerJ*, 2021. **9**: p. e11199.
105. Ancillao, A., S. Tedesco, J. Barton, et al., *Indirect Measurement of Ground Reaction Forces and Moments by Means of Wearable Inertial Sensors: A Systematic Review*. *Sensors (Basel)*, 2018. **18**(8): p. 2564.
106. LeBlanc, B., E.M. Hernandez, R.S. McGinnis, et al., *Continuous estimation of ground reaction force during long distance running within a fatigue monitoring framework: A Kalman filter-based model-data fusion approach*. *Journal of Biomechanics*, 2021. **115**: p. 110130.
107. Pavei, G., E. Seminati, D. Cazzola, et al., *On the Estimation Accuracy of the 3D Body Center of Mass Trajectory during Human Locomotion: Inverse vs. Forward Dynamics*. *Frontiers in Physiology*, 2017. **8**.
108. Leardini, A., L. Chiari, U. Della Croce, et al., *Human movement analysis using stereophotogrammetry. Part 3. Soft tissue artifact assessment and compensation*. *Gait & Posture*, 2005. **21**(2): p. 212-25.
109. Della Croce, U., A. Leardini, L. Chiari, et al., *Human movement analysis using stereophotogrammetry. Part 4: assessment of anatomical landmark misplacement and its effects on joint kinematics*. *Gait & Posture*, 2005. **21**(2): p. 226-37.
110. Chiari, L., U. Della Croce, A. Leardini, et al., *Human movement analysis using stereophotogrammetry. Part 2: instrumental errors*. *Gait & Posture*, 2005. **21**(2): p. 197-211.
111. Hanavan, E., *A mathematical model of the human body*. AMRL-TR. Aerospace Medical Research Laboratories, 1964. **1**: p. 1-149.
112. Dempster, W.T., *Space requirements of the seated operator: geometrical, kinematic, and mechanical aspects of the body with special reference to the limbs*. 1955, Wright-Patterson Air Force Base, Ohio: Wright Air Development Center.

-
113. Napier, C., X. Jiang, C.L. MacLean, et al., *The use of a single sacral marker method to approximate the centre of mass trajectory during treadmill running*. Journal of Biomechanics, 2020. **108**: p. 109886.
 114. Pavei, G., E. Seminati, J.L.L. Storniolo, et al., *Estimates of Running Ground Reaction Force Parameters from Motion Analysis*. Journal of Applied Biomechanics, 2017. **33**(1): p. 69-75.
 115. Patoz, A., T. Lussiana, B. Breine, et al., *Both a single sacral marker and the whole-body center of mass accurately estimate peak vertical ground reaction force in running*. Gait & Posture, 2021. **89**: p. 186-192.
 116. Verheul, J., W. Gregson, P. Lisboa, et al., *Whole-body biomechanical load in running-based sports: The validity of estimating ground reaction forces from segmental accelerations*. Journal of Science and Medicine in Sport, 2019. **22**(6): p. 716-722.
 117. Flaction, P., J. Quievre, and J.B. Morin, *An Athletic Performance Monitoring Device*. 2013: Washington, DC: U.S. Patent and Trademark Office.
 118. Gindre, C., T. Lussiana, K. Hebert-Losier, et al., *Reliability and validity of the Myotest® for measuring running stride kinematics*. Journal of Sports Sciences, 2016. **34**(7): p. 664-670.
 119. Lee, J.B., R.B. Mellifont, and B.J. Burkett, *The use of a single inertial sensor to identify stride, step, and stance durations of running gait*. Journal of Science and Medicine in Sport, 2010. **13**(2): p. 270-273.
 120. Moe-Nilssen, R., *A new method for evaluating motor control in gait under real-life environmental conditions. Part 1: The instrument*. Clinical Biomechanics, 1998. **13**(4): p. 320-327.
 121. Falbriard, M., F. Meyer, B. Mariani, et al., *Accurate Estimation of Running Temporal Parameters Using Foot-Worn Inertial Sensors*. Frontiers in Physiology, 2018. **9**(610).
 122. Norris, M., R. Anderson, and I.C. Kenny, *Method analysis of accelerometers and gyroscopes in running gait: A systematic review*. Proceedings of the Institution of Mechanical Engineers, Part P: Journal of Sports Engineering and Technology, 2014. **228**(1): p. 3-15.
 123. Falbriard, M., F. Meyer, B. Mariani, et al., *Drift-Free Foot Orientation Estimation in Running Using Wearable IMU*. Frontiers in Bioengineering and Biotechnology, 2020. **8**(65).
 124. Giandolini, M., T. Poupard, P. Gimenez, et al., *A simple field method to identify foot strike pattern during running*. Journal of Biomechanics, 2014. **47**(7): p. 1588-1593.
 125. Giandolini, M., N. Horvais, J. Rossi, et al., *Foot strike pattern differently affects the axial and transverse components of shock acceleration and attenuation in downhill trail running*. Journal of Biomechanics, 2016. **49**(9): p. 1765-1771.

-
126. Chew, D.-K., K.J.-H. Ngoh, D. Gouwanda, et al., *Estimating running spatial and temporal parameters using an inertial sensor*. Sports Engineering, 2018. **21**(2): p. 115-122.
 127. Patoz, A., T. Lussiana, B. Breine, et al., *Estimating effective contact and flight times using a sacral-mounted inertial measurement unit*. Journal of Biomechanics, 2021. **127**: p. 110667.
 128. Dewolf, A.H., T. Lejeune, and P.A. Willems, *The on-off ground asymmetry during running on sand*. Computer Methods in Biomechanics and Biomedical Engineering, 2019. **22**(sup1): p. S291-S293.
 129. Cavagna, G.A., *The two asymmetries of the bouncing step*. European Journal of Applied Physiology, 2009. **107**(6): p. 739.
 130. Mai, P. and S. Willwacher, *Effects of low-pass filter combinations on lower extremity joint moments in distance running*. Journal of Biomechanics, 2019. **95**: p. 109311.
 131. Kiernan, D., R.H. Miller, B.S. Baum, et al., *Amputee locomotion: Frequency content of prosthetic vs. intact limb vertical ground reaction forces during running and the effects of filter cut-off frequency*. Journal of Biomechanics, 2017. **60**: p. 248-252.
 132. Cavagna, G.A., P. Franzetti, N.C. Heglund, et al., *The determinants of the step frequency in running, trotting and hopping in man and other vertebrates*. The Journal of Physiology, 1988. **399**(1): p. 81-92.
 133. Cavagna, G.A., M.A. Legramandi, and L.A. Peyré-Tartaruga, *The landing–take-off asymmetry of human running is enhanced in old age*. Journal of Experimental Biology, 2008. **211**(10): p. 1571.
 134. Kiernan, D., D.A. Hawkins, M.A.C. Manoukian, et al., *Accelerometer-based prediction of running injury in National Collegiate Athletic Association track athletes*. Journal of Biomechanics, 2018. **73**: p. 201-209.
 135. Edwards, W.B., *Modeling Overuse Injuries in Sport as a Mechanical Fatigue Phenomenon*. Exercise and Sport Sciences Reviews, 2018. **46**(4): p. 224-231.
 136. Malisoux, L., P. Gette, N. Delattre, et al., *Spatiotemporal and Ground-Reaction Force Characteristics as Risk Factors for Running-Related Injury: A Secondary Analysis of a Randomized Trial Including 800+ Recreational Runners*. The American Journal of Sports Medicine, 2022. **50**(2): p. 537-544.
 137. Patoz, A., T. Lussiana, B. Breine, et al., *A Single Sacral-Mounted Inertial Measurement Unit to Estimate Peak Vertical Ground Reaction Force, Contact Time, and Flight Time in Running*. Sensors, 2022. **22**(3): p. 784.
 138. Xu, D., W. Quan, H. Zhou, et al., *Explaining the differences of gait patterns between high and low-mileage runners with machine learning*. Scientific Reports, 2022. **12**(1): p. 2981.

-
139. Derie, R., P. Robberechts, P. Van den Berghe, et al., *Tibial Acceleration-Based Prediction of Maximal Vertical Loading Rate During Overground Running: A Machine Learning Approach*. *Frontiers in Bioengineering and Biotechnology*, 2020. **8**.
 140. Matijevich, E.S., L.R. Scott, P. Volgyesi, et al., *Combining wearable sensor signals, machine learning and biomechanics to estimate tibial bone force and damage during running*. *Human Movement Science*, 2020. **74**: p. 102690.
 141. Wouda, F.J., M. Giuberti, G. Bellusci, et al., *Estimation of Vertical Ground Reaction Forces and Sagittal Knee Kinematics During Running Using Three Inertial Sensors*. *Frontiers in Physiology*, 2018. **9**(218).
 142. Halilaj, E., A. Rajagopal, M. Fiterau, et al., *Machine learning in human movement biomechanics: Best practices, common pitfalls, and new opportunities*. *Journal of Biomechanics*, 2018. **81**: p. 1-11.
 143. Backes, A., S.D. Skejød, P. Gette, et al., *Predicting cumulative load during running using field-based measures*. *Scandinavian Journal of Medicine & Science in Sports*, 2020. **30**(12): p. 2399-2407.
 144. Chambers, J., *Chapter 4: linear models.*, in *Statistical models in S*, J. Chambers and T. Hastie, Editors. 1992, Wadsworth & Brooks/Cole.: Pacific Grove, California.
 145. Divert, C., H. Baur, G. Mornieux, et al., *Stiffness adaptations in shod running*. *Journal of Applied Biomechanics*, 2005. **21**(4): p. 311-21.
 146. Arnold, B.J.W., B.K. Weeks, and S.A. Horan, *An examination of treadmill running familiarisation in barefoot and shod conditions in healthy men*. *Journal of Sports Science*, 2019. **37**(1): p. 5-12.
 147. Lindorfer, J., J. Kröll, and H. Schwameder, *Familiarisation of novice and experienced treadmill users during a running session: Group specific evidence, time and individual patterns*. *Human Movement Science*, 2020. **69**: p. 102530.
 148. Riazati, S., N. Caplan, and P.R. Hayes, *The number of strides required for treadmill running gait analysis is unaffected by either speed or run duration*. *Journal of Biomechanics*, 2019. **97**: p. 109366.
 149. Tranberg, R., T. Saari, R. Zügner, et al., *Simultaneous measurements of knee motion using an optical tracking system and radiostereometric analysis (RSA)*. *Acta Orthopaedica*, 2011. **82**(2): p. 171-176.
 150. Hoogkamer, W., S. Kipp, J.H. Frank, et al., *A comparison of the energetic cost of running in marathon racing shoes*. *Sports Medicine*, 2018. **48**(4): p. 1009-1019.
 151. ISO/IEC, *ISO International Standard ISO/IEC 14882:2020(E) Programming languages — C++*. 2020: Geneva, Switzerland: International Organization for Standardization
 152. Lieberman, D.E., A.G. Warrener, J. Wang, et al., *Effects of stride frequency and foot position at landing on braking force, hip torque, impact peak force and the metabolic*

- cost of running in humans*. Journal of Experimental Biology, 2015. **218**(Pt 21): p. 3406-14.
153. Luo, Z., X. Zhang, J. Wang, et al., *Changes in Ground Reaction Forces, Joint Mechanics, and Stiffness during Treadmill Running to Fatigue*. Applied Sciences, 2019. **9**(24): p. 5493.
154. Gill, N., S.J. Preece, and R. Baker, *Using the spring-mass model for running: Force-length curves and foot-strike patterns*. Gait & Posture, 2020. **80**: p. 318-323.
155. Nilsson, J. and A. Thorstensson, *Ground reaction forces at different speeds of human walking and running*. Acta Physiologica Scandinavica, 1989. **136**(2): p. 217-27.
156. Nagahara, R., Y. Takai, H. Kanehisa, et al., *Vertical Impulse as a Determinant of Combination of Step Length and Frequency During Sprinting*. International Journal of Sports Medicine, 2018.
157. Atkinson, G. and A.M. Nevill, *Statistical methods for assessing measurement error (reliability) in variables relevant to sports medicine*. Sports Medicine, 1998. **26**(4): p. 217-38.
158. Bland, J.M. and D.G. Altman, *Comparing methods of measurement: why plotting difference against standard method is misleading*. Lancet, 1995. **346**(8982): p. 1085-7.
159. Cohen, J., *Statistical Power Analysis for the Behavioral Sciences*. 1988: Routledge.
160. Zar, J.H., *Biostatistical Analysis*. 1999: Prentice Hall. 960.
161. McMahon, T.A. and G.C. Cheng, *The mechanics of running: How does stiffness couple with speed?* Journal of Biomechanics, 1990. **23**: p. 65-78.
162. Breine, B., P. Malcolm, I. Van Caekenberghe, et al., *Initial foot contact and related kinematics affect impact loading rate in running*. Journal of Sports Sciences, 2017. **35**(15): p. 1556-1564.
163. Sinclair, J., J. Fau-Goodwin, J. Richards, et al., *The influence of minimalist and maximalist footwear on the kinetics and kinematics of running*. Footwear Science, 2016. **8**(1): p. 33-39.
164. Hébert-Losier, K., S.J. Finlayson, M.W. Driller, et al., *Metabolic and performance responses of male runners wearing 3 types of footwear: Nike Vaporfly 4%, Saucony Endorphin racing flats, and their own shoes*. Journal of Sport and Health Science, 2020.
165. Tam, N., R. Tucker, and J.L. Astephen Wilson, *Individual Responses to a Barefoot Running Program: Insight Into Risk of Injury*. American Journal of Sports Medicine, 2016. **44**(3): p. 777-84.
166. Tung, K.D., J.R. Franz, and R. Kram, *A test of the metabolic cost of cushioning hypothesis during unshod and shod running*. Medicine and Science in Sports and Exercise, 2014. **46**(2): p. 324-9.

167. Hinkle, D.E., W. Wiersma, and S.G. Jurs, *Applied Statistics for the Behavioral Sciences*. 2002, Boston: Houghton Mifflin.
168. van Oeveren, B.T., C.J. de Ruiter, M.J.M. Hoozemans, et al., *Inter-individual differences in stride frequencies during running obtained from wearable data*. *Journal of Sports Sciences*, 2019. **37**(17): p. 1996-2006.
169. Morin, J.-B., G. Dalleau, H. Kyröläinen, et al., *A simple method for measuring stiffness during running*. *Journal of Applied Biomechanics*, 2005. **21**(2): p. 167-180.
170. Willson, J.D., J.S. Bjorhus, D.S. Williams, 3rd, et al., *Short-term changes in running mechanics and foot strike pattern after introduction to minimalistic footwear*. *Physical Medicine & Rehabilitation Journal*, 2014. **6**(1): p. 34-43.
171. Clark, K.P., L.J. Ryan, and P.G. Weyand, *A general relationship links gait mechanics and running ground reaction forces*. *Journal of Experimental Biology*, 2017. **220**(2): p. 247-258.
172. Udofa, A.B., K.P. Clark, L.J. Ryan, et al., *Running ground reaction forces across footwear conditions are predicted from the motion of two body mass components*. *Journal of Applied Physiology (Bethesda, Md.: 1985)*, 2019. **126**(5): p. 1315-1325.
173. Weyand, P.G., D.B. Sternlight, M.J. Bellizzi, et al., *Faster top running speeds are achieved with greater ground forces not more rapid leg movements*. *Journal of Applied Physiology*, 2000. **89**(5): p. 1991-1999.
174. Nordin, A.D., J.S. Dufek, and J.A. Mercer, *Three-dimensional impact kinetics with foot-strike manipulations during running*. *Journal of Sport and Health Science*, 2017. **6**(4): p. 489-497.
175. Schache, A.G., T.W. Dorn, G.P. Williams, et al., *Lower-Limb Muscular Strategies for Increasing Running Speed*. *Journal of Orthopaedic and Sports Physical Therapy*, 2014. **44**(10): p. 813-824.
176. Schepens, B., P.A. Willems, and G.A. Cavagna, *The mechanics of running in children*. *The Journal of physiology*, 1998. **509**(3): p. 927-940.
177. Vogt, M. and H.H. Hoppeler, *Eccentric exercise: mechanisms and effects when used as training regime or training adjunct*. *Journal of Applied Physiology*, 2014. **116**(11): p. 1446-1454.
178. Johnson, W.R., A. Mian, M.A. Robinson, et al., *Multidimensional Ground Reaction Forces and Moments From Wearable Sensor Accelerations via Deep Learning*. *IEEE Transactions on Biomedical Engineering*, 2021. **68**(1): p. 289-297.
179. Pogson, M., J. Verheul, M.A. Robinson, et al., *A neural network method to predict task- and step-specific ground reaction force magnitudes from trunk accelerations during running activities*. *Medical Engineering & Physics*, 2020. **78**: p. 82-89.
180. Charry, E., W. Hu, M. Umer, et al. *Study on estimation of peak Ground Reaction Forces using tibial accelerations in running*. in *2013 IEEE Eighth International Conference on Intelligent Sensors, Sensor Networks and Information Processing*. 2013.

181. Firminger, C.R., G. Vernillo, A. Savoldelli, et al., *Joint kinematics and ground reaction forces in overground versus treadmill graded running*. *Gait & Posture*, 2018. **63**: p. 109-113.
182. García-Pinillos, F., P.Á. Latorre-Román, R. Ramirez-Campillo, et al., *Agreement between spatiotemporal parameters from a photoelectric system with different filter settings and high-speed video analysis during running on a treadmill at comfortable velocity*. *Journal of Biomechanics*, 2019. **93**: p. 213-219.
183. Favre, J., B.M. Jolles, R. Aissaoui, et al., *Ambulatory measurement of 3D knee joint angle*. *Journal of Biomechanics*, 2008. **41**(5): p. 1029-35.
184. Swinnen, W., I. Mylle, W. Hoogkamer, et al., *Changing Stride Frequency Alters Average Joint Power and Power Distributions during Ground Contact and Leg Swing in Running*. *Medicine and Science in Sports and Exercise*, 2021. **53**(10): p. 2111-2118.
185. Willwacher, S., M. Kurz, J. Robbin, et al., *Running-Related Biomechanical Risk Factors for Overuse Injuries in Distance Runners: A Systematic Review Considering Injury Specificity and the Potentials for Future Research*. *Sports Medicine*, 2022. **52**(8): p. 1863-1877.
186. Mo, S., F.O.Y. Lau, A.K.Y. Lok, et al., *Bilateral asymmetry of running gait in competitive, recreational and novice runners at different speeds*. *Human Movement Science*, 2020. **71**: p. 102600.
187. Van Hooren, B., J.T. Fuller, J.D. Buckley, et al., *Is Motorized Treadmill Running Biomechanically Comparable to Overground Running? A Systematic Review and Meta-Analysis of Cross-Over Studies*. *Sports Medicine*, 2020. **50**(4): p. 785-813.
188. Selinger, J.C., J.L. Hicks, R.W. Jackson, et al., *Running in the wild: Energetics explain ecological running speeds*. *Current Biology*, 2022. **32**(10): p. 2309-2315.e3.
189. Bailey, J.P., T. Mata, and J.D. Mercer, *Is the relationship between stride length, frequency, and velocity influenced by running on a treadmill or overground?* *International Journal of Exercise Science*, 2017. **10**(7): p. 1067 - 1075.

8. List of publications

Study 1

Patoz, A., Lussiana, T., Breine, B., Gindre, C., & Malatesta, D. (2022). Duty factor and foot-strike pattern do not represent similar running pattern at the individual level. *Scientific Reports*, 12, 13061. <http://doi.org/10.1038/s41598-022-17274-0>

Patoz A. designed the study, performed the experiment, analyzed the data, interpreted the results, and wrote the manuscript.

Funding: This study was supported by Innosuisse grant no. 35793.1 IP-LS.

Study 2

Patoz, A., Lussiana, T., Breine, B., Gindre, C., Malatesta, D., & Hébert-Losier, K. (2022). Examination of running pattern consistency across speeds. *Sports Biomechanics*, ahead-of-print. <http://doi.org/10.1080/14763141.2022.2094825>

Patoz A. analyzed the data, interpreted the results, and wrote the manuscript.

Funding: This study was financially supported by the University of Bourgogne Franche-Comté (France) and the National Sports Institute of Malaysia.

Study 3

Patoz, A., Lussiana, T., Breine, B., Piguet, E., Gyuriga, J., Gindre, C., & Malatesta, D. (2022). Using statistical parametric mapping to assess the association of duty factor and step frequency on running kinetic. *Frontiers in Physiology*, <http://doi.org/10.3389/fphys.2022.1044363>

Patoz A. designed the study, performed the experiment, analyzed the data, interpreted the results, and wrote the manuscript.

Funding: This study was supported by Innosuisse grant no. 35793.1 IP-LS.

Study 4

Patoz, A., Lussiana, T., Gindre, C., & Malatesta, D. (2021). A novel kinematic detection of foot-strike and toe-off events during non-instrumented treadmill running to estimate contact time. *Journal of Biomechanics*, 128, 110737. <http://doi.org/10.1016/j.jbiomech.2021.110737>

Patoz A. designed the study, performed the experiment, analyzed the data, interpreted the results, and wrote the manuscript.

Funding: This study was supported by Innosuisse grant no. 35793.1 IP-LS.

Study 5

Patoz, A., Lussiana, T., Breine, B., Gindre, C., & Malatesta, D. (2021). Both a single sacral marker and the whole-body center of mass accurately estimate peak vertical ground reaction force in running. *Gait & Posture*, 89, 186-192. <http://doi.org/10.1016/j.gaitpost.2021.07.013>

Patoz A. designed the study, performed the experiment, analyzed the data, interpreted the results, and wrote the manuscript.

Funding: This study was supported by Innosuisse grant no. 35793.1 IP-LS.

Study 6

Patoz, A., Lussiana, T., Breine, B., Gindre, C., & Malatesta, D. (2022) A single sacral-mounted inertial measurement unit to estimate peak vertical ground reaction force, contact time, and flight time in running. *Sensors*, 22, 784. <http://doi.org/10.3390/s22030784>

Patoz A. designed the study, performed the experiment, analyzed the data, interpreted the results, and wrote the manuscript.

Funding: This study was supported by Innosuisse grant no. 35793.1 IP-LS.

Study 7

Patoz, A., Lussiana, T., Breine, B., Gindre, C., & Malatesta, D. (2021). Estimating effective contact and flight times using a sacral-mounted inertial measurement unit. *Journal of Biomechanics*, 127, 110667. <http://doi.org/10.1016/j.jbiomech.2021.110667>

Patoz A. designed the study, performed the experiment, analyzed the data, interpreted the results, and wrote the manuscript.

Funding: This study was supported by Innosuisse grant no. 35793.1 IP-LS.

Study 8

Patoz, A., Lussiana, T., Breine, B., Gindre, C., & Malatesta, D. (2022). Comparison of different machine learning models to enhance sacral acceleration-based estimations of running stride temporal variables and peak vertical ground reaction force. Accepted in *Sports Biomechanics*

Patoz A. designed the study, performed the experiment, analyzed the data, interpreted the results, and wrote the manuscript.

Funding: This study was supported by Innosuisse grant no. 35793.1 IP-LS.

8.1 Duty factor and foot-strike pattern do not represent similar running pattern at the individual level

Aurélien Patoz^{1,2,*}, Thibault Lussiana^{2,3,4}, Bastiaan Breine^{2,5}, Cyrille Gindre^{2,3}, Davide Malatesta¹

¹ Institute of Sport Sciences, University of Lausanne, 1015 Lausanne, Switzerland

² Research and Development Department, Volodalen Swiss Sport Lab, 1860 Aigle, Switzerland

³ Research and Development Department, Volodalen, 39270 Chavéria, France

⁴ Research Unit EA3920 Prognostic Markers and Regulatory Factors of Cardiovascular Diseases and Exercise Performance, Health, Innovation platform, University of Franche-Comté, Besançon, France

⁵ Department of Movement and Sports Sciences, Ghent University, 9000 Ghent, Belgium

* Corresponding author

Published in **Scientific Reports**

DOI: 10.1038/s41598-022-17274-0



OPEN

Duty factor and foot-strike pattern do not represent similar running pattern at the individual level

Aurélien Patoz^{1,2,✉}, Thibault Lussiana^{1,2,3,4}, Bastiaan Breine^{1,2,5}, Cyrille Gindre^{2,3} & Davide Malatesta¹

Runners were classified using their duty factor (DF) and using their foot-strike pattern (FSP; rearfoot, midfoot, or forefoot strikers), determined from their foot-strike angle (FSA). High and low DF runners showed different FSPs but DF was assumed to not only reflect what happens at initial contact with the ground (more global than FSP/FSA). Hence, FSP and DF groups should not necessarily be constituted by the same runners. However, the relation between FSP and DF groups has never been investigated, leading to the aim of this study. One hundred runners ran at 9, 11, and 13 km/h. Force data (1000 Hz) and whole-body kinematics (200 Hz) were acquired by an instrumented treadmill and optoelectronic system and were used to classify runners according to their FSA and DF. Weak correlations were obtained between FSA and DF values and a sensitivity of 50% was reported between FSP and DF groups, i.e., only one in two runners was attributed to the DF group supposedly corresponding to the FSP group. Therefore, 'local' FSP/FSA and DF do not represent similar running pattern information when investigated at the individual level and DF should be preferred to FSP/FSA when evaluating the global running pattern of a runner.

Runners are usually classified into one of three discrete categories depending on their preferred foot-strike pattern (FSP). A runner is categorized as a (1) rearfoot striker (RFS) when the foot initially contacts the ground with the heel or rear third of the sole, (2) a midfoot striker (MFS) when the heel and toes contact the ground simultaneously, or (3) a forefoot striker (FFS) when the foot initially contacts the ground with the forefoot or front half of the sole¹. This classification can be obtained using the foot-strike angle (FSA) following the procedure proposed by Altman and Davis². These FSPs involve different neuromuscular activation patterns³ and impact attenuation strategies⁴⁻⁷. They were also shown to induce different loads on the lower limb and different three-dimensional (3D) stress patterns in the ankle, knee, and hip joints⁸⁻¹¹, as well as different sagittal plane joint angles during stance^{10,12}. Moreover, no differences in running economy have been reported among different FSAs¹³ or FSPs¹⁴⁻¹⁶, and changing FSPs is not necessarily recommended for RFS^{10,15,17,18}.

More recently, runners have been categorized using the duty factor (DF)^{19,20}, i.e., the ratio of ground contact time (t_c) to stride time [t_c + swing time (t_s)], with a higher DF reflecting a greater relative contribution of t_c to the running stride^{21,22}. Considering both t_c and t_s simultaneously provides a better understanding of the global running pattern compared with when these temporal variables are considered separately^{19,20}. The authors observed that the 20 subjects with highest DF values and 20 subjects with lowest DF values (among a cohort of 54 participants) used different running strategies but had a similar running economy, showing that these two strategies are energetically equivalent at endurance running speeds¹⁹. A more symmetrical running pattern between braking and propulsion phases in terms of time and vertical center of mass displacement, anterior FSP (MFS and FFS), and extended lower limb during t_c at the hip, knee, and ankle joints were observed for low than for high DF runners^{19,20}. On the contrary, high DF runners exhibited greater lower limb flexion during t_c at the hip, knee, and ankle joints, more RFS, and less work against gravity to generate forward propulsion than low DF runners^{19,20}. Hence, high and low DF runners reflected different FSPs^{19,20}, most likely because t_c is related to FSP^{1,23}. Nonetheless, DF was thought to not only be directly related to the angle at the initial ground contact (via t_c) as is FSP but to also be functionally representative of a more global running behavior because it takes

¹Institute of Sport Sciences, University of Lausanne, 1015 Lausanne, Switzerland. ²Research and Development Department, Volodalen Swiss Sport Lab, 1860 Aigle, Switzerland. ³Research and Development Department, 39270 Volodalen, Chavéria, France. ⁴Research Unit EA3920 Prognostic Markers and Regulatory Factors of Cardiovascular Diseases and Exercise Performance, Health, Innovation Platform, University of Franche-Comté, Besançon, France. ⁵Department of Movement and Sports Sciences, Ghent University, 9000 Ghent, Belgium. ✉email: aurelien.patoz@unil.ch

both the duration of force production (t_c) and the cycle frequency of running into account^{19,20,24}. For this reason, although FSA and DF values should be different among DF (high, mid, and low DF runners) and FSP (RFS, MFS, FFS) groups, respectively, FSP and DF groups should not necessarily be constituted by the same runners. This would confirm that DF should be preferred to FSP/FSA when evaluating the global running pattern of a runner. Nonetheless, to the best of our knowledge, the relationship between the groups created using FSA and DF values has not yet been considered.

Hence, the purpose of the present study was to compare these two different classification methods in analyzing running gait at several running speeds. We hypothesized that (i) FSP groups should have significantly different DF values; (ii) DF groups should have significantly different FSA values; and (iii) FSP and DF groups should not be constituted by the same runners because of weak correlations between FSA and DF values and, thus, leading to weak agreement in the classification of runners between FSP and DF groups.

Materials and methods

Participants. One hundred recreational runners, 75 males (age: 31 ± 8 years, height: 180 ± 6 cm, body mass: 70 ± 7 kg, weekly running sessions: 3 ± 2 , and weekly running distance: 37 ± 24 km) and 25 females (age: 30 ± 7 years, height: 169 ± 5 cm, body mass: 61 ± 6 kg, weekly running sessions: 3 ± 1 , and weekly running distance: 20 ± 14 km), were randomly selected from an existing database consisting of 115 participants²⁵ for the purpose of this study. Participants voluntarily participated in the present study, and to be included, they were required to be in good self-reported general health with no current or recent lower-extremity injuries (≤ 1 month), to run at least once a week, and to have an estimated maximal aerobic speed ≥ 14 km/h. The study protocol was approved by the ethics committee of the Vaud canton (commission cantonale d'éthique de la recherche sur l'être humain CER-VD 2020-00334) and adhered to the latest version of the Declaration of Helsinki of the World Medical Association.

Experimental procedure. After the participants provided written informed consent, retroreflective markers were positioned on the participants (described in Subsec. Data Collection) to record their running biomechanics. For each participant, a 5-s static trial was first recording while he or she stood in a standard anatomical position on an instrumented treadmill (Arsalis T150 – FMT-MED, Louvain-la-Neuve, Belgium) for calibration purposes. Then, a 7-min warm-up run was performed on the same treadmill. The speed was set to 9 km/h for the first 3 min and was then increased by 0.5 km/h every 30 s. Then, after a short break (< 5 min), three 1-min runs (9, 11, 13 km/h) were performed in a randomized order (1-min recovery between each run where runners just stand). 3D kinematic and kinetic data were collected during the static trial and the first 10 strides following the 30-s mark of the running trials. All participants were familiar with running on a treadmill, as it was part of their usual training program, and they wore their habitual running shoes during testing (shoe mass: 257 ± 49 g and shoe heel-to-toe drop: 7 ± 3 mm).

Data collection. Whole-body 3D kinematic data were collected at 200 Hz using motion capture (8 cameras) and Vicon Nexus software v2.9.3 (Vicon, Oxford, UK). The laboratory coordinate system was oriented such that the x -, y -, and z -axes denoted the mediolateral (pointing towards the right side of the body), posterior-anterior, and inferior-superior axes, respectively. Forty-three and 39 retroreflective markers of 12.5 mm diameter were used for the static and running trials, respectively. They were affixed to the skin and shoes of the individuals on anatomical landmarks using double-sided tape following standard guidelines²⁶. Synchronized kinetic data (1000 Hz) were also collected using the force plate embedded into the treadmill.

The 3D marker and ground reaction force data (analog signal) were exported in the .c3d format and processed in Visual3D Professional software v6.01.12 (C-Motion Inc., Germantown, MD, USA). The 3D marker data were interpolated using a third-order polynomial least-square fit algorithm (using three frames of data before and after the “gap” to calculate the coefficients of the polynomial), allowing a maximum of 20 frames for gap filling, and were subsequently low-pass filtered at 20 Hz using a fourth-order Butterworth filter. The 3D ground reaction force signal was filtered using the same filter²⁷ and down sampled to 200 Hz to match the sampling frequency of the marker data.

Data analysis. For each running trial, the foot-strike (FS) and toe-off (TO) events were identified with Visual3D. These events were detected by applying a 20 N threshold to the z -component of the ground reaction force²⁸. More explicitly, FS was detected as the first data point greater than or equal to 20 N within a running step, while TO was detected at the last data point greater than or equal to 20 N within the same running step. t_c and t_s were defined as the times from FS to TO and from TO to FS of the same foot, respectively. DF was calculated as follows²¹:

$$DF = \frac{t_c}{t_c + t_s} = t_c SF, \quad (1)$$

where SF denotes the stride frequency. In addition, a full-body biomechanical model with six degrees of freedom and 15 rigid segments was constructed from the marker set. The segments included the head, upper arms, lower arms, hands, thorax, pelvis, thighs, shanks, and feet. In Visual3D, the segments were treated as geometric objects, assigned inertial properties and center of mass locations based on their shape²⁹, and attributed relative masses based on standard regression equations³⁰. The foot segment angle was defined as the angle of the foot segment relative to the laboratory coordinate system and computed using an x - y - z Cardan sequence. The foot segment was obtained using five markers which were placed at the apex of both the lateral and medial malleolus, foot

calcaneus (aspect of the Achilles tendon insertion), and head of the first and fifth metatarsals. The x -component of the foot segment angle at FS was used to determine FSP following the procedure proposed by Altman and Davis². In brief, the average foot segment angle of the standing static trial was subtracted from that of running trials such that 0° corresponded to a foot parallel to the ground. Then, the angle at FS, i.e., FSA, was computed using the x -component of the rescaled foot segment angle (negative and positive angle values represented plantar flexion and dorsiflexion, respectively).

For all biomechanical measures, the values extracted from the 10 strides for each participant were averaged for subsequent analyses. Data analysis was performed using Python (v3.7.4, available at <http://www.python.org>).

Runners' classification. High (DF_{high}), mid (DF_{mid}), and low (DF_{low}) DF groups were created using the terciles of the group (i.e., the 33 highest, 33 middle, and 34 lowest DF values at each speed). Of note, DF_{low} group was composed of one extra runner but attributing this extra runner to DF_{mid} or DF_{high} group or removing their data from the study would not have had an impact on the results. In addition, runners were classified as RFS, MFS, and FFS if FSA values were $\geq 8^\circ$, $< 8^\circ$ but $\geq -1.6^\circ$, and $< -1.6^\circ$, respectively, at each speed². A similar analysis was also performed using FSP groups created based on an absolute classification of runners, i.e., RFS, MFS, and FFS being represented by the 33 highest, 33 middle, and 34 lowest FSA values at each speed, and is presented in section S1 of supplementary materials. The relative² and absolute classifications to create FSP groups led to similar results because both classifications classified most of the runners in the same group. Indeed, on average, 1 participant (4%) was attributed to a different FSP group when using the absolute rather than the relative classification.

Statistical analysis. All data are presented as the mean \pm standard deviation. A chi-squared test was used to compare the foot-strike distribution at the different speeds.

Then, after the residual plots were inspected, and no obvious deviations from homoscedasticity or normality were observed, a linear mixed model fitted by restricted maximum likelihood was used to compare DF values for the different FSP groups and speeds. The within-subject nature was controlled for by including random effects for participants. Pairwise post hoc comparisons were performed using Holm corrections. The differences between groups were quantified using Cohen's d effect size³¹. The effect sizes were interpreted as very small, small, moderate, or large when $|d|$ values were close to 0.01, 0.2, 0.5, or 0.8, respectively³¹.

A similar linear mixed model was used to compare FSA values for the different DF groups and speeds. Linear mixed models were also used to compare DF and FSA values among DF and FSP groups (considering all groups together) and speeds. These tests were used to investigate the difference in DF and FSA values between the three group pairs (RFS and DF_{high} , MFS and DF_{mid} , FFS and DF_{low}). Therefore, only the group \times running speed interaction effect was investigated, and, if significant, the pairwise comparisons between these three group pairs at each running speed were reported.

Agreement between FSP and DF groups as well as sensitivity and specificity of the agreement were calculated for the three speeds³². As participants were classified in three FSP and DF groups, agreement, sensitivity, and specificity were obtained for each of the three group pairs by collapsing to three 2×2 classifications, i.e., RFS and DF_{high} vs non-RFS and non- DF_{high} , MFS and DF_{mid} vs non-MFS and non- DF_{mid} , and FFS and DF_{low} vs non-FFS and non- DF_{low} . Agreement was defined as the sum of the number of runners in a DF group that were attributed to the corresponding FSP group and the number of runners in the corresponding non-DF group that were attributed to the non-FSP group over the total number of runners, e.g., the sum of DF_{high} runners in RFS and non- DF_{high} runners in non-RFS over all runners. Sensitivity was defined as the number of runners in a DF group that were attributed to the corresponding FSP group over the total number of runners in the corresponding FSP group, e.g., DF_{high} runners among RFS. Specificity was defined as the number of runners in a non-DF group that were attributed to the corresponding non-FSP group over the total number of runners in the corresponding non-FSP group, e.g., non- DF_{high} runners among non-RFS. The 95% confidence intervals (lower, upper) of the agreement between FSP and DF groups and of the sensitivity and specificity values, were estimated using binomial exact calculation.

The Pearson's correlation coefficient (r) and its corresponding 95% confidence interval (lower, upper) and P -values were computed for the relation between FSA and DF, as well as t_c and SR, i.e., the variables constituting DF, for the three speeds. In addition, correlations among shoe mass, shoe heel-to-toe drop, DF, and FSA were computed to investigate if footwear could affect DF and FSA. Very high, high, moderate, low, and negligible correlations were given by $|r|$ values of 0.90–1.00, 0.70–0.90, 0.50–0.70, 0.30–0.50, and 0.00–0.30, respectively³³.

Statistical analysis was performed using Jamovi (v1.2, retrieved from <https://www.jamovi.org>) with a level of significance set at $P \leq 0.05$.

Results

Distribution of runners within foot-strike pattern groups. The number of RFS, MFS, and FFS together with their corresponding FSAs at all speeds examined are given in Table 1. The chi-squared test showed no differences in the foot-strike distribution at the different speeds employed ($\chi^2 = 4.6$, $P = 0.34$), revealing homogeneity among groups at all speeds. On average, 2 participants per group (7%) changed their FSP group with running speed while 4 participants per group (12%) changed their DF group. The complete analysis is provided in section S2 of supplementary materials.

Duty factor values within foot-strike pattern groups. The linear mixed model revealed a significant FSP group effect on DF ($P < 0.001$). The Holm post hoc tests indicated a significantly higher DF for RFS than for MFS and FFS ($P \leq 0.005$), and for MFS than for FFS ($P = 0.001$). A significant effect of speed was reported

Running speed (km/h)	RFS		MFS		FFS	
	Count	Angle (°)	Count	Angle (°)	Count	Angle (°)
9	27	13.3 ± 2.9	34	4.3 ± 4.2	39	-6.7 ± 4.7
11	31	13.2 ± 2.8	33	3.4 ± 2.7	36	-7.7 ± 3.3
13	38	11.7 ± 4.1	23	1.4 ± 4.1	39	-5.9 ± 5.6

Table 1. Number of rearfoot (RFS), midfoot (MFS), and forefoot (FFS) strikers observed in the cohort of participants ($N=100$) and their corresponding foot-strike angles at three running speeds. The values are presented as the mean ± standard deviation.

Running speed (km/h)		DF _{high}	DF _{mid}	DF _{low}
9	RFS	15	8	4
	MFS	11	12	11
	FFS	7	13	19
	Agreement (%)	70 (61, 79)	76 (68, 84)	65 (56, 74)
	Sensitivity (%)	56 (37, 74)	35 (19, 51)	49 (33, 64)
	Specificity (%)	75 (65, 85)	68 (57, 79)	75 (65, 86)
11	RFS	18	8	5
	MFS	9	14	10
	FFS	6	11	19
	Agreement (%)	72 (63, 81)	81 (73, 89)	68 (59, 77)
	Sensitivity (%)	58 (41, 75)	42 (26, 59)	53 (36, 69)
	Specificity (%)	78 (69, 88)	72 (61, 82)	77 (66, 87)
13	RFS	21	9	8
	MFS	5	11	7
	FFS	7	13	19
	Agreement (%)	71 (62, 80)	85 (78, 92)	65 (56, 74)
	Sensitivity (%)	55 (39, 71)	48 (27, 68)	49 (33, 64)
	Specificity (%)	81 (71, 90)	71 (61, 82)	75 (65, 86)

Table 2. Number of runners in foot-strike pattern (FSP) [rearfoot (RFS), midfoot (MFS), and forefoot (FFS) strikers] and duty factor (DF) [high (DF_{high}), mid (DF_{mid}), and low (DF_{low}) DF runners] groups, as well as the agreement, sensitivity, and specificity between FSP and DF groups together with their 95% confidence intervals in parentheses (lower, upper) at three running speeds.

on DF ($P < 0.001$). A significantly smaller DF was obtained at a faster speed, as depicted by the Holm post hoc tests ($P < 0.001$). There was no FSP group x speed interaction ($P < 0.66$). The Cohen's d effect sizes were moderate ($|d| \leq 0.66$), except for those corresponding to the RFS-FFS pairs, which were large at all speeds ($|d| \geq 0.96$).

Foot-strike angle values within duty factor groups. The DF ranges for DF_{low}, DF_{mid}, and DF_{high} groups were [31.6%, 36.3%], [36.4%, 38.4%], and [38.6%, 45.3%] at 9 km/h, [28.5%, 33.4%], [33.4%, 35.7%], and [35.8%, 40.2%] at 11 km/h, and [27.0%, 31.4%], [31.5%, 33.5%], and [33.5%, 37.6%] at 13 km/h, respectively. The linear mixed model revealed a significant DF group effect on FSA ($P < 0.001$). The Holm post hoc tests indicated a significantly higher FSA for DF_{high} than for DF_{mid} and DF_{low} ($P < 0.001$), and for DF_{mid} than for DF_{low} ($P = 0.005$). A significant effect of speed was reported on FSA ($P < 0.001$). A significantly higher FSA was obtained at a faster speed, as reported by the Holm post hoc tests ($P \leq 0.01$). There was no DF group x speed interaction ($P < 0.42$). The Cohen's d effect sizes were moderate ($|d| \leq 0.68$), except for those corresponding to the DF_{high}-DF_{low} pairs, which were large at all speeds ($|d| \geq 0.86$).

Duty factor and foot-strike angle values within all (duty factor and foot-strike pattern) groups together. When considering all groups together, a significant group x running speed interaction effect was reported by the linear mixed models for both DF and FSA values ($P \leq 0.013$). Pairwise post hoc comparisons between the three group pairs (RFS and DF_{high}, MFS and DF_{mid}, FFS and DF_{low}) at each running speed revealed no significant differences for DF and FSA values ($P \geq 0.16$).

Agreement between foot-strike pattern and duty factor groups. The number of runners in FSP and DF groups as well as the agreement, sensitivity, and specificity between FSP and DF groups are given in Table 2. The average (over speed and group) agreement, sensitivity, and specificity were 73, 49, and 75%, respectively.

	Running Speed (km/h)	<i>r</i>	<i>P</i>
DF	9	0.39 (0.21, 0.55)	<0.001
	11	0.42 (0.24, 0.57)	<0.001
	13	0.48 (0.31, 0.62)	<0.001
<i>t_c</i>	9	0.43 (0.26, 0.58)	<0.001
	11	0.47 (0.30, 0.61)	<0.001
	13	0.50 (0.34, 0.63)	<0.001
SF	9	-0.13 (-0.32, 0.06)	0.18
	11	-0.14 (-0.28, 0.11)	0.36
	13	-0.11 (-0.30, 0.09)	0.29

Table 3. Pearson's correlation coefficients (*r*) and the corresponding 95% confidence intervals (lower, upper) and *P*-values for the relationships between the foot-strike angle and duty factor (DF), contact time (*t_c*), and stride frequency (SF) for three tested speeds. The statistically significant correlations ($P \leq 0.05$) are indicated in bold font.

Variables	Running speed (km/h)	Shoe mass		Shoe heel-to-toe drop	
		<i>r</i>	<i>P</i>	<i>R</i>	<i>P</i>
DF	9	0.13 (-0.07, 0.32)	0.21	0.14 (-0.06, 0.33)	0.16
	11	0.13 (-0.07, 0.32)	0.2	0.14 (-0.06, 0.33)	0.16
	13	0.20 (0.01, 0.38)	0.04	0.11 (-0.09, 0.30)	0.26
FSA	9	0.18 (-0.02, 0.36)	0.08	0.21 (0.01, 0.39)	0.04
	11	0.15 (-0.05, 0.34)	0.14	0.16 (-0.03, 0.35)	0.1
	13	0.18 (-0.02, 0.36)	0.08	0.16 (-0.04, 0.34)	0.12

Table 4. Pearson's correlation coefficients (*r*) and the corresponding 95% confidence intervals (lower, upper) and *P*-values for the relationships among shoe mass, shoe heel-to-toe drop, foot-strike angle (FSA), and duty factor (DF) for three tested speeds. The statistically significant correlations ($P \leq 0.05$) are indicated in bold font.

The DF and FSA values of runners attributed to a DF group but not being classified in the supposedly corresponding FSP group, for instance DF_{high} runners but classified as MFS and FFS, are given in Fig. 2A. Similarly, Fig. 2B depicts FSA and DF values of runners attributed to a FSP group but not being classified in the supposedly corresponding DF group, for instance RFS but classified as DF_{mid} or DF_{low}.

Relationships between foot-strike angle and duty factor, contact time, and stride frequency. The correlations between FSA and DF, *t_c*, and SF, together with their 95% confidence intervals, are given in Table 3. For DF and *t_c*, the correlation was weak (low) but statistically significant ($r \leq 0.50$; $P < 0.001$) for all speeds, while the correlation between DF and SF was negligible and not statistically significant ($|r| \leq 0.14$; $P \geq 0.18$).

Relationships between shoe mass, shoe heel-to-toe drop, foot-strike angle, and duty factor. The correlation between shoe mass and shoe heel-to-toe drop was low but significant [$r = 0.52$ (0.37, 0.65); $P < 0.001$]. However, the correlations between shoe mass and DF, shoe heel-to-toe drop and DF, shoe mass and FSA, and shoe heel-to-toe drop and FSA were negligible and not statistically significant ($|r| \leq 0.18$; $P \geq 0.08$; Table 4) except between DF and shoe mass at 13 km/h ($r = 0.20$; $P = 0.04$) and between FSA and shoe heel-to-toe drop at 9 km/h ($r = 0.21$; $P = 0.04$) which were significant.

Discussion

The purpose of the present study was to compare two different classification methods (either based on DF or FSA) in analyzing running gait at several running speeds. In the present study, a significantly higher DF was obtained for RFS than for MFS and FFS and for MFS than for FFS, supporting our first hypothesis. Moreover, a significantly higher FSA was reported for DF_{high} than for DF_{mid} and DF_{low} and for DF_{mid} than for DF_{low}, supporting our second hypothesis. Furthermore, the three group pairs (RFS and DF_{high}, MFS and DF_{mid}, FFS and DF_{low}) did not report any significant difference in DF and FSA values at each tested speed. However, although weak correlations were obtained between FSA and DF values, the agreement between FSP and DF groups was 73%, which did not fully support our third hypotheses. Nonetheless, the sensitivity between FSP and DF groups was 50%, meaning that only one in two runners was attributed to the DF group supposedly corresponding to the FSP group. Therefore, although DF and FSA values were not statistically different between each of the three group pairs (at a group level), the runners constituting these groups were not the same in 50% of the cases and DF should be preferred to FSP/FSA when evaluating the global running pattern of a runner.

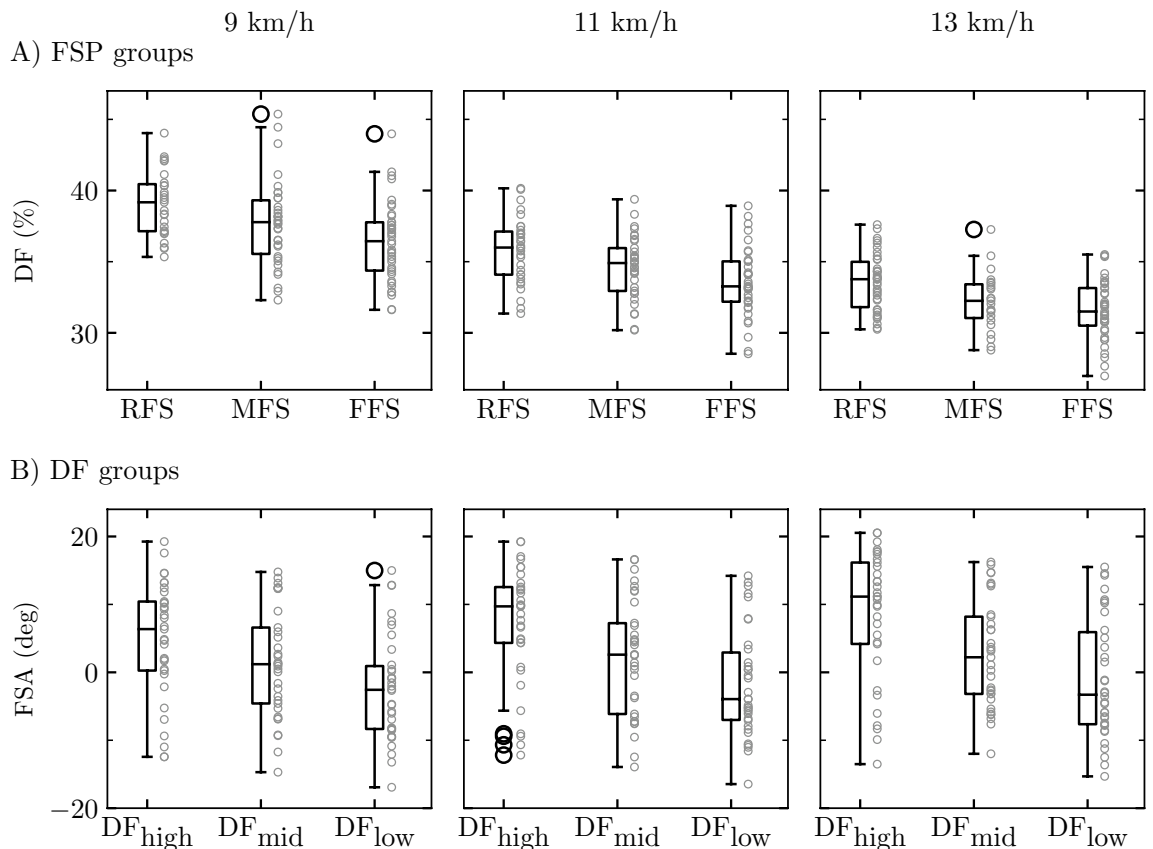


Figure 1. Boxplots of (A) the duty factor (DF) for the different foot-strike pattern (FSP) groups, i.e., rearfoot (RFS), midfoot (MFS), and forefoot (FFS) strikers, and (B) the foot-strike angle (FSA) for the different DF groups, i.e., high (DF_{high}), mid (DF_{mid}), and low (DF_{low}) DF runners, at 9, 11, and 13 km/h. The box extends from the lower to upper quartile values of the data, with a line at the median. The whiskers extend from the box to show the range of the data while flier points (black empty circles) are those past the end of the whiskers. The upper whisker extends to the last data less than $Q3 + 1.5(Q3 - Q1)$, where $Q1$ and $Q3$ are the first and third quartile. Similarly, the lower whisker extends to the first data greater than $Q1 - 1.5(Q3 - Q1)$. The small gray empty circles denote the data of each participant.

Homogeneous foot-strike pattern distribution. The groups created based on FSP were homogeneous at all speeds, although FSP was not a criterion for recruiting participants. Larson, et al.³⁴ reported that ~90% of recreational runners in a road race were RFS, which makes the FSP distribution of ~33% observed for each group surprising and unexpected (Table 1). One possible explanation is that the participants of this study followed the popular advice given by coaches over the past decade promoting a more mid- to forefoot pattern than a rearfoot strike pattern^{35–37}. Although recent reviews^{15,18} concluded that there is no scientific foundation to recommend non-injured rearfoot strikers to change their RFS. Another explanation is the young age of the participants of this study (30 ± 7 years). In fact, older people were shown to run with a more rearfoot strike pattern than younger people^{38,39}. Finally, though shoe mass and shoe heel-to-toe drop were not associated to DF and FSA (Table 4), other footwear characteristics not assessed as part of this study could impact DF or FSA values, such as midsole cushioning and/or the longitudinal bending stiffness⁴⁰. Nevertheless, the homogeneity of the FSP groups made the results of this study more robust when comparing FSP groups due to similar group sizes.

Duty factor and foot-strike pattern differ at the individual level. DF was significantly lower for FFS than for RFS and MFS and for MFS than for RFS, with a moderate to large effect size (Fig. 1). These results confirm previous observations that there should be a trend towards a more forefoot strike pattern with a decreasing DF value^{19,20}. Similarly, FSA was significantly lower for DF_{low} than for DF_{high} and DF_{mid} and for DF_{mid} than for DF_{high}, with also a moderate to large effect size (Fig. 1). Moreover, no significant difference was revealed between the three group pairs at each tested speed. However, the sensitivity between DF and FSP groups was 50%, reflecting that only one in two runners in a DF group (50%) were classified in the supposedly corresponding FSP group, although there was a slightly greater chance of matching among RFS (56%) and FFS (50%) than among MFS (42%).

This might be explained by the fact that the DF range corresponding to DF_{mid} runners and FSA range corresponding to MFS are smaller than the DF ranges corresponding to DF_{high} and DF_{low} runners and FSA ranges corresponding to RFS and FFS. Besides, the DF values of runners attributed to a DF group but not being classified in the supposedly corresponding FSP group mostly span the entire range of DF values of this DF group (Fig. 2A).

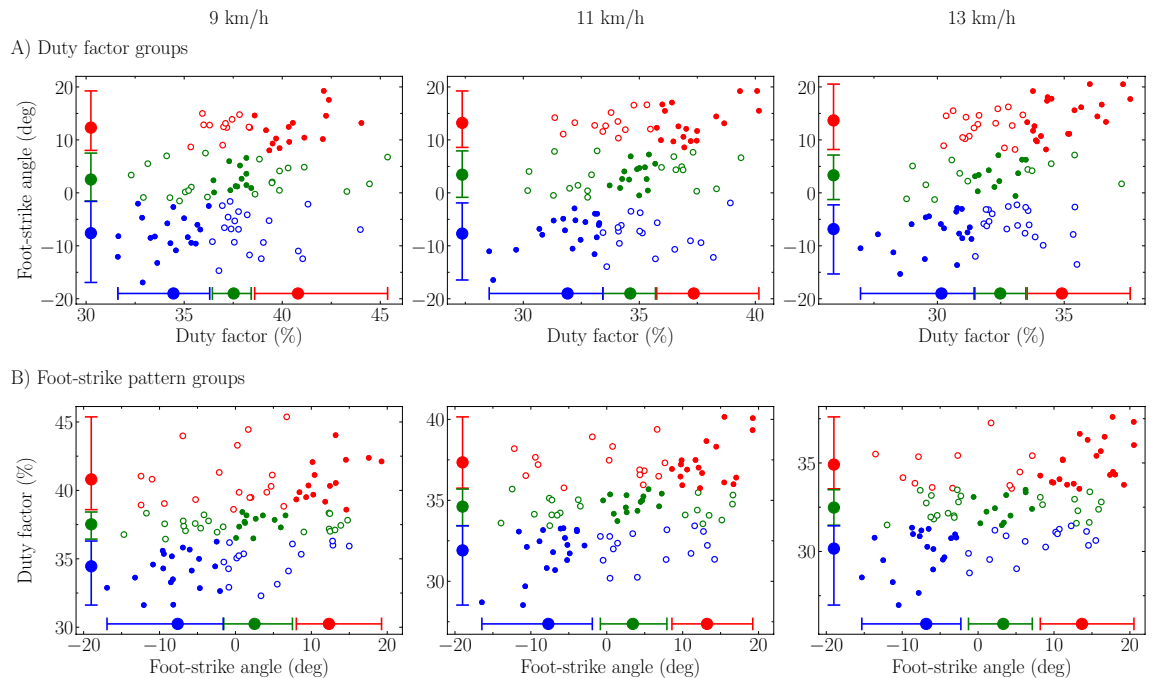


Figure 2. Duty factor (DF) and foot-strike angle (FSA) values of runners attributed to (A) a DF group but not being classified in the supposedly corresponding foot-strike pattern (FSP) group and (B) a FSP group but not being classified in the supposedly corresponding DF group at each tested running speed. Mean DF and FSA value (filled circle) and range of values (whiskers) for each DF and FSP group, i.e., high DF runners and rearfoot strikers (RFS; red), mid DF runners and midfoot strikers (MFS; green), and low DF runners and forefoot strikers (FFS; blue). The upper whisker extends to the maximum while the lower whisker extends to the minimum value. Empty circles denote the runners attributed to a DF or FSP group but not being classified in the supposedly corresponding FSP or DF group, respectively, e.g., high DF runners but classified as MFS or FFS (green and blue empty circles within the red whiskers of the high DF runners) in (A) and RFS but classified as mid or low DF runners (green and blue empty circles within the red whiskers of RFS) in (B).

A similar observation is made for FSA values of runners attributed to a FSP group but not being classified in the supposedly corresponding DF group (Fig. 2B). Thereby, these results suggest that 'local' FSP/FSA and DF do not represent similar running pattern information when investigated at the individual level.

Weak association between duty factor and foot-strike angle. Weak but significant correlations were observed between DF and FSA at all speeds ($r \leq 0.48$ and $P < 0.001$; Table 3). Nonetheless, FSA was only able to explain ~20% of the variance of DF. The angle of the lower limb at initial ground contact relative to the vertical axis⁴¹ can be estimated using t_c and therefore DF (indirectly). In addition, according to the observations of Breine et al.⁴² which showed that RFS have a less vertical leg at the point of contact than do runners landing further forward on their foot (MFS and FFS), FSP is indirectly related to the lower limb angle at initial contact. As RFS position their foot to be much more forward than their pelvis to strike the ground with their heel, these runners have a higher lower limb angle at initial contact than do FFS. Therefore, the lower limb angle at initial contact may be indirectly related to FSA. Hence, there is an indirect relationship between FSA and DF which is supported by the indirect relationship between the lower limb angle at initial contact and both DF and FSA. Besides, the 50% sensitivity reported between FSP and DF groups can be partly explained by the weak correlations between DF and FSA, which also corroborate that FSP represents only a portion of DF. Indeed, DF is computed from t_c and SF (Eq. 1), which makes it to be functionally representative of a more global biomechanical behavior^{19,20,24}. For instance, DF has been shown to represent the trade-off between muscle contractile mechanics and energetics in running as a valid estimate of the muscle force-length-velocity related to mechanical work, total active muscle volume, and energy expenditure in running²⁴.

Correlation coefficients between DF and FSA increased with increasing running speed (+20% from 9 to 13 km/h; Table 3), depicting that FSA was more strongly correlated with DF with increasing speed. These results suggest that FSA and DF should be more similar at faster speeds. This might partly be attributed to the smaller ranges of DF and FSA values with increasing speed. Nonetheless, the present study did not report an increase in sensitivity with increasing speed except for DF_{mid} runners (Table 2). The increase in sensitivity for DF_{mid} runners could partly be explained by the fact the DF range of DF_{mid} runners relatively increased compared to the DF ranges of DF_{high} and DF_{low} runners with increasing speed. Nevertheless, the relation between FSP and DF groups as well as FSA and DF values at faster running speeds should further be investigated.

The correlations between t_c and FSA were weak but statistically significant and slightly stronger than those between DF and FSA (+4%; Table 3). Nonetheless, FSA was only able to explain up to 25% of the variance of t_c ,

confirming that t_c (as DF) does not only represent what happens at initial contact with the ground as does FSP. The weaker correlation between DF and FSA than that between t_c and FSA can be explained by the negligible correlations between SF and FSA ($|r| \leq 0.14$; Table 3) coupled to the fact that DF is given by the product between t_c and SF (Eq. 1).

Limitations. A few limitations of the present study exist. An unexpected high proportion of runners were classified as FFS, indicating that the study population may not be representative of the general population. The speeds were limited to endurance speeds, and running trials were only performed on a treadmill. Furthermore, participants wore their own running shoes during testing, which could be confounding our results. Given that differences in footwear characteristics can underpin differences in running biomechanics⁴³, using a standardized shoe might have led to different study outcomes in terms of FSA and DF. Noteworthy, however, is that there were no significant correlations between shoe mass and DF and FSA and between shoe heel-to-toe drop and DF and FSA. Recreational runners are more comfortable wearing their own shoes⁴⁴, and show individual responses to novel footwear^{44,45} and cushioning properties⁴⁶. Nevertheless, it is possible that other footwear characteristics not assessed as part of this study correlate to DF or FSA, such as midsole cushioning and/or the longitudinal bending stiffness⁴⁰. Moreover, very few studies on DF exist. Therefore, it is difficult to determine how DF may be affected by confounding variables such as footwear or the running surface. Therefore, future studies should focus on the relation between DF and FSP under additional conditions (i.e., faster speeds, different types of ground, and different shoes). Nonetheless, the presented results are strong due to the use of a large dataset.

Conclusion

This study revealed that RFS depict higher DF than MFS and FFS and similarly for MFS than FFS. Moreover, DF_{high} showed higher FSA than DF_{mid} and DF_{low} and similarly for DF_{mid} than DF_{low}. However, weak correlations were obtained between FSA and DF values as well as a sensitivity of 50% between FSP and DF groups, meaning that only one in two runners was attributed to the DF group supposedly corresponding to the FSP group. Therefore, though DF and FSA values were not statistically different between each of the three group pairs (at a group level), these results suggest that the runners constituting these groups were not the same. In other words, 'local' FSP/FSA and DF do not represent similar running pattern information when investigated at an individual level and DF should be preferred to FSP/FSA when evaluating the global running pattern of a runner.

Data availability

The datasets supporting this article are available upon request by the corresponding author.

Received: 2 September 2021; Accepted: 22 July 2022

Published online: 29 July 2022

References

- Hasegawa, H., Yamauchi, T. & Kraemer, W. J. Foot strike patterns of runners at the 15-km point during an elite-level half marathon. *J. Strength Cond. Res.* **21**, 888–893. <https://doi.org/10.1519/R-22096.1> (2007).
- Altman, A. R. & Davis, I. S. A kinematic method for footstrike pattern detection in barefoot and shod runners. *Gait Posture* **35**, 298–300. <https://doi.org/10.1016/j.gaitpost.2011.09.104> (2012).
- Ahn, A. N., Brayton, C., Bhatia, T. & Martin, P. Muscle activity and kinematics of forefoot and rearfoot strike runners. *J. Sport Health Sci.* **3**, 102–112. <https://doi.org/10.1016/j.jshs.2014.03.007> (2014).
- Wei, Z., Zhang, Z., Jiang, J., Zhang, Y. & Wang, L. Comparison of plantar loads among runners with different strike patterns. *J. Sports Sci.* **37**, 2152–2158. <https://doi.org/10.1080/02640414.2019.1623990> (2019).
- Ruder, M., Jamison, S. T., Tenforde, A., Mulloy, F. & Davis, I. S. Relationship of Foot Strike Pattern and Landing Impacts during a Marathon. *Med. Sci. Sports Exerc.* **51** (2019).
- Gruber, A. H., Boyer, K. A., Derrick, T. R. & Hamill, J. Impact shock frequency components and attenuation in rearfoot and forefoot running. *J. Sport Health Sci.* **3**, 113–121. <https://doi.org/10.1016/j.jshs.2014.03.004> (2014).
- Breine, B., Malcolm, P., Frederick, E. C. & De Clercq, D. Relationship between running speed and initial foot contact patterns. *Med. Sci. Sports Exerc.* **46**, 1595–1603. <https://doi.org/10.1249/mss.000000000000267> (2014).
- Knorz, S. *et al.* Three-dimensional biomechanical analysis of rearfoot and forefoot running. *Orthop J. Sports Med.* **5**, 2325967117719065. <https://doi.org/10.1177/2325967117719065> (2017).
- Sun, X., Yang, Y., Wang, L., Zhang, X. & Fu, W. Do strike patterns or shoe conditions have a predominant influence on foot loading? *J. Hum. Kinet.* **64**, 13–23. <https://doi.org/10.1515/hukin-2017-0205> (2018).
- Anderson, L. M., Bonanno, D. R., Hart, H. F. & Barton, C. J. What are the benefits and risks associated with changing foot strike pattern during running? A systematic review and meta-analysis of injury, running economy, and biomechanics. *Sports Med.* <https://doi.org/10.1007/s40279-019-01238-y> (2019).
- Kulmala, J.-P., Avela, J., Pasanen, K. & Parkkari, J. Forefoot strikers exhibit lower running-induced knee loading than rearfoot strikers. *Med. Sci. Sports Exerc.* **45**, 2306–2313. <https://doi.org/10.1249/MSS.0b013e31829efcf7> (2013).
- Almeida, M. O., Davis, I. S. & Lopes, A. D. Biomechanical differences of foot-strike patterns during running: A systematic review with meta-analysis. *J. Orthop. Sports Phys. Ther.* **45**, 738–755. <https://doi.org/10.2519/jospt.2015.6019> (2015).
- Forrester, S. E. & Townend, J. The effect of running velocity on footstrike angle—a curve-clustering approach. *Gait Posture* **41**, 26–32. <https://doi.org/10.1016/j.gaitpost.2014.08.004> (2015).
- Craighead, D. H., Lehecka, N. & King, D. L. A novel running mechanic's class changes kinematics but not running economy. *J. Strength Cond. Res.* **28**, 3137–3145. <https://doi.org/10.1519/JSC.0000000000000500> (2014).
- Hamill, J. & Gruber, A. H. Is changing footstrike pattern beneficial to runners?. *J. Sport Health Sci.* **6**, 146–153. <https://doi.org/10.1016/j.jshs.2017.02.004> (2017).
- Ekizos, A., Santuz, A. & Arampatzis, A. Short- and long-term effects of altered point of ground reaction force application on human running energetics. *J. Exp. Biol.* **221**, 1–15. <https://doi.org/10.1242/jeb.176719> (2018).
- Anderson, L., Barton, C. & Bonanno, D. The effect of foot strike pattern during running on biomechanics, injury and performance: A systematic review and meta-analysis. *J. Sci. Med. Sport* **20**, e54. <https://doi.org/10.1016/j.jsams.2017.01.145> (2017).

18. Alexander, J. L. N., Willy, R. W., Napier, C., Bonanno, D. R. & Barton, C. J. Infographic. Running myth: switching to a non-rearfoot strike reduces injury risk and improves running economy. *Br. J. Sports Med.* **55**, 175–176. <https://doi.org/10.1136/bjsports-2020-102262> (2021).
19. Lussiana, T., Patoz, A., Gindre, C., Mourot, L. & Hébert-Losier, K. The implications of time on the ground on running economy: Less is not always better. *J. Exp. Biol.* **222**, jeb192047, <https://doi.org/10.1242/jeb.192047> (2019).
20. Patoz, A., Lussiana, T., Thouvenot, A., Mourot, L. & Gindre, C. Duty factor reflects lower limb kinematics of running. *Appl. Sci.* **10**, 8818 (2020).
21. Minetti, A. E. A model equation for the prediction of mechanical internal work of terrestrial locomotion. *J. Biomech.* **31**, 463–468. [https://doi.org/10.1016/S0021-9290\(98\)00038-4](https://doi.org/10.1016/S0021-9290(98)00038-4) (1998).
22. Folland, J. P., Allen, S. J., Black, M. I., Handsaker, J. C. & Forrester, S. E. Running technique is an important component of running economy and performance. *Med. Sci. Sports Exerc.* **49**, 1412–1423 (2017).
23. Hayes, P. & Caplan, N. Foot strike patterns and ground contact times during high-calibre middle-distance races. *J. Sports Sci.* **30**, 1275–1283. <https://doi.org/10.1080/02640414.2012.707326> (2012).
24. Beck, O. N., Gosyne, J., Franz, J. R. & Sawicki, G. S. Cyclically producing the same average muscle-tendon force with a smaller duty increases metabolic rate. *Proc. Royal Soc. B* **287**, 20200431. <https://doi.org/10.1098/rspb.2020.0431> (2020).
25. Patoz, A., Lussiana, T., Breine, B., Gindre, C. & Malatesta, D. Both a single sacral marker and the whole-body center of mass accurately estimate peak vertical ground reaction force in running. *Gait Posture* **89**, 186–192. <https://doi.org/10.1016/j.gaitpost.2021.07.013> (2021).
26. Tranberg, R., Saari, T., Zügner, R. & Kärrholm, J. Simultaneous measurements of knee motion using an optical tracking system and radiostereometric analysis (RSA). *Acta Orthop.* **82**, 171–176. <https://doi.org/10.3109/17453674.2011.570675> (2011).
27. Mai, P. & Willwacher, S. Effects of low-pass filter combinations on lower extremity joint moments in distance running. *J. Biomech.* **95**, 109311. <https://doi.org/10.1016/j.jbiomech.2019.08.005> (2019).
28. Smith, L., Preece, S., Mason, D. & Bramah, C. A comparison of kinematic algorithms to estimate gait events during overground running. *Gait Posture* **41**, 39–43. <https://doi.org/10.1016/j.gaitpost.2014.08.009> (2015).
29. Hanavan, E. A mathematical model of the human body. *AMRL-TR. Aerosp. Med. Res. Lab.* **1**, 1–149 (1964).
30. Dempster, W. T. *Space requirements of the seated operator: Geometrical, kinematic, and mechanical aspects of the body with special reference to the limbs.* (Wright Air Development Center, 1955).
31. Cohen, J. *Statistical power analysis for the behavioral sciences.* (Routledge, 1988).
32. Gaddis, G. M. & Gaddis, M. L. Introduction to biostatistics: Part 3, sensitivity, specificity, predictive value, and hypothesis testing. *Ann. Emerg. Med.* **19**, 591–597. [https://doi.org/10.1016/S0196-0644\(05\)82198-5](https://doi.org/10.1016/S0196-0644(05)82198-5) (1990).
33. Hinkle, D. E., Wiersma, W. & Jurs, S. G. *Applied statistics for the behavioral sciences.* 768 (Houghton Mifflin (p. 109), 2002).
34. Larson, P. *et al.* Foot strike patterns of recreational and sub-elite runners in a long-distance road race. *J. Sports Sci.* **29**, 1665–1673. <https://doi.org/10.1080/02640414.2011.610347> (2011).
35. Arendse, R. E. *et al.* Reduced eccentric loading of the knee with the pose running method. *Med. Sci. Sports Exerc.* **36**, 272–277. <https://doi.org/10.1249/01.MSS.0000113684.61351.B0> (2004).
36. Fitzgerald, M. *Runner's world the cutting-edge runner: How to use the latest science and technology to run longer, stronger, and faster.* (Rodale Books, 2005).
37. Glover, B. & Glover, S.-I. F. *The competitive runner's handbook: The bestselling guide to running 5Ks through marathons.* (Penguin, 1999).
38. Paquette, M. R., Powell, D. W. & DeVita, P. Age and training volume influence joint kinetics during running. *Scand. J. Med. Sci. Sports* **31**, 380–387. <https://doi.org/10.1111/sms.13857> (2021).
39. Paquette, M. R., Devita, P. & Williams, D. S. B. 3rd. Biomechanical implications of training volume and intensity in aging runners. *Med. Sci. Sports Exerc.* **50**, 510–515. <https://doi.org/10.1249/mss.0000000000001452> (2018).
40. Sun, X., Lam, W.-K., Zhang, X., Wang, J. & Fu, W. Systematic review of the role of footwear constructions in running biomechanics: Implications for running-related injury and performance. *J. Sports Sci. Med.* **19**, 20–37 (2020).
41. McMahon, T. A. & Cheng, G. C. The mechanics of running: How does stiffness couple with speed?. *J. Biomech.* **23**, 65–78. [https://doi.org/10.1016/0021-9290\(90\)90042-2](https://doi.org/10.1016/0021-9290(90)90042-2) (1990).
42. Breine, B. *et al.* Initial foot contact and related kinematics affect impact loading rate in running. *J. Sports Sci.* **35**, 1556–1564. <https://doi.org/10.1080/02640414.2016.1225970> (2017).
43. Sinclair, J., Fau-Goodwin, J., Richards, J. & Shore, H. The influence of minimalist and maximalist footwear on the kinetics and kinematics of running. *Footwear Sci.* **8**, 33–39. <https://doi.org/10.1080/19424280.2016.1142003> (2016).
44. Hébert-Losier, K. *et al.* Metabolic and performance responses of male runners wearing 3 types of footwear: Nike Vaporfly 4%, Saucony Endorphin racing flats, and their own shoes. *J. Sport Health Sci.* <https://doi.org/10.1016/j.jshs.2020.11.012> (2020).
45. Tam, N., Tucker, R. & Astephen Wilson, J. L. Individual responses to a barefoot running program: Insight into risk of injury. *Am. J. Sports Med.* **44**, 777–784. <https://doi.org/10.1177/0363546515620584> (2016).
46. Tung, K. D., Franz, J. R. & Kram, R. A test of the metabolic cost of cushioning hypothesis during unshod and shod running. *Med. Sci. Sports Exerc.* **46**, 324–329. <https://doi.org/10.1249/MSS.0b013e3182a63b81> (2014).

Acknowledgements

This study was supported by the University of Lausanne (Switzerland). The authors warmly thank the participants for their time and cooperation.

Author contributions

Conceptualization, A.P., T.L., C.G., and D.M.; methodology, A.P., T.L., C.G., and D.M.; investigation, A.P., T.L., and B.B.; formal analysis, A.P. and B.B.; writing—original draft preparation, A.P.; writing—review and editing, A.P., T.L., C.G., and D.M.; supervision, A.P., T.L., C.G., and D.M.

Funding

This study was supported by Innosuisse grant no. 35793.1 IP-LS.

Competing interest

The authors declare no competing interests.

Additional information

Supplementary Information The online version contains supplementary material available at <https://doi.org/10.1038/s41598-022-17274-0>.

Correspondence and requests for materials should be addressed to A.P.

Reprints and permissions information is available at www.nature.com/reprints.

Publisher's note Springer Nature remains neutral with regard to jurisdictional claims in published maps and institutional affiliations.



Open Access This article is licensed under a Creative Commons Attribution 4.0 International License, which permits use, sharing, adaptation, distribution and reproduction in any medium or format, as long as you give appropriate credit to the original author(s) and the source, provide a link to the Creative Commons licence, and indicate if changes were made. The images or other third party material in this article are included in the article's Creative Commons licence, unless indicated otherwise in a credit line to the material. If material is not included in the article's Creative Commons licence and your intended use is not permitted by statutory regulation or exceeds the permitted use, you will need to obtain permission directly from the copyright holder. To view a copy of this licence, visit <http://creativecommons.org/licenses/by/4.0/>.

© The Author(s) 2022

Supplementary Materials for:

Duty factor and foot-strike pattern do not represent similar running pattern at the individual level

S1. Absolute classification of runners to create foot-strike pattern groups

Runners were classified as rearfoot (RFS), midfoot (MFS), and forefoot (FFS) strikers using the 33 highest, 33 middle, and 34 lowest foot-strike angle (FSA) values at each speed. Noteworthy, FFS group was composed of one extra runner but attributing this extra runner to MFS or RFS group or removing him from the study would not have had an impact on the results.

Both relative and absolute classifications classified most of the runners in the same foot-strike pattern (FSP) group. On average, 1 participant (4%) was attributed to a different FSP group when using the absolute rather than the relative classification reported in the manuscript. The complete analysis of the number of runners that were attributed to a different FSP group between the relative and absolute classifications at the different running speeds is provided in Table S1.

Table S1. Number and percentage (in parentheses) of runners that were attributed to a different foot-strike pattern (FSP) group, i.e., rearfoot (RFS), midfoot (MFS), or forefoot (FFS) group, between the relative and absolute classifications at the different running speeds.

Relative classification	Absolute classification	9 km/h	11 km/h	13 km/h
FFS	MFS	5 (15%)	2 (6%)	5 (15%)
MFS	FFS	0 (0%)	0 (0%)	0 (0%)
MFS	RFS	6 (18%)	2 (6%)	0 (0%)
RFS	MFS	0 (0%)	0 (0%)	5 (15%)
FFS	RFS	0 (0%)	0 (0%)	0 (0%)
RFS	FFS	0 (0%)	0 (0%)	0 (0%)

The FSA ranges for FFS, MFS, and RFS groups were [-16.9°, -2.7°], [-2.5°, 5.5°], and [6.0°, 19.3°] at 9km/h, [-16.9°, -3.5°], [-2.9°, 7.7°], and [7.8°, 19.2°] at 11km/h, and [-15.3°, -3.0°], [-2.9°, 9.7°], and [9.9°, 20.5°] at 13km/h, respectively. The linear mixed model revealed a significant FSP group effect on duty factor (DF) ($P < 0.001$). The Holm post hoc tests indicated a significantly higher DF for RFS than for MFS and FFS ($P \leq 0.001$), and for MFS than for FFS ($P = 0.004$). A significant effect of speed was reported on DF ($P < 0.001$). A significantly smaller DF was obtained at a faster speed, as depicted by the Holm post hoc tests ($P < 0.001$). There was no FSP group x speed interaction ($P < 0.81$). The Cohen's d effect sizes were moderate ($|d| \leq 0.62$), except for those corresponding to the RFS-FFS pairs, which were large at all speeds ($|d| \geq 0.92$).

When considering all groups together, a significant group x running speed interaction effect was reported by the linear mixed models for both DF and FSA values ($P \leq 0.018$). Pairwise post hoc comparisons between the three group pairs at each running speed revealed no significant differences for DF and FSA values ($P \geq 0.18$).

The number of runners in FSP and DF groups as well as the agreement, sensitivity, and specificity between FSP and DF groups are given in Table S2. The average (over speed and group) agreement, sensitivity, and specificity were 72, 50, and 75%, respectively.

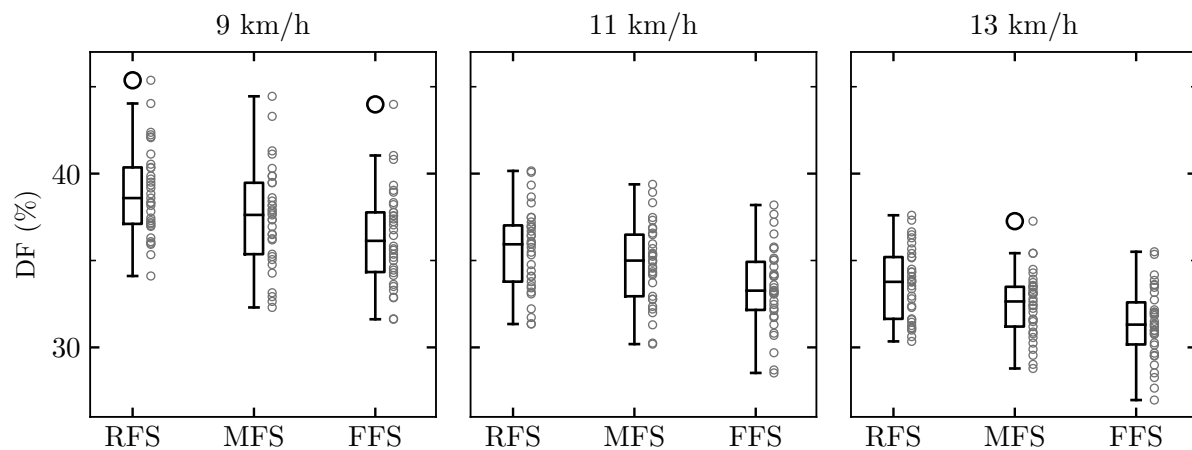


Figure S1. Boxplots of the duty factor (DF) for the different foot-strike pattern groups, i.e., rearfoot (RFS), midfoot (MFS), and forefoot (FFS) strikers, at 9, 11, and 13 km/h. The box extends from the lower to upper quartile values of the data, with a line at the median. The whiskers (black empty circles) extend from the box to show the range of the data while flier points are those past the end of the whiskers. The upper whisker extends to the last data less than $Q3 + 1.5(Q3 - Q1)$, where $Q1$ and $Q3$ are the first and third quartile. Similarly, the lower whisker extends to the first data greater than $Q1 - 1.5(Q3 - Q1)$. The small gray empty circles denote the data of each participant.

The DF and FSA values of runners attributed to a DF group but not being classified in the supposedly corresponding FSP group, for instance DF_{high} runners but classified as MFS and FFS, are given in Fig. S2A. Similarly, Fig. S2B depicts FSA and DF values of runners attributed to a FSP group but not being classified in the supposedly corresponding DF group, for instance RFS but classified as DF_{mid} or DF_{low} .

On average, 2 participants (6%) changed their FSP group with running speed. The complete analysis of the number of runners that switched group between the different running speeds is provided in Table S3.

Table S2. Number of runners in foot-strike pattern (FSP) [rearfoot (RFS), midfoot (MFS), and forefoot (FFS) strikers] and duty factor (DF) [high (DF_{high}), mid (DF_{mid}), and low (DF_{low}) DF runners] groups, as well as the agreement, sensitivity, and specificity between FSP and DF groups together with their 95% confidence intervals in parenthesis at three running speeds.

Running Speed (km/h)		DF _{high}	DF _{mid}	DF _{low}
9	RFS	17	10	6
	MFS	10	12	11
	FFS	6	11	17
	Agreement (%)	68 (59, 77)	75 (67, 83)	66 (57, 75)
	Sensitivity (%)	52 (34, 69)	36 (20, 53)	50 (33, 67)
	Specificity (%)	76 (66, 86)	69 (58, 80)	74 (64, 85)
	11	RFS	18	8
MFS		10	14	9
FFS		5	11	18
Agreement (%)		70 (61, 79)	80 (72, 88)	68 (59, 77)
Sensitivity (%)		55 (38, 72)	42 (26, 59)	53 (36, 70)
Specificity (%)		78 (68, 88)	72 (61, 82)	76 (65, 86)
13		RFS	19	7
	MFS	8	16	9
	FFS	6	10	18
	Agreement (%)	72 (63, 81)	84 (77, 91)	68 (59, 77)
	Sensitivity (%)	58 (41, 74)	48 (31, 66)	53 (36, 70)
	Specificity (%)	79 (69, 89)	75 (64, 85)	76 (65, 86)

Table S3. Number and percentage (in parentheses) of runners that changed from one foot-strike pattern (FSP) group, i.e., rearfoot (RFS), midfoot (MFS), or forefoot (FFS) group, to another FSP group with changing running speed.

	9 to 11 km/h	11 to 13 km/h	9 to 13 km/h
FFS to MFS	1 (3%)	5 (15%)	3 (9%)
MFS to FFS	3 (9%)	3 (9%)	3 (9%)
MFS to RFS	2 (6%)	3 (9%)	2 (6%)
RFS to MFS	4 (12%)	1 (3%)	2 (6%)
FFS to RFS	1 (3%)	0 (0%)	0 (0%)
RFS to FFS	0 (0%)	2 (6%)	1 (3%)

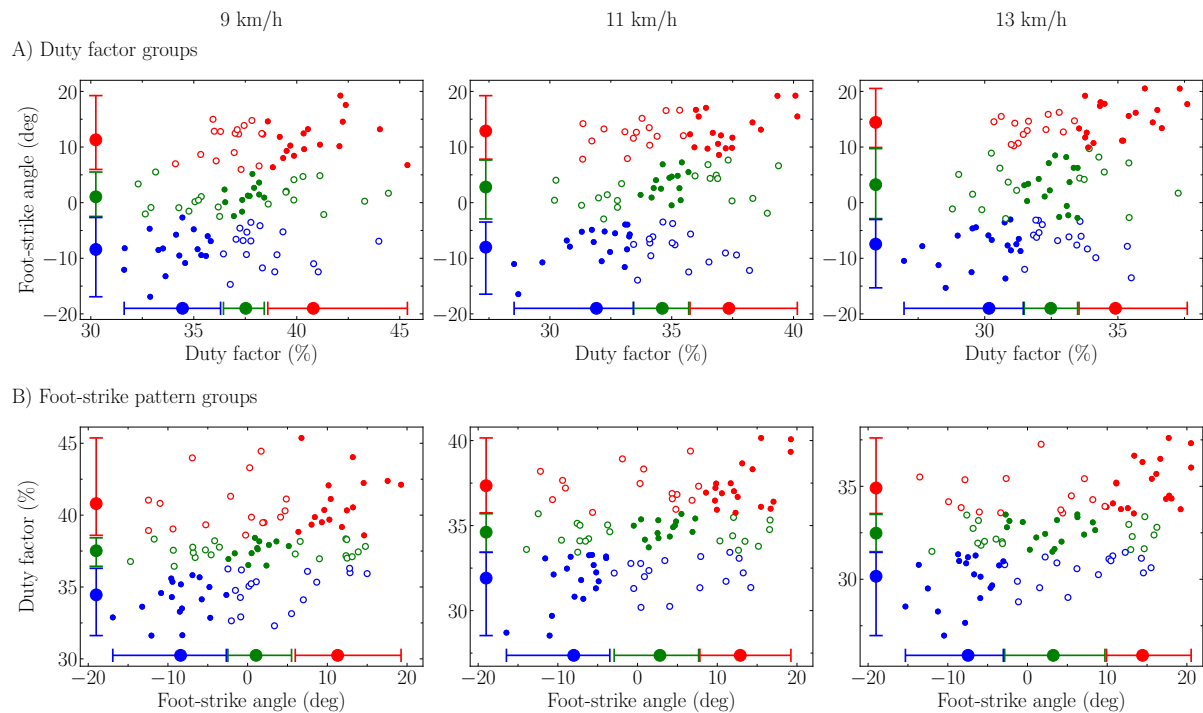


Figure S2. Duty factor (DF) and foot-strike angle (FSA) values of runners attributed to (A) a DF group but not being classified in the supposedly corresponding foot-strike pattern (FSP) group and (B) a FSP group but not being classified in the supposedly corresponding DF group at each tested running speed. Mean DF and FSA value (filled circle) and range of values (whiskers) for each DF and FSP group, i.e., high DF runners and rearfoot strikers (RFS; red), mid DF runners and midfoot strikers (MFS; green), and low DF runners and forefoot strikers (FFS; blue). The upper whisker extends to the maximum while the lower whisker extends to the minimum value. Empty circles denote the runners attributed to a DF or FSP group but not being classified in the supposedly corresponding FSP or DF group, respectively, e.g., high DF runners but classified as MFS or FFS (green and blue empty circles within the red whiskers of the high DF runners) in (A) and RFS but classified as mid or low DF runners (green and blue empty circles within the red whiskers of RFS) in (B).

S2. Runners attributed to a different foot-strike pattern and duty factor group depending on the running speed

Table S4. Number and percentage (in parentheses) of runners that changed from one foot-strike pattern (FSP) group, i.e., rearfoot (RFS), midfoot (MFS), or forefoot (FFS) group, to another FSP group with changing running speed.

	9 to 11 km/h	11 to 13 km/h	9 to 13 km/h
FFS to MFS	4 (10%)	2 (5%)	3 (8%)
MFS to FFS	1 (3%)	4 (12%)	2 (6%)
MFS to RFS	5 (15%)	8 (24%)	12 (35%)
RFS to MFS	1 (4%)	0 (0%)	0 (0%)
FFS to RFS	0 (0%)	0 (0%)	0 (0%)
RFS to FFS	0 (0%)	1 (4%)	1 (4%)

Table S5. Number and percentage (in parentheses) of runners that changed from one duty factor (DF) group, i.e., high (DF_{high}), mid (DF_{mid}), or low (DF_{low}) DF, to another DF group with changing running speed.

	9 to 11 km/h	11 to 13 km/h	9 to 13 km/h
DF_{low} to DF_{mid}	6 (18%)	6 (18%)	6 (18%)
DF_{mid} to DF_{low}	6 (18%)	5 (15%)	6 (18%)
DF_{mid} to DF_{high}	5 (15%)	5 (15%)	7 (21%)
DF_{high} to DF_{mid}	5 (15%)	4 (12%)	7 (21%)
DF_{low} to DF_{high}	0 (0%)	0 (0%)	1 (3%)
DF_{high} to DF_{low}	0 (0%)	1 (3%)	1 (3%)

8.2 Examination of running pattern consistency across speeds

Aurélien Patoz^{1,2,*}, Thibault Lussiana^{2,3,4}, Bastiaan Breine^{2,5}, Cyrille Gindre^{2,3}, Davide Malatesta¹, Kim Hébert-Losier^{6,7}

¹ Institute of Sport Sciences, University of Lausanne, Lausanne, Switzerland

² Research and Development Department, Volodalen Swiss Sport Lab, Aigle, Switzerland

³ Research and Development Department, Volodalen, Chavéria, France

⁴ Research Unit EA3920 Prognostic Markers and Regulatory Factors of Cardiovascular Diseases and Exercise Performance, Health, Innovation platform, University of Bourgogne Franche-Comté, Besançon, France

⁵ Department of Movement and Sports Sciences, Ghent University, Ghent, Belgium

⁶ Division of Health, Engineering, Computing and Science, Te Huataki Waiora School of Health, University of Waikato, Adams Centre for High Performance, Tauranga, New Zealand

⁷ Department of Sports Science, National Sports Institute of Malaysia, Kuala Lumpur, Malaysia

* Corresponding author

Published in **Sports Biomechanics**

DOI: 10.1080/14763141.2022.2094825



Examination of running pattern consistency across speeds

Aurélien Patoz ^{a,b}, Thibault Lussiana ^{b,c,d}, Bastiaan Breine ^{b,e}, Cyrille Gindre ^{b,c}, Davide Malatesta ^a and Kim Hébert-Losier ^{f,g}

^aInstitute of Sport Sciences, University of Lausanne, Lausanne, Switzerland; ^bResearch and Development Department, Volodalen Swiss Sport Lab, Aigle, Switzerland; ^cVolodalen, Research and Development Department, Chavéria, France; ^dResearch Unit EA3920 Prognostic Markers and Regulatory Factors of Cardiovascular Diseases and Exercise Performance, Health, Innovation Platform, University of Bourgogne Franche-Comté, Besançon, France; ^eDepartment of Movement and Sports Sciences, Ghent University, Ghent, Belgium; ^fDivision of Health, Engineering, Computing and Science, Te Huataki Waiora School of Health, University of Waikato, Adams Centre for High Performance, Tauranga, New Zealand; ^gDepartment of Sports Science, National Sports Institute of Malaysia, Kuala Lumpur, Malaysia

ABSTRACT

Duty factor (DF) and step frequency (SF) are key running pattern determinants. However, running patterns may change with speed if DF and SF changes are inconsistent across speeds. We examined whether the relative positioning of runners was consistent: 1) across five running speeds (10–18 km/h) for four temporal variables [DF, SF, and their subcomponents: contact (t_c) and flight (t_f) time]; and 2) across these four temporal variables at these five speeds. Three-dimensional whole-body kinematics were acquired from 52 runners, and deviations from the median for each variable (normalised to minimum-maximum values) were extracted. Across speeds for all variables, correlations on the relative positioning of individuals were *high* to *very high* for 2–4 km/h speed differences, and *moderate* to *high* for 6–8 km/h differences. Across variables for all speeds, correlations were *low* between DF-SF, *very high* between DF- t_c , and *low* to *high* between DF- t_c , SF- t_c , and SF- t_c . Hence, the consistency in running patterns decreased as speed differences increased, suggesting that running patterns be assessed using a range of speeds. Consistency in running patterns at a given speed was low between DF and SF, corroborating suggestions that using both variables can encapsulate the full running pattern spectrum.

ARTICLE HISTORY

Received 23 November 2021

Accepted 22 June 2022

KEYWORDS

Gait analysis; motion analysis; biomechanics; temporal variables; Relative positioning

Introduction

The spring-mass model represents running as a ‘bouncing’ gait modelled using a mass connected to a massless spring (Blickhan, 1989). In this model, the supporting leg behaves like a spring during stance and each stance is separated by a flight time (t_f), i.e., a period where the limbs are not in contact with the ground. The presence of this flight phase distinguishes running from walking (Novacheck, 1998).

Each runner adopts a unique and natural running pattern that is challenging to describe using a single variable (Folland et al., 2017). As early as 1985, the running pattern was viewed as a global system with several interconnected variables (Subotnick,

1985). More recently, the synthetic review of van Oeveren et al. (2021) proposed that the full spectrum of running patterns could be described combining two temporal variables: step frequency (SF) and duty factor (DF), where DF reflects the relative contribution of the ground contact time (t_c) to the running stride (Folland et al., 2017; Minetti, 1998). According to van Oeveren et al. (2021), knowing DF and SF allows to categorise running patterns in one of five distinct categories, namely ‘stick’, ‘bounce’, ‘push’, ‘hop’, and ‘sit’, but keeping in mind that running patterns operate along a continuum. Individuals spontaneously and subconsciously adopt their own running pattern, a choice shown to be self-optimised and central in the development of an economical and safe running gait (Cavanagh & Williams, 1982; Moore et al., 2016; Moore, 2016; Williams & Cavanagh, 1987). The understanding of the individual running patterns might be important for improving performance, optimising training, and preventing running-related injuries.

The importance of DF and SF in determining running patterns (van Oeveren et al., 2021) corroborates previous findings. On the one hand, DF has been used to categorise runners with distinct running patterns (Lussiana et al., 2019; Patoz et al., 2020). Runners with a low DF exhibit a more symmetrical stance phase (similar brake and push times), anterior (midfoot and forefoot) strike pattern, and extended lower limb during t_c than runners with a high DF. In contrast, runners with a high DF exhibit greater lower limb flexion during t_c , a more rearfoot strike pattern, and lesser work against gravity to generate forward propulsion (Lussiana et al., 2019; Patoz et al., 2020). Despite these biomechanical differences, the running economy of runners within these two DF groups are similar (Lussiana et al., 2019), suggesting two energetically equivalent strategies at endurance running speeds. On the other hand, SF can reveal individual muscle recruitment patterns of runners and strategies to increase running speed (Dorn et al., 2012) or achieve top-end running speeds (Salo et al., 2011). Even in subgroups of individuals with similar sprint velocities, a range of SF and step length combinations are present (Hunter et al., 2004).

Running speed affects DF and SF, with an increase in running speed decreasing DF (Lussiana et al., 2019; Minetti, 1998; van Oeveren et al., 2021) and increasing SF (Dorn et al., 2012; Ogueta-Alday et al., 2014; van Oeveren et al., 2021). These changes are likely related to changes in their subcomponent variables t_c and t_f . Indeed, t_c decreases with an increase in running speed, whereas t_f increases (da Rosa et al., 2019; Lussiana et al., 2019; Ogueta-Alday et al., 2014; van Oeveren et al., 2021). Given the speed-dependency of these variables, van Oeveren et al. (2021) suggested using an absolute speed to define running patterns as stick, bounce, push, hop, and sit.

Worth noting is the large interindividual variations in temporal variables (DF, t_c , t_f , and SF) reported at absolute running speeds (Lussiana et al., 2019; Ogueta-Alday et al., 2014) and the large interindividual variations in the individual strategies adopted to adapt to changes in running speeds (Forrester & Townend, 2015; Hébert-Losier et al., 2015; Salo et al., 2011). For instance, a curve-clustering approach on the footstrike angle of runners across speeds revealed three subgroups: those that maintained a rearfoot strike pattern, those that maintained a forefoot or midfoot strike pattern, and those that transitioned from a rearfoot to a less rearfoot strike pattern with increasing speed (Forrester & Townend, 2015). Therefore, the running pattern of an individual could also change with speed if the relationship between or changes in the underlying temporal

variables are inconsistent across running speeds. Such understanding would then allow us assessing if the evaluation of running patterns could be generalised across speeds and studies.

Hence, our first aim was to assess if running patterns are consistent across running speeds by examining the consistency in four temporal variables (DF, SF, t_c , and t_f). For instance, we investigated whether a runner with a high DF (with respect to the group median) at a slow running speed also exhibits a high DF at a faster running speed. We hypothesised that consistency would be greater when differences in running speeds were smaller, as previously observed for footstrike angle (Forrester & Townend, 2015).

Our second aim was to assess the consistency across the four temporal variables at an absolute running speed. Given that DF and SF are proposed to be two independent key running pattern determinants (van Oeveren et al., 2021), the association between these two variables should be low. Hence, we hypothesised that consistency would be low between DF and SF. On the other hand, we anticipated greater consistency between DF and its subcomponent variables (t_c and t_f) as well as between SF and t_c and t_f .

Material and methods

Participants

Fifty-two runners, 32 men (age: 32 ± 9 yr, mass: 66 ± 11 kg, height: 175 ± 7 cm, running distance: 53 ± 21 km/week, running experience: 8 ± 8 yr, and best half-marathon time: 92 ± 10 min) and 20 women (age: 32 ± 9 yr, mass: 52 ± 6 kg, height: 162 ± 4 cm, running distance: 50 ± 22 km/week, running experience: 7 ± 4 yr, and best half-marathon time: 102 ± 12 min) participated in this study. For study inclusion, participants were required to be in good self-reported general health with no current or recent (<3 months) musculoskeletal injuries and to meet a certain level of running performance. More specifically, in the last year, runners were required to have competed in a road race with finishing times of ≤ 50 min for 10 km or ≤ 2 h for 21.1 km. The ethical committee of the

National Sports Institute of Malaysia approved the study protocol prior to participant recruitment (ISNRP: 26/2015, which adhered to the latest version of the Declaration of Helsinki of the World Medical Association.

Experimental procedure

Each participant completed one experimental laboratory session. After providing written informed consent, participants ran 16 min (4 min at 9 km/h, 10 km/h, 12 km/h, and 14 km/h in that order) on a treadmill (h/p/cosmos mercury®, h/p/cosmos sports & medical gmbh, Nussdorf-Traunstein, Germany) as a warm-up ensuring stabilisation of shoe stiffness properties (Divert et al., 2005) and promoting treadmill familiarisation (Arnold et al., 2019; Lindorfer et al., 2020). Then, retro-reflective markers were positioned on individuals (described in *Data Collection* section) to assess running kinematics. For each participant, a 1-s static calibration trial was recorded, which was followed by 5×30 -s runs at 10, 12, 14, 16, and 18 km/h (with 1-min recovery periods between each run) to collect three-dimensional (3D) kinematic data in the last 10-s segment of these runs

(30 ± 2 running steps), resulting in at least 20 steps being analysed (Riazati et al., 2019). All participants were familiar with running on a treadmill as part of their usual training programs and wore their habitual running shoes during testing (shoe mass: 226 ± 37 g, stack height: 25 ± 3 mm, and heel-to-toe drop: 7 ± 3 mm).

Data collection

3D kinematic data were collected at 200 Hz using seven infrared Oqus cameras (five Oqus 300+, one Oqus 310+, and one Oqus 311+) and Qualisys Track Manager software version 2.1.1 build 2902 together with the Project Automation Framework Running package version 4.4 (Qualisys AB, Göteborg, Sweden). Thirty-five retro-reflective markers of 12 mm in diameter were used for static calibration and running trials, and were affixed to the skin and shoes of individuals over anatomical landmarks using double-sided tape following standard guidelines from the Project Automation Framework Running package (Tranberg et al., 2011) as already reported elsewhere (Lussiana et al., 2019). The 3D marker data were exported in .c3d format and processed in Visual3D Professional software version 5.02.25 (C-Motion Inc., Germantown, MD, USA). More explicitly, the 3D marker data were interpolated using a third-order polynomial least-square fit algorithm, allowing a maximum of 20 frames for gap filling, and subsequently low-pass filtered at 20 Hz using a fourth-order Butterworth filter.

Temporal variables

Running events were derived from the trajectories of the 3D marker data using similar procedures to those previously reported (Lussiana et al., 2019; Maiwald et al., 2009). More explicitly, a mid-foot landmark was generated midway between the heel and toe markers. Footstrike was defined as the instance when the mid-foot landmark reached a local minimal vertical velocity prior to it reaching a peak vertical velocity reflecting the start of swing. Toe-off was defined as the instance when the toe marker attained a peak vertical acceleration before reaching a 7 cm vertical position. All events were verified to ensure correct identification and were manually adjusted when required.

t_c was defined as the time from footstrike to toe-off of the same foot while t_f was defined as the time from toe-off of one foot to footstrike of the contralateral foot. SF was calculated as $SF = 1/(t_c + t_f)$, and DF as $DF = t_c SF/2$. For all temporal variables, the values extracted from the 10-s data collection for each participant were averaged. To express the temporal variables as relative, each variable was normalised using the min-max scaler approach, i.e., $(x - x_{\min})/(x_{\max} - x_{\min})$ where x represents the value for a given participant and $x_{\min/\max}$ the minimum/maximum among all participants at a given speed. The normalised variables were used in subsequent statistical analyses.

Statistical analysis

Descriptive statistics are presented using mean \pm standard deviation. The consistency in running patterns across running speeds was evaluated by examining the relative positioning of runners for each temporal variable and tested speed. The relative positioning

was obtained by calculating the deviations from the median of the temporal values. These datasets were normally distributed based on Kolmogorov–Smirnov tests ($P \geq 0.34$). Pearson's correlation coefficients (r) on the relative values together with corresponding 95% CI [lower, upper] and P -values were extracted to explore the consistency between each pair of running speeds for each of the four temporal variables. The same statistical approach was used to explore the consistency between each pair of temporal variables for each of the five running speeds. Correlations were considered *very high*, *high*, *moderate*, *low*, and *negligible* when absolute r values were between 0.90–1.00, 0.70–0.89, 0.50–0.69, 0.30–0.49, and 0.00–0.29, respectively (Hinkle et al., 2002). Statistical analyses were performed using Jamovi (version 1.6, <https://www.jamovi.org>) with a level of significance set at $P \leq 0.05$ for all analyses.

Results

As speed increased from 10 to 18 km/h, DF and t_c decreased by $8.5 \pm 2.8\%$ and 87 ± 20 ms, while t_f and SF increased by 42 ± 20 ms and 0.42 ± 0.16 Hz, respectively (Table 1 and Figure 1). The relative DF, SF, t_c , and t_f values for all participants and each running speed are depicted in Figure 2.

Consistency across running speeds for each temporal variable

Correlations for each one of the four relative temporal variables were *high* to *very high* for each pair of running speeds when changes were 2–4 km/h ($P < 0.001$, Table 2), except for the correlation between 10 and 14 km/h for t_c being *moderate*. Correlations were *moderate* to *high* for each pair of running speeds when changes were 6–8 km/h for the four relative temporal variables ($P < 0.001$; Table 2).

The relative DF values for all participants and each running speed are depicted in Figure 3. According to the correlations reported in Table 2, similar figures and corresponding interpretations would result using the three other variables (t_c , t_f , and SF).

Consistency across temporal variables for each running speed

Correlations were *low* between relative DF and SF at all tested speeds ($P \leq 0.02$; Table 3). Correlations were *very high* between relative DF and t_f at all tested speeds ($P < 0.001$); and *high* between relative DF and t_c at 10 and 12 km/h ($P < 0.001$), but *moderate* at 14, 16, and 18 km/h ($P < 0.001$; Table 3).

Table 1. Duty factor, contact time, flight time, and step frequency at five running speeds.

Running speed (km/h)	Duty factor (%)	Contact time (ms)	Flight time (ms)	Step frequency (Hz)
10	38.6 ± 3.4	274 ± 24	81 ± 27	2.83 ± 0.16
12	35.1 ± 2.8	242 ± 19	103 ± 23	2.91 ± 0.18
14	33.2 ± 1.5	220 ± 18	112 ± 21	3.02 ± 0.19
16	31.2 ± 2.4	201 ± 17	121 ± 20	3.12 ± 0.21
18	30.1 ± 2.3	186 ± 15	124 ± 20	3.24 ± 0.24

Values are means \pm standard deviations.

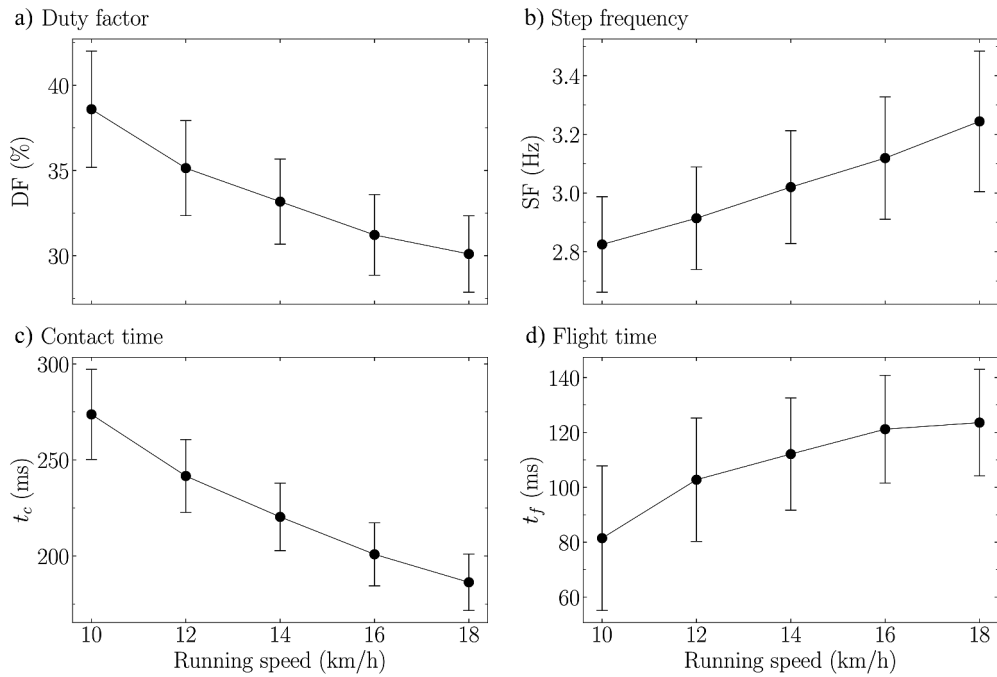


Figure 1. a) Duty factor (DF), b) step frequency (SF), c) contact time (t_c), and d) flight time (t_f) at five running speeds. Circles and error bars represent means and standard deviations, respectively.

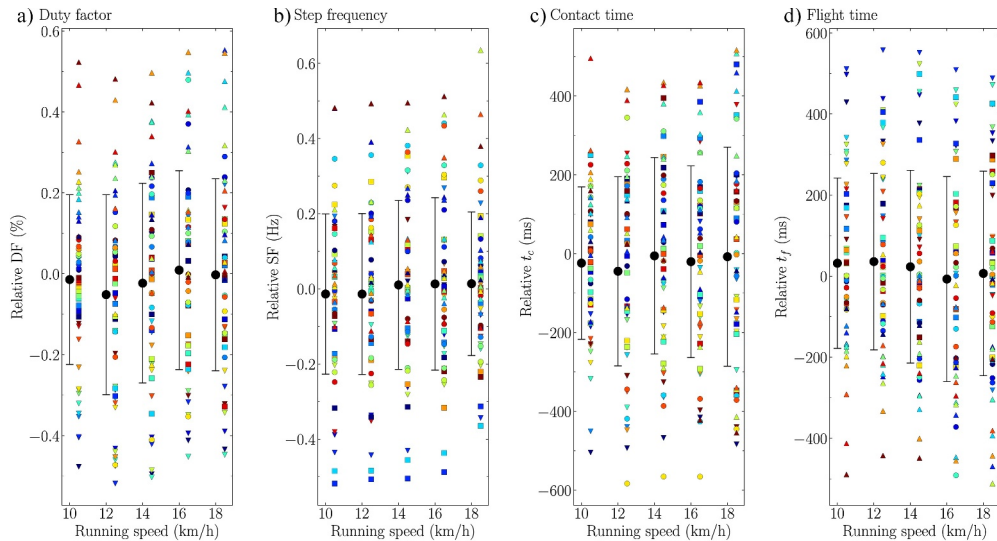


Figure 2. Relative (deviations from the median) a) duty factor (DF), b) step frequency (SF), c) contact time (t_c), and d) flight time (t_f) values at five running speeds for all participants. Circles and error bars represent means and standard deviations, respectively. The combination of a colour and symbol represents a given participant and allows to observe the interindividual differences across both running speeds and temporal variables.

Table 2. Pearson's correlation coefficients (r) and corresponding 95% confidence intervals [lower, upper] and P -values for the relationships of the relative values for pair of running speeds among five different speeds (10, 12, 14, 16, and 18 km/h) and for four temporal variables (duty factor, contact time, flight time, and step frequency).

Running speed pair (km/h)	Statistics	Duty factor	Contact time	Flight time	Step frequency
10 - 12	r	0.86 [0.76, 0.92]	0.83 [0.73, 0.90]	0.89 [0.81, 0.93]	0.98 [0.96, 0.99]
	P	<0.001	<0.001	<0.001	<0.001
10 - 14	r	0.72 [0.56, 0.83]	0.69 [0.51, 0.81]	0.78 [0.64, 0.87]	0.93 [0.88, 0.96]
	P	<0.001	<0.001	<0.001	<0.001
10 - 16	r	0.64 [0.45, 0.78]	0.63 [0.44, 0.77]	0.73 [0.56, 0.83]	0.86 [0.77, 0.92]
	P	<0.001	<0.001	<0.001	<0.001
10 - 18	r	0.58 [0.37, 0.74]	0.54 [0.32, 0.71]	0.66 [0.47, 0.79]	0.77 [0.63, 0.86]
	P	<0.001	<0.001	<0.001	<0.001
12 - 14	r	0.91 [0.84, 0.95]	0.90 [0.83, 0.94]	0.93 [0.88, 0.96]	0.97 [0.94, 0.98]
	P	<0.001	<0.001	<0.001	<0.001
12 - 16	r	0.79 [0.66, 0.88]	0.83 [0.72, 0.90]	0.83 [0.73, 0.90]	0.92 [0.87, 0.96]
	P	<0.001	<0.001	<0.001	<0.001
12 - 18	r	0.68 [0.51, 0.81]	0.71 [0.54, 0.82]	0.73 [0.57, 0.84]	0.83 [0.71, 0.90]
	P	<0.001	<0.001	<0.001	<0.001
14 - 16	r	0.86 [0.77, 0.92]	0.90 [0.83, 0.94]	0.90 [0.83, 0.94]	0.97 [0.95, 0.98]
	P	<0.001	<0.001	<0.001	<0.001
14 - 18	r	0.73 [0.57, 0.83]	0.82 [0.70, 0.89]	0.77 [0.63, 0.86]	0.88 [0.80, 0.93]
	P	<0.001	<0.001	<0.001	<0.001
16 - 18	r	0.86 [0.77, 0.92]	0.91 [0.85, 0.95]	0.90 [0.83, 0.94]	0.93 [0.88, 0.96]
	P	<0.001	<0.001	<0.001	<0.001

Statistically significant correlations ($P \leq 0.05$) are in bold font. Correlations were considered *very high*, *high*, *moderate*, *low*, and *negligible* when absolute r values were between 0.90–1.00, 0.70–0.89, 0.50–0.69, 0.30–0.49, and 0.00–0.29, respectively (Hinkle et al. 2002). Cells were coloured according to the intensity of the correlations, i.e., the larger the correlation, the darker the shaded area.

Correlations between relative SF and t_f were *moderate* at all speeds ($P < 0.001$), except for being *high* at 18 km/h ($P < 0.001$). Correlations were *low* between relative SF and t_c at 10, 12, and 14 km/h ($P \leq 0.03$), and *moderate* at 16 and 18 km/h ($P < 0.001$; Table 3).

Correlations between relative t_c and t_f were *moderate* at 10 km/h ($P < 0.001$), *low* at 12, 14, and 16 km/h ($P \leq 0.04$). Correlations were *negligible* at 18 km/h ($P = 0.21$; Table 3)

The relative temporal variables are depicted in Figure 4 for all participants running at 10 km/h. According to the correlations reported in Table 3, similar figures and corresponding interpretations would result using the four other running speeds (12, 14, 16, and 18 km/h).

Discussion and implications

In agreement with our first hypothesis, smaller differences between two running speeds were associated with greater consistency in running patterns, i.e., greater consistency in the four temporal variables examined (DF, SF, t_c , and t_f). Correlations of the relative values were *high* to *very high* for 2–4 km/h speed differences, whereas *moderate* to *high* for 6–8 km/h differences. In agreement with our second hypothesis, the consistency between DF and SF variables was low at each tested speed, and greater between DF

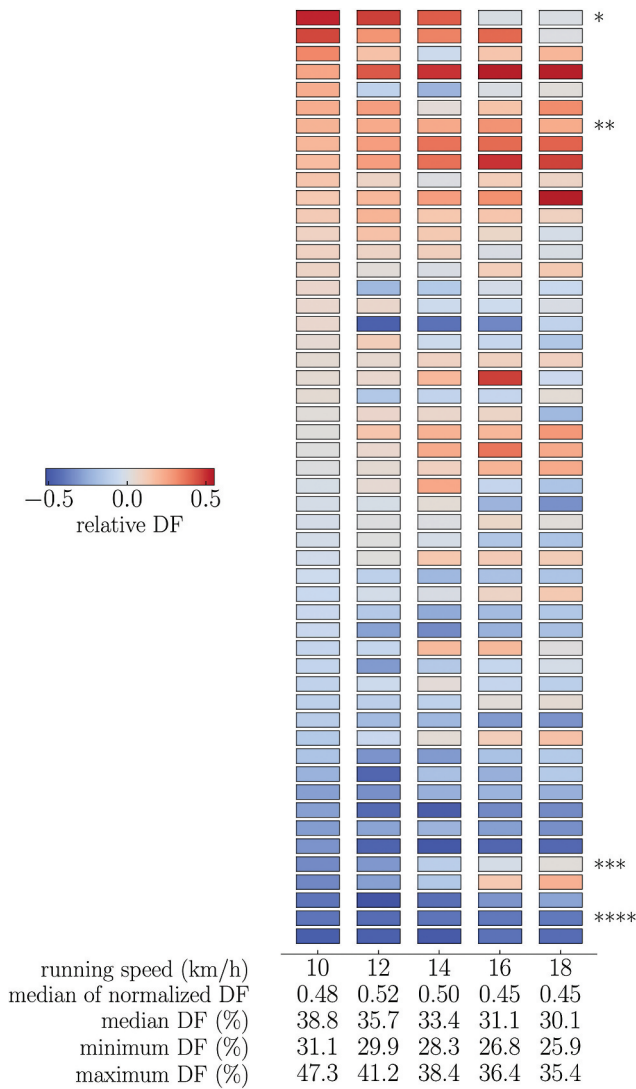


Figure 3. Relative (deviations from the median) duty factor (DF) values for all participants and five running speeds. Runners were relatively positioned according to their relative DF values at 10 km/h. The star symbols depict four participants with distinct behaviours. * participant with a DF much higher than the median at 10 km/h, but a decreasing DF with increasing speed resulting in a DF closer to the median at 18 km/h. ** participant with a DF higher than the median at all tested speeds. *** participant with a DF lower than the median at 10 km/h, but an increasing DF with increasing speed resulting in a DF closer to the median at 18 km/h. **** participant with a DF much lower than the median at all tested speeds.

and both its subcomponents as well as between SF and both its subcomponents than between DF and SF variables. Across speeds, correlations were *low* between relative DF and SF, *very high* between relative DF and t_f , and *low to high* between relative DF and t_c , SF and t_f , and SF and t_f . From a practical perspective, the lower consistency in running patterns observed as speed differences increased suggests that running patterns should be

Table 3. Pearson's correlation coefficients (r) and corresponding 95% confidence intervals [lower, upper] and P -values for the relationships of the relative values for pair of temporal variables among duty factor (DF), contact time (t_c), flight time (t_f), and step frequency (SF), and for five running speeds.

Variable pair	Statistics	10 km/h	12 km/h	14 km/h	16 km/h	18 km/h
DF – SF	r	0.38 [0.11, 0.59]	0.38 [0.13, 0.60]	0.34 [0.07, 0.56]	0.32 [0.05, 0.55]	0.41 [0.16, 0.62]
	P	0.006	0.005	0.01	0.02	0.002
DF – t_f	r	-0.98 [-0.99, -0.97]	-0.96 [-0.98, -0.93]	-0.94 [-0.96, -0.89]	-0.91 [-0.95, -0.85]	-0.91 [-0.95, -0.85]
	P	< 0.001	< 0.001	< 0.001	< 0.001	< 0.001
DF – t_c	r	0.77 [0.63, 0.86]	0.71 [0.54, 0.82]	0.67 [0.48, 0.80]	0.65 [0.46, 0.79]	0.57 [0.35, 0.73]
	P	< 0.001	< 0.001	< 0.001	< 0.001	< 0.001
SF – t_f	r	-0.53 [-0.70, -0.30]	-0.62 [-0.76, -0.41]	-0.64 [-0.78, -0.44]	-0.67 [-0.80, -0.49]	-0.74 [-0.85, -0.59]
	P	< 0.001	< 0.001	< 0.001	< 0.001	< 0.001
SF – t_c	r	-0.30 [-0.53, -0.03]	-0.38 [-0.59, -0.12]	-0.47 [-0.66, -0.23]	-0.50 [-0.68, -0.27]	-0.51 [-0.69, -0.28]
	P	0.03	0.006	< 0.001	< 0.001	< 0.001
t_c – t_f	r	-0.65 [-0.79, -0.46]	-0.49 [-0.67, -0.25]	-0.37 [-0.58, -0.11]	-0.29 [-0.52, -0.02]	-0.18 [-0.43, 0.10]
	P	< 0.001	< 0.001	0.007	0.04	0.21

Statistically significant correlations ($P \leq 0.05$) are in bold font. Correlations were considered *very high*, *high*, *moderate*, *low*, and *negligible* when absolute r values were between 0.90–1.00, 0.70–0.89, 0.50–0.69, 0.30–0.49, and 0.00–0.29, respectively (Hinkle et al., 2002). Cells were coloured according to the intensity of the correlations, i.e., the closer to one the correlation, the darker the red shaded area and the closer to minus one the correlation, the darker the blue shaded area.

assessed at a range of speeds or at a specific speed. In other words, the generalisation of running patterns across speeds may not be valid. Noteworthy is the considerable inter-individual differences observed in terms of the evolution of the relative variables with changes in speed, with some runners demonstrating similar running patterns across speeds and others changing running patterns. The low consistency between DF and SF at a given running speed corroborates previous findings that SF does not necessarily encapsulate the same running pattern information than DF. As proposed by van Oeveren et al. (2021), the full spectrum of running patterns can be described using both DF and SF. Individuals spontaneously and subconsciously adopt their own running pattern. This spontaneous choice was shown to be self-optimised, which is a central element in the development of an economical and safe running gait (Cavanagh & Williams, 1982; Moore et al., 2016; Moore, 2016; Williams & Cavanagh, 1987). Hence, being able to analyse the full spectrum of running patterns may be important to interpret measurements, to design and test specific coaching interventions, and to conduct research to answer questions regarding performance, running economy, and injury risk.

The stronger correlations of the relative temporal variables (DF, SF, t_c , and t_f) for 2–4 km/h than 6–8 km/h speed differences (Table 2) indicate greater consistency in variables when changes in running speeds are smaller. In other words, the running pattern is less consistent when measured over a larger speed range (Figures 2 and 3). This result supports that the running pattern should be defined at a given speed (van Oeveren et al., 2021). Moreover, large interindividual variations in the consistency in running patterns across running speeds were observed (Figure 3). For instance, there were runners with a DF higher than the median at 10 km/h, but a decreasing DF with increasing speed resulting in a DF closer to the median at 18 km/h; runners with a DF higher than the median at all tested speeds; runners with a DF lower than the median at 10 km/h, but an increasing DF with increasing speed resulting in a DF closer to the median at 18 km/h; and runners with a DF much lower than the median at all tested

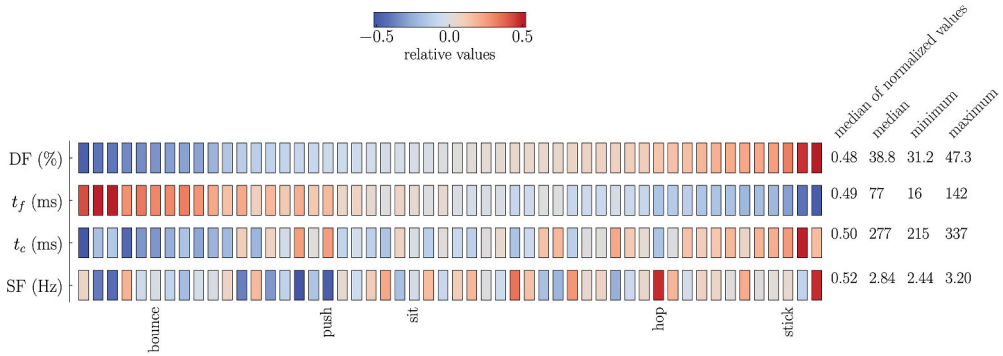


Figure 4. Relative (deviations from the median) duty factor (DF), contact time (t_c), flight time (t_f), and step frequency (SF) values for all participants at 10 km/h. Runners were relatively positioned according to their relative DF values at 10 km/h. The relative t_f values are almost the exact opposite to the relative DF values (Pearson correlation coefficient: -0.98). One participant representing each of the five running pattern categories proposed by van Oeveren et al. (2021) based on the combination of DF and SF is identified, namely bounce (low DF and median SF), push (low SF and median DF), sit (median DF and SF), hop (high SF and median DF), and stick (high DF and median SF).

speeds. This agrees with previous observations that individuals adapt to running speeds differently (Forrester & Townend, 2015; Hébert-Losier et al., 2015; Salo et al., 2011), which might be linked to differences in anthropometric characteristics, age, and running training (van Oeveren et al., 2019). Performing a more detailed analysis that incorporates clustering approaches might reveal subgroups that respond similarly to changes in running speeds. As absolute running speeds were used rather than relative speeds (based on the level of participants), it would not be possible to identify whether sudden changes in DF and/or SF take place at given relative intensities. Overall, coaches should evaluate the running pattern of their athletes using a range of speeds or at a specific speed.

As indicates the *low* correlations between relative DF and SF values at all tested speeds (Table 3), the consistency between these two variables was low. Similarly, Figure 4 depicts how runners with a low/high DF can present with either a low/high SF. These results again reflect previous ones wherein SF does not necessarily encapsulate the same running pattern information than DF, and that combining DF and SF information should allow to describe the full running pattern spectrum (van Oeveren et al., 2021). As depicted in Figure 4, each of the five categories proposed by van Oeveren et al. (2021) were represented herein. Specifically, there were stick (high DF and median SF), bounce (low DF and median SF), hop (high SF and median DF), push (low SF and median DF), and sit (median DF and SF) runners. Moreover, there were runners in between these categories, which also confirms that running patterns operate along a spectrum (Figure 4) (van Oeveren et al., 2021).

Given that the risk of injury was shown greater in runners with a lower DF, especially in softer shoes (Malisoux et al., 2022), quantifying DF might be informative for lower-limb injury prevention. The present study found *very high* correlations between relative DF and t_f values at all tested speed (Table 3 and Figure 4), suggesting that the relative t_f is equivalent to the relative DF. In other words, individual variations in t_f are equivalent to variations in DF. The interrelatedness of DF and t_f and their importance in running are

further highlighted by their established correlations to ground reaction force metrics. Indeed, DF and t_f are related to the average vertical ground reaction force during t_f (Beck et al., 2020) and effective vertical impulse during t_f (Dorn et al., 2012), respectively. Both the average vertical ground reaction force during t_f and effective vertical impulse during t_f are proportional to the peak vertical ground reaction force, as supports the sine wave model of the vertical ground reaction force (Morin et al., 2005) and experimental data (Bonnaerens et al., 2021). The present study reported lower association between relative t_c and DF values (correlations were *moderate* to *high*; Table 3 and Figure 4) than relative t_c to DF values. This result is primarily driven by the midrange DF runners (Figure 4). Altogether, these observations indicate that runners with a relatively long t_f (or short t_c) are runners with a relatively low DF within a group of runners, i.e., DF is mainly controlled by t_f and less by t_c . Overall, the kinematic differences previously observed between high and low DF runners (Lussiana et al., 2019; Patoz et al., 2020) should generalise well to runners with short and long t_f , but might not generalise as well to runners with long and short t_c . Among these three variables (DF, t_c , and t_f), one might be easier to evaluate subjectively, which would be ideal for track and field running coaches, athletes, and practitioners seeking to describe running patterns along a spectrum. Indeed, running coaches could then subjectively evaluate their runners and identify the low DF runners using either DF, t_f , or t_c . Nevertheless, further studies comparing subjective and objective evaluations of runners using DF, t_f , and t_c would be needed to assess if one of these variables is easier to subjectively evaluate than the others.

The *moderate* to *high* correlations between relative SF and t_f values and *low* to *moderate* correlations between relative SF and t_c values (Table 3 and Figure 4) follow the same trend than those between relative DF and t_f or t_c , i.e., correlations were larger with t_f than with t_c . Hence, t_f also determines more of the variation of SF than t_c .

Bear in mind that the running trials were performed on a treadmill, hence generalisation to overground running is not guaranteed (Bailey et al., 2017). Nevertheless, as temporal variables between treadmill and overground running are largely comparable (Van Hooren et al., 2020), our results may still apply to overground running. In addition, absolute running speeds were used, which enables generalisability with findings from other studies using absolute speeds. However, future studies might seek to examine the consistency in running patterns based on DF and SF variables across relative speeds [i.e., percent of maximal aerobic speed or maximal oxygen uptake, or percent of maximal lactate steady state to avoid influencing motor unit recruitment strategy (Burnley & Jones, 2018; Fletcher et al., 2009)] to establish whether sudden changes in DF and/or SF could take place at given relative intensities. Moreover, the eligibility criteria about the level of running performance was independent of the sex of the runners, implying that women were of a higher relative standard than men. Furthermore, no sex distinction was considered in the present study. Although a relatively large sample size was employed ($n = 52$), which would have allowed us to separate out men ($n = 32$) and women ($n = 20$), we preferred to not do such separation to increase the statistical power as well as to keep the method as simple as possible to have an easy-to-read manuscript. Besides, even though correlations are known to be affected by the range of the sample (a large range could lead to very high

correlations), the present study reported only a $13 \pm 12\%$ larger range for men than women when considering the four temporal variables at all tested speeds. The larger range reported for men than women could not be explained by the difference in relative performance standard between men and women. Indeed, even though women reported a 10% slower best half-marathon racing time than men, their range of best racing time was 20% larger than men, which is opposed to the 10% smaller range obtained for the temporal variables compared to men. Nevertheless, future work should focus on the impact of sex when examining the running pattern consistency across running speeds.

Conclusion

This study revealed that the consistency in running patterns decreased as speed differences increased. Therefore, running patterns should be assessed using a range of speeds or at a specific speed. Moreover, there were large interindividual differences across the relative temporal variables examined (DF, SF, t_c , and t_f), highlighting individualised strategies to adapt in running speed changes. In accordance with a previously proposed running pattern model, relative DF and SF were weakly related, indicating that both variables encapsulate different information on running patterns.

Acknowledgments

The authors thank Mr. Chris Tee Chow Li for assistance during the data collection process. The authors also thank the participants for their time and participation.

Authors' contribution

TL carried out the lab work and collected data; AP and BB performed the data analysis, carried out the statistical analysis, and wrote the original draft of the manuscript; AP, TL, BB, CG, DM, and KH-L critically revised the manuscript; TL, CG, DM, and KH-L conceived of the study, designed the study, and coordinated the study. All authors gave final approval for publication and agreed to be held accountable for the work performed therein.

Data availability statement

The datasets supporting this article are available on request to the corresponding author.

Disclosure statement

The authors declare no conflicts of interest.

Funding

This study was financially supported by the University of Bourgogne Franche-Comté (France) and the National Sports Institute of Malaysia.

ORCID

Aurélien Patoz  <http://orcid.org/0000-0002-6949-7989>
 Thibault Lussiana  <http://orcid.org/0000-0002-1782-401X>
 Bastiaan Breine  <http://orcid.org/0000-0002-7959-7721>
 Davide Malatesta,  <http://orcid.org/0000-0003-3905-5642>
 Kim Hébert-Losier  <http://orcid.org/0000-0003-1087-4986>

References

- Arnold, B. J. W., Weeks, B. K., & Horan, S. A. (2019). An examination of treadmill running familiarisation in barefoot and shod conditions in healthy men. *Journal of Sports Science*, 37(1), 5–12. <https://doi.org/10.1080/02640414.2018.1479533>
- Bailey, J. P., Mata, T., & Mercer, J. D. (2017). Is the relationship between stride length, frequency, and velocity influenced by running on a treadmill or overground? *International Journal of Exercise Science*, 10(7), 1067–1075.
- Beck, O. N., Gosyne, J., Franz, J. R., & Sawicki, G. S. (2020). Cyclically producing the same average muscle-tendon force with a smaller duty increases metabolic rate. *Proceedings of the Royal Society B: Biological Sciences*, 287(1933), 20200431. <https://doi.org/10.1098/rspb.2020.0431>
- Blickhan, R. (1989). The spring-mass model for running and hopping. *Journal of Biomechanics*, 22(11), 1217–1227. [https://doi.org/10.1016/0021-9290\(89\)90224-8](https://doi.org/10.1016/0021-9290(89)90224-8)
- Bonnaerens, S., Fiers, P., Galle, S., Derie, R., Aerts, P., Frederick, E., Kaneko, Y., Kaneko, Y., Derave, W., De Clercq, D., Segers, V. (2021). Relationship between duty factor and external forces in slow recreational runners. *BMJ Open Sport & Exercise Medicine*, 7(1), e000996. <https://doi.org/10.1136/bmjsem-2020-000996>
- Burnley, M., & Jones, A. M. (2018). Power–duration relationship: Physiology, fatigue, and the limits of human performance. *European Journal of Sport Science*, 18(1), 1–12. <https://doi.org/10.1080/17461391.2016.1249524>
- Cavanagh, P. R., & Williams, K. R. (1982). The effect of stride length variation on oxygen uptake during distance running. *Medicine and Science in Sports and Exercise*, 14(1), 30–35. <https://doi.org/10.1249/00005768-198201000-00006>
- da Rosa, R. G., Oliveira, H. B., Gomeñuka, N. A., Masiero, M. P. B., da Silva, E. S., Zanardi, A. P. J., & Peyré-Tartaruga, L. A. (2019). Landing-Takeoff asymmetries applied to running mechanics: A new perspective for performance. *Frontiers in Physiology*, 10(415). <https://doi.org/10.3389/fphys.2019.00415>
- Divert, C., Baur, H., Mornieux, G., Mayer, F., & Belli, A. (2005). Stiffness adaptations in shod running. *Journal of Applied Biomechanics*, 21(4), 311–321. <https://doi.org/10.1123/jab.21.4.311>
- Dorn, T. W., Schache, A. G., & Pandy, M. G. (2012). Muscular strategy shift in human running: Dependence of running speed on hip and ankle muscle performance. *The Journal of Experimental Biology*, 215(11), 1944–1956. <https://doi.org/10.1242/jeb.064527>
- Fletcher, J. R., Esau, S. P., & MacIntosh, B. R. (2009). Economy of running: Beyond the measurement of oxygen uptake. *Journal of Applied Physiology*, 107(6), 1918–1922. <https://doi.org/10.1152/jappphysiol.00307.2009>
- Folland, J. P., Allen, S. J., Black, M. I., Handsaker, J. C., & Forrester, S. E. (2017). Running technique is an important component of running economy and performance. *Medicine & Science in Sports & Exercise*, 49(7), 1412–1423. <https://doi.org/10.1249/MSS.0000000000001245>
- Forrester, S. E., & Townend, J. (2015). The effect of running velocity on footstrike angle—a curve-clustering approach. *Gait & Posture*, 41(1), 26–32. <https://doi.org/10.1016/j.gaitpost.2014.08.004>
- Hébert-Losier, K., Mourot, L., & Holmberg, H. C. (2015). Elite and amateur orienteers' running biomechanics on three surfaces at three speeds. *Medicine & Science in Sports & Exercise*, 47(2), 381–389. <https://doi.org/10.1249/mss.00000000000000413>
- Hinkle, D. E., Wiersma, W., & Jurs, S. G. (2002). *Applied statistics for the behavioral sciences*. Houghton Mifflin.

- Hunter, J. P., Marshall, R. N., & McNair, P. J. (2004). Interaction of step length and step rate during sprint running. *Medicine and Science in Sports and Exercise*, 36(2), 261–271. <https://doi.org/10.1249/01.Mss.0000113664.15777.53>
- Lindorfer, J., Kröll, J., & Schwameder, H. (2020). Familiarisation of novice and experienced treadmill users during a running session: Group specific evidence, time and individual patterns. *Human Movement Science*, 69, 102530. <https://doi.org/10.1016/j.humov.2019.102530>
- Lussiana, T., Patoz, A., Gindre, C., Mourot, L., & Hébert-Losier, K. (2019). The implications of time on the ground on running economy: Less is not always better. *The Journal of Experimental Biology*, 222(6), jeb192047. <https://doi.org/10.1242/jeb.192047>
- Maiwald, C., Sterzing, T., Mayer, T. A., & Milani, T. L. (2009). Detecting foot-to-ground contact from kinematic data in running. *Footwear Science*, 1(2), 111–118. <https://doi.org/10.1080/19424280903133938>
- Malisoux, L., Gette, P., Delattre, N., Urhausen, A., & Theisen, D. (2022). Spatiotemporal and ground-reaction force characteristics as risk factors for running-related injury: A secondary analysis of a randomized trial including 800+ recreational runners. *The American Journal of Sports Medicine*, 50(2), 537–544. <https://doi.org/10.1177/03635465211063909>
- Minetti, A. E. (1998). A model equation for the prediction of mechanical internal work of terrestrial locomotion. *Journal of Biomechanics*, 31(5), 463–468. [https://doi.org/10.1016/S0021-9290\(98\)00038-4](https://doi.org/10.1016/S0021-9290(98)00038-4)
- Moore, I. S. (2016). Is there an economical tuning technique? a review of modifiable biomechanical factors affecting running economy. *Sports Medicine*, 46(6), 793–807. <https://doi.org/10.1007/s40279-016-0474-4>
- Moore, I. S., Jones, A. M., & Dixon, S. J. (2016). Reduced oxygen cost of running is related to alignment of the resultant GRF and leg axis vector: A pilot study. *Scandinavian Journal of Medicine & Science in Sports*, 26(7), 809–815. <https://doi.org/10.1111/sms.12514>
- Morin, J.-B., Dalleau, G., Kyröläinen, H., Jeannin, T., & Belli, A. (2005). A simple method for measuring stiffness during running. *Journal of Applied Biomechanics*, 21(2), 167–180. <https://doi.org/10.1123/jab.21.2.167>
- Novacheck, T. F. (1998). The biomechanics of running. *Gait & Posture*, 7(1), 77–95. [https://doi.org/10.1016/S0966-6362\(97\)00038-6](https://doi.org/10.1016/S0966-6362(97)00038-6)
- Ogueta-Alday, A. N. A., Rodriguez-Marroyo, J. A., & Garcia-Lopez, J. (2014). Rearfoot striking runners are more economical than midfoot strikers. *Medicine & Science in Sports & Exercise*, 46(3), 580–585. <https://doi.org/10.1249/MSS.0000000000000139>
- Patoz, A., Lussiana, T., Thouvenot, A., Mourot, L., & Gindre, C. (2020). Duty factor reflects lower limb kinematics of running. *Applied Sciences*, 10(24), 8818. <https://doi.org/10.3390/app10248818>
- Riazati, S., Caplan, N., & Hayes, P. R. (2019). The number of strides required for treadmill running gait analysis is unaffected by either speed or run duration. *Journal of Biomechanics*, 97, 109366. <https://doi.org/10.1016/j.jbiomech.2019.109366>
- Salo, A. I. T., Bezodis, I. N., Batterham, A. M., & Kerwin, D. G. (2011). Elite sprinting: Are athletes individually step-frequency or step-length reliant? *Medicine & Science in Sports & Exercise*, 43(6), 1055–1062. <https://doi.org/10.1249/MSS.0b013e318201f6f8>
- Subotnick, S. I. (1985). The biomechanics of running. Implications for the prevention of foot injuries. *Sports Medicine*, 2(2), 144–153. <https://doi.org/10.2165/00007256-198502020-00006>
- Tranberg, R., Saari, T., Zügner, R., & Kärrholm, J. (2011). Simultaneous measurements of knee motion using an optical tracking system and radiostereometric analysis (RSA). *Acta Orthopaedica*, 82(2), 171–176. <https://doi.org/10.3109/17453674.2011.570675>
- Van Hooren, B., Fuller, J. T., Buckley, J. D., Miller, J. R., Sewell, K., Rao, G., Barton, C., Barton, C., Bishop, C., Willy, R. W. (2020). Is motorized treadmill running biomechanically comparable to overground running? A systematic review and meta-analysis of cross-over studies. *Sports Medicine*, 50(4), 785–813. <https://doi.org/10.1007/s40279-019-01237-z>
- van Overen, B. T., de Ruiter, C. J., Hoozemans, M. J. M., Beek, P. J., & van Dieën, J. H. (2019). Inter-Individual differences in stride frequencies during running obtained from wearable data. *Journal of Sports Sciences*, 37(17), 1996–2006. <https://doi.org/10.1080/02640414.2019.1614137>

- van Oeveren, B. T., de Ruiter, C. J., Beek, P. J., & van Dieën, J. H. (2021). The biomechanics of running and running styles: A synthesis. *Sports Biomechanics*, 1–39. <https://doi.org/10.1080/14763141.2021.1873411>
- Williams, K. R., & Cavanagh, P. R. (1987). Relationship between distance running mechanics, running economy, and performance. *Journal of Applied Physiology*, 63(3), 1236–1245. <https://doi.org/10.1152/jappl.1987.63.3.1236>

8.3 Using statistical parametric mapping to assess the association of duty factor and step frequency on running kinetic

Aurélien Patoz^{1,2,*}, Thibault Lussiana^{2,3,4}, Bastiaan Breine^{2,5}, Elliott Piguët¹, Jonathan Gyuriga¹, Cyrille Gindre^{2,3}, and Davide Malatesta¹

¹ Institute of Sport Sciences, University of Lausanne, 1015 Lausanne, Switzerland

² Research and Development Department, Volodalen Swiss Sport Lab, 1860 Aigle, Switzerland

³ Research and Development Department, Volodalen, 39270 Chavéria, France

⁴ Research Unit EA3920 Prognostic Markers and Regulatory Factors of Cardiovascular Diseases and Exercise Performance, Health, Innovation platform, University of Franche-Comté, Besançon, France

⁵ Department of Movement and Sports Sciences, Ghent University, 9000 Ghent, Belgium

* Corresponding author

Published in **Frontiers in Physiology**

DOI: 10.3389/fphys.2022.1044363



OPEN ACCESS

EDITED BY
Paul Stapley,
University of Wollongong, Australia

REVIEWED BY
Diego Jaén-Carrillo,
Universidad San Jorge, Spain
Jonathan Goodwin,
Charleston Southern University,
United States

*CORRESPONDENCE
Aurélien Patoz,
aurelien.patoz@unil.ch

SPECIALTY SECTION
This article was submitted to
Exercise Physiology,
a section of the journal
Frontiers in Physiology

RECEIVED 14 September 2022
ACCEPTED 23 November 2022
PUBLISHED 05 December 2022

CITATION
Patoz A, Lussiana T, Breine B, Piguet E,
Gyuriga J, Gindre C and Malatesta D
(2022), Using statistical parametric
mapping to assess the association of
duty factor and step frequency on
running kinetic.
Front. Physiol. 13:1044363.
doi: 10.3389/fphys.2022.1044363

COPYRIGHT
© 2022 Patoz, Lussiana, Breine, Piguet,
Gyuriga, Gindre and Malatesta. This is an
open-access article distributed under
the terms of the [Creative Commons
Attribution License \(CC BY\)](https://creativecommons.org/licenses/by/4.0/). The use,
distribution or reproduction in other
forums is permitted, provided the
original author(s) and the copyright
owner(s) are credited and that the
original publication in this journal is
cited, in accordance with accepted
academic practice. No use, distribution
or reproduction is permitted which does
not comply with these terms.

Using statistical parametric mapping to assess the association of duty factor and step frequency on running kinetic

Aurélien Patoz^{1,2*}, Thibault Lussiana^{2,3,4}, Bastiaan Breine^{2,5},
Elliott Piguet¹, Jonathan Gyuriga¹, Cyrille Gindre^{2,3} and
Davide Malatesta¹

¹Institute of Sport Sciences, University of Lausanne, Lausanne, Switzerland, ²Research and Development Department, Volodalen Swiss Sport Lab, Aigle, Switzerland, ³Research and Development Department, Volodalen, France, ⁴Research Unit EA3920 Prognostic Markers and Regulatory Factors of Cardiovascular Diseases and Exercise Performance, Health, Innovation Platform, University of Franche-Comté, Besançon, France, ⁵Department of Movement and Sports Sciences, Ghent University, Ghent, Belgium

Duty factor (DF) and step frequency (SF) were previously defined as the key running pattern determinants. Hence, this study aimed to investigate the association of DF and SF on 1) the vertical and fore-aft ground reaction force signals using statistical parametric mapping; 2) the force related variables (peaks, loading rates, impulses); and 3) the spring-mass characteristics of the lower limb, assessed by computing the force-length relationship and leg stiffness, for treadmill runs at several endurance running speeds. One hundred and fifteen runners ran at 9, 11, and 13 km/h. Force data (1000 Hz) and whole-body three-dimensional kinematics (200 Hz) were acquired by an instrumented treadmill and optoelectronic system, respectively. Both lower DF and SF led to larger vertical and fore-aft ground reaction force fluctuations, but to a lower extent for SF than for DF. Besides, the linearity of the force-length relationship during the leg compression decreased with increasing DF or with decreasing SF but did not change during the leg decompression. These findings showed that the lower the DF and the higher the SF, the more the runner relies on the optimization of the spring-mass model, whereas the higher the DF and the lower the SF, the more the runner promotes forward propulsion.

KEYWORDS

biomechanics, running pattern, spring-mass model, leg stiffness, ground reaction force

Introduction

The running pattern was defined to be multifactorial and as being the product of overall action of human body as early as 1985 (Subotnick, 1985). Indeed, foot placement, arm swing, body angle, rear leg lift, and stride length were suggested to be considered together (Subotnick, 1985). The running pattern was also described as a global and dynamic system (Gindre et al., 2016). For this reason, the running pattern has been analyzed globally by some researchers. For instance, McMahon et al. (1987) defined running with increased knee flexion and long ground contact time (t_c) as *Groucho running* while Arendse et al. (2004) defined running with aligned acromion, greater trochanter, and lateral malleolus as well as short t_c as *Pose running*. As another example, running with either a midfoot or forefoot strike pattern, short stride length, and with the body slightly leaning forward has been named *Chi running* (Dreyer and Dreyer, 2009).

More recently, the synthetic review of van Oeveren et al. (2021) proposed that the full spectrum of running patterns could be described by combining two temporal variables: step frequency (SF) and duty factor (DF). The DF variable represents the product of t_c and stride frequency, where stride frequency is equivalent to approximately half of SF, with less than 4% differences in step times between right and left sides seen in competitive, recreational, and novice runners between 8 and 12 km/h (Mo et al., 2020). Hence, DF reflects the relative contribution of t_c to the running stride (Minetti, 1998; Folland et al., 2017). According to van Oeveren et al. (2021), knowing DF and SF allows to categorize running patterns in one of five distinct categories, namely “stick”, “bounce”, “push”, “hop”, and “sit”, but keeping in mind that running patterns operate along a continuum.

The importance of DF and SF in determining running patterns corroborates previous findings. For instance, Beck et al. (2020) showed that DF is functionally representative of global biomechanical behavior, considering the duration of force production (which takes place during t_c) and its cycle frequency (stride frequency). Moreover, DF was used to categorize runners with distinct running patterns (Lussiana et al., 2019; Patoz et al., 2019; Patoz et al., 2020). High and low DF runners were shown to use different running strategies (Lussiana et al., 2019; Patoz et al., 2020). Indeed, low DF runners exhibited a more symmetrical running step, anterior (midfoot and forefoot) strike pattern, and extended lower limb during t_c than high DF runners, whereas the latter exhibited greater lower limb flexion during t_c , more rearfoot strike pattern, and less vertical oscillation of the whole-body center of mass (COM) to promote forward propulsion than low DF runners (Lussiana et al., 2019; Patoz et al., 2020). Despite these spatiotemporal and kinematic differences, the two DF groups demonstrated similar running economy, indicating the two strategies are energetically equivalent at endurance running speeds (Lussiana et al.,

2019). This would suggest that the two DF groups may optimize differently their running pattern, i.e., high DF runners promotes forward propulsion (pulley system) whereas low DF runners optimized the spring-mass model (Lussiana et al., 2019). This statement was further explored by investigating the relationships between DF and force-length relationship and leg stiffness (k_{leg}).

In relation to SF, this variable can reveal individual strategies to increase running speed (Dorn et al., 2012) or achieve top-end running speeds (Salo et al., 2011). Indeed, the consistency in SF was shown to decrease as speed differences increased (tested running speeds: 10–18 km/h) (Patoz et al., 2022) and each runner was shown to self-optimize his step length over SF ratio (Hunter et al., 2017; van Oeveren et al., 2021). Even in subgroups of individuals with similar sprint velocities, a range of SF and step length combinations are present (Hunter et al., 2004). In addition, SF was shown to be more variable in novice than expert runners, independently of the running speed (10 and 15 km/h) (Fadillioğlu et al., 2022). Furthermore, Bonnaerens et al. (2021) demonstrated that external forces were lower in recreational runners that run with higher DF and SF values (although non-significant for SF).

These previous studies investigated the association of DF or SF on running biomechanics using summary metrics, i.e., specific temporal focus like foot-strike, mid-stance, or toe-off, of signals such as the whole-body COM trajectory or the lower limb angles during t_c (Lussiana et al., 2019; Patoz et al., 2020). This reduction to summary-metric space is not strictly necessary because statistical hypothesis testing can also be conducted in a continuous manner (Pataky, 2012). Indeed, one-dimensional biomechanical curves such as the ground reaction force signals are registrable and their fluctuations can be described and, then, compared expressing them as a function of the normalized stance phase duration (Cavanagh and LaFortune, 1980; Sadeghi et al., 2003). In this case, statistical analysis can be conducted on the original registered curves using statistical parametric mapping (SPM) (Friston et al., 2007), which was recently applied to the field of biomechanics (Pataky, 2010). SPM has the advantages to consider the signal as a whole and presents the results directly in the original sampling space. For this reason, the spatiotemporal biomechanical context is immediately apparent, and allows direct visualization of where do significant differences occur during t_c (Pataky, 2012).

Therefore, the first purpose of the present study was to investigate the association of DF and SF on the vertical and fore-aft ground reaction force signals for treadmill runs at several endurance running speeds using SPM. The second purpose of this study was to investigate the association of DF and SF on variables derived from the vertical and fore-aft ground reaction force signals, i.e., impact ($F_{z,impact}$), active ($F_{z,max}$), braking ($F_{brake,min}$), and propulsive ($F_{prop,max}$) peaks (Luo et al., 2019).

Besides, force related variables that additionally consider the temporal aspect of the running step were also considered because the latter can vary with DF and SF. The third purpose of the present study was to investigate the association of DF and SF on the force-length relationship (Gill et al., 2020) and k_{leg} (Liew et al., 2017).

We hypothesized that 1) a lower DF should be associated to higher vertical and fore-aft ground reaction force fluctuations, and that a lower SF should be associated to higher vertical and fore-aft ground reaction force fluctuations but to a lower extent than for DF (Bonnaerens et al., 2021). Moreover, we hypothesized that 2) both a lower DF and lower SF should be associated to higher peak forces ($F_{z,impact}$, $F_{z,max}$, $F_{brake,min}$, $F_{prop,max}$). Besides, higher DF runners demonstrated a more rearfoot strike pattern (Lussiana et al., 2019; Patoz et al., 2020) but should show lower vertical force than lower DF runners. Hence, we hypothesized that 3) the linearity of the force-length relationship should decrease with increasing DF, due to the higher chance to observe an impact peak when increasing DF, and that a higher DF should be associated to a lower k_{leg} . Furthermore, we hypothesized that 4) a higher SF should correspond to a greater k_{leg} and smaller leg compression, as previously observed (Morin et al., 2007; Coleman et al., 2012; Hobara et al., 2020).

Materials and methods

Participant characteristics

An existing database of 115 recreational runners (Patoz et al., 2021) including 87 males (age: 30 ± 8 y, height: 180 ± 6 cm, leg length, measured from motion capture: 86 ± 4 cm, body mass: 70 ± 7 kg, weekly running distance: 38 ± 24 km, and running experience: 10 ± 8 y) and 28 females (age: 30 ± 7 years, height: 169 ± 5 cm, leg length: 82 ± 4 cm, body mass: 61 ± 6 kg, weekly running distance: 22 ± 16 km, and running experience: 11 ± 8 y) was used in this study. For study inclusion, participants were required to not have current or recent lower-extremity injury (≤ 1 month), to run at least once a week, and to have an estimated maximal aerobic speed ≥ 14 km/h (individual estimation). The study protocol was approved by the local Ethics Committee (CER-VD 2020-00334).

Experimental procedure

After the participants provided written informed consent, retroreflective markers were positioned on the participants (described in Subsec. *Data Collection*) to record their running biomechanics. For each participant, a 1-s static trial was first recorded while he or she stood in a standard anatomical position on an instrumented treadmill (Arsalis T150-FMT-MED,

Louvain-la-Neuve, Belgium) for calibration purposes. Then, a 7-min warm-up run was performed on the same treadmill (9–13 km/h). After a short break (<5 min), three 1-min runs (9, 11, and 13 km/h) were performed in a randomized order (1-min recovery between each run). Three-dimensional (3D) kinematic and kinetic data were collected during the static trial and the last 30 s of the running trials (83 ± 5 running steps), resulting in more than 20 steps being analyzed (Riazati et al., 2019). All participants were familiar with running on a treadmill, as it was part of their usual training program, and they wore their habitual running shoes (shoe mass: 256 ± 48 g and shoe heel-to-toe drop: 7 ± 3 mm).

Data collection

Whole-body 3D kinematic data were collected at 200 Hz using motion capture (8 cameras) and Vicon Nexus software v2.9.3 (Vicon, Oxford, United Kingdom). The laboratory coordinate system was oriented such that the x -, y -, and z -axes denoted the mediolateral (pointing towards the right side of the body), posterior-anterior, and inferior-superior axes, respectively. Forty-three and 39 retroreflective markers of 12.5 mm diameter were used for the static and running trials, respectively. They were affixed to the skin and shoes of individuals on anatomical landmarks using double-sided tape following standard guidelines (Tranberg et al., 2011). Synchronized kinetic data (1000 Hz) were also collected using the force plate embedded into the treadmill.

The 3D marker and ground reaction force data (analog signal) were exported in the .c3d format and processed in Visual3D Professional software v6.01.12 (C-Motion Inc., Germantown, MD, United States). The 3D marker data were interpolated using a third-order polynomial least-square fit algorithm, allowing a maximum of 20 frames for gap filling, and were subsequently low-pass filtered at 20 Hz using a fourth-order Butterworth filter. The 3D ground reaction force signal was filtered using the same filter, and down sampled to 200 Hz to match the sampling frequency of the marker data.

A full-body biomechanical model with six degrees of freedom and 15 rigid segments was constructed from the marker set. The segments included the head, upper arms, lower arms, hands, thorax, pelvis, thighs, shanks, and feet. In Visual3D, the segments were treated as geometric objects, assigned inertial properties and COM locations based on their shape (Hanavan, 1964), and attributed relative masses based on standard regression equations (Dempster, 1955). The whole-body COM location was calculated from the parameters of all 15 segments (the whole-body COM was directly provided by Visual3D).

For all biomechanical measures, the values extracted from the 30-s data collection for each participant, including both right and left steps, were averaged for subsequent statistical analyses.

Event detection

For each running trial, foot-strike, toe-off, and mid-stance events were identified with Visual3D. Foot-strike and toe-off were detected by applying a 20N threshold to the vertical ground reaction force (Smith et al., 2015). Mid-stance was placed at the instant where the fore-aft ground reaction force changed from negative to positive, which permitted to separate the stance phase in a braking and propulsive phase.

Temporal Variables t_c , flight time (t_f), and swing time (t_s) were defined as the time from foot-strike to toe-off of the same foot, from toe-off of one foot to foot-strike of the contralateral foot, and from toe-off to foot-strike of the same foot, respectively.

DF was calculated as $DF = t_c / (t_c + t_s)$, where $1 / (t_c + t_s)$ represents the stride frequency (Minetti, 1998). SF was defined as the inverse of the sum of t_c and t_f , i.e., $SF = 1 / (t_c + t_f)$. Furthermore, SF was normalized by $\sqrt{g/L_0}$ (Lieberman et al., 2015; van Oeveren et al., 2021), where g is the gravitational constant and L_0 the leg length, calculated as the distance between hip and ankle joint center using the static (calibration) trial.

Braking (t_{brake}) and propulsive (t_{prop}) times were given as the time from foot-strike to mid-stance and mid-stance to toe-off of the same foot, respectively.

Compression (t_{comp}) and decompression (t_{decomp}) times were given as the time from foot-strike to the time where the vertical position of the whole-body COM is at its minimum, i.e., where the vertical ground reaction force is maximum, and from the time where the vertical position of the whole-body COM is at its minimum to toe-off, respectively.

Ground reaction force variables

$F_{z,\text{impact}}$ and $F_{z,\text{max}}$ were obtained from the vertical ground reaction force signal (Luo et al., 2019). Noteworthy, an impact peak was not always observed, $F_{z,\text{impact}}$ was quantified in 80% of the running trials. Besides, $F_{\text{brake},\text{min}}$ and $F_{\text{prop},\text{max}}$ were given by the minimum and maximum values of the fore-aft ground reaction force signal (Luo et al., 2019).

The instantaneous vertical loading rate (LR_z) was calculated as the largest slope of the vertical ground reaction force signal between 20 and 80% of the first 15% of the stance phase (Willson et al., 2014). The 15% limit was chosen because an impact peak was not always identified and so that the loading rate of every runner was in the same relative temporal window (Willson et al., 2014). The braking (LR_{brake}) and propulsive (LR_{prop}) loading rates, because of their relation to running-related injuries (Daoud et al., 2012; Willson et al., 2014; Davis et al., 2016; Johnson et al., 2020), were calculated as the largest slopes of the fore-aft ground reaction force signal between foot-strike and the instant of $F_{\text{brake},\text{min}}$ and between mid-stance and the instant of $F_{\text{prop},\text{max}}$, respectively.

The braking (I_{brake}) and propulsive (I_{prop}) impulses were calculated as the integral of the fore-aft ground reaction force signal from foot-strike to mid-stance and from mid-stance to toe-off, respectively (Gottschall and Kram, 2005).

Force variables were all normalized by BW.

Stiffness related variables

The spring-mass characteristics of the lower limb were assessed by computing the force-length relationship (Gill et al., 2020), i.e., the force vector projected along the leg as function of the leg compression/decompression during stance, and k_{leg} (Liew et al., 2017), calculated using both the compression and decompression of the human body (Gill et al., 2020) and adapted from Liew et al. (2017). More explicitly, compressive ($k_{\text{leg, comp}}$) and decompressive ($k_{\text{leg, decomp}}$) leg stiffnesses were given by the maximum of the force vector projected along the leg ($F_{\text{leg,max}}$) divided by the maximum leg compression (ΔL_{comp}) and decompression (ΔL_{decomp}) during stance, respectively. Following the definition of the spring-mass model, i.e., a massless spring attached to a point mass located at the whole-body COM (Blickhan, 1989), the leg length was represented by the magnitude of a 3D leg vector defined from the whole-body COM to the center of pressure of the foot. The center of pressure being subject to large fluctuations for low vertical force values, a 200N vertical threshold was used for foot-strike and toe-off events in this specific case (see supplementary materials). ΔL_{comp} and ΔL_{decomp} were given by the difference between the leg length at foot-strike and the minimum value of the leg length and by the difference between the leg length at toe-off and the minimum value of the leg length, respectively. A leg angle (θ_{leg}) was calculated as the angle between the leg vector and anterior-posterior axis, and evaluated at foot-strike ($\theta_{\text{leg,FS}}$) and toe-off ($\theta_{\text{leg,TO}}$) (Coleman et al., 2012).

$F_{\text{leg,max}}$ was normalized by BW, ΔL_{comp} and ΔL_{decomp} were expressed in absolute and relative (as a percentage of participant's height) units and similarly for $k_{\text{leg, comp}}$ and $k_{\text{leg, decomp}}$.

Statistical analysis

All data are presented as the mean \pm standard deviation. Pearson correlation coefficient (r) between DF and SF together with corresponding 95% confidence interval (lower, upper) were computed at the three running speeds separately. Correlations were considered *very high*, *high*, *moderate*, *low*, and *negligible* when absolute r values were between 0.90–1.00, 0.70–0.89, 0.50–0.69, 0.30–0.49, and 0.00–0.29, respectively (Hinkle et al., 2002). In this study, collinearity between DF and SF was prevented because r was smaller than 0.7 (Table 1) (Van Oeveren et al., 2019). The association of DF and SF on the

TABLE 1 Duty factor (DF) and step frequency (SF), as well as their Pearson's correlation coefficient (r) together with their 95% confidence interval (lower, upper) and statistical significance ($P \leq 0.05$), indicated in bold, for three tested speeds.

Running speed (km/h)	DF (%)	SF (-)	r	P
9	37.7 \pm 3.1	0.80 \pm 0.04	0.32 (0.14, 0.47)	<0.001
11	34.7 \pm 2.5	0.82 \pm 0.04	0.33 (0.15, 0.48)	<0.001
13	32.6 \pm 2.2	0.84 \pm 0.04	0.32 (0.14, 0.47)	<0.001

Note: values are presented as mean \pm standard deviation. SF was normalized by $\sqrt{g/L_0}$, where g is the gravitational constant and L_0 the leg length.

TABLE 2 Temporal variables for runners at endurance running speeds. Significant differences ($P \leq 0.05$) identified by linear mixed effects modeling are indicated in bold. Note: values are presented as mean \pm standard deviation. DF: duty factor, SF: step frequency, t_c : contact time, t_{brake} : brake time, t_{prop} : propulsion time, t_{comp} : compression time, t_{decomp} : decompression time, and t_f : flight time. SF covariate was normalized by $\sqrt{g/L_0}$, where g is the gravitational constant and L_0 the leg length. Up (\uparrow) and down (\downarrow) arrows indicate positive and negative effects of the covariate, respectively. \dagger and \ddagger Significantly different from the value at 13 km/h.

Running speed (km/h)	t_c (ms)	t_{brake} (ms)	t_{prop} (ms)	t_{comp} (ms)	t_{decomp} (ms)	t_f (ms)
9	279 \pm 24	139 \pm 13	140 \pm 14	113 \pm 12	166 \pm 18	92 \pm 24 [†]
11	250 \pm 19	126 \pm 11	124 \pm 10	104 \pm 11	146 \pm 13	111 \pm 20 [‡]
13	228 \pm 17	116 \pm 10	112 \pm 9	96 \pm 10	132 \pm 12	122 \pm 18
Running speed effect (P)	<0.001	0.33	0.39	0.26	0.02	<0.001
DF covariate effect (P)	\uparrow <0.001	\uparrow <0.001	\uparrow <0.001	\uparrow <0.001	\uparrow <0.001	\downarrow <0.001
SF covariate effect (P)	\downarrow <0.001	\downarrow <0.001	\downarrow <0.001	\downarrow <0.001	\downarrow <0.001	\downarrow <0.001

vertical and fore-aft ground reaction force signals (along the entire stance phase) was examined using SPM and linear regression for each tested speed. Bonferroni correction was employed to consider that three running speeds were tested. To compare participants, the stance phase was normalized and therefore expressed in percentage. Besides, residual plots were inspected and no obvious deviations from homoscedasticity or normality were observed. Hence, the association of DF and SF (covariates) and running speed on temporal, ground reaction force, and stiffness related variables was evaluated using a linear mixed effects model fitted by restricted maximum likelihood. The within-subject nature was controlled for by including random effects for participants (individual differences in the intercept of the model). The fixed effects included running speed (categorical variable) and DF and SF (continuous variables). The linearity of the force-length relationship was quantified using the coefficient of determination (R^2) during both leg compression (R^2_{comp}) and decompression (R^2_{decomp}). However, the calculation of R^2 was modified so that R^2_{comp} and R^2_{decomp} values were computed by comparing the compression and decompression force-length relationships to the perfectly elastic compression and decompression lines, i.e., linear relations obtained using slopes equal to $k_{\text{leg, comp}}$ and $k_{\text{leg, decomp}}$, respectively (Gill et al., 2020). In other words, R^2 evaluates how far the force-length relationship is from a linear model obtained using k_{leg} . Statistical analysis was performed using spm1D (v0.4.6, <https://spm1d.org>) (Pataky,

2012), Python (v3.7.4, <http://www.python.org>), and Jamovi (v1.6.23, <https://www.jamovi.org>) with a level of significance set at $p \leq 0.05$.

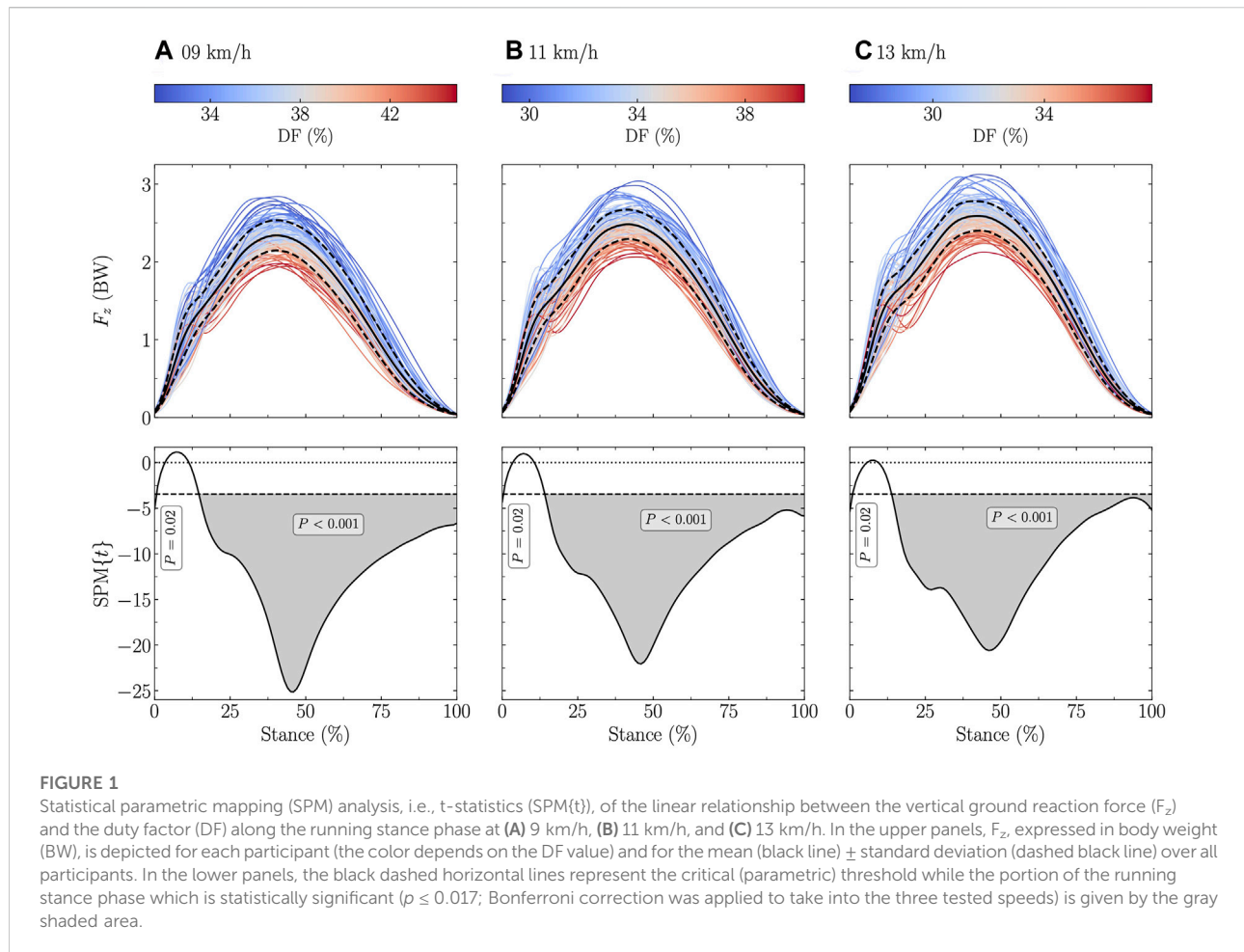
Results

The increase of the running speed from 9 to 13 km/h was accompanied with a decrease of DF of $13.3 \pm 3.8\%$ and an increase of SF of $5.9 \pm 3.1\%$. The correlation between DF and SF was low but significant at all tested speeds ($r \leq 0.32$; $p < 0.001$; Table 1).

t_c , t_{brake} , t_{prop} , t_{comp} , and t_{decomp} significantly increased with increasing DF while t_f decreased ($p < 0.001$; Table 2). These six variables significantly decreased with increasing SF ($p < 0.001$; Table 2). Besides, t_c and t_{decomp} decreased with increasing speed while t_f increased with increasing speed ($p \leq 0.02$; Table 2).

The vertical ground reaction force signal was significantly negatively related to DF at all tested speeds (stance range: 0 and 15–100% at 9 and 11 km/h, and 0 and 14–100% at 13 km/h; Figure 1). Similar findings were obtained for SF but to a lower extent (stance range: 60–99% at 9 km/h, 59–99% at 11 km/h, and 67–83% at 13 km/h; Figure 2).

The fore-aft ground reaction force signal was significantly positively related to both DF and SF in the first 50% of the stance (negative fore-aft force) and negatively related to both DF and SF



in the last 50% of the stance at all tested speeds (stance range for DF: 5–11, 27–34, and 69–100% at 9 km/h, 7–12, 29–35, and 71–100% at 11 km/h, and 6–13 and 68–100% at 13 km/h; **Figure 3**; stance range for SF: 15–33 and 68–95% at 9 km/h, 14, 19–35, 47–52, and 70–98% at 11 km/h, and 14–28 and 71–89% at 13 km/h; **Figure 4**).

$F_{z,max}$, $F_{z,impact}$, $F_{prop,max}$, LR_{prop} , and I_{brake} significantly decreased with increasing DF while $F_{brake,min}$, LR_{brake} , and I_{prop} significantly increased ($p \leq 0.01$; **Table 3**). $F_{z,impact}$, $F_{brake,min}$, LR_{prop} , and I_{brake} significantly increased with increasing SF while, $F_{prop,max}$ and I_{prop} significantly decreased ($p \leq 0.02$; **Table 3**). Considering absolute values, all the ground reaction force variables significantly increased with increasing speed ($p \leq 0.005$; **Table 3**).

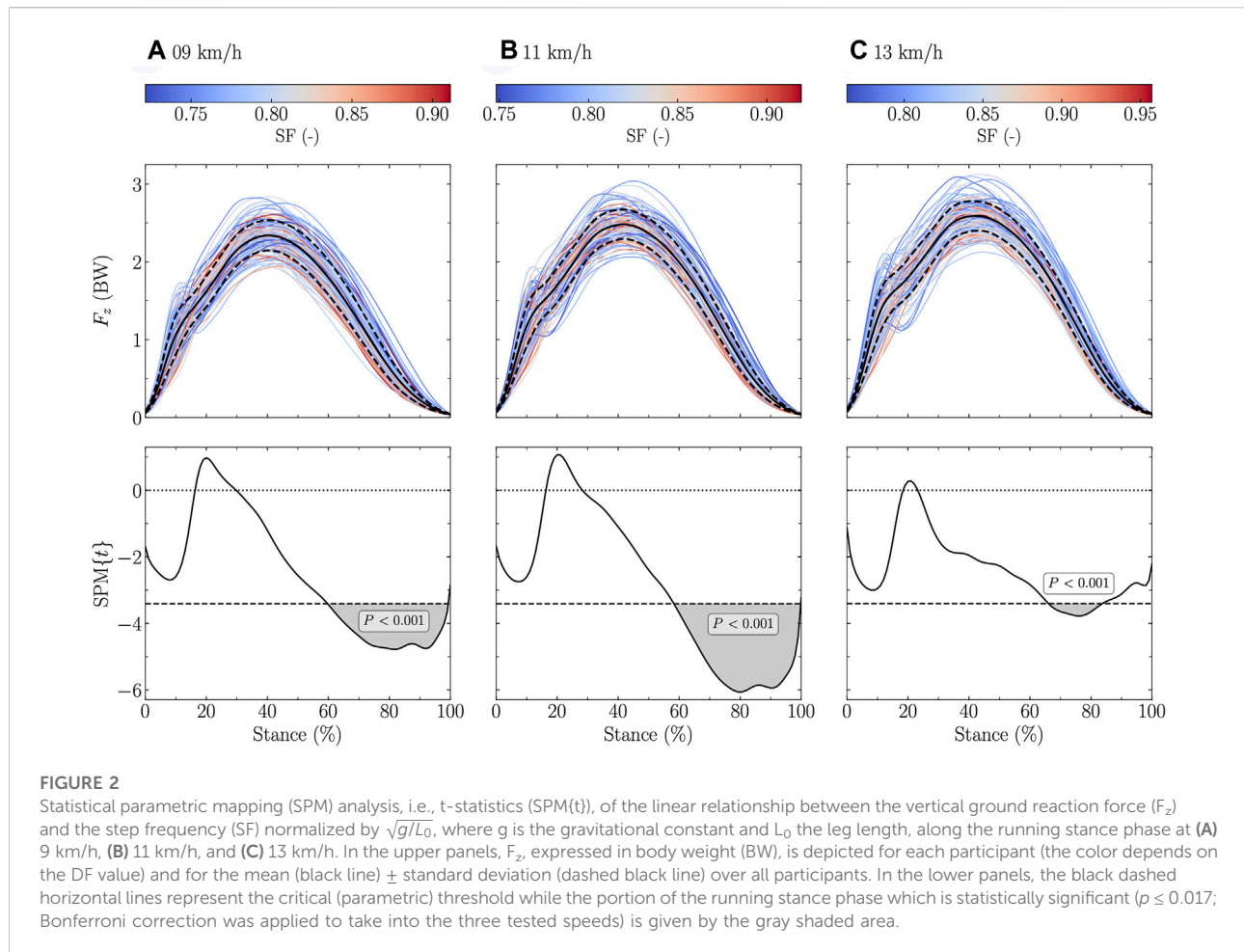
The force-length relationships of all participants, colored according to their DF and SF, are depicted in **Figures 5, 6**, respectively, for each tested speeds and separately for the compression and decompression phases. R_{comp}^2 significantly

decreased with increasing DF or running speed, and increased with increasing SF ($p \leq 0.007$; **Table 4**), while there was no change of R_{decomp}^2 with DF, SF, and speed.

$F_{z,max}$, ΔL_{comp} , $k_{leg, comp}$, and $k_{leg, decomp}$ significantly decreased with increasing DF while ΔL_{decomp} and $\theta_{leg,TO}$ significantly increased ($p \leq 0.03$; **Table 5**). ΔL_{comp} , ΔL_{decomp} , and $\theta_{leg,TO}$ significantly decreased with increasing SF while $k_{leg, comp}$, and $k_{leg, decomp}$ significantly increased ($p < 0.001$; **Table 5**). $F_{leg,max}$, ΔL_{decomp} , $k_{leg, decomp}$, $|\theta_{leg,FS}|$, and $\theta_{leg,TO}$ significantly increased with increasing speed ($p \leq 0.005$; **Table 5**).

Discussion

According to the first hypothesis, lower DF and lower SF were associated to higher vertical and fore-aft ground reaction force fluctuations, but SF to a lower extent than DF. Besides, according to the second hypothesis, larger $F_{z,max}$, $F_{z,impact}$, |



$F_{\text{brake,min}}$, and $F_{\text{prop,max}}$ were reported for lower DF values as well as larger $|F_{\text{brake,min}}|$, and $F_{\text{prop,max}}$ for lower SF values. However, there was no association between SF and $F_{z,\text{max}}$ and a larger $F_{z,\text{impact}}$ was reported for higher SF values, which partly refuted the second hypothesis. The linearity of the force-length relationship during the leg compression decreased with increasing DF but did not change during the leg decompression, partly refuting the third hypothesis. According to the fourth hypothesis, a higher SF was associated to a larger k_{leg} and a smaller leg compression.

DF was previously analytically shown to be inversely proportional to the maximum of an approximated, based on a sine-wave model (Beck et al., 2020), vertical ground reaction force signal (Morin et al., 2005). This previous knowledge is further expanded by the present results which showed that $F_{z,\text{max}}$ is significantly negatively related to DF (Table 3), and corroborates previous findings which showed that DF was negatively correlated to $F_{z,\text{max}}$ (Bonnaerens et al., 2021). This

suggests that DF should be inversely related to $F_{z,\text{max}}$ without using a sine-wave model to approximate the vertical ground reaction force. Moreover, the present study extends to the fact that a lower DF results in a larger vertical ground reaction force during most of the stance (~15–100%; Figure 1) but after the 15% temporal window representative of the “impact” phase (Willson et al., 2014). Therefore, the SPM analysis additionally revealed that the association between DF and the vertical ground reaction force signal is not only given at $F_{z,\text{max}}$ but through almost the entire stance (after the impact phase; $\geq 15\%$). This result suggests that the shape of the vertical ground reaction force during the impact phase is not affected by the DF. This result might be attributed to the fact that the vertical ground reaction force signal is given by the force contributions of two discrete body mass components, i.e., a distal mass composed of the foot and shank and the remaining mass (Clark et al., 2017; Udofa et al., 2019). Hence, the impact phase, represented by the distal mass in this model, might not be affected by the DF. This study also showed

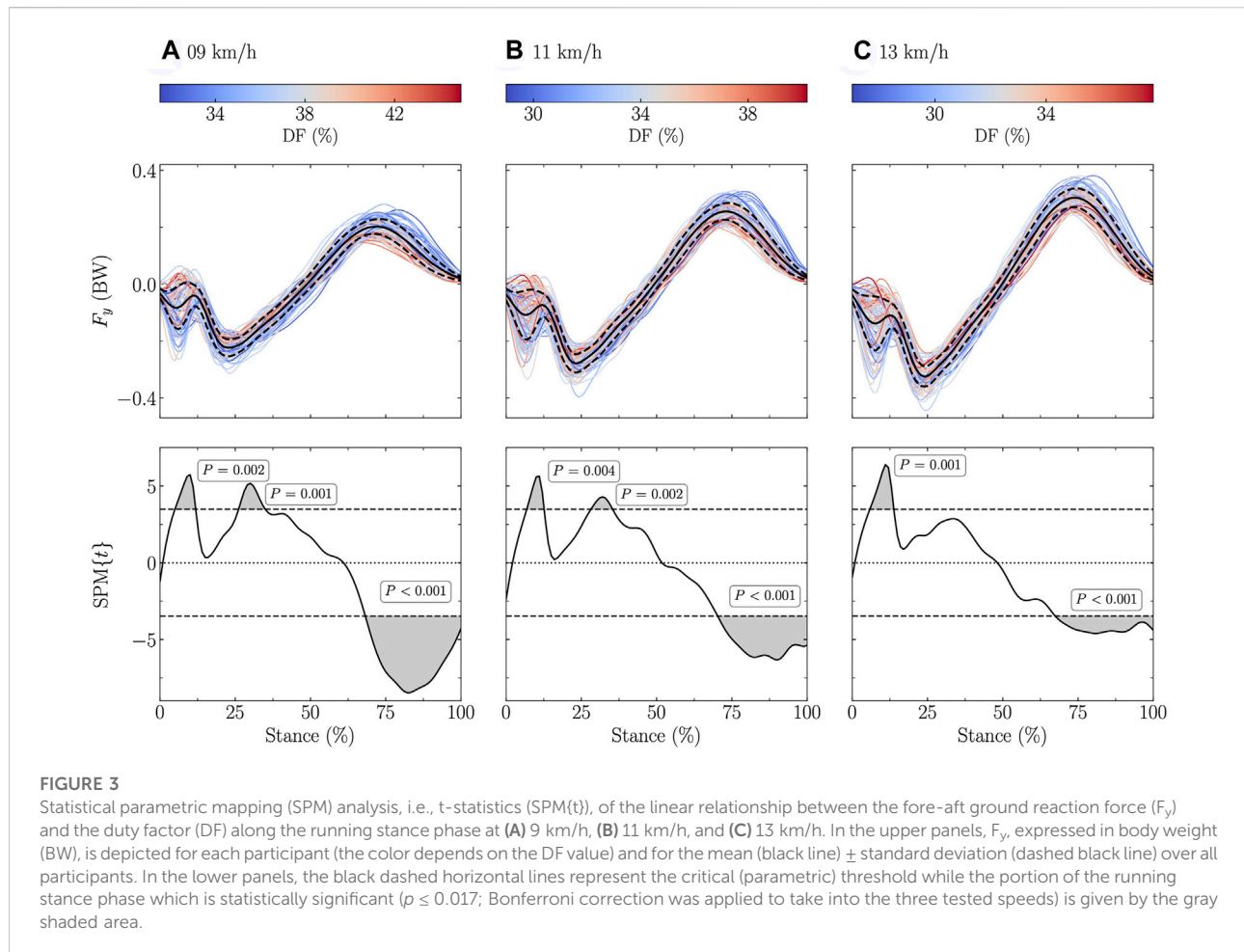


FIGURE 3

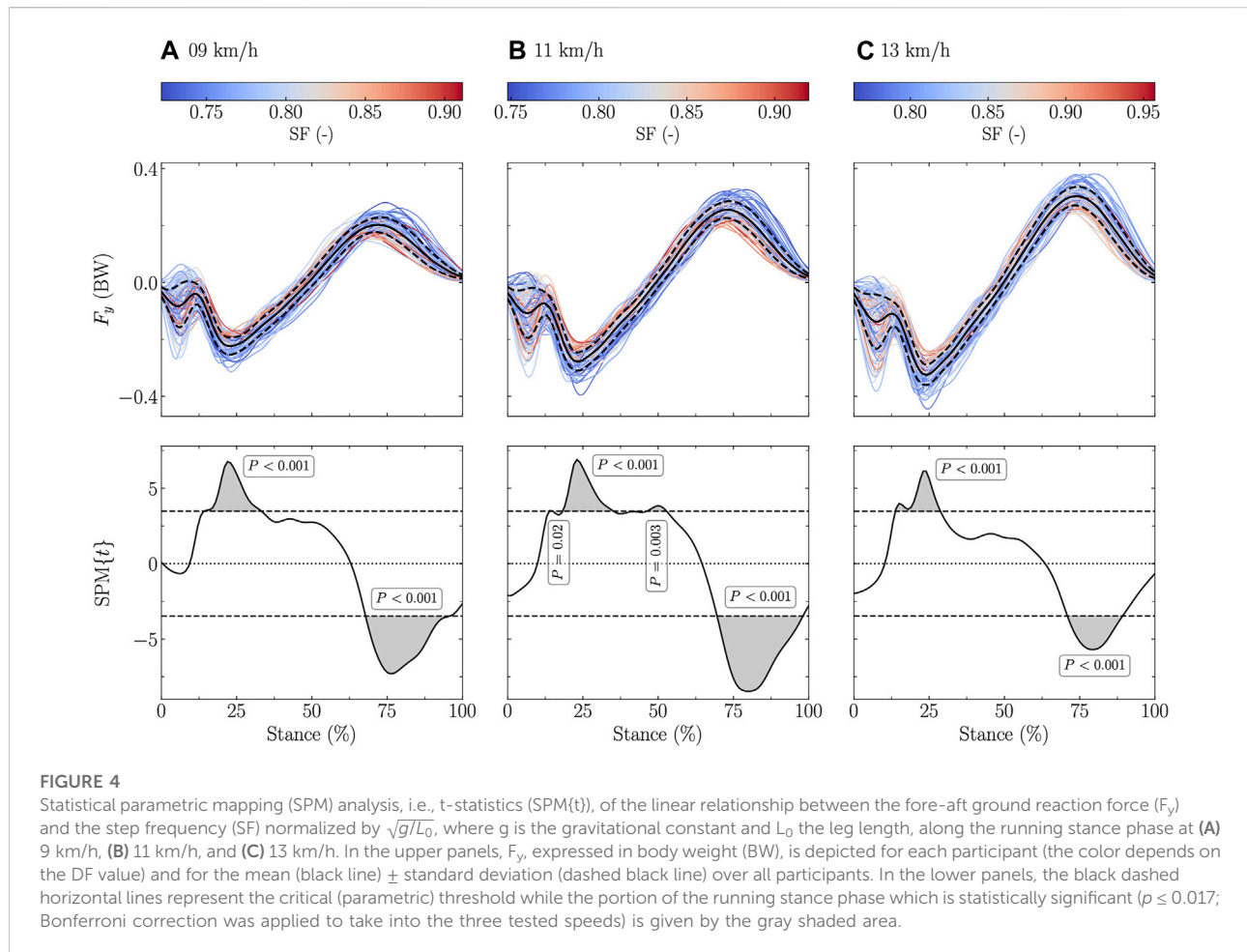
Statistical parametric mapping (SPM) analysis, i.e., t-statistics (SPM(t)), of the linear relationship between the fore-aft ground reaction force (F_y) and the duty factor (DF) along the running stance phase at (A) 9 km/h, (B) 11 km/h, and (C) 13 km/h. In the upper panels, F_y , expressed in body weight (BW), is depicted for each participant (the color depends on the DF value) and for the mean (black line) \pm standard deviation (dashed black line) over all participants. In the lower panels, the black dashed horizontal lines represent the critical (parametric) threshold while the portion of the running stance phase which is statistically significant ($p \leq 0.017$; Bonferroni correction was applied to take into the three tested speeds) is given by the gray shaded area.

that for the runners having a visible $F_{z, \text{impact}}$, this $F_{z, \text{impact}}$ was significantly larger for lower than higher DF values (Table 3). This discrepancy could be explained by fact that the impact peak might be happening at a different instant of the running stance phase (within the first 15%) depending on individuals.

Similarly, a lower SF resulted in a larger vertical ground reaction force, but only at the end of the stance (~65–95%; Figure 2). This was likely related to the longer step length for running at the same speed. In fact, it has previously been shown that a larger vertical ground reaction force (i.e., support force) produces a larger step length (Weyand et al., 2000; Dorn et al., 2012). Our SPM analysis demonstrated that this larger support force was located only at the end of the stance. Indeed, $F_{z, \text{max}}$ was not related to SF (Table 3). Nonetheless, the reason why this larger support force was located at the end of the stance could not readily be explained. Besides, $F_{z, \text{impact}}$ significantly increased with increasing SF (Table 3). This result contradicts previous findings which observed a

decrease of the impact peak with increasing SF (Lieberman et al., 2015). However, these findings were obtained when asking individuals to voluntarily increase their SF. Hence, this could lead to a different running pattern than the spontaneous running pattern of runners with a naturally high SF.

The present study reported no association of DF and SF on LR_z (Table 3). This could partly follow from the fact that the SPM analysis did not report any significant association between DF and SF and the vertical ground reaction force during the impact phase (the first 15% of the stance). This result corroborates the absence of correlation between LR_z and both DF and SF at slow running speeds, as reported by Bonnaerens et al. (2021). However, assuming that DF is partly related to foot-strike pattern, i.e., the higher the DF, the more likely that this runner is a rearfoot striker (Lussiana et al., 2019; Patoz et al., 2020), this result contradicts the result of a meta-analysis which reported higher LR_z for rearfoot than non-rearfoot strikers (Almeida et al., 2015).



The fore-aft ground reaction force signal was positively related to DF around ~5–10% of the stance and to both DF and SF around ~25–35% (positively) and ~70–90% (negatively; Figures 3, 4). The positive association of DF on the fore-aft ground reaction force signal reported by the SPM analysis around ~5–10% of the stance can be explained by the foot-strike pattern. Indeed, fore-foot strikers were shown to have a negative spike on the fore-aft ground reaction force signal around ~5–10% of the stance (Nordin et al., 2017) and DF was related to the footstrike pattern (Lussiana et al., 2019; Patoz et al., 2020). However, the association of DF on the fore-aft force signal around ~5–10% of the stance was not accompanied by an association of DF on the vertical force signal at the same percentage of the stance. This suggests that the effect of DF during the impact phase was more important in the fore-aft than vertical force signal. The other two significant regions are around the braking and propulsive peaks ($F_{\text{brake,min}}$ and $F_{\text{prop,max}}$), which were also significantly related to DF and SF (Table 3). These

results partly corroborate previous observations, which showed that the peak braking force was correlated to DF but not to SF (Bonnaerens et al., 2021). Moreover, they confirm that larger ground reaction forces during propulsion are needed to lift and accelerate the body during stance to generate longer step lengths (Schache et al., 2014). As previously suggested (van Oeveren et al., 2021), combining vertical and horizontal ground reaction forces into a single vector could be useful to properly characterize their orientations and actions and carefully describe the relationship of this single vector with DF and SF, especially at the end of the stance.

The linearity of the force-length relationship was higher for lower DF and SF than for higher DF and SF runners during the leg compression but there was no difference during the leg decompression (Table 4). This means that higher DF and SF values were associated to more variations of the instantaneous compressive stiffness, i.e., the slope for each pair of point during the leg compression. However, the decompressive stiffness

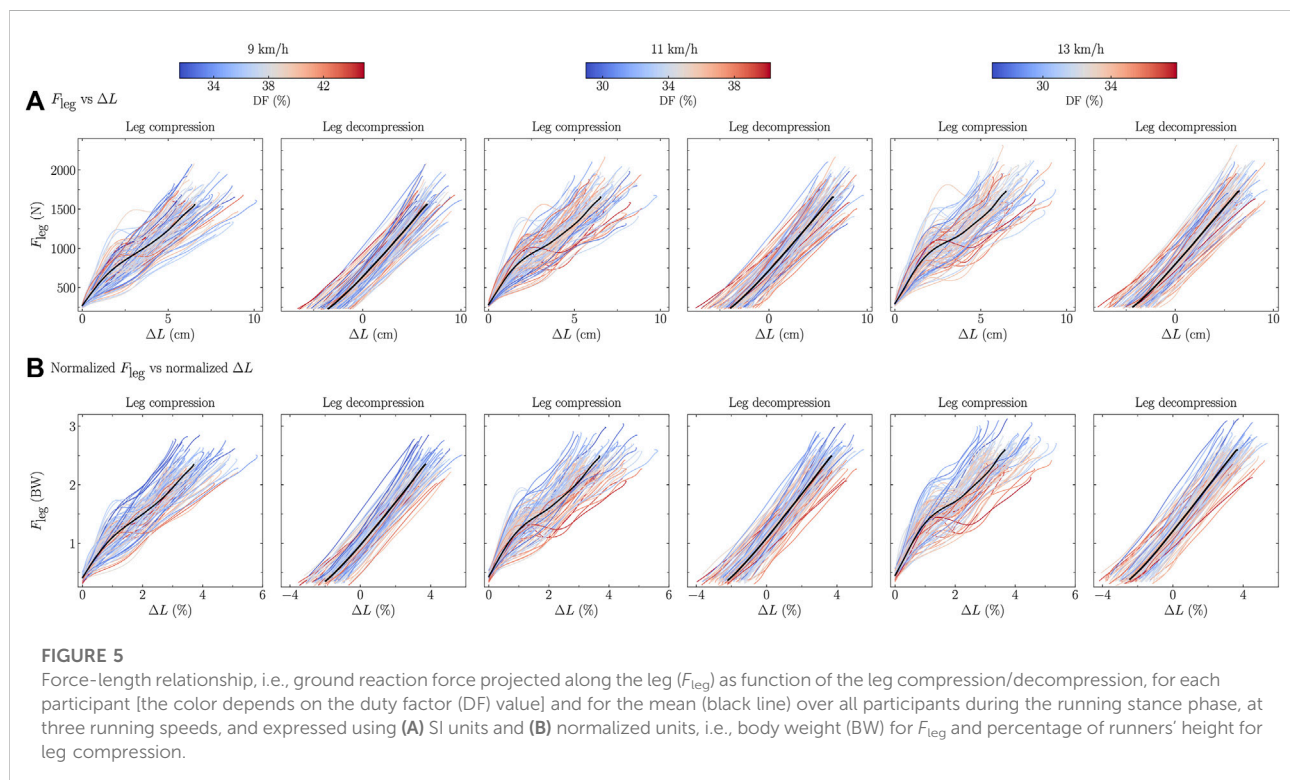
TABLE 3 Ground reaction force variables for runners at endurance running speeds. Significant differences ($P \leq 0.05$) identified by linear mixed effects modeling are indicated in bold.

Running speed (km/h)	$F_{z,max}$ (BW)	$F_{z,impact}$ (BW)	$F_{brake,min}$ (BW)	$F_{prop,max}$ (BW)	LR_z (BW/s)	LR_{brake} (BW/s)	LR_{prop} (BW/s)	I_{brake} (BW · s)	I_{prop} (BW · s)
9	2.36 ± 0.19 ^{a,b}	1.53 ± 0.28 ^{a,b}	-0.24 ± 0.03 ^{a,b}	0.21 ± 0.03 ^{a,b}	49.0 ± 11.9 ^{a,b}	-13.4 ± 2.7 ^{a,b}	5.7 ± 0.8 ^{a,b}	-0.016 ± 0.002 ^{a,b}	0.017 ± 0.002 ^{a,b}
11	2.50 ± 0.19	1.63 ± 0.30	-0.29 ± 0.03 ^b	0.26 ± 0.03 ^b	58.7 ± 13.4 ^b	-16.2 ± 3.1 ^b	7.5 ± 1.0 ^b	-0.018 ± 0.002 [‡]	0.019 ± 0.002 ^b
13	2.62 ± 0.19	1.81 ± 0.32	-0.34 ± 0.03	0.31 ± 0.03	68.4 ± 15.2	-18.1 ± 3.4	9.7 ± 1.4	-0.019 ± 0.002	0.021 ± 0.002
Running speed effect (P)	0.005	<0.001	<0.001	<0.001	<0.001	<0.001	<0.001	<0.001	<0.001
DF covariate effect (P)	↓ <0.001	↓ <0.001	↑ 0.01	↓ <0.001	0.34	↑ <0.001	↓ <0.001	↓ 0.004	↑ <0.001
SF covariate effect (P)	0.33	↑ <0.001	↑ <0.001	↓ <0.001	0.11	0.17	↑ 0.02	↑ <0.001	↓ <0.001

Note: values are presented as mean ± standard deviation. DF: duty factor, SF: step frequency, $F_{z,max}$ and $F_{z,impact}$: active and impact peaks, $F_{brake,min}$: minimum braking force, $F_{prop,max}$: maximum propulsive force, LR_z : instantaneous vertical loading rate, LR_{brake} : instantaneous braking loading rate, LR_{prop} : instantaneous propulsive loading rate, and I_{brake} and I_{prop} : braking and propulsive impulses. Ground reaction force variables were normalized by body weight (BW) and SF covariate was normalized by $\sqrt{g/L_0}$, where g is the gravitational constant and L_0 the leg length. Up (↑) and down (↓) arrows indicate positive and negative effects of the covariate, respectively.

^aSignificantly different from the value at 11 km/h.

^bSignificantly different from the value at 13 km/h.



during the leg decompression was independent of DF and SF (Table 4). This result corroborates the choice made by several authors to use the decompression phase instead of the compression one to calculate the vertical stiffness (Cavagna et al., 1988; Schepens et al., 1998). Deviation from linearity of the force-length relationship among individuals was also

reported by Gill et al. (2020). Indeed, these authors reported that the linearity of the force-length curve was foot-strike index (foot-strike pattern) dependent and that this curve should be investigated before using the spring-mass model. Furthermore, these authors suggested that for $R^2 < 0.95$, it may be more appropriate to segment the stance phase and to individually

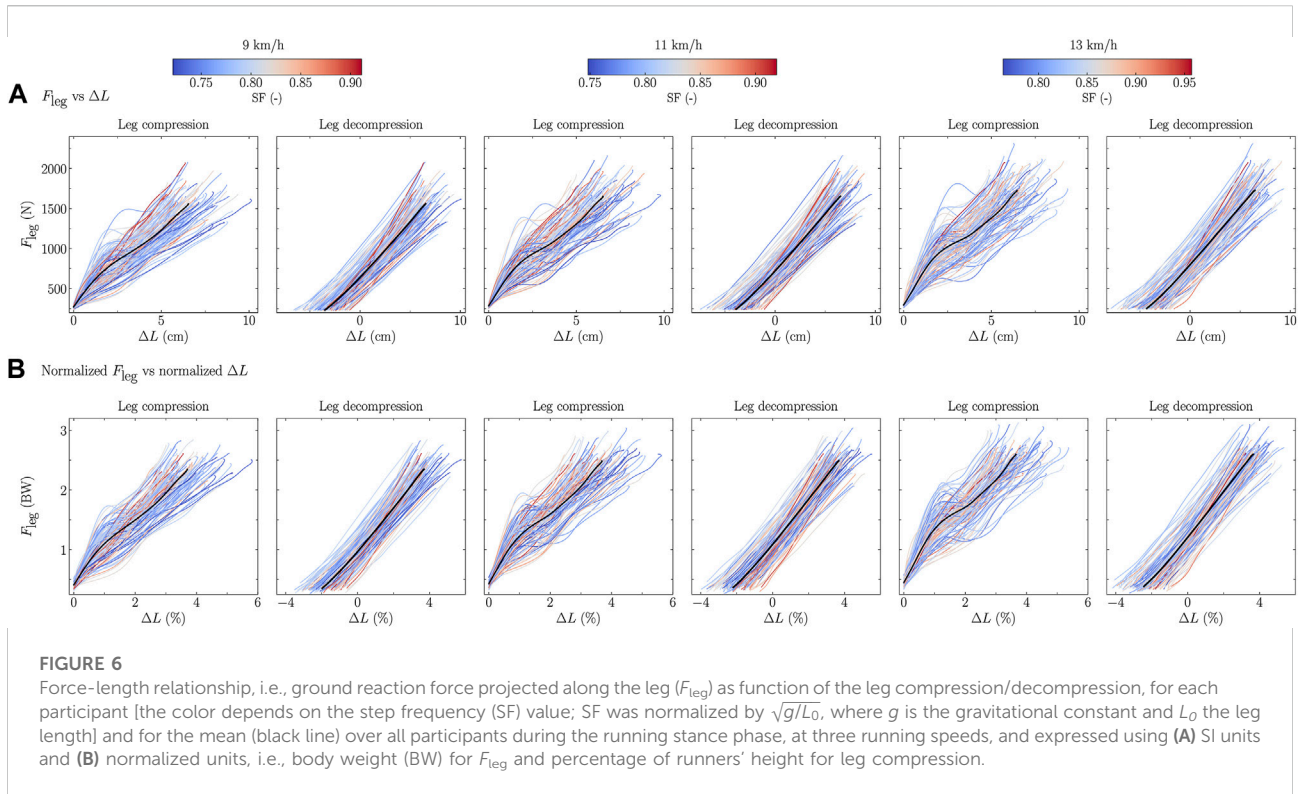


TABLE 4 Linearity of the force-length relationship during leg compression (R^2_{comp}) and decompression (R^2_{decomp}). Significant differences ($p \leq 0.05$) identified by linear mixed effects modeling are indicated in bold.

Running speed (km/h)	R^2_{comp}	R^2_{decomp}
9	$0.95 \pm 0.06^{a,b}$	0.99 ± 0.02
11	0.93 ± 0.08^b	0.99 ± 0.01
13	0.90 ± 0.10	0.99 ± 0.01
Running speed effect (P)	<0.001	0.14
DF covariate effect (P)	↓ <0.001	0.06
SF covariate effect (P)	↑ 0.007	0.85

Note: values are presented as mean \pm standard deviation. DF: duty factor, SF: step frequency, SF covariate was normalized by $\sqrt{g/L_0}$, where g is the gravitational constant and L_0 the leg length. Up (↑) and down (↓) arrows indicate negative effects of the covariate.

^aSignificantly different from the value at 11 km/h.

^bSignificantly different from the value at 13 km/h.

investigate the different subphases. Hence, the deviation from linearity observed herein during the leg compression for higher than lower DF and SF runners suggest that the stiffness should be split into several phases during the leg compression and thus invalidate the usage of $k_{leg, comp}$ for these runners. However, the linearity observed during leg decompression for all participants suggest that $k_{leg, decomp}$ could be used.

This study reported that $k_{leg, decomp}$ and $F_{leg, max}$ significantly increased with decreasing DF while ΔL_{decomp} decreased (Table 5).

Hence, the elastic energy (E_{el}), which could be calculated as $E_{el} = \frac{F_{leg, max}^2 k_{leg, decomp}}{2}$ using the definition of the spring-mass model, increased with decreasing DF. Furthermore, the compression was more vertical and t_c was shorter for lower than higher DF runners. High DF runners could be characterized by a slow stretch-shortening cycle (runners with t_c longer than 250 m) while low DF runners by a fast one (Vogt and Hoppeler, 2014). These results, together with the higher linearity of the force-length curve during the compression phase observed for lower than higher DF runners suggest that a lower DF runner better optimizes the spring-mass model than a higher DF runner. On the contrary, $\theta_{leg, TO}$ significantly increased with increasing DF (Table 5). These results suggest that the higher the DF, the higher the promotion of forward propulsion of the body. This compensates for the lower utilization of the spring-mass model of higher than lower DF runners and corroborates previous findings (Lussiana et al., 2019; Patoz et al., 2020). These findings bring further evidence and reinforce previous statements that low DF runners rely more on the optimization of the spring-mass model whereas high DF runners promotes forward propulsion (pulley system) (Lussiana et al., 2019; Patoz et al., 2020).

This study further revealed that the higher the SF, the larger $k_{leg, decomp}$ and the smaller ΔL_{decomp} (Table 5), which corroborates previous findings (Coleman et al., 2012; Hobara et al., 2020). Moreover, $\theta_{leg, TO}$ significantly decreased with increasing SF (Table 5). These results suggest that higher SF

TABLE 5 Stiffness variables for runners at endurance running speeds. Significant differences ($P \leq 0.05$) identified by linear mixed effects modeling are indicated in bold.

Running speed (km/h)	$F_{leg,max}$ (BW)	ΔL_{comp} (cm)	ΔL_{decomp} (cm)	ΔL_{comp} (%)	ΔL_{decomp} (%)	$k_{leg,comp}$ (kN/m)	$k_{leg,decomp}$ (kN/m)	$k_{leg,comp}$ (BW/%)	$k_{leg,decomp}$ (BW/%)	$\theta_{leg,FS}$ (deg)	$\theta_{leg,TO}$ (deg)
9	2.36 ± 0.19 ^{a,b}	6.5 ± 1.1	10.0 ± 1.0 ^{a,b}	3.7 ± 0.6	5.7 ± 0.6 ^{a,b}	24.6 ± 4.5	15.8 ± 2.4 ^{a,b}	0.66 ± 0.11	0.42 ± 0.06 ^{a,b}	-8.1 ± 2.6 ^{a,b}	13.4 ± 1.6 ^{a,b}
11	2.50 ± 0.19	6.5 ± 1.1	10.4 ± 1.1 ^b	3.7 ± 0.6	5.9 ± 0.6 ^b	26.3 ± 5.0	16.2 ± 2.4 ^b	0.70 ± 0.13	0.43 ± 0.06 ^b	-9.2 ± 2.5 ^b	15.0 ± 1.5 ^b
13	2.62 ± 0.19	6.4 ± 1.1	10.7 ± 1.1	3.6 ± 0.6	6.1 ± 0.6	27.8 ± 5.3	16.3 ± 2.3	0.74 ± 0.13	0.44 ± 0.06	-10.2 ± 2.4	16.5 ± 1.5
Running speed effect (P)	0.005	0.38	<0.001	0.39	<0.001	0.30	<0.001	0.13	<0.001	<0.001	<0.001
DF covariate effect (P)	↓ <0.001	↓ 0.02	↑ 0.03	↓ 0.01	↑ 0.01	↓ <0.001	↓ <0.001	↓ <0.001	↓ <0.001	0.59	↑ <0.001
SF covariate effect (P)	0.36	↓ <0.001	↓ <0.001	↓ <0.001	↓ <0.001	↑ <0.001	↑ <0.001	↑ <0.001	↑ <0.001	0.83	↓ <0.001

Note: values are presented as mean ± standard deviation. DF: duty factor, SF: step frequency, $F_{leg,max}$: maximum of the force vector projected along the leg, ΔL_{comp} and ΔL_{decomp} : maximum leg compression and decompression during stance, $k_{leg,comp}$ and $k_{leg,decomp}$: compressive and decompressive leg stiffnesses, $\theta_{leg,FS}$ and $\theta_{leg,TO}$: leg angle at foot-strike and toe-off. $F_{leg,max}$ was normalized by body weight (BW). ΔL_{comp} and ΔL_{decomp} were expressed in absolute and relative (as a percentage of participant's height) units and similarly for $k_{leg,comp}$ and $k_{leg,decomp}$. SF covariate was normalized by $\sqrt{g/L_0}$, where g is the gravitational constant and L_0 the leg length. Up (↑) and down (↓) arrows indicate positive and negative effects of the covariate, respectively.

^aSignificantly different from the value at 11 km/h.

^bSignificantly different from the value at 13 km/h.

runners better optimize the spring-mass model than lower SF runners, confirming that SF seems to be an indirect factor influencing k_{leg} through its effect on t_c (Morin et al., 2007).

Most of the variables studied herein reported an opposite association of DF and SF covariates (Tables 3-5). In other words, for most of the variables, if DF had a positive association on a given variable, then SF had a negative association on the same variable, and vice versa. This observation sounds counter-intuitive because SF is analytically associated to DF, i.e., $DF = 0.5 t_c SF$. However, though significant, correlations between DF and SF were low at all tested speeds (Table 1). Hence, the direct association of SF covariate on a given variable is more important than the indirect association caused by the relationship between SF and DF. Besides, the low correlations between SF and DF tend to reduce the direct association of a covariate on a given variable. Noteworthy, correlations between DF and t_c were high ($r \geq 0.78$) and significant ($p < 0.001$) and correlations between DF and t_f were very high ($r \geq 0.95$) and significant ($p < 0.001$). Hence, these results corroborate that DF and SF can be viewed as two variables that complement each other and that should be used together to describe the full spectrum of running patterns (van Oeveren et al., 2021).

A few limitations to the present study exist. Few findings of this study were obtained using the spring-mass model, which include many assumptions and limitations (Blickhan, 1989; McMahon and Cheng, 1990; Farley and González, 1996) that may restrict our conclusion on the underlying mechanisms. However, due to the methodological challenges associated to *in vivo* measurements under dynamic conditions to understand the role of muscle-tendon unit during running, the use of spring-loaded inverted pendulum model

seems rational and relevant. In addition, the running speeds were limited to endurance speeds representative of the running speeds employed by recreational runners during endurance running training (Selinger et al., 2022) and experimental trials were performed on a treadmill. Similar results might also be obtained using overground running trials because spatiotemporal parameters between motorized treadmill and overground running are largely comparable (Van Hooren et al., 2020). However, it was also concluded that participants behaved differently when attempting to achieve faster speeds overground than on a treadmill (Bailey et al., 2017). Therefore, further studies should investigate the association of DF and SF on running kinetic using additional conditions, i.e., faster speeds, positive and negative slopes, and different types of ground.

To conclude, this study revealed that the lower the DF and the higher the SF, the more the runner relies on the optimization of the spring-mass model, whereas the higher the DF and the lower the SF, the more the runner promotes forward propulsion.

Data availability statement

The raw data supporting the conclusions of this article will be made available by the authors, without undue reservation.

Ethics statement

The studies involving human participants were reviewed and approved by the local Ethics Committee (CER-VD 2020-00334).

The patients/participants provided their written informed consent to participate in this study.

Author contributions

Conceptualization, AP, TL, CG, and DM; methodology, AP, TL, CG, and DM; investigation, AP, TL, BB, EP, and JG; formal analysis, AP and BB; writing—original draft preparation, AP and BB; writing—review and editing, AP, TL, BB, CG, and DM; supervision, AP, TL, CG, and DM.

Funding

This study was supported by Innosuisse grant no. 35793.1 IP-LS. This study was supported by the University of Lausanne (Switzerland).

Acknowledgments

The authors warmly thank the participants for their time and cooperation.

References

- Almeida, M. O., Davis, I. S., and Lopes, A. D. (2015). Biomechanical differences of foot-strike patterns during running: A systematic review with meta-analysis. *J. Orthop. Sports Phys. Ther.* 45, 738–755. doi:10.2519/jospt.2015.6019
- Arendse, R. E., Noakes, T. D., Azevedo, L. B., Romanov, N., Schweltnus, M. P., and Fletcher, G. (2004). Reduced eccentric loading of the knee with the pose running method. *Med. Sci. Sports Exerc.* 36, 272–277. doi:10.1249/01.MSS.0000113684.61351.B0
- Bailey, J. P., Mata, T., and Mercer, J. D. (2017). Is the relationship between stride length, frequency, and velocity influenced by running on a treadmill or overground? *Int. J. Exerc. Sci.* 10, 1067–1075.
- Beck, O. N., Gosyne, J., Franz, J. R., and Sawicki, G. S. (2020). Cyclically producing the same average muscle-tendon force with a smaller duty increases metabolic rate. *Proc. Biol. Sci.* 287, 20200431. doi:10.1098/rspb.2020.0431
- Blickhan, R. (1989). The spring-mass model for running and hopping. *J. Biomech.* 22, 1217–1227. doi:10.1016/0021-9290(89)90224-8
- Bonnaerens, S., Fiers, P., Galle, S., Derie, R., Aerts, P., Frederick, E., et al. (2021). Relationship between duty factor and external forces in slow recreational runners. *BMJ Open Sport Exerc. Med.* 7, e000996. doi:10.1136/bmjsem-2020-000996
- Cavagna, G. A., Franzetti, P., Heglund, N. C., and Willems, P. (1988). The determinants of the step frequency in running, trotting and hopping in man and other vertebrates. *J. Physiol.* 399, 81–92. doi:10.1113/jphysiol.1988.sp017069
- Cavanagh, P. R., and Lafortune, M. A. (1980). Ground reaction forces in distance running. *J. Biomech.* 13, 397–406. doi:10.1016/0021-9290(80)90033-0
- Clark, K. P., Ryan, L. J., and Weyand, P. G. (2017). A general relationship links gait mechanics and running ground reaction forces. *J. Exp. Biol.* 220, 247–258. doi:10.1242/jeb.138057
- Coleman, D. R., Cannavan, D., Horne, S., and Blazevich, A. J. (2012). Leg stiffness in human running: Comparison of estimates derived from previously published models to direct kinematic-kinetic measures. *J. Biomech.* 45, 1987–1991. doi:10.1016/j.jbiomech.2012.05.010
- Daoud, A. I., Geissler, G. J., Wang, F., Saretzky, J., Daoud, Y. A., and Lieberman, D. E. (2012). Foot strike and injury rates in endurance runners: A retrospective study. *Med. Sci. Sports Exerc.* 44, 1325–1334. doi:10.1249/MSS.0b013e3182465115

Conflict of interest

The authors declare that the research was conducted in the absence of any commercial or financial relationships that could be construed as a potential conflict of interest.

Publisher's note

All claims expressed in this article are solely those of the authors and do not necessarily represent those of their affiliated organizations, or those of the publisher, the editors and the reviewers. Any product that may be evaluated in this article, or claim that may be made by its manufacturer, is not guaranteed or endorsed by the publisher.

Supplementary material

The Supplementary Material for this article can be found online at: <https://www.frontiersin.org/articles/10.3389/fphys.2022.1044363/full#supplementary-material>

- Davis, I. S., Bowser, B. J., and Mullineaux, D. R. (2016). Greater vertical impact loading in female runners with medically diagnosed injuries: A prospective investigation. *Br. J. Sports Med.* 50, 887–892. doi:10.1136/bjsports-2015-094579
- Dempster, W. T. (1955). *Space requirements of the seated operator: Geometrical, kinematic, and mechanical aspects of the body with special reference to the limbs*. Ohio: Wright-Patterson Air Force Base/Wright Air Development Center.
- Dorn, T. W., Schache, A. G., and Pandy, M. G. (2012). Muscular strategy shift in human running: Dependence of running speed on hip and ankle muscle performance. *J. Exp. Biol.* 215, 1944–1956. doi:10.1242/jeb.064527
- Dreyer, D., and Dreyer, K. (2009). *ChiRunning: A revolutionary approach to effortless, injury-free running. Revised and fully*. Updated ed. New York, USA: Simon & Schuster.
- Fadillioglu, C., Möhler, F., Reuter, M., and Stein, T. (2022). Changes in key biomechanical parameters according to the expertise level in runners at different running speeds. *Bioengineering* 9, 616. doi:10.3390/bioengineering9110616
- Farley, C. T., and González, O. (1996). Leg stiffness and stride frequency in human running. *J. Biomech.* 29, 181–186. doi:10.1016/0021-9290(95)00029-1
- Folland, J. P., Allen, S. J., Black, M. I., Handsaker, J. C., and Forrester, S. E. (2017). Running technique is an important component of running economy and performance. *Med. Sci. Sports Exerc.* 49, 1412–1423. doi:10.1249/MSS.0000000000001245
- Friston, K. J., Ashburner, J. T., Kiebel, S. J., Nichols, T. E., and Penny, W. D. (2007). *Statistical parametric mapping: The analysis of functional brain images*. Amsterdam: Elsevier Academic Press.
- Gill, N., Preece, S. J., and Baker, R. (2020). Using the spring-mass model for running: Force-length curves and foot-strike patterns. *Gait Posture* 80, 318–323. doi:10.1016/j.gaitpost.2020.06.023
- Gindre, C., Lussiana, T., Hébert-Losier, K., and Mourot, L. (2016). Aerial and terrestrial patterns: A novel approach to analyzing human running. *Int. J. Sports Med.* 37, 25–29. doi:10.1055/s-0035-1555931
- Gottschall, J. S., and Kram, R. (2005). Ground reaction forces during downhill and uphill running. *J. Biomech.* 38, 445–452. doi:10.1016/j.jbiomech.2004.04.023
- Hanavan, E. (1964). A mathematical model of the human body. *AMRL-TR. Aerosp. Med. Res. Laboratories* 1, 1–149.

- Hinkle, D. E., Wiersma, W., and Jurs, S. G. (2002). *Applied statistics for the behavioral sciences*. Boston: Houghton Mifflin.
- Hobara, H., Sakata, H., Namiki, Y., Hisano, G., Hashizume, S., and Usui, F. (2020). Effect of step frequency on leg stiffness during running in unilateral transfemoral amputees. *Sci. Rep.* 10, 5965. doi:10.1038/s41598-020-62964-2
- Hunter, I., Lee, K., Ward, J., and Tracy, J. (2017). Self-optimization of stride length Among experienced and inexperienced runners. *Int. J. Exerc. Sci.* 10, 446–453.
- Hunter, J. P., Marshall, R. N., and Mcnair, P. J. (2004). Interaction of step length and step rate during sprint running. *Med. Sci. Sports Exerc.* 36, 261–271. doi:10.1249/01.MSS.0000113664.15777.53
- Johnson, C. D., Tenforde, A. S., Outerleys, J., Reilly, J., and Davis, I. S. (2020). Impact-related ground reaction forces are more strongly associated with some running injuries than others. *Am. J. Sports Med.* 48, 3072–3080. doi:10.1177/0363546520950731
- Lieberman, D. E., Warrener, A. G., Wang, J., and Castillo, E. R. (2015). Effects of stride frequency and foot position at landing on braking force, hip torque, impact peak force and the metabolic cost of running in humans. *J. Exp. Biol.* 218, 3406–3414. doi:10.1242/jeb.125500
- Liew, B. X. W., Morris, S., Masters, A., and Netto, K. (2017). A comparison and update of direct kinematic-kinetic models of leg stiffness in human running. *J. Biomech.* 64, 253–257. doi:10.1016/j.jbiomech.2017.09.028
- Luo, Z., Zhang, X., Wang, J., Yang, Y., Xu, Y., and Fu, W. (2019). Changes in ground reaction forces, joint mechanics, and stiffness during treadmill running to fatigue. *Appl. Sci.* 9, 5493. doi:10.3390/app9245493
- Lussiana, T., Patoz, A., Gindre, C., Mourot, L., and Hébert-Losier, K. (2019). The implications of time on the ground on running economy: Less is not always better. *J. Exp. Biol.* 222, jeb192047. doi:10.1242/jeb.192047
- McMahon, T. A., and Cheng, G. C. (1990). The mechanics of running: How does stiffness couple with speed? *J. Biomech.* 23, 65–78. doi:10.1016/0021-9290(90)90042-2
- McMahon, T. A., Valiant, G., and Frederick, E. C. (1987), 62. Bethesda, Md, 2326–2337. doi:10.1152/jappl.1987.62.6.2326Groucho running. *J. Appl. Physiol.*
- Minetti, A. E. (1998). A model equation for the prediction of mechanical internal work of terrestrial locomotion. *J. Biomech.* 31, 463–468. doi:10.1016/s0021-9290(98)00038-4
- Mo, S., Lau, F. O. Y., Lok, A. K. Y., Chan, Z. Y. S., Zhang, J. H., Shum, G., et al. (2020). Bilateral asymmetry of running gait in competitive, recreational and novice runners at different speeds. *Hum. Mov. Sci.* 71, 102600. doi:10.1016/j.humov.2020.102600
- Morin, J.-B., Dalleau, G., Kyröläinen, H., Jeannin, T., and Belli, A. (2005). A simple method for measuring stiffness during running. *J. Appl. Biomech.* 21, 167–180. doi:10.1123/jab.21.2.167
- Morin, J. B., Samozino, P., Zameziati, K., and Belli, A. (2007). Effects of altered stride frequency and contact time on leg-spring behavior in human running. *J. Biomech.* 40, 3341–3348. doi:10.1016/j.jbiomech.2007.05.001
- Nordin, A. D., Dufek, J. S., and Mercer, J. A. (2017). Three-dimensional impact kinetics with foot-strike manipulations during running. *J. Sport Health Sci.* 6, 489–497. doi:10.1016/j.jshs.2015.11.003
- Pataky, T. C. (2010). Generalized n-dimensional biomechanical field analysis using statistical parametric mapping. *J. Biomech.* 43, 1976–1982. doi:10.1016/j.jbiomech.2010.03.008
- Pataky, T. C. (2012). One-dimensional statistical parametric mapping in Python. *Comput. Methods Biomech. Biomed. Engin.* 15, 295–301. doi:10.1080/10255842.2010.527837
- Patoz, A., Gindre, C., Thouvenot, A., Mourot, L., Hébert-Losier, K., and Lussiana, T. (2019). Duty factor is a viable measure to classify spontaneous running forms. *Sports* 7, 233. doi:10.3390/sports7110233
- Patoz, A., Lussiana, T., Breine, B., Gindre, C., and Malatesta, D. (2021). Both a single sacral marker and the whole-body center of mass accurately estimate peak vertical ground reaction force in running. *Gait Posture* 89, 186–192. doi:10.1016/j.gaitpost.2021.07.013
- Patoz, A., Lussiana, T., Breine, B., Gindre, C., Malatesta, D., and Hébert-Losier, K. (2022). Examination of running pattern consistency across speeds. *Sports Biomech.*, 1–15. doi:10.1080/14763141.2022.2094825
- Patoz, A., Lussiana, T., Thouvenot, A., Mourot, L., and Gindre, C. (2020). Duty factor reflects lower limb kinematics of running. *Appl. Sci.* 10, 8818. doi:10.3390/app10248818
- Riazati, S., Caplan, N., and Hayes, P. R. (2019). The number of strides required for treadmill running gait analysis is unaffected by either speed or run duration. *J. Biomech.* 97, 109366. doi:10.1016/j.jbiomech.2019.109366
- Sadeghi, H., Mathieu, P. A., Sadeghi, S., and Labelle, H. (2003). Continuous curve registration as an intertrial gait variability reduction technique. *IEEE Trans. Neural Syst. Rehabil. Eng.* 11, 24–30. doi:10.1109/TNSRE.2003.810428
- Salo, A. I. T., Bezodis, I. N., Batterham, A. M., and Kerwin, D. G. (2011). Elite sprinting: Are athletes individually step-frequency or step-length reliant? *Med. Sci. Sports Exerc.* 43, 1055–1062. doi:10.1249/MSS.0b013e318201f6f8
- Schache, A. G., Dorn, T. W., Williams, G. P., Brown, N. A. T., and Pandy, M. G. (2014). Lower-limb muscular strategies for increasing running speed. *J. Orthop. Sports Phys. Ther.* 44, 813–824. doi:10.2519/jospt.2014.5433
- Schepens, B., Willems, P. A., and Cavagna, G. A. (1998). The mechanics of running in children. *J. Physiol.* 509, 927–940. doi:10.1111/j.1469-7793.1998.927bm.x
- Selinger, J. C., Hicks, J. L., Jackson, R. W., Wall-Scheffler, C. M., Chang, D., and Delp, S. L. (2022). Running in the wild: Energetics explain ecological running speeds. *Curr. Biol.* 32, 2309–2315.e3. doi:10.1016/j.cub.2022.03.076
- Smith, L., Preece, S., Mason, D., and Bramah, C. (2015). A comparison of kinematic algorithms to estimate gait events during overground running. *Gait Posture* 41, 39–43. doi:10.1016/j.gaitpost.2014.08.009
- Subotnick, S. I. (1985). The biomechanics of running. Implications for the prevention of foot injuries. *Sports Med.* 2, 144–153. doi:10.2165/00007256-198502020-00006
- Tranberg, R., Saari, T., Zügner, R., and Kärrholm, J. (2011). Simultaneous measurements of knee motion using an optical tracking system and radiostereometric analysis (RSA). *Acta Orthop.* 82, 171–176. doi:10.3109/17453674.2011.570675
- Udofa, A. B., Clark, K. P., Ryan, L. J., and Weyand, P. G. (2019), 126. Bethesda, Md, 1315–1325. doi:10.1152/japplphysiol.00925.2018Running ground reaction forces across footwear conditions are predicted from the motion of two body mass components. *J. Appl. Physiol.*
- Van Hooren, B., Fuller, J. T., Buckley, J. D., Miller, J. R., Sewell, K., Rao, G., et al. (2020). Is motorized treadmill running biomechanically comparable to overground running? A systematic review and meta-analysis of cross-over studies. *Sports Med.* 50, 785–813. doi:10.1007/s40279-019-01237-z
- Van Overen, B. T., De Ruiter, C. J., Beek, P. J., and Van Dieën, J. H. (2021). The biomechanics of running and running styles: A synthesis. *Sports Biomech.*, 1–39. doi:10.1080/14763141.2021.1873411
- Van Overen, B. T., De Ruiter, C. J., Hoozemans, M. J. M., Beek, P. J., and Van Dieën, J. H. (2019). Inter-individual differences in stride frequencies during running obtained from wearable data. *J. Sports Sci.* 37, 1996–2006. doi:10.1080/02640414.2019.1614137
- Vogt, M., and Hoppeler, H. H. (2014). Eccentric exercise: Mechanisms and effects when used as training regime or training adjunct. *J. Appl. Physiol.* 116, 1446–1454. doi:10.1152/japplphysiol.00146.2013
- Weyand, P. G., Sternlight, D. B., Bellizzi, M. J., and Wright, S. (2000). Faster top running speeds are achieved with greater ground forces not more rapid leg movements. *J. Appl. Physiol.* 89, 1991–1999. doi:10.1152/jappl.2000.89.5.1991
- Willson, J. D., Bjorhus, J. S., Williams, D. S., 3rd, Butler, R. J., Porcari, J. P., and Kernozek, T. W. (2014). Short-term changes in running mechanics and foot strike pattern after introduction to minimalist footwear. *Phys. Med. Rehabilitation J.* 6, 34–43. doi:10.1016/j.pmrj.2013.08.602

Supplementary Materials:

Using statistical parametric mapping to assess the association of duty factor and step frequency on running kinetic

S1 Trajectory of the Center of Pressure during the Stance Running Phase

Figure S1 shows the trajectory of the center of pressure for one representative right foot contact at 11km/h. This figure depicts that the center of pressure calculated with low vertical ground reaction force values, i.e., below 200N, are not reliable. This can be explained because the vertical ground reaction force is present in the denominator of the equations required to calculate the anterior-posterior and mediolateral trajectories of the center of pressure and therefore cannot be too low (reference: <http://www.kwon3d.com/theory/grf/cop.html>).

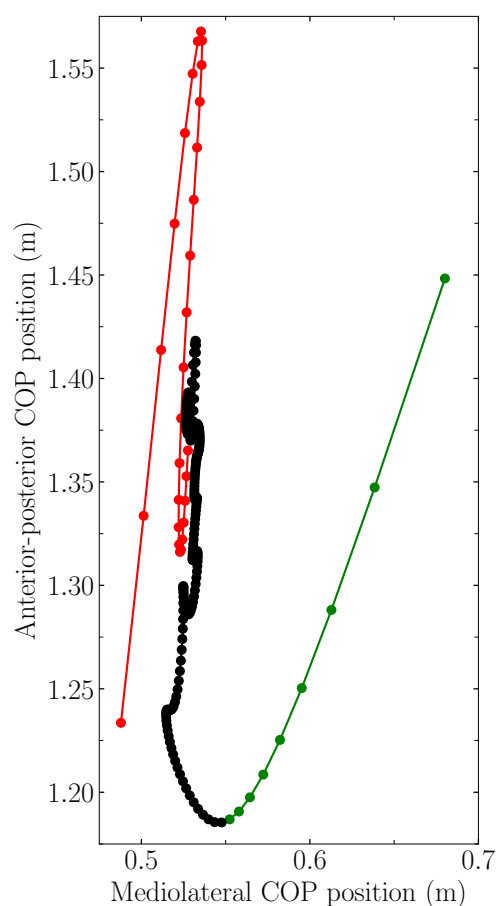


Figure S1. Example of the trajectory of the center of pressure (COP) for one representative right foot contact at 11km/h. The green and red colors show the trajectory of the COP at the initial and final instant of the stance running phase, respectively, i.e., when the vertical ground reaction force was below 200N. The vertical axis is the anterior-posterior COP position while the horizontal axis is the mediolateral COP position.

8.4 A novel kinematic detection of foot-strike and toe-off events during non-instrumented treadmill running to estimate contact time

Aurélien Patoz^{1,2,*}, Thibault Lussiana^{2,3,4}, Cyrille Gindre^{2,3}, Davide Malatesta¹

¹ Institute of Sport Sciences, University of Lausanne, 1015 Lausanne, Switzerland

² Research and Development Department, Volodalen Swiss Sport Lab, 1860 Aigle, Switzerland

³ Research and Development Department, Volodalen, 39270 Chavéria, France

⁴ Research Unit EA3920 Prognostic Markers and Regulatory Factors of Cardiovascular Diseases and Exercise Performance, Health, Innovation platform, University of Franche-Comté, Besançon, France

* Corresponding author

Published in **Journal of Biomechanics**

DOI: 10.1016/j.jbiomech.2021.110737



A novel kinematic detection of foot-strike and toe-off events during noninstrumented treadmill running to estimate contact time

Aurélien Patoz^{a,b,*}, Thibault Lussiana^{b,c,d}, Cyrille Gindre^{b,c}, Davide Malatesta^a

^a Institute of Sport Sciences, University of Lausanne, 1015 Lausanne, Switzerland

^b Research and Development Department, Volodalen Swiss Sport Lab, 1860 Aigle, Switzerland

^c Research and Development Department, Volodalen 39270, Chavéria, France

^d Research Unit EA3920 Prognostic Markers and Regulatory Factors of Cardiovascular Diseases and Exercise Performance, Health, Innovation Platform, University of Franche-Comté, Besançon, France

ARTICLE INFO

Keywords:

Gait analysis
Gait events
Event detection
Rearfoot running
Midfoot running
Forefoot running

ABSTRACT

Contact time (t_c) relies upon the accuracy of foot-strike and toe-off events, for which ground reaction force (GRF) is the gold standard. However, force plates are not always available, e.g., when running on a noninstrumented treadmill. In this situation, a kinematic algorithm (KA) – an algorithm based on motion capture data – might be used if it performs equally for all foot-strike angles across speeds. The purpose of this study was to propose a novel KA, using a combination of heel and toe kinematics (three markers per foot), to detect foot-strike and toe-off and compare it to GRF at different speeds and across foot-strike angles. One hundred runners ran at 9 km/h, 11 km/h, and 13 km/h. Force data and whole-body kinematic data were acquired by an instrumented treadmill and optoelectronic system. Foot-strike and toe-off showed small systematic biases between GRF and KA at all speeds (≤ 5 ms), except toe-off at 11 km/h (no bias). The root mean square error (RMSE) was ≤ 9 ms and was mostly constant across foot-strike angles for toe-off (7.4 ms) but not for foot-strike (4.1–11.1 ms). Small systematic biases (≤ 8 ms) and significant differences ($P \leq 0.01$) were reported for t_c at all speeds, and the RMSE was ≤ 14 ms ($\leq 5\%$). The RMSE for t_c increased with increasing foot-strike angle (3.5–5.4%). Nonetheless, this novel KA computed smaller errors than existing methods for foot-strike, toe-off, and t_c . Therefore, this study supports the use of this novel KA to accurately estimate foot-strike, toe-off, and t_c from kinematic data obtained during noninstrumented treadmill running independent of the foot-strike angle.

1. Introduction

Running is defined by a duty factor, i.e., a ratio of contact time (t_c) over stride duration, under 50% (Folland et al., 2017; Minetti, 1998), which makes t_c a key parameter of running biomechanics. This parameter is computed from foot-strike and toe-off events, obtained from the ground reaction force (GRF). However, force plates are not always available (Abendroth-Smith, 1996; Maiwald et al., 2009), e.g., when running on a noninstrumented treadmill. In this situation, foot-strike and toe-off, and therefore t_c , can be obtained with a kinematic algorithm (KA) based on motion capture data.

Several algorithms were developed and compared to the use of GRF (De Witt, 2010; Fellin et al., 2010; Hreljac and Stergiou, 2000; Leitch et al., 2011; Maiwald et al., 2009; Milner and Paquette, 2015; Smith et al., 2015) or a footswitch device (Alvim et al., 2015), but they did not

all offer the same accuracy. Moreover, previous datasets were limited to < 30 runners (Alvim et al., 2015; Leitch et al., 2011), which may be too small to allow generalizing the algorithm to every runner. In addition, rearfoot, midfoot, and forefoot strike patterns (Hasegawa et al., 2007), which can be determined based on the foot-strike angle (Altman and Davis, 2012), can impact kinematic data and algorithm accuracy because they involve different biomechanical strategies (Ruder et al., 2019; Wei et al., 2019). Relatively different errors (up to 30 ms) were reported for both foot-strike and toe-off among rearfoot, midfoot, and forefoot strikers using five methods (Smith et al., 2015). Similarly, Leitch et al. (2011) showed that the most accurate algorithm for detecting foot-strike was dependent on the foot-strike pattern but not on toe-off detection. These previous algorithms were based on heel kinematics, which differ based on foot-strike patterns. Indeed, Milner and Paquette (2015) and Smith et al. (2015) reported larger errors for non-

* Corresponding author at: Institute of Sport Sciences, University of Lausanne, 1015 Lausanne, Switzerland.

E-mail address: aurelien.patoz@unil.ch (A. Patoz).

rearfoot strikers than for rearfoot strikers when using these heel-based algorithms.

It also seems necessary to compare t_c based on GRF and KAs, due to its biomechanical importance (Moore et al., 2019). For instance, a larger error in t_c was observed for an algorithm that was more precise in foot-strike and toe-off detection than for those that were less precise (Smith et al., 2015) due to the accumulation of errors in foot-strike and toe-off detection.

Hence, the purpose of this study was to propose a novel KA to detect foot-strike and toe-off and compare it to the use of GRF at several treadmill speeds and across foot-strike angles. In addition, foot-strike and toe-off were used to estimate t_c which was then compared to that based on GRF. This algorithm uses a combination of heel and toe kinematics to detect foot-strike. We hypothesized that i) no systematic bias would be reported between GRF and KA for foot-strike and toe-off at any of the speeds examined and that the error in foot-strike and toe-off would be similar independent of foot-strike angle and ii) no systematic bias, significant difference between t_c derived from GRF and KA, or effect of foot-strike angle would be obtained.

2. Materials and methods

2.1. Participant characteristics

One hundred recreational runners participated in this study, including 75 males (age: 31 ± 8 years, height: 180 ± 6 cm, body mass: 70 ± 7 kg, foot size: 270 ± 4 mm, and weekly running distance: 37 ± 24 km) and 25 females (age: 30 ± 7 years, height: 169 ± 5 cm, body mass: 61 ± 6 kg, foot size: 244 ± 6 mm, and weekly running distance: 20 ± 14 km). For study inclusion, participants were required to be in good self-reported general health with no lower-extremity injury (≤ 1 month) and to have an estimated maximal aerobic speed ≥ 14 km/h. The study protocol was approved by the Ethics Committee (CER-VD 2020–00334) and adhered to the latest version of the Declaration of Helsinki of the World Medical Association.

2.2. Experimental procedure

After providing written informed consent, retroreflective markers were positioned on participants to assess their running biomechanics (Appendix A). For calibration purposes, a 5-second standing static trial using a standard anatomical position was recorded on an instrumented treadmill (Arsalis T150–FMT-MED, Louvain-la-Neuve, Belgium) for each participant. Then, a 7-minute warm-up run was performed (9 km/h). After a short break (< 5 min) participants completed three 1-minute runs (9 km/h, 11 km/h, and 13 km/h) performed in a randomized order with a 1-minute recovery between each run. These speeds were chosen because they are like those used in prior studies (Alvim et al., 2015; Leitch et al., 2011; Milner and Paquette, 2015). Three-dimensional (3D) kinematic (200 Hz) and kinetic (1000 Hz) data were collected during the static trial and for the first 10 strides following the 30-second mark of the running trials. The 3D kinetic data were down sampled to 200 Hz to match the sampling frequency of 3D kinematic data. Participants were familiar with running on a treadmill and wore their habitual running shoes during testing (shoe mass: 257 ± 49 g and shoe heel-to-toe drop: 7 ± 3 mm).

2.3. Ground reaction force for events detection

The gold standard foot-strike and toe-off were identified with Visual3D Professional software v6.01.12 (C-Motion Inc., Germantown, MD, USA) by applying a 20 N threshold to the z-component of the GRF (Smith et al., 2015).

2.4. Kinematic algorithm for events detection

The KA was implemented within Visual3D to detect foot-strike and toe-off from kinematic data. A mid-toe landmark was created midway between markers placed at the head of the first and fifth metatarsals. The mid-toe landmark position was rescaled by subtracting its respective global minimum (within the 10 strides) to overcome bias due to shoe height. Heel and mid-toe accelerations were calculated as the second derivative (second order central method) of the heel marker (foot calcaneus: aspect of the Achilles tendon insertion) and rescaled mid-toe landmark positions, respectively. Following visual observations of heel and mid-toe z-acceleration curves, an approach similar to that of Hreljac and Stergiou (2000), was followed. The KA was constructed such that foot-strike was detected within a time window of 120 ms centered around the instant when the mid-toe z-position reached 3.5 cm on descent. Foot-strike was defined as the first occurring maximum between the maxima of the heel marker and mid-toe landmark on z-acceleration curves within this time window (Figs. 1 and 2A). Toe-off was detected at the instance when the mid-toe z-position reached 3.5 cm on ascent after the preceding foot-strike, following a similar approach to that of Alvim et al. (2015). If such a threshold did not exist, 4 and 4.5 cm thresholds were used instead (Figs. 1 and 2B). The distance between the mid-toe landmark and the end part of the shoe (on the toe-side) being close to 5.5 cm, the global minimum of the mid-toe landmark being close to 2 cm, and the foot angle at toe-off being close to 90° justified the 3.5 cm threshold. The KA requires three markers per foot to detect foot-strike and toe-off but 39 markers were used because a whole-body biomechanical model was needed to construct foot segment angles to obtain the foot-strike angle (see Appendix A), which permitted to validate the KA across foot-strike angles.

2.5. Statistical analysis

All data are presented as mean \pm standard deviation. Bland-Altman plots were constructed to examine the presence of systematic bias in foot-strike, toe-off, and t_c obtained based on GRF and the KA for each speed (Atkinson and Nevill, 1998; Bland and Altman, 1995). The corresponding lower and upper limits of agreement and 95% confidence intervals were calculated. Positive systematic biases indicate overestimation by the KA, while negative values indicate underestimation. The root mean square error (RMSE) was calculated for foot-strike, toe-off, and t_c for each participant and each running trial. The RMSE was also calculated in relative units for t_c , i.e., by normalizing by the mean t_c value obtained using the GRF for each participant and running trial. In addition, the RMSE for foot-strike, toe-off, and t_c (averaged over speed) were given for forefoot, midfoot, and rearfoot strikers using the classification proposed by Altman and Davis (2012), i.e., using foot-strike angles $< -1.6^\circ$, $\geq -1.6^\circ$ but $< 8^\circ$, and $\geq 8^\circ$, respectively.

A linear mixed model (a model including both random and fixed factors fitted by restricted maximum likelihood) was used to compare t_c obtained using the GRF and KA for the different speeds and across foot-strike angles. The fixed factors were speed (ordinal variable), method (GRF vs KA; nominal variable), and foot-strike angle (continuous variable). The within-subject nature was controlled for by including random effects for participants. Pairwise post hoc comparisons were performed using Holm corrections, and only those comparing the GRF and KA methods for a given speed were investigated. Statistical analysis was performed using Python (v3.7.4, <http://www.python.org>) and Jamovi (v1.6.23, <https://www.jamovi.org>), with the level of significance set at $P \leq 0.05$.

3. Results

Systematic biases were obtained for both foot-strike and toe-off at all speeds (Table 1 and Fig. 3) and were ≤ 5 ms (≤ 1 frame), except for toe-off at 11 km/h (no bias; the zero line is between the 95% confidence

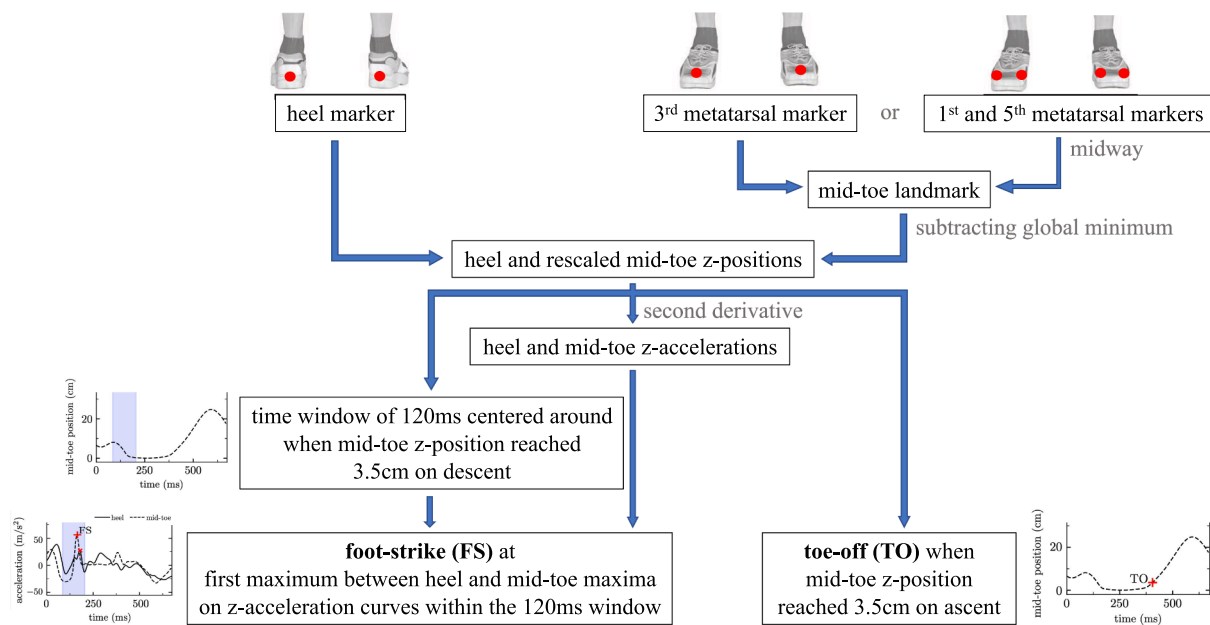


Fig. 1. Description of the kinematic algorithm for detecting foot-strike and toe-off. The mid-toe landmark could be a mid-toe marker (third metatarsal) in a simplified marker set.

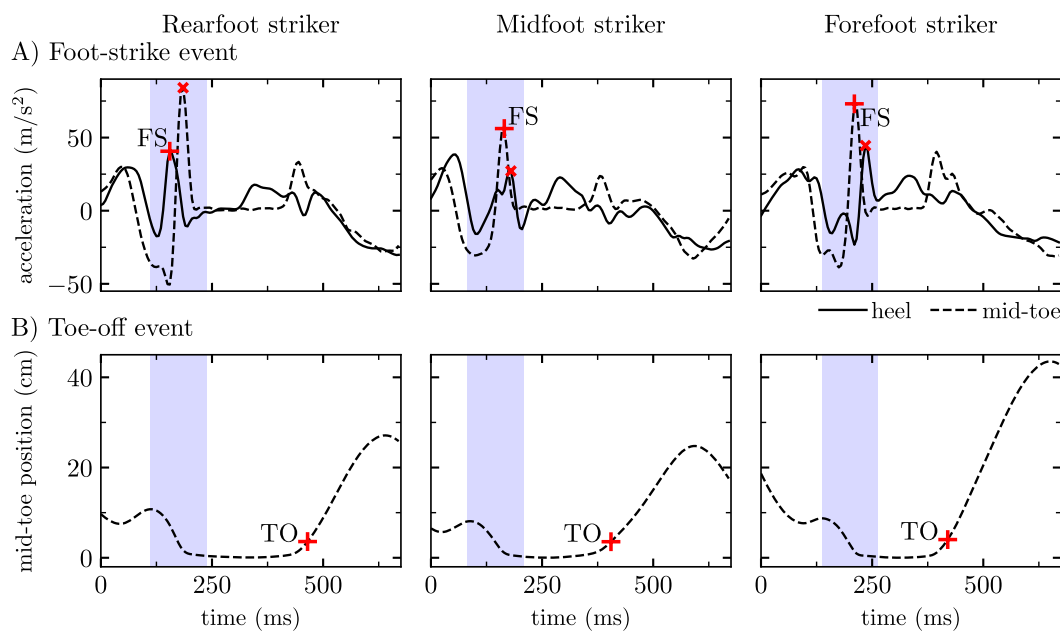


Fig. 2. Typical trajectory characteristics for a portion of a stride for three different runners at 11 km/h [rearfoot striker with foot-strike angle = 19.2° , midfoot striker with foot-strike angle = 1.4° , and forefoot striker with foot-strike angle = -16.5°] used by the kinematic algorithm to detect (A) foot-strike (FS) and (B) toe-off (TO; + sign; in red). The blue shaded area depicts the 120 ms time window during which foot-strike is examined. This time window is centered around the instant where the mid-toe z-position reached 3.5 cm on descent. The × sign (in red) denotes the second maximum detected by the algorithm during this time window. The first maximum defined foot-strike (+ sign; in red) and corresponded to a spike in heel z-acceleration for rearfoot strikers and in mid-toe z-acceleration for both midfoot and forefoot strikers. (For interpretation of the references to colour in this figure legend, the reader is referred to the web version of this article.)

interval).

The RMSE was ≤ 9 ms for both foot-strike and toe-off and decreased slightly with increasing speed (Table 2). The RMSE for foot-strike increased with increasing foot-strike angle while the RMSE was mostly constant across foot-strike angles for toe-off (Fig. 4). The RMSE (averaged over speed) was 4.1 ± 2.2 , 10.0 ± 3.5 , and 11.1 ± 2.3 ms for foot-strike and 7.1 ± 3.1 ms, 8.2 ± 3.6 ms, and 6.9 ± 3.2 ms for toe-off for forefoot, midfoot, and rearfoot strikers, respectively.

Systematic biases were reported for t_c at all speeds (< 8 ms), and the

corresponding RMSE was ≤ 14 ms ($\leq 5\%$; Table 3). The RMSE for t_c increased with increasing foot-strike angle (Fig. 5). Forefoot, midfoot, and rearfoot strikers had RMSEs for t_c (averaged over speed) of 8.6 ± 3.6 ms ($3.5 \pm 1.4\%$), 13.0 ± 6.2 ms ($5.1 \pm 2.3\%$), and 13.9 ± 5.3 ms ($5.4 \pm 1.9\%$), respectively.

The linear mixed model depicted significant effects of method, speed, foot-strike angle, and method \times speed interaction ($P \leq 0.004$). t_c was significantly overestimated by the KA, decreased with increasing speed, and increased with increasing foot-strike angle. Holm post hoc tests

Table 1

Systematic bias, lower limit of agreement (lloa), and upper limit of agreement (uloa) for foot-strike and toe-off detected using ground reaction force and the kinematic algorithm at three running speeds. 95% confidence intervals are given in square brackets [lower, upper].

	9 km/h			11 km/h			13 km/h		
	Bias (ms)	lloa (ms)	uloa (ms)	bias (ms)	lloa (ms)	uloa (ms)	bias (ms)	lloa (ms)	uloa (ms)
Foot-strike	-4.4 [-4.8, -4.0]	-20.8 [-21.4, -20.2]	12.0 [11.3, 12.6]	-4.8 [-5.2, -4.5]	-20.1 [-20.7, -19.6]	10.5 [9.9, 11.0]	-4.6 [-5.0, -4.3]	-19.1 [-19.7, -18.6]	9.9 [9.3, 10.4]
Toe-off	3.5 [3.1, 3.9]	-13.9 [-14.6, -13.2]	20.9 [20.2, 21.6]	0.2 [-0.1, 0.5]	-13.6 [-14.1-13.1]	14.1 [13.5, 14.6]	-1.8 [-2.1, -1.5]	-15.9 [-16.4-15.4]	12.3 [11.7, 12.8]

Note: for bias, positive and negative values indicate that the kinematic algorithm overestimated and underestimated gait events, respectively.

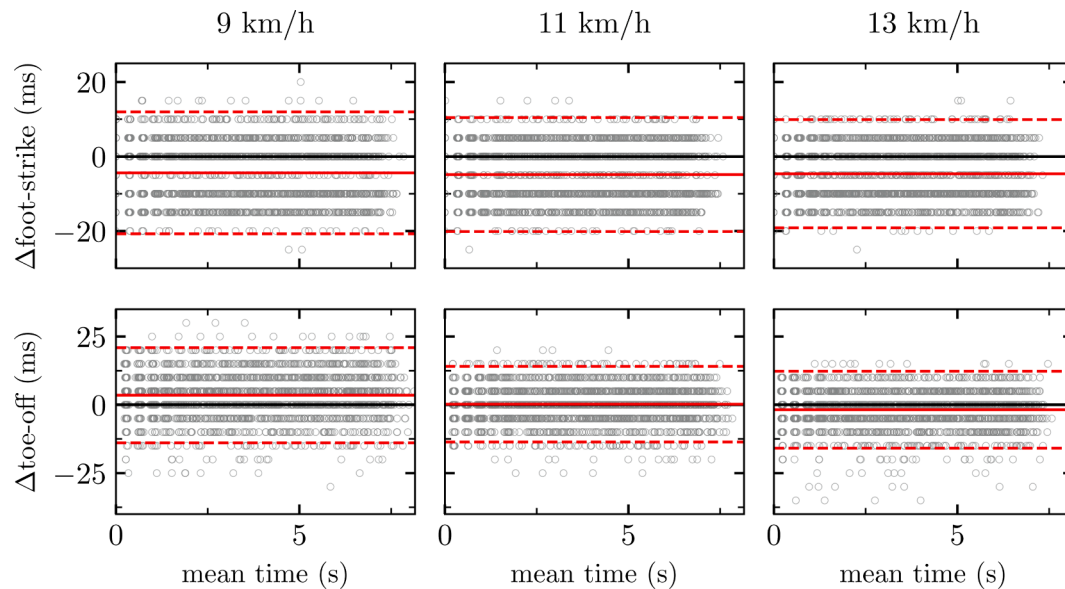


Fig. 3. Comparison of foot-strike and toe-off detection using ground reaction force and the kinematic algorithm [differences (Δ) as a function of mean values for the 10 analyzed strides of each participant (gray empty circles; 2000 values) together with systematic bias (red solid line), lower and upper limit of agreements (red dashed lines), and the zero line (black solid line), i.e., a Bland-Altman plot] for three running speeds. (For interpretation of the references to colour in this figure legend, the reader is referred to the web version of this article.)

Table 2

Root mean square error (RMSE) for foot-strike and toe-off events at three running speeds.

Running speed (km/h)	RMSE for foot-strike (ms)	RMSE for toe-off (ms)
9	8.4 ± 4.4	8.6 ± 4.0
11	8.2 ± 4.2	6.6 ± 2.6
13	7.8 ± 3.9	6.9 ± 2.8

Values are presented as mean ± standard deviation.

yielded significantly higher t_c when calculated by the KA than by the GRF at all speeds ($P \leq 0.01$; Table 3).

4. Discussion

Systematic biases were reported for foot-strike and toe-off at all speeds, refuting the first hypothesis. The RMSE was mostly constant across foot-strike angles for toe-off (7.4 ms) but not for foot-strike (4.1–11.1 ms), which partly refuted the first hypothesis. Systematic biases, as well as significant differences, were reported for t_c at all speeds. The RMSE for t_c increased with increasing foot-strike angle (3.5–5.4%), thus refuting the second hypothesis. Nonetheless, smaller errors than those obtained by existing methods were obtained for foot-strike, toe-off, and t_c . Therefore, this novel KA can be applied to accurately estimate foot-strike, toe-off, and t_c from kinematic data obtained

during noninstrumented treadmill running independent of foot-strike angle.

The RMSEs for foot-strike were ≤ 8 ms at all speeds (Table 2). These errors were smaller than those obtained with existing algorithms (Alvim et al., 2015; Fellin et al., 2010; Leitch et al., 2011; Milner and Paquette, 2015; Smith et al., 2015). However, the RMSE increased with increasing foot-strike angle and was ~ 3 times smaller in forefoot strikers (RMSE = 4.1 ms) than in rearfoot strikers (RMSE = 11.1 ms; Fig. 4). Milner and Paquette (2015) showed that algorithms based solely on heel kinematics (position, velocity, or acceleration) were less accurate in foot-strike detection for midfoot or forefoot strikers than for rearfoot strikers because heel kinematics around foot-strike differ according to foot-strike pattern, i.e., a non-rearfoot striker does not initiate contact with the ground using the heel. In addition, the heel-based algorithm reported in Smith et al. (2015) had poorer foot-strike detection abilities in non-rearfoot strikers than in rearfoot strikers (RMSE: 22 to 6 ms). Their results are opposed to those of this study, most likely because Smith et al. (2015) used a heel-based algorithm. Moreover, the range of RMSE reported here was less than that in Smith et al. (2015) (4.1–11.1 ms for forefoot to rearfoot strikers; Fig. 4). Leitch et al. (2011) demonstrated that heel-based and mid-foot-based algorithms were best suited for rearfoot and forefoot strikers. Therefore, the novel KA proposed here, which accounts for this recommendation and combines heel and toe kinematic data to detect foot-strike, proved to be useful and showed a smaller error than existing methods.

The algorithm proposed by Milner and Paquette (2015) was based on

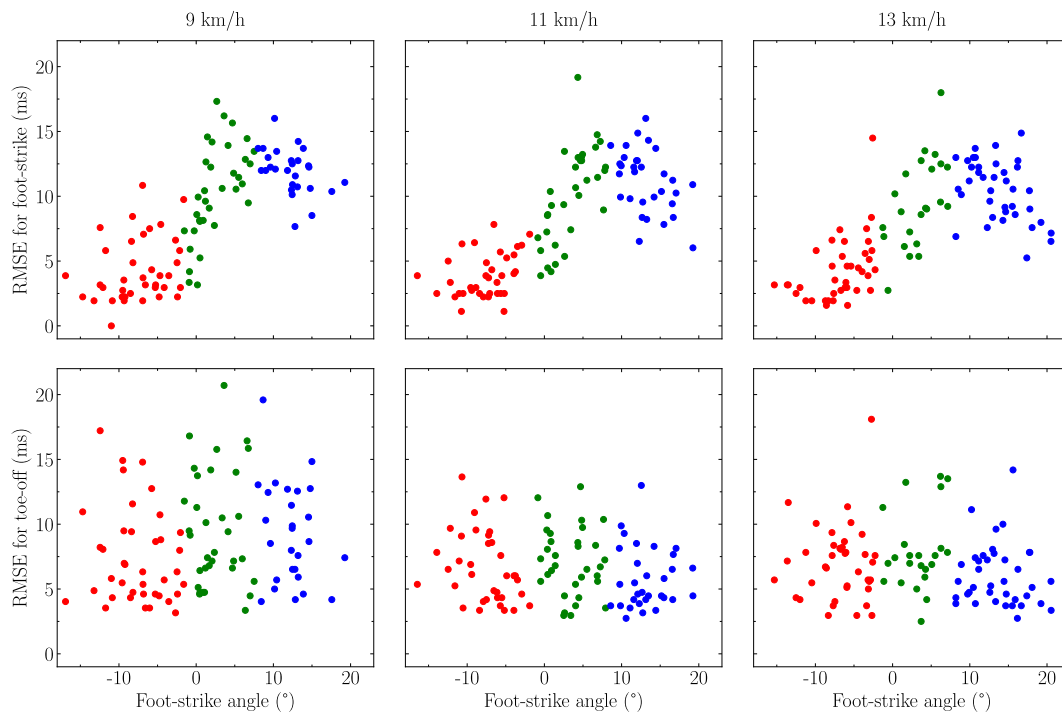


Fig. 4. The root mean square error (RMSE) for foot-strike and toe-off as a function of foot-strike angle for three running speeds. Each dot represents a participant, and colors indicate different foot-strike patterns according to Altman and Davis (2012), i.e., forefoot (red), midfoot (green), and rearfoot (blue) strikers for foot-strike angles $<-1.6^\circ$, $\geq-1.6^\circ$ but $<8^\circ$, and $\geq 8^\circ$, respectively. (For interpretation of the references to colour in this figure legend, the reader is referred to the web version of this article.)

Table 3

Contact time (t_c) calculated based on foot-strike and toe-off detected using ground reaction force (GRF) and the kinematic algorithm together with systematic bias, 95% confidence intervals (in square brackets [lower, upper]), and root mean square error [RMSE; both in absolute (ms) and relative (%) units]. Data are presented for three running speeds. The linear mixed model revealed a significant method (kinematic algorithm vs GRF) \times speed interaction effect ($P = 0.004$). *Significant difference ($P \leq 0.01$) between the t_c calculated based on GRF and that calculated based on the kinematic algorithm, as determined by Holm post hoc tests.

	9 km/h	11 km/h	13 km/h
t_c (ms)	286.6 \pm 27.5*	255.4 \pm 23.7*	230.7 \pm 20.5*
t_c GRF (ms)	278.6 \pm 24.9	250.3 \pm 20.7	227.9 \pm 18.4
bias (ms)	7.9 [7.3, 8.5]	5.1 [4.6, 5.6]	2.8 [2.4, 3.3]
RMSE (ms)	13.7 \pm 7.0	11.2 \pm 4.8	9.9 \pm 3.9
RMSE (%)	4.9 \pm 2.5	4.5 \pm 1.9	4.4 \pm 1.7

Values are presented as mean \pm standard deviation. Note: for bias, positive and negative values indicate that the kinematic algorithm overestimated and underestimated t_c , respectively.

the velocity of the center of mass of the pelvis and had a 15 ms offset for foot-strike. Similarly, the algorithm of Dingwell et al. (2001), originally designed for walking gait and based on knee extension spikes and used by Smith et al. (2015), depicted a 28 ms RMSE for foot-strike. These algorithms performed worse than the KA proposed here for foot-strike detection ($\text{RMSE} \leq 8$ ms or $|\text{bias}| \leq 5$ ms). One reason could be that these algorithms used more proximal segments, which might be temporally shifted compared to what is happening directly at the foot.

Toe-off necessarily occurs based on the toes moving away from the ground, suggesting that a toe-based algorithm should accurately detect toe-off. The RMSE for toe-off was mostly constant across foot-strike angles (7.4 ms; Fig. 4), which corroborates the findings of Leitch et al. (2011). This RMSE was similar to the RMSE of rearfoot strikers given by the algorithm proposed by Smith et al. (2015) (ms) but slightly higher

than the modified version of the algorithm of Alton et al. (1998) (3 ms) (Smith et al., 2015). However, the RMSE was obtained here was smaller than that obtained for forefoot strikers [7 vs 17 (Smith et al., 2015) or 12 ms (Alton et al., 1998)]. Therefore, toe-off detection with the novel KA showed similar or better accuracy than existing methods.

Small systematic biases, as well as significant differences, were reported for t_c at all speeds (Table 3). Even though the novel KA yielded smaller errors for foot-strike than the algorithm of Smith et al. (2015), those authors did not report significant differences in t_c between methods. The discrepancy might be due to a combination of under- and overestimations in foot-strike and toe-off. Moreover, a high speed (20 km/h) was used in Smith et al. (2015), which makes t_c smaller than that observed in this study, implicitly reducing observed differences and affecting the outcomes of statistical tests. In this study, the RMSE decreased with increasing speed [13.7–9.9 ms (5–4.5%) for 9–13 km/h] and was smaller than that in Smith et al. (2015) [18.4 ms (11%) at 20 km/h]. Hence, the algorithm of Smith et al. (2015) could be less effective at slower speeds because the time scale of kinematic trajectories might be slower, thus resulting in larger errors (i.e., greater differences in the number of frames) than in this study at similar speeds.

The proposed method could further be simplified and reduced to a two-dimensional analysis (Appendix B) though requiring future studies to evaluate its reliability. The strength and limitations of this study are specified in Appendix C.

5. Conclusion

This study proposed a novel KA that uses a combination of heel and toe kinematics (three markers per foot) to detect foot-strike and toe-off. Small systematic biases were reported for foot-strike and toe-off at all speeds. The RMSE was constant across foot-strike angles for toe-off but not for foot-strike. Small systematic biases were reported for t_c at all speeds, and the RMSE for t_c increased with increasing foot-strike angle. However, this novel KA yielded smaller errors than existing methods for foot-strike, toe-off, and t_c . Therefore, it can be applied to accurately

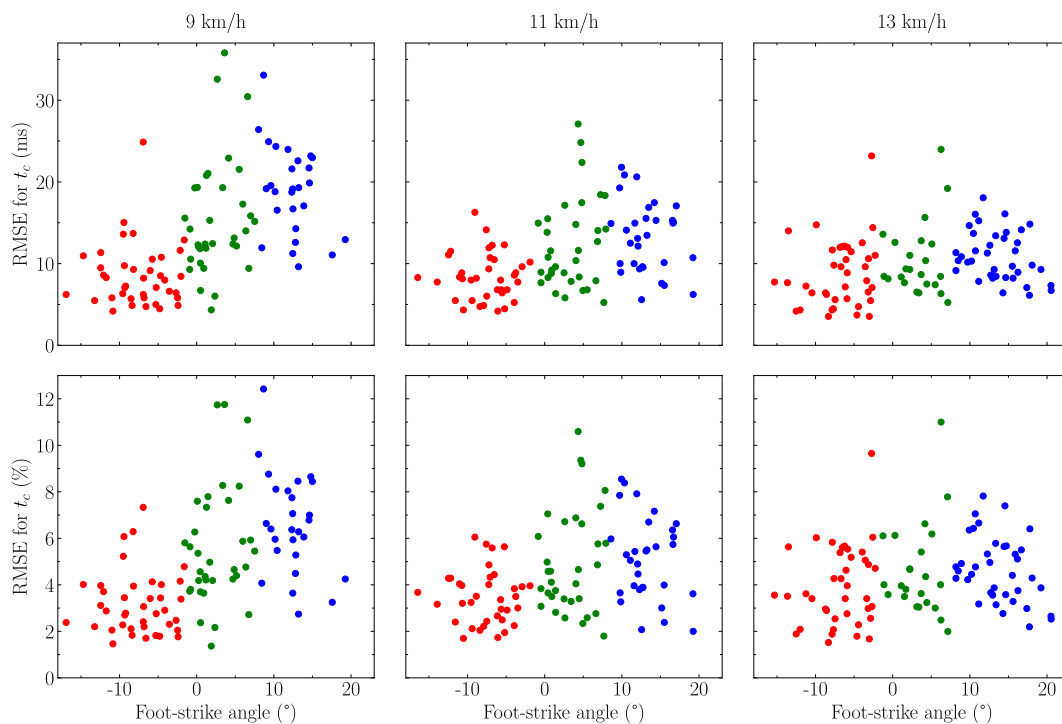


Fig. 5. The root mean square error (RMSE) for contact time (t_c) in both absolute (ms) and relative (%) units as a function of foot-strike angle for three running speeds. Each dot represents a participant, and colors indicate different foot-strike patterns according to Altman and Davis (2012), i.e., forefoot (red), midfoot (green), and rearfoot (blue) strikers for foot-strike angles $<-1.6^\circ$, $\geq-1.6^\circ$ but $<8^\circ$, and $\geq8^\circ$, respectively. (For interpretation of the references to colour in this figure legend, the reader is referred to the web version of this article.)

estimate foot-strike, toe-off, and t_c from kinematic data obtained during treadmill running, independent of foot-strike angle.

CRediT authorship contribution statement

Aurélien Patoz: Conceptualization, Methodology, Investigation, Formal analysis, Writing – original draft, Writing – review & editing, Supervision. **Thibault Lussiana:** Conceptualization, Methodology, Investigation, Writing – review & editing, Supervision. **Cyrille Gindre:** Conceptualization, Methodology, Writing – review & editing, Supervision. **Davide Malatesta:** Conceptualization, Methodology, Writing – review & editing, Supervision.

Declaration of Competing Interest

The authors declare that they have no known competing financial

interests or personal relationships that could have appeared to influence the work reported in this paper.

Acknowledgments

The authors warmly thank the participants for their time and cooperation.

Availability of Data and Code

The datasets and codes supporting this article are available upon request from the corresponding author.

Funding

This study was supported by Innosuisse grant no. 35793.1 IP-LS.

Appendix A. . Data collection and processing

Whole-body three-dimensional (3D) kinematic data were collected at 200 Hz using motion capture (8 cameras) and Vicon Nexus software v2.9.3 (Vicon, Oxford, UK). The laboratory coordinate system was oriented such that the x -, y -, and z -axes denoted the mediolateral (pointing toward the right side of the body), anterior-posterior, and inferior-superior axes, respectively. Forty-three and 39 retroreflective markers of 12.5 mm diameter were used for the static and running trials, respectively. They were affixed to the skin and shoes of participants over anatomical landmarks using double-sided tape following standard guidelines (Tranberg et al., 2011). Synchronized kinetic data (1000 Hz) were also collected using the force plate embedded in the treadmill.

3D markers and force (analog signal) were exported in .c3d format and processed in Visual3D. 3D marker data were interpolated using a third-order polynomial least-square fit algorithm, allowing a maximum of 20 frames for gap filling, and subsequently low-pass filtered at 20 Hz using a fourth-order Butterworth filter (Lussiana et al., 2019). The 3D force signal was down sampled to 200 Hz to match the sampling frequency of marker data and filtered using the same filter.

From the marker set, a full-body biomechanical model with six degrees of freedom and 15 rigid segments was constructed. Segments included the head, upper arms, lower arms, hands, thorax, pelvis, thighs, shanks, and feet. In Visual3D, segments were treated as geometric objects, assigned

inertial properties and center of mass locations based on their shape (Hanavan, 1964), and attributed relative mass based on standard regression equations (Dempster, 1955). The foot segment angle was defined as the orientation of the foot segment relative to the laboratory coordinate system and computed using an x - y - z Cardan sequence. The foot segment angle at foot-strike defined the foot-strike angle.

Appendix B. . Simplification of the proposed method

The proposed KA used three markers per foot to estimate t_c . This can be simplified by using only two markers. First, assuming that t_c is symmetric between right and left running steps (symmetry index $\sim 3\%$) (Mo et al., 2020), markers could be positioned on a single of both feet. Second, the two markers placed on the head of the first and fifth metatarsals could be replaced by a single marker placed on the head of the third metatarsal. In this case, the 3D analysis could further be simplified to a two-dimensional analysis (in the sagittal plane), which could then more easily be used outside the laboratory and by non-scientific teams (e.g., podiatrists, coaches, etc.). Nonetheless, future studies should be performed to assess the reliability of this simplified method.

Appendix C. Strengths and limitations

The strength of the results is due to the large dataset employed. This dataset allows better generalization of the results than datasets obtained with the smaller cohorts of 10 (Leitch et al., 2011) to 30 (Alvim et al., 2015) runners used previously. Nonetheless, a few limitations to this study exist. The KA was compared to the use of GRF using only treadmill runs, and speeds were limited to endurance speeds. The KA might also perform well for overground running trials because spatiotemporal parameters between motorized treadmill and overground running are largely comparable (Van Hooren et al., 2020). However, it was also concluded that participants behaved differently when attempting to achieve faster speeds overground than on a treadmill (Bailey et al., 2017). Therefore, further studies should focus on comparing this novel KA to the use of GRF using additional conditions, i. e., faster speeds, positive and negative slopes, and different types of ground. Finally, toe-off detection is based on an absolute threshold (3.5 cm), and its accuracy might be influenced by marker placement, shoe size, and footwear characteristics. Nonetheless, the toe-off detection method proposed herein yielded equivalent or smaller errors than existing methods.

References

- Abendroth-Smith, J., 1996. Stride adjustments during a running approach toward a force plate. *Res. Q. Exerc. Sport* 67 (1), 97–101.
- Altman, A.R., Davis, I.S., 2012. A kinematic method for footstrike pattern detection in barefoot and shod runners. *Gait Posture* 35 (2), 298–300.
- Alton, F., Baldey, L., Caplan, S., Morrissey, M.C., 1998. A kinematic comparison of overground and treadmill walking. *Clin. Biomech.* 13 (6), 434–440.
- Alvim, F., Cerqueira, L., Netto, A.D., Leite, G., Muniz, A., 2015. Comparison of Five Kinematic-Based Identification Methods of Foot Contact Events During Treadmill Walking and Running at Different Speeds. *J. Appl. Biomech.* 31, 383–388.
- Atkinson, G., Nevill, A.M., 1998. Statistical methods for assessing measurement error (reliability) in variables relevant to sports medicine. *Sports Med.* 26 (4), 217–238.
- Bailey, J.P., Mata, T., Mercer, J.D., 2017. Is the relationship between stride length, frequency, and velocity influenced by running on a treadmill or overground? *Int. J. Exercise Sci.* 10, 1067–1075.
- Bland, J.M., Altman, D.G., 1995. Comparing methods of measurement: why plotting difference against standard method is misleading. *Lancet* 346 (8982), 1085–1087.
- De Witt, J.K., 2010. Determination of toe-off event time during treadmill locomotion using kinematic data. *J. Biomech.* 43 (15), 3067–3069.
- Dempster, W.T., 1955. Space requirements of the seated operator: geometrical, kinematic, and mechanical aspects of the body with special reference to the limbs. Wright Air Development Center, Wright-Patterson Air Force Base, Ohio.
- Dingwell, J.B., Cusumano, J.P., Cavanagh, P.R., Sternad, D., 2001. Local dynamic stability versus kinematic variability of continuous overground and treadmill walking. *J. Biomech. Eng.* 123, 27–32.
- Fellin, R.E., Rose, W.C., Royer, T.D., Davis, I.S., 2010. Comparison of methods for kinematic identification of footstrike and toe-off during overground and treadmill running. *J. Sci. Med. Sport* 13 (6), 646–650.
- Folland, J.P., Allen, S.J., Black, M.I., Handsaker, J.C., Forrester, S.E., 2017. Running Technique is an Important Component of Running Economy and Performance. *Med. Sci. Sports Exerc.* 49, 1412–1423.
- Hanavan, E., 1964. A mathematical model of the human body. AMRL-TR. Aerospace Medical Research Laboratories 1, 1–149.
- Hasegawa, H., Yamauchi, T., Kraemer, W.J., 2007. Foot strike patterns of runners at the 15-km point during an elite-level half marathon. *J. Strength Cond. Res.* 21 (3), 888–893.
- Hreljac, A., Stergiou, N., 2000. Phase determination during normal running using kinematic data. *Med. Biol. Eng. Comput.* 38 (5), 503–506.
- Leitch, J., Stebbins, J., Paolini, G., Zavatsky, A.B., 2011. Identifying gait events without a force plate during running: A comparison of methods. *Gait Posture* 33 (1), 130–132.
- Lussiana, T., Patoz, A., Gindre, C., Mourot, L., Hébert-Losier, K., 2019. The implications of time on the ground on running economy: less is not always better. *J. Exp. Biol.* 222, jeb192047.
- Maiwald, C., Sterzing, T., Mayer, T.A., Milani, T.L., 2009. Detecting foot-to-ground contact from kinematic data in running. *Footwear Science* 1 (2), 111–118.
- Milner, C.E., Paquette, M.R., 2015. A kinematic method to detect foot contact during running for all foot strike patterns. *J. Biomech.* 48 (12), 3502–3505.
- Minetti, A.E., 1998. A model equation for the prediction of mechanical internal work of terrestrial locomotion. *J. Biomech.* 31 (5), 463–468.
- Mo, S., Lau, F.O.Y., Lok, A.K.Y., Chan, Z.Y.S., Zhang, J.H., Shum, G., Cheung, R.T.H., 2020. Bilateral asymmetry of running gait in competitive, recreational and novice runners at different speeds. *Hum. Mov. Sci.* 71, 102600. <https://doi.org/10.1016/j.humov.2020.102600>.
- Moore, I.S., Ashford, K.J., Cross, C., Hope, J., Jones, H.S.R., McCarthy-Ryan, M., 2019. Humans Optimize Ground Contact Time and Leg Stiffness to Minimize the Metabolic Cost of Running. *Front. Sports Act. Living* 1.
- Ruder, M., Jamison, S.T., Tenforde, A., Mulloy, F., Davis, I.S., 2019. Relationship of Foot Strike Pattern and Landing Impacts during a Marathon. *Med. Sci. Sports Exerc.* 51.
- Smith, L., Preece, S., Mason, D., Bramah, C., 2015. A comparison of kinematic algorithms to estimate gait events during overground running. *Gait Posture* 41 (1), 39–43.
- Tranberg, R., Saari, T., Zügner, R., Kärrholm, J., 2011. Simultaneous measurements of knee motion using an optical tracking system and radiostereometric analysis (RSA). *Acta Orthop.* 82 (2), 171–176.
- Van Hooren, B., Fuller, J.T., Buckley, J.D., Miller, J.R., Sewell, K., Rao, G., Barton, C., Bishop, C., Willy, R.W., 2020. Is Motorized Treadmill Running Biomechanically Comparable to Overground Running? A Systematic Review and Meta-Analysis of Cross-Over Studies. *Sports Med.* 50 (4), 785–813.
- Wei, Z., Zhang, Z., Jiang, J., Zhang, Y.u., Wang, L., 2019. Comparison of plantar loads among runners with different strike patterns. *J. Sports Sci.* 37 (18), 2152–2158.

8.5 Both a single sacral marker and the whole-body center of mass accurately estimate peak vertical ground reaction force in running

Aurélien Patoz^{1,2,*}, Thibault Lussiana^{2,3,4}, Bastiaan Breine^{2,5}, Cyrille Gindre^{2,3}, Davide Malatesta¹

¹ Institute of Sport Sciences, University of Lausanne, 1015 Lausanne, Switzerland

² Research and Development Department, Volodalen Swiss Sport Lab, 1860 Aigle, Switzerland

³ Research and Development Department, Volodalen, 39270 Chavéria, France

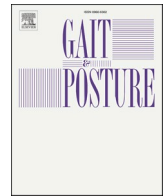
⁴ Research Unit EA3920 Prognostic Markers and Regulatory Factors of Cardiovascular Diseases and Exercise Performance, Health, Innovation platform, University of Franche-Comté, Besançon, France

⁵ Department of Movement and Sports Sciences, Ghent University, 9000 Ghent, Belgium

* Corresponding author

Published in **Gait & Posture**

DOI: 10.1016/j.gaitpost.2021.07.013



Both a single sacral marker and the whole-body center of mass accurately estimate peak vertical ground reaction force in running

Aurélien Patoz^{a,b,*}, Thibault Lussiana^{b,c,d}, Bastiaan Breine^{b,e}, Cyrille Gindre^{b,c}, Davide Malatesta^a

^a Institute of Sport Sciences, University of Lausanne, Lausanne, 1015, Switzerland

^b Research and Development Department, Volodalen Swiss Sport Lab, Aigle, 1860, Switzerland

^c Research and Development Department, Volodalen, Chavéria, 39270, France

^d Research Unit EA3920 Prognostic Markers and Regulatory Factors of Cardiovascular Diseases and Exercise Performance, Health, Innovation Platform, University of Franche-Comté, Besançon, France

^e Department of Movement and Sports Sciences, Ghent University, Ghent, 9000, Belgium

ARTICLE INFO

Keywords:

Biomechanics
Gait analysis
Motion capture
Treadmill
Endurance

ABSTRACT

Background: While running, the human body absorbs repetitive shocks with every step. These shocks can be quantified by the peak vertical ground reaction force ($F_{v,max}$). To measure so, using a force plate is the gold standard method (GSM), but not always at hand. In this case, a motion capture system might be an alternative if it accurately estimates $F_{v,max}$.

Research question: The purpose of this study was to estimate $F_{v,max}$ based on motion capture data and validate the obtained estimates with force plate-based measures.

Methods: One hundred and fifteen runners participated at this study and ran at 9, 11, and 13 km/h. Force data (1000 Hz) and whole-body kinematics (200 Hz) were acquired with an instrumented treadmill and an optoelectronic system, respectively. The vertical ground reaction force was reconstructed from either the whole-body center of mass (COM-M) or sacral marker (SACR-M) accelerations, calculated as the second derivative of their respective positions, and further low-pass filtered using several cutoff frequencies (2–20 Hz) and a fourth-order Butterworth filter.

Results: The most accurate estimations of $F_{v,max}$ were obtained using 5 and 4 Hz cutoff frequencies for the filtering of COM and sacral marker accelerations, respectively. GSM, COM-M, and SACR-M were not significantly different at 11 km/h but were at 9 and 13 km/h. The comparison between GSM and COM-M or SACR-M for each speed depicted root mean square error (RMSE) smaller or equal to 0.17BW ($\leq 6.5\%$) and no systematic bias at 11 km/h but small systematic biases at 9 and 13 km/h (≤ 0.09 BW). COM-M gave systematic biases three times smaller than SACR-M and two times smaller RMSE.

Significance: The findings of this study support the use of either COM-M or SACR-M using data filtered at 5 and 4 Hz, respectively, to estimate $F_{v,max}$ during level treadmill runs at endurance speeds.

1. Introduction

Even though running can offer many health benefits, the incidence of running related injuries remains high [1]. These injuries often occur when the loading of the musculoskeletal system exceeds its load bearing capacities. This loading corresponds to the repetitive shocks associated with every step that the human body must absorb by adopting a specific running biomechanics. Although the magnitude of these shocks are relatively insubstantial, in the order of 1.5–2.5 body weights (BW) for

the active peak [2], their quantity can be significant. For instance, an individual running an average of 20 km/week produces more than one million of active peaks during a one year period [3].

Although the internal forces contribute most to the experienced loading [4,5], the external forces are often used as substitute measures to estimate the loading of the musculoskeletal system [5–8]. For instance, moderate correlation was observed between the active peak force, i.e., peak vertical ground reaction force ($F_{v,max}$), and peak axial tibial compressive force [6]. It was also suggested that the peak tibial

* Corresponding author at: Institute of Sport Sciences, University of Lausanne, Lausanne, 1015, Switzerland.

E-mail address: aurelien.patoz@unil.ch (A. Patoz).

<https://doi.org/10.1016/j.gaitpost.2021.07.013>

Received 17 May 2021; Received in revised form 20 July 2021; Accepted 22 July 2021

Available online 24 July 2021

0966-6362/© 2021 The Author(s).

Published by Elsevier B.V. This is an open access article under the CC BY-NC-ND license

(<http://creativecommons.org/licenses/by-nc-nd/4.0/>).

bone loading occurs during midstance at $F_{v,max}$ [5,8] and that $F_{v,max}$ is representative of the magnitude of external bone loading during the stance running phase [5]. For these reasons, $F_{v,max}$ proved to be one important biomechanical parameter to accurately measure, though this variable alone should not be used to assess running related injuries [9].

The measurement of $F_{v,max}$ is usually performed using force plates, which is considered as the gold standard method (GSM). However, an instrumented treadmill would be required to conduct such measurement in the laboratory, which could not always be affordable or at hand [10, 11]. In such case, alternatives would be to use a sacral-mounted inertial measurement unit (IMU) [12–15] or a motion capture system [16,17]. The former is low-cost and practical to use in a coaching environment [18] while the latter, though more expensive, allows an in-depth assessment of running kinematics and is the alternative employed in the present study.

Using Newton's second law, which states that the sum of the forces applied to the human body is given by the body mass (m) multiplied by the acceleration of its center of mass (COM), vertical ground reaction force (F_v) can easily be recovered when assuming no air resistance and is given by Eq. 1

$$F_v(t) = m[a_v(t) + g] \quad (1)$$

where mg represents body weight and a_v is the whole-body COM vertical acceleration. The latter is the last piece of missing information in the previous equation and can be provided by the outcome of the motion capture system. Indeed, based on the three-dimensional (3D) kinematics of the entire body, the COM trajectory is computed as a weighted sum of the COM of each body segments (segmental analysis) [19], which ultimately allows obtaining the whole-body COM acceleration by computing the second derivative of the COM trajectory.

Although the segmental analysis is quite widespread, it is not a perfect estimation. For instance, it is subject to soft tissue artefact [20] and relies on accurate markers placement [21]. Moreover, this methods is time-consuming due to the large number of markers required to approximate each segment as a rigid body, where the choice of each rigid body, i.e., the schematic model of each body segment, is essential to correctly estimate the whole-body COM [22]. Furthermore, body segments need to be assigned inertial properties and COM locations based on their shape [23], and attributed relative mass based on standard regression equations [24], which add extra approximations. For these reasons, Napier, Jiang, MacLean, Menon and Hunt [25] approximated the whole-body COM trajectory by the trajectory of a single marker placed on the sacrum at the midpoint of the posterior superior iliac spines. These authors demonstrated that this very simple alternative was a valid proxy for the COM trajectory in vertical and fore-aft directions at specific events of the running cycle [25]. However, to the best of our knowledge, using the vertical acceleration of a single sacral marker to estimate $F_{v,max}$ has never been investigated while using the whole-body vertical COM acceleration has already been attempted but using a single participant [26].

Alternatively, sacral acceleration directly recorded using sacral-mounted IMU were used to estimate $F_{v,max}$ [12–15]. For instance, Alcantara, Day, Hahn and Grabowski [13] predicted $F_{v,max}$ using machine learning and reported a root mean square error (RMSE) of 0.15 BW. Moreover, weak to moderate correlations were obtained between $F_{v,max}$ measured using GSM and estimated using IMU data [12]. These authors observed an effect of the low-pass cutoff frequency used for the IMU data, where a better correlation was depicted for a 10 Hz than a 5 or 30 Hz cutoff frequency.

The previous findings suggest that the choice of the cutoff frequency proved to be important. Indeed, a substantial filtering method is required to avoid unrealistic peaks in the acceleration signal [19]. However, the effect of the cutoff frequency was not investigated when estimating $F_{v,max}$ from whole-body COM [26]. Hence, the purpose of this study was to 1) estimate $F_{v,max}$ based on whole-body COM (COM

method; COM-M) and sacral marker (sacral marker method: SACR-M) accelerations filtered using several cutoff frequencies (2–20 Hz), and 2) compare these estimations against GSM at several treadmill speeds. We hypothesized that 1) a single cutoff frequency should minimize RMSE and that this cutoff frequency should be different for each method and 2) a similar RMSE than in Alcantara, Day, Hahn and Grabowski [13] should be obtained, i.e., ~ 0.15 BW.

2. Materials and methods

2.1. Participant characteristics

Hundred and fifteen recreational runners, 87 males (age: 30 ± 8 years, height: 180 ± 6 cm, body mass: 70 ± 7 kg, and weekly running distance: 38 ± 24 km) and 28 females (age: 30 ± 7 years, height: 169 ± 5 cm, body mass: 61 ± 6 kg, and weekly running distance: 22 ± 16 km) voluntarily participated in this study. For study inclusion, participants were required to not have current or recent lower-extremity injury (≤ 1 month), to run at least once a week, and to have an estimated maximal aerobic speed ≥ 14 km/h. The study protocol was approved by the local Ethics Committee (CER-VD 2020–00334).

2.2. Experimental procedure

After providing written informed consent, retroreflective markers were positioned on participants (described in Subsec. 2.3 Data collection and processing) to assess their running biomechanics. As for each participant, a 7-min warm-up run was performed on an instrumented treadmill (Arsalis T150 – FMT-MED, Louvain-la-Neuve, Belgium). Speed was set to 9 km/h for the first 3 min and was then increased by 0.5 km/h every 30 s. This was followed, after a short break (< 5 min), by a 1-s static trial on the same treadmill for calibration. Then, three 1-min runs (9, 11, and 13 km/h) were performed in a randomized order (1-min recovery between each run). 3D kinematic and kinetic data were collected during the first 10 strides following the 30-s mark of running trials. All participants were familiar with running on a treadmill as part of their usual training program and wore their habitual running shoes.

2.3. Data collection and processing

Whole-body 3D kinematic data were collected at 200 Hz using motion capture (8 cameras) and Vicon Nexus software v2.9.3 (Vicon, Oxford, UK). Forty-three and 39 retro-reflective markers of 12.5 mm diameter were used for static and running trials, respectively. They were affixed to skin and shoes of individuals over anatomical landmarks using double-sided tape following standard guidelines [27]. Synchronized kinetic data (1000 Hz) were collected using the force plate embedded into the treadmill.

3D marker and ground reaction force (analog signal) were exported in .c3d format and processed in Visual3D Professional software v6.01.12 (C-Motion Inc., Germantown, MD, USA). 3D marker data were interpolated using a third-order polynomial least-square fit algorithm (using three frames of data before and after the “gap” to calculate the coefficients of the polynomial), allowing a maximum of 20 frames for gap filling, and subsequently low-pass filtered at 20 Hz using a fourth-order Butterworth filter. 3D ground reaction force signal was filtered using the same filter and downsampled to 200 Hz to match the sampling frequency of marker data.

From the marker set, a full-body biomechanical model with six degrees of freedom and 15 rigid segments was constructed. Segments included the head, upper arms, lower arms, hands, thorax, pelvis, thighs, shanks, and feet. Whole-body COM trajectory was calculated from the parameters of all 15 segments (directly provided by Visual3D). A sacral marker was reconstructed (virtual marker) at the midpoint between the two markers affixed to the posterior superior iliac spines [25]. Noteworthy, similar results would have been obtained by using a real marker

at this same location because marker placement error and soft tissue movement artefact are expected to be low in this region (prominence of bony landmarks and lack of soft tissue) [25].

The acceleration of the COM and sacral marker trajectories were calculated by computing their second derivative and were subsequently low-pass filtered using a fourth-order Butterworth filter. Several cutoff frequencies have been tested: 20, 10, 5, 4, 3, and 2 Hz. This choice of cutoff frequencies follows from the fact that any frequency above 20 Hz should arise due to vibration [3] while 3 Hz spike is considered to be reflective of step frequencies (vertical sinusoidal pelvic motion) [28]. For each low-pass filtered acceleration of both COM and sacral marker, the ground reaction force was reconstructed using Eq. 1. Finally, $F_{v,max}$ was given by the maximum of the measured (GSM) and both estimated (COM-M and SACR-M) vertical ground reaction force signals between foot-strike and toe-off events. These events were identified within visual3D and detected by applying a 20 N threshold to the vertical component of the ground reaction force [29]. The body mass of each participant was obtained from body weight recorded during the static trial and was used in Eq. 1 and to express force-like data in BW. For further analyses, each $F_{v,max}$ (from GSM, COM-M, and SACR-M) of each participant was given by the average over the 20 consecutive $F_{v,max}$ values corresponding to the 10 analyzed strides. Errors in estimating $F_{v,max}$ with respect to GSM using either COM-M or SACR-M were calculated using RMSE (in absolute and relative units, i.e., normalized by the mean $F_{v,max}$ value over all participants and obtained using GSM). The best cutoff frequency for COM-M and SACR-M was determined as the frequency which minimized RMSE. Statistical analysis was performed on $F_{v,max}$ estimated by the most accurate COM-M and SACR-M. Data analysis was performed using Python (v3.7.4, available at <http://www.python.org>).

2.4. Statistical analysis

All data are presented as mean \pm standard deviation. Bland-Altman plots were constructed to examine the presence of systematic bias on $F_{v,max}$ between COM-M and GSM as well as between SACR-M and GSM for each running speed [30,31]. Corresponding lower and upper limit of agreements and 95 % confidence intervals (CI) were calculated. Systematic biases have a direction, i.e., positive values indicate overestimations of COM-M or SACR-M while negative values indicate underestimations. Then, after having inspected residual plots and having observed no obvious deviations from homoscedasticity or normality, two-way [method of calculation (GSM vs COM-M vs SACR-M) \times running speed (9 vs 11 vs 13)] repeated measures ANOVA with Mauchly's correction for sphericity and employing Holm corrections for pairwise post hoc comparisons were performed. Differences between GSM,

COM-M, and SACR-M were quantified using Cohen's d effect size and interpreted as very small, small, moderate, and large when $|d|$ values were close to 0.01, 0.2, 0.5, and 0.8, respectively [32]. Statistical analysis was performed using Jamovi (v1.2, retrieved from <http://www.jamovi.org>) with a level of significance set at $P \leq 0.05$.

3. Results

RMSE of the estimation of $F_{v,max}$ with respect to GSM using either COM-M or SACR-M as function of the cutoff frequency of the fourth-order Butterworth filter is depicted in Fig. 1 for the three running speeds. The filter frequencies which minimized RMSE were 5 and 4 Hz for COM-M and SACR-M, respectively, for the three speeds. RMSE for COM-M with a 5 Hz cutoff frequency at 9, 11, and 13 km/h were 0.06, 0.07, and 0.08 BW, respectively, while RMSE for SACR-M with a 4 Hz cutoff frequency at 9, 11, and 13 km/h were 0.14, 0.13, and 0.17 BW, respectively (RMSE for all cutoff frequencies and running speeds are reported in Table S1). $F_{v,max}$ estimated by COM-M and SACR-M using these best frequencies were kept for the following analyses.

Fig. 2 depicts the vertical ground reaction force obtained using GSM (force plate) as well as COM-M and SACR-M using data filtered at 5 and 4 Hz, respectively.

No systematic bias was reported for $F_{v,max}$ at 11 km/h for both COM-M and SACR-M compared to GSM (the zero line lied within the 95 % CI) while small biases were obtained at 9 and 13 km/h [≤ 0.09 BW (≤ 61.8 N for a 70 kg person); Fig. 3 and Table 1]. RMSE was smaller or equal to 0.06 BW (≤ 2.6 %) and 0.17 BW (≤ 6.5 %) for the comparison between GSM and COM-M and between GSM and SACR-M, respectively (Table 1). Estimations of $F_{v,max}$ using COM-M and SACR-M in Fig. 3 and Tables 1–3 were obtained using data filtered at 5 and 4 Hz, respectively.

Repeated measures ANOVA depicted significant effects for both running speed and method of calculation \times running speed interaction ($P < 0.001$; Table 2) but there was no effect of the method of calculation ($P = 0.41$; Table 2). Holm post hoc tests yielded significant differences between $F_{v,max}$ obtained using pair of methods at 9 and 13 km/h ($P \leq 0.003$) but not at 11 km/h ($P \geq 0.23$). The other pairwise post hoc comparisons were all statistically significant ($P \leq 0.03$) except the pair GSM at 11 km/h and SACR-M at 13 km/h ($P = 0.23$). Besides, while a linear increase in $F_{v,max}$ with increasing speed is reported for GSM and COM-M, this is less true for SACR-M (Table 2).

Cohen's d effect sizes were very small for the comparison of each pair of methods at 11 km/h and GSM and COM-M at 9 km/h, small for GSM and COM-M at 13 km/h and COM-M and SACR-M at 9 and 13 km/h, and moderate for GSM and SACR-M at 9 and 13 km/h were moderate (Table 3).

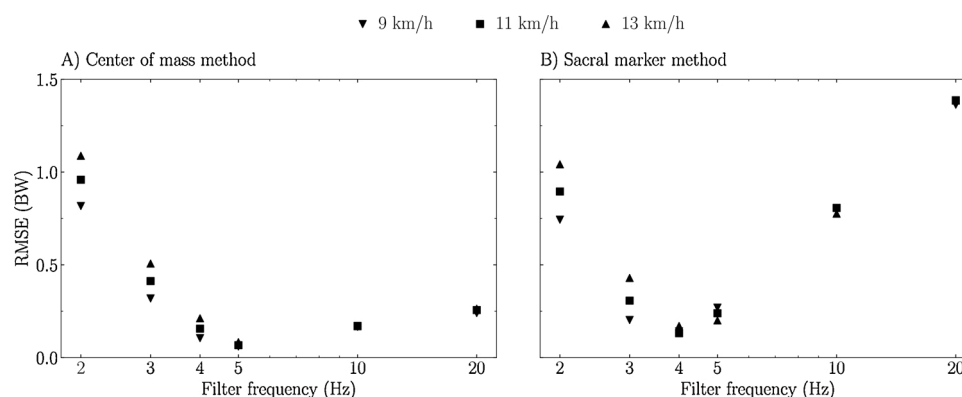


Fig. 1. Root mean square error [RMSE; in body weight (BW)] of the estimation of the peak vertical ground reaction force with respect to the gold standard method using A) the center of mass method (COM-M) and B) the sacral marker method (SACR-M), as function of the cutoff frequency of the fourth-order Butterworth low-pass filter and for three running speeds. Noteworthy, a log-scale was used on the x-axis to improve readability and vertical force was filtered at 20 Hz.

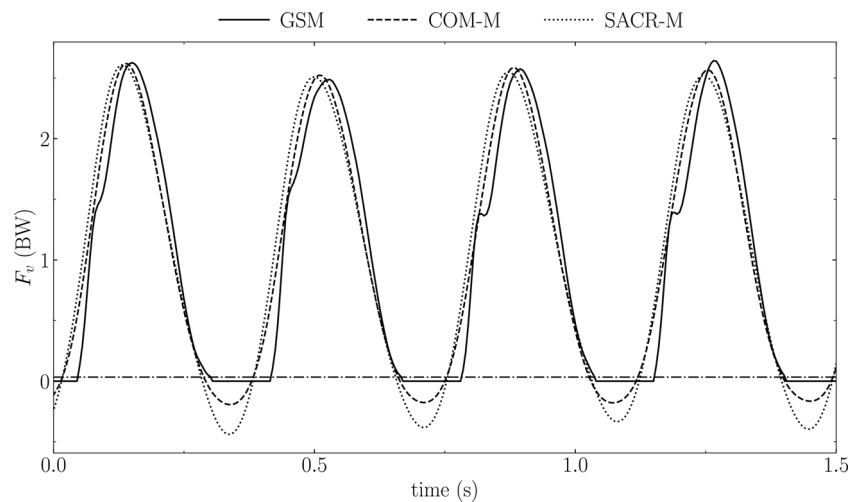


Fig. 2. Vertical ground reaction force [F_v ; in body weight (BW)] obtained using force plate and filtered at 20 Hz, i.e., gold standard method (GSM; solid line), center of mass method using a 5 Hz filter (COM-M; dashed line), and sacral marker method using a 4 Hz filter (SACR-M; dotted line) during two running strides for a representative participant at 11 km/h. The gray dash-dotted line represents the 20 N threshold used to detect foot-strike and toe-off events on the GSM.

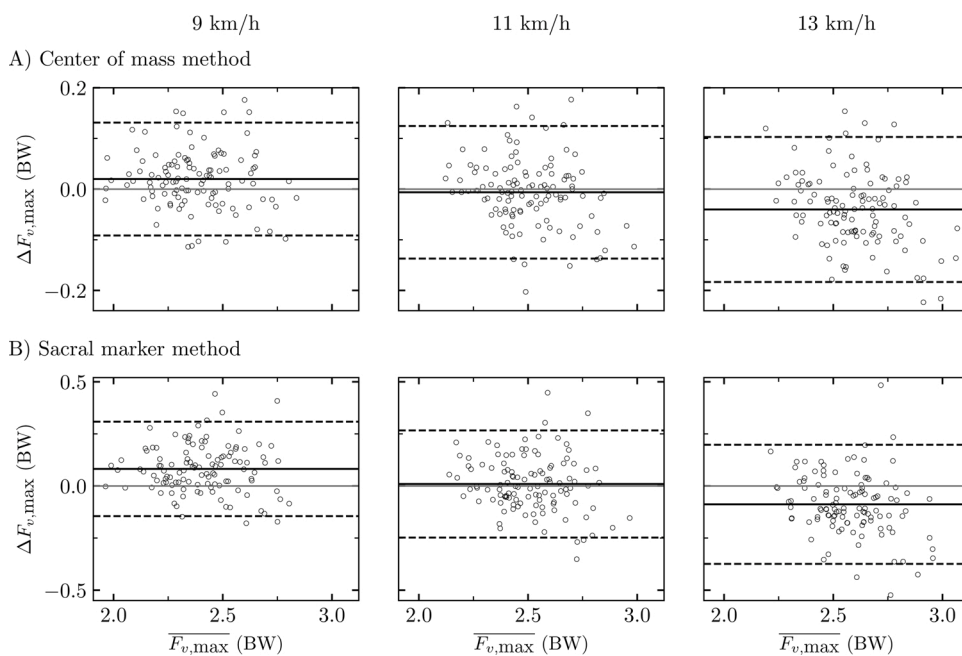


Fig. 3. Comparison of peak vertical ground reaction force [$F_{v,max}$; in body weight (BW)] obtained using gold standard method and A) center of mass method and B) sacral marker method [differences (Δ) as function of mean values together with systematic bias (black solid line) as well as lower and upper limit of agreements (black dashed lines), i.e., Bland-Altman plots] for three running speeds. COM and sacral marker data were filtered at 5 and 4 Hz, respectively, while vertical force was filtered at 20 Hz. Each dot represents the average over the 10 analyzed strides from one subject.

4. Discussion

According to the first hypothesis, a single cutoff frequency minimized RMSE and was different for each method. Indeed, the most accurate estimations of $F_{v,max}$ were obtained using a 5 and 4 Hz cutoff frequency for the fourth order Butterworth low-pass filtering of COM and sacral marker accelerations, respectively. Besides, according to the second hypothesis, RMSE close to 0.15 BW were obtained for both COM-M and SACR-M at each tested speed (RMSE \leq 0.17 BW). Conventional statistical approaches demonstrated no systematic bias and no significant difference of $F_{v,max}$ between GSM, COM-M, and SACR-M at 11 km/h. However, systematic biases and significant differences were obtained at 9 and 13 km/h, though COM-M gave systematic biases three times smaller than SACR-M as well as two times smaller RMSE. Nonetheless, systematic biases at 9 and 13 km/h were small (\leq 0.09 BW) and accompanied with \leq 6.5 % RMSE.

COM-M and SACR-M depicted the smallest RMSE for a cutoff

frequency of 5 and 4 Hz, respectively (Fig. 1). As the body segments were not considered in the sacral acceleration, this might not attenuate and “smooth” the signal compared to COM acceleration (the whole-body COM trajectory being a weighted sum of all body segments, its overall shape should be smoother than the sacral marker trajectory). This suggests that the vertical peaks in the unfiltered sacral acceleration signal were slightly higher than in COM acceleration (see Fig. S1). Therefore, a smaller cutoff frequency was required to filter the sacral than COM acceleration to decrease the magnitude of the vertical peaks and to make them match with the ones of GSM. Nonetheless, as the sacral marker should be close to COM location [25], the corresponding acceleration signals should be similar, i.e., the noise in the sacral acceleration was not drastically larger than in the COM one, justifying the small difference of 1 Hz in optimal cutoff frequencies.

Different RMSE between speeds were reported at lower than optimal cutoff frequencies while similar RMSE were obtained at larger than optimal cutoff frequencies (Fig. 1). In other words, the effect of speed on

Table 1

Systematic bias, lower limit of agreement (lloa), upper limit of agreement (uloa), and root mean square error [RMSE; both in absolute (body weight; BW) and relative (%) units] between peak vertical ground reaction force ($F_{v,max}$) obtained using center of mass (COM-M) and gold standard (GSM) method as well as using sacral marker method (SACR-M) and GSM at three running speeds. 95 % confidence intervals are given in square brackets [lower, upper].

	Running Speed (km/h)	Systematic Bias (BW)	Lloa (BW)	Uloa (BW)	RMSE (BW)
COM-M vs GSM	9	0.02 [0.01, 0.03]	-0.09 [-0.11, -0.07]	0.13 [0.11, 0.15]	0.06 (2.6 %)
	11	-0.01 [-0.02, 0.01]	-0.14 [-0.16, -0.12]	0.12 [0.10, 0.15]	0.07 (2.7 %)
	13	-0.04 [-0.05, -0.03]	-0.18 [-0.21, -0.16]	0.10 [0.08, 0.13]	0.08 (3.2 %)
SACR-M vs GSM	9	0.08 [0.06, 0.10]	-0.14 [-0.18, -0.11]	0.31 [0.27, 0.34]	0.14 (6.0 %)
	11	0.01 [-0.01, 0.03]	-0.25 [-0.29, -0.21]	0.27 [0.23, 0.31]	0.13 (5.3 %)
	13	-0.09 [-0.11, -0.06]	-0.37 [-0.42, -0.33]	0.20 [0.15, 0.24]	0.17 (6.5 %)

Note: for systematic bias, positive and negative values indicate the COM-M and SACR-M methods overestimated and underestimated $F_{v,max}$, respectively. COM and sacral marker data were filtered at 5 and 4 Hz, respectively, while vertical force was filtered at 20 Hz.

Table 2

Peak vertical ground reaction force [$F_{v,max}$; in body weight (BW)] obtained using gold standard (GSM), center of mass (COM-M), and sacral marker (SACR-M) methods for three running speeds. Significant ($P \leq 0.05$) method of calculation, running speed, and interaction effect, as determined by repeated measures ANOVA, are reported in bold font. *, †, and ‡ depict significant differences between $F_{v,max}$ obtained using GSM and COM-M, GSM and SACR-M, and COM-M and SACR-M, respectively, at a given running speed and as determined by Holm post hoc tests. Noteworthy, the other pairwise post hoc comparisons were all statistically significant ($P \leq 0.03$) except the pair GSM at 11 km/h and SACR-M at 13 km/h ($P = 0.23$) but not represented by a symbol in the table.

	Running Speed (km/h)	GSM	COM-M	SACR-M
$F_{v,max}$ (BW)	9	2.25 ± 0.28*†	2.27 ± 0.28‡	2.33 ± 0.29
	11	2.39 ± 0.30	2.38 ± 0.29	2.40 ± 0.30
	13	2.50 ± 0.31*†	2.46 ± 0.30‡	2.41 ± 0.30
Method of calculation effect		$P = 0.41$		
Running speed effect		$P < 0.001$		
Interaction effect		$P < 0.001$		

Note: values are presented as mean ± standard deviation. COM and sacral marker data were filtered at 5 and 4 Hz, respectively, while vertical force was filtered at 20 Hz.

RMSE increased as cutoff frequency decreased. This might be explained by the fact that the 2–4 Hz cutoff frequencies were close to the oscillatory behavior of COM or sacral marker. Indeed, 3 Hz is considered as the frequency corresponding to the vertical sinusoidal pelvic motion, reflective of step frequencies [28]. Besides, the higher the speed, the higher the step rate, and thus the even more likely to be close to the oscillatory behavior of the COM or sacral marker, further explaining the higher RMSE reported at 13 km/h than at 11 km/h and 9 km/h at lower than optimal cutoff frequencies.

A previous study evaluating the effect of the cutoff frequency to filter sacral-mounted IMU data to estimate $F_{v,max}$ reported that the smallest RMSE was obtained using a 10 Hz cutoff [12]. The present study reported optimal cutoff frequencies that were two times smaller (4 and 5 Hz). The discrepancy might be explained by the fact that the authors were directly measuring the sacral acceleration, which might be more prone to high frequency noise [12]. Furthermore, ground reaction force was filtered at 30 Hz whereas a 20 Hz cutoff was used in this study. In addition, the authors recorded treadmill runs from 13.7 to 19.4 km/h, which is faster than the endurance speeds used in the present study. Therefore, as the present study slightly overestimated and underestimated $F_{v,max}$ at 9 and 13 km/h, respectively, this suggests that a larger cutoff frequency should be used at a faster speed and a smaller one at a slower speed, which goes in the direction of the previous findings [12]. Indeed, increasing/decreasing the cutoff frequency

increases/decreases the magnitude of the filtered signal [12]. Moreover, a significant effect of running speed was observed (Table 2). Therefore, a speed-dependent cutoff frequency would probably provide better results. However, future studies should focus on testing several slower and faster running speeds to further decipher the running speed effect. Besides, a more complicated model could be constructed to better estimate $F_{v,max}$, for instance following recent research [13,33,34], which use artificial intelligence to estimate the vertical ground reaction force. Then, in practice, a systematic addition of the bias corresponding to the given speed could be applied when estimating $F_{v,max}$.

The differences between GSM and COM-M or SACR-M obtained in this study reported the same level of accuracy than in the study based on a single participant [26] [≤ 100 N (≤ 0.15 BW for a 70 kg person) at 7–20 km/h]. Moreover, $F_{v,max}$ estimated using sacral-mounted inertial sensors reported similar differences [12] [≤ 20 N (≤ 0.03 BW for a 70 kg person) at 14–19 km/h] and RMSE [13] (0.15 BW at 13.5–19.5 km/h) with respect to GSM than COM-M and SACR-M used in the present study. In addition, a 6 % error on $F_{v,max}$ (6–21 km/h) was reported using an inertial sensor placed on the leg along the tibial axis [35] while a 3 % error (10–14 km/h) was achieved using three IMUs (two on lower legs and one on pelvis) and two artificial neural networks [36]. Thus, estimated $F_{v,max}$ depicted similar error (~5 %) than previous estimations which used whole-body COM trajectory or inertial sensors. Nonetheless,

Table 3

Cohen's *d* effect size for peak vertical ground reaction force obtained using gold standard method (GSM) and center of mass method (COM-M), GSM and sacral marker method (SACR-M), and COM-M and GSM-M for three running speeds.

	Running Speed (km/h)	GSM vs COM-M	GSM vs SACR-M	COM-M vs SACR-M
<i>d</i>	9	-0.10	-0.42	-0.33
	11	0.03	-0.05	-0.09
	13	0.22	0.49	0.29

Note: COM and sacral marker data were filtered at 5 and 4 Hz, respectively, while vertical force was filtered at 20 Hz.

the present study only tested running speeds ranging between 9 and 13 km/h, thus not permitting to generalize on the accuracy of COM-M and SACR-M at faster running speeds, especially because a significant effect of running speed was observed (Table 2).

No systematic bias and significant difference were reported for both COM-M and SACR-M at 11 km/h (Fig. 3 and Tables 1 and 2). However, systematic but small biases were reported at 9 and 13 km/h (Fig. 3 and Table 1), which were accompanied with significant differences (Table 2). The systematic bias of SACR-M was almost three times larger than the one of COM-M at 9 and 13 km/h while RMSE and effect size were two times larger (Fig. 3, Tables 1 and 3). Besides, a less important linear increase in $F_{v,max}$ with increasing speed was reported for SACR-M than for GSM and COM-M (Table 2). These results could be explained by the fact that the speed-dependence of the cutoff frequency might be more important for SACR-M than COM-M, which is depicted by the larger range of RMSE over the three running speeds at a given cutoff frequency for SACR-M than COM-M (Fig. 1). Therefore, SACR-M might require a more pronounced variation of the cutoff frequency with running speed than COM-M, i.e., the cutoff frequency for SACR-M might need to vary (even if <1 Hz) when speed changes by 2 km/h while the one of COM-M might not. This might allow to obtain a similar linear increase of $F_{v,max}$ with increasing speed for SACR-M than for GSM and COM-M. Nonetheless, further studies should be conducted to validate this assumption.

No significant difference was reported between COM-M and SACR-M at 11 km/h but were at 9 and 13 km/h (Table 2), which follows the differences between GSM and both COM-M and SACR-M. However, SACR-M depicted larger deviations around the mean than COM-M, as reported by the larger lower and upper limit of agreements (Fig. 3) and 95 % CI (Table 1). These larger deviations could be explained by the fact that the whole-body COM trajectory is a weighted sum of all body segments while the sacral marker trajectory is obviously not. Indeed, the overall shape of the whole-body COM trajectory being smoother than the sacral marker one (see Fig. S1), the difference between participants tends to be smaller for the COM trajectory, which is then reflected in the acceleration signals obtained by double differentiation. These findings showed that COM-M is more consistent amongst participants than SACR-M and might be a preferred choice but is not reflected by the statistical analysis. Therefore, we suggest researchers with access to a motion capture system but not to a force plate to use COM-M or SACR-M with data filtered at 5 and 4 Hz, respectively, to estimate $F_{v,max}$. Furthermore, similar methods but employing a sacral-mounted IMU might be used to estimate $F_{v,max}$ overground, as long as an optimal cutoff frequency has been determined [12].

As a limitation to the present study, a single cutoff frequency was used to filter the vertical ground reaction force, i.e., 20 Hz. Though this choice of cutoff frequency is quite widespread [37,38], other cutoff frequencies (e.g., 30 or 80 Hz) are also used in the literature [12,13,39]. In this case, the optimal cutoff frequencies reported in this study and of 5 and 4 Hz for COM-M and SACR-M, respectively, might not be valid anymore because $F_{v,max}$ calculated using GSM might be different. Hence, further studies investigating the effect of the cutoff frequency of the gold standard signal should be conducted.

5. Conclusion

To conclude, this study proposed to estimate $F_{v,max}$ by reconstructing the vertical ground reaction force from either the whole-body COM or sacral marker accelerations (Eq. 1), themselves obtained by double differentiations of their respective trajectories and further low-pass filtered using a fourth-order Butterworth filter. The most accurate estimations of $F_{v,max}$ were obtained using a 5 and 4 Hz cutoff frequency for the filtering of COM and sacral marker accelerations, respectively. The comparison between GSM and COM-M or SACR-M, using data filtered at 5 and 4 Hz, respectively, depicted RMSE ≤ 0.17 BW (≤ 6.5 %), together

with no systematic bias at 11 km/h and systematic but small biases at 9 and 13 km/h (≤ 0.09 BW). No significant difference was reported between each pair of methods at 11 km/h but were at 9 and 13 km/h, The findings of this study support the use of either COM-M or SACR-M using data filtered at 5 and 4 Hz, respectively, to estimate $F_{v,max}$ during level treadmill runs at endurance speeds.

Author contributions

Conceptualization, A.P., T.L., C.G., and D.M.; methodology, A.P., T.L., C.G., and D.M.; investigation, A.P., T.L., and B.B.; formal analysis, A.P. and B.B.; writing—original draft preparation, A.P.; writing—review and editing, A.P., T.L., B.B., C.G., and D.M.; supervision, A.P., T.L., C.G., and D.M.

Funding

This study was supported by the Innosuisse grant no. 35793.1 IP-LS.

Availability of data and material

The datasets supporting this article are available on request to the corresponding author.

Declaration of Competing Interest

The authors declare no conflict of interest.

Acknowledgments

The authors warmly thank the participants for their time and cooperation.

Appendix A. Supplementary data

Supplementary material related to this article can be found, in the online version, at doi:<https://doi.org/10.1016/j.gaitpost.2021.07.013>.

References

- [1] M.L. Bertelsen, A. Hulme, J. Petersen, R.K. Brund, H. Sørensen, C.F. Finch, et al., A framework for the etiology of running-related injuries, *Scand. J. Med. Sci. Sports* 27 (11) (2017) 1170–1180.
- [2] D.I. Miller, Ground reaction forces in distance running, in: P.R. Cavanagh (Ed.), *Biomechanics of Distance Running*, Human Kinetics, Champaign, IL, 1990, pp. 203–224.
- [3] T.R. Derrick, D. Dereu, S.P. McLean, Impacts and kinematic adjustments during an exhaustive run, *Med. Sci. Sports Exerc.* 34 (6) (2002) 998–1002.
- [4] W.B. Edwards, J.C. Gillette, J.M. Thomas, T.R. Derrick, Internal femoral forces and moments during running: implications for stress fracture development, *Clin. Biomech.* 23 (10) (2008) 1269–1278. <https://www.sciencedirect.com/science/article/pii/S0268003308002234>.
- [5] S.H. Scott, D.A. Winter, Internal forces of chronic running injury sites, *Med. Sci. Sports Exerc.* 22 (3) (1990) 357–369.
- [6] E.S. Matijevich, L.M. Branscombe, L.R. Scott, K.E. Zelik, Ground reaction force metrics are not strongly correlated with tibial bone load when running across speeds and slopes: implications for science, sport and wearable tech, *PLoS One* 14 (1) (2019), e0210000, <https://doi.org/10.1371/journal.pone.0210000>.
- [7] R.L. Lenhart, D.G. Thelen, C.M. Wille, E.S. Chumanov, B.C. Heiderscheit, Increasing running step rate reduces patellofemoral joint forces, *Med. Sci. Sports Exerc.* 46 (3) (2014) 557–564.
- [8] S. Sasimontonkul, B.K. Bay, M.J. Pavol, Bone contact forces on the distal tibia during the stance phase of running, *J. Biomech.* 40 (15) (2007) 3503–3509. <https://www.sciencedirect.com/science/article/pii/S0021929007002576>.
- [9] H. van der Worp, J.W. Vrielink, S.W. Bredeweg, Do runners who suffer injuries have higher vertical ground reaction forces than those who remain injury-free? A systematic review and meta-analysis, *Br. J. Sports Med.* 50 (8) (2016) 450. <http://bjsm.bmj.com/content/50/8/450.abstract>.
- [10] C. Maiwald, T. Sterzing, T.A. Mayer, T.L. Milani, Detecting foot-to-ground contact from kinematic data in running, *Footwear Sci.* 1 (2) (2009) 111–118, <https://doi.org/10.1080/19424280903133938>.
- [11] J. Abendroth-Smith, Stride adjustments during a running approach toward a force plate, *Res. Q. Exerc. Sport* 67 (1) (1996) 97–101.

- [12] E.M. Day, R.S. Alcantara, M.A. McGeehan, A.M. Grabowski, M.E. Hahn, Low-pass filter cutoff frequency affects sacral-mounted inertial measurement unit estimations of peak vertical ground reaction force and contact time during treadmill running, *J. Biomech.* 119 (2021), 110323. <https://www.sciencedirect.com/science/article/pii/S0021929021001032>.
- [13] R.S. Alcantara, E.M. Day, M.E. Hahn, A.M. Grabowski, Sacral acceleration can predict whole-body kinetics and stride kinematics across running speeds, *PeerJ* 9 (2021), e11199.
- [14] A. Ancillao, S. Tedesco, J. Barton, B. O'Flynn, Indirect measurement of ground reaction forces and moments by means of wearable inertial sensors: a systematic review, *Sensors (Basel)* 18 (8) (2018).
- [15] B. LeBlanc, E.M. Hernandez, R.S. McGinnis, R.D. Gurchiek, Continuous estimation of ground reaction force during long distance running within a fatigue monitoring framework: a Kalman filter-based model-data fusion approach, *J. Biomech.* 115 (2021), 110130. <https://www.sciencedirect.com/science/article/pii/S0021929020305546>.
- [16] T. Lussiana, A. Patoz, C. Gindre, L. Mourot, K. Hébert-Losier, The implications of time on the ground on running economy: less is not always better, *J. Exp. Biol.* 222 (6) (2019), jeb192047. <https://jeb.biologists.org/content/jebio/222/6/jeb192047.full.pdf>.
- [17] A. Patoz, T. Lussiana, A. Thouvenot, L. Mourot, C. Gindre, Duty factor reflects lower limb kinematics of running, *Appl. Sci.* 10 (24) (2020), 8818. <https://www.mdpi.com/2076-3417/10/24/8818>.
- [18] V. Camomilla, E. Bergamini, S. Fantozzi, G. Vannozzi, Trends supporting the in-field use of wearable inertial sensors for sport performance evaluation: a systematic review, *Sensors* 18 (3) (2018) 873. [https://pubmed.ncbi.nlm.nih.gov/pmc/articles/PMC5877384/](https://www.ncbi.nlm.nih.gov/pmc/articles/PMC5877384/).
- [19] G. Pavei, E. Seminati, D. Cazzola, A.E. Minetti, On the estimation accuracy of the 3D body center of mass trajectory during human locomotion: inverse vs. forward dynamics, *Front. Physiol.* 8 (2017) 129.
- [20] A. Leardini, L. Chiari, U. Della Croce, A. Cappozzo, Human movement analysis using stereophotogrammetry. Part 3. Soft tissue artifact assessment and compensation, *Gait Posture* 21 (2) (2005) 212–225.
- [21] U. Della Croce, A. Leardini, L. Chiari, A. Cappozzo, Human movement analysis using stereophotogrammetry. Part 4: assessment of anatomical landmark misplacement and its effects on joint kinematics, *Gait Posture* 21 (2) (2005) 226–237.
- [22] L. Chiari, U. Della Croce, A. Leardini, A. Cappozzo, Human movement analysis using stereophotogrammetry. Part 2: instrumental errors, *Gait Posture* 21 (2) (2005) 197–211.
- [23] E. Hanavan, A mathematical model of the human body, AMRL-TR, AMRL. 1 (1964) 1–149. <http://www.ncbi.nlm.nih.gov/pubmed/14243640>, files/1506/14243640.html, <https://europepmc.org/article/med/14243640>.
- [24] W.T. Dempster, Space Requirements of the Seated Operator: Geometrical, Kinematic, and Mechanical Aspects of the Body With Special Reference to the Limbs, Wright Air Development Center, Wright-Patterson Air Force Base, Ohio, 1955.
- [25] C. Napier, X. Jiang, C.L. MacLean, C. Menon, M.A. Hunt, The use of a single sacral marker method to approximate the centre of mass trajectory during treadmill running, *J. Biomech.* 108 (2020), 109886. <https://www.sciencedirect.com/science/article/pii/S0021929020303092>.
- [26] G. Pavei, E. Seminati, J.L.L. Stornio, L.A. Peyré-Tartaruga, Estimates of running ground reaction force parameters from motion analysis, *J. Appl. Biomech.* 33 (1) (2017) 69–75. <http://journals.humankinetics.com/view/journals/jab/33/1/article-p69.xml>.
- [27] R. Tranberg, T. Saari, R. Zügner, J. Kärrholm, Simultaneous measurements of knee motion using an optical tracking system and radiostereometric analysis (RSA), *Acta. Orthop.* 82 (2) (2011) 171–176. <http://www.ncbi.nlm.nih.gov/pubmed/21463221>.
- [28] W. Hoogkamer, S. Kipp, J.H. Frank, E.M. Farina, G. Luo, R. Kram, A comparison of the energetic cost of running in marathon racing shoes, *Sports Med.* 48 (4) (2018) 1009–1019. <https://doi.org/10.1007/s40279-017-0811-2>.
- [29] L. Smith, S. Preece, D. Mason, C. Bramah, A comparison of kinematic algorithms to estimate gait events during overground running, *Gait Posture* 41 (1) (2015) 39–43.
- [30] J.M. Bland, D.G. Altman, Comparing methods of measurement: why plotting difference against standard method is misleading, *Lancet* 346 (8982) (1995) 1085–1087. <https://www.ncbi.nlm.nih.gov/pubmed/7564793>.
- [31] G. Atkinson, A.M. Nevill, Statistical methods for assessing measurement error (reliability) in variables relevant to sports medicine, *Sports Med.* 26 (4) (1998) 217–238. <https://www.ncbi.nlm.nih.gov/pubmed/9820922>.
- [32] J. Cohen, *Statistical Power Analysis for the Behavioral Sciences*, Routledge, 1988.
- [33] W.R. Johnson, A. Mian, M.A. Robinson, J. Verheul, D.G. Lloyd, J.A. Alderson, Multidimensional ground reaction forces and moments from wearable sensor accelerations via deep learning, *IEEE Trans. Biomed. Eng.* 68 (1) (2021) 289–297.
- [34] M. Pogson, J. Verheul, M.A. Robinson, J. Vanrenterghem, P. Lisboa, A neural network method to predict task- and step-specific ground reaction force magnitudes from trunk accelerations during running activities, *Med. Eng. Phys.* 78 (2020) 82–89. <https://www.sciencedirect.com/science/article/pii/S135045332030028X>.
- [35] E. Charry, W. Hu, M. Umer, A. Ronchi, S. Taylor, Study on estimation of peak ground reaction forces using tibial accelerations in running, in: 2013 IEEE Eighth International Conference on Intelligent Sensors, Sensor Networks and Information Processing, 2013, pp. 288–293.
- [36] F.J. Wouda, M. Giuberti, G. Bellusci, E. Maartens, J. Reenalda, B.-J.F. van Beijnum, et al., Estimation of vertical ground reaction forces and sagittal knee kinematics during running using three inertial sensors, *Front. Physiol.* 9 (218) (2018). <https://www.frontiersin.org/article/10.3389/fphys.2018.00218>.
- [37] P. Mai, S. Willwacher, Effects of low-pass filter combinations on lower extremity joint moments in distance running, *J. Biomech.* 95 (2019), 109311. <https://www.sciencedirect.com/science/article/pii/S0021929019305238>.
- [38] W. Swinnen, I. Mylle, W. Hoogkamer, F. De Groot, B. Vanwanseele, Changing stride frequency alters average joint power and power distributions during ground contact and leg swing in running, *Med. Sci. Sports Exerc.* (2021).
- [39] B. Breine, P. Malcolm, I. Van Caekenberghe, P. Fiers, E.C. Frederick, D. De Clercq, Initial foot contact and related kinematics affect impact loading rate in running, *J. Sports Sci.* 35 (15) (2017) 1556–1564. <https://doi.org/10.1080/02640414.2016.1225970>.

Supplementary materials for

Both a single sacral marker and the whole-body center of mass accurately estimate peak vertical ground reaction force in running

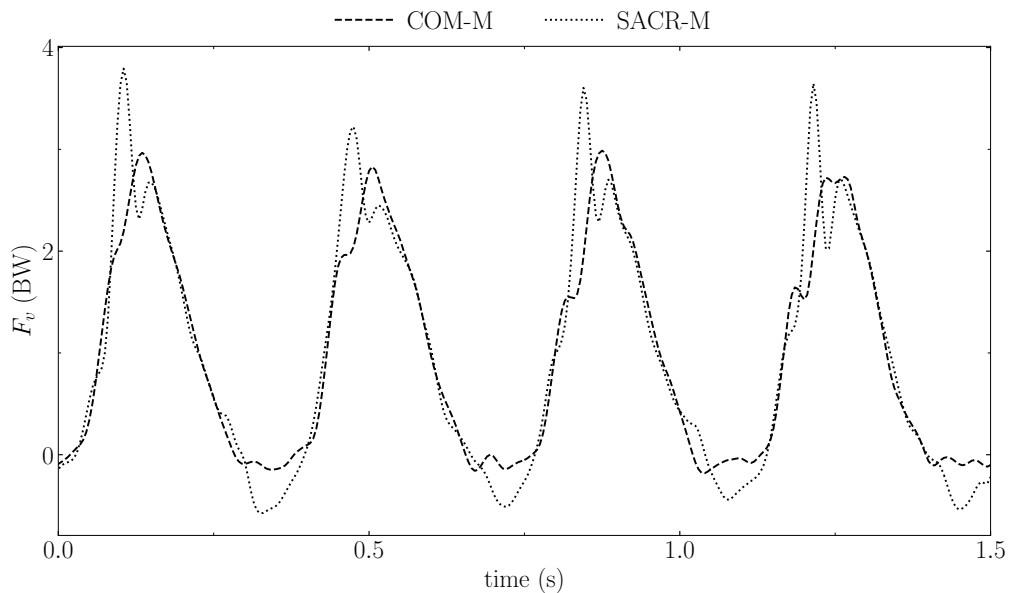


Figure S1. Vertical ground reaction force [F_v ; in body weight (BW)] obtained using center of mass method (COM-M; dashed line) and sacral marker method (SACR-M; dotted line) without applying a low-pass filter to the underlying COM and sacral marker acceleration signals. F_v is shown for two running strides and for a representative participant at 11km/h.

Table S1. Root mean square error [both in absolute (body weight; BW) and relative (%) units] between peak vertical ground reaction force obtained using center of mass (COM-M) and gold standard (GSM) method as well as using sacral marker method (SACR-M) and GSM at three running speeds and for all cutoff frequencies.

Cutoff frequency (Hz)	RMSE	COM-M vs GSM			SACR-M vs GSM		
		9 km/h	11 km/h	13 km/h	9 km/h	11 km/h	13 km/h
2	BW	0.82	0.96	1.09	0.74	0.90	1.04
	(%)	(34.6)	(38.3)	(41.5)	(31.4)	(35.7)	(39.8)
3	BW	0.32	0.41	0.51	0.20	0.31	0.43
	(%)	(13.5)	(16.5)	(19.4)	(8.6)	(12.3)	(16.4)
4	BW	0.11	0.16	0.21	0.14	0.13	0.17
	(%)	(4.5)	(6.2)	(8.1)	(6.0)	(5.3)	(6.5)
5	BW	0.06	0.07	0.08	0.27	0.24	0.20
	(%)	(2.6)	(2.7)	(3.2)	(11.4)	(9.6)	(7.7)
10	BW	0.17	0.17	0.17	0.81	0.81	0.78
	(%)	(7.0)	(6.8)	(6.5)	(34.1)	(32.2)	(29.6)
20	BW	0.24	0.26	0.26	1.36	1.39	1.38
	(%)	(10.2)	(10.2)	(10.1)	(57.6)	(55.4)	(52.3)

8.6 A single sacral-mounted inertial measurement unit to estimate peak vertical ground reaction force, contact time, and flight time in running

Aurélien Patoz^{1,2,*}, Thibault Lussiana^{2,3,4}, Bastiaan Breine^{2,5}, Cyrille Gindre^{2,3}, Davide Malatesta¹

¹ Institute of Sport Sciences, University of Lausanne, 1015 Lausanne, Switzerland; aurelien.patoz@unil.ch; davide.malatesta@unil.ch

² Research and Development Department, Volodalen Swiss Sport Lab, 1860 Aigle, Switzerland; thibault@volodalen.com; bastiaan@volodalen.com; cyrille@volodalen.com

³ Research and Development Department, Volodalen, 39270 Chavéria, France

⁴ Research Unit EA3920 Prognostic Markers and Regulatory Factors of Cardiovascular Diseases and Exercise Performance, Health, Innovation platform, University of Franche-Comté, Besançon, France

⁵ Department of Movement and Sports Sciences, Ghent University, 9000 Ghent, Belgium

* Corresponding author

Published in **Sensors**

DOI: 10.3390/s22030784

Article

A Single Sacral-Mounted Inertial Measurement Unit to Estimate Peak Vertical Ground Reaction Force, Contact Time, and Flight Time in Running

Aurélien Patoz ^{1,2,*}, Thibault Lussiana ^{2,3,4} , Bastiaan Breine ^{2,5}, Cyrille Gindre ^{2,3} and Davide Malatesta ¹ ¹ Institute of Sport Sciences, University of Lausanne, 1015 Lausanne, Switzerland; davide.malatesta@unil.ch² Volodalen Swiss Sport Lab, Research and Development Department, 1860 Aigle, Switzerland; thibault@volodalen.com (T.L.); bastiaan@volodalen.com (B.B.); cyrille@volodalen.com (C.G.)³ Volodalen, Research and Development Department, 39270 Chavéria, France⁴ Research Unit EA3920 Prognostic Markers and Regulatory Factors of Cardiovascular Diseases and Exercise Performance, Health, Innovation Platform, University of Franche-Comté, 25000 Besançon, France⁵ Department of Movement and Sports Sciences, Ghent University, 9000 Ghent, Belgium* Correspondence: aurelien.patoz@unil.ch; Tel.: +41-79-535-07-16

Abstract: Peak vertical ground reaction force ($F_{z,max}$), contact time (t_c), and flight time (t_f) are key variables of running biomechanics. The gold standard method (GSM) to measure these variables is a force plate. However, a force plate is not always at hand and not very portable overground. In such situation, the vertical acceleration signal recorded by an inertial measurement unit (IMU) might be used to estimate $F_{z,max}$, t_c , and t_f . Hence, the first purpose of this study was to propose a method that used data recorded by a single sacral-mounted IMU (IMU method: IMUM) to estimate $F_{z,max}$. The second aim of this study was to estimate t_c and t_f using the same IMU data. The vertical acceleration threshold of an already existing IMUM was modified to detect foot-strike and toe-off events instead of effective foot-strike and toe-off events. Thus, t_c and t_f estimations were obtained instead of effective contact and flight time estimations. One hundred runners ran at 9, 11, and 13 km/h. IMU data (208 Hz) and force data (200 Hz) were acquired by a sacral-mounted IMU and an instrumented treadmill, respectively. The errors obtained when comparing $F_{z,max}$, t_c , and t_f estimated using the IMUM to $F_{z,max}$, t_c , and t_f measured using the GSM were comparable to the errors obtained using previously published methods. In fact, a root mean square error (RMSE) of 0.15 BW (6%) was obtained for $F_{z,max}$ while a RMSE of 20 ms was reported for both t_c and t_f (8% and 18%, respectively). Moreover, even though small systematic biases of 0.07 BW for $F_{z,max}$ and 13 ms for t_c and t_f were reported, the RMSEs were smaller than the smallest real differences [$F_{z,max}$: 0.28 BW (11%), t_c : 32.0 ms (13%), and t_f : 32.0 ms (30%)], indicating no clinically important difference between the GSM and IMUM. Therefore, these results support the use of the IMUM to estimate $F_{z,max}$, t_c , and t_f for level treadmill runs at low running speeds, especially because an IMU has the advantage to be low-cost and portable and therefore seems very practical for coaches and healthcare professionals.

Keywords: gait analysis; biomechanics; sensor; accelerometer

Citation: Patoz, A.; Lussiana, T.; Breine, B.; Gindre, C.; Malatesta, D. A Single Sacral-Mounted Inertial Measurement Unit to Estimate Peak Vertical Ground Reaction Force, Contact Time, and Flight Time in Running. *Sensors* **2022**, *22*, 784. <https://doi.org/10.3390/s22030784>

Academic Editors: Robert Crowther and Dimitrios A. Patikas

Received: 2 November 2021

Accepted: 18 January 2022

Published: 20 January 2022

Publisher's Note: MDPI stays neutral with regard to jurisdictional claims in published maps and institutional affiliations.



Copyright: © 2022 by the authors. Licensee MDPI, Basel, Switzerland. This article is an open access article distributed under the terms and conditions of the Creative Commons Attribution (CC BY) license (<https://creativecommons.org/licenses/by/4.0/>).

1. Introduction

Running is defined as a cyclic alternance of support and flight phases, where at most one limb is in contact with the ground. Indeed, Novacheck [1] postulated that the presence of this flight phase (t_f) marks the distinction between walking and running gaits. In other words, the duty factor, i.e., the ratio of ground contact time (t_c) over stride duration, should be under 50% to observe a running gait [2,3]. Though running provides many health benefits, it is also associated with lower limb injuries [4,5], with a yearly incidence of running related injuries of up to 85% across novice to competitive runners [6,7]. Several biomechanical variables such as the peak vertical ground reaction force ($F_{z,max}$,

i.e., the maximum of the vertical ground reaction force during stance) and t_c were used to identify runners at risk of developing a running related injury [8–13]. In fact, $F_{z,max}$ is representative of the magnitude of external bone loading during the stance running phase while t_c measures the time during which this force is applied [14]. Therefore, $F_{v,max}$, t_c , and t_f are key variables of running biomechanics.

A force plate is the gold standard method (GSM) to measure $F_{z,max}$, t_c , and t_f . However, a force plate could not always be available and used [15,16]. In such a case, alternatives would be to use a motion capture system [17,18] or a light-based optical technology [19]. Nevertheless, even though these three systems can be used outside the laboratory [20–22], they suffer from a lack of portability and are restricted to a specific and small capture volume. To overcome such limitation, techniques were developed to estimate $F_{z,max}$, t_c , and t_f using portable tools such as inertial measurement units (IMUs), which are low-cost and practical to use in a coaching environment [23].

$F_{z,max}$ was previously estimated using the vertical acceleration signal recorded by a sacral-mounted IMU [24,25]. For instance, a root mean square error (RMSE) of 0.15 BW was reported when using a machine learning algorithm that used data filtered using a 10 Hz 8th order low-pass Butterworth filter [25]. Another method calculated the center of mass and sacral marker vertical accelerations from their corresponding three-dimensional (3D) kinematic trajectories, and reported an RMSE ≤ 0.17 BW when estimating $F_{z,max}$ from these acceleration signals [26]. The whole-body center of mass acceleration calculated from the kinematic trajectories was also used by Pavei, et al. [27] to estimate $F_{z,max}$, but for a single participant, and by Verheul, et al. [28] to estimate the resultant ground reaction force impact peak (within the first 30% of the stance). Pavei, Seminati, Storniolo and Peyré-Tartaruga [27] reported an RMSE of ~ 0.15 BW for running speeds ranging from 7 to 20 km/h, while an error of ~ 0.20 BW was reported by Verheul, Gregson, Lisboa, Vanrenterghem and Robinson [28] for speeds between 7 and 18 km/h.

t_c and t_f are calculated from foot-strike (FS) and toe-off (TO) events, which can themselves be identified using different available techniques that used IMU data [24,25,29–39]. When using a sacral-mounted IMU, which is a natural choice as it approximates the location of the center of mass [40], either the forward [31] or the vertical acceleration [24,25] were used to estimate t_c and t_f . On the one hand, Lee, Mellifont and Burkett [31] detected specific spikes in their unfiltered forward acceleration signals sampled at 100 Hz to identify FS and TO events. On the other hand, the vertical ground reaction force was estimated from the vertical acceleration signal recorded by the IMU (using Newton's second law), which allowed detecting FS and TO events using a 0 N threshold [24,25]. A 5 Hz low-pass Butterworth filter (8th order) was shown to result in the best correlation between t_c , obtained from GSM and IMU data (sampled at 500 Hz) [24], while a machine learning algorithm that used data filtered using a 10 Hz 8th order low-pass Butterworth filter, resulted in an RMSE of 11 ms for t_c [25]. The vertical acceleration (sampled at 208 Hz) was also used to estimate the effective contact and flight times [39], two variables that allow deciphering the landing-take-off asymmetry of running [41–43]. The authors estimated these effective timings by using a body weight threshold instead of a 0 N threshold, which allowed detecting effective FS and TO events and thus estimating effective contact and flight times. Moreover, the vertical acceleration was filtered using a Fourier series truncated to 5 Hz instead of the usual low-pass Butterworth filter. The authors reported an RMSE ≤ 22 ms for both effective contact and flight times.

As previously stated, more research investigating the effect of different filtering methods are needed when estimating biomechanical variables such as $F_{z,max}$ and t_c [24], especially because the low-pass cutoff frequency could affect the estimation of biomechanical variables [44,45]. For this reason, the first purpose of this study was to estimate $F_{z,max}$ using a Fourier series truncated to 5 Hz to filter the acceleration signal recorded by a sacral-mounted IMU (IMU method: IMUM). The second aim of this study was to estimate t_c and t_f using the same filtered acceleration signal. We previously used this filter to estimate both effective contact and flight times [39], but this filter has never been used, to the best of

the authors knowledge, to estimate $F_{z,\max}$, t_c , and t_f . In the present study, t_c and t_f were estimated from FS and TO events, themselves detected by modifying the body weight threshold we previously used [39]. We hypothesized that (i) an RMSE smaller than or equal to the 0.15 BW reported in Alcantara, Day, Hahn and Grabowski [25] should be obtained for $F_{z,\max}$, even if the IMUM is a simple method which does not rely on machine learning, as was the 3D kinematic method [26], and (ii) t_c and t_f should have an RMSE smaller than or equal to that we previously reported for effective contact and flight times (i.e., 0.22 ms) [39].

2. Materials and Methods

2.1. Participant Characteristics

One hundred recreational runners, which consisted of 27 females (age: 29 ± 7 years, height: 169 ± 5 cm, body mass: 61 ± 6 kg, and weekly running distance: 22 ± 16 km) and 73 males (age: 30 ± 8 years, height: 180 ± 6 cm, body mass: 71 ± 7 kg, and weekly running distance: 38 ± 24 km), were randomly selected from an existing database consisting of 115 participants [26] for the purpose of the present study. Participants voluntarily participated in this study, and to be included, they were required to run at least once a week and to not have current or recent lower-extremity injury (≤ 1 month). The study protocol was conducted according to the guidelines of the latest declaration of Helsinki and approved by the local Ethics Committee of the Vaud canton (CER-VD 2020-00334). Written informed consent was obtained for all subjects involved in the study.

2.2. Experimental Procedure and Data Collection

The experimental procedure and data collection has already been described elsewhere [39]. Briefly, an IMU of 9.4 g (Movesense sensor, Suunto, Vantaa, Finland) was firmly attached to the sacrum of participants using an elastic strap belt (Movesense, Suunto, Vantaa, Finland; see first figure in [39]). Then, after a warm-up run of 7-min, performed between 9 and 13 km/h on an instrumented treadmill (Arsalis T150-FMT-MED, Louvain-la-Neuve, Belgium), three 1-min running trials using speeds of 9, 11, and 13 km/h were recorded in a randomized order. Three-dimensional IMU and kinetic data corresponding to the first 10 strides following the 30-s mark of the running trials were kept for data analysis. Kinetic and IMU data were not exactly synchronized. However, the synchronization delay between kinetic and IMU data was small (≤ 50 ms). Therefore, kinetic and IMU data corresponded to the same 10 strides.

IMU data (saturation range: ± 8 g) were collected at 208 Hz (manufacturing specification) using a home-made iOS application running on an iPhone SE (Apple, Cupertino, CA, USA). The IMU orientation was such that its medio-lateral (pointing towards the right side of the IMU), posterior–anterior, and inferior–superior axes were denoted as the x -, y -, and z -axis, respectively. These IMU data were transferred to a personal computer for post processing.

The force plate embedded into the treadmill together with the Vicon Nexus software (v2.9.3, Vicon, Oxford, UK) were used to collect kinetic data (200 Hz). In the laboratory coordinate system (LCS), medio-lateral (pointing towards the right side of the body), posterior–anterior, and inferior–superior axes were denoted as the x -, y -, and z -axis, respectively. The Visual3D Professional software (v6.01.12, C-Motion Inc., Germantown, MD, USA) was used to process the 3D ground reaction forces (analog signal), which were first exported in .c3d format. Then, the forces were low-pass filtered at 20 Hz using a 4th order Butterworth filter.

2.3. Gold Standard Method

For each running trial, FS and TO events were identified within Visual3D. These events were detected by applying a 20 N threshold to the vertical ground reaction force [46]. t_c and t_f were defined by the time between FS and TO events and between TO and FS events, respectively, while $F_{z,\max}$ was defined by the maximum of the vertical ground reaction force between FS and TO events and was expressed in body weights.

2.4. Inertial Measurement Unit Method

The custom c++ code [47] used to process IMU data has already been described elsewhere [39]. Briefly, the average angle between the z-axis of the IMU and LCS was calculated using the median values of the 3D raw acceleration data filtered using a truncated Fourier series to 0.5 Hz in each dimension. This angle was used to align (reorient) the z-axis of the IMU with the LCS. This reorientation process was not considered in previous research that used a sacral-mounted IMU to estimate $F_{z,\max}$ and t_c [24,25,31]. Then, 3D reoriented data were filtered using a truncated Fourier series to 5 Hz in each dimension. The vertical ground reaction force was approximated by the filtered vertical acceleration signal multiplied by body mass. FS and TO events were detected using a 20 N threshold, which allowed to estimate t_c and t_f . This 20 N threshold replaced the body weight threshold used in the original custom code described in [39] and is the only change made herein. $F_{z,\max}$ was estimated as the maximum of the approximated vertical ground reaction force between FS and TO events.

2.5. Data Analysis

The RMSE, both in absolute (ms and BW) and relative units, i.e., normalized by the corresponding mean value over all participants and obtained using the GSM, was calculated for $F_{z,\max}$, t_c , and t_f averaged over the 10 analyzed strides for each participant and each running trial. Data analysis was performed using Python (v3.7.4, available at <http://www.python.org> (accessed on 25 October 2021)).

2.6. Statistical Analysis

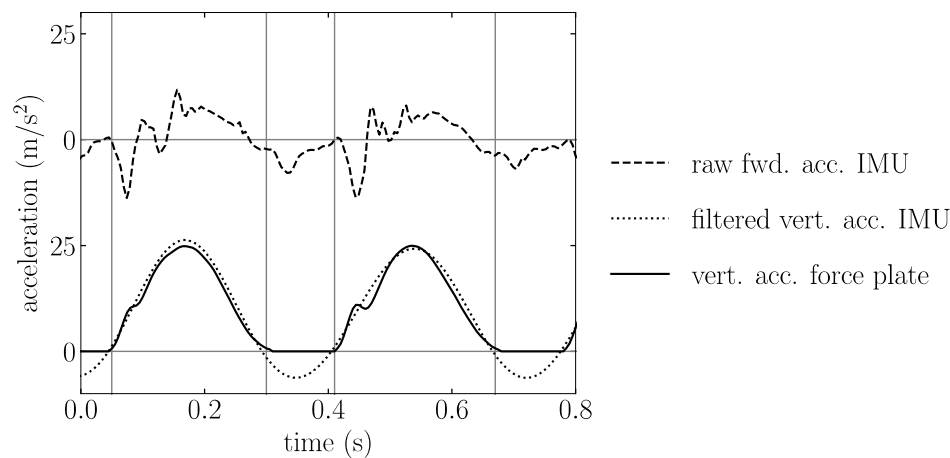
All data are presented as mean \pm standard deviation. To examine the presence of systematic bias on $F_{z,\max}$, t_c , and t_f obtained from the GSM and IMUM for each speed, Bland–Altman plots were constructed [48,49]. In case of a systematic bias, a positive value indicates an overestimation of the IMUM compared to the GSM, while a negative value indicates an underestimation. In addition, lower and upper limit of agreements and 95% confidence intervals were calculated. The limits of agreements were calculated as the bias \pm the smallest real difference (SRD). SRD defines the smallest change that indicates a clinically important difference and is calculated as $\text{SRD} = 1.96 \sigma$, where σ is the standard deviation of the difference between the gold standard and estimated values [50,51]. Besides, a significant slope of the regression line indicates the presence of a proportional bias (heteroscedasticity). Then, as no obvious deviations from homoscedasticity and normality were observed in the residual plots, two-way [method of calculation (GSM vs. IMUM) \times running speed (9 vs. 11 vs. 13)] repeated measures ANOVA using Mauchly's correction for sphericity were performed for $F_{z,\max}$, t_c , and t_f . Holm corrections were employed for pairwise post hoc comparisons. The differences between the GSM and IMUM were quantified using Cohen's d effect size, where $|d|$ values close to 0.01, 0.2, 0.5, and 0.8 reflect a very small, small, moderate, and large effect size, respectively [52]. Statistical analysis was performed using Jamovi (v1.2, <https://www.jamovi.org> (accessed on 25 October 2021)) with a level of significance set at $p \leq 0.05$.

3. Results

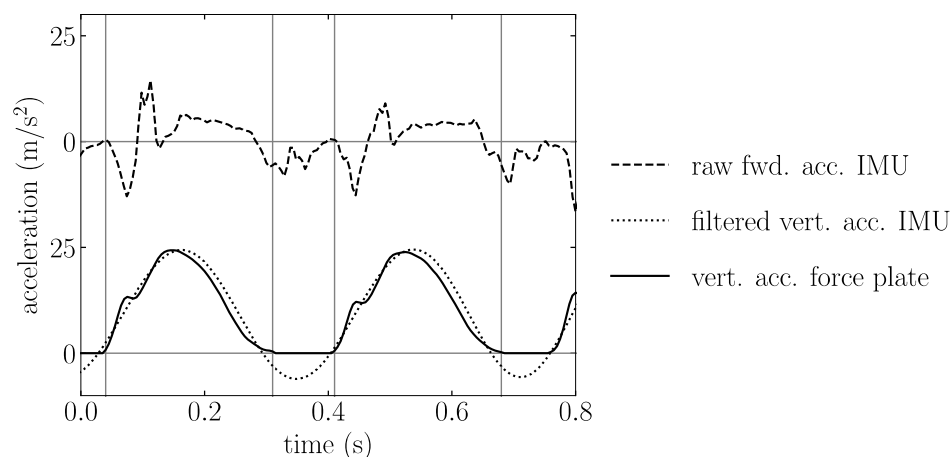
The raw forward acceleration recorded by the IMU and the filtered vertical acceleration recorded by the IMU, as well as the vertical acceleration recorded by the force plate during a running stride for three representative participants running at 11 km/h, are depicted in Figure 1.

Systematic biases (average over running speeds) were obtained for $F_{z,\max}$ (0.07 BW) and t_c and t_f (13 ms), and 11 km/h gave the smallest absolute bias, followed by 9 km/h and 13 km/h (Table 1). The three variables reported a significant negative proportional bias at all speeds and the proportional bias of t_f was larger than that of t_c (Table 1).

(A) Example for a first participant



(B) Example for a second participant



(C) Example for a third participant

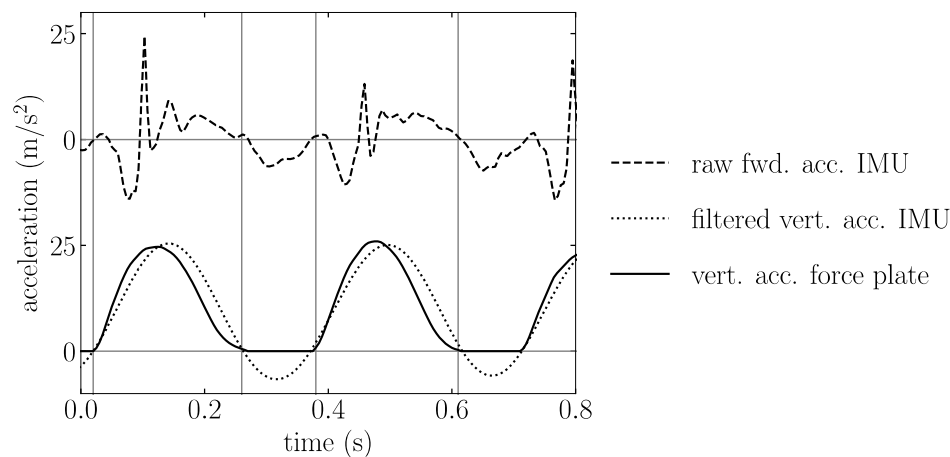


Figure 1. Raw forward acceleration from inertial measurement unit (IMU), filtered vertical acceleration from IMU, and vertical acceleration from force plate during a running stride for three representative participants at 11 km/h are reported in (A–C). The vertical lines represent foot-strike and toe-off events as determined using a 20 N threshold on force plate data.

Table 1. Systematic bias, lower limit of agreement (Lloa), upper limit of agreement (Uloa), and proportional bias \pm residual random error together with its corresponding p -value between peak vertical ground reaction force ($F_{z,max}$), contact time (t_c), and flight time (t_f) obtained using inertial measurement unit method and gold standard method at three running speeds. Confidence intervals of 95% are given in square brackets [lower, upper]. Significant ($p \leq 0.05$) proportional biases are reported in bold font.

	Speed (km/h)	Systematic Bias	Lloa	Uloa	Proportional Bias (p)
$F_{z,max}$ (BW)	9	0.05 [0.04, 0.05]	−0.21 [−0.22, −0.20]	0.30 [0.29, 0.31]	−0.28 \pm 0.02 (<0.001)
	11	−0.04 [−0.04, −0.03]	−0.31 [−0.32, −0.30]	0.23 [0.22, 0.24]	−0.41 \pm 0.02 (<0.001)
	13	−0.13 [−0.13, −0.12]	−0.45 [−0.46, −0.43]	0.19 [0.18, 0.20]	−0.51 \pm 0.02 (<0.001)
t_c (ms)	9	−9.9 [−10.6, −9.1]	−43.7 [−45.0, −42.4]	23.9 [22.6, 25.2]	−0.38 \pm 0.02 (<0.001)
	11	7.3 [6.5, 8.0]	−24.6 [−25.8, −23.4]	39.1 [37.9, 40.3]	−0.37 \pm 0.02 (<0.001)
	13	20.2 [19.5, 20.9]	−10.1 [−11.3, −9.0]	50.6 [49.4, 51.7]	−0.29 \pm 0.02 (<0.001)
t_f (ms)	9	9.9 [9.1, 10.7]	−23.8 [−25.0, −22.5]	43.5 [42.3, 44.8]	−0.79 \pm 0.02 (<0.001)
	11	−7.4 [−8.1, −6.6]	−39.2 [−40.5, −38.0]	24.5 [23.3, 25.8]	−0.86 \pm 0.02 (<0.001)
	13	−20.4 [−21.1, −19.7]	−50.8 [−52.0, −49.7]	10.0 [8.9, 11.2]	−0.91 \pm 0.02 (<0.001)

Note: For systematic biases, positive and negative values indicate the inertial measurement unit method overestimated and underestimated $F_{z,max}$, t_c , and t_f , respectively.

Repeated measures ANOVA depicted significant effects for both methods and running speed, as well as an interaction effect for $F_{z,max}$, t_c , and t_f ($p \leq 0.002$; Table 2). Holm post hoc tests yielded significant differences between $F_{z,max}$, t_c , and t_f obtained using the GSM and IMUM at all speeds ($p \leq 0.006$). The average RMSE over running speed was 0.15 BW for $F_{z,max}$ (6%), while it was 20 ms for t_c and t_f , corresponding to 8% and 18%, respectively (Table 2). Cohen's d effect sizes were small for $F_{z,max}$ and moderate for t_c and t_f , except at 13 km/h which was large for the three variables (Table 2). The average SRD over running speed was 0.28 BW for $F_{z,max}$ (11%), while it was 32.0 ms for t_c and t_f , corresponding to 13% and 30%, respectively (Table 2).

Table 2. Peak vertical ground reaction force ($F_{z,max}$), contact time (t_c), and flight time (t_f) obtained using the gold standard method (GSM) and inertial measurement unit method (IMUM) together with the root mean square error [RMSE; both in absolute (ms or BW) and relative (%) units], as well as Cohen's d effect size and smallest real difference (SRD) for three running speeds. Significant ($p \leq 0.05$) method of calculation, running speed, and interaction effect, as determined by repeated measures ANOVA, are reported in bold font. * Significant difference between $F_{z,max}$, t_c , and t_f obtained using the GSM and IMUM at a given running speed, as determined by Holm post hoc tests.

Speed (km/h)	Parameter	$F_{z,max}$ (BW)	t_c (ms)	t_f (ms)
9	GSM	2.37 \pm 0.19 *	278.3 \pm 22.2 *	92.8 \pm 22.4 *
	IMUM	2.42 \pm 0.14	268.4 \pm 15.5	102.7 \pm 10.8
	RMSE (absolute)	0.13	18.5	18.6
	RMSE (%)	5.3	6.7	20.1
	d	−0.27	0.49	−0.54
	SRD	0.26 (11%)	33.8 (12%)	33.7 (36%)
11	GSM	2.51 \pm 0.19 *	249.7 \pm 19.2 *	111.5 \pm 19.7 *
	IMUM	2.47 \pm 0.13	256.9 \pm 13.9	104.1 \pm 9.1
	RMSE (absolute)	0.13	16.4	16.5
	RMSE (%)	5.1	6.6	14.8
	d	0.22	−0.41	0.45
	SRD	0.27 (11%)	31.8 (13%)	31.9 (29%)

Table 2. Cont.

Speed (km/h)	Parameter	$F_{z,max}$ (BW)	t_c (ms)	t_f (ms)
13	GSM	2.62 ± 0.20 *	227.6 ± 16.5 *	122.8 ± 17.5 *
	IMUM	2.49 ± 0.11	247.8 ± 12.8	102.4 ± 8.0
	RMSE (absolute)	0.19	24.4	24.5
	RMSE (%)	7.4	10.7	20.0
	d	0.73	−1.26	1.37
	SRD	0.32 (12%)	30.3 (13%)	30.4 (25%)
Method of calculation effect		$p = 0.002$	$p < 0.001$	$p < 0.001$
Running speed effect		$p < 0.001$	$p < 0.001$	$p < 0.001$
Interaction effect		$p < 0.001$	$p < 0.001$	$p < 0.001$

Note: Values are presented as mean ± standard deviation.

4. Discussion

According to the first hypothesis, an RMSE equal to 0.15 BW was reported for $F_{z,max}$. Moreover, according to the second hypothesis, an RMSE equal to 20 ms was obtained for t_c and t_f . Our findings demonstrated systematic and proportional biases, as well as significant differences between gold standard and estimated $F_{z,max}$, t_c , and t_f at each speed employed. Nonetheless, systematic biases averaged over running speeds were small (0.07 BW and 13 ms) and the RMSEs were smaller than the SRDs, indicating no clinically important difference between the GSM and IMUM. Hence, the present findings support the use of the IMUM to estimate $F_{z,max}$, t_c , and t_f for level treadmill runs at low running speeds.

A systematic bias of 0.07 BW and an RMSE of 0.15 BW (6%) were reported for $F_{z,max}$. These errors seemed to be comparable to those obtained using a 10 Hz low-pass cutoff frequency [24], though the bias and RMSE were not explicitly reported [\sim 0.15 BW by visual inspection of the fourth figure in [24] (14–19 km/h)]. In addition, the RMSE found for $F_{z,max}$ in the present study was equal to the RMSE obtained using two different machine learning algorithms (linear regression and quantile regression forest) [25]. This result suggests that combining IMU data with machine learning algorithms seems to not necessarily be advantageous to estimate $F_{z,max}$. Using inertial sensors placed on the legs along the tibial axis, Charry, et al. [53] obtained a 6% error on $F_{z,max}$ (6–21 km/h), while Wouda, et al. [54] achieved a 3% error (10–14 km/h) by using three IMUs (two on lower legs and one on pelvis) and two artificial neural networks. Besides, an RMSE \leq 0.17 BW was reported when estimating $F_{z,max}$ using 3D kinematic data of the center of mass or sacral marker trajectory [26]. An RMSE close to 0.15 BW was reported by Pavei, Seminati, Storniolo and Peyré-Tartaruga [27] when the whole-body center of mass acceleration, obtained using kinematic data to estimate $F_{z,max}$ for running speeds ranging from 7 to 20 km/h, was used for a single participant. Thus, the errors reported for $F_{z,max}$ in the present study were comparable to those obtained using previously published methods [24–27,53,54]. Moreover, the RMSE of $F_{z,max}$ was smaller than its SRD for each tested speed (Table 2), indicating no clinically important difference between $F_{z,max}$ values obtained using the GSM and IMUM.

The IMUM reported a systematic bias of 13 ms and an RMSE of 20 ms (8%) for t_c (Tables 1 and 2). These errors seemed to be smaller than those obtained using a 5 Hz low-pass cutoff frequency [24], though the bias and RMSE were not explicitly reported [\sim 30 ms by visual inspection of the fifth figure in [24] (14–19 km/h)]. The IMUM employed in the present study might be advantageous compared to that previously used [24] because the present IMUM utilized a single low-pass cutoff frequency (5 Hz) to estimate both $F_{z,max}$ and t_c while the previous method required two different cutoff frequencies (10 Hz for $F_{z,max}$ and 5 Hz for t_c). However, the present errors were much higher than those reported by Lee, Mellifont and Burkett [31] (0 ms). These authors used specific spikes in an unfiltered forward acceleration signal recorded by a sacral-mounted IMU sampled at 100 Hz to detect FS and TO events. However, these spikes were not present in most of the data recorded in the present study [see the first figure in in Lee, Mellifont and Burkett [31] vs. Figure 1 herein]. One possible explanation could be that the 10 national

level runners recruited by these authors shared a very similar running pattern with specific acceleration spikes that were not always observed in the present study. As a side note, the anterior–posterior acceleration signal recorded by the IMU (Figure 1) was quite different from that depicted in Lee, Mellifont and Burkett [31], and both anterior–posterior IMU signals were different from that assessed using the gold standard anterior–posterior ground reaction force signal [55]. This was also previously observed when reconstructing the anterior–posterior acceleration signal using 3D kinematic trajectories [27]. Besides, the 20 ms RMSE obtained in our study is almost two times larger than the 10 ms RMSE reported by Alcantara, Day, Hahn and Grabowski [25]. Such a difference might be explained by the fact that these authors predicted t_c using two different machine learning algorithms (linear regression and quantile regression forest) while the present study estimates t_c directly from the post-processing of the vertical acceleration signal recorded by the sacral-mounted IMU. Moreover, such a difference suggests that combining IMU data with a machine learning algorithm may improve the estimations of t_c and t_f compared to those obtained using IMU data alone. However, the robustness of the machine learning algorithms employed by these authors might be questioned as these algorithms were trained on 28 runners and tested on 9 runners, which is below the median value of 40 participants used for this kind of research question [56]. Nonetheless, further studies would be required to evaluate if applying a machine learning algorithm on our IMU data, which contains 100 participants, would be more accurate in estimating t_c and t_f . Using foot-worn inertial sensors, the systematic bias on t_c was ~ 10 ms (10–20 km/h) [33] and the RMSE was ~ 10 ms (11 km/h) [38]. Hence, the errors reported for the IMUM [systematic bias: 7 ms; RMSE: 15 ms (6%) at 11 km/h] were comparable to those previously reported using foot-worn inertial sensors. In addition, Falbriard, Meyer, Mariani, Millet and Aminian [33] reported a proportional bias for t_c , as in the present study. Using 3D kinematic data, the RMSE was larger or equal to 15 ms for t_c (20 km/h) [46] while using a photoelectric system, a bias of ~ 1 ms was reported for t_c , though validated against motion capture (12 km/h) [57]. Therefore, the error reported for the IMUM when estimating t_c was comparable to the error obtained using an optoelectronic system [46], but was much larger than the error obtained using a photoelectric system [57]. However, even though these two systems can be used outside the laboratory [20,21], they suffer from a lack of portability and do not allow continuous data collection. For this reason, using a single IMU was advantageous by its portability, and was shown to be quite accurate to estimate t_c , and therefore t_f . Indeed, when the error is calculated for many running steps, as t_c and t_f are based on the same TO events, the bias of t_f is the negative of the bias of t_c , and the RMSEs for t_c and t_f are mostly the same in absolute (ms) units. Furthermore, t_c and t_f reported smaller RMSEs than their corresponding SRDs for each tested speed (Table 2), indicating no clinically important differences between t_c and t_f values obtained using the GSM and IMUM.

A significant effect of running speed was observed for $F_{z,max}$, t_c , and t_f (Table 2). Moreover, the most accurate estimation was given at 11 km/h (Tables 1 and 2). These findings could not readily be explained. However, further studies should focus on testing several slower and faster running speeds to further decipher the running speed effect. Then, future studies could focus on constructing a more sophisticated model, considering the running speed to try to improve the estimations of $F_{z,max}$, t_c , and t_f .

A few limitations to this study exist. The IMUM was compared to the GSM only at low running speeds during treadmill runs. However, the IMUM might also perform well overground because spatiotemporal variables between treadmill and overground running are largely comparable [58], although controversial [59]. Nonetheless, further studies should focus on comparing the IMUM to the GSM using additional conditions (i.e., faster speeds, positive and negative slopes, and different types of ground). Moreover, kinetic and IMU data were not exactly synchronized. Therefore, further studies should focus on synchronizing these data and performing FS and TO events comparisons between the GSM and IMUM. This may be useful if the assessment of metrics at specific FS and TO

events is needed, e.g., knee angle at FS, using additional IMUs [60] synchronized with the sacral-mounted IMU providing FS and TO events.

5. Conclusions

This study estimated $F_{z,max}$, t_c , and t_f using the vertical acceleration signal recorded by a single sacral-mounted IMU, which was filtered using a truncated Fourier series to 5 Hz. The comparison between the GSM and IMUM depicted an RMSE of 0.15 BW for $F_{z,max}$, and of 20 ms for t_c and t_f , and small systematic biases of 0.07 BW for $F_{z,max}$, and 13 ms for t_c and t_f (average over running speeds). These errors were comparable to those obtained using previously published methods. Moreover, the RMSEs were smaller than the SRDs, indicating no clinically important difference between the GSM and IMUM. Therefore, the findings of this study support the use of the IMUM to estimate $F_{z,max}$, t_c , and t_f for level treadmill runs at low running speeds, especially because an IMU has the advantage to be low-cost and portable, and therefore seems very practical for coaches and healthcare professionals.

Author Contributions: Conceptualization, A.P., T.L., C.G. and D.M.; methodology, A.P., T.L., C.G. and D.M.; investigation, A.P., T.L. and B.B.; formal analysis, A.P. and B.B.; writing—original draft preparation, A.P. and B.B.; writing—review and editing, A.P., T.L., B.B., C.G. and D.M.; supervision, A.P., T.L., C.G. and D.M. All authors have read and agreed to the published version of the manuscript.

Funding: This research was funded by Innosuisse, grant number 35793.1 IP-LS.

Institutional Review Board Statement: The study was conducted according to the guidelines of the Declaration of Helsinki, and approved by the local Ethics Committee of the Vaud canton (CER-VD 2020-00334).

Informed Consent Statement: Written informed consent was obtained from all subjects involved in the study.

Data Availability Statement: The datasets supporting this article are available on request to the corresponding author.

Acknowledgments: The authors warmly thank the participants for their time and cooperation.

Conflicts of Interest: The authors declare no conflict of interest. The funders had no role in the design of the study; in the collection, analyses, or interpretation of data; in the writing of the manuscript, or in the decision to publish the results.

References

1. Novacheck, T.F. The biomechanics of running. *Gait Posture* **1998**, *7*, 77–95. [[CrossRef](#)]
2. Minetti, A.E. A model equation for the prediction of mechanical internal work of terrestrial locomotion. *J. Biomech.* **1998**, *31*, 463–468. [[CrossRef](#)]
3. Folland, J.P.; Allen, S.J.; Black, M.I.; Handsaker, J.C.; Forrester, S.E. Running Technique is an Important Component of Running Economy and Performance. *Med. Sci. Sports Exerc.* **2017**, *49*, 1412–1423. [[CrossRef](#)] [[PubMed](#)]
4. Hreljac, A. Impact and overuse injuries in runners. *Med. Sci. Sports Exerc.* **2004**, *36*, 845–849. [[CrossRef](#)]
5. Hreljac, A.; Marshall, R.N.; Hume, P.A. Evaluation of lower extremity overuse injury potential in runners. *Med. Sci. Sports Exerc.* **2000**, *32*, 1635–1641. [[CrossRef](#)] [[PubMed](#)]
6. Nielsen, R.O.; Buist, I.; Sørensen, H.; Lind, M.; Rasmussen, S. Training errors and running related injuries: A systematic review. *Int. J. Sports Phys. Ther.* **2012**, *7*, 58–75.
7. Fredette, A.; Roy, J.S.; Perreault, K.; Dupuis, F.; Napier, C.; Esculier, J.F. The association between running injuries and training parameters: A systematic review. *J. Athl. Train.* **2021**. [[CrossRef](#)]
8. Kiernan, D.; Hawkins, D.A.; Manoukian, M.A.C.; McKallip, M.; Oelsner, L.; Caskey, C.F.; Coolbaugh, C.L. Accelerometer-based prediction of running injury in National Collegiate Athletic Association track athletes. *J. Biomech.* **2018**, *73*, 201–209. [[CrossRef](#)]
9. Scott, S.H.; Winter, D.A. Internal forces of chronic running injury sites. *Med. Sci. Sports Exerc.* **1990**, *22*, 357–369. [[CrossRef](#)]
10. Edwards, W.B. Modeling Overuse Injuries in Sport as a Mechanical Fatigue Phenomenon. *Exerc. Sport Sci. Rev.* **2018**, *46*, 224–231. [[CrossRef](#)]
11. Matijevich, E.S.; Branscombe, L.M.; Scott, L.R.; Zelik, K.E. Ground reaction force metrics are not strongly correlated with tibial bone load when running across speeds and slopes: Implications for science, sport and wearable tech. *PLoS ONE* **2019**, *14*, e0210000. [[CrossRef](#)] [[PubMed](#)]

12. Lenhart, R.L.; Thelen, D.G.; Wille, C.M.; Chumanov, E.S.; Heiderscheit, B.C. Increasing running step rate reduces patellofemoral joint forces. *Med. Sci. Sports Exerc.* **2014**, *46*, 557–564. [[CrossRef](#)] [[PubMed](#)]
13. Sasimontokul, S.; Bay, B.K.; Pavol, M.J. Bone contact forces on the distal tibia during the stance phase of running. *J. Biomech.* **2007**, *40*, 3503–3509. [[CrossRef](#)]
14. van der Worp, H.; Vrielink, J.W.; Bredeweg, S.W. Do runners who suffer injuries have higher vertical ground reaction forces than those who remain injury-free? A systematic review and meta-analysis. *Br. J. Sports Med.* **2016**, *50*, 450. [[CrossRef](#)]
15. Maiwald, C.; Sterzing, T.; Mayer, T.A.; Milani, T.L. Detecting foot-to-ground contact from kinematic data in running. *Footwear Sci.* **2009**, *1*, 111–118. [[CrossRef](#)]
16. Abendroth-Smith, J. Stride adjustments during a running approach toward a force plate. *Res. Q. Exerc. Sport* **1996**, *67*, 97–101. [[CrossRef](#)] [[PubMed](#)]
17. Lussiana, T.; Patoz, A.; Gindre, C.; Mourot, L.; Hébert-Losier, K. The implications of time on the ground on running economy: Less is not always better. *J. Exp. Biol.* **2019**, *222*, jeb192047. [[CrossRef](#)]
18. Patoz, A.; Lussiana, T.; Thouvenot, A.; Mourot, L.; Gindre, C. Duty Factor Reflects Lower Limb Kinematics of Running. *Appl. Sci.* **2020**, *10*, 8818. [[CrossRef](#)]
19. Debaere, S.; Jonkers, I.; Delecluse, C. The Contribution of Step Characteristics to Sprint Running Performance in High-Level Male and Female Athletes. *J. Strength Cond. Res.* **2013**, *27*, 116–124. [[CrossRef](#)] [[PubMed](#)]
20. Hébert-Losier, K.; Mourot, L.; Holmberg, H.C. Elite and amateur orienteers' running biomechanics on three surfaces at three speeds. *Med. Sci. Sports Exerc.* **2015**, *47*, 381–389. [[CrossRef](#)]
21. Lussiana, T.; Gindre, C. Feel your stride and find your preferred running speed. *Biol. Open* **2016**, *5*, 45–48. [[CrossRef](#)]
22. Logan, S.; Hunter, I.; Ty Hopkins, J.T.J.; Feland, J.B.; Parcell, A.C. Ground reaction force differences between running shoes, racing flats, and distance spikes in runners. *J. Sports Sci. Med.* **2010**, *9*, 147–153. [[PubMed](#)]
23. Camomilla, V.; Bergamini, E.; Fantozzi, S.; Vannozzi, G. Trends Supporting the In-Field Use of Wearable Inertial Sensors for Sport Performance Evaluation: A Systematic Review. *Sensors* **2018**, *18*, 873. [[CrossRef](#)]
24. Day, E.M.; Alcantara, R.S.; McGeehan, M.A.; Grabowski, A.M.; Hahn, M.E. Low-pass filter cutoff frequency affects sacral-mounted inertial measurement unit estimations of peak vertical ground reaction force and contact time during treadmill running. *J. Biomech.* **2021**, *119*, 110323. [[CrossRef](#)]
25. Alcantara, R.S.; Day, E.M.; Hahn, M.E.; Grabowski, A.M. Sacral acceleration can predict whole-body kinetics and stride kinematics across running speeds. *PeerJ* **2021**, *9*, e11199. [[CrossRef](#)] [[PubMed](#)]
26. Patoz, A.; Lussiana, T.; Breine, B.; Gindre, C.; Malatesta, D. Both a single sacral marker and the whole-body center of mass accurately estimate peak vertical ground reaction force in running. *Gait Posture* **2021**, *89*, 186–192. [[CrossRef](#)] [[PubMed](#)]
27. Pavei, G.; Seminati, E.; Storniolo, J.L.L.; Peyré-Tartaruga, L.A. Estimates of Running Ground Reaction Force Parameters from Motion Analysis. *J. Appl. Biomech.* **2017**, *33*, 69–75. [[CrossRef](#)]
28. Verheul, J.; Gregson, W.; Lisboa, P.; Vanrenterghem, J.; Robinson, M.A. Whole-body biomechanical load in running-based sports: The validity of estimating ground reaction forces from segmental accelerations. *J. Sci. Med. Sport* **2019**, *22*, 716–722. [[CrossRef](#)]
29. Flaction, P.; Quievre, J.; Morin, J.B. An Athletic Performance Monitoring Device. 2013. Available online: <https://patents.justia.com/patent/9536134> (accessed on 25 October 2021).
30. Gindre, C.; Lussiana, T.; Hébert-Losier, K.; Morin, J.-B. Reliability and validity of the Myotest[®] for measuring running stride kinematics. *J. Sports Sci.* **2016**, *34*, 664–670. [[CrossRef](#)]
31. Lee, J.B.; Mellifont, R.B.; Burkett, B.J. The use of a single inertial sensor to identify stride, step, and stance durations of running gait. *J. Sci. Med. Sport* **2010**, *13*, 270–273. [[CrossRef](#)]
32. Moe-Nilssen, R. A new method for evaluating motor control in gait under real-life environmental conditions. Part 1: The instrument. *Clin. Biomech.* **1998**, *13*, 320–327. [[CrossRef](#)]
33. Falbriard, M.; Meyer, F.; Mariani, B.; Millet, G.P.; Aminian, K. Accurate Estimation of Running Temporal Parameters Using Foot-Worn Inertial Sensors. *Front. Physiol.* **2018**, *9*, 610. [[CrossRef](#)]
34. Norris, M.; Anderson, R.; Kenny, I.C. Method analysis of accelerometers and gyroscopes in running gait: A systematic review. *Proc. Inst. Mech. Eng. Part P J. Sports Eng. Technol.* **2014**, *228*, 3–15. [[CrossRef](#)]
35. Falbriard, M.; Meyer, F.; Mariani, B.; Millet, G.P.; Aminian, K. Drift-Free Foot Orientation Estimation in Running Using Wearable IMU. *Front. Bioeng. Biotechnol.* **2020**, *8*, 65. [[CrossRef](#)] [[PubMed](#)]
36. Giandolini, M.; Poupard, T.; Gimenez, P.; Horvais, N.; Millet, G.Y.; Morin, J.-B.; Samozino, P. A simple field method to identify foot strike pattern during running. *J. Biomech.* **2014**, *47*, 1588–1593. [[CrossRef](#)]
37. Giandolini, M.; Horvais, N.; Rossi, J.; Millet, G.Y.; Samozino, P.; Morin, J.-B. Foot strike pattern differently affects the axial and transverse components of shock acceleration and attenuation in downhill trail running. *J. Biomech.* **2016**, *49*, 1765–1771. [[CrossRef](#)]
38. Chew, D.-K.; Ngoh, K.J.-H.; Gouwanda, D.; Gopalai, A.A. Estimating running spatial and temporal parameters using an inertial sensor. *Sports Eng.* **2018**, *21*, 115–122. [[CrossRef](#)]
39. Patoz, A.; Lussiana, T.; Breine, B.; Gindre, C.; Malatesta, D. Estimating effective contact and flight times using a sacral-mounted inertial measurement unit. *J. Biomech.* **2021**, *127*, 110667. [[CrossRef](#)] [[PubMed](#)]
40. Napier, C.; Jiang, X.; MacLean, C.L.; Menon, C.; Hunt, M.A. The use of a single sacral marker method to approximate the centre of mass trajectory during treadmill running. *J. Biomech.* **2020**, *108*, 109886. [[CrossRef](#)]
41. Cavagna, G.A. The landing–take-off asymmetry in human running. *J. Exp. Biol.* **2006**, *209*, 4051. [[CrossRef](#)] [[PubMed](#)]

42. Cavagna, G.A.; Legramandi, M.A.; Peyré-Tartaruga, L.A. Old men running: Mechanical work and elastic bounce. *Proc. Biol. Sci.* **2008**, *275*, 411–418. [[CrossRef](#)]
43. Cavagna, G.A.; Legramandi, M.A.; Peyré-Tartaruga, L.A. The landing–take-off asymmetry of human running is enhanced in old age. *J. Exp. Biol.* **2008**, *211*, 1571. [[CrossRef](#)] [[PubMed](#)]
44. Mai, P.; Willwacher, S. Effects of low-pass filter combinations on lower extremity joint moments in distance running. *J. Biomech.* **2019**, *95*, 109311. [[CrossRef](#)] [[PubMed](#)]
45. Kiernan, D.; Miller, R.H.; Baum, B.S.; Kwon, H.J.; Shim, J.K. Amputee locomotion: Frequency content of prosthetic vs. intact limb vertical ground reaction forces during running and the effects of filter cut-off frequency. *J. Biomech.* **2017**, *60*, 248–252. [[CrossRef](#)]
46. Smith, L.; Preece, S.; Mason, D.; Bramah, C. A comparison of kinematic algorithms to estimate gait events during overground running. *Gait Posture* **2015**, *41*, 39–43. [[CrossRef](#)] [[PubMed](#)]
47. ISO/IEC 14882:2020; ISO International Standard ISO/IEC 14882:2020(E) Programming Languages—C++. International Organization for Standardization: Geneva, Switzerland, 2020.
48. Bland, J.M.; Altman, D.G. Comparing methods of measurement: Why plotting difference against standard method is misleading. *Lancet* **1995**, *346*, 1085–1087. [[CrossRef](#)]
49. Atkinson, G.; Nevill, A.M. Statistical methods for assessing measurement error (reliability) in variables relevant to sports medicine. *Sports Med.* **1998**, *26*, 217–238. [[CrossRef](#)]
50. Hopkins, W.G. Measures of Reliability in Sports Medicine and Science. *Sports Med.* **2000**, *30*, 1–15. [[CrossRef](#)] [[PubMed](#)]
51. Beckerman, H.; Roebroek, M.E.; Lankhorst, G.J.; Becher, J.G.; Bezemer, P.D.; Verbeek, A.L.M. Smallest real difference, a link between reproducibility and responsiveness. *Qual. Life Res.* **2001**, *10*, 571–578. [[CrossRef](#)] [[PubMed](#)]
52. Cohen, J. *Statistical Power Analysis for the Behavioral Sciences*; Routledge: London, UK, 1988.
53. Charry, E.; Hu, W.; Umer, M.; Ronchi, A.; Taylor, S. Study on estimation of peak Ground Reaction Forces using tibial accelerations in running. In Proceedings of the 2013 IEEE Eighth International Conference on Intelligent Sensors, Sensor Networks and Information Processing, Melbourne, VIC, Australia, 2–5 April 2013; pp. 288–293.
54. Wouda, F.J.; Giuberti, M.; Bellusci, G.; Maartens, E.; Reenalda, J.; van Beijnum, B.-J.F.; Veltink, P.H. Estimation of Vertical Ground Reaction Forces and Sagittal Knee Kinematics During Running Using Three Inertial Sensors. *Front. Physiol.* **2018**, *9*, 218. [[CrossRef](#)]
55. Firminger, C.R.; Vernillo, G.; Savoldelli, A.; Stefanyshyn, D.J.; Millet, G.Y.; Edwards, W.B. Joint kinematics and ground reaction forces in overground versus treadmill graded running. *Gait Posture* **2018**, *63*, 109–113. [[CrossRef](#)] [[PubMed](#)]
56. Halilaj, E.; Rajagopal, A.; Fiterau, M.; Hicks, J.L.; Hastie, T.J.; Delp, S.L. Machine learning in human movement biomechanics: Best practices, common pitfalls, and new opportunities. *J. Biomech.* **2018**, *81*, 1–11. [[CrossRef](#)] [[PubMed](#)]
57. García-Pinillos, F.; Latorre-Román, P.Á.; Ramirez-Campillo, R.; Roche-Seruendo, L.E. Agreement between spatiotemporal parameters from a photoelectric system with different filter settings and high-speed video analysis during running on a treadmill at comfortable velocity. *J. Biomech.* **2019**, *93*, 213–219. [[CrossRef](#)]
58. Van Hooren, B.; Fuller, J.T.; Buckley, J.D.; Miller, J.R.; Sewell, K.; Rao, G.; Barton, C.; Bishop, C.; Willy, R.W. Is Motorized Treadmill Running Biomechanically Comparable to Overground Running? A Systematic Review and Meta-Analysis of Cross-Over Studies. *Sports Med.* **2020**, *50*, 785–813. [[CrossRef](#)]
59. Bailey, J.P.; Mata, T.; Mercer, J.D. Is the relationship between stride length, frequency, and velocity influenced by running on a treadmill or overground? *Int. J. Exerc. Sci.* **2017**, *10*, 1067–1075. [[PubMed](#)]
60. Favre, J.; Jolles, B.M.; Aissaoui, R.; Aminian, K. Ambulatory measurement of 3D knee joint angle. *J. Biomech.* **2008**, *41*, 1029–1035. [[CrossRef](#)] [[PubMed](#)]

8.7 Estimating effective contact and flight times using a sacral-mounted inertial measurement unit

Aurélien Patoz^{1,2,*}, Thibault Lussiana^{2,3,4}, Bastiaan Breine^{2,5}, Cyrille Gindre^{2,3}, Davide Malatesta¹

¹ Institute of Sport Sciences, University of Lausanne, 1015 Lausanne, Switzerland

² Research and Development Department, Volodalen Swiss Sport Lab, 1860 Aigle, Switzerland

³ Research and Development Department, Volodalen, 39270 Chavéria, France

⁴ Research Unit EA3920 Prognostic Markers and Regulatory Factors of Cardiovascular Diseases and Exercise Performance, Health, Innovation platform, University of Franche-Comté, Besançon, France

⁵ Department of Movement and Sports Sciences, Ghent University, 9000 Ghent, Belgium

* Corresponding author

Published in **Journal of Biomechanics**

DOI: 10.1016/j.jbiomech.2021.110667



Estimating effective contact and flight times using a sacral-mounted inertial measurement unit

Aurélien Patoz^{a,b,*}, Thibault Lussiana^{b,c,d}, Bastiaan Breine^{b,e}, Cyrille Gindre^{b,c}, Davide Malatesta^a

^a Institute of Sport Sciences, University of Lausanne, Lausanne 1015, Switzerland

^b Research and Development Department, Volodalen Swiss Sport Lab, Aigle 1860, Switzerland

^c Research and Development Department, Volodalen, Chavéria 39270, France

^d Research Unit EA3920 Prognostic Markers and Regulatory Factors of Cardiovascular Diseases and Exercise Performance, Health, Innovation platform, University of Franche-Comté, Besançon, France

^e Department of Movement and Sports Sciences, Ghent University, Ghent 9000, Belgium

ARTICLE INFO

Keywords:

Gait analysis
Running
Biomechanics
Sensor
Accelerometer

ABSTRACT

Effective ground contact (t_{ce}) and flight (t_{fe}) times were proven to be more appropriate to decipher the landing-take-off asymmetry of running than usual ground contact (t_c) and flight (t_f) times. To measure these effective timings, force plate is the gold standard method (GSM), though not very portable overground. In such situation, alternatives could be to use portable tools such as inertial measurement unit (IMU). Therefore, the purpose of this study was to propose a method that uses the vertical acceleration recorded using a sacral-mounted IMU to estimate t_{ce} and t_{fe} and to compare these estimations to those from GSM. Besides, t_{ce} and t_{fe} were used to evaluate the landing-take-off asymmetry, which was further compared to GSM. One hundred runners ran at 9, 11, and 13 km/h. Force data (200 Hz) and IMU data (208 Hz) were acquired by an instrumented treadmill and a sacral-mounted IMU, respectively. The comparison between GSM and IMU method depicted root mean square error ≤ 22 ms ($\leq 14\%$) for t_{ce} and t_{fe} along with small systematic biases (≤ 20 ms) for each tested speed. These errors are similar to previously published methods that estimated usual t_c and t_f . The systematic biases on t_{ce} and t_{fe} were subtracted before calculating the landing-take-off asymmetry, which permitted to correctly evaluate it at a group level. Therefore, the findings of this study support the use of this method based on vertical acceleration recorded using a sacral-mounted IMU to estimate t_{ce} and t_{fe} for level treadmill runs and to evaluate the landing-take-off asymmetry but only after subtraction of systematic biases and at a group level.

1. Introduction

Back in 1988, Cavagna et al. (1988) defined two key running parameters denoted as effective ground contact (t_{ce}) and flight (t_{fe}) times. They differ from the usual ground contact (t_c) and flight (t_f) times by the fact that t_{ce} and t_{fe} correspond to the amount of time where the vertical ground reaction force is above and below body weight, respectively, rather than where the foot is in contact with the ground or not (Cavagna et al., 2008a). These effective timings were proven to be more appropriate to decipher the landing-take-off asymmetry of running than the usual timings (i.e., t_c and t_f) (Cavagna, 2006; Cavagna et al., 2008a, b).

These two parameters are usually obtained from effective foot-strike (eFS) and toe-off (eTO) events, i.e., when vertical ground reaction force

goes over and below body weight, respectively. To obtain such events, the use of force plates is considered as the gold standard method (GSM). However, force plates are not always available and not very portable overground (Abendroth-Smith, 1996; Maiwald et al., 2009). To overcome such limitation, gait events detection methods were developed using inertial measurement units (IMU) (Chew et al., 2018; Day et al., 2021; Falbriard et al., 2018, 2020; Flaction et al., 2013; Giandolini et al., 2016; Giandolini et al., 2014; Gindre et al., 2016; Lee et al., 2010; Moenilssen, 1998; Norris et al., 2014). Amongst them, a natural choice is a sacral-mounted IMU, the reason being that such placement approximates the location of the center of mass (Napier et al., 2020).

On the one hand, Flaction et al. (2013) determined effective timings using the Myotest® but did not explicitly mentioned the exact procedure

* Corresponding author.

E-mail address: aurelien.patoz@unil.ch (A. Patoz).

<https://doi.org/10.1016/j.jbiomech.2021.110667>

Accepted 28 July 2021

Available online 31 July 2021

0021-9290/© 2021 The Authors. Published by Elsevier Ltd. This is an open access article under the CC BY license (<http://creativecommons.org/licenses/by/4.0/>).

to go from raw IMU data to effective timings. Moreover, the Myotest® outcomes were compared to t_c and t_f from photocell- and optical-based systems instead of t_{ce} and t_{fe} from GSM, leading to an “unusable” validity assessment (Gindre et al., 2016). On the other hand, Day et al. (2021) calculated t_c and t_f from usual foot-strike and toe-off events obtained using a 0 N threshold applied to an estimation of the vertical ground reaction force (using Newton’s second law of motion). However, the authors did not attempt to calculate t_{ce} and t_{fe} . Nonetheless, they showed that a 5 Hz low-pass filter was resulting in the best correlation between t_c obtained from GSM and their method, though mentioning that more research investigating the effect of different filtering methods is needed. For this reason, the purpose of this study was to estimate t_{ce} and t_{fe} using a different filtering method than the one proposed by Day et al. (2021), i. e., a Fourier series truncated to 5 Hz instead of a 5 Hz low-pass filter, to filter the sacral-mounted IMU data (IMU method; IMUM) and to compare these estimations to those from GSM. Besides, estimated t_{ce} and t_{fe} were used to evaluate the landing-take-off asymmetry of running and compare it to that obtained using GSM.

2. Materials and methods

2.1. Participant characteristics

Hundred recreational runners, 74 males (age: 30 ± 8 years, height: 180 ± 6 cm, body mass: 71 ± 7 kg, and weekly running distance: 37 ± 22 km) and 26 females (age: 30 ± 7 years, height: 169 ± 5 cm, body mass: 61 ± 6 kg, and weekly running distance: 22 ± 16 km) voluntarily participated in this study. For study inclusion, participants were required to do not have current or recent lower-extremity injury (≤ 1 month). The study protocol was approved by the local Ethics Committee (CER-VD 2020-00334) and each participant gave written informed consent.

2.2. Experimental procedure and data collection

After providing written informed consent, an IMU of 9.4 g (Movesense, Vantaa, Finland) was firmly attached to the sacrum at the midpoint between the posterior superior iliac spinae (Fig. 1) using an elastic strap belt (Movesense, Vantaa, Finland). Then, a 7-min warm-up run (9–13 km/h) was performed on an instrumented treadmill (Arsalis T150-FMT-MED, Louvain-la-Neuve, Belgium), followed by three 1-min runs (9, 11, and 13 km/h) performed in a randomized order. Three-dimensional (3D) kinetic and IMU data were collected during the first 10 strides following the 30-s mark of running trials.



Fig. 1. The Movesense inertial measurement unit attached to the sacrum of a representative participant using an elastic strap belt.

3D kinetic data were collected at 200 Hz using the force plate embedded into the treadmill and Vicon Nexus software v2.9.3 (Vicon, Oxford, United-Kingdom), and processed in Visual3D Professional software v6.01.12 (C-Motion, Germantown, USA). Ground reaction forces were interpolated using a third-order polynomial least-square fit algorithm and low-pass filtered at 20 Hz using a fourth-order Butterworth filter (Swinnen et al., 2021).

IMU data were collected at 208 Hz (manufacturing specification) with a saturation range of ± 8 g, and using an iPhone SE (Apple, Cupertino, USA) and a home-made iOS application that communicated with the IMU via Bluetooth. During each running trial, the iPhone was kept close to the participant (≤ 1 m) to avoid losing the Bluetooth connection. Kinetic and IMU data were not exactly synchronized (Fig. 2).

2.3. Gold standard method

eFS and eTO were identified within Visual3D by applying a body weight threshold to the vertical ground reaction force (Cavagna et al., 1988). Then, t_{ce} was given by the time between eFS and eTO while t_{fe} by

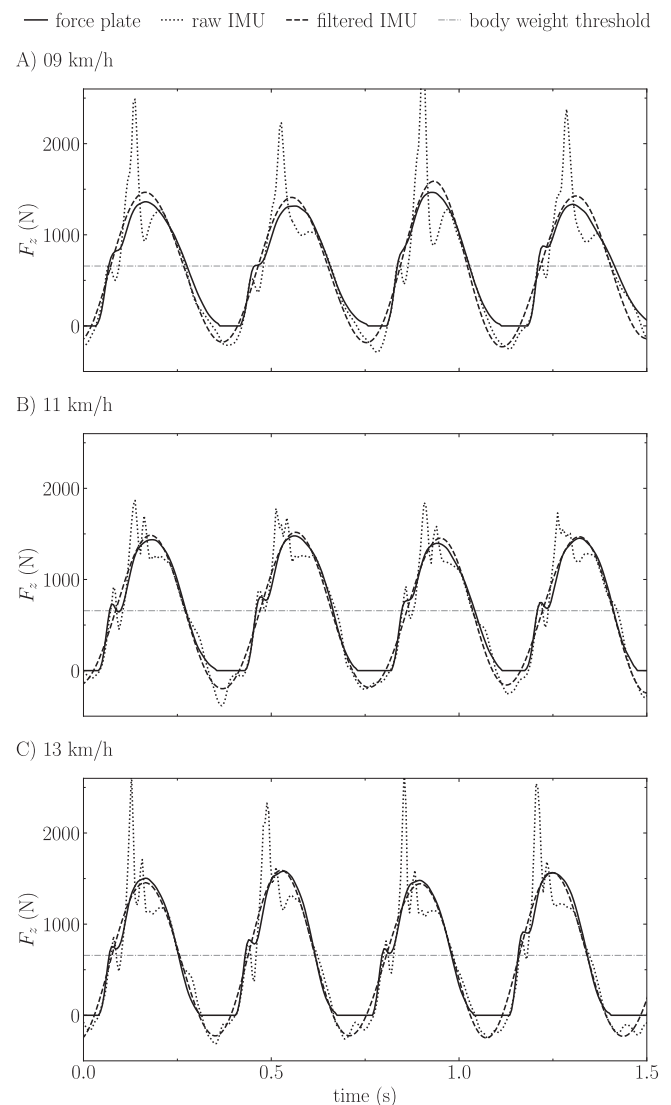


Fig. 2. Vertical ground reaction force (F_z) obtained using force plate (gold standard; solid line) and inertial measurement unit (IMU; raw: dotted line and filtered: dashed line) during two running strides for a given participant at A) 9 km/h, B) 11 km/h, and C) 13 km/h. The gray dash-dotted line represents the body weight threshold used to detect effective foot-strike and toe-off events.

the time between eTO and eFS.

2.4. Inertial measurement unit method

A custom c++ code (ISO/IEC, 2020) was used to process IMU data. First, the z-axis of IMU was aligned with z-axis of local coordinate system (Appendix A). Then, aligned raw acceleration data were filtered using a truncated Fourier series to 5 Hz. This cut-off frequency was chosen because it led to the best estimation of t_c in Day et al. (2021). Filtered data were used to detect eFS and eTO using a $g = 9.81 \text{ m/s}^2$ threshold (equivalent to the body weight threshold of GSM), and to reconstruct vertical ground reaction force by multiplying it by body mass. Besides, t_{ce} and t_{fe} were calculated from eFS and eTO (Appendix B).

2.5. Data analysis

Root mean square error [RMSE; in absolute (ms) and relative units, i. e., normalized by the corresponding mean value over all participants and obtained using GSM] was calculated for t_{ce} and t_{fe} . RMSE was computed from t_{ce} and t_{fe} averaged over the 10 analyzed strides for each participant and each running trial. Data analysis was performed using Python (v3.7.4, available at <http://www.python.org>).

2.6. Statistical analysis

All data are presented as mean \pm standard deviation. Systematic bias, lower and upper limit of agreements, and 95% confidence intervals between GSM and IMUM for t_{ce} and t_{fe} were examined using Bland-Altman plots for each speed (Atkinson and Nevill, 1998; Bland and Altman, 1995). Systematic biases have a direction, i.e., positive values indicate overestimations of IMUM while negative values indicate

underestimations. Proportional bias was identified by a significant slope of the regression line. Coefficients of determination (R^2) were computed to assess the quality of the linear fit. t_{ce} and t_{fe} obtained using IMUM and GSM were compared using two-way [method of calculation (GSM vs. IMUM) \times running speed (9 vs. 11 vs. 13)] repeated measures ANOVA with Mauchly's correction for sphericity and employing Holm corrections for pairwise post hoc comparisons. Differences between GSM and IMUM were quantified using Cohen's d effect size and interpreted as very small, small, moderate, and large when $|d|$ values were close to 0.01, 0.2, 0.5, and 0.8, respectively (Cohen, 1988). The landing-take-off asymmetry was evaluated as the difference between t_{fe} and t_{ce} (Δ) (Cavagna, 2006; Cavagna et al., 2008a, b). Δ obtained using IMUM and GSM were compared using two-way repeated measures ANOVA and differences between GSM and IMUM were also quantified using Cohen's d effect size. Statistical analysis was performed using Jamovi (v1.2, retrieved from <https://www.jamovi.org>) with a level of significance set at $P \leq 0.05$.

3. Results

Fig. 2 depicts the vertical ground reaction force obtained using GSM (force plate) and IMUM (raw and filtered IMU).

t_{ce} and t_{fe} depicted small systematic biases ($\leq 20 \text{ ms}$) at all speeds. The smallest absolute bias was given for 9 km/h, followed by 11 km/h and 13 km/h (Fig. 3 and Table 1). Both effective timings reported a significant negative proportional bias at all speeds but were accompanied with small R^2 (Table 1).

Significant effects for both method of calculation and running speed as well as an interaction effect were depicted by repeated measures ANOVA for t_{ce} and t_{fe} ($P < 0.001$; Table 2). Significant differences between GSM and IMUM for t_{ce} and t_{fe} at all speeds ($P < 0.001$) were

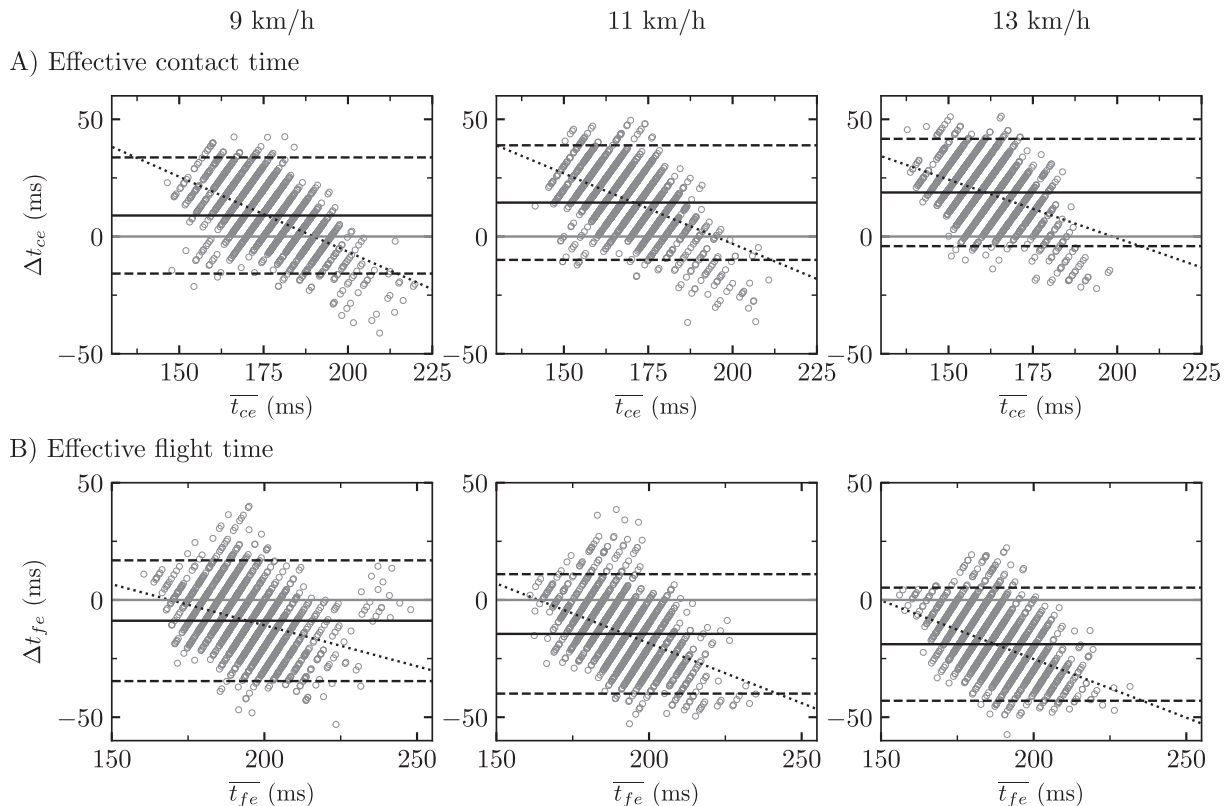


Fig. 3. Comparison of A) effective contact time (t_{ce}) and B) effective flight time (t_{fe}) obtained using inertial measurement unit method and gold standard method [differences (Δ) as function of mean values together with systematic bias (black solid line) as well as lower and upper limit of agreements (black dashed lines), and proportional bias (black dotted line), i.e., Bland-Altman plots] for three running speeds. For systematic bias, positive and negative values indicate the inertial measurement unit method overestimated and underestimated t_{ce} and t_{fe} , respectively.

Table 1

Systematic bias, lower limit of agreement (lloa), upper limit of agreement (uloa), proportional bias \pm residual random error together with its corresponding *P*-value, and coefficient of determination (R^2) between effective contact (t_{ce}) and flight (t_{fe}) times obtained using inertial measurement unit method and gold standard method at three running speeds. 95% confidence intervals are given in square brackets [lower, upper]. Significant ($P \leq 0.05$) proportional bias are reported in bold font. For systematic bias, positive and negative values indicate the inertial measurement unit method overestimated and underestimated t_{ce} and t_{fe} , respectively.

	Running Speed (km/h)	Systematic Bias	lloa	uloa	Proportional Bias (<i>P</i>)	R^2
t_{ce} (ms)	9	9.0 [8.4, 9.5]	-15.8 [-16.7, -14.9]	33.7 [32.8, 34.7]	-0.64 \pm 0.02 (<0.001)	0.30
	11	14.5 [13.9, 15.0]	-10.0 [-10.9, -9.0]	38.9 [38.0, 39.8]	-0.60 \pm 0.02 (<0.001)	0.25
	13	18.8 [18.3, 19.3]	-4.1 [-5.0, -3.2]	41.7 [40.8, 42.5]	-0.50 \pm 0.03 (<0.001)	0.15
t_{fe} (ms)	9	-8.9 [-9.4, -8.3]	-34.6 [-35.6, -33.6]	16.9 [15.9, 17.9]	-0.35 \pm 0.02 (<0.001)	0.10
	11	-14.5 [-15.0, -13.9]	-39.9 [-40.9, -39.0]	11.0 [10.0, 12.0]	-0.51 \pm 0.02 (<0.001)	0.18
	13	-18.9 [-19.4, -18.3]	-43.0 [-43.9, -42.1]	5.3 [4.3, 6.2]	-0.50 \pm 0.02 (<0.001)	0.19

Table 2

Effective contact (t_{ce}) and flight (t_{fe}) times obtained using gold standard method (GSM) and inertial measurement unit method (IMUM) together with root mean square error [RMSE; both in absolute (ms or N) and relative (%) units], as well as Cohen's *d* effect size for three running speeds. Significant ($P \leq 0.05$) method of calculation, running speed, and interaction effect, as determined by repeated measures ANOVA, are reported in bold font. *Significant difference between t_{ce} and t_{fe} obtained using GSM and IMUM, as determined by Holm post hoc tests.

Running Speed (km/h)		t_{ce} (ms)	t_{fe} (ms)
9	GSM	172.2 \pm 14.4*	198.6 \pm 14.3*
	IMUM	181.2 \pm 8.0	189.8 \pm 10.3
	RMSE (ms)	14.7	14.8
	RMSE (%)	8.5	7.4
	<i>d</i>	-0.71	0.65
11	GSM	162.5 \pm 13.6*	198.7 \pm 13.8*
	IMUM	177.0 \pm 8.1	184.2 \pm 8.4
	RMSE (ms)	18.5	18.6
	RMSE (%)	11.4	9.4
	<i>d</i>	-1.21	1.14
13	GSM	152.7 \pm 12.0*	197.3 \pm 13.3*
	IMUM	171.5 \pm 7.9	178.4 \pm 8.0
	RMSE (ms)	21.6	21.7
	RMSE (%)	14.2	11.0
	<i>d</i>	-1.72	1.51
Method of calculation effect		<i>P</i> < 0.001	<i>P</i> < 0.001
Running speed effect		<i>P</i> < 0.001	<i>P</i> < 0.001
Interaction effect		<i>P</i> < 0.001	<i>P</i> < 0.001

Values are presented as mean \pm standard deviation.

reported by Holm post hoc tests. RMSE was ≤ 22 ms ($\leq 14\%$) for t_{ce} and t_{fe} (Table 2) and Cohen's *d* effect size was large for t_{ce} and t_{fe} except at 9 km/h which was moderate (Table 2).

Due to the presence of systematic biases for t_{ce} and t_{fe} obtained by IMUM (Table 1), Δ was also estimated from these t_{ce} and t_{fe} but with further subtracting the systematic biases (corrected IMUM). Significant effects for both method of calculation and running speed as well as an interaction effect were depicted by repeated measures ANOVA for Δ ($P < 0.001$; Table 3). Holm post hoc tests reported significantly larger Δ for GSM than IMUM and for corrected IMUM than IMUM at all speeds ($P < 0.001$) whereas GSM and corrected IMUM were not statistically different ($P = 1.0$). Cohen's *d* effect size was large between GSM and IMUM but very small between GSM and corrected IMUM at all speeds (Table 3). Noteworthy, proportional biases were not taken into account because their corresponding R^2 (≤ 0.30) were not satisfactory. Indeed, using proportional biases to correct t_{ce} and t_{fe} resulted in a worse estimation of Δ than with corrected IMUM (data not shown).

4. Discussion

Our findings demonstrated systematic and proportional biases between GSM and IMUM for t_{ce} and t_{fe} at each speed employed as well as significant differences between GSM and IMUM. Nonetheless, systematic biases were small (≤ 20 ms). In addition, after subtraction of these systematic biases, the landing-take-off asymmetry was correctly

Table 3

Landing-take-off asymmetry (Δ), i.e., the difference between effective flight and effective contact times, obtained using gold standard method (GSM), inertial measurement unit method (IMUM), and corrected IMUM (subtraction of systematic biases on effective flight and effective contact times), as well as Cohen's *d* effect size between GSM and IMUM and between GSM and corrected IMUM for three running speeds. Significant ($P \leq 0.05$) method of calculation, running speed, and interaction effect, as determined by repeated measures ANOVA, are reported in bold font. * and † denote a significant difference between Δ obtained using GSM and IMUM and using IMUM and corrected IMUM, respectively, as determined by Holm post hoc tests.

Running Speed (km/h)		Δ (ms)
9	GSM	26.4 \pm 23.0*
	IMUM	8.6 \pm 7.0
	corrected IMUM	26.5 \pm 7.0 [†]
	<i>d</i> (IMUM)	0.96
	<i>d</i> (corrected IMUM)	0.00
11	GSM	36.2 \pm 22.1*
	IMUM	7.2 \pm 3.7
	corrected IMUM	36.2 \pm 3.7 [†]
	<i>d</i> (IMUM)	1.67
	<i>d</i> (corrected IMUM)	0.00
13	GSM	44.6 \pm 20.1*
	IMUM	6.9 \pm 2.4
	corrected IMUM	44.6 \pm 3.4 [†]
	<i>d</i> (IMUM)	-2.32
	<i>d</i> (corrected IMUM)	0.0
Method of calculation effect		<i>P</i> < 0.001
Running speed effect		<i>P</i> < 0.001
Interaction effect		<i>P</i> < 0.001

Values are presented as mean \pm standard deviation.

evaluated by corrected IMUM at a group level. However, as revealed by the small standard deviations obtained for corrected IMUM, the landing-take-off asymmetry was not as correctly evaluated at an individual than at a group level.

IMUM reported systematic biases ≤ 20 ms and RMSE ≤ 22 ms ($\leq 14\%$) for t_{ce} (Tables 1 and 2). Noteworthy, error in t_{fe} (in absolute units) tends to be equal to the one in t_{ce} when the number of strides per individual tends to infinity. Indeed, the only difference to calculate t_{ce} and t_{fe} being in the first eFS and last eTO. In addition, errors in t_{ce} and t_{fe} could not directly be compared to the actual literature because, to the best of our knowledge, no study comparing several methods to calculate these effective timings was conducted so far. Indeed, we are only aware of the comparison between t_{ce} and t_{fe} obtained using Myotest® and t_c and t_f obtained from photocell- and optical-based systems (Gindre et al., 2016), which makes this comparison useless as different outcomes (t_{ce} vs. t_c and t_{fe} vs. t_f) were actually being compared. Nevertheless, the authors were aware of this limitation and clearly stated this limitation (Gindre et al., 2016).

Errors in t_{ce} and t_{fe} could be compared to those obtained for usual timings (t_c and t_f). For instance, the errors reported in this study seemed to be smaller than the one obtained for t_c by Day et al. (2021) though bias and RMSE were not explicitly given [~ 30 ms by visual inspection

of their Fig. 5 (14–19 km/h)]. As for foot-worn inertial sensors, a systematic bias on t_c of ~ 10 ms (10–20 km/h) (Falbriard et al., 2018) and RMSE of ~ 10 ms (11 km/h) (Chew et al., 2018) were reported, which placed IMUM at a similar level of accuracy. In addition, Falbriard et al. (2018) depicted a proportional bias for t_c , as in this study for t_{ce} . Besides, IMUM showed similar accuracy than an opoelectronic system (3D kinematic data), which reported RMSE ≥ 15 ms for t_c (20 km/h) (Smith et al., 2015). However, such system suffers from a lack of portability and do not allow continuous data collection. For this reason, using a single IMU was advantageous by its portability, and was shown to be quite accurate to estimate t_{ce} (and t_{fe}). Moreover, in practice, a systematic subtraction of the bias corresponding to the given speed could be applied when estimating t_{ce} and t_{fe} .

Due to the inexact synchronization between kinetic and IMU data, eFS and eTO could not be compared between GSM and IMUM. However, we suspect that even under perfect synchronization, eFS and eTO from GSM and IMUM would not exactly coincide as vertical force used in IMUM is an approximation of ground truth vertical force recorded by force plate. Nonetheless, further studies involving synchronized kinetic and IMU data would prove useful, especially if one is interested in assessing metrics at specific eFS and eTO, for instance using additional IMUs (Favre et al., 2008) themselves synchronized with the sacral-mounted one which would provide eFS and eTO.

A single cut-off frequency was used to filter the vertical ground reaction force, i.e., 20 Hz. Though this choice of cut-off frequency is quite widespread (Mai and Willwacher, 2019; Swinnen et al., 2021), other cut-off frequencies (e.g., 30 or 80 Hz) are also used in the literature (Alcantara et al., 2021; Breine et al., 2017). In this case, the error of IMUM might increase because the cut-off frequency affects the magnitude of the vertical ground reaction force and thus the time at which eFS and eTO occur. Hence, it would also be useful to explore the effect of the cut-off frequency of the truncated Fourier series on the accuracy of IMUM, as already explored by Day et al. (2021) for a low-pass filter. Additionally, the effect of the filter itself (e.g., truncated Fourier series, 4th order low-pass Butterworth filter, 8th order low-pass Butterworth filter, etc.) might also be worth exploring. Therefore, further studies investigating the effect of the cut-off frequency of both the gold standard and IMU signals as well as the kind of filter should be conducted. Furthermore, a significant effect of running speed was observed for t_{ce} and t_{fe} (Table 2). The most accurate estimation (smallest systematic bias and RMSE) was given at 9 km/h (Fig. 3 and Tables 1 and 2). These findings suggests that the cut-off frequency that estimates best t_{ce} and t_{fe} might be speed dependent and reinforce the need to further explore the effect of the cut-off frequency of both GSM and IMUM, and to explore slower and faster speeds.

The landing-take-off asymmetry was reported to increase from ~ 20 to ~ 50 ms with increasing running speed (8–20 km/h) (Cavagna, 2006; Cavagna et al., 2008a, b). The present study depicted that Δ increased from 25 to 45 ms with running speed (9–13 km/h) for GSM and for corrected IMUM while Δ was ~ 7 ms at all tested speeds for IMUM. Due to the systematic biases reported for t_{fe} and t_{ce} , though similar than previously published methods that estimated usual t_f and t_c , IMUM was not able to evaluate the landing-take-off asymmetry. The main reason was that t_{fe} and t_{ce} were underestimated and overestimated, respectively, leading to an accumulation of errors. Moreover, the deviation from GSM increased with increasing speed because the error on t_{fe} and t_{ce} also increased with speed. However, after subtraction of these systematic biases, the landing-take-off asymmetry was correctly evaluated by corrected IMUM at a group level. Nonetheless, even though these biases might be generalizable due to the large dataset employed, i.e., 100 runners, they might still be dependent on the given dataset. Therefore, we suggest researchers willing to employ this method to first calculate these biases using their own dataset and then subtract these calculated biases to evaluate the landing-take-off asymmetry. Finally, the landing-

take-off-asymmetry evaluated by corrected IMUM reported small standard deviations (Table 3), meaning that the landing-take-off asymmetry was not as correctly evaluated at an individual than at a group level. Indeed, corrected IMUM was not totally able to provide insights into the inter-individual variation of the landing-take-off asymmetry.

This study presents few limitations. The comparison between IMUM and GSM was performed using treadmill runs. As spatiotemporal parameters between overground and treadmill running are largely comparable, IMUM might also perform well overground (Van Hooren et al., 2020). However, it was concluded that participants behaved differently when attempting to achieve faster speeds overground than on a treadmill (Bailey et al., 2017). Therefore, the comparison between IMUM and GSM using additional conditions (i.e., faster speeds, positive and negative slopes, and different types of ground) should be further studied.

5. Conclusion

A IMUM was provided to estimate t_{ce} and t_{fe} . These timings were obtained by filtering the vertical acceleration recorded by a sacral-mounted IMU using a truncated Fourier series to 5 Hz. GSM and IMUM depicted RMSE ≤ 22 ms ($\leq 14\%$) together with small systematic biases (≤ 20 ms) for t_{ce} and t_{fe} at each speed. These errors are similar to previously published methods that estimated usual t_c and t_f . To avoid that the errors on t_{ce} and t_{fe} accumulate when evaluating the landing-take-off asymmetry, the systematic biases on t_{ce} and t_{fe} were subtracted before calculating the landing-take-off asymmetry, which permitted to correctly evaluate it at a group level. Therefore, the findings of this study support the use of this method based on vertical acceleration recorded using a sacral-mounted IMU to estimate t_{ce} and t_{fe} for level treadmill runs and to evaluate the landing-take-off asymmetry of running but only after subtraction of systematic biases and at a group level.

CRedit authorship contribution statement

Aurélien Patoz: Conceptualization, Methodology, Investigation, Formal analysis, Writing – original draft, Writing – review & editing, Supervision. **Thibault Lussiana:** Conceptualization, Methodology, Investigation, Writing – review & editing, Supervision. **Bastiaan Breine:** Investigation, Formal analysis, Writing – original draft, Writing – review & editing. **Cyrille Gindre:** Conceptualization, Methodology, Writing – review & editing, Supervision. **Davide Malatesta:** Conceptualization, Methodology, Writing – review & editing, Supervision.

Declaration of Competing Interest

The authors declare that they have no known competing financial interests or personal relationships that could have appeared to influence the work reported in this paper.

Acknowledgements

The authors warmly thank the participants for their time and cooperation.

Funding

This study was supported by the Innosuisse grant no. 35793.1 IP-LS.

Availability of Data and Material

The datasets supporting this article are available on request to the corresponding author.

Appendix A. . Aligning the IMU z-axis with the z-axis of the local coordinate system

The laboratory coordinate system (LCS) was oriented such that x -, y -, and z -axis denoted medio-lateral (pointing towards the right side of the body), posterior-anterior, and inferior-superior axis, respectively. The IMU was oriented such that its own x -, y -, and z -axes denoted medio-lateral (pointing towards the right side of the IMU), posterior-anterior, and inferior-superior axis, respectively.

Raw acceleration data was filtered using a truncated Fourier series to 0.5 Hz in each dimension, allowing to remove any acceleration due to movement of the IMU (vibrations and body motion) (Day et al., 2021). Indeed, a truncated Fourier series allows removing any frequency component within the original signal that are above the requested cut-off. Noteworthy, the number of terms to include in the truncated Fourier series is given by $N = nF/f$, where n is the number of IMU data points, F is the requested truncation frequency, and f is the IMU sampling frequency. Then, the median of each component of the filtered 3D signal was computed. Knowing that the average acceleration should be equal to g in the z -axis of LCS and 0 in the other two axes, the average angle between the z -axis of IMU and LCS could be calculated based on the previously computed medians. This average angle corresponds to the average tilt of the IMU with respect to the z -axis of LCS. Therefore, the IMU can be reoriented using this average angle so that its z -axis is, in average, aligned with the one of LCS. However, it was assumed that the rotational motion of the sensor around any of the three axes was negligible so that no complicated reorientation of the IMU had to be performed at each timestamp, which would anyway require several approximations (see for instance Falbriard et al. (2020) for foot-worn IMU). This reorientation process is usually not taken into account when using sacral-mounted IMU and signals from sacral-mounted IMU are usually analyzed along the IMU's coordinate system and compared to ground reaction forces analyzed in LCS (Alcantara et al., 2021; Day et al., 2021; Lee et al., 2010).

Appendix B. . Computing t_{ce} and t_{fe} from eFS and eTO obtained using the sacral-mounted IMU

t_{ce} was given by the time between eFS and eTO data points while t_{fe} by the time between eTO data point $+1$ and eFS data point -1 . Doing so, two timesteps were missing when computing t_{ce} and t_{fe} for a running step. However, this was corrected by using a linear interpolation to calculate the “exact” timing of the threshold for eFS and eTO, using eFS data point and previous data point and eTO data point and next data point, respectively. Then, the duration between exact eFS threshold and eFS data point as well as between eTO data point and exact eTO threshold were added to t_{ce} while the duration between eFS data point -1 and exact eFS threshold as well as between exact eTO threshold and eTO data point $+1$ were added to t_{fe} . This procedure allowed to obtain the exact (under linear interpolation) t_{ce} and t_{fe} falling above and below the threshold, respectively.

References

- Abendroth-Smith, J., 1996. Stride adjustments during a running approach toward a force plate. *Res. Q. Exerc. Sport* 67 (1), 97–101.
- Alcantara, R.S., Day, E.M., Hahn, M.E., Grabowski, A.M., 2021. Sacral acceleration can predict whole-body kinetics and stride kinematics across running speeds. *e11199 PeerJ* 9.
- Atkinson, G., Nevill, A.M., 1998. Statistical methods for assessing measurement error (reliability) in variables relevant to sports medicine. *Sports Med.* 26 (4), 217–238.
- Bailey, J.P., Mata, T., Mercer, J.D., 2017. Is the relationship between stride length, frequency, and velocity influenced by running on a treadmill or overground? *International Journal of Exercise Science* 10, 1067–1075.
- Bland, J.M., Altman, D.G., 1995. Comparing methods of measurement: why plotting difference against standard method is misleading. *Lancet* 346 (8982), 1085–1087.
- Breine, B., Malcolm, P., Van Caekenbergh, I., Fiers, P., Frederick, E.C., De Clercq, D., 2017. Initial foot contact and related kinematics affect impact loading rate in running. *J. Sports Sci.* 35 (15), 1556–1564.
- Cavagna, G.A., 2006. The landing–take-off asymmetry in human running. *J. Exp. Biol* 209 (20), 4051–4060.
- Cavagna, G.A., Franzetti, P., Heglund, N.C., Willems, P., 1988. The determinants of the step frequency in running, trotting and hopping in man and other vertebrates. *The Journal of Physiology* 399, 81–92.
- Cavagna, G.A., Legramandi, M.A., Peyré-Tartaruga, L.A., 2008a. The landing–take-off asymmetry of human running is enhanced in old age. *J. Exp. Biol* 211 (10), 1571–1578.
- Cavagna, G.A., Legramandi, M.A., Peyré-Tartaruga, L.A., 2008b. Old men running: mechanical work and elastic bounce. *Proc. Biol. Sci.* 275 (1633), 411–418.
- Chew, D.-K., Ngoh, K.-H., Gouwanda, D., Gopalai, A.A., 2018. Estimating running spatial and temporal parameters using an inertial sensor. *Sports Eng.* 21 (2), 115–122.
- Cohen, J., 1988. *Statistical Power Analysis for the Behavioral Sciences*. Routledge.
- Day, E.M., Alcantara, R.S., McGeehan, M.A., Grabowski, A.M., Hahn, M.E., 2021. Low-pass filter cutoff frequency affects sacral-mounted inertial measurement unit estimations of peak vertical ground reaction force and contact time during treadmill running. *J. Biomech.* 119, 110323.
- Falbriard, M., Meyer, F., Mariani, B., Millet, G.P., Aminian, K., 2018. Accurate Estimation of Running Temporal Parameters Using Foot-Worn Inertial Sensors. *Front Physiol* 9.
- Falbriard, M., Meyer, F., Mariani, B., Millet, G.P., Aminian, K., 2020. Drift-Free Foot Orientation Estimation in Running Using Wearable IMU. *Frontiers in Bioengineering and Biotechnology* 8.
- Favre, J., Jolles, B.M., Aissaoui, R., Aminian, K., 2008. Ambulatory measurement of 3D knee joint angle. *J. Biomech.* 41 (5), 1029–1035.
- Flaction, P., Quievre, J., Morin, J.B., 2013. *An Athletic Performance Monitoring Device*, Washington, DC: U.S. Patent and Trademark Office.
- Giandolini, M., Horvais, N., Rossi, J., Millet, G.Y., Samozino, P., Morin, J.-B., 2016. Foot strike pattern differently affects the axial and transverse components of shock acceleration and attenuation in downhill trail running. *J. Biomech.* 49 (9), 1765–1771.
- Giandolini, M., Poupard, T., Gimenez, P., Horvais, N., Millet, G.Y., Morin, J.-B., Samozino, P., 2014. A simple field method to identify foot strike pattern during running. *J. Biomech.* 47 (7), 1588–1593.
- Gindre, C., Lussiana, T., Hebert-Losier, K., Morin, J.-B., 2016. Reliability and validity of the Myotest® for measuring running stride kinematics. *J. Sports Sci.* 34 (7), 664–670.
- ISO, IEC, 2020. *ISO International Standard ISO/IEC 14882:2020(E) Programming languages — C++*. International Organization for Standardization, Geneva, Switzerland.
- Lee, James B., Mellifont, Rebecca B., Burkett, Brendan J., 2010. The use of a single inertial sensor to identify stride, step, and stance durations of running gait. *J. Clin. Med. Sport* 13 (2), 270–273.
- Mai, Patrick, Willwacher, Steffen, 2019. Effects of low-pass filter combinations on lower extremity joint moments in distance running. *J. Biomech.* 95, 109311.
- Maiwald, C., Sterzing, T., Mayer, T.A., Milani, T.L., 2009. Detecting foot-to-ground contact from kinematic data in running. *Footwear Science* 1 (2), 111–118.
- Moe-Nilssen, R., 1998. A new method for evaluating motor control in gait under real-life environmental conditions. Part 1: The instrument. *Clin. Biomech.* 13 (4-5), 320–327.
- Napier, Christopher, Jiang, Xianta, MacLean, Christopher L., Menon, Carlo, Hunt, Michael A., 2020. The use of a single sacral marker method to approximate the centre of mass trajectory during treadmill running. *J. Biomech.* 108, 109886.
- Norris, Michelle, Anderson, Ross, Kenny, Ian C., 2014. Method analysis of accelerometers and gyroscopes in running gait: A systematic review. *Proceedings of the Institution of Mechanical Engineers, Part P. Journal of Sports Engineering and Technology* 228 (1), 3–15.
- Smith, Laura, Preece, Stephen, Mason, Duncan, Bramah, Christopher, 2015. A comparison of kinematic algorithms to estimate gait events during overground running. *Gait Posture* 41 (1), 39–43.
- Swinnen, W., Mylle, I., Hoogkamer, W., De Groot, F., Vanwansseele, B., 2021. Changing Stride Frequency Alters Average Joint Power and Power Distributions during Ground Contact and Leg Swing in Running. *Med. Sci. Sports Exerc.*
- Van Hooren, Bas, Fuller, Joel T., Buckley, Jonathan D., Miller, Jayme R., Sewell, Kerry, Rao, Guillaume, Barton, Christian, Bishop, Chris, Willy, Richard W., 2020. Is Motorized Treadmill Running Biomechanically Comparable to Overground Running? A Systematic Review and Meta-Analysis of Cross-Over Studies. *Sports Med.* 50 (4), 785–813.

8.8 Comparison of different machine learning models to enhance sacral acceleration-based estimations of running stride temporal variables and peak vertical ground reaction force

Aurélien Patoz^{1,2,*}, Thibault Lussiana^{2,3,4}, Bastiaan Breine^{2,5}, Cyrille Gindre^{2,3}, Davide Malatesta¹

¹ Institute of Sport Sciences, University of Lausanne, 1015 Lausanne, Switzerland

² Research and Development Department, Volodalen Swiss Sport Lab, 1860 Aigle, Switzerland

³ Research and Development Department, Volodalen, 39270 Chavéria, France

⁴ Research Unit EA3920 Prognostic Markers and Regulatory Factors of Cardiovascular Diseases and Exercise Performance, Health, Innovation platform, University of Franche-Comté, Besançon, France

⁵ Department of Movement and Sports Sciences, Ghent University, 9000 Ghent, Belgium

* Corresponding author

Accepted in **Sports Biomechanics**

Comparison of different machine learning models to enhance sacral acceleration-based estimations of running stride temporal variables and peak vertical ground reaction force

Aurélien Patoz^{1,2,*}, Thibault Lussiana^{2,3,4}, Bastiaan Breine^{2,5}, Cyrille Gindre^{2,3}, Davide Malatesta¹

¹ Institute of Sport Sciences, University of Lausanne, 1015 Lausanne, Switzerland

² Research and Development Department, Volodalen Swiss Sport Lab, 1860 Aigle, Switzerland

³ Research and Development Department, Volodalen, 39270 Chavéria, France

⁴ Research Unit EA3920 Prognostic Markers and Regulatory Factors of Cardiovascular Diseases and Exercise Performance, Health, Innovation platform, University of Franche-Comté, Besançon, France

⁵ Department of Movement and Sports Sciences, Ghent University, 9000 Ghent, Belgium

* Correspondence:

Dr. Aurélien Patoz, Institute of Sport Sciences, University of Lausanne, 1015 Lausanne, Switzerland, email: aurelien.patoz@unil.ch, tel: +41 79 535 07 16

Author Contributions: Conceptualization, A.P., T.L., C.G., and D.M.; methodology, A.P., T.L., C.G., and D.M.; investigation, A.P., T.L., and B.B.; formal analysis, A.P. and B.B.; writing—original draft preparation, A.P.; writing—review and editing, A.P., T.L., B.B., C.G., and D.M.; supervision, A.P., T.L., C.G., and D.M.

Funding: This study was supported by the Innosuisse grant no. 35793.1 IP-LS.

Acknowledgments: The authors warmly thank the participants for their time and cooperation.

Conflicts of Interest: The authors declare no conflict of interest.

ORCID:

Aurélien Patoz: 0000-0002-6949-7989

Thibault Lussiana: 0000-0002-1782-401X

Bastiaan Breine: 0000-0002-7959-7721

Davide Malatesta: 0000-0003-3905-5642

Abstract

Machine learning (ML) was used to predict contact (t_c) and flight (t_f) time, duty factor (DF), and peak vertical force ($F_{v,max}$) from IMU-based estimations. One hundred runners ran on an instrumented treadmill (9-13km/h) while wearing a sacral-mounted IMU. Linear regression (LR), support vector regression, and two-layers neural-network were trained (80 participants) using IMU-based estimations, running speed, stride frequency, and body mass. Predictions (remaining 20 participants) were compared to gold standard (kinetic data collected using the force plate) by calculating the mean absolute percentage error (MAPE). MAPEs of $F_{v,max}$ did not significantly differ among its estimation and predictions ($P=0.37$) while prediction MAPEs for t_c , t_f , and DF were significantly smaller than corresponding estimation MAPEs ($P\leq 0.003$). There were no significant differences among prediction MAPEs obtained from the three ML models ($P\geq 0.80$). Errors of the ML models were equal to or smaller than ($\leq 32\%$) the smallest real difference for the four variables while errors of the estimations were not (15-45%), indicating that ML models were sufficiently accurate to detect a clinically important difference. The simplest ML model (LR) should be used to improve the accuracy of the IMU-based estimations. These improvements may be beneficial when monitoring running-related injury risk factors in real-world settings.

Keywords: biomechanics, gait, locomotion, inertial measurement unit, duty factor, contact time, running injuries

Introduction

While providing many health benefits, running is also associated with lower limb overuse injuries (Fredette et al., 2021; Hreljac, 2004; Hreljac, Marshall, & Hume, 2000; Nielsen, Buist, Sørensen, Lind, & Rasmussen, 2012). These injuries often occur when a repetitive stress is applied to the system beyond its maximum tolerance (Hreljac, 2004). The peak vertical ground reaction force ($F_{v,max}$), contact time (t_c), and duty factor (DF), i.e., the product of t_c and stride frequency (SF) (Folland, Allen, Black, Handsaker, & Forrester, 2017; Minetti, 1998) were shown to play a role in running-related injury development (Edwards, 2018; Kiernan et al., 2018; Lenhart, Thelen, Wille, Chumanov, & Heiderscheit, 2014; Malisoux, Gette, Delattre, Urhausen, & Theisen, 2022; Matijevich, Branscombe, Scott, & Zelik, 2019; Sasimontokul, Bay, & Pavol, 2007; Scott & Winter, 1990). Flight time (t_f) might also play a role as it takes both the vertical ground reaction force and its time of production into account (Appendix).

These variables have often been estimated using inertial measurement units (IMUs) (Chew, Ngho, Gouwanda, & Gopalai, 2018; Day, Alcantara, McGeehan, Grabowski, & Hahn, 2021; Falbriard, Meyer, Mariani, Millet, & Aminian, 2018; Lee, Mellifont, & Burkett, 2010; Norris, Anderson, & Kenny, 2014; Patoz, Lussiana, Breine, Gindre, & Malatesta, 2022), which are effective devices to longitudinally monitor these variables outside of a laboratory (Camomilla, Bergamini, Fantozzi, & Vannozzi, 2018). However, obtaining accurate estimations based on IMU data depends on several factors such as the number of sensors, sensor position, or signal filtering (Alcantara, Day, Hahn, & Grabowski, 2021). For instance, error on t_c was ~10ms when using foot-worn inertial sensors (Chew et al., 2018; Falbriard et al., 2018). Using a single sacral-mounted IMU to estimate t_c , t_f , and $F_{v,max}$ led to root mean square errors (RMSEs) of 20ms and 0.15BW compared to gold standard values (force plate) (Patoz et al., 2022). Similarly, Day et al. (2021) reported Pearson correlation coefficients (r) of ~0.65 between IMU

estimations and gold standard values for t_c and $F_{v,\max}$. A sacral-mounted IMU is a natural choice because it approximates the location of the center of mass (Napier, Jiang, MacLean, Menon, & Hunt, 2020) but led to error two times larger for t_c . However, applying advanced analysis methods such as machine learning (ML) on top of these estimations may provide more accurate predictions.

ML was used to explain the differences of gait patterns between high and low-mileage runners (Xu et al., 2022) as well as to estimate biomechanical variables based on IMU data (Alcantara et al., 2021; Derie et al., 2020; Matijevich, Scott, Volgyesi, Derry, & Zelik, 2020; Wouda et al., 2018). ML has the advantage to provide an analytical model which is trained and tested using different subsets of the dataset (Halilaj et al., 2018) and built from physics-based variables, i.e., variables that demonstrated to provide changes in running biomechanics (Alcantara et al., 2021). The modeling of the relationships between clinical outcomes and biomechanical measures was attempted using ML models like linear regressions (LRs), support vector machines, and artificial neural networks (NNs) (Backes et al., 2020; Halilaj et al., 2018). Though limited to linear relationships, LRs are widely used because the regression coefficients are useful for model interpretability (Chambers, 1992). On the other hand, support vector machines and NNs are used to model non-linear relationships. Although they usually provide better accuracies than LRs, their coefficients are difficult to interpret because of their large numbers (Halilaj et al., 2018). Therefore, using both basic and complex ML models might illustrate the tradeoff between interpretability and accuracy and give the option to prioritize between the former and the latter.

Hence, the purpose of this study was to apply ML to predict t_c , t_f , DF, and $F_{v,\max}$ from their respective IMU-based estimations. It was hypothesized that further applying ML to these IMU-

based estimations should provide predictions with higher accuracies than those previously reported for the estimations (Patoz et al., 2022). Errors of the ML models were also compared to the smallest real difference (SRD) for the four variables, i.e., it was investigated if the ML models were sufficiently accurate to detect a clinically important difference. The comparison among the predictions of several ML models would allow defining which model has the best tradeoff between interpretability and accuracy.

Materials and Methods

Participant Characteristics

An existing database of 100 recreational runners (Patoz et al., 2022) (females: 27, age: 29 ± 7 years, height: 169 ± 5 cm, body mass: 61 ± 6 kg, and weekly running distance: 22 ± 16 km; males: 73, age: 30 ± 8 years, height: 180 ± 6 cm, body mass: 71 ± 7 kg, and weekly running distance: 38 ± 24 km) was used in the present study. Participants were required to run at least once a week and to not have current or recent lower-extremity injury (≤ 1 month) to be involved in this study. The local Ethics Committee of the XXX approved the study protocol prior to data collection (XXX) and adhered to the latest version of the Declaration of Helsinki of the World Medical Association. Written informed consent was obtained for all subjects.

Experimental Procedure, Data Collection, and Estimations from Inertial Measurement Unit

Data

The experimental procedure, data collection, and IMU-based estimations have already been described elsewhere (Patoz et al., 2022) and are briefly summarized herein.

An IMU of 9.4g (Movesense sensor, Suunto, Vantaa, Finland) was attached to the sacrum of participants. Then, after a warm-up run of 7-min (9-13km/h) on an instrumented treadmill

(Arsalis T150–FMT-MED, Louvain-la-Neuve, Belgium), three 1-min running trials (9, 11, and 13 km/h) were recorded in a randomized order. These speeds were chosen because they represent the most commonly adopted speeds of recreational runners (Selinger et al., 2022). Data analysis was performed on the IMU and kinetic data corresponding to the first 10 strides following the 30-s mark. IMU and kinetic data were not exactly synchronized (technical limitation), but the same 10 strides were used for each running trial of each participant because the synchronization delay between IMU and kinetic data was small (≤ 50 ms).

A home-made iOS application running on an iPhone SE (Apple, Cupertino, CA, USA) was used to collect IMU data (saturation range: $\pm 8g$) at 208Hz (manufacturing specification). IMU data were then transferred to a personal computer for post processing.

Kinetic data were collected at 200Hz using the force plate embedded into the treadmill (Arsalis, Louvain-la-Neuve, Belgium) together with the Vicon Nexus software (v2.9.3, Vicon, Oxford, UK). The Visual3D Professional software (v6.01.12, C-Motion Inc., Germantown, MD, USA) was used to process the 3D ground reaction forces (analog signal), which were first exported in .c3d format. The forces were low-pass filtered at 20Hz using a fourth-order Butterworth filter.

Gold standard t_c and t_f were given by the time during which the vertical ground reaction force was above and below 20N, respectively (Smith, Preece, Mason, & Bramah, 2015). Gold standard DF was given by the product of t_c and SF. Gold standard $F_{v,max}$ was given by the maximum of the vertical ground reaction force during t_c and was expressed in body weight units. The gold standard variables were computed within Visual3D and given as the average over the 10 analyzed strides.

A custom c++ code (ISO/IEC, 2020) was used to process IMU data and has already been described elsewhere (Patoz et al., 2022). Briefly, the vertical ground reaction force was approximated by the vertical acceleration (previously reoriented and filtered using a truncated Fourier series to 5Hz) multiplied by body mass. Then, t_c , t_f , DF, and $F_{v,max}$ were estimated as in the gold standard case but using the approximated vertical ground reaction force. In other words, t_c and t_f were given by the time during which the approximated vertical ground reaction force was above and below 20N, respectively, DF was given by the product of t_c and SF, and $F_{v,max}$ was given by the maximum of the approximated vertical ground reaction force during t_c . The custom c++ code provided the estimated variables as the average over the 10 analyzed strides.

Predicted Variables Obtained using Machine Learning Models

Three ML models: LR, support vector regression (SVR) – the regression analog of support vector machine – with the radial basis function kernel, and two-layers NN (NN2), were constructed to predict t_c , t_f , DF, and $F_{v,max}$ using a train/test method (80%–20% split; 80 and 20 runners in the training and testing set, respectively). All the running trials from one subject were included in only one set to ensure that the models generalize well to new data and a similar distribution of male (72.5%) and female (27.5%) was maintained in both subsets to avoid introducing bias in the model during training (Halilaj et al., 2018). For each variable predicted by the three models, four features were used as predictors: running speed, runner's body mass, SF, and corresponding IMU-based estimation. This choice follows from their relationship with changes in running biomechanics (Alcantara et al., 2021; Nagahara, Takai, Kanehisa, & Fukunaga, 2018; Nilsson & Thorstensson, 1989) and to keep the models relatively simple. The SF included in the features was the IMU-based estimation and was almost identical to the gold standard (Fig. 1). The features were standardized by removing the mean and by scaling to unit

variance. The different models were trained using a 5-fold cross validation approach for hyperparameter optimization. Hyperparameters are given in Table 1. The trained models were used to make predictions on the testing set, which was previously standardized based on the mean and standard deviation (SD) of the training set, leading to a total of 60 predictions (three running speeds x 20 individuals). The accuracy between gold standard and predicted values was quantified using r , RMSE, and mean absolute percentage error (MAPE). Besides, RMSE was compared to the SRD to evaluate if the precision of a model is sufficient to detect a clinically important difference. Indeed, SRD can be defined as the smallest change that indicates a clinically important difference and was calculated as $SRD = 1.96 \sigma$, where σ is the within-subject standard deviation of the gold standard values. The analysis was performed using Python (v3.7.4, available at <http://www.python.org>).

Statistical Analysis

All data are presented as mean \pm SD. To examine the presence of systematic bias between gold standard t_c , t_f , DF, and $F_{v,max}$ values and corresponding predicted or estimated values, Bland-Altman plots were constructed (Atkinson & Nevill, 1998; Bland & Altman, 1995). In case of a systematic bias, a positive value indicates the estimated or predicted variable is overestimated. In addition, lower and upper limit of agreements and 95% confidence intervals were calculated. Moreover, residual plots were inspected and no obvious deviations from homoscedasticity and normality were observed; therefore, one-way [model (no model vs LR vs SVR vs NN2)] repeated measures ANOVA with Mauchly's correction for sphericity and employing Holm corrections for pairwise post hoc comparisons were used to compare MAPE between models. This comparison was possible because an MAPE was calculated for each estimation/prediction made in the testing set. Statistical analysis was performed using Jamovi (v1.6.23, available at <https://www.jamovi.org>) with a level of significance set at $P \leq 0.05$.

Results

Participant characteristics and biomechanical variables within training and testing sets

Participant characteristics were not significantly different between training and testing sets ($P \geq 0.24$; Table 2). Gold standard values in the training set and gold standard, estimated (using IMU data, no ML), and predicted values in the testing set are reported in Tables 3 and 4, respectively.

Accuracy of the machine learning models (predictions) and estimations

The ML models predicted t_c with an r of 0.89 ± 0.01 , RMSE of 12.2 ± 0.2 ms, and MAPE of $3.6 \pm 0.1\%$ (mean \pm SD for the three models). As for t_f , the r , RMSE, and MAPE were 0.86 ± 0.01 , 11.7 ± 0.4 ms, and $9.3 \pm 0.4\%$. DF was predicted with an r of 0.84 ± 0.03 , RMSE of $1.7 \pm 0.1\%$, and MAPE of $3.6 \pm 0.2\%$. As for $F_{v,\max}$, the r , RMSE, and MAPE were 0.77 ± 0.01 , 0.13 ± 0.01 BW, and $3.8 \pm 0.1\%$ (Fig. 2). For completeness, Fig. 2 also depicts the gold standard as function of estimated values for the testing set together with their corresponding r , RMSE, and MAPE.

A significant model effect was reported for the MAPE of t_c , t_f , and DF ($P \leq 0.001$) but not of $F_{v,\max}$ ($P = 0.37$). Post hoc tests revealed that the MAPEs obtained using the three ML models were significantly smaller than the MAPE obtained without ML for t_c , t_f , and DF ($P \leq 0.003$; Fig. 2). However, there was no significant difference among the MAPEs obtained using the three ML models for these three variables ($P \geq 0.80$).

Bland-Altman plots between gold standard and predicted or estimated values are given in Fig. 3, and systematic bias as well as lower and upper limit agreements are reported in Table 5. The smallest bias was reported for LR.

Accuracy improvement between the predictions and estimations

Using ML allowed increasing r by $28\pm 1\%$, $59\pm 2\%$, $65\pm 5\%$, and $15\pm 1\%$, for t_c , t_f , DF, and $F_{v,max}$, respectively, compared to those obtained from IMU-based estimations. As for the RMSEs, they decreased by $37\pm 1\%$, $39\pm 2\%$, $37\pm 4\%$, and $16\pm 4\%$ for t_c , t_f , DF, and $F_{v,max}$, respectively, while the MAPEs decreased by $40\pm 1\%$, $40\pm 3\%$, $41\pm 3\%$, and $9\pm 1\%$ (Table 6).

Ability to detect a clinically important difference

SRD were equal to 13.2ms, 15.4ms, 1.8%, and 0.13BW for t_c , t_f , DF, and $F_{v,max}$, respectively. RMSE of the ML models were equal to or smaller than ($\leq 32\%$) the SRDs of the four variables. However, RMSE of the estimated values were larger than the SRDs of the four variables (15-45%).

Optimal coefficients of the linear regression models

The optimal coefficients obtained for the predictors used in the LR models are given in Table 7. Among all predictors, SF did not contribute significantly to the predictions ($P \geq 0.69$; Table 7). Hence, new LR models which did not include SF as a predictor were optimized, and optimal coefficients are reported in Table 8. These new LR models predicted t_c with an r of 0.88, RMSE of 12.9ms, and MAPE of $3.9\pm 3.3\%$. As for t_f , r , RMSE, and MAPE were 0.85, 12.2ms,

and $9.9\pm 8.9\%$. DF was predicted with an r of 0.82, RMSE of 1.8%, and MAPE of $4.1\pm 3.1\%$, while $F_{v,\max}$ with an r , RMSE, and MAPE of 0.77, 0.13BW, and $3.8\pm 3.0\%$.

Discussion and Implications

The purpose of the present study was to apply ML to predict t_c , t_f , DF, and $F_{v,\max}$ from their respective IMU-based estimations. According to the hypothesis, further applying ML to IMU-based estimations of t_c , t_f , DF, and $F_{v,\max}$ increased the accuracy of their predictions. However, the enhancement was not significant for $F_{v,\max}$. The simplest ML model (LR) was characterized by a similar prediction accuracy than more complicated models (SVR and NN2). Therefore, the simplest ML model (LR) should be used to improve the accuracy of the estimations of t_c , t_f , DF and $F_{v,\max}$ obtained using a sacral-mounted IMU across a range of running speeds. These improvements may be beneficial when monitoring running-related injury risk factors in real-world settings.

ML was able to improve the prediction accuracy, as reported by the higher r and lower RMSE and MAPE compared to those of the IMU-based estimations (Figs. 2 and 3 and Table 6). Nonetheless, the enhancement reported for $F_{v,\max}$ was not significant. Using more complicated ML models (SVR and NN2) did not further improve the prediction accuracy compared to the simple LR (Fig. 2 and Table 6). These results corroborate previous findings which observed similar errors for LR and quantile regression forest when predicting t_c , $F_{v,\max}$, and vertical impulse with an accelerometer (Alcantara et al., 2021). Moreover, the present RMSE and MAPE of t_c and $F_{v,\max}$ were similar to those previously obtained (t_c : $\sim 10\text{ms}$ and $\sim 4\%$ and $F_{v,\max}$: $\sim 0.14\text{BW}$ and $\sim 4\%$) using a different algorithm to estimate t_c and $F_{v,\max}$ from IMU data (Alcantara et al., 2021). Nonetheless, these previous results might suffer from generalization due to the small sample size ($N=37$). Using three inertial sensors placed on the

lower limb (two on lower leg and one on pelvis), Wouda et al. (2018) achieved a 3% error with a NN (10-14km/h), which is similar to the present accuracy (MAPE~4%, Fig. 2). Despite their low prediction error, their results were harder to interpret because of the experimental setup (three IMUs instead of one) and more complicated ML model than the model employed herein. Practically, the improvements reported herein may be beneficial for practitioners seeking to monitor running-related injury risk factors in real-world settings, though keeping in mind that there exists only limited evidence for most running-related injury-specific risk factors (Willwacher et al., 2022). Besides, as asymmetry level might be an important factor to consider for injured runner (Russell Esposito, Choi, Owens, Blanck, & Wilken, 2015), a ML model should be used to predict the biomechanical variables of the right and left lower limbs separately. Moreover, as the biomechanical variables of an injured lower limb might give different values than the ones used in the current training set (healthy individuals), the ML model should further be trained using injured runners and by separating the values of the biomechanical variables of the injured and non-injured lower limb in the training process.

ML was able to decrease the confidence limits (95% confidence intervals and lower and upper limit of agreements) compared to those of the IMU-based estimations (Table 5). In addition, the systematic bias reported for the simple linear regression was smaller than the bias obtained without ML (Table 5). Moreover, Fig. 3 suggests that the IMU-based estimations have a proportional bias (i.e., the error depends on the value of the estimated parameter). This proportional bias drastically decreased when using ML. Hence, these results strengthen the use of ML to obtain more accurate predictions.

SF was not reported as a predictor of the four variables ($P \geq 0.69$; Table 7). Hence, LRs which consider only the body mass, running speed, and IMU-based estimation should be used to

improve the prediction accuracy (see Table 8 for the coefficients). The optimal coefficients of a ML model might be specific to the IMU-based estimations used in the training and testing sets because each algorithm used to obtain these IMU-based estimations might have its own bias. Hence, these LRs can be used to predict t_c , t_f , and DF, and $F_{v,\max}$ to a lower extent, as long as the IMU-based estimations were obtained using the present algorithm, which is described elsewhere (Patoz et al., 2022). Nonetheless, further studies should try to create a ML model based on IMU-based estimations obtained from different algorithms, so that its usage could largely be generalized.

Previously, ML was also used to predict the vertical impulse from its IMU-based estimation as well as body mass, running speed, and step frequency (Alcantara et al., 2021). The authors reported an almost perfect correlation between gold standard and predicted vertical impulse values ($r=0.995$) and obtained that the intercept and step frequency of the LR were the only significant predictors of the vertical impulse. However, this was not necessarily needed. Indeed, as the integral of the vertical external forces during a running step is null (Eq. 1):

$$\int_0^{t_c} F_z(t)dt - mg(t_c + t_f) = 0, \quad (1)$$

we get

$$t_{\text{step}} = \frac{\int_0^{t_c} F_z(t)dt}{mg} = \frac{I_z}{mg}, \quad (2)$$

where $t_{\text{step}} = t_c + t_f$ and I_z represent the step time and vertical impulse, respectively. Therefore, according to Eq. 2, the step frequency, i.e., the inverse of t_{step} , is given by the inverse of the vertical impulse expressed in body weight units. Hence, the model created by Alcantara et al. (2021) to predict the vertical impulse was redundant and not necessarily needed. First, the vertical impulse is directly given by t_{step} and thus by the inverse of the step frequency (Eq. 2). Second, they assumed that the step frequency estimated using IMU data is

a valid surrogate to its gold standard counterpart (they used the step frequency estimated using IMU data as a predictor for the vertical impulse, t_c , and $F_{z,max}$). Thus, they already indirectly assumed that the estimated vertical impulse, i.e., t_{step} (the inverse of the step frequency), is equivalent to its gold standard counterpart. In the present study, gold standard and estimated SF were shown to be equivalent ($r=0.998$; Fig. 1), which corroborates what has just been explained. Indeed, t_{step} could be approximated by half of the stride time because small symmetry indices $\leq 4\%$ were previously reported for t_{step} of competitive, recreational, and novice runners at running speeds ranging from 8 to 12km/h (Mo et al., 2020).

As expected, as gold standard and estimated SF were equivalent ($r=0.998$; Fig. 1), similar MAPEs were reported between t_c and DF ($\sim 4\%$; Fig. 2). Thus, the DF prediction is almost only dependent on the t_c prediction. Finally, it is worth mentioning that using predicted t_c values and IMU-based estimations of SF to predict DF instead of constructing a specific LR led to a slightly larger prediction accuracy. Indeed, using predicted t_c values from the LR reported in Table 8, DF was predicted with an r of 0.82, RMSE of 1.8%, and MAPE of $3.9 \pm 3.3\%$.

The strength of the present results is due to the large dataset employed ($N=100$). This dataset allows better generalization of the results than those previously obtained with the smaller cohorts of 37 runners (Alcantara et al., 2021), though the generalization might not apply to populations not represented in the training set. Hence, further studies should include a broader population (increase N) by including elite athletes and less experienced runners. Moreover, injured runners should also be included in the training set, and the values of the biomechanical variables of the left and right lower limb should be separated in the training process, especially in the case of an asymmetry-based injury. In this case, the dataset would contain as much

different running gaits as possible, which would make the trained ML models as much generalizable as possible. Further studies could also apply other ML models and even more complex models such as deep learning models, though their complexity make them very difficult to interpret (Halilaj et al., 2018). Furthermore, running trials were performed only at level, endurance speeds, and on a treadmill. However, predictions obtained using ML might also perform well overground because spatiotemporal parameters between treadmill and overground running are largely comparable (Van Hooren et al., 2020). Nonetheless, running speed must be known to use the ML models. In real-life situation, the ML model could use the instantaneous running speed provided by the gps of the smartwatch or smartphone to predict the biomechanical variables in real-time. Finally, further studies should focus on improving the predictions by using additional conditions (i.e., faster speeds, positive and negative slopes, and different types of ground) when training the ML models.

Conclusion

Further applying ML to IMU-based estimations of t_c , t_f , DF, and $F_{v,max}$ increased the accuracy of their predictions, though the enhancement was not significant for $F_{v,max}$. The simplest ML model (LR) was characterized by a similar prediction accuracy than more complicated models (SVR and NN2). Moreover, errors of the ML models were equal to or smaller than the SRD for the four variables while errors of the estimations were not, indicating that ML models were sufficiently accurate to detect a clinically important difference. Therefore, the simplest ML model (LR) should be used to improve the accuracy of the estimations of t_c , t_f , DF and $F_{v,max}$ obtained using a sacral-mounted IMU across a range of running speeds. These improvements may be beneficial for practitioners seeking to monitor running-related injury risk factors in real-world settings.

Availability of Data and Material: The datasets and codes supporting this article are available online at <https://github.com/aurelienPatoz/predictions-of-tc-tf-DF-Fvmax-using-machine-learning>.

Appendix. The Relation between Flight Time and Net Vertical Impulse

The integral of the vertical external forces during a running step is null. Hence, t_f relates to the net vertical impulse ($I_{z,net}$), i.e., the integral of the vertical ground reaction force (F_z) which is above body weight during t_c (Eqs. A1 and A2) (Heise & Martin, 2001)

$$\int_0^{t_c} (F_z(t) - mg)dt - mg t_f = 0, \quad (\text{A1})$$

$$t_f = \frac{\int_0^{t_c} (F_z(t) - mg)dt}{mg} = \frac{I_{z,net}}{mg}. \quad (\text{A2})$$

Therefore, t_f takes both the vertical ground reaction force and its time of production into account. Hence, t_f might play a role in running-related injury development.

References

- Alcantara, R. S., Day, E. M., Hahn, M. E., & Grabowski, A. M. (2021). Sacral acceleration can predict whole-body kinetics and stride kinematics across running speeds. *PeerJ*, 9, e11199. doi: 10.7717/peerj.11199
- Atkinson, G., & Nevill, A. M. (1998). Statistical methods for assessing measurement error (reliability) in variables relevant to sports medicine. *Sports Medicine*, 26(4), 217-238. doi: 10.2165/00007256-199826040-00002
- Backes, A., Skej , S. D., Gette, P., Nielsen, R.  ., S rensen, H., Morio, C., & Malisoux, L. (2020). Predicting cumulative load during running using field-based measures. *Scandinavian Journal of Medicine & Science in Sports*, 30(12), 2399-2407. doi: <https://doi.org/10.1111/sms.13796>
- Bland, J. M., & Altman, D. G. (1995). Comparing methods of measurement: why plotting difference against standard method is misleading. *Lancet*, 346(8982), 1085-1087. doi: 10.1016/s0140-6736(95)91748-9

- Camomilla, V., Bergamini, E., Fantozzi, S., & Vannozzi, G. (2018). Trends Supporting the In-Field Use of Wearable Inertial Sensors for Sport Performance Evaluation: A Systematic Review. *Sensors*, *18*(3), 873. doi: 10.3390/s18030873
- Chambers, J. (1992). Chapter 4: linear models. In J. Chambers & T. Hastie (Eds.), *Statistical models in S*. Pacific Grove, California: Wadsworth & Brooks/Cole.
- Chew, D.-K., Ngoh, K. J.-H., Gouwanda, D., & Gopalai, A. A. (2018). Estimating running spatial and temporal parameters using an inertial sensor. *Sports Engineering*, *21*(2), 115-122. doi: 10.1007/s12283-017-0255-9
- Day, E. M., Alcantara, R. S., McGeehan, M. A., Grabowski, A. M., & Hahn, M. E. (2021). Low-pass filter cutoff frequency affects sacral-mounted inertial measurement unit estimations of peak vertical ground reaction force and contact time during treadmill running. *Journal of Biomechanics*, *119*, 110323. doi: <https://doi.org/10.1016/j.jbiomech.2021.110323>
- Derie, R., Robberechts, P., Van den Berghe, P., Gerlo, J., De Clercq, D., Segers, V., & Davis, J. (2020). Tibial Acceleration-Based Prediction of Maximal Vertical Loading Rate During Overground Running: A Machine Learning Approach. *Frontiers in Bioengineering and Biotechnology*, *8*. doi: 10.3389/fbioe.2020.00033
- Edwards, W. B. (2018). Modeling Overuse Injuries in Sport as a Mechanical Fatigue Phenomenon. *Exercise and Sport Sciences Reviews*, *46*(4), 224-231
- Falbriard, M., Meyer, F., Mariani, B., Millet, G. P., & Aminian, K. (2018). Accurate Estimation of Running Temporal Parameters Using Foot-Worn Inertial Sensors. *Frontiers in Physiology*, *9*(610). doi: 10.3389/fphys.2018.00610
- Folland, J. P., Allen, S. J., Black, M. I., Handsaker, J. C., & Forrester, S. E. (2017). Running Technique is an Important Component of Running Economy and Performance. *Medicine & Science in Sports & Exercise*, *49*(7), 1412-1423
- Fredette, A., Roy, J. S., Perreault, K., Dupuis, F., Napier, C., & Esculier, J. F. (2021). The association between running injuries and training parameters: A systematic review. *Journal of Athletic Training*. doi: 10.4085/1062-6050-0195.21
- Halilaj, E., Rajagopal, A., Fiterau, M., Hicks, J. L., Hastie, T. J., & Delp, S. L. (2018). Machine learning in human movement biomechanics: Best practices, common pitfalls, and new opportunities. *Journal of Biomechanics*, *81*, 1-11. doi: <https://doi.org/10.1016/j.jbiomech.2018.09.009>
- Heise, G. D., & Martin, P. E. (2001). Are variations in running economy in humans associated with ground reaction force characteristics? *European Journal of Applied Physiology*, *84*(5), 438-442. doi: 10.1007/s004210100394
- Hreljac, A. (2004). Impact and overuse injuries in runners. *Medicine and Science in Sports and Exercise*, *36*(5), 845-849. doi: 10.1249/01.mss.0000126803.66636.dd
- Hreljac, A., Marshall, R. N., & Hume, P. A. (2000). Evaluation of lower extremity overuse injury potential in runners. *Medicine and Science in Sports and Exercise*, *32*(9), 1635-1641. doi: 10.1097/00005768-200009000-00018

- ISO/IEC. (2020). *ISO International Standard ISO/IEC 14882:2020(E) Programming languages — C++*: Geneva, Switzerland: International Organization for Standardization
- Kiernan, D., Hawkins, D. A., Manoukian, M. A. C., McKallip, M., Oelsner, L., Caskey, C. F., & Coolbaugh, C. L. (2018). Accelerometer-based prediction of running injury in National Collegiate Athletic Association track athletes. *Journal of Biomechanics*, *73*, 201-209. doi: 10.1016/j.jbiomech.2018.04.001
- Lee, J. B., Mellifont, R. B., & Burkett, B. J. (2010). The use of a single inertial sensor to identify stride, step, and stance durations of running gait. *Journal of Science and Medicine in Sport*, *13*(2), 270-273. doi: <https://doi.org/10.1016/j.jsams.2009.01.005>
- Lenhart, R. L., Thelen, D. G., Wille, C. M., Chumanov, E. S., & Heiderscheit, B. C. (2014). Increasing running step rate reduces patellofemoral joint forces. *Medicine and Science in Sports and Exercise*, *46*(3), 557-564. doi: 10.1249/MSS.0b013e3182a78c3a
- Malisoux, L., Gette, P., Delattre, N., Urhausen, A., & Theisen, D. (2022). Spatiotemporal and Ground-Reaction Force Characteristics as Risk Factors for Running-Related Injury: A Secondary Analysis of a Randomized Trial Including 800+ Recreational Runners. *The American Journal of Sports Medicine*, *50*(2), 537-544. doi: 10.1177/03635465211063909
- Matijevich, E. S., Branscombe, L. M., Scott, L. R., & Zelik, K. E. (2019). Ground reaction force metrics are not strongly correlated with tibial bone load when running across speeds and slopes: Implications for science, sport and wearable tech. *PloS One*, *14*(1), e0210000. doi: 10.1371/journal.pone.0210000
- Matijevich, E. S., Scott, L. R., Volgyesi, P., Derry, K. H., & Zelik, K. E. (2020). Combining wearable sensor signals, machine learning and biomechanics to estimate tibial bone force and damage during running. *Human Movement Science*, *74*, 102690. doi: <https://doi.org/10.1016/j.humov.2020.102690>
- Minetti, A. E. (1998). A model equation for the prediction of mechanical internal work of terrestrial locomotion. *Journal of Biomechanics*, *31*(5), 463-468. doi: 10.1016/S0021-9290(98)00038-4
- Mo, S., Lau, F. O. Y., Lok, A. K. Y., Chan, Z. Y. S., Zhang, J. H., Shum, G., & Cheung, R. T. H. (2020). Bilateral asymmetry of running gait in competitive, recreational and novice runners at different speeds. *Human Movement Science*, *71*, 102600. doi: <https://doi.org/10.1016/j.humov.2020.102600>
- Nagahara, R., Takai, Y., Kanehisa, H., & Fukunaga, T. (2018). Vertical Impulse as a Determinant of Combination of Step Length and Frequency During Sprinting. *International Journal of Sports Medicine*. doi: 10.1055/s-0043-122739
- Napier, C., Jiang, X., MacLean, C. L., Menon, C., & Hunt, M. A. (2020). The use of a single sacral marker method to approximate the centre of mass trajectory during treadmill running. *Journal of Biomechanics*, *108*, 109886. doi: <https://doi.org/10.1016/j.jbiomech.2020.109886>

- Nielsen, R. O., Buist, I., Sørensen, H., Lind, M., & Rasmussen, S. (2012). Training errors and running related injuries: a systematic review. *International Journal of Sports Physical Therapy*, 7(1), 58-75
- Nilsson, J., & Thorstensson, A. (1989). Ground reaction forces at different speeds of human walking and running. *Acta Physiologica Scandinavica*, 136(2), 217-227. doi: 10.1111/j.1748-1716.1989.tb08655.x
- Norris, M., Anderson, R., & Kenny, I. C. (2014). Method analysis of accelerometers and gyroscopes in running gait: A systematic review. *Proceedings of the Institution of Mechanical Engineers, Part P: Journal of Sports Engineering and Technology*, 228(1), 3-15. doi: 10.1177/1754337113502472
- Patoz, A., Lussiana, T., Breine, B., Gindre, C., & Malatesta, D. (2022). A Single Sacral-Mounted Inertial Measurement Unit to Estimate Peak Vertical Ground Reaction Force, Contact Time, and Flight Time in Running. *Sensors*, 22(3), 784. doi: 10.3390/s22030784
- Russell Esposito, E., Choi, H. S., Owens, J. G., Blanck, R. V., & Wilken, J. M. (2015). Biomechanical response to ankle-foot orthosis stiffness during running. *Clinical Biomechanics (Bristol, Avon)*, 30(10), 1125-1132. doi: 10.1016/j.clinbiomech.2015.08.014
- Sasimontongkul, S., Bay, B. K., & Pavol, M. J. (2007). Bone contact forces on the distal tibia during the stance phase of running. *Journal of Biomechanics*, 40(15), 3503-3509. doi: <https://doi.org/10.1016/j.jbiomech.2007.05.024>
- Scott, S. H., & Winter, D. A. (1990). Internal forces of chronic running injury sites. *Medicine and Science in Sports and Exercise*, 22(3), 357-369
- Selinger, J. C., Hicks, J. L., Jackson, R. W., Wall-Scheffler, C. M., Chang, D., & Delp, S. L. (2022). Running in the wild: Energetics explain ecological running speeds. *Current Biology*, 32(10), 2309-2315.e2303. doi: <https://doi.org/10.1016/j.cub.2022.03.076>
- Smith, L., Preece, S., Mason, D., & Bramah, C. (2015). A comparison of kinematic algorithms to estimate gait events during overground running. *Gait & Posture*, 41(1), 39-43. doi: 10.1016/j.gaitpost.2014.08.009
- Van Hooren, B., Fuller, J. T., Buckley, J. D., Miller, J. R., Sewell, K., Rao, G., . . . Willy, R. W. (2020). Is Motorized Treadmill Running Biomechanically Comparable to Overground Running? A Systematic Review and Meta-Analysis of Cross-Over Studies. *Sports Medicine*, 50(4), 785-813. doi: 10.1007/s40279-019-01237-z
- Willwacher, S., Kurz, M., Robbin, J., Thelen, M., Hamill, J., Kelly, L., & Mai, P. (2022). Running-Related Biomechanical Risk Factors for Overuse Injuries in Distance Runners: A Systematic Review Considering Injury Specificity and the Potentials for Future Research. *Sports Medicine*, 52(8), 1863-1877. doi: 10.1007/s40279-022-01666-3
- Wouda, F. J., Giuberti, M., Bellusci, G., Maartens, E., Reenalda, J., van Beijnum, B.-J. F., & Veltink, P. H. (2018). Estimation of Vertical Ground Reaction Forces and Sagittal

Knee Kinematics During Running Using Three Inertial Sensors. *Frontiers in Physiology*, 9(218). doi: 10.3389/fphys.2018.00218

Xu, D., Quan, W., Zhou, H., Sun, D., Baker, J. S., & Gu, Y. (2022). Explaining the differences of gait patterns between high and low-mileage runners with machine learning. *Scientific Reports*, 12(1), 2981. doi: 10.1038/s41598-022-07054-1

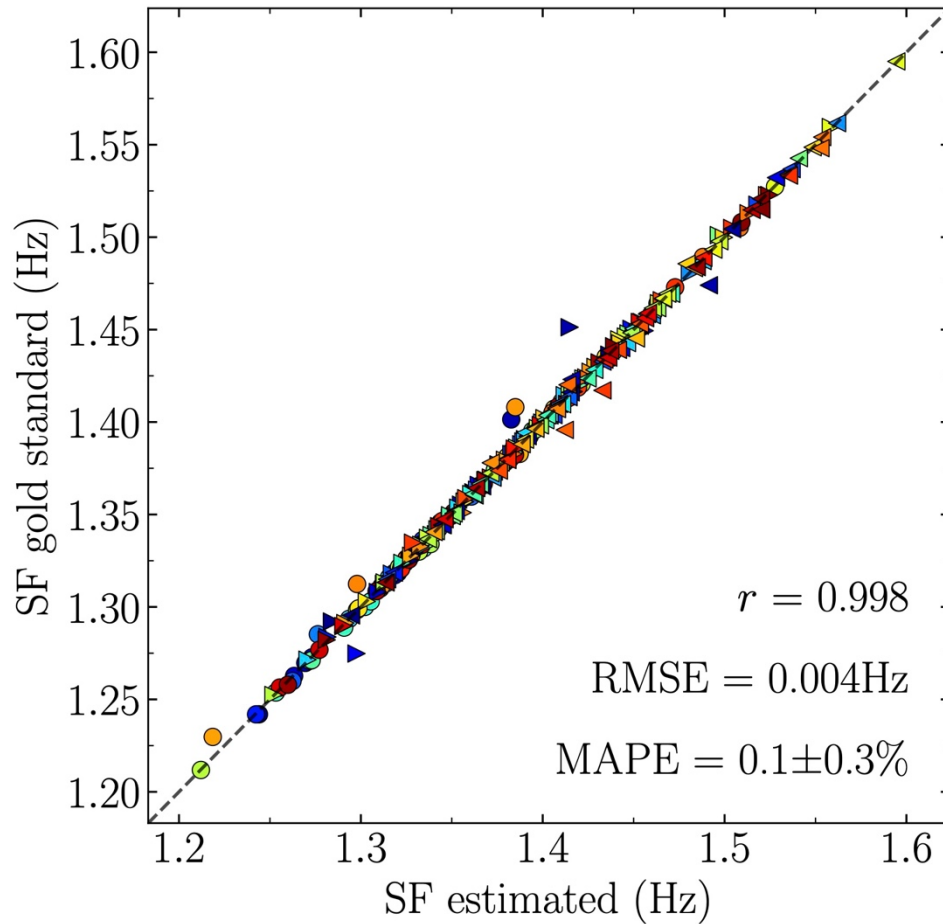


Figure 1. Gold standard (obtained using force plate data) stride frequency (SF) as function of estimated SF (obtained using inertial measurement unit data, no machine learning) for the entire set of data and corresponding Pearson correlation coefficient (r), root mean square error (RMSE), and mean absolute percentage error (MAPE). Each point represents the value for a given participant-running speed combination (300 points: three running speeds x 100 runners). Colors represent different participants while the three symbols represent different running speeds (o: 9km/h, \triangleright : 11km/h, \triangleleft : 13km/h).

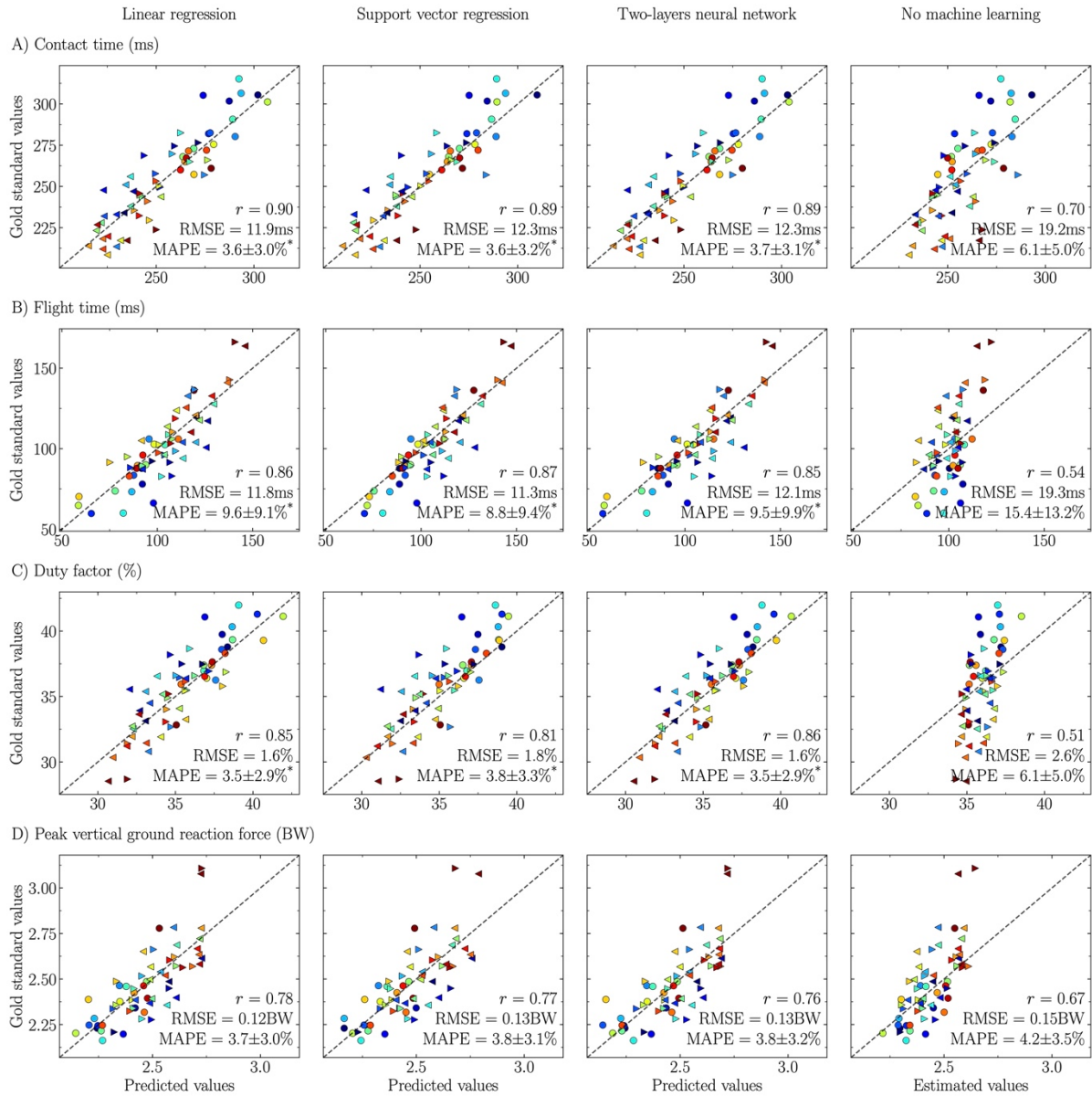


Figure 2. Gold standard (obtained using force plate data) as function of predicted (obtained using three different machine learning models) and estimated (obtained using inertial measurement unit data, no machine learning) (A) contact time, (B) flight time, (C) duty factor, and (D) peak vertical ground reaction force for the testing set and corresponding Pearson correlation coefficient (r), root mean square error (RMSE), and mean absolute percentage error (MAPE). The one-way repeated measures ANOVA revealed a significant model effect (no model vs linear regression vs support vector regression with the radial basis function kernel vs two-layers neural network) for contact time, flight time, and duty factor when comparing the MAPE among the models. *Significant difference ($P \leq 0.003$) between the MAPE of the predictions obtained using a given machine learning model and the MAPE of the estimations obtained using inertial measurement unit data, as determined by Holm post hoc tests. Each point represents the value for a given participant-running speed combination (60 points: three running speeds x 20 runners). Colors represent different participants while the three symbols represent different running speeds (o: 9km/h, \triangleright : 11km/h, \triangleleft : 13km/h).

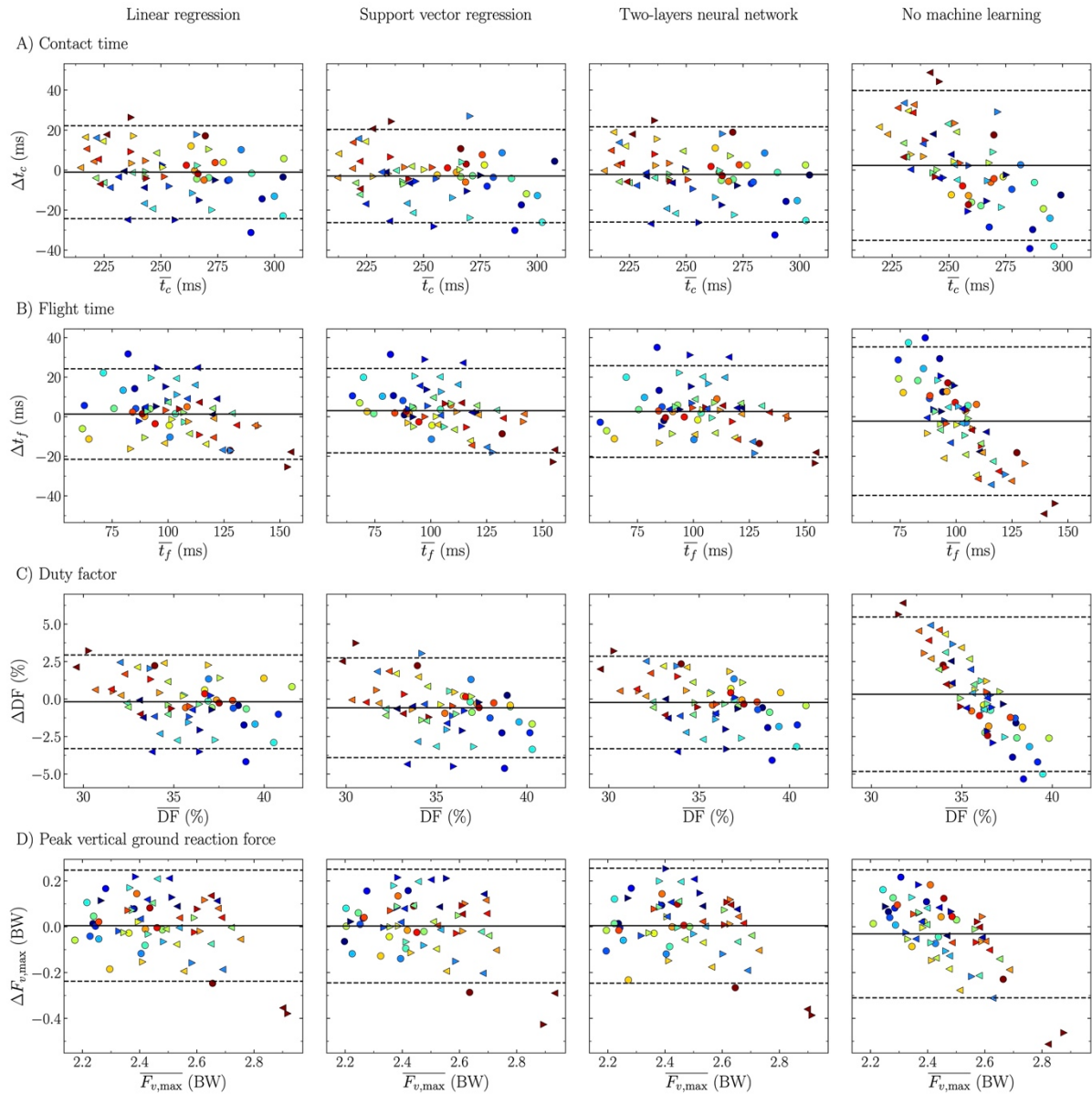


Figure 3. Comparison between gold standard (obtained using force plate data) and predicted (obtained using three different machine learning models) as well as estimated (obtained using inertial measurement unit data, no machine learning) (A) contact time, (B) flight time, (C) duty factor, and (D) peak vertical ground reaction force for the testing set [differences (Δ) as a function of mean values together with systematic bias (solid line) as well as lower and upper limit of agreements (dashed lines), i.e., a Bland-Altman plot]. Each point represents the value for a given participant-running speed combination (60 points: three running speeds \times 20 runners). Colors represent different participants while the three symbols represent different running speeds (o: 9km/h, \triangleright : 11km/h, \triangleleft : 13km/h). For systematic bias, positive values indicate the estimated or predicted variable is overestimated.

Table 1. Hyperparameters optimized during the 5-fold cross validation for the three machine learning models employed.

Machine learning model	Hyperparameter	Values
Linear regression	Intercept in the model	True and False
	C (inversely proportional to the strength of the regularization)	20 points (logarithmic scale between 0.001 and 10000)
Support vector regression	Epsilon (specifies the epsilon-tube within which no penalty is associated in the training loss function with points predicted within a distance epsilon from the actual value)	20 points (logarithmic scale between 0.001 and 100)
	Activation function of the first layer	relu, tanh, sigmoid, and softmax
Two-layers neural network	Dimensionality of the inner layer	8, 16, 32, and 64
	Batch size	2, 4, 8, and 16
	Loss function	mean absolute error and mean squared error

Table 2. Participant characteristics for the training (80 runners) and testing (20 runners) sets.

Characteristics	Training set	Testing set	<i>p</i>-value
Sex	M = 58; F = 22	M = 15; F = 5	NA
Age (yr)	30 ± 7	30 ± 8	0.96
Height (cm)	177 ± 8	177 ± 7	0.89
Body mass (kg)	68 ± 8	70 ± 6	0.29
Running distance (km/week)	32 ± 24	39 ± 20	0.24

Note. The values are presented as mean ± standard deviation. M: male, F: female, and NA: not applicable.

Table 3. Gold standard (obtained using force plate data) contact time (t_c), flight time (t_f), duty factor (DF), and peak vertical ground reaction force ($F_{v,max}$) for the training set (80 runners) at three running speeds.

Running speed (km/h)	t_c (ms)	t_f (ms)	DF (%)	$F_{v,max}$ (BW)
9	277 ± 23	95 ± 23	37.3 ± 2.9	2.4 ± 0.2
11	249 ± 20	113 ± 19	34.4 ± 2.4	2.5 ± 0.2
13	227 ± 17	124 ± 17	32.3 ± 2.2	2.6 ± 0.2

Note. The values are presented as mean ± standard deviation.

Table 4. Gold standard (obtained using force plate data) contact time (t_c), flight time (t_f), duty factor (DF), and peak vertical ground reaction force ($F_{v,max}$) as well as corresponding estimated (obtained using inertial measurement unit data, no machine learning) and predicted [obtained using three machine learning models: linear regression (LR), support vector regression with the radial basis function kernel (SVR), and two-layers neural network (NN2)] values for the testing set (20 runners) at three running speeds.

Variable	Running speed (km/h)	Gold standard	Estimated	Predicted LR	Predicted SVR	Predicted NN2
t_c (ms)	9	282 ± 18	268 ± 14	279 ± 13	278 ± 13	278 ± 13
	11	253 ± 17	257 ± 13	253 ± 12	251 ± 15	252 ± 11
	13	229 ± 14	246 ± 11	229 ± 9	227 ± 10	228 ± 9
t_f (ms)	9	86 ± 19	100 ± 9	89 ± 15	91 ± 14	89 ± 17
	11	105 ± 21	101 ± 9	105 ± 16	107 ± 15	108 ± 16
	13	117 ± 18	100 ± 8	118 ± 13	119 ± 13	119 ± 14
DF (%)	9	38.4 ± 2.3	36.4 ± 1.0	38.0 ± 1.7	37.5 ± 1.3	37.8 ± 1.3
	11	35.4 ± 2.4	35.9 ± 0.9	35.3 ± 1.6	34.9 ± 1.5	35.4 ± 1.5
	13	33.2 ± 2.1	35.6 ± 0.7	33.1 ± 1.4	32.8 ± 1.4	33.1 ± 1.4
$F_{v,max}$ (BW)	9	2.35 ± 0.15	2.39 ± 0.10	2.34 ± 0.11	2.34 ± 0.11	2.33 ± 0.12
	11	2.47 ± 0.20	2.45 ± 0.11	2.48 ± 0.13	2.48 ± 0.13	2.50 ± 0.13
	13	2.59 ± 0.18	2.47 ± 0.09	2.60 ± 0.10	2.59 ± 0.11	2.58 ± 0.09

Note. The values are presented as mean ± standard deviation.

Table 5. Systematic bias, lower limit of agreement (Lloa), and upper limit of agreement (Uloa) between contact time (t_c), flight time (t_f), duty factor (DF), and peak vertical ground reaction force ($F_{v,max}$) obtained using a force plate (gold standard method) and machine learning models (predictions; linear regression, support vector regression with the radial basis function kernel, and two-layers neural network) as well as an inertial measurement unit (estimations; no machine learning) for the testing set (20 runners).

Variable	Method	Systematic Bias	Lloa	Uloa
t_c (ms)	Linear regression	-1.0 [-4.0, 2.0]	-24.3 [-29.4, -19.1]	22.2 [17.1, 27.3]
	Support vector regression	-3.0 [-6.0, 0.0]	-26.3 [-31.4, -21.1]	20.3 [15.2, 25.5]
	2-layers neural network	-2.2 [-5.3, 0.9]	-26.0 [-31.3, -20.7]	21.7 [16.4, 26.9]
	No machine learning	2.3 [-2.5, 7.2]	-35.1 [-43.4, -26.9]	39.8 [31.5, 48.0]
t_f (ms)	Linear regression	1.3 [-1.6, 4.3]	-21.6 [-26.6, -16.5]	24.2 [19.2, 29.3]
	Support vector regression	3.1 [0.3, 5.8]	-18.3 [-23.0, -13.6]	24.4 [19.7, 29.1]
	2-layers neural network	2.6 [-0.4, 5.6]	-20.5 [-25.6, -15.4]	25.8 [20.7, 30.9]
	No machine learning	-2.2 [-7.1, 2.6]	-39.8 [-48.0, -31.5]	35.3 [27.0, 43.6]
DF (%)	Linear regression	-0.2 [-0.6, 0.2]	-3.3 [-4.0, -2.6]	2.9 [2.3, 3.6]
	Support vector regression	-0.6 [-1.0, -0.2]	-3.9 [-4.6, -3.2]	2.7 [2.0, 3.5]
	2-layers neural network	-0.2 [-0.6, 0.2]	-3.3 [-4.0, -2.6]	2.9 [2.2, 3.5]
	No machine learning	0.3 [-0.3, 1.0]	-4.8 [-6.0, -3.7]	5.5 [4.3, 6.6]
$F_{v,max}$ (BW)	Linear regression	0.00 [-0.03, 0.04]	-0.24 [-0.29, -0.18]	0.25 [0.19, 0.30]
	Support vector regression	0.00 [-0.03, 0.04]	-0.24 [-0.30, -0.19]	0.25 [0.20, 0.31]
	2-layers neural network	0.00 [-0.03, 0.04]	-0.25 [-0.30, -0.19]	0.26 [0.20, 0.31]
	No machine learning	-0.03 [-0.07, 0.01]	-0.31 [-0.37, -0.25]	0.25 [0.19, 0.31]

Note. Confidence intervals of 95% are given in square brackets [lower, upper]. For systematic bias, positive values indicate the estimated or predicted variable is overestimated.

Table 6. Percentage difference of the Pearson correlation coefficient (r), root mean square error (RMSE), and mean absolute percentage error (MAPE) between those obtained using estimations based on inertial-measurement unit data and those obtained using a machine learning model among linear regression, support vector regression with the radial basis function kernel, and two-layers neural network, for four predicted variables, i.e., contact time, flight time, duty factor, and peak vertical ground reaction force.

Variable	Metrics	Linear regression (%)	Support vector regression (%)	Two-layers neural network (%)
Contact time	r	29	27	27
	RMSE	-38	-36	-36
	MAPE	-40	-42	-40
Flight time	r	59	61	57
	RMSE	-39	-41	-37
	MAPE	-38	-43	-38
Duty factor	r	67	59	69
	RMSE	-40	-32	-40
	MAPE	-42	-37	-43
Peak vertical ground reaction force	r	16	15	13
	RMSE	-20	-13	-13
	MAPE	-11	-9	-8

Table 7. Optimal coefficients, standard error, and p -values (P) obtained for the predictors used in the linear regression models, i.e., intercept, runner's body mass, stride frequency, running speed, and estimated variable obtained using inertial measurement unit data, constructed to predict contact time (t_c), flight time (t_f), duty factor (DF), and peak vertical ground reaction force ($F_{v,max}$).

Variable	Metrics	Coefficient	Standard error	P
t_c (ms)	intercept	251.08	56.09	<0.001
	runner's body mass	5.40	0.11	<0.001
	stride frequency	9.40	23.22	0.69
	running speed	-13.71	0.60	<0.001
	estimated t_c	22.20	0.10	<0.001
t_f (ms)	intercept	110.64	28.24	<0.001
	runner's body mass	-5.33	0.11	<0.001
	stride frequency	-3.35	15.80	0.83
	running speed	13.80	0.61	<0.001
	estimated t_f	12.50	0.10	<0.001
DF (%)	intercept	34.68	4.67	<0.001
	runner's body mass	0.74	0.02	<0.001
	stride frequency	0.67	1.92	0.73
	running speed	-1.92	0.08	<0.001
	estimated DF	1.56	0.10	<0.001
$F_{v,max}$ (BW)	intercept	2.51	0.27	<0.001
	runner's body mass	0.01	0.00	<0.001
	stride frequency	-0.01	0.14	0.93
	running speed	0.07	0.01	<0.001
	estimated $F_{v,max}$	0.15	0.07	0.02

Note. Significant coefficients ($P \leq 0.05$) are reported in bold font.

Table 8. Optimal coefficients, standard error, and p -values (P) obtained for the linear regression models which excluded stride frequency as a predictor to predict contact time (t_c), flight time (t_f), duty factor (DF), and peak vertical ground reaction force ($F_{v,max}$).

Variable	Metrics	Coefficient	Standard error	P
t_c (ms)	intercept	251.08	20.84	< 0.001
	runner's body mass	5.29	0.11	< 0.001
	running speed	-13.27	0.64	< 0.001
	estimated t_c	14.42	0.06	< 0.001
t_f (ms)	intercept	110.64	13.43	< 0.001
	runner's body mass	-4.79	0.11	< 0.001
	running speed	12.27	0.53	< 0.001
	estimated t_f	13.88	0.09	< 0.001
DF (%)	intercept	34.68	4.17	< 0.001
	runner's body mass	0.63	0.02	< 0.001
	running speed	-1.61	0.08	< 0.001
	estimated DF	1.56	0.11	< 0.001
$F_{v,max}$ (BW)	intercept	2.51	0.19	< 0.001
	runner's body mass	0.01	0.00	< 0.001
	running speed	0.07	0.01	< 0.001
	estimated $F_{v,max}$	0.15	0.07	0.02

Note. Significant coefficients ($P \leq 0.05$) are reported in bold font.

9. Annexes

9.1 Critical speed estimated by statistically appropriate fitting procedures

Aurélien Patoz^{1,2,*}, Romain Spicher¹, Nicola Pedrani¹, Davide Malatesta^{1,†}, Fabio Borrani^{1,†}

¹ Institute of Sport Sciences, University of Lausanne, Lausanne, Switzerland

² Research and Development Department, Volodalen Swiss Sport Lab, Aigle, Switzerland

† These authors contributed equally to this work

* Corresponding author

Published in **European Journal of Applied Physiology**

DOI: 10.1007/s00421-021-04675-8



Critical speed estimated by statistically appropriate fitting procedures

Aurélien Patoz^{1,2} · Romain Spicher¹ · Nicola Pedrani¹ · Davide Malatesta¹ · Fabio Borrani¹

Received: 17 November 2020 / Accepted: 28 March 2021

© The Author(s) 2021

Abstract

Purpose Intensity domains are recommended when prescribing exercise. The distinction between heavy and severe domains is made by the critical speed (CS), therefore requiring a mathematically accurate estimation of CS. The different model variants (distance versus time, running speed versus time, time versus running speed, and distance versus running speed) are mathematically equivalent. Nevertheless, error minimization along the correct axis is important to estimate CS and the distance that can be run above CS (d'). We hypothesized that comparing statistically appropriate fitting procedures, which minimize the error along the axis corresponding to the properly identified dependent variable, should provide similar estimations of CS and d' but that different estimations should be obtained when comparing statistically appropriate and inappropriate fitting procedure.

Methods Sixteen male runners performed a maximal incremental aerobic test and four exhaustive runs at 90, 100, 110, and 120% of their peak speed on a treadmill. Several fitting procedures (a combination of a two-parameter model variant and regression analysis: weighted least square) were used to estimate CS and d' .

Results Systematic biases ($P < 0.001$) were observed between each pair of fitting procedures for CS and d' , even when comparing two statistically appropriate fitting procedures, though negligible, thus corroborating the hypothesis.

Conclusion The differences suggest that a statistically appropriate fitting procedure should be chosen beforehand by the researcher. This is also important for coaches that need to prescribe training sessions to their athletes based on exercise intensity, and their choice should be maintained over the running seasons.

Keywords Running · Curve fitting · Linear model · Hyperbolic model · Exercise prescription · Intensity domains

Abbreviations

CP	Critical power
CS	Critical speed
d'	Distance that can be run above critical speed
LS	Least squares
$s\dot{V}O_{2\max}$	Speed associated with maximum oxygen consumption
PS	Peak speed of the incremental test
WLS	Weighted least squares

Communicated by Guido Ferretti.

Davide Malatesta and Fabio Borrani authors contributed equally to this work.

✉ Aurélien Patoz
aurelien.patoz@unil.ch

¹ Institute of Sport Sciences, University of Lausanne, 1015 Lausanne, Switzerland

² Research and Development Department, Volodalen Swiss Sport Lab, Aigle, Switzerland

Introduction

Exercise intensity, one of the most important criteria for obtaining the desired metabolic stimulus and inducing specific adaptations to training (MacInnis and Gibala 2017), is often prescribed based on the percentage of the maximal rate of oxygen uptake or maximal heart rate (American College of Sports Medicine 2000; Roy et al. 2018). However, there is a large variability in the characteristics of the metabolic responses and the duration of exercise at a common percentage of the maximum between individuals. For example, Fontana et al. (2015) showed that the lactate threshold as well as critical power/speed (CP/CS) can occur at different percentages of the maximum oxygen consumption between individuals. Therefore, the control of exercise intensity is not guaranteed when the prescription is based on percentages of maximum values (DiMenna and Jones 2009; Lansley et al. 2011). Instead, Iannetta et al. (2020) recommended the use of a model that considers exercise intensity domains for exercise prescription. These different intensity domains can

be defined based on the oxygen uptake kinetics (Whipp and Mahler 1980), maximum lactate steady-state (Iannetta et al. 2018), ventilatory threshold (Wasserman et al. 1973), or CP/CS (Vanhatalo et al. 2007; Jones et al. 2019).

Exercising above or below such thresholds leads to considerable differences in the physiological responses (Black et al. 2017). Therefore, training across disparate specific work intensities spanning different intensity domains is important to improve athletic performance. The CP/CS concept is widely used to evaluate the threshold intensity associated with the lower extremity of the severe intensity domain (Galán-Rioja et al. 2020; Jones et al. 2019). Therefore, having an accurate estimation of CP/CS, i.e., a very good approximation of the critical intensity but not the critical intensity per se, is important. This is usually obtained using the relationship between power/speed and time to exhaustion.

This relationship has been characterized with a number of models that differ in their mathematical form and number of parameters (Monod and Scherrer 1965; Moritani et al. 1981; Whipp et al. 1982; Morton 1996, 1986; Wilkie 1980; Peronet and Thibault 1989). The original linear model formulation was proposed by Monod and Scherrer (1965) and relates the work performed during an exhaustive bout and the actual time to exhaustion through two parameters: the highest sustainable oxidative metabolic rate and the fixed anaerobic work capacity. The first parameter, known as CP (Monod and Scherrer 1965) or threshold of fatigue (Bigland-Ritchie and Woods 1984), separates power outputs for which exercise tolerance is predictably limited (exercise > CP) from those that can be sustained for longer periods (exercise < CP). The second parameter represents the energy reserve located in the muscle that can be utilized above CP as fast or as slow as needed (i.e., the sustainable work of exercise above that metabolic rate) (Monod and Scherrer 1965). Later, some authors related power and time to exhaustion by dividing the variables of the original model by the exercise duration (Poole et al. 1986; Gaesser and Wilson 1988; Housh et al. 1989). As exercise duration is the dependent variable and power the independent variable when considering bouts of fixed power, Gaesser et al. (1990) proposed expressing this exercise duration as a function of the power, which led to the well-known hyperbolic model (Morton and Hodgson 1996). Another model variant, proposed by Morton (2006), expresses the work performed as function of power, since this work (power multiplied by time to exhaustion) is also a dependent variable. However, this model has, to our knowledge, never been used so far.

A straightforward transposition of CP to running has been studied by several researchers (Hughson et al. 1984; Housh et al. 1991, 2001; McDermott et al. 1993). By analogy to the power versus time relationship, the running speed and time variables are related through critical speed

(CS; the running analogue of CP for cycle ergometry) and anaerobic running capacity (d' ; the running analogue of the anaerobic work capacity) (Hill and Ferguson 1999; Housh et al. 1991; Hughson et al. 1984; Pepper et al. 1992). The latter was more recently and accurately defined as the distance that can be run above CS (Jones and Vanhatalo 2017). It implicitly follows that the work performed during an exhaustive bout becomes the distance travelled. These different two-parameter model variants are still extensively used to assess CS and d' (for review see Jones and Vanhatalo (2017) and Jones et al. (2019)).

The estimation of CS and d' are usually obtained from data provided by the critical speed test procedure (Poole et al. 1988), where the number and duration of the exhaustive runs were shown to play an important role in these estimations (Bishop et al. 1998; Mattioni Maturana et al. 2018). Based on the data provided by this test, CS and d' could be estimated using a regression fitting routine. In general, the least squares (LS) loss function is used to minimize the error. In that case, the dependent variable must be observed with additive error (white noise) while the independent variable does not (Morton and Hodgson 1996). As heteroscedasticity is taking place (a smaller error is most likely to occur in the measurement of time to exhaustion for high running speeds, i.e., for short times to exhaustion (McLellan and Skinner 1985; Poole et al. 1988; Faude et al. 2017)), Morton and Hodgson (1996) suggested using weighted LS (WLS) in the regression analysis with weights proportional to the inverse of the variance of time to exhaustion, where the variance is itself proportional to the time to exhaustion.

The different model variants (distance versus time, running speed versus time, time versus running speed, and distance versus speed) are mathematically equivalent. Nevertheless, error minimization along the correct axis is important to estimate CS and d' , as already highlighted but not yet investigated by Gaesser et al. (1995). Therefore, the purpose of this study was to compare the estimations of CS and d' obtained using statistically appropriate fitting procedures (which minimize the error along the axis corresponding to the properly identified dependent variables (Vinetti et al. 2020)), and statistically inappropriate fitting procedures (which do not minimize the error along the axis that contain the dependent variable) but are frequently used in the literature (Jones et al. 2019; Jones and Vanhatalo 2017). These estimations were obtained using several combinations of a linear two-parameter model variant and a regression analysis (fitting procedure). We hypothesized that the comparison of statistically appropriate fitting procedures should provide similar estimations of CS and d' . On the other hand, different estimations of CS and d' should be obtained when comparing a statistically appropriate with a statistically inappropriate fitting procedure.

Materials and methods

Participant characteristics

Sixteen male runners participated in the present experiment (age: 25.6 ± 3.9 years old; height: 1.79 ± 0.05 m; body mass: 69.2 ± 5.3 kg; speed associated with maximum oxygen consumption ($s_{\dot{V}O_{2\max}}$): 18.2 ± 1.4 km/h; maximum oxygen consumption: 63.0 ± 4.9 ml/min/kg). For study inclusion, participants were required to be in good self-reported general health with no symptoms of cardiovascular disease or major coronary risk factors, no current or recent lower-extremity injury that could prevent them from giving 100% of their capacity during the test and to meet a certain level of running performance. More specifically, runners were required to have an $s_{\dot{V}O_{2\max}}$ greater or equal to 16 km/h.

Experimental procedure

Each participant completed five experimental sessions interspersed by at least two days in the laboratory. All participants were advised to avoid strenuous exercise the day before a test but to maintain their usual training programme otherwise. During the first session, participants completed a maximal incremental aerobic test on a treadmill (Arsalis T150—FMT-MED, Louvain-la-Neuve, Belgium). This test consisted of a 10-min warm-up at 10 km/h followed by an incremental increase in the running speed of 1 km/h every two minutes until exhaustion. This test was used to determine the peak speed (PS) of the incremental test of each participant. PS is defined as the running speed of the last fully completed increment ($s_{\dot{V}O_{2\max}}$) plus the fraction of time spent in the following uncompleted increment (α) multiplied by the running speed increment ($\Delta s = 1$ km/h) (Kuipers et al. 2003): $PS = s_{\dot{V}O_{2\max}} + \alpha \Delta s$.

The other four tests were performed in a randomized order and consisted of exhaustive runs at a given percentage of the participant's PS (90, 100, 110, or 120%). These tests were as follows: after a 10-min warm-up at 10 km/h and a 5-min rest period, the running speed was increased to a given percentage of PS, and the participant had to maintain the pace until exhaustion. The time to exhaustion was collected for each of the four sessions. No information about the timings or running speed was given to any participant during any of the five experimental sessions. All participants were familiar with running on a treadmill.

Mathematical modelling

The estimations of CS and d' were obtained from the following four different but mathematically equivalent equations

$$t(s) = \frac{d'}{s - CS} \quad (1)$$

$$d(s) = s \frac{d'}{s - CS} \quad (2)$$

$$s(t) = \frac{d'}{t} + CS \quad (3)$$

$$d(t) = d' + CS t \quad (4)$$

where t , s , and d stand for time to exhaustion, running speed, and distance, respectively. Equation 4 represents the original linear model of Monod and Scherrer (1965). Whipp et al. (1982) and Gaesser et al. (1990) proposed the models given by Eqs. 3 and 1, respectively. Equation 2 denotes the distance as function of running speed model proposed by Morton (2006).

Data analysis

Four different fitting procedures were used on the data set obtained for each subject to estimate CS and d' . More specifically, $t(s)$ (Eq. 1) using WLS and $d(s)$ (Eq. 2) using WLS were evaluated. These first two fitting procedures are statistically appropriate. The two other fitting procedures that have been evaluated were $s(t)$ (Eq. 3) using LS and $d(t)$ (Eq. 4) using LS. These two fitting procedures are statistically inappropriate but are frequently used in the literature (Jones et al. 2019; Jones and Vanhatalo 2017). In the first case, time to exhaustion should be considered as the dependent variable and not speed. In the second case, both distance and time to exhaustion should be considered as dependent variables and not only distance. However, the errors of both variables are correlated, i.e., the error of distance is given by the product of speed and the error of time to exhaustion variable, since speed does not carry any error. This is known as endogeneity and, to the best of our knowledge, there exists no regression method that can handle such case (Antonakis et al. 2014). Weights were applied to corresponding dependent variables (time to exhaustion or distance) only in the statistically appropriate fitting procedures. Error minimization was performed iteratively using the Levenberg–Marquardt algorithm (Levenberg 1944; Marquardt 1963) for (W)LS regression. The standard error of the estimate (SEE) in

absolute numbers for both CS and d' , the combined SEE (%SEE), i.e., the sum of SEE of CS and d' transformed to percent units, and the residual standard error (RSE) of the fitting procedure were computed to assess the quality of the fit. Data analysis was performed using Python (version 3.7.4, Python Software Foundation. Available at <http://www.python.org>).

Statistical analysis

Descriptive statistics are presented using mean \pm standard deviation (SD) unless otherwise indicated. The normality of the data was confirmed through the Shapiro–Wilk test. Bland–Altman plots were constructed to examine the presence of systematic and proportional bias on CS and d' estimated from two different fitting procedures (Bland and Altman 1995; Atkinson and Nevill 1998). Systematic bias was also identified by a significant difference obtained from a paired two-sided Student's t -test. After confirming no correlation amongst the residuals using the Durbin-Watson test (Durbin-Watson statistic between 1.5 and 2.5), the proportional bias (heteroscedasticity) was identified by a significant slope of the regression line. In addition, the estimations of CS and d' obtained from the two statistically appropriate fitting procedures as well as from a statistically appropriate and both statistically inappropriate fitting procedures were compared using one-way repeated measures ANOVA (RM-ANOVA) with Mauchly's correction for sphericity and employing Holm corrections for pairwise post hoc comparisons. Statistical analysis was performed using Jamovi (version 1.0.8, [Computer Software], retrieved from <https://www.jamovi.org>) and R (version 3.5.0, The R Foundation for Statistical

Computing, Vienna, Austria) with a level of significance set at $P \leq 0.05$.

Results

Table 1 depicts the time to exhaustion corresponding to the four exhaustive runs performed at 90, 100, 110, and 120% of the participant's PS.

Table 2 depicts the estimations of CS and d' obtained from the two statistically appropriate [$t(s)$ using WLS and $d(s)$ using WLS] and the two statistically inappropriate but frequently used [$s(t)$ using LS and $d(t)$ using LS] fitting procedures together with their corresponding %SEE and RSE. Note that as the units of the residual sum of squares depend on the fitting procedure itself, the RSE cannot be compared between the different fitting procedures employed. The smallest to largest estimations of CS were given by $t(s)$ using WLS and $d(s)$ using WLS (same CS), $d(t)$ using LS, and $s(t)$ using LS, while those for d' were ordered as $s(t)$ using LS, $d(t)$ using LS, $d(s)$ using WLS, and $t(s)$ using WLS (Table 2).

Comparison between statistically appropriate [$t(s)$ using WLS and $d(s)$ using WLS] fitting procedures

Bland–Altman plots comparing statistically appropriate fitting procedures for both CS and d' are depicted in Fig. 1, while Table 3 reports their systematic and proportional biases.

Table 1 Means \pm standard deviations of the time to exhaustion corresponding to the four exhaustive runs performed at 90, 100, 110, and 120% of the participant's peak aerobic speed (PS)

Running speed (%PS)	90	100	110	120
Time to exhaustion (min)	14.8 \pm 2.57	5.94 \pm 1.21	2.78 \pm 0.78	1.68 \pm 0.50

Table 2 Means \pm standard deviations of the critical speed (CS) and distance that can be run above CS (d') and their corresponding standard error of estimate (SEE, in parenthesis) obtained from statistically appropriate [$t(s)$ using weighted least squares (WLS) and $d(s)$ using

WLS] and statistically inappropriate [$s(t)$ and $d(t)$ both using LS] fitting procedures together with the combined SEE (%SEE), i.e., the sum of SEE of CS and d' transformed to percent units, as well as the residual standard errors (RSE)

Statistically appropriate	Fitting procedure	CS (m/s)	d' (m)	%SEE	RSE
Yes	$t(s)$ using WLS	4.39 \pm 0.41 (0.03 \pm 0.01)	226.0 \pm 57.0 (20.3 \pm 8.0)	9.8 \pm 3.4	37.0 \pm 14.5
	$d(s)$ using WLS	4.39 \pm 0.40 (0.03 \pm 0.01)	222.3 \pm 56.0 (19.8 \pm 7.6)	9.7 \pm 3.4	201.5 \pm 79.3
No	$s(t)$ using LS	4.59 \pm 0.43 (0.07 \pm 0.02)	167.3 \pm 46.2 (11.2 \pm 4.3)	8.3 \pm 2.6	0.11 \pm 0.04
	$d(t)$ using LS	4.42 \pm 0.39 (0.04 \pm 0.02)	210.2 \pm 50.5 (19.7 \pm 7.7)	10.5 \pm 3.9	34.4 \pm 11.9

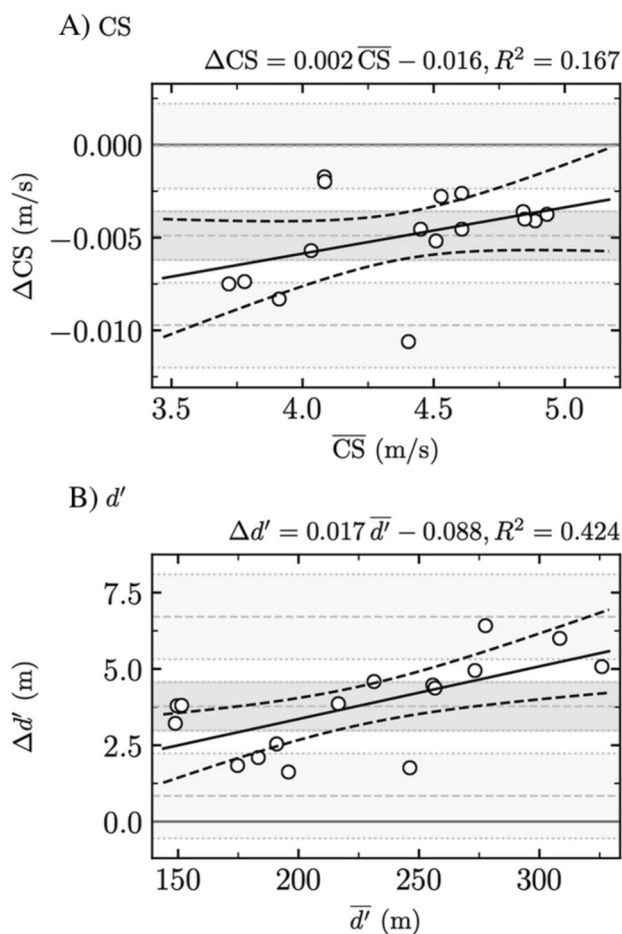


Fig. 1 Comparison between statistically appropriate fitting procedures. Bland–Altman plots comparing $t(s)$ using weighted least squares (WLS) and $d(s)$ using WLS for (i) critical speed (CS) and (ii) distance that can be run above CS (d')

Table 3 Systematic bias \pm random error (RE, i.e., 1.6 standard deviation) and proportional bias \pm residual standard error (RSE) for critical speed (CS) and distance that can be run above CS (d') when comparing statistically appropriate fitting procedures, i.e., $t(s)$ using weighted least squares (WLS) and $d(s)$ using WLS

	$t(s)$ using WLS vs. $d(s)$ using WLS	
	CS	d'
Systematic bias \pm RE	-0.005 ± 0.001	3.8 ± 0.8
<i>P</i>	< 0.001	< 0.001
Proportional bias \pm RSE	0.002 ± 0.001	0.02 ± 0.005
<i>P</i>	0.12	0.006

Significant differences ($P \leq 0.05$) are depicted in bold font

Comparison between the statistically appropriate $t(s)$ using WLS and the two statistically inappropriate $s(t)$ and $d(t)$ both using LS fitting procedures

Bland–Altman plots comparing the statistically appropriate $t(s)$ using WLS fitting procedure to the two frequently used but statistically inappropriate fitting procedures for both CS and d' are depicted in Fig. 2, while Table 4 reports their systematic and proportional biases.

The comparison of the three fitting procedures using RM-ANOVA yielded a significant main effect ($P < 0.001$) for both CS and d' . In addition, post hoc comparisons gave significant differences between each pair of fitting procedures and for both CS and d' ($P \leq 0.01$). Notably, the pair [$t(s)$ using WLS, $d(t)$ using LS] was the only comparison giving P values larger than 0.001 for CS, i.e., 0.01.

Comparison between the statistically appropriate $d(s)$ using WLS and the two statistically inappropriate $s(t)$ and $d(t)$ both using LS fitting procedures

Bland–Altman plots comparing the statistically appropriate $d(s)$ using WLS fitting procedure to the two frequently used but statistically inappropriate fitting procedures are depicted in Fig. 3, while Table 5 reports their systematic and proportional biases.

The comparison of the three fitting procedures using RM-ANOVA yielded a significant main effect ($P < 0.001$) for both CS and d' . In addition, post hoc comparisons yielded significant differences between each pair of fitting procedures and for both CS and d' ($P \leq 0.02$). Notably, the pair [$d(s)$ using WLS, $d(t)$ using LS] was the only comparison giving P values larger than 0.001 for CS and d' , i.e., 0.02 and 0.006, respectively.

Discussion

Conventional statistical approaches demonstrated a systematic bias between each pair of fitting procedures for the estimation of both CS and d' . These results were in line with the hypothesis that different estimations of CS and d' should have been obtained when comparing a statistically appropriate with a statistically inappropriate fitting procedure. Although these findings seem to refute the hypothesis that similar estimations of CS and d' should have been obtained when comparing statistically appropriate fitting procedures, the differences for these estimations between statistically appropriate fitting procedures were negligible.

As pointed out by Iannetta et al. (2020), coaches are recommended to prescribe exercise based on intensity domains.

Fig. 2 Comparison between the statistically appropriate [$t(s)$ using weighted least squares (WLS)] and the two statistically inappropriate fitting procedures. Bland–Altman plots comparing **a** $t(s)$ using WLS and $s(t)$ using LS and **b** $t(s)$ using WLS and $d(t)$ using LS for (i) critical speed (CS) and (ii) distance that can be run above CS (d')

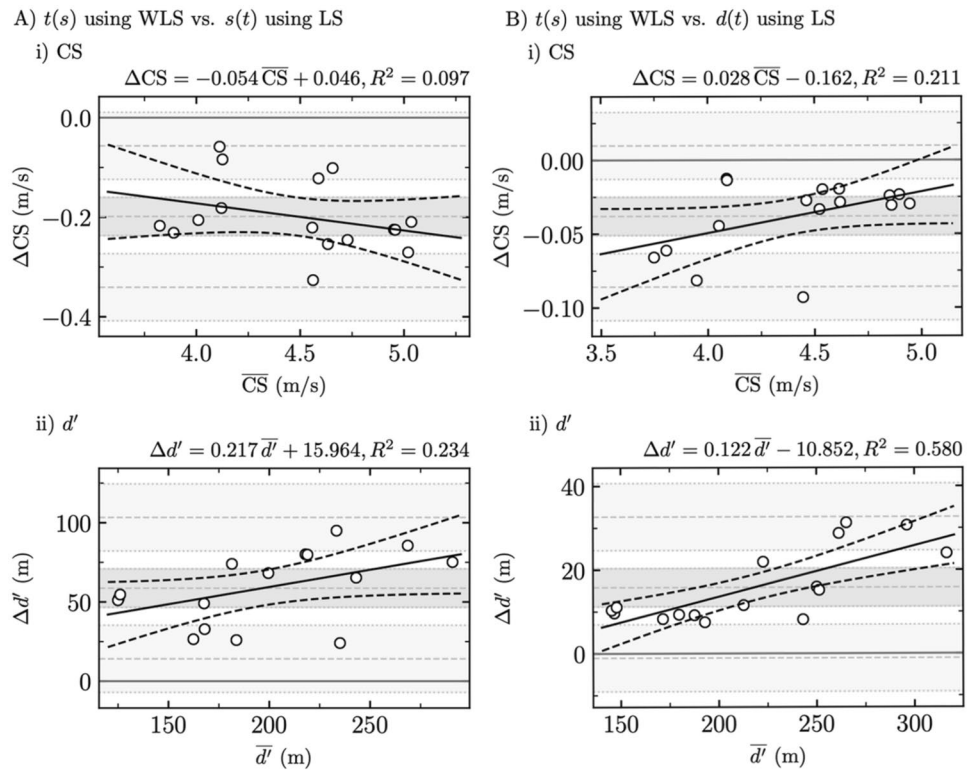


Table 4 Systematic bias \pm random error (RE, i.e., 1.6 standard deviation) and proportional bias \pm residual standard error (RSE) for critical speed (CS) and distance that can be run above CS (d') when compar-

ing $t(s)$ using weighted least squares (WLS) with both $s(t)$ using least squares (LS) and $d(t)$ using LS

	$t(s)$ using WLS vs. $s(t)$ using LS		$t(s)$ using WLS vs. $d(t)$ using LS	
	CS	d'	CS	d'
Systematic bias \pm RE	-0.20 ± 0.04	58.7 ± 12.2	-0.04 ± 0.01	15.8 ± 4.6
<i>P</i>	< 0.001	< 0.001	< 0.001	< 0.001
Proportional bias \pm RSE	-0.05 ± 0.04	0.22 ± 0.11	0.03 ± 0.01	0.12 ± 0.03
<i>P</i>	0.24	0.06	0.07	< 0.001

Significant differences ($P \leq 0.05$) are depicted in bold font

To do so, one possibility is to estimate CS and use it as a limit between the heavy and severe intensity domains (Jones et al. 2019). Therefore, an accurate estimation of CS is required. There exist two statistically appropriate fitting procedures for the two-parameter model variants that allow us to estimate CS: $t(s)$ using WLS and $d(s)$ using WLS. The comparison of these two fitting procedures yielded significant systematic biases -0.005 ± 0.001 m/s (0.018 ± 0.004 km/h) and 3.8 ± 0.8 m for CS and d' , respectively ($P < 0.001$). However, the bias for CS was less than treadmills' speed resolution. Therefore, these differences could be assumed to be negligible when prescribing a training session based on exercise intensity because they would be practically meaningless. Nonetheless, they could be due to the specific data set used in this study and could potentially be larger with

another data set, other choices of running speeds, a larger number of exhaustive runs, or another underlying model (e.g., three-parameters or exponential). In addition, even though the estimated CS should be a very good approximation of the critical intensity but not the critical intensity per se, we suggest coaches to physiologically verify that the estimated CS represents the upper boundary of sustainable exercise. Moreover, there is a day-to-day variation in human performance and given the SEE of CS (0.03 ± 0.01 m/s or 0.11 ± 0.04 km/h, Table 2), its confidence limits are about 10% of its value. Therefore, it would be justified to prescribe exercise intensity outside these confidence limits to avoid being in a range of values that are uncertain due to measurement error, which could be defined as the phase transition between heavy and severe intensity domains (Anderson et al.

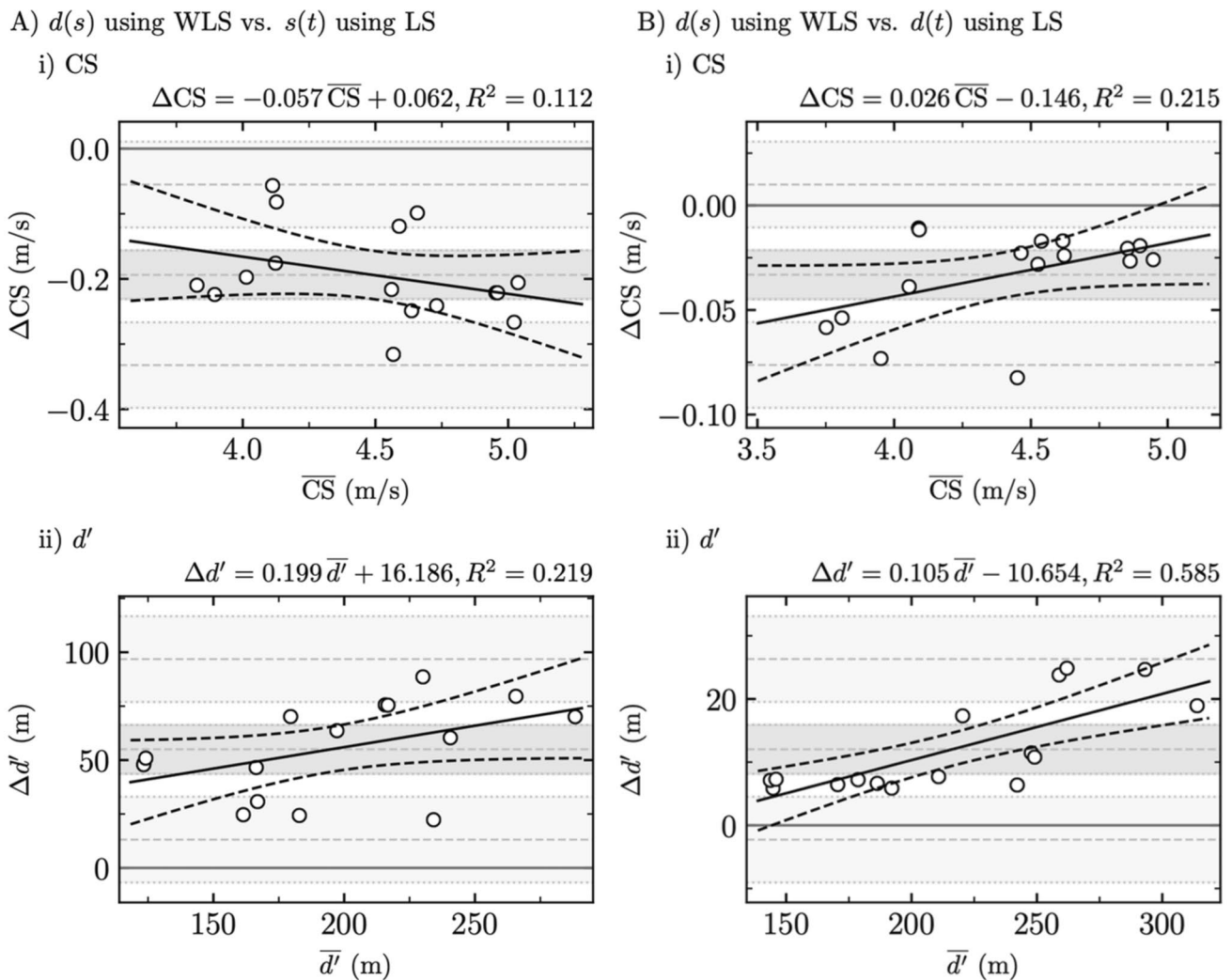


Fig. 3 Comparison between the statistically appropriate [$d(s)$ using weighted least squares (WLS)] and the two statistically inappropriate fitting procedures. Bland–Altman plots comparing **a** $d(s)$ using WLS

and $s(t)$ using LS and **b** $d(s)$ using WLS and $d(t)$ using LS for (i) critical speed (CS) and (ii) distance that can be run above CS (d')

Table 5 Systematic bias \pm random error (RE, i.e., 1.6 standard deviation) and proportional bias \pm residual standard error (RSE) for critical speed (CS) and distance that can be run above CS (d') when compar-

ing $d(s)$ using weighted least squares (WLS) with both $s(t)$ using least squares (LS) and $d(t)$ using LS

	$d(s)$ using WLS vs. $s(t)$ using LS		$d(s)$ using WLS vs. $d(t)$ using LS	
	CS	d'	CS	d'
Systematic bias \pm RE	-0.19 ± 0.04	55.0 ± 11.3	-0.03 ± 0.01	12.0 ± 3.9
<i>P</i>	< 0.001	< 0.001	< 0.001	< 0.001
Proportional bias \pm RSE	-0.06 ± 0.04	0.20 ± 0.10	0.03 ± 0.01	0.11 ± 0.02
<i>P</i>	0.21	0.07	0.07	< 0.001

Significant differences ($P \leq 0.05$) are depicted in bold font

2019). From a practical perspective, coaches could still prescribe exercise intensity at CS, but should acknowledge that there might be a source of error, especially if no physiological verification was performed.

The comparison between the statistically appropriate $t(s)$ using WLS [or $d(s)$ using WLS] and statistically inappropriate $d(t)$ using LS fitting procedures produced systematic but reasonably small biases for both CS ($< -0.04 \pm 0.01$ m/s;

0.14 ± 0.04 km/h) and d' ($< 15.8 \pm 4.6$ m). These differences are quite small and could be assumed to be negligible. The largest biases were obtained between the statistically appropriate $t(s)$ using WLS [or $d(s)$ using WLS] and statistically inappropriate $s(t)$ using LS fitting procedures (CS: $< -0.20 \pm 0.04$ m/s or 0.72 ± 0.14 km/h, d' : $< 58.7 \pm 12.2$ m). In this case, the observed differences could have an impact when prescribing a training session based on exercise intensity. Nonetheless, as previously mentioned already, the magnitude of all the observed differences could be due to the specific data set and could potentially be smaller or larger. Moreover, as all comparisons of fitting procedures yielded systematic biases, it suggests that each fitting procedure produced specific estimations of CS and d' . Therefore, we encourage coaches to verify that the estimated CS coincide with the physiological CS and make small adjustments based on the observed performance.

The coefficient of determination is not a reliable measure to assess the goodness of fit when using WLS (Willet and Singer 1988; Kvalseth 1985). Therefore, one possibility is to use the residual sum of squares or a parameter that depends on it, such as RSE. However, the units of RSE depend on the fitting procedure and, more specifically, on the choice of the vertical and horizontal axes for the model variant and on which axes the errors are being minimized, making it impossible to compare the RSE of different fitting procedures. Moreover, when the time to exhaustion is assumed to be the independent variable, a lower RSE is necessarily observed because the data points mostly lied in the region where there was a high difference between the measured and predicted data in the horizontal axis (time to exhaustion variable) but a small difference in the vertical axis (running speed or distance variable). Therefore, a lower RSE and thus a perception of a better fitting procedure is likely to be provided by assuming the running speed or distance as the dependent variable instead of the time to exhaustion (Vinetti et al. 2020). In the case of distance as function of time, even if distance is indeed a dependent variable, error minimization only along the vertical axis (distance variable) is not statistically appropriate and there exists no regression method that can take into account the fact the errors are actually correlated. On the other hand, one could use %SEE and assume that the smallest %SEE provides the best fit quality (Triska et al. 2021). However, obtaining lower RSE or %SEE are not consistent with the experiment generating the data set but with the representation of the data set itself, as already pointed out by Vinetti et al. (2020). Therefore, based on these observations, we suggest deciding the choice of regression analysis and model variant beforehand. Moreover, this choice should be based on the specific data set (the sources of experimental error) to lead to a statistically appropriate fitting procedure. Then, we suggest to physiologically verify that the estimated CS represents a very good approximation of the actual CS.

Heteroscedasticity of the dependent variable was explicitly depicted by Hinckson and Hopkins (2005) when using usual LS fitting procedure. Indeed, these authors demonstrated systematic and nonuniform deviation from their models by showing the residuals as function of predicted values. In this study, the suggestion made by Morton and Hodgson (1996) to include weights to overcome heteroscedasticity was applied.

Practical applications

The preferred choice between model variants is not clear (Gaesser et al. 1990; Hill 1993) and researchers/coaches might be confused on which model variant to select and the corresponding regression analysis to apply based on their data set. Therefore, a methodology to select a statistically appropriate fitting procedure is provided. The following methodology specifically addresses running speed and distance, but any occurrence of these terms can be replaced by power and work, respectively. Moreover, special cases that need to be taken into account when dealing with power or work are explicitly mentioned. Furthermore, the methodology is presented using WLS regression applied to the two-parameter model variants. This methodology can be generalized to other choices of loss functions and more complicated (e.g., three-parameter or exponential) models.

First, an experiment that fixes running speed (independent variable: s) and measures time to exhaustion and distance (dependent variables: t and d) is considered (Fig. 4a). Special consideration exists in the case of extremely high power on an ergometer or when cycling outdoors (Vinetti et al. 2020; Maier et al. 2017). In such cases, power should be considered as a dependent variable and geometric mean regression should be employed. The recommendations on the choice of the regression analysis are as follows:

1. No regression analysis should be used with the models $s(t)$ and $s(d)$ [the inverse function of $d(s)$] because in these cases, t and d , respectively, should be the dependent variables, but they are not. In the case of extremely high power on an ergometer or when cycling outdoors, geometric mean regression should be used (Vinetti et al. 2020).
2. WLS should be used with the models $t(s)$ and $d(s)$ with weights applied to t and d , respectively. In the case of extremely high power on an ergometer or when cycling outdoors, geometric mean regression should be used (Vinetti et al. 2020).
3. No regression should be used with the models $d(t)$ and $t(d)$ [the inverse function of $d(t)$] as the errors are correlated and no regression method exists to handle such case.

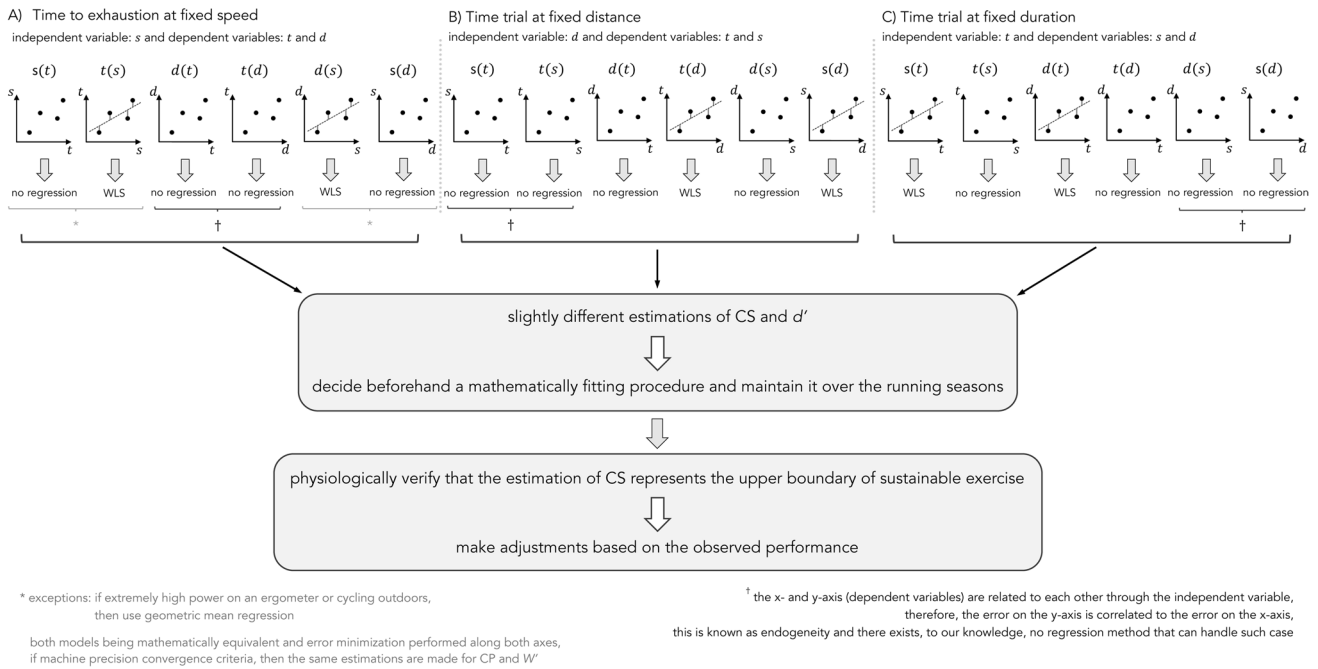


Fig. 4 Recommendations on the choice of regression analysis. **a** Time to exhaustion (dependent variable: t) is measured for a fixed running speed (s). Distance (d) is by induction a dependent variable. **b** Time trial and running speed (dependent variables) are measured for a fixed distance (independent variable). **c** Distance and running speed (dependent variables) are measured for a fixed time trial (independent

variable). For sake of clarity, the models represented in the figures are not representative of the outcome of the measurements. They are only given to demonstrate where a regression method can be applied. *WLS* weighted least squares, *CS* critical speed, d' distance that can be run above *CS*, *CP* critical power, W' anaerobic work capacity

Second, an experiment that fixes distance (independent variable: d) and measures time trial and running speed (dependent variables: t and s) is considered (Fig. 4b). The recommendations are as follows:

1. No regression analysis should be used with the models $d(t)$ and $d(s)$ because in these cases, t and s , respectively, should be the dependent variables, but they are not.
2. WLS should be used with the models $t(d)$ and $s(d)$ with weights applied to t and s , respectively.
3. No regression should be used with the models $s(t)$ and $t(s)$ as the errors are correlated and no regression method exists to handle such case.

Third, an experiment that fixes time (independent variable: t) and measures running speed and distance (dependent variables: s and d) is considered (Fig. 4c). The recommendations are as follows:

1. No regression analysis should be used with the models $t(s)$ and $t(d)$ because in these cases, s and d , respectively, should be the dependent variables, but they are not.
2. WLS should be used with the models $s(t)$ and $d(t)$ with weights applied to s and d , respectively.

3. No regression should be used with the models $d(s)$ and $s(d)$ as the errors are correlated and no regression method exists to handle such case.

Of note, we did not consider WLS that estimates parameters based on an error minimization along the horizontal axis of a given model $f(\cdot)$. The reason being that using WLS based on an error minimization along the horizontal axis is equivalent to applying the usual WLS regression on $f(\cdot)^{-1}$, i.e., the inverse of the model variant. However, it should be pointed out that if $f(\cdot)^{-1}$ does not exist (the function is not invertible), then WLS based on an error minimization along the horizontal axis of the model variant $f(\cdot)$ should be used.

Finally, potential error in the model should be acknowledged and a physiological verification that the estimated *CS* represents the upper boundary of sustainable exercise should be made. In addition, small adjustments based on the observed performance could be applied.

Methodological limitations

A few limitations to the present study are worth noting. First, no test–retest repeatability of time to exhaustion has been performed. However, even if repeatability was shown to have

up to 15% error (Laursen et al. 2007), correctly assigning variables being dependent on time to exhaustion, as the dependent variables, automatically takes into account the fact that they carry error. Nonetheless, familiarization was shown to increase reliability but tends to be quite unpractical for the participant (Triska et al. 2017). Second, no runs below, at, and above CS whilst assessing oxygen uptake responses to exercise were performed to physiologically verify that the estimated CS obtained with statistically appropriate fitting procedures represents the threshold intensity associated with the lower extremity of the severe intensity domain. Although this is beyond the aim of this study, future studies, using these runs, may determine it. Third, the selected percent of PS (90, 100, 110, and 120%) resulted in time distributions that were relatively unbalanced. Therefore, the estimated CS might not represent the physiological CS (Bishop et al. 1998; Mattioni Maturana et al. 2018). However, this did not affect the present study as the main goal was not to show that estimated and physiological CS coincide. Nevertheless, when using the estimated CS to prescribe exercise intensity, a careful choice of percent of PS is important to make sure the estimated CS is a very good approximation of the physiological CS.

Conclusion

Systematic biases were observed between each pair of fitting procedures for the estimations of both CS and d' , though negligible when comparing statistically appropriate fitting procedures. The observed differences suggest that a statistically appropriate fitting procedure should be chosen beforehand by the researcher. Indeed, even if these differences could be negligible when prescribing a training session based on exercise intensity, they might vary depending on the data set or the underlying model. This statement is also particularly important for coaches using CS and d' for prescribing training session intensity: the fitting procedure should be maintained over the running seasons. Moreover, we suggest coaches to physiologically verify that the estimated CS represents a very good approximation of the actual CS, to acknowledge the error in the model, and make adjustments when they seem necessary. In addition, this study provides a methodology to determine the statistically appropriate fitting procedures that can be considered based on a specific data set.

Acknowledgements This study was supported by the University of Lausanne (Switzerland). The authors warmly thank the participants for their time and cooperation.

Author contributions RS, NP, DM, and FB carried out the lab work and collected data; AP performed the data analysis, carried out the statistical analysis, and wrote the original draft of the manuscript; AP,

DM, and FB critically revised the manuscript; FB and DM conceived of the study, designed the study, and coordinated the study. All authors gave final approval for publication and agree to be held accountable for the work performed therein.

Funding Open Access funding provided by Université de Lausanne. This research received no external funding.

Availability of data and materials The datasets supporting this article are available on request to the corresponding author.

Code availability The code supporting this article is available on request to the corresponding author.

Declarations

Conflict of interest The authors declare no competing interests.

Ethics approval The study protocol was approved by the Ethics Committee (CER-VD 2018-01814) and adhered to the latest Declaration of Helsinki of the World Medical Association.

Informed consent Informed consent was obtained from all individual participants included in the study.

Open Access This article is licensed under a Creative Commons Attribution 4.0 International License, which permits use, sharing, adaptation, distribution and reproduction in any medium or format, as long as you give appropriate credit to the original author(s) and the source, provide a link to the Creative Commons licence, and indicate if changes were made. The images or other third party material in this article are included in the article's Creative Commons licence, unless indicated otherwise in a credit line to the material. If material is not included in the article's Creative Commons licence and your intended use is not permitted by statutory regulation or exceeds the permitted use, you will need to obtain permission directly from the copyright holder. To view a copy of this licence, visit <http://creativecommons.org/licenses/by/4.0/>.

References

- American College of Sports Medicine (2000) ACSM's guidelines for exercise testing and prescription, 9th edn. Lippincott Williams & Wilkins, Philadelphia
- Anderson LM, Bonanno DR, Hart HF, Barton CJ (2019) What are the benefits and risks associated with changing foot strike pattern during running? A systematic review and meta-analysis of injury, running economy, and biomechanics. *Sports Med* (Auckland, NZ). <https://doi.org/10.1007/s40279-019-01238-y>
- Antonakis J, Bendahan S, Jacquart P, Lalive R (2014) Causality and endogeneity: problems and solutions. *The Oxford handbook of leadership and organizations*. Oxford University Press, New York, pp 93–117
- Atkinson G, Nevill AM (1998) Statistical methods for assessing measurement error (reliability) in variables relevant to sports medicine. *Sports Med* 26(4):217–238. <https://doi.org/10.2165/00007256-199826040-00002>
- Bigland-Ritchie B, Woods JJ (1984) Changes in muscle contractile properties and neural control during human muscular fatigue. *Muscle Nerve* 7(9):691–699. <https://doi.org/10.1002/mus.880070902>

- Bishop D, Jenkins DG, Howard A (1998) The critical power function is dependent on the duration of the predictive exercise tests chosen. *Int J Sports Med* 19(2):125–129. <https://doi.org/10.1055/s-2007-971894>
- Black MI, Jones AM, Blackwell JR, Bailey SJ, Wylie LJ, McDonagh ST, Thompson C, Kelly J, Summers P, Mileva KN, Bowtell JL, Vanhatalo A (2017) Muscle metabolic and neuromuscular determinants of fatigue during cycling in different exercise intensity domains. *J Appl Physiol* 122(3):446–459. <https://doi.org/10.1152/jappphysiol.00942.2016>
- Bland JM, Altman DG (1995) Comparing methods of measurement: why plotting difference against standard method is misleading. *Lancet* 346(8982):1085–1087. [https://doi.org/10.1016/s0140-6736\(95\)91748-9](https://doi.org/10.1016/s0140-6736(95)91748-9)
- DiMenna FJ, Jones AM (2009) “Linear” versus “nonlinear” VO₂ responses to exercise: reshaping traditional beliefs. *J Exerc Sci Fit* 7(2):67–84. [https://doi.org/10.1016/s1728-869x\(09\)60009-5](https://doi.org/10.1016/s1728-869x(09)60009-5)
- Faude O, Hecksteden A, Hammes D, Schumacher F, Besenius E, Sperlich B, Meyer T (2017) Reliability of time-to-exhaustion and selected psycho-physiological variables during constant-load cycling at the maximal lactate steady-state. *Appl Physiol Nutr Metab* 42(2):142–147. <https://doi.org/10.1139/apnm-2016-0375>
- Fontana FY, Keir DA, Bellotti C, De Roia GF, Murias JM, Pogliaghi S (2015) Determination of respiratory point compensation in healthy adults: Can non-invasive near-infrared spectroscopy help? *J Sci Med Sport* 18(5):590–595. <https://doi.org/10.1016/j.jsams.2014.07.016>
- Gaesser GA, Wilson LA (1988) Effects of continuous and interval training on the parameters of the power-endurance time relationship for high-intensity exercise. *Int J Sports Med* 9(6):417–421. <https://doi.org/10.1055/s-2007-1025043>
- Gaesser GA, Carnevale TJ, Garfinkel A, Walter DO (1990) Modeling of the power-endurance relationship for high-intensity exercise. *Med Sci Sports Exerc* 22:S16
- Gaesser GA, Carnevale TJ, Garfinkel A, Walter DO, Womack CJ (1995) Estimation of critical power with nonlinear and linear models. *Med Sci Sports Exerc* 27(10):1430–1438
- Galán-Rioja MÁ, González-Mohino F, Poole DC, González-Ravé JM (2020) Relative proximity of critical power and metabolic/ventilatory thresholds: systematic review and meta-analysis. *Sports Med*. <https://doi.org/10.1007/s40279-020-01314-8>
- Hill DW (1993) The critical power concept. A review. *Sports Med* 16(4):237–254. <https://doi.org/10.2165/00007256-199316040-00003>
- Hill DW, Ferguson CS (1999) A physiological description of critical velocity. *Eur J Appl Physiol Occup Physiol* 79(3):290–293. <https://doi.org/10.1007/s004210050509>
- Hinckson EA, Hopkins WG (2005) Reliability of time to exhaustion analyzed with critical-power and log-log modeling. *Med Sci Sports Exerc* 37(4):696–701. <https://doi.org/10.1249/01.mss.0000159023.06934.53>
- Housh DJ, Housh TJ, Bauge SM (1989) The accuracy of the critical power test for predicting time to exhaustion during cycle ergometry. *Ergonomics* 32(8):997–1004. <https://doi.org/10.1080/00140138908966860>
- Housh TJ, Johnson GO, McDowell SL, Housh DJ, Pepper M (1991) Physiological responses at the fatigue threshold. *Int J Sports Med* 12(3):305–308. <https://doi.org/10.1055/s-2007-1024686>
- Housh TJ, Cramer JT, Bull AJ, Johnson GO, Housh DJ (2001) The effect of mathematical modeling on critical velocity. *Eur J Appl Physiol* 84(5):469–475. <https://doi.org/10.1007/s004210000375>
- Hughson RL, Orok CJ, Staudt LE (1984) A high velocity treadmill running test to assess endurance running potential. *Int J Sports Med* 5(1):23–25. <https://doi.org/10.1055/s-2008-1025875>
- Iannetta D, Fontana FY, Maturana FM, Inglis EC, Pogliaghi S, Keir DA, Murias JM (2018) An equation to predict the maximal lactate steady state from ramp-incremental exercise test data in cycling. *J Sci Med Sport* 21(12):1274–1280. <https://doi.org/10.1016/j.jsams.2018.05.004>
- Iannetta D, Inglis EC, Mattu AT, Fontana FY, Pogliaghi S, Keir DA, Murias JM (2020) A critical evaluation of current methods for exercise prescription in women and men. *Med Sci Sports Exerc* 52(2):466–473. <https://doi.org/10.1249/MSS.0000000000002147>
- Jones AM, Vanhatalo A (2017) The “critical power” concept: applications to sports performance with a focus on intermittent high-intensity exercise. *Sports Med* 47(Suppl 1):65–78. <https://doi.org/10.1007/s40279-017-0688-0>
- Jones AM, Burnley M, Black MI, Poole DC, Vanhatalo A (2019) The maximal metabolic steady state: redefining the “gold standard.” *Physiol Rep* 7(10):e14098. <https://doi.org/10.14814/phy2.14098>
- Kuipers H, Rietjens G, Verstappen F, Schoenmakers H, Hofman G (2003) Effects of stage duration in incremental running tests on physiological variables. *Int J Sports Med* 24(7):486–491. <https://doi.org/10.1055/s-2003-42020>
- Kvalseth TO (1985) Cautionary note about R₂. *Amer Stat* 39(4):279–285
- Lansley KE, DiMenna FJ, Bailey SJ, Jones AM (2011) A “new” method to normalise exercise intensity. *Int J Sports Med* 32(7):535–541. <https://doi.org/10.1055/s-0031-1273754>
- Laursen PB, Francis GT, Abbiss CR, Newton MJ, Nosaka K (2007) Reliability of time-to-exhaustion versus time-trial running tests in runners. *Med Sci Sports Exerc* 39(8):1374–1379. <https://doi.org/10.1249/mss.0b013e31806010f5>
- Levenberg K (1944) A method for the solution of certain non-linear problems in least squares. *Q Appl Math* 2(2):164–168
- MacInnis MJ, Gibala MJ (2017) Physiological adaptations to interval training and the role of exercise intensity. *J Physiol* 595(9):2915–2930. <https://doi.org/10.1113/JP273196>
- Maier T, Schmid L, Muller B, Steiner T, Wehrli JP (2017) Accuracy of cycling power meters against a mathematical model of treadmill cycling. *Int J Sports Med* 38(6):456–461. <https://doi.org/10.1055/s-0043-102945>
- Marquardt DW (1963) An algorithm for least-squares estimation of nonlinear parameters. *J Soc Ind Appl Math* 11(2):431–441
- Mattioni Maturana F, Fontana FY, Pogliaghi S, Passfield L, Murias JM (2018) Critical power: how different protocols and models affect its determination. *J Sci Med Sport* 21(7):742–747. <https://doi.org/10.1016/j.jsams.2017.11.015>
- McDermott KS, Forbes MR, Hill DW (1993) Application of the critical power concept to outdoor running. *Med Sci Sports Exerc* 25:S109
- McLellan TM, Skinner JS (1985) Submaximal endurance performance related to the ventilation thresholds. *Can J Appl Sport Sci* 10(2):81–87
- Monod H, Scherrer J (1965) The work capacity of a synergic muscular group. *Ergonomics* 8(3):329–338. <https://doi.org/10.1080/00140136508930810>
- Moritani T, Nagata A, Devries HA, Muro M (1981) Critical power as a measure of physical work capacity and anaerobic threshold. *Ergonomics* 24(5):339–350. <https://doi.org/10.1080/00140138108924856>
- Morton RH (1986) A three component model of human bioenergetics. *J Math Biol* 24(4):451–466. <https://doi.org/10.1007/bf01236892>
- Morton HR (1996) A 3-parameter critical power model. *Ergonomics* 39(4):611–619. <https://doi.org/10.1080/00140139608964484>
- Morton RH (2006) The critical power and related whole-body bioenergetic models. *Eur J Appl Physiol* 96(4):339–354. <https://doi.org/10.1007/s00421-005-0088-2>
- Morton RH, Hodgson DJ (1996) The relationship between power output and endurance: a brief review. *Eur J Appl Physiol Occup Physiol* 73(6):491–502. <https://doi.org/10.1007/bf00357670>
- Pepper ML, Housh TJ, Johnson GO (1992) The accuracy of the critical velocity test for predicting time to exhaustion during treadmill

- running. *Int J Sports Med* 13(2):121–124. <https://doi.org/10.1055/s-2007-1021242>
- Peronnet F, Thibault G (1989) Mathematical analysis of running performance and world running records. *J Appl Physiol* 67(1):453–465. <https://doi.org/10.1152/jappl.1989.67.1.453>
- Poole DC, Ward SA, Ward BJ (1986) Effects of training on the metabolic and respiratory profile of high-intensity exercise. *Eur J Appl Physiol Occup Physiol* 29:161
- Poole DC, Ward SA, Gardner GW, Whipp BJ (1988) Metabolic and respiratory profile of the upper limit for prolonged exercise in man. *Ergonomics* 31(9):1265–1279. <https://doi.org/10.1080/00140138808966766>
- Roy M, Williams SM, Brown RC, Meredith-Jones KA, Osborne H, Jospe M, Taylor RW (2018) High-intensity interval training in the real world: outcomes from a 12-month intervention in overweight adults. *Med Sci Sports Exerc* 50(9):1818–1826. <https://doi.org/10.1249/MSS.0000000000001642>
- Triska C, Karsten B, Heidegger B, Koller-Zeisler B, Prinz B, Nimmerichter A, Tschan H (2017) Reliability of the parameters of the power-duration relationship using maximal effort time-trials under laboratory conditions. *PLoS ONE* 12(12):e0189776. <https://doi.org/10.1371/journal.pone.0189776>
- Triska C, Hopker J, Wessner B, Reif A, Tschan H, Karsten B (2021) A 30-min rest protocol does not affect W' , critical power, and systemic response. *Med Sci Sports Exerc* 53(2):404–412. <https://doi.org/10.1249/mss.0000000000002477>
- Vanhatalo A, Doust JH, Burnley M (2007) Determination of critical power using a 3-min all-out cycling test. *Med Sci Sports Exerc* 39(3):548–555. <https://doi.org/10.1249/mss.0b013e31802dd3e6>
- Vinetti G, Taboni A, Ferretti G (2020) A regression method for the power-duration relationship when both variables are subject to error. *Eur J Appl Physiol* 120(4):765–770. <https://doi.org/10.1007/s00421-020-04314-8>
- Wasserman K, Whipp BJ, Koysl SN, Beaver WL (1973) Anaerobic threshold and respiratory gas exchange during exercise. *J Appl Physiol* 35(2):236–243. <https://doi.org/10.1152/jappl.1973.35.2.236>
- Whipp BJ, Mahler M (1980) Dynamics of pulmonary gas exchange during exercise. In: West JB (ed) *Pulmonary gas exchange*, vol 2. Academic Press, New York
- Whipp B, Huntsman D, Storer T, Lamarra N, Wasserman K (1982) A constant which determines the duration of tolerance to high-intensity work. *Fed Proc* 41(5):1591
- Wilkie DR (1980) Equations describing power input by humans as a function of duration of exercise. In: Whipp BJ (ed) *Exercise bioenergetics and gas exchange*. Elsevier/North-Holland Biomedical, Amsterdam
- Willet JB, Singer JD (1988) Another cautionary note about R²: its use in weighted least-squares regression analysis. *Am Stat* 42(3):236–238

Publisher's Note Springer Nature remains neutral with regard to jurisdictional claims in published maps and institutional affiliations.

9.2 Effect of mathematical modeling and fitting procedures on the assessment of critical speed and its relationship with aerobic fitness parameters

Aurélien Patoz^{1,2,*}, Nicola Pedrani¹, Romain Spicher¹, André Berchtold³, Fabio Borrani^{1,†}, Davide Malatesta^{1,†}

¹ Institute of Sport Sciences, University of Lausanne, Lausanne, Switzerland

² Research and Development Department, Volodalen Swiss Sport Lab, Aigle, Switzerland

³ Institute of Social Sciences & NCCR LIVES, University of Lausanne, Lausanne, Switzerland

† These authors contributed equally to this work

* Corresponding author

Published in **Frontiers in Physiology**

DOI: 10.3389/fphys.2021.613066



Effect of Mathematical Modeling and Fitting Procedures on the Assessment of Critical Speed and Its Relationship With Aerobic Fitness Parameters

Aurélien Patoz^{1,2*}, Nicola Pedrani¹, Romain Spicher¹, André Berchtold³, Fabio Borrani[†] and Davide Malatesta[†]

¹ Institute of Sport Sciences, University of Lausanne, Lausanne, Switzerland, ² Research and Development Department, Volodalen Swiss Sport Lab, Aigle, Switzerland, ³ Institute of Social Sciences and National Centre of Competence in Research LIVES, University of Lausanne, Lausanne, Switzerland

OPEN ACCESS

Edited by:

Martin Burtscher,
University of Innsbruck, Austria

Reviewed by:

Leonardo Alexandre
Peyré-Tartaruga,
Federal University of Rio Grande do
Sul, Brazil
Robert Eberle,
University of Innsbruck, Austria

*Correspondence:

Aurélien Patoz
aurelien@volodalen.com

[†] These authors have contributed
equally to this work

Specialty section:

This article was submitted to
Exercise Physiology,
a section of the journal
Frontiers in Physiology

Received: 01 October 2020

Accepted: 05 May 2021

Published: 31 May 2021

Citation:

Patoz A, Pedrani N, Spicher R,
Berchtold A, Borrani F and
Malatesta D (2021) Effect
of Mathematical Modeling and Fitting
Procedures on the Assessment
of Critical Speed and Its Relationship
With Aerobic Fitness Parameters.
Front. Physiol. 12:613066.
doi: 10.3389/fphys.2021.613066

An accurate estimation of critical speed (CS) is important to accurately define the boundary between heavy and severe intensity domains when prescribing exercise. Hence, our aim was to compare CS estimates obtained by statistically appropriate fitting procedures, i.e., regression analyses that correctly consider the dependent variables of the underlying models. A second aim was to determine the correlations between estimated CS and aerobic fitness parameters, i.e., ventilatory threshold, respiratory compensation point, and maximal rate of oxygen uptake. Sixteen male runners performed a maximal incremental aerobic test and four exhaustive runs at 90, 100, 110, and 120% of the peak speed of the incremental test on a treadmill. Then, two mathematically equivalent formulations (time as function of running speed and distance as function of running speed) of three different mathematical models (two-parameter, three-parameter, and three-parameter exponential) were employed to estimate CS, the distance that can be run above CS (d'), and if applicable, the maximal instantaneous running speed (s_{max}). A significant effect of the mathematical model was observed when estimating CS, d' , and s_{max} ($P < 0.001$), but there was no effect of the fitting procedure ($P > 0.77$). The three-parameter model had the best fit quality (smallest Akaike information criterion) of the CS estimates but the highest 90% confidence intervals and combined standard error of estimates (%SEE). The 90% CI and %SEE were similar when comparing the two fitting procedures for a given model. High and very high correlations were obtained between CS and aerobic fitness parameters for the three different models ($r \geq 0.77$) as well as reasonably small SEE ($SEE \leq 6.8\%$). However, our results showed no further support for selecting the best mathematical model to estimate critical speed. Nonetheless, we suggest coaches choosing a mathematical model beforehand to define intensity domains and maintaining it over the running seasons.

Keywords: running, curve fitting, linear model, hyperbolic model, exponential model, exercise prescription

INTRODUCTION

The prescription of exercise intensity, one of the most important criteria to induce specific adaptations to training (MacInnis and Gibala, 2017), is often based on the percentage of the maximal rate of oxygen uptake ($\dot{V}O_{2max}$) or maximal heart rate (American College of Sports Medicine, 2000; Burgomaster et al., 2007; Roy et al., 2018). However, among individuals, the lactate threshold, the respiratory compensation point (RCP), and critical power (CP)/speed (CS) were located at different percentages of $\dot{V}O_{2max}$ (Fontana et al., 2015), leading to substantial differences between participants in terms of characteristics of metabolic responses and duration of exercise at a common percentage of the maximum. Therefore, using an exercise prescription based on percentages of maximum values does not guarantee control of exercise intensity (DiMenna and Jones, 2009; Lansley et al., 2011). Instead, a model considering exercise intensity domains for exercise prescription has been recommended (Iannetta et al., 2020). Parameters such as oxygen uptake kinetics (Whipp and Mahler, 1980), ventilatory threshold (VT) (Wasserman et al., 1973), maximum lactate steady-state (Iannetta et al., 2018), and CP/CS (Vanhatalo et al., 2007; Constantini et al., 2014; Jones et al., 2019) can be used to define these various intensity domains.

CP/CS allows defining of the boundary between heavy and severe intensity domains (Jones et al., 2019; Galán-Rioja et al., 2020). Therefore, having an accurate estimation of CP/CS is important. This is obtained by fitting the experimental data to a mathematical model, chosen among several possibilities that differ with respect to their mathematical forms and number of parameters (Monod and Scherrer, 1965; Wilkie, 1980; Moritani et al., 1981; Whipp et al., 1982; Morton, 1986, 1990, 1996; Peronnet and Thibault, 1989). The original linear model formulation was proposed by Monod and Scherrer (1965). This model was applied to cycle ergometry and relates the work performed during an exhaustive bout and its duration through two parameters (two-parameter model): CP (Monod and Scherrer, 1965) or threshold of fatigue (Bigland-Ritchie and Woods, 1984) and the sustainable work of exercise above that metabolic rate (W') (Monod and Scherrer, 1965). Power has been related to time by dividing the original formulation by the exercise duration (Poole et al., 1986; Gaesser and Wilson, 1988; Housh et al., 1989) while Gaesser et al. (1990) proposed expressing this exercise duration as function of power, which led to the well-known hyperbolic formulation (Morton and Hodgson, 1996). Another model variant, proposed by Morton (2006), expresses the work performed as function of power, since this work (power multiplied by time to exhaustion) is also a dependent variable. However, this model has, to our knowledge, never been used so far.

A straightforward transposition of CP to running was studied by several researchers (Ettema, 1966; Hughson et al., 1984; Housh et al., 1991, 2001; Sid-Ali et al., 1991; McDermott et al., 1993). The CS and distance that can be run above CS (d') are the running analogs of CP and W' , respectively (Hughson et al., 1984; Housh et al., 1991; Pepper et al., 1992; Hill and Ferguson, 1999; Jones and Vanhatalo, 2017). CS is thought to reflect an inherent characteristic of the aerobic energy supply

system (Hughson et al., 1984; Gaesser and Wilson, 1988; Poole et al., 1988) and is observed to be correlated with $\dot{V}O_{2max}$ (Hughson et al., 1984; Gaesser and Wilson, 1988; Poole et al., 1988), as well as lactate thresholds (Poole et al., 1988) and RCP (Moritani et al., 1981).

Major shortcomings of the two-parameter model are the assumptions 1) of infinite running speed as time to exhaustion approaches zero, and 2) that at the point of fatigue, d' has been completely covered (Gaesser et al., 1995; Morton, 1996). To overcome these limitations, Morton (1996) proposed a three-parameter model including an additional parameter, the maximal instantaneous running speed (s_{max}), and a d' that can be only partly covered for a running speed between CS and s_{max} . Alternatively, Hopkins et al. (1989) proposed a three-parameter exponential model based on CS and s_{max} , but where d' was replaced by an undefined time constant (τ). The authors reported that their three-parameter exponential model gave better fits than the two-parameter model for inclined treadmill running of short duration (<3 min) (Hopkins et al., 1989). These two- or three-parameter models can be formulated as either distance as function of time, time as function of distance, running speed as function of time, time as function of running speed, distance as function of running speed, and running speed as function of distance, which are mathematically equivalent.

To obtain a statistically appropriate estimation of the model parameters, the correct choice of model formulation and regression analysis should be chosen (Patoz et al., 2021). Such choice is based on the data provided by the experiment and the knowledge of the independent and dependent variables. For the treadmill CS test, running speed is the independent variable while time to exhaustion and distance (implicitly, because it is given by running speed multiplied by time to exhaustion) are the dependent variables. To minimize the error of a model formulation expressing the dependent and independent variables on the vertical and horizontal axes, respectively, the least squares (LS) loss function can be used and requires that the dependent variable be observed with additive error while the independent one would have no additive error (Morton and Hodgson, 1996). Statistical theory has shown that errors in the independent variable are of minor importance, making error minimization in the dependent variable sufficient (Morton and Hodgson, 1996). However, due to heteroscedasticity of the dependent variable (McLellan and Skinner, 1985; Poole et al., 1988; Faude et al., 2017), Morton and Hodgson (1996) suggested to use weighted LS (WLS).

Several researchers have compared the estimation of the parameters provided by the three different models (two-parameter, three-parameter, and three-parameter exponential) and some of their different formulations for cycle ergometry (Gaesser et al., 1995; Bull et al., 2000; Bergstrom et al., 2014) and running on a treadmill (Housh et al., 2001). Significant differences were obtained between the different formulations of the two-parameter model (Gaesser et al., 1995; Bull et al., 2000; Housh et al., 2001; Bergstrom et al., 2014). The three models also differed significantly from one another and the three-parameter model gave the lowest estimation of CP (Gaesser et al., 1995; Bull et al., 2000; Bergstrom et al., 2014) and CS

(Housh et al., 2001). However, these studies (Gaesser et al., 1995; Bull et al., 2000; Housh et al., 2001; Bergstrom et al., 2014) did not consider time to exhaustion as the dependent variable, as honestly highlighted by Gaesser et al. (1995). Moreover, these previous studies (Gaesser et al., 1995; Bull et al., 2000; Housh et al., 2001; Bergstrom et al., 2014) are not methodologically exhaustive. Indeed, none of these studies acknowledged heteroscedasticity of the dependent variable.

Hence, the purpose of this study was twofold. First, we compared the estimations of the model parameters obtained by statistically appropriate fitting procedures (the combination of model formulation and regression analysis) applied to the three different models (two-parameter, three-parameter, and three-parameter exponential). We hypothesized that the estimations of CS, d' , and s_{max} would be significantly different between the mathematical models employed, but not between the fitting procedures. We also hypothesized that the three-parameter model would give the lowest estimation of CS, as already observed by Housh et al. (2001) for statistically inappropriate fitting procedures. Second, we determined the correlations between estimated CS and aerobic fitness parameters, i.e., VT, RCP, and $\dot{V}O_{2max}$, as well as the standard error of estimate (SEE) of these relations. We hypothesized that lower quality of the fit [determined by Akaike information criterion (AIC)] would be associated with lower correlations between CS and aerobic fitness parameters and higher SEE.

MATERIALS AND METHODS

Participant Characteristics

Sixteen male runners gave written informed consent to participate in the present experiment (age: 25.6 ± 3.9 years old; height: 1.79 ± 0.05 m; body mass: 69.2 ± 5.3 kg). For study inclusion, participants were required to be in good self-reported general health with no symptoms of cardiovascular disease or major coronary risk factors, no current or recent lower-extremity injury that could prevent them from giving 100% of their capacity during the test or from meeting a certain level of running performance. More specifically, runners were required to have a speed associated with $\dot{V}O_{2max}$ ($s_{\dot{V}O_{2max}}$) greater or equal to 4.44 m/s (16 km/h). The study protocol was approved by the Ethics Committee (CER-VD 2018-01814) and adhered to the latest Declaration of Helsinki of the World Medical Association.

Experimental Procedure

Each participant completed five experimental sessions interspersed by at least 2 days in the laboratory. All participants were advised to avoid strenuous exercise the day before a test but to maintain their usual training program otherwise. During the first session, participants completed a maximal incremental aerobic test on a treadmill (Arsalis T150—FMT-MED, Louvain-la-Neuve, Belgium). This test consisted of a 10-min warm-up at 2.78 m/s followed by an incremental increase in the running speed of 0.28 m/s every 2 min until exhaustion. Throughout the test, participants breathed into a mask connected to a gas analyzer (Quark, Cosmed, Italy). Pulmonary gas exchange

variables [expired minute ventilation ($\dot{V}E$), oxygen uptake ($\dot{V}O_2$), and carbon dioxide output ($\dot{V}CO_2$)] were measured breath-by-breath and subsequently averaged over 10-s intervals throughout the test. Before each test, the O_2 and CO_2 analyzers were calibrated using room air and known concentrations of calibration gas (16.00% O_2 , 5.02% CO_2 , and the remainder N_2), and the turbine was calibrated using a 3-L syringe (Hans Rudolph, Germany).

This test was used, first, to determine the peak speed (PS) of the incremental test of each participant. PS is defined as the running speed of the last fully completed increment ($s_{\dot{V}O_{2max}}$) plus the fraction of time spent in the following uncompleted increment (α) multiplied by the running speed increment ($\Delta s = 0.28$ m/s) (Kuipers et al., 2003): $PS = s_{\dot{V}O_{2max}} + \alpha \Delta s$. Second, the $\dot{V}O_{2max}$ was defined as the highest measured $\dot{V}O_2$ value corresponding to (1) a plateau of $\dot{V}O_2$ with increased running speed ($\Delta \dot{V}O_2$ between the last two increments smaller than 50% of the average $\Delta \dot{V}O_2$ during the submaximal phase of the test) and/or (2) an heart rate greater than 90% of the theoretical maximum heart rate given by 220—age associated with a respiratory quotient greater than 1.1 and a rate of perceived exertion greater than 17. Third, VT and RCP were determined based on gas exchange data and using the method proposed by Wasserman et al. (1973).

The other four tests were performed in a randomized order and consisted of exhaustive runs at a given percentage of the participant's PS (90, 100, 110, or 120%). These tests were as follows: after a 10-min warm-up at 2.78 m/s and a 5-min rest period, the running speed was increased to a given percentage of PS, and the participant had to maintain the pace until exhaustion. The time to exhaustion was collected for each of the four sessions. No information about the timings or running speed was given to any participant, who were strongly encouraged, during any of the five experimental sessions. All participants were familiar with running on a treadmill.

Mathematical Modeling

The estimations of CS, d' , and s_{max} were obtained from two different but mathematically equivalent formulations for the three different models. Gaesser et al. (1990) proposed the two-parameter model formulation given by Eq. 1 (non-linear, time-running speed) while Eq. 2 (non-linear, distance-running speed) represents the formulation proposed by Morton (2006). The three-parameter model formulation proposed by Morton (1996) and the inverse of the three-parameter exponential model formulation proposed by Hopkins et al. (1989) are given by Eqs. 3 and 5 (non-linear, time-running speed), respectively, while Eqs. 4 and 6 (non-linear, distance-running speed) represent their distances as a function of running speed formulations.

$$t(s) = \frac{d'}{s - CS} \quad (1)$$

$$d(s) = s t(s) = \frac{s d'}{s - CS} \quad (2)$$

$$t(s) = \frac{(s - s_{max}) d'}{(s - CS)(CS - s_{max})} \quad (3)$$

$$d(s) = s t(s) = s \frac{(s - s_{\max})d'}{(s - CS)(CS - s_{\max})} \quad (4)$$

$$t(s) = \tau \log \left(\frac{s_{\max} - CS}{s - CS} \right) \quad (5)$$

$$d(s) = s t(s) = s \tau \log \left(\frac{s_{\max} - CS}{s - CS} \right) \quad (6)$$

t , s , and d stand for time, running speed, and distance, respectively. Of note, distance as a function of running speed was simply given by multiplying time as function of running speed by running speed, i.e., $d(s) = s t(s)$.

The three-parameter exponential model does not provide a direct estimation of d' because the distance that can be run above CS is time-dependent in such a model. Indeed, rearranging the two-parameter model formulation proposed by Whipp et al. (1982) and given by Eq. 7 (i.e., the inverse of Eq. 1)

$$s(t) = \frac{d'}{t} + CS \quad (7)$$

leads to $d' = t[s(t) - CS] = d(t) - tCS$. Then, applying this result to the three-parameter exponential model gives an equation where the left-hand side is time-dependent, i.e., $d'(t) = t(s_{\max} - CS)e^{-t/\tau}$. The maximum (d'_{\max}) of this equation appears where its first derivative is equal to zero, which is at $t = \tau$ and is given by $d'_{\max} = \tau(s_{\max} - CS)e^{-1}$. This parameter (d'_{\max}) was used as an estimate of d' for the three-parameter exponential model when comparing the d' provided by the different models.

Data Analysis

Two different fitting procedures were used on the data set obtained for each participant to estimate CS, d' , and s_{\max} . More specifically, $t(s)$ and $d(s)$ using WLS were evaluated. These two fitting procedures are statistically appropriate, i.e., they minimize the error along the axes corresponding to the dependent variables (Vinetti et al., 2020) and should overcome heteroscedasticity Morton and Hodgson (1996). Weights were applied to the corresponding dependent variables, i.e., time to exhaustion in $t(s)$, and distance in $d(s)$. Following Morton and Hodgson (1996), weights were set proportional to the inverse of the variance of the dependent variable, where the variance was itself set proportional to the dependent variable. Noteworthy, the model variants $d(t)$ and $t(d)$ have not been used. The reason being that in these cases, distance and time to exhaustion should be considered as dependent variables. However, the errors of both variables are correlated, i.e., the error of distance is given by the product of speed and the error of time to exhaustion variable, since speed does not carry any error. This is known as endogeneity and, to the best of our knowledge, there exists no regression method that can handle such case (Antonakis et al., 2014). Error minimization was performed iteratively using the Levenberg-Marquardt algorithm (Levenberg, 1944; Marquardt, 1963). After inspecting residual plots, deviations from homoscedasticity were present for the two fitting procedures applied to the three different models, the

three-parameter model with $d(s)$ and the two-parameter model with $t(s)$ showing the least and the most heteroscedasticity, respectively (**Supplementary Figure 1**).

To obtain the $\dot{V}O_2$ values at the CS estimates for each participant, first the CS estimates were converted to the times at which these running speeds occurred during the maximal incremental aerobic test assuming a linear relation between running speed and time [i.e., $s = 2.78 + 0.14t$, leading to $t = (s - 2.78)/0.14$, where t and s stand for time and running speed, respectively]. Then, the $\dot{V}O_2$ values at the CS estimates were simply given by placing these corresponding times into the computed linear regression of $\dot{V}O_2$ as a function of time recorded during the maximal incremental aerobic test. Data analysis was performed using Python (version 3.7.4, Python Software Foundation¹).

Statistical Analysis

Descriptive statistics were expressed as the mean \pm standard deviation. The 90% confidence intervals (CI) of CS, d' and if applicable, s_{\max} , the combined standard error of the estimate (%SEE), i.e., the sum of SEE preliminary transformed to percent units of CS, d' and if applicable, s_{\max} , and the AIC of the fitting procedure were computed to assess the quality of the fit. For the linear regression of $\dot{V}O_2$ as a function of time, its coefficient of determination (R^2) was calculated to examine its accuracy.

After inspecting residual plots, no obvious deviations from homoscedasticity and normality were present. Linear mixed models fitted by restricted maximum likelihood were used to compare CS, d' , and s_{\max} obtained from the three mathematical models (two-parameter if applicable, three-parameter, and three-parameter exponential) and two fitting procedures [$t(s)$ and $d(s)$]. The fixed effects included the mathematical models, fitting procedures, and their interaction. The within-subject nature was controlled for by including random effects for participants. The variance explained by the fixed effects over the total expected variance was given by R^2_{marginal} while $R^2_{\text{conditional}}$ represented the variance explained by the fixed and random effects together over the total variance (Johnson, 2014). Intraclass correlation coefficients (ICC) of the random effects were computed as the ratios of the variance of the random coefficient divided by the sum of itself and the residual variance. On the basis of commonly used thresholds, poor, moderate, good, and excellent ICCs are given by ICC values <0.5 , $0.5-0.75$, $0.75-0.90$, and ≥ 0.90 , respectively (Koo and Li, 2016). Pairwise *post hoc* comparisons of any significant fixed effects were performed using Holm corrections.

Correlations, 90% CI, SEE (in %), and systematic differences of predicted value (Δ , in %) were computed among the three mathematical models and two fitting procedures with regard to CS, d' , and s_{\max} and similarly between CS and aerobic fitness parameters. Data were log transformed as suggested by Hopkins et al. (2009). Correlations were computed using Pearson's correlation coefficients (r). Very high, high, moderate, low, and negligible correlations were given by r values of $0.90-1.00$, $0.70-0.90$, $0.50-0.70$, $0.30-0.50$, and $0.00-0.30$, respectively

¹<http://www.python.org>

(Hinkle et al., 2003). Statistical analysis was performed using Python, Jamovi (version 1.0.8, [Computer Software]²), and R 3.5.0 (The R Foundation for Statistical Computing, Vienna, Austria) with a level of significance set at $P \leq 0.05$.

RESULTS

The variables determined by the incremental test were $s\dot{V}O_{2max}$: 5.05 ± 0.38 m/s, PS: 5.16 ± 0.39 m/s, $\dot{V}O_{2max}$: 63.0 ± 4.9 ml/min/kg, VT: 47.1 ± 3.9 ml/min/kg (74.8 ± 4.1 % $\dot{V}O_{2max}$), and RCP: 56.3 ± 4.8 ml/min/kg (89.3 ± 3.6 % $\dot{V}O_{2max}$). The average R^2 obtained for the linear regression of the $\dot{V}O_2$ as a function of time relationship recorded during the maximal incremental aerobic test was 0.94 ± 0.04 .

The regression analysis for one representative participant and for each of the three mathematical models as well as the two fitting procedures [$t(s)$ and $d(s)$] is presented in **Figure 1**.

Table 1 depicts the time to exhaustion corresponding to the four exhaustive runs performed at 90, 100, 110, and 120% of the participant's PS.

Table 2 depicts CS, d' , and s_{max} , together with their corresponding 90% CI, %SEE, and AIC obtained from the three mathematical models and two fitting procedures.

The linear mixed model with random effects explained almost all variance in the data for CS while a large part of variance in the data was still unexplained for d' and s_{max} even with random effects (**Table 3**). These results were reinforced by the ICC of the random effects, which was excellent for CS but poor and moderate for d' and s_{max} , respectively (**Table 3**).

A significant mathematical model effect was obtained for CS, d' , and s_{max} ($P < 0.001$; **Table 3**). CS was significantly faster for the three-parameter exponential model compared with CS determined by two- ($P < 0.001$) and three-parameter ($P < 0.001$) models and it was significantly faster for the two- than for the three-parameter model ($P < 0.001$; **Table 2**). d' was significantly lower for the two- and three-parameter exponential model than for the three-parameter model ($P < 0.001$; **Table 2**). The three-parameter exponential model had a significant slower estimation of s_{max} than the three-parameter model ($P < 0.001$; **Table 2**).

No significant fitting procedure effect or significant mathematical model x fitting procedure interaction effect were reported for CS, d' , and s_{max} ($P \geq 0.77$; **Table 3**).

On a group level, the average AIC was lower for the three-parameter model for both fitting procedures; however, it was very close to the average AIC for the three-parameter exponential model (**Table 2**). Note that, because the units of the residual sum of squares error (RSS) depend on the fitting procedure itself, the AICs can be compared between models within a given fitting procedure but not between the two fitting procedures. On an individual level, $t(s)$ and $d(s)$ fitting procedures gave the lowest AIC when using the three-parameter model for 12 participants while 4 participants obtained the lowest AIC when using the three-parameter exponential model.

The three-parameter model reported the highest 90% CI as well as the highest %SEE (**Table 2**). However, %SEE can in general not be compared between the two- and three-parameter models because they do not have the same number of parameters to estimate. Nevertheless, the 90% CI of CS and d' in the three-parameter and three-parameter exponential models were higher than in the two-parameter model, even if expressed in percent units. Therefore, the two models with three parameters carried more error on their estimates than the two-parameter model. The 90% CI and %SEE were similar when comparing the two fitting procedures for a given model (**Table 2**).

SEE and Δ between CS obtained from the three mathematical models and two fitting procedures ranged from 0.06 to 3.95% and from -0.10 to 0.03%, respectively, while correlations were very high ($0.93 \leq r \leq 1.00$; 90% CI: [≥ 0.84 , ≤ 1.00]) and were all statistically significant ($P < 0.001$). For d' , SEE and Δ ranged from 0.58 to 20.2% and from -1.89 to 1.37%, respectively, while correlations were high and very high ($0.77 \leq r \leq 1.00$; 90% CI: [≥ 0.52 , ≤ 1.00]) and statistically significant ($P < 0.001$). For s_{max} , SEE and Δ ranged from 0.62 to 9.09% and from -0.06 to 0.14%, respectively, while correlations were moderate to very high ($0.67 \leq r \leq 1.00$; 90% CI: [≥ 0.34 , ≤ 1.00]) and statistically significant ($P \leq 0.004$).

The $\dot{V}O_2$ at the CS estimates expressed as a percentage of $\dot{V}O_{2max}$ as well as the CS expressed as a percentage of $s\dot{V}O_{2max}$ for the three mathematical models and two fitting procedures are given in **Table 4**. The $\dot{V}O_2$ corresponding to the CS estimates were based on linear regression, therefore, the significant differences between $\dot{V}O_2$ values were the same as those for the CV estimates (**Table 2**; Housh et al., 2001).

Correlations, 90% CI, SEE, and Δ between CS and aerobic fitness parameters are given in **Table 5**. Correlations were high and very high, and all statistically significant ($P \leq 0.001$).

DISCUSSION

Conventional statistical approaches demonstrated a significant effect of the mathematical model when estimating CS, d' , and s_{max} , but no significant effect of the fitting procedure. These results validated our first hypothesis that the estimates of CS, d' , and s_{max} would be significantly different between mathematical models employed, but not between fitting procedures. Moreover, the three-parameter model gave the lowest estimation of CS, in accordance with our first hypothesis. Lower SEE and higher correlations between aerobic fitness parameters and CS estimated using a given mathematical model and fitting procedure were not necessarily associated with a lower AIC for these models and procedures, which refuted our second hypothesis.

The linear mixed model showed interindividual differences in CS, d' , and s_{max} , as depicted by the larger $R^2_{conditional}$ than $R^2_{marginal}$ (**Table 3**), but with a higher impact for CS than for d' and s_{max} , as depicted by the excellent ICC of the random effects for CS but poor and moderate ICCs for d' and s_{max} , respectively (**Table 3**). In addition, a large part of the variance was still unexplained for d'

²<https://www.jamovi.org>

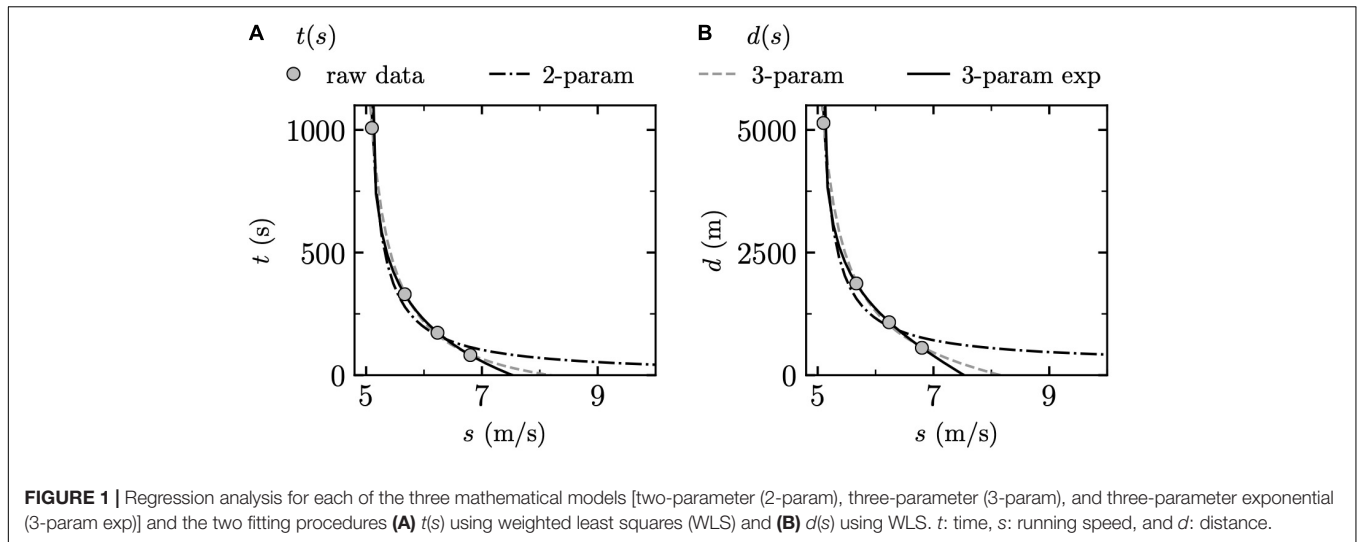


TABLE 1 | Means \pm standard deviations of the time to exhaustion corresponding to the four exhaustive runs performed at 90, 100, 110, and 120% of the participant's peak speed (PS).

Running speed (%PS)	90	100	110	120
Time to exhaustion (min)	14.8 \pm 2.57	5.94 \pm 1.21	2.78 \pm 0.78	1.68 \pm 0.50

TABLE 2 | Mean \pm standard deviation of the critical speed (CS), distance that can be run above CS (d'), and maximal instantaneous running speed (s_{max}), and their corresponding 90% confidence interval (in parenthesis) obtained from the three mathematical models [two-parameter (2-param), three-parameter (3-param), and three-parameter exponential (3-param exp)] and two fitting procedures [$t(s)$ and $d(s)$ using weighted least squares] together with the combined standard error of the estimate (%SEE) and the Akaike information criterion (AIC) assessing the quality of the fit.

Mathematical model	Fitting procedure	CS (m/s)	d' (m)	s_{max} (m/s)	%SEE	AIC
2-param	$t(s)$	4.39 \pm 0.41 (0.10 \pm 0.05)	226.0 \pm 57.0 (66.9 \pm 26.31)	–	9.8 \pm 3.4	32.3 \pm 3.4
	$d(s)$	4.39 \pm 0.40 (0.10 \pm 0.05)	222.3 \pm 56.0 (65.2 \pm 25.1)	–	9.7 \pm 3.4	45.8 \pm 3.4
3-param	$t(s)$	4.12 \pm 0.52 (0.27 \pm 0.28)	556.9 \pm 289.8 (360.6 \pm 386.0)	7.72 \pm 0.85 (1.50 \pm 1.44)	24.8 \pm 15.2	24.1 \pm 5.3
	$d(s)$	4.12 \pm 0.52 (0.27 \pm 0.27)	546.6 \pm 279.1 (352.3 \pm 367.7)	7.76 \pm 0.88 (1.58 \pm 1.59)	25.2 \pm 15.3	37.8 \pm 5.2
3-param exp	$t(s)$	4.55 \pm 0.41 (0.12 \pm 0.15)	219.5 \pm 59.2 (151.6 \pm 112.4)	6.96 \pm 0.43 (0.55 \pm 0.34)	23.9 \pm 15.1	24.4 \pm 9.0
	$d(s)$	4.56 \pm 0.41 (0.12 \pm 0.15)	217.7 \pm 58.0 (150.7 \pm 110.0)	6.98 \pm 0.43 (0.55 \pm 0.35)	24.1 \pm 15.2	38.2 \pm 8.7

TABLE 3 | Percentage of variance explained, fixed effects, and random effects [intraclass correlation coefficient (ICC)] when assessing the effect of the mathematical model and fitting procedure on critical speed (CS), distance that can be run above CS (d'), and maximal instantaneous running speed (s_{max}) using a linear mixed model.

	CS	d'	s_{max}
Variance explained	%	%	%
R^2_{marginal}	14.0	45.7	24.5
$R^2_{\text{conditional}}$	96.0	72.0	75.6
Fixed effects	P	P	P
Mathematical model	<0.001	<0.001	<0.001
Fitting procedure	0.79	0.83	0.77
Mathematical model x fitting procedure interaction	1.00	0.99	0.90
Random effects	–	–	–
ICC for intercept	0.95	0.48	0.68

The variance explained by the fixed effects over the total expected variance was given by R^2_{marginal} while $R^2_{\text{conditional}}$ represented the variance explained by the fixed and random effects together over the total variance. Statistical significances ($P \leq 0.05$) are indicated in bold.

TABLE 4 | Oxygen uptake [$\dot{V}O_2$; expressed as a percentage of maximal rate of oxygen uptake ($\dot{V}O_{2max}$)] at the critical speed (CS) estimates as well as CS [expressed as a percentage of speed associated with $\dot{V}O_{2max}$ ($s_{\dot{V}O_{2max}}$)] for the three mathematical models [two-parameter (2-param), three-parameter (3-param), and three-parameter exponential (3-param exp)] and the two fitting procedures [$t(s)$ and $d(s)$ using weighted least squares].

	2-param		3-param		3-param exp	
	$t(s)$	$d(s)$	$t(s)$	$d(s)$	$t(s)$	$d(s)$
$\dot{V}O_2$ (% $\dot{V}O_{2max}$)	88.2 ± 4.4	88.3 ± 4.4	83.1 ± 6.7	83.2 ± 6.6	91.3 ± 4.1	91.4 ± 4.1
CS (% $s_{\dot{V}O_{2max}}$)	86.7 ± 2.5	86.8 ± 2.5	81.3 ± 6.2	81.4 ± 6.1	90.1 ± 2.9	90.1 ± 2.8

TABLE 5 | Pearson's correlations coefficients (r) together with their corresponding 90% confidence intervals (CI), standard error of estimate (SEE, in %), and systematic differences of predicted value (Δ , in %) between critical speed (CS) obtained from the three mathematical models [two-parameter (2-param), three-parameter (3-param), and three-parameter exponential (3-param exp)] and two fitting procedures [$t(s)$ and $d(s)$ using weighted least squares] and aerobic fitness parameters [ventilatory threshold and respiratory compensation point (VT and RCP), and maximal rate of oxygen uptake ($\dot{V}O_{2max}$)].

		2-param		3-param		3-param exp	
		$t(s)$	$d(s)$	$t(s)$	$d(s)$	$t(s)$	$d(s)$
VT	r	0.85	0.85	0.77	0.77	0.83	0.83
	CI	0.66–0.94	0.66–0.94	0.50–0.90	0.51–0.90	0.63–0.93	0.63–0.93
	P	<0.001	<0.001	<0.001	0.001	<0.001	<0.001
	SEE	4.37	4.36	5.50	5.43	4.70	4.67
	Δ	–0.13	0.05	–1.46	2.40	1.07	–0.93
RCP	r	0.90	0.90	0.77	0.78	0.88	0.88
	CI	0.77–0.96	0.76–0.96	0.52–0.90	0.53–0.91	0.73–0.95	0.73–0.95
	P	<0.001	<0.001	<0.001	0.001	<0.001	<0.001
	SEE	3.90	3.88	5.82	5.73	4.27	4.23
	Δ	0.01	–0.01	1.99	–2.56	–1.95	2.61
$\dot{V}O_{2max}$	r	0.91	0.90	0.85	0.85	0.91	0.91
	CI	0.79–0.96	0.78–0.96	0.66–0.94	0.66–0.94	0.79–0.96	0.80–0.97
	P	<0.001	<0.001	<0.001	<0.001	<0.001	<0.001
	SEE	3.63	6.84	4.49	4.43	3.40	3.38
	Δ	0.27	–0.01	–1.38	–2.56	0.40	0.33

Data were log transformed as suggested by Hopkins et al. (2009). Statistical significance of the correlations ($P \leq 0.05$) are indicated in bold.

and s_{max} ($R^2_{conditional} \leq 72.0\%$; Table 3). Therefore, CS could be well estimated by using the mathematical model and fitting procedure, but this is not the case for d' and s_{max} . Furthermore, the high and very high between-model correlations ($r \geq 0.93$) obtained for CS suggest that the estimation of CS provided by each model qualitatively represents the same, as already pointed out by Gaesser et al. (1995). By contrast, some between-model correlations were high and moderate for d' and s_{max} , respectively ($r \geq 0.67$), suggesting less link between estimations of d' and s_{max} from the different regression analyses. Overall, the regression analyses provided more robust estimates of CS than of d' and s_{max} .

The three-parameter model gave the lowest AIC on a group level as well as for 75% of the participants for both $t(s)$ and $d(s)$ fitting procedures. Nevertheless, the AICs of both three-parameter models were very close to one another (Table 2). The AICs for the two-parameter model were 34% and 21% higher than the three-parameter model ones for $t(s)$ and $d(s)$, respectively. Therefore, the two-parameter model gave the lowest quality of the fit, while the three-parameter model seemed to be the most accurate one for both fitting procedures even though it was only slightly better than the three-parameter exponential

model. These observations contradict previous findings that obtained similar R^2 values between different mathematical models (Gaesser et al., 1995; Bull et al., 2000; Housh et al., 2001; Bergstrom et al., 2014) [except for a two-parameter linear model expressing power as function of 1/time (Gaesser et al., 1995; Bull et al., 2000)]; this might be explained several ways. First, comparing the accuracy of regression analyses for models based on a different number of parameters (e.g., two vs. three parameters) requires an adjusted R^2 to normalize with respect to the number of parameters within the model. However, these studies (Gaesser et al., 1995; Bull et al., 2000; Housh et al., 2001; Bergstrom et al., 2014) did not mention such usage. Second, R^2 was shown to be an unfavorable measure to describe the validity of a non-linear regression (e.g., both model formulations of the three-parameter model) (Spiess and Neumeyer, 2010) and when using weights in the regression analysis (Willett and Singer, 1988). Therefore, one remaining possibility to compare the quality of the fit of different mathematical models is to use RSS or a parameter that depends on it such as AIC. However, the units of RSS (and thus AIC) being dependent on the fitting procedure (i.e., on the choice of model formulation and axes on which the errors are minimized), the AICs of the various fitting procedures

cannot be compared, i.e., AIC of $t(s)$ cannot be compared to the one of $d(s)$.

Another option to compare the quality of the fit of different mathematical models is to use %SEE (Triska et al., 2021). However, as already mentioned, %SEE depends on the number of parameters to estimate and is therefore not optimal to compare two- and three-parameter models. Nevertheless, in our case, the 90% CI of CS and d' in the three-parameter and three-parameter exponential models were higher than in the two-parameter model, even if expressed in percent units. Therefore, the two-parameter model gave the lowest %SEE (9.7%) and SEE for CS (0.7%) and d' (9%), while the three-parameter gave the highest %SEE (25%; CS: 2.2%, d' :17%, and s_{max} : 5.8%), but only 1% higher than the three-parameter exponential model (24%; CS: 0.8%, d' :20.8%, and s_{max} :2.4%). Based on %SEE, the three-parameter model seemed to be the least accurate model, which is in contradiction with the results based on AIC.

CS was thought to reflect an inherent characteristic of the aerobic energy supply system (Hughson et al., 1984; Gaesser and Wilson, 1988; Poole et al., 1988). Such a characteristic is supported by the small SEE and high and very high correlations obtained between CS and aerobic fitness parameters such as VT, RCP, and $\dot{V}O_2max$ ($SEE \leq 6.84$; $r \geq 0.77$; **Table 5**). These results additionally confirm previous observations that showed that CS correlated with $\dot{V}O_2max$ (Hughson et al., 1984; Gaesser and Wilson, 1988; Poole et al., 1988) and RCP (Moritani et al., 1981). However, the three-parameter model reported the highest SEE [if we do not consider SEE for the two-parameter model and $d(s)$] and smallest correlations, which were associated with the largest 90% CI ($4.43 \leq SEE \leq 5.82$; $0.77 \leq r \leq 0.85$; **Table 5**). This is in line with the fact that the three-parameter model reported the highest %SEE (**Table 2**). Nonetheless, SEE and correlations were still small and high, respectively, for this model.

The linear mixed model provided a significant effect of the mathematical model when estimating CS, d' , and s_{max} (**Table 3**). These results accord with those of previous observations that depicted considerable differences in the estimation of parameters among different models (Gaesser et al., 1995; Bull et al., 2000; Housh et al., 2001; Bergstrom et al., 2014). The three-parameter model provided the lowest estimation of CS on a group level (**Table 2**) as well as on an individual level. CS estimated using the three-parameter model were 6% and 9% smaller than when using the two-parameter and three-parameter exponential models, respectively. The two-parameter model was shown to produce overestimated CS (Pepper et al., 1992). The authors observed that the time to exhaustion at a running speed set at CS estimated by the two-parameter model was much smaller than expected. Indeed, participants were able to run only 16 min instead of a theoretically indefinite time. Because CS predicted by the three-parameter exponential model was faster than CS predicted by the two-parameter model (+3%; **Table 2**), we could conclude that the three-parameter exponential model also produced overestimated CS.

The observed between model differences for the CS estimates (up to 0.44 m/s, **Table 2**) are not negligible and would certainly

have an impact when prescribing a training session based on exercise intensity. Therefore, we encourage coaches prescribing exercise based on critical intensity to choose a mathematical model beforehand to estimate CS and maintain it over the running seasons, so that CS is always estimated in the same way. Moreover, even though the estimated CS should be a very good approximation of the critical intensity but not the critical intensity *per se*, we suggest to physiologically verify that the estimated CS represents the upper boundary of sustainable exercise. In addition, coaches should not hesitate to make small adjustments based on the observed performance. Moreover, given the day-to-day variation of human performance and the CI of the estimated CS, i.e., about 5% of its value (**Table 2**), it would be justified to prescribe exercise intensity outside these confidence limits to avoid being in the phase transition between the heavy and severe intensity domains (Anderson et al., 2019).

Jones and Vanhatalo (2017) found that CS occurred at 70–90% of $\dot{V}O_2max$, depending on training status (the higher the training status, the higher the CS in % $\dot{V}O_2max$). In the present study, the $\dot{V}O_2$ at the CS estimates for the three-parameter model were close to the middle of the range defined by Jones and Vanhatalo (2017) (83%; **Table 4**), while the $\dot{V}O_2$ at the CS estimates for the two-parameter and three-parameter exponential models were in the higher end of the range (≥ 88.2 % $\dot{V}O_2max$; **Table 4**). Higher $\dot{V}O_2$ at the CS estimates were already reported by Housh et al. (2001) for the two-parameter and three-parameter exponential models (≥ 94 % $\dot{V}O_2max$) than for the three-parameter model (89 % $\dot{V}O_2max$). These authors even reported $\dot{V}O_2$ at the CS estimates that exceeded $\dot{V}O_2max$ for the exponential model (105 % $\dot{V}O_2max$). In the present study, CS corresponded to 81, 87, and 90 % $s_{\dot{V}O_2max}$ for the three-parameter, two-parameter, and three-parameter exponential models, respectively. Billat et al. (1995) observed that CS corresponded to 86% of $s_{\dot{V}O_2max}$ for runners having 75 ml/min/kg of $\dot{V}O_2max$ and 6.22 m/s of $s_{\dot{V}O_2max}$. These values were higher than those of the participants of this study (+16 and +19%, respectively). Therefore, we could speculate that CS estimated by the three-parameter model (81 % $s_{\dot{V}O_2max}$) is closer to reality than CS estimated by the other two models (≥ 87 % $s_{\dot{V}O_2max}$). Both arguments reinforce the idea that both two-parameter and three-parameter exponential models overestimate CS. In any case, a future study involving exhaustive runs below, at, and above CS whilst assessing oxygen uptake responses to exercise would be needed to quantitatively validate this suggestion.

The estimation of d' using the three-parameter model were roughly 2.5 times larger than those from the other two models. These findings are consistent with those of previous studies (Gaesser et al., 1995; Morton, 1996; Bull et al., 2000; Housh et al., 2001; Bergstrom et al., 2014). Morton (1996) suggested that such a model overcomes physiological assumptions of the two-parameter model such as an infinite power when time approaches zero and that at d' , the muscular energy reserve is empty. Assuming an $s_{\dot{V}O_2max}$ of 6 m/s and a time to exhaustion of ~ 5 min at 100% of $s_{\dot{V}O_2max}$ (Billat et al., 1995), the corresponding total distance covered is 1,800 m. The anaerobic contribution was shown to represent approximately 10% of the total distance

covered, i.e., approximately 200 m (Billat, 2001). Therefore, because Morton (1996) suggested that the three-parameter model allows d' to be only partly covered for a running speed between CS and s_{max} , this statement causes the estimate of d' that is larger in the three-parameter model than in the other two models to not be unrealistically high. This idea is reinforced by an explanation based on anaerobic energy calculation by Gaesser et al. (1995).

Buchheit and Laursen (2013) found that athletes with similar $s\dot{V}O_{2max}$ to those of the present study had a s_{max} ranging from 161 to 183 % $s\dot{V}O_{2max}$. Higher level athletes ($s\dot{V}O_{2max} = 6.36$ m/s) were shown to have a lower relative s_{max} (149 % $s\dot{V}O_{2max}$) (Sandford and Stellingwerff, 2019). Therefore, the estimation of s_{max} using the three-parameter exponential model seemed to be unrealistically too small (~ 136 % $s\dot{V}O_{2max}$) whereas the one obtained using the three-parameter model seemed closer to reality (~ 155 % $s\dot{V}O_{2max}$). Nonetheless, this has to be nuanced by the fact that most of the running trials at 120 %PS gave a time to exhaustion below 2 min, which is below the usual recommendation (Jones and Vanhatalo, 2017) and could have influenced the estimation of the parameters present in the mathematical models. In addition, participants were long distance runners, meaning that they are not accustomed to running at high speeds (i.e., > 100 % $s\dot{V}O_{2max}$) and that they actually did not have a high s_{max} . This assumption is supported by the observations of Sandford and Stellingwerff (2019), who showed that a 400-m elite runner ($s\dot{V}O_{2max} = 6.23$ m/s) had a s_{max} of 158 % $s\dot{V}O_{2max}$ while a 1,500-m elite runner ($s\dot{V}O_{2max} = 6.45$ m/s) had a s_{max} of 141 % $s\dot{V}O_{2max}$.

No significant fitting procedure or mathematical model \times fitting procedure interaction effects were reported for the estimations of CS, d' , and s_{max} (Table 3). Gaesser et al. (1995) proposed that differences between the estimation of parameters among models could come from the designation of the dependent and independent variables, the number of parameters in each model, and the choice of model (e.g., two-parameter, three-parameter, or three-parameter exponential). Moreover, two mathematically equivalent model formulations requiring linear vs. non-linear regressions were shown to provide different estimations of their underlying parameters (Colquhoun, 1971). In this study, we observed that using different but statistically appropriate fitting procedures, i.e., that correctly attribute the dependent and independent variables, applied to a given model did not have an impact on the estimations of CS, d' , and s_{max} , as long as all the model formulations are non-linear or linear.

Heteroscedasticity of the dependent variable was explicitly depicted by Hinckson and Hopkins (2005) when using usual LS fitting procedure. Indeed, these authors demonstrated systematic and non-uniform deviation from their models by showing the residuals as function of predicted values. In this study, the suggestion made by Morton and Hodgson (1996) to overcome heteroscedasticity, i.e., weights proportional to the inverse of the values of the dependent variable, were applied. However, the absolute weighted residuals as function of predicted values for the two fitting procedures applied to the three different models depicted clear deviations from homoscedasticity (Supplementary Figure 1). Therefore, considering weights in the fitting procedure did not overcome the heteroscedasticity problem. Nonetheless, a future study considering different

weighting schemes should be performed in order to observe if a specific weighting scheme, different from the one proposed by Morton and Hodgson (1996), could overcome heteroscedasticity of the dependent variable.

Some limitations to the present study exist and need to be addressed. On the one hand, the participant should complete five experimental sessions interspersed by at least 2 days, which could be slightly unpractical. On the other hand, performing a regression analysis with only four measurement points is already quite few, especially when dealing with heteroscedasticity. Nonetheless, the estimation of CS based on four points is considered as the best practice (Poole et al., 2021). Moreover, there is a well-known large variability in the time to exhaustion during treadmill running at CS (Pepper et al., 1992). Furthermore, due to the proximity between CS and RCP in terms of % $\dot{V}O_{2max}$ (CS: 87.6 % $\dot{V}O_{2max}$; RCP: 89.3 % $\dot{V}O_{2max}$) and the high and very high correlations between them ($r \geq 0.85$), one could wonder the relevance of CS. However, the recent meta-analysis of Galán-Rioja et al. (2020) showed that CS and RCP are not synonymous. Besides, CS can be estimated using personal best times, which does not require the participant to go to the laboratory (Jones et al., 2019). Finally, a recent study demonstrated that using estimations of CS from raw training data can be sufficient to successfully predict marathon performance and provide useful pacing information (Smyth and Muniz-Pumares, 2020).

To conclude, this study demonstrated that CS, d' , and s_{max} estimated from three different mathematical models (two-parameter, three-parameter, and three-parameter exponential model) differed significantly, but that no difference in the estimation of CS, d' , and s_{max} was reported between different statistically appropriate fitting procedures applied to a given model. Weights did not help overcoming heteroscedasticity of the dependent variable. CS estimates from the three different models were correlated with aerobic fitness parameters, i.e., VT, RCP, and $\dot{V}O_{2max}$. Moreover, small SEE was obtained. The three-parameter model gave the lowest AIC on a group level and the smallest CS estimates. However, the three-parameter model reported the highest %SEE and 90% CI. Therefore, our results showed no further support for selecting the best mathematical model to estimate critical speed. Nevertheless, our results showed that statistically appropriate fitting procedures gave the same estimates for a given model. For these reasons, we suggest coaches choosing a mathematical model with appropriate fitting procedure beforehand to define CS and intensity domains and maintaining it over the running seasons. Moreover, our findings suggest that each CS estimation during season should be physiologically verified and training prescription should be done around CS ($\pm 10\%$) for taking into account CI of its estimation and the day-to-day variation of human performance.

DATA AVAILABILITY STATEMENT

The raw data supporting the conclusions of this article will be made available by the authors, without undue reservation.

ETHICS STATEMENT

The studies involving human participants were reviewed and approved by CER-VD 2018-01814. The patients/participants provided their written informed consent to participate in this study.

AUTHOR CONTRIBUTIONS

FB and DM: conceptualization and supervision. FB, DM, and AP: methodology. FB, DM, RS, and NP: investigation. AP and AB: formal analysis. AP: writing—original draft preparation. AP, AB, FB, and DM: writing—review and editing. All authors contributed to the article and approved the submitted version.

REFERENCES

- American College of Sports Medicine (2000). *ACSM's Guidelines for Exercise Testing and Prescription*. Philadelphia, PA: Lippincott Williams & Wilkins.
- Anderson, L. M., Bonanno, D. R., Hart, H. F., and Barton, C. J. (2019). What are the benefits and risks associated with changing foot strike pattern during running? A systematic review and meta-analysis of injury, running economy, and biomechanics. *Sports Med.* 50, 885–917. doi: 10.1007/s40279-019-01238-y
- Antonakis, J., Bendahan, S., Jacquart, P., and Lalive, R. (2014). *Causality and Endogeneity: Problems and Solutions*. New York, NY: Oxford University Press.
- Bergstrom, H. C., Housh, T. J., Zuniga, J. M., Traylor, D. A., Lewis, R. W. Jr., Camic, C. L., et al. (2014). Differences among estimates of critical power and anaerobic work capacity derived from five mathematical models and the three-minute all-out test. *J. Stren. Condit. Res.* 28, 592–600. doi: 10.1519/jsc.0b013e31829b576d
- Bigland-Ritchie, B., and Woods, J. J. (1984). Changes in muscle contractile properties and neural control during human muscular fatigue. *Muscle Nerve* 7, 691–699. doi: 10.1002/mus.880070902
- Billat, L. V. (2001). Interval training for performance: a scientific and empirical practice. special recommendations for middle- and long-distance running. part I: aerobic interval training. *Sports Med.* 31, 13–31. doi: 10.2165/00007256-200131010-00002
- Billat, V., Renoux, J. C., Pinoteau, J., Petit, B., and Koralsztein, J. P. (1995). Times to exhaustion at 90, 100 and 105% of velocity at $\dot{V}O_2$ max (Maximal aerobic speed) and critical speed in elite long distance runners. *Arch. Physiol. Biochem.* 103, 129–135. doi: 10.3109/13813459508996126
- Buchheit, M., and Laursen, P. B. (2013). High-intensity interval training, solutions to the programming puzzle. *Sports Med.* 43, 313–338. doi: 10.1007/s40279-013-0029-x
- Bull, A. J., Housh, T. J., Johnson, G. O., and Perry, S. R. (2000). Effect of mathematical modeling on the estimation of critical power. *Med. Sci. Sports Exerc.* 32, 526–530. doi: 10.1097/00005768-200002000-00040
- Burgomaster, K. A., Cermak, N. M., Phillips, S. M., Benton, C. R., Bonen, A., and Gibala, M. J. (2007). Divergent response of metabolite transport proteins in human skeletal muscle after sprint interval training and detraining. *Am. J. Physiol. Regulatory Integr. Comparat. Physiol.* 292, R1970–R1976.
- Colquhoun, D. (1971). *Lectures on Biostatistics*. Oxford: Clarendon Press.
- Constantini, K., Sabapathy, S., and Cross, T. J. (2014). A single-session testing protocol to determine critical power and W' . *Eur. J. Appl. Physiol.* 114, 1153–1161. doi: 10.1007/s00421-014-2827-8
- DiMenna, F. J., and Jones, A. M. (2009). Linear versus “nonlinear” $\dot{V}O_2$ responses to exercise: reshaping traditional beliefs. *J. Exerc. Sci. Fitness* 7, 67–84. doi: 10.1016/s1728-869x(09)60009-5
- Ettema, J. H. (1966). Limits of human performance and energy-production. *Int. Zeitschrift für Angewandte Physiol. Einschliesslich Arbeitsphysiologie* 22, 45–54. doi: 10.1007/bf00694796

FUNDING

This study was supported by the University of Lausanne (Switzerland).

ACKNOWLEDGMENTS

We warmly thank the participants for their time and cooperation.

SUPPLEMENTARY MATERIAL

The Supplementary Material for this article can be found online at: <https://www.frontiersin.org/articles/10.3389/fphys.2021.613066/full#supplementary-material>

- Faude, O., Hecksteden, A., Hammes, D., Schumacher, F., Besenius, E., Sperlich, B., et al. (2017). Reliability of time-to-exhaustion and selected psycho-physiological variables during constant-load cycling at the maximal lactate steady-state. *Appl. Physiol. Nut. Metabol.* 42, 142–147. doi: 10.1139/apnm-2016-0375
- Fontana, F. Y., Keir, D. A., Bellotti, C., De Roia, G. F., Murias, J. M., and Pogliaghi, S. (2015). Determination of respiratory point compensation in healthy adults: Can non-invasive near-infrared spectroscopy help? *J. Sci. Med. Sport* 18, 590–595. doi: 10.1016/j.jsams.2014.07.016
- Gaesser, G. A., Carnevale, T. J., Garfinkel, A., and Walter, D. O. (1990). Modeling of the power-endurance relationship for high-intensity exercise. *Med. Sci. Sports Exerc.* 22:S16.
- Gaesser, G. A., Carnevale, T. J., Garfinkel, A., Walter, D. O., and Womack, C. J. (1995). Estimation of critical power with nonlinear and linear models. *Med. Sci. Sports Exerc.* 27, 1430–1438.
- Gaesser, G. A., and Wilson, L. A. (1988). Effects of continuous and interval training on the parameters of the power-endurance time relationship for high-intensity exercise. *Int. J. Sports Med.* 9, 417–421. doi: 10.1055/s-2007-1025043
- Galán-Rioja, M. Á., González-Mohino, F., Poole, D. C., and González-Ravé, J. M. (2020). Relative proximity of critical power and metabolic/ventilatory thresholds: systematic review and meta-analysis. *Sports Med.* 50, 1771–1783. doi: 10.1007/s40279-020-01314-8
- Hill, D. W., and Ferguson, C. S. (1999). A physiological description of critical velocity. *Eur. J. Appl. Physiol. Occupational. Physiol.* 79, 290–293. doi: 10.1007/s004210050509
- Hinckson, E. A., and Hopkins, W. G. (2005). Reliability of time to exhaustion analyzed with critical-power and log-log modeling. *Med. Sci. Sports Exerc.* 37, 696–701. doi: 10.1249/01.mss.0000159023.06934.53
- Hinkle, D. E., Wiersma, W., and Jurs, S. G. (2003). *Applied Statistics for the Behavioral Sciences*. Boston: Houghton Mifflin, 109.
- Hopkins, W. G., Edmond, I. M., Hamilton, B. H., Macfarlane, D. J., and Ross, B. H. (1989). Relation between power and endurance for treadmill running of short duration. *Ergonomics* 32, 1565–1571. doi: 10.1080/00140138908966925
- Hopkins, W. G., Marshall, S. W., Batterham, A. M., and Hanin, J. (2009). Progressive statistics for studies in sports medicine and exercise science. *Med. Sci. Sports Exerc.* 41, 3–13. doi: 10.1249/mss.0b013e31818cb278
- Housh, D. J., Housh, T. J., and Bauge, S. M. (1989). The accuracy of the critical power test for predicting time to exhaustion during cycle ergometry. *Ergonomics* 32, 997–1004. doi: 10.1080/00140138908966860
- Housh, T. J., Cramer, J. T., Bull, A. J., Johnson, G. O., and Housh, D. J. (2001). The effect of mathematical modeling on critical velocity. *Eur. J. Appl. Physiol.* 84, 469–475.
- Housh, T. J., Johnson, G. O., Mcdowell, S. L., Housh, D. J., and Pepper, M. (1991). Physiological responses at the fatigue threshold. *Int. J. Sports Med.* 12, 305–308. doi: 10.1055/s-2007-1024686
- Hughson, R. L., Orok, C. J., and Staudt, L. E. (1984). A high velocity treadmill running test to assess endurance running potential. *Int. J. Sports Med.* 5, 23–25. doi: 10.1055/s-2008-1025875

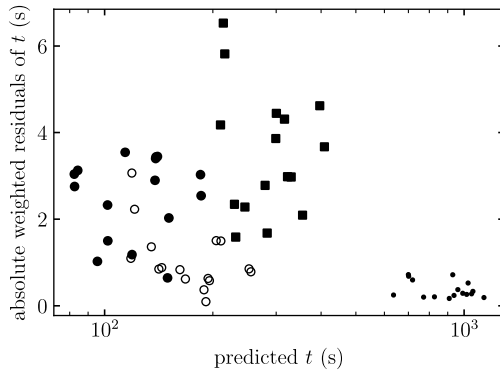
- Iannetta, D., Fontana, F. Y., Maturana, F. M., Inglis, E. C., Pogliaghi, S., Keir, D. A., et al. (2018). An equation to predict the maximal lactate steady state from ramp-incremental exercise test data in cycling. *J. Sci. Med. Sport* 21, 1274–1280. doi: 10.1016/j.jsams.2018.05.004
- Iannetta, D., Inglis, E. C., Mattu, A. T., Fontana, F. Y., Pogliaghi, S., Keir, D. A., et al. (2020). A critical evaluation of current methods for exercise prescription in women and men. *Med. Sci. Sports Exerc.* 52, 466–473. doi: 10.1249/mss.0000000000002147
- Johnson, P. C. D. (2014). Extension of Nakagawa & Schielzeth's R2GLMM to random slopes models. *Methods Ecol. Evol.* 5, 944–946. doi: 10.1111/2041-210x.12225
- Jones, A. M., Burnley, M., Black, M. I., Poole, D. C., and Vanhatalo, A. (2019). The maximal metabolic steady state: redefining the 'gold standard'. *Physiol. Rep.* 7:e14098. doi: 10.14814/phy2.14098
- Jones, A. M., and Vanhatalo, A. (2017). The 'critical power' concept: applications to sports performance with a focus on intermittent high-intensity exercise. *Sports Med.* 47, 65–78. doi: 10.1007/s40279-017-0688-0
- Koo, T. K., and Li, M. Y. (2016). A guideline of selecting and reporting intraclass correlation coefficients for reliability research. *J. Chiropractic Med.* 15, 155–163. doi: 10.1016/j.jcm.2016.02.012
- Kuipers, H., Rietjens, G., Verstappen, F., Schoenmakers, H., and Hofman, G. (2003). Effects of stage duration in incremental running tests on physiological variables. *Int. J. Sports Med.* 24, 486–491. doi: 10.1055/s-2003-42020
- Lansley, K. E., Dimenna, F. J., Bailey, S. J., and Jones, A. M. (2011). A 'new' method to normalise exercise intensity. *Int. J. Sports Med.* 32, 535–541. doi: 10.1055/s-0031-1273754
- Levenberg, K. (1944). A method for the solution of certain non-linear problems in least squares. *Q. Appl. Mathemat.* 2, 164–168. doi: 10.1090/qam/10666
- MacInnis, M. J., and Gibala, M. J. (2017). Physiological adaptations to interval training and the role of exercise intensity. *J. Physiol.* 595, 2915–2930. doi: 10.1113/jp273196
- Marquardt, D. W. (1963). An algorithm for least-squares estimation of nonlinear parameters. *J. Soc. Indust. Appl. Mathemat.* 11, 431–441. doi: 10.1137/0111030
- McDermott, K. S., Forbes, M. R., and Hill, D. W. (1993). Application of the critical power concept to outdoor running. *Med. Sci. Sports Exerc.* 25:S109.
- McLellan, T. M., and Skinner, J. S. (1985). Submaximal endurance performance related to the ventilation thresholds. *Can. J. Appl. Sport Sci. J. Can. des Sci. Appl. Au Sport* 10, 81–87.
- Monod, H., and Scherrer, J. (1965). The work capacity of a synergic muscular group. *Ergonomics* 8, 329–338. doi: 10.1080/00140136508930810
- Moritani, T., Nagata, A., Devries, H. A., and Muro, M. (1981). Critical power as a measure of physical work capacity and anaerobic threshold. *Ergonomics* 24, 339–350. doi: 10.1080/00140138108924856
- Morton, H. R. (1996). A 3-parameter critical power model. *Ergonomics* 39, 611–619. doi: 10.1080/00140139608964484
- Morton, R. H. (1986). A three component model of human bioenergetics. *J. Mathemat. Biol.* 24, 451–466. doi: 10.1007/bf01236892
- Morton, R. H. (1990). Modelling human power and endurance. *J. Mathemat. Biol.* 28, 49–64.
- Morton, R. H. (2006). The critical power and related whole-body bioenergetic models. *Eur. J. Appl. Physiol.* 96, 339–354. doi: 10.1007/s00421-005-0088-2
- Morton, R. H., and Hodgson, D. J. (1996). The relationship between power output and endurance: a brief review. *Eur. J. Appl. Physiol. Occupational Physiol.* 73, 491–502. doi: 10.1007/bf00357670
- Patoz, A., Spicher, R., Pedrani, N., Malatesta, D., and Borrani, F. (2021). Critical speed estimated by statistically appropriate fitting procedures. *Eur. J. Appl. Physiol.* doi: 10.1007/s00421-021-04675-8
- Pepper, M. L., Housh, T. J., and Johnson, G. O. (1992). The accuracy of the critical velocity test for predicting time to exhaustion during treadmill running. *Int. J. Sports Med.* 13, 121–124. doi: 10.1055/s-2007-1021242
- Peronnet, F., and Thibault, G. (1989). Mathematical analysis of running performance and world running records. *J. Appl. Physiol.* 67, 453–465. doi: 10.1152/jappl.1989.67.1.453
- Poole, D. C., Rossiter, H. B., Brooks, G. A., and Gladden, L. B. (2021). The anaerobic threshold: 50+ years of controversy. *J. Physiol.* 599, 737–767. doi: 10.1113/jp279963
- Poole, D. C., Ward, S. A., Gardner, G. W., and Whipp, B. J. (1988). Metabolic and respiratory profile of the upper limit for prolonged exercise in man. *Ergonomics* 31, 1265–1279. doi: 10.1080/00140138808966766
- Poole, D. C., Ward, S. A., and Ward, B. J. (1986). Effects of training on the metabolic and respiratory profile of high-intensity exercise. *Eur. J. Appl. Physiol. Occupat. Physiol.* 29:161.
- Roy, M., Williams, S. M., Brown, R. C., Meredith-Jones, K. A., Osborne, H., Jospe, M., et al. (2018). High-intensity interval training in the real world: outcomes from a 12-month intervention in overweight adults. *Med. Sci. Sports Exerc.* 50, 1818–1826. doi: 10.1249/mss.0000000000001642
- Sandford, G. N., and Stellingwerff, T. (2019). 'Question Your Categories': the misunderstood complexity of middle-distance running profiles with implications for research methods and application. *Front. Sports Active Living* 1:28. doi: 10.3389/fspor.2019.00028
- Sid-Ali, B., Vandewalle, H., Chair, K., Moreaux, A., and Monod, H. (1991). Lactate steady state velocity and distance-exhaustion time relationship in running. *Arch. Int. de Physiol. de Biochimie et de Biophysique* 99, 297–301. doi: 10.3109/13813459109146940
- Smyth, B., and Muniz-Pumares, D. (2020). Calculation of critical speed from raw training data in recreational marathon runners. *Med. Sci. Sports Exerc.* 52, 2637–2645. doi: 10.1249/mss.0000000000002412
- Spieß, A.-N., and Neumeyer, N. (2010). An evaluation of R2 as an inadequate measure for nonlinear models in pharmacological and biochemical research: a Monte Carlo approach. *BMC Pharmacology* 10:6.
- Triska, C., Hopker, J., Wessner, B., Reif, A., Tschan, H., and Karsten, B. (2021). A 30-min rest protocol does not affect W'. *Crit. Power Syst. Res. Med. Sci. Sports Exerc.* 53, 404–412. doi: 10.1249/mss.0000000000002477
- Vanhatalo, A., Doust, J. H., and Burnley, M. (2007). Determination of critical power using a 3-min all-out cycling test. *Med. Sci. Sports Exerc.* 39, 548–555. doi: 10.1249/mss.0b013e31802dd3e6
- Vinetti, G., Taboni, A., and Ferretti, G. (2020). A regression method for the power-duration relationship when both variables are subject to error. *Eur. J. Appl. Physiol.* 120, 765–770. doi: 10.1007/s00421-020-04314-8
- Wasserman, K., Whipp, B. J., Koyle, S. N., and Beaver, W. L. (1973). Anaerobic threshold and respiratory gas exchange during exercise. *J. Appl. Physiol.* 35, 236–243. doi: 10.1152/jappl.1973.35.2.236
- Whipp, B., Huntsman, D., Storer, T., Lamarra, N., and Wasserman, K. (1982). A constant which determines the duration of tolerance to high-intensity work. *Federat. Proc.* 41:1591.
- Whipp, B. J., and Mahler, M. (1980). *Dynamics of Pulmonary Gas Exchange During Exercise. in Pulmonary Gas Exchange.* New York, NY: Academic Press.
- Wilkie, D. R. (1980). *Equations Describing Power input by Humans as a Function of Duration of Exercise. in Exercise Bioenergetics and Gas Exchange.* Amsterdam: Elsevier.
- Willet, J. B., and Singer, J. D. (1988). Another cautionary note about R²: its use in weighted least-squares regression analysis. *Am. Statist.* 42, 236–238. doi: 10.2307/2685031

Conflict of Interest: The authors declare that the research was conducted in the absence of any commercial or financial relationships that could be construed as a potential conflict of interest.

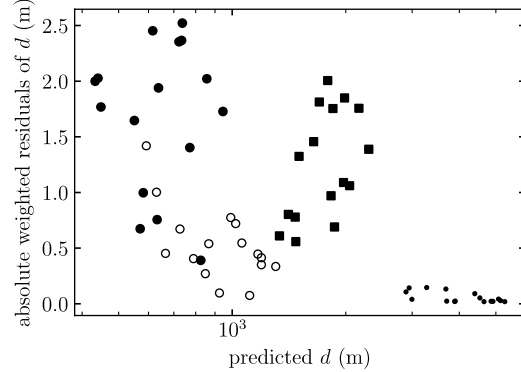
Copyright © 2021 Patoz, Pedrani, Spicher, Berchtold, Borrani and Malatesta. This is an open-access article distributed under the terms of the Creative Commons Attribution License (CC BY). The use, distribution or reproduction in other forums is permitted, provided the original author(s) and the copyright owner(s) are credited and that the original publication in this journal is cited, in accordance with accepted academic practice. No use, distribution or reproduction is permitted which does not comply with these terms.

Supplementary Material

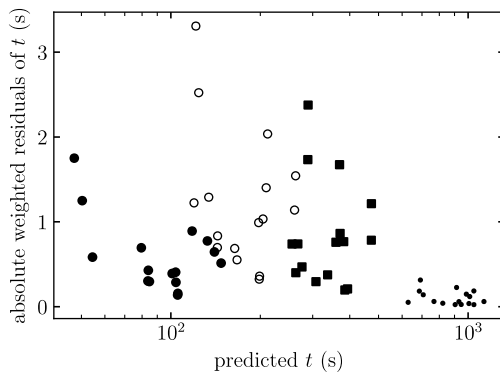
A) $t(s)$ and two-parameter model



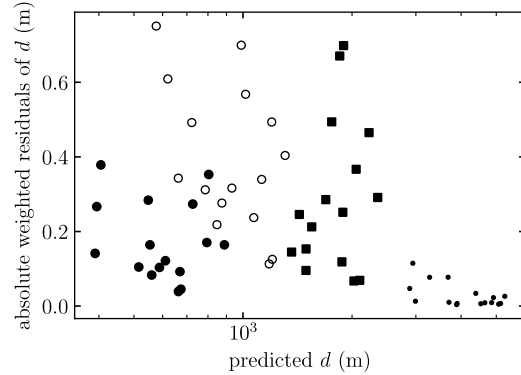
B) $d(s)$ and two-parameter model



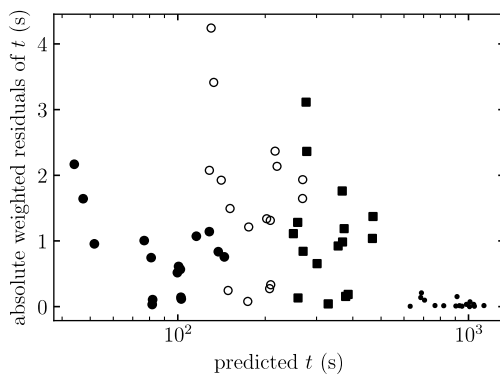
C) $t(s)$ and three-parameter model



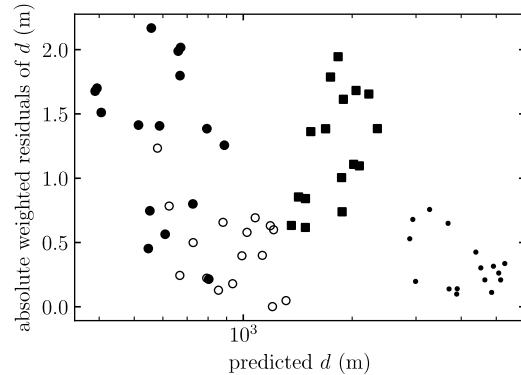
D) $d(s)$ and three-parameter model



E) $t(s)$ and three-parameter exponential model



F) $d(s)$ and three-parameter exponential model



Supplementary Figure 1. Residuals as function of predicted values for (A) $t(s)$ and two-parameter model, (B) $d(s)$ and two-parameter model, (C) $t(s)$ and three-parameter model, (D) $d(s)$ and three-parameter model, (E) $t(s)$ and three-parameter exponential model, and (F) $d(s)$ and three-parameter exponential model. The fitting was performed using weighted least square regression. The four symbols represent the set of four exhaustive runs of each runner: 90% (\circ), 100% (\blacksquare), 110% (\odot), and 120% (\bullet) peak speed of the incremental test.

9.3 The oxygen uptake at critical speed and power in running: perspectives and practical applications

Aurélien Patoz^{1,2,*}, Thomas Blokker¹, Nicola Pedrani¹, Romain Spicher¹, Fabio Borrani^{1,†}, Davide Malatesta^{1,†}

¹ Institute of Sport Sciences, University of Lausanne, Lausanne, Switzerland

² Research and Development Department, Volodalen Swiss Sport Lab, Aigle, Switzerland

† These authors contributed equally to this work

* Corresponding author

Published in **International Journal of Sports Physiology and Performance**

DOI: 10.1123/ijsp.2021-0207

Oxygen Uptake at Critical Speed and Power in Running: Perspectives and Practical Applications

Aurélien Patoz, Thomas Blokker, Nicola Pedrani, Romain Spicher, Fabio Borrani, and Davide Malatesta

Purpose: Intensity domains are recommended when prescribing exercise, and critical power/speed (CP/CS) was designated the “gold standard” when determining maximal metabolic steady state. CS is the running analog of CP for cycle ergometry. However, a CP for running could be useful for controlling intensity when training in any type of condition. Therefore, this study aimed to estimate external, internal, and total CP (CP_{ext} , CP_{int} , and CP_{tot}), obtained based on running power calculations, and verified whether they occurred at the same percentage of peak oxygen uptake as the usual CS. Furthermore, this study examined whether selecting strides at the start, half, or end of the exhaustive runs to calculate running power influenced the estimation of the 3 CPs. **Methods:** Thirteen male runners performed a maximal incremental aerobic test and 4 exhaustive runs (90%, 100%, 110%, 120% peak speed) on a treadmill. The estimations of CS and CPs were obtained using a 3-parameter mathematical model fitted using weighted least square. **Results:** CS was estimated at 4.3 m/s while the estimates of CP_{ext} , CP_{int} , and CP_{tot} were 5.2, 2.6, and 7.8 W/kg, respectively. The corresponding $\dot{V}O_2$ for CS was 82.5 percentage of peak oxygen uptake and 81.3, 79.7, and 80.6 percentage of peak oxygen uptake for CP_{ext} , CP_{int} , and CP_{tot} , respectively. No systematic bias was reported when comparing CS and CP_{ext} , as well as the 3 different CPs, whereas systematic biases of 2.8% and 1.8% were obtained for the comparison among CS and CP_{int} and CP_{tot} , respectively. Nonetheless, the $\dot{V}O_2$ for CS and CPs were not statistically different ($P = .09$). Besides, no effect of the time stride selection for CPs as well as their resulting $\dot{V}O_2$ was obtained ($P \geq .44$). **Conclusions:** The systematic biases among $\dot{V}O_2$ at CS and CP_{int} and CP_{tot} were not clinically relevant. Therefore, CS and CPs closely represent the same fatigue threshold in running. The knowledge of CP in running might prove to be useful for both athletes and coaches, especially when combined with instantaneous running power. Indeed, this combination might help athletes controlling their targeted training intensity and coaches prescribing a training session in any type of condition.

Keywords: hyperbolic model, mechanical work, intensity domains, fatigue, critical intensity

The importance of exercise intensity in training adaptations is well established.¹ The intensity is often prescribed based on the percentage of maximal oxygen uptake ($\dot{V}O_{2max}$) or maximal heart rate.¹⁻³ However, due to a large intersubject variability, the recommendation of exercise intensity based on these parameters has been criticized by several authors.⁴⁻⁶ Indeed, inequivalent metabolic responses were obtained for the same given percentage. Instead, exercise intensity domains have been recommended⁷ and shown to trigger targeted adaptations.⁸ Among several possibilities,⁹⁻¹² critical power/speed (CP/CS)¹¹⁻¹⁴ can be used, which is described as the highest power/speed output at which metabolic homeostasis is achieved,¹⁵ and may be considered the most important fatigue threshold in exercise physiology.¹⁶

The CP/CS is considered a better individualization method for training, provides a useful insight in the best possible performance for a given work/distance and power/speed for athletes,¹⁷ and permits the separation of heavy from severe intensity domains.^{12,15} For this reason, the calculation of CP/CS was designated the “gold standard” when determining maximal metabolic steady state.¹² CP/CS is usually obtained by the typical CP/CS test, that is, several exhaustive cycling/running tests between 90% and 130% $\dot{V}O_{2max}$.¹⁸

The CS is considered as the running analog of CP for cycle ergometry.¹⁸ However, speed could become a nonrelevant metric for separating between intensity domains, for example, when training on a variable terrain with uphill, flat, and downhill parts, or in a very windy condition, where air resistance starts playing an important role. In these cases, controlling running power sounds more suitable. Such metrics are available from several commercial power meters (eg, Runscribe [Scribe Lab Inc, Half Moon Bay, CA], Stryd [Stryd Inc Boulder, CO], or Myotest [Myotest SA, Sion, Switzerland]), which are based on inertial measurement units.¹⁹ Nonetheless, training that targets a specific power-based intensity domain requires an estimation of a running CP. Fortunately, performing the CP/CS test on an instrumented treadmill provides the measure of ground reaction forces, which allow calculating positive external work (W_{ext}) and thus external power (P_{ext}).²⁰ Besides, internal power (P_{int}) can be derived from the equation proposed by Nardello et al²¹ and summing these 2 leads to the total power (P_{tot}). Each of these 3 different powers could be used to estimate a corresponding running CP: CP_{ext} , CP_{int} , and CP_{tot} . These calculations had, to the best of our knowledge, never been investigated so far, therefore constituting the first aim of this study. Moreover, this study verified whether CPs and CS were at the same physiological state, for example, the same percentage of peak $\dot{V}O_2$ ($\% \dot{V}O_{2peak}$). As it sounds mechanically logical, we hypothesized that (1) each CP and CS would occur at the same $\% \dot{V}O_{2peak}$, that is, no systematic bias would be reported between $\dot{V}O_2$ ($\% \dot{V}O_{2peak}$) at CS and at each of the 3 different CPs. Moreover, this would also be true for the different pairs of CPs

The authors are with the Inst of Sport Sciences, University of Lausanne, Lausanne, Switzerland. Patoz is also with the Research and Development Dept, Volodalen Swiss Sport Lab, Aigle, Switzerland. Patoz (aurelien.patoz@unil.ch) is corresponding author.

because $\dot{V}O_2$ at CP represents a specific metabolic rate (ie, specific parameter of aerobic function) achieved at different combinations of P_{ext} and P_{int} outputs as previously reported in cycling at different pedaling frequency.²² Therefore, we hypothesized that (2) no systematic bias would be reported among $\dot{V}O_2$ at the 3 different CPs.²³

Although CP/CS technically ought to be a defined precise value, research has established that determining that value may not be as accurate as theoretical beliefs.^{23–27} More specifically, a day-to-day intrasubject variability of up to 5% to 6% when defining CP/CS was highlighted.²³ In addition, a decrease of CP was obtained when it was assessed using a 3-minute all-out test (up to 10%) on a cycle ergometer following a prolonged (120 min) submaximal exercise.²⁵ Besides, a decrease in the internal work (W_{int}), due to a decrease of both stride frequency and contact time, was observed close to the end of an exhaustive run at a speed corresponding to 95% $\dot{V}O_{2max}$.²⁴ Similarly, Candau et al²⁶ observed a slight decrease of the step frequency at the end of an exhaustive treadmill run performed at a speed corresponding to the participants' personal record over 3000 m, thus supporting the idea of a decrease in W_{int} . On the contrary, Avogadro et al²⁷ obtained no difference in W_{int} at the third and last minute of an exhaustive run at a speed corresponding to 90% $\dot{V}O_{2max}$. As for W_{ext} , no change during the exhaustive run was reported by Borrani et al²⁴ and by Avogadro et al,²⁷ while Candau et al²⁶ observed its increase at the end of the run. Therefore, these results depict conflicting evidence in the scientific literature about the changes in W_{ext} and W_{int} , and thus in total work (W_{tot}), through the time course of an exhaustive run. Moreover, it might be that a different exercise intensity, that is, a supramaximal intensity, is also affecting the changes in W_{ext} , W_{int} , and W_{tot} through the exhaustive run. Altogether, this could ultimately lead to different estimations of CP_{int} , CP_{ext} , and CP_{tot} when calculated using strides selected at different time points of the exhaustive run. Hence, the second aim of this study was to examine whether selecting strides at the start, half, and end of the exhaustive runs influenced the estimation of the 3 different CPs. We hypothesized that (3) time stride selection would influence the estimation of the 3 different CPs.

Methods

Subjects

Thirteen male runners gave written informed consent to participate in the present experiment (age 25.7 [4.4] y; height 179 [5] cm; body mass 68 [5] kg). For study inclusion, participants were required to be in good self-reported general health with no symptoms of cardiovascular disease or major coronary risk factors, no current or recent lower-extremity injury that could prevent them from giving 100% of their capacity during the test, and to meet a certain level of running performance. More specifically, runners were required to have a speed associated with $\dot{V}O_{2max}$ greater or equal to 4.44 m/s (16 km/h). The study protocol was approved by the *Commission cantonale d'éthique de la recherche sur l'être humain* (CER-VD 2018-01814) and adhered to the latest Declaration of Helsinki of the World Medical Association.

Design

Each participant completed 5 experimental sessions interspersed by at least 2 days in the laboratory. All participants were advised to avoid strenuous exercise the day before a test but to maintain their usual training program otherwise. During the first session,

participants completed a maximal incremental aerobic test on an instrumented treadmill (Arsalis T150—FMT-MED; Arsalis, Louvain-la-Neuve, Belgium). This test consisted of a 10-minute warm-up at 2.78 m/s followed by an incremental increase in the running speed of 0.28 m/s every 2 minutes until exhaustion. Throughout the test, participants breathed into a mask connected to a gas analyzer (Quark; COSMED, Rome, Italy). Pulmonary gas exchange variables (expired minute ventilation, $\dot{V}O_2$, and carbon dioxide output) were measured breath-by-breath and subsequently averaged over 10-second intervals throughout the test. Before each test, the O_2 and CO_2 analyzers were calibrated using room air and known concentrations of calibration gas (16.00% O_2 , 5.02% CO_2 , and balanced N_2), and the turbine was calibrated using a 3-L syringe (Hans Rudolph, Shawnee, KS).

This test was used, first, to determine the peak speed (PS) of the maximal incremental aerobic test of each participant. PS is defined as the running speed of the last fully completed increment ($s_{last-inc}$) plus the fraction of time spent in the following uncompleted increment (α) multiplied by the running speed increment ($\Delta s = 0.28$ m/s)²⁸: $PS = s_{last-inc} + \alpha \Delta s$. Second, the $\dot{V}O_{2peak}$ was defined as the highest measured $\dot{V}O_2$.

The other 4 tests were performed in a randomized order and consisted of exhaustive runs at a given percentage of the participant's PS (90%, 100%, 110%, and 120%). These tests were as follows: after a 10-minute warm-up at 2.78 m/s and a 5-minute rest period, the running speed was increased to a given percentage of PS, and the participant had to maintain the pace until exhaustion. The time to exhaustion was collected for each of the 4 sessions. No information about the timings or running speed was given to any of the participants, who were strongly encouraged, during any of the 5 experimental sessions. All participants were familiar with running on a treadmill.

Ground reaction forces (1000 Hz) were collected using the force plate embedded into the treadmill during the last 30 seconds of each minute passed in each of the 4 exhaustive runs, as well as in the maximal incremental aerobic test. Forces were subsequently low-pass filtered at 20 Hz using a fifth-order Butterworth filter. From these data, 10 successive strides were selected and chosen to be at the first (start), middle (half), and last (end) minute of each exhaustive run and at every 2 minutes (corresponding to the timing of the speed increment) of the maximal incremental aerobic test. This allowed assessing running biomechanics. More specifically, W_{ext} , that is, the sum of positive potential and kinetic works,²⁰ W_{int} ,²¹ and W_{tot} were computed (in joule per kilogram per meter) using the 3-D force plate software (Arsalis), which further facilitated obtaining P_{ext} , P_{int} , and P_{tot} (ie, by multiplying work with running speed).

Methodology

The estimations of CPs and CS were obtained from the 3-parameter model formulation proposed by Morton,²⁹ that is, by expressing power (P_{ext} , P_{int} , and P_{tot})/speed as function of time:

$$P(t) = CP + \frac{W'}{t + \frac{W'}{P_{max} - CS}},$$

$$s(t) = CS + \frac{d'}{t + \frac{d'}{s_{max} - CS}}, \quad (\text{Equation 1})$$

where P_{max}/s_{max} are the maximal instantaneous power/running speed. However, time being the dependent variable, error minimization was performed on this variable, that is, on the x -axis,³⁰ using

weighted least square (iteratively using Levenberg–Marquardt algorithm)^{31,32} with weights proportional to the inverse of the time to exhaustion, as suggested by Morton and Hodgson.¹⁸

To obtain the $\dot{V}O_2$ at the CS estimates for each participant, first the $\dot{V}O_2$ recorded during the maximal incremental aerobic test was averaged during the last 30 seconds of each 2-minute increment. Then, a linear relation between these $\dot{V}O_2$'s and corresponding running speeds was constructed. Finally, the $\dot{V}O_2$ at the CS estimates was simply given by placing these CSs on the previously computed linear regressions. Similarly, to obtain the $\dot{V}O_2$ at the CP estimates for each participant, a linear regression of $\dot{V}O_2$ as function of power (both obtained during the maximal incremental aerobic test) was computed. Then, the $\dot{V}O_2$ at the CP estimates were given by inserting these CPs into the previously mentioned linear regressions. Data analysis was performed using Python (version 3.7.4; Python Software Foundation. available at <http://www.python.org>).

Statistical Analysis

All data are presented as mean (SD). Comparison among the $\dot{V}O_2$ at CS and CPs calculated using strides selected at the start of the exhaustive runs and between pairs of CPs were performed using a Bland–Altman analysis. Corresponding 95% confidence intervals were calculated. Besides, after having inspected residual plots and having observed no obvious deviations from homoscedasticity and normality, these $\dot{V}O_2$'s were compared using 1-way repeated-measures analysis of variance (RM-ANOVA) with Mauchly correction for sphericity and employing Holm corrections for pairwise post hoc comparisons. Then, 1-way RM-ANOVA were used to investigate the effect of the time stride selection (start, half, and end) on the estimation of CP_{ext} , CP_{int} , and CP_{tot} , and their corresponding $\dot{V}O_2$. Finally, the effect of the time stride selection and percentage of PS (%PS) on the calculation of P_{ext} , P_{int} , and P_{tot} were investigated using 2-way ([start, half, end time stride selection] \times [90%PS, 100%PS, 110%PS, 120%PS]) RM-ANOVA. Statistical analysis was performed using Jamovi (version 1.6.18; [computer software], retrieved from <https://www.jamovi.org>) with a level of significance set at $P \leq .05$.

Results

The variables determined by the maximal incremental aerobic test were $\dot{V}O_{2peak}$: 64.2 (4.2) mL/min/kg, $S_{last-inc}$: 5.2 (0.3) m/s, and PS: 5.3 (0.3) m/s. The average R^2 obtained for the linear regression of the $\dot{V}O_2$ as a function of time relationship recorded during the maximal incremental aerobic test was 0.98 (0.03), while those for the linear regressions of P_{ext} , P_{int} , and P_{tot} as function of $\dot{V}O_2$ were 0.97 (0.04), 0.95 (0.05), and 0.97 (0.04), respectively.

The regression analyses for one representative participant and for the 3 powers as function of time, speed as function of time, $\dot{V}O_2$ as function of time of the maximal incremental aerobic test, and powers as function $\dot{V}O_2$ recorded during the maximal incremental aerobic test are presented in Figure 1, together with the $\dot{V}O_2$ corresponding to the 3 CPs as well as CS.

Bland–Altman plots comparing the $\dot{V}O_2$ (% $\dot{V}O_{2peak}$) at CS with the one at the 3 CPs calculated using strides selected at the start of the exhaustive runs and between pairs of CPs are depicted in Figures 2 and 3, respectively.

No systematic bias (the zero line lies between the 95% confidence interval) was reported when comparing CS and CP_{ext} , that is, 1.1% (–1.0% to 3.3%), whereas small systematic biases of

2.8% (95% CI, 1.2% to 4.3%) and 1.8% (0.6% to 3.0%) were obtained for the comparison among CS and CP_{int} and CP_{tot} , respectively. No significant systematic biases were reported when comparing the different CPs, that is, CP_{ext} versus CP_{int} : 1.6% (–1.1% to 4.3%); CP_{tot} versus CP_{ext} : –0.7% (–2.4% to 0.9%); and CP_{tot} versus CP_{int} : 0.9% (–0.2% to 2.0%). The 1-way RM-ANOVA reported no significant difference among the $\dot{V}O_2$ for CS and CPs at the start ($P = .09$; Table 1).

The CS and CPs estimated using strides recorded at the start, half, and end of the exhaustive runs as well as their corresponding $\dot{V}O_2$ (% $\dot{V}O_{2peak}$) are given in Table 1. There was no main effect of the time stride selection when estimating the 3 CPs as well as for their resulting $\dot{V}O_2$ ($P \geq .44$).

Table 2 depicts the time to exhaustion corresponding to the 4 exhaustive runs performed at 90%, 100%, 110%, and 120% of the participant's PS as well as P_{ext} , P_{int} , and P_{tot} computed at the start, half, and end of the exhaustive runs. There was no significant main effect of the time stride selection on the calculation of the 3 powers ($P \geq .11$), while there was a significant main effect of %PS ($P < .001$), with each of the 3 powers being statistically higher at a higher %PS than at previous one, as reported by post hoc tests ($P < .001$). A significant interaction effect was obtained only for P_{tot} ($P = .03$), leading to a statistically higher P_{tot} at the end than at the start ($P = .03$) and half ($P = .05$) for 110%PS as well as a statistically higher P_{tot} for all comparisons between a higher %PS and a lower one ($P < .001$; 54 comparisons).

Discussion

Conventional statistical approaches demonstrated no systematic bias between the $\dot{V}O_2$ at CS and CP_{ext} , whereas systematic biases were obtained among the $\dot{V}O_2$ at CS and at CP_{int} and CP_{tot} , which partly refuted the first hypothesis. In accordance with the second hypothesis, no systematic biases were reported among the $\dot{V}O_2$ at the 3 different CPs. Besides, the 4 $\dot{V}O_2$'s (at CS, CP_{ext} , CP_{int} , and CP_{tot}) were not statistically different. In addition, this study observed no effect of the time stride selection when estimating CPs, their resulting $\dot{V}O_2$, as well as the underlying powers used for the CPs calculations, which refuted the third hypothesis.

On the one hand, the $\dot{V}O_2$ at CS and CPs were not statistically different. Moreover, no systematic bias was reported between the $\dot{V}O_2$ at CS and CP_{ext} . However, systematic biases were obtained among the $\dot{V}O_2$ at CS and CP_{int} and CP_{tot} (Table 1 and Figure 2). Nonetheless, these differences were reasonably small, that is, smaller than 3%, and thus not clinically relevant. Furthermore, these differences might be explained by the accuracy of the linear regressions used to estimate the relation between $\dot{V}O_2$ and running speed as well as between $\dot{V}O_2$ and each of the 3 different powers. In fact, even though the R^2 were quite high ($\geq .95$ [.05]), they were not perfect and could have led to these small discrepancies. These differences might also be explained by the mathematical model employed to estimate CS and CPs (Equation 1). Indeed, these estimations were based on a model simplifying a more complex system, hence necessarily introducing some errors. In addition, the highest difference was obtained between the $\dot{V}O_2$ at CS and CP_{int} , which might be explained by the fact that P_{int} was calculated using a model equation²¹ and not using the motion of the body segments relative to the center of mass, further introducing some errors. Therefore, these results suggest that CS and CPs closely represent the same fatigue threshold in running. Nonetheless, the message of Jones et al,³³ which states that CS and CP should not be grouped together under a nebulous “critical intensity” term but that the

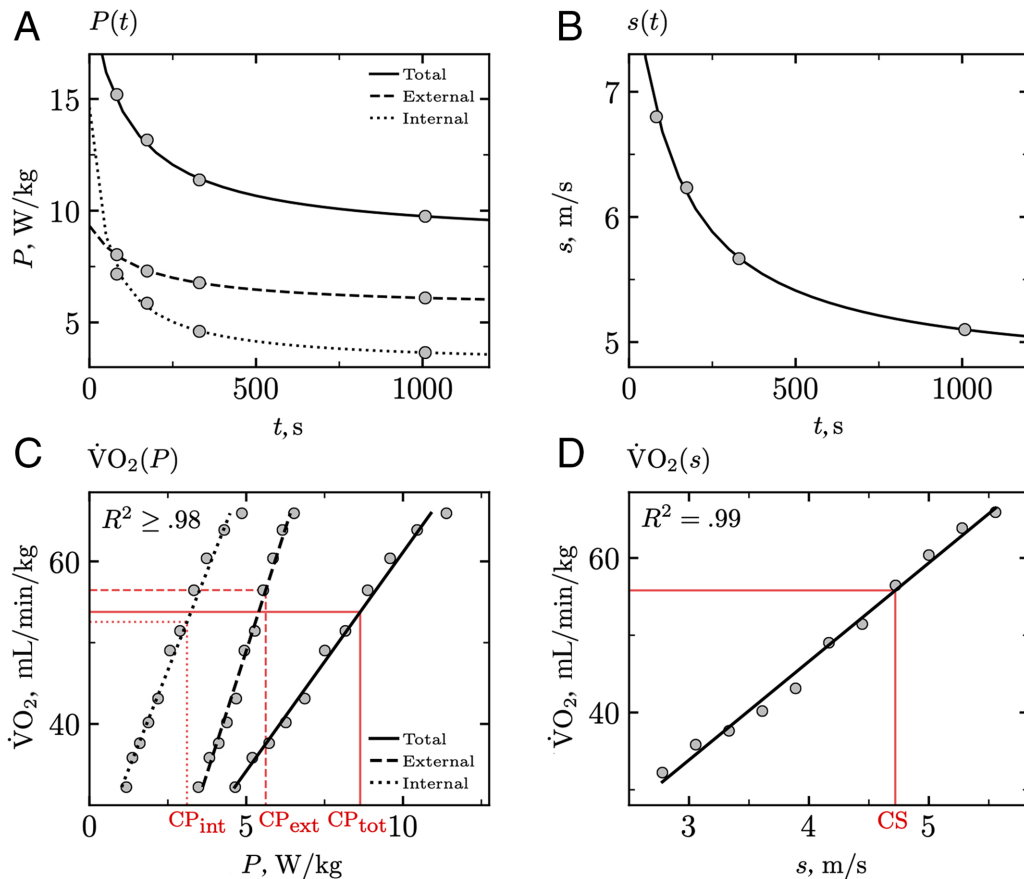


Figure 1 — Regression analyses of 1 representative participant for (A) the 3 different P_{ext} , P_{int} , and P_{tot} as function of t obtained using powers calculated using strides selected at the start of the time trials and corresponding times to exhaustion (3-parameter model); (B) s as function of time obtained using fixed speeds (90%PS, 100%PS, 110%PS, and 120%PS) and corresponding times to exhaustion (3-parameter model); (C) $\dot{V}O_2$ averaged during the last 30 seconds of each 2-minute increment of the maximal incremental aerobic test as function of corresponding running speed (linear regression); and (D) $\dot{V}O_2$ averaged during the last 30 seconds of each 2-minute increment of the maximal incremental aerobic test as function of corresponding powers calculated using strides selected at every 2-minutes of the maximal incremental aerobic test (linear regression). In addition, $\dot{V}O_2$ corresponding to internal, external, and total critical powers (CP_{int} , CP_{ext} , and CP_{tot}) as well as CS are depicted in (C) and (D), respectively. CP indicates critical power; CP_{ext} , external CP; CP_{int} , internal CP; CP_{tot} , total CP; CS, critical speed; P , power, P_{ext} , external P ; P_{int} , internal P ; PS, peak speed; P_{tot} , total P ; s , speed; t , time; $\dot{V}O_2$, oxygen uptake.

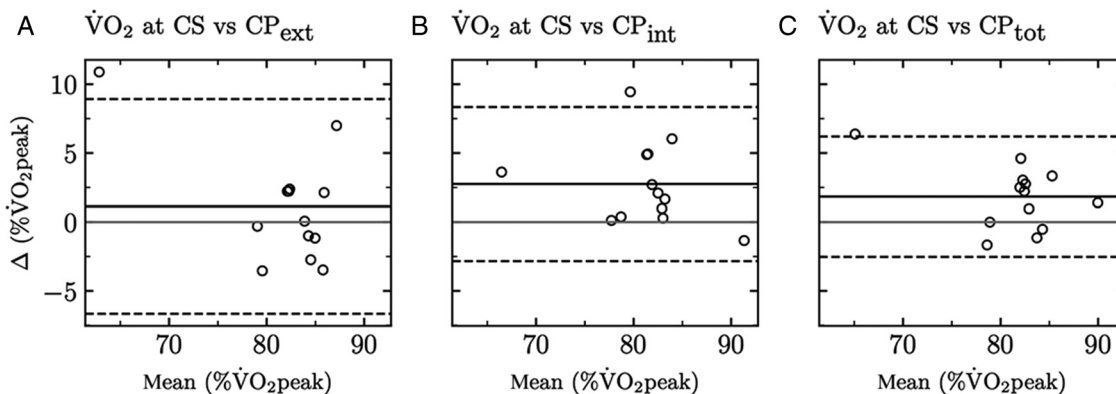


Figure 2 — Bland–Altman plots comparing $\dot{V}O_2$ (expressed as a $\% \dot{V}O_{2\text{peak}}$) at CS with (A) CP_{ext} , (B) CP_{int} , and (C) CP_{tot} . CP indicates critical power; CP_{ext} , external CP; CP_{int} , internal CP; CP_{tot} , total CP; CS, critical speed; $\dot{V}O_2$, oxygen uptake; $\% \dot{V}O_{2\text{peak}}$, percentage of peak rate of oxygen uptake.

proper term (CS, CP, critical force, critical tension, or critical torque) should be used depending on the corresponding measured quantity, must continue to spread. Indeed, the similarity between CS and CPs reported in the present study may only be true because

CS and CPs were both determined during running and thus represent a specific intensity threshold for the same exercise mode. On the contrary, CS and CP assessed during 2 different exercise modes (ie, running and cycling, respectively) do not

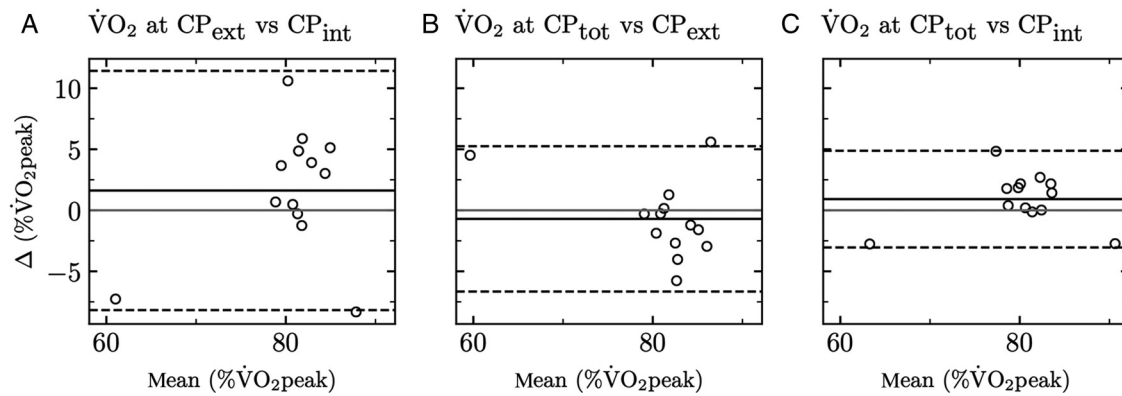


Figure 3 — Bland–Altman plots comparing $\dot{V}O_2$ (expressed as a $\% \dot{V}O_{2peak}$) between (A) CP_{ext} and CP_{int} , (B) CP_{tot} and CP_{ext} , and (C) CP_{tot} and CP_{int} . CP indicates critical power; CP_{ext} , external CP; CP_{int} , internal CP; CP_{tot} , total CP; $\dot{V}O_2$, oxygen uptake; $\% \dot{V}O_{2peak}$, percentage of peak rate of oxygen uptake.

Table 1 Mean (SD) of CS Estimated Using Time to Exhaustion and CP_{ext} , CP_{int} , and CP_{tot} Estimated Using Strides Recorded During First (Start), Middle (Half), and Last (End) Minute of Each Time to Exhaustion, As Well As $\dot{V}O_2$ (Expressed as a $\% \dot{V}O_{2peak}$) at the CS/CPs

Critical intensity	Critical intensity value, m/s or W/kg	$\dot{V}O_2$, $\% \dot{V}O_{2peak}$
CS	4.27 (0.40)	82.5 (5.3)
CP_{ext}		
Start	5.16 (0.56)	81.3 (7.6)
Half	5.26 (0.46)	82.6 (5.2)
End	5.28 (0.49)	83.1 (6.0)
CP_{int}		
Start	2.60 (0.54)	79.7 (6.0)
Half	2.53 (0.62)	78.9 (6.9)
End	2.53 (0.43)	78.9 (4.2)
CP_{tot}		
Start	7.78 (1.01)	80.6 (6.3)
Half	7.77 (0.94)	80.5 (5.6)
End	7.81 (0.79)	80.8 (3.9)

Abbreviations: CP, critical power; CP_{ext} , external CP; CP_{int} , internal CP; CP_{tot} , total CP; CS, critical speed; RM-ANOVA, repeated-measures analysis of variance; $\dot{V}O_2$, oxygen uptake; $\% \dot{V}O_{2peak}$, percentage of peak rate of oxygen uptake. Note: One-way RM-ANOVA reported no significant difference between the $\dot{V}O_2$ for CS and CPs at the start ($P = .09$). One-way RM-ANOVA reported no significant main effect of the time stride selection when estimating CP_{ext} , CP_{int} , and CP_{tot} , as well as for the resulting $\dot{V}O_2$ ($P \geq .44$).

necessarily correspond to the same specific intensity threshold for everyone.

On the other hand, consistent $\dot{V}O_2$ were obtained among the 3 different CPs (Table 1), and no systematic biases were reported (Figure 3), which proved that using P_{ext} , P_{int} , and P_{tot} to estimate corresponding CPs led to similar $\dot{V}O_2$. Our findings corroborate those of Barker et al.²² who report that CP represents a specific $\dot{V}O_2$, which can be achieved at different combinations of P_{ext} and P_{int} (pedaling frequencies) outputs in cycling. Therefore, the present study is the first to show that $\dot{V}O_2$ at CP represents a specific metabolic rate independent of the type of power output considered (internal vs external vs total) in running. Practically, this

means that if one is only interested in the $\dot{V}O_2$ associated with CP, it can be obtained simply by using an inertial sensor. Indeed, this sensor would provide the spatiotemporal parameters required to calculate P_{int} during the 4 exhaustive runs, that is, ground contact time, stride frequency, and duty factor. These P_{int} s would then be used to estimate CP_{int} , which would finally be matched to the P_{int} s computed during the maximal incremental aerobic test to obtain the $\dot{V}O_2$ associated to CP_{int} . Therefore, this would avoid the need for an expensive instrumented treadmill as well as the more complicated analysis of the ground reaction force to obtain P_{ext} to estimate CP_{ext} . However, typical power meters¹⁹ provide P_{ext} or P_{tot} but not P_{int} , which makes the estimation of CP_{ext} or CP_{tot} essential to perform training based on power-based intensity domains. Besides, Vassallo et al.³⁴ recently estimated a running CP_{tot} from a 3-minute all-out test performed on an outdoor athletic track. The authors obtained a CP_{tot} of 6.64 W/kg (assuming a body mass of 68 kg), which is 15% smaller than the one reported in the present study. Nonetheless, the difference might be explained by the different methodology employed: CP_{tot} was given by the running power averaged during the last 30 seconds of the 3-minute test and running power was computed from speed data recorded using a global positioning system sampling at 10 Hz. Moreover, participants were less trained, that is, they reported a 20% smaller $\dot{V}O_{2peak}$ (51.1 mL/kg/min) than in the present study, which obviously lead to a smaller CP.

No effect of time stride selection was obtained when estimating CP_{ext} , CP_{int} , and CP_{tot} , as well as for their resulting $\dot{V}O_2$ (Table 1). Indeed, using the first, half, or last minute of the exhaustive runs to calculate P_{ext} , P_{int} , and P_{tot} were equivalent, except for the 110%PS intensity, though the difference could be assumed negligible (0.15 W/kg, ie, 10 W for a 70-kg person; Table 2). Therefore, using the average of the powers calculated at the first, half, and last minute of the exhaustive runs would have led to similar estimations of CPs than when using these time stride selections separately. Besides, the similar P_{ext} , P_{int} , and P_{tot} obtained in this study within each exhaustive run and independently of the intensity of the run (submaximal or supramaximal) is consistent with the observations of Avogadro et al.²⁷ which depicted similar W_{ext} , W_{int} , and W_{tot} at the third and last minute of an exhaustive run at a speed corresponding to 90% $\dot{V}O_{2max}$ and with similar W_{ext} at the end of an exhaustive run at 95% $\dot{V}O_{2max}$ than at the beginning of the slow component of $\dot{V}O_2$ (~120 s).²⁴ However, these results disagreed with the fact that the same

Table 2 Mean (SD) of the Time to Exhaustion Corresponding to the 4 Exhaustive Runs Performed at 90%, 100%, 110%, and 120% of the Participant's PS, As Well As P_{ext} , P_{int} , and P_{tot} Power Computed Using Strides Recorded During the First (Start), Middle (Half), and Last (End) Minute of Each Time to Exhaustion

Running speed (%PS)	90	100	110	120
Time to exhaustion (min)	15.25 (2.50)	5.68 (1.10)	2.65 (0.78)	1.58 (0.49)
P_{ext} , W/kg				
Start	5.77 (0.35)	6.38 (0.44)	6.94 (0.43)	7.56 (0.45)
Half	5.74 (0.39)	6.29 (0.42)	6.90 (0.43)	7.51 (0.46)
End	5.77 (0.37)	6.32 (0.39)	6.95 (0.40)	7.52 (0.39)
P_{int} , W/kg				
Start	3.26 (0.44)	4.12 (0.58)	5.14 (0.72)	6.39 (0.99)
Half	3.26 (0.42)	4.15 (0.56)	5.19 (0.71)	6.41 (0.90)
End	3.24 (0.41)	4.16 (0.56)	5.28 (0.71)	6.51 (0.92)
P_{tot} , W/kg				
Start	9.03 (0.73)	10.50 (0.96)	12.08 (1.06)*	13.95 (1.37)
Half	9.00 (0.74)	10.44 (0.91)	12.09 (1.07)*	13.92 (1.29)
End	9.02 (0.69)	10.48 (0.85)	12.23 (1.05)	14.03 (1.25)

Abbreviations: P , power; P_{ext} , external P; P_{int} , internal P; PS, peak speed; P_{tot} , total P; RM-ANOVA, repeated-measures analysis of variance. Note: Two-way RM-ANOVA reported no significant main effect of the time stride selection on the calculation of P_{ext} , P_{int} , and P_{tot} ($P \geq .11$), while there was a significant main effect of %PS ($P < .001$), with each of the 3 powers at %PS being statistically higher compared with those at previous %PS, as reported by Holm post hoc tests ($P < .001$). Significant differences as determined by post hoc tests for the time stride selection \times %PS interaction effect obtained for P_{tot} ($P = .03$): *significantly different from the end at 110%PS. Note that, a statistically higher P_{tot} was obtained for all comparisons between an higher %PS and a lower one ($P < .001$; 54 comparisons) but was not represented by a symbol in the table.

authors²⁴ as well as Candau et al²⁶ observed a lower W_{int} at the end of the exhaustive run than at its beginning and that a larger W_{ext} was obtained right before exhaustion.²⁶ Although these discrepancies with previous findings may be due to methodological differences associated with the device used to assess the mechanical power output (kinematic arm vs instrumented treadmill) and the running speed tested (submaximal vs supramaximal), the present study depicted no effect of the time stride selection when calculating running powers at intensities ranging from 90%PS to 120%PS. Thus, these results further extended the knowledge of the effect of the time stride selection on power calculations, especially at supramaximal intensities.

Practical Applications

Power is becoming a widely used external metric in running, and is especially useful when speed is no longer a relevant metric to separate between intensity domains (running on a variable terrain or in a very windy condition). In such case, commercial systems (eg, Runscribe, Stryd, or Myotest) provide coaches and athletes an easy-to-use tool to monitor running power.¹⁹ Thereby, combining this outcome with the knowledge of CP could allow athletes to control their targeted training intensity and coaches to prescribe a training session in any type of condition.

Conclusions

To conclude, the present study estimated the usual CS as well as CP_{ext} , CP_{int} , and CP_{tot} in running. The $\dot{V}O_2$ at CS and CPs were not statistically different. No systematic bias was reported between the $\dot{V}O_2$ at CS and CP_{ext} as well as among the $\dot{V}O_2$ at the 3 different CPs, whereas systematic biases were obtained among the $\dot{V}O_2$ at CS and internal and total CP. Nonetheless, these differences were small ($\leq 3\%$) and thus not clinically relevant. Therefore, these

results suggest that CS and CPs closely represent the same fatigue threshold in running. Furthermore, this study reported no effect of the time stride selection when calculating P_{ext} , P_{int} , and P_{tot} , when estimating CP_{ext} , CP_{int} , and CP_{tot} , as well as when calculating their resulting $\dot{V}O_2$, which further extends the knowledge of the effect of the time stride selection on power calculations.

Acknowledgments

This study was supported by the University of Lausanne (Switzerland). The authors warmly thank the participants for their time and cooperation.

References

- Garber CE, Blissmer B, Deschenes MR, et al. American College of Sports Medicine position stand. Quantity and quality of exercise for developing and maintaining cardiorespiratory, musculoskeletal, and neuromotor fitness in apparently healthy adults: guidance for prescribing exercise. *Med Sci Sports Exerc.* 2011;43(7):1334–1359. PubMed ID: [21694556](#) doi:[10.1249/MSS.0b013e318213febf](#)
- Sjödín B, Svedenhag J. Applied physiology of marathon running. *Sports Med.* 1985;2(2):83–99. PubMed ID: [3890068](#) doi:[10.2165/00007256-198502020-00002](#)
- Billat LV, Koralsztein JP. Significance of the velocity at $\dot{V}O_{2\text{max}}$ and time to exhaustion at this velocity. *Sports Med.* 1996;22(2):90–108. PubMed ID: [8857705](#) doi:[10.2165/00007256-199622020-00004](#)
- Swain DP, Leutholtz BC, King ME, Hass LA, Branch JD. Relationship between % heart rate reserve and % $\dot{V}O_2$ reserve in treadmill exercise. *Med Sci Sports Exerc.* 1998;30(2):318–321. PubMed ID: [9502363](#) doi:[10.1097/00005768-199802000-00022](#)
- Scharhag-Rosenberger F, Meyer T, Gabler N, Faude O, Kindermann W. Exercise at given percentages of $\dot{V}O_{2\text{max}}$: heterogeneous metabolic responses between individuals. *J Sci Med Sport.* 2010;13(1):74–79. PubMed ID: [19230766](#) doi:[10.1016/j.jsams.2008.12.626](#)

6. Lansley KE, Dimeena FJ, Bailey SJ, Jones AM. A 'new' method to normalise exercise intensity. *Int J Sports Med.* 2011;32(7):535–541. PubMed ID: [21563028](#) doi:[10.1055/s-0031-1273754](#)
7. Iannetta D, Inglis EC, Mattu AT, et al. A critical evaluation of current methods for exercise prescription in women and men. *Med Sci Sports Exerc.* 2020;52(2):466–473. PubMed ID: [31479001](#) doi:[10.1249/MSS.0000000000002147](#)
8. Burnley M, Jones AM. Oxygen uptake kinetics as a determinant of sports performance. *Eur J Sport Sci.* 2007;7(2):63–79. doi:[10.1080/17461390701456148](#)
9. Whipp BJ, Mahler M. Dynamics of pulmonary gas exchange during exercise. In: West JB ed. *Pulmonary gas exchange*. Vol. 2. New York, NY: Academic Press; 1980.
10. Wasserman K, Whipp BJ, Koysl SN, Beaver WL. Anaerobic threshold and respiratory gas exchange during exercise. *J Appl Physiol.* 1973; 35(2):236–243. PubMed ID: [4723033](#) doi:[10.1152/jappl.1973.35.2.236](#)
11. Vanhatalo A, Doust AH, Burnley M. Determination of critical power using a 3-min all-out cycling test. *Med Sci Sports Exerc.* 2007; 39(3):548–555. PubMed ID: [17473782](#) doi:[10.1249/mss.0b013e31802dd3e6](#)
12. Jones AM, Burnley M, Black MI, Poole DC, Vanhatalo A. The maximal metabolic steady state: redefining the 'gold standard.' *Physiol Rep.* 2019;7(10):e14098. PubMed ID: [31124324](#) doi:[10.14814/phy2.14098](#)
13. Monod H, Scherrer J. The work capacity of a synergic muscular group. *Ergonomics.* 1965;8(3):329–338. doi:[10.1080/00140136508930810](#)
14. Poole DC, Ward SA, Gardner GW, Whipp BJ. Metabolic and respiratory profile of the upper limit for prolonged exercise in man. *Ergonomics.* 1988;31(9):1265–1279. PubMed ID: [3191904](#) doi:[10.1080/00140138808966766](#)
15. Jones AM, Vanhatalo A, Burnley M, Morton RH, Poole DC. Critical power: implications for determination of V'O₂max and exercise tolerance. *Med Sci Sports Exerc.* 2010;42(10):1876–1890. PubMed ID: [20195180](#) doi:[10.1249/MSS.0b013e3181d9cf7f](#)
16. Craig JC, Vanhatalo A, Burnley M, et al. Critical power: Possibly the most important fatigue threshold in exercise physiology. In: Zoladz JA, ed. *Muscle and Exercise Physiology*. Academic Press; 2019: 159–181.
17. Jones AM, Vanhatalo A. The 'critical power' concept: applications to sports performance with a focus on intermittent high-intensity exercise. *Sports Med.* 2017;47(suppl 1):65–78. doi:[10.1007/s40279-017-0688-0](#)
18. Morton RH, Hodgson DJ. The relationship between power output and endurance: a brief review. *Eur J Appl Physiol Occup Physiol.* 1996;73(6):491–502. PubMed ID: [8817118](#) doi:[10.1007/BF00357670](#)
19. Jaén-Carrillo D, Roche-Seruendo LE, Carton-Llorente A, Ramirez-Campillo R, Garcia-Pinillos F. Mechanical power in endurance running: a scoping review on sensors for power output estimation during running. *Sensors.* 2020;20(22):6482. doi:[10.3390/s20226482](#)
20. Cavagna GA. Force platforms as ergometers. *J Appl Physiol.* 1975; 39(1):174–179. PubMed ID: [1150585](#) doi:[10.1152/jappl.1975.39.1.174](#)
21. Nardello F, Ardigo LP, Minetti AE. Measured and predicted mechanical internal work in human locomotion. *Hum Mov Sci.* 2011;30(1): 90–104. PubMed ID: [21056491](#) doi:[10.1016/j.humov.2010.05.012](#)
22. Barker T, Poole DC, Noble ML, Barstow BJ. Human critical power–oxygen uptake relationship at different pedalling frequencies. *Exp Physiol.* 2006;91(3):621–632. PubMed ID: [16527863](#) doi:[10.1113/expphysiol.2005.032789](#)
23. Smith JC, Hill DW. Stability of parameter estimates derived from the power/time relationship. *Can J Appl Physiol.* 1993;18(1):43–47. PubMed ID: [8471993](#) doi:[10.1139/h93-005](#)
24. Borrani F, Candau R, Perrey S, Millet GY, Millet GP, Rouillon J-D. Does the mechanical work in running change during the VO₂ slow component? *Med Sci Sports Exerc.* 2003;35(1):50–57. PubMed ID: [12544635](#) doi:[10.1097/00005768-200301000-00009](#)
25. Clark IE, Vanhatalo A, Thompson P, et al. Dynamics of the power-duration relationship during prolonged endurance exercise and influence of carbohydrate ingestion. *J Appl Physiol.* 2019;127(3):726–736. PubMed ID: [31295069](#) doi:[10.1152/jappphysiol.00207.2019](#)
26. Candau R, Belli A, Millet GY, Geroges D, Barbier B, Rouillon JD. Energy cost and running mechanics during a treadmill run to voluntary exhaustion in humans. *Eur J Appl Physiol Occup Physiol.* 1998; 77(6):479–485. PubMed ID: [9650730](#) doi:[10.1007/s004210050363](#)
27. Avogadro P, Dolenc A, Belli A. Changes in mechanical work during severe exhausting running. *Eur J Appl Physiol.* 2003;90(1–2): 165–170. PubMed ID: [14504949](#) doi:[10.1007/s00421-003-0846-y](#)
28. Kuipers H, Rietjens G, Verstappen F, Schoenmakers H, Hofman G. Effects of stage duration in incremental running tests on physiological variables. *Int J Sports Med.* 2003;24(7):486–491. PubMed ID: [12968205](#) doi:[10.1055/s-2003-42020](#)
29. Morton HR. A 3-parameter critical power model. *Ergonomics.* 1996; 39(4):611–619. PubMed ID: [8854981](#) doi:[10.1080/00140139608964484](#)
30. Patoz A, Spicher R, Pedrani N, Malatesta D, Borrani F. Critical speed estimated by statistically appropriate fitting procedures. *Eur J Appl Physiol.* 2021;121(7):2027–2038.
31. Levenberg K. A method for the solution of certain non-linear problems in least squares. *Q Appl Math.* 1944;2(2):164–168. doi:[10.1090/qam/10666](#)
32. Marquardt DW. An algorithm for least-squares estimation of non-linear parameters. *J Soc Ind Appl Math.* 1963;11(2):431–441. doi:[10.1137/0111030](#)
33. Jones AM, Vanhatalo A, Burnley M, Morton RH, Poole DC. Response. *Med Sci Sports Exerc.* 2011;43(3):553. doi:[10.1249/MSS.0b013e3182075485](#)
34. Vassallo C, Gray A, Cummins C, Murphy A, Waldron M. Exercise tolerance during flat over-ground intermittent running: modelling the expenditure and reconstitution kinetics of work done above critical power. *Eur J Appl Physiol.* 2020;120(1):219–230. PubMed ID: [31776696](#) doi:[10.1007/s00421-019-04266-8](#)

9.4 A multivariate polynomial regression to reconstruct ground contact and flight times based on a sine-wave model for vertical ground reaction force and measured effective timings

Aurélien Patoz^{1,2,*}, Thibault Lussiana^{2,3,4}, Bastiaan Breine^{2,5}, Cyrille Gindre^{2,3}, Davide Malatesta¹

¹ Institute of Sport Sciences, University of Lausanne, 1015 Lausanne, Switzerland

² Research and Development Department, Volodalen Swiss Sport Lab, 1860 Aigle, Switzerland

³ Research and Development Department, Volodalen, 39270 Chavéria, France

⁴ Research Unit EA3920 Prognostic Markers and Regulatory Factors of Cardiovascular Diseases and Exercise Performance, Health, Innovation platform, University of Franche-Comté, Besançon, France

⁵ Department of Movement and Sports Sciences, Ghent University, 9000 Ghent, Belgium

* Corresponding author

Published in **Frontiers in Bioengineering and Biotechnology**

DOI: 10.3389/fbioe.2021.687951



A Multivariate Polynomial Regression to Reconstruct Ground Contact and Flight Times Based on a Sine Wave Model for Vertical Ground Reaction Force and Measured Effective Timings

Aurélien Patoz^{1,2*}, Thibault Lussiana^{2,3,4}, Bastiaan Breine^{2,5}, Cyrille Gindre^{2,3} and Davide Malatesta¹

¹Institute of Sport Sciences University of Lausanne, Lausanne, Switzerland, ²Research and Development Department Volodalen Swiss Sport Lab, Aigle, Switzerland, ³Research and Development Department Volodalen, Chavéria, France, ⁴Research Unit EA3920 Prognostic Markers and Regulatory Factors of Cardiovascular Diseases and Exercise Performance Health Innovation Platform University of Franche-Comté, Besançon, France, ⁵Department of Movement and Sports Sciences Ghent University, Ghent, Belgium

OPEN ACCESS

Edited by:

Yang Liu,
Hong Kong Polytechnic University,
Hong Kong, SAR China

Reviewed by:

Weiwei Yan,
China Jiliang University, China
Shuo Chen,
Tongji University, China

*Correspondence:

Aurélien Patoz
aurelien.patoz@unil.ch

Specialty section:

This article was submitted to
Biomechanics,
a section of the journal
Frontiers in Bioengineering and
Biotechnology

Received: 30 March 2021

Accepted: 29 September 2021

Published: 04 November 2021

Citation:

Patoz A, Lussiana T, Breine B, Gindre C and Malatesta D (2021) A Multivariate Polynomial Regression to Reconstruct Ground Contact and Flight Times Based on a Sine Wave Model for Vertical Ground Reaction Force and Measured Effective Timings. *Front. Bioeng. Biotechnol.* 9:687951. doi: 10.3389/fbioe.2021.687951

Effective contact (t_{ce}) and flight (t_{fe}) times, instead of ground contact (t_c) and flight (t_f) times, are usually collected outside the laboratory using inertial sensors. Unfortunately, t_{ce} and t_{fe} cannot be related to t_c and t_f because the exact shape of vertical ground reaction force is unknown. However, using a sine wave approximation for vertical force, t_{ce} and t_c as well as t_{fe} and t_f could be related. Indeed, under this approximation, a transcendental equation was obtained and solved numerically over a $t_{ce} \times t_{fe}$ grid. Then, a multivariate polynomial regression was applied to the numerical outcome. In order to reach a root-mean-square error of 0.5 ms, the final model was given by an eighth-order polynomial. As a direct application, this model was applied to experimentally measured t_{ce} values. Then, reconstructed t_c (using the model) was compared to corresponding experimental ground truth. A systematic bias of 35 ms was depicted, demonstrating that ground truth t_c values were larger than reconstructed ones. Nonetheless, error in the reconstruction of t_c from t_{ce} was coming from the sine wave approximation, while the polynomial regression did not introduce further error. The presented model could be added to algorithms within sports watches to provide robust estimations of t_c and t_f in real time, which would allow coaches and practitioners to better evaluate running performance and to prevent running-related injuries.

Keywords: running, biomechanics, sensors, inertial measurement unit, machine learning

INTRODUCTION

Ground contact (t_c) and flight (t_f) times are key temporal parameters of running biomechanics. Indeed, Novacheck (1998) postulated that the presence of t_f allowed distinguishing walking from running gaits. In other words, the duty factor (the ratio of t_c over stride duration) is under 50% for running (Minetti, 1998; Folland et al., 2017). Moreover, t_c was shown to be self-optimized to minimize the metabolic cost of running (Moore et al., 2019). These two parameters are obtained from foot-strike (FS) and toe-off (TO) events. More specifically, t_c represents the time from FS to TO of the

same foot, while t_f is the time from TO of one foot to FS of the contralateral foot. Therefore, t_c and t_f rely on the accuracy of FS and TO detections, for which the use of force plates is considered the gold standard method. However, force plates could not always be available and used (Abendroth-Smith, 1996; Maiwald et al., 2009). In such case, alternatives would be to use a motion capture system (Lussiana et al., 2019; Patoz et al., 2020) or a light-based optical technology (Debaere et al., 2013). Nevertheless, even though these three systems can be used outside the laboratory (Purcell et al., 2006; Hébert-Losier et al., 2015; Ammann et al., 2016; Lussiana and Gindre, 2016), they suffer a lack of portability and are restricted to a specific and small capture volume, that is, they do not allow continuous temporal gait data collection throughout the entire training or race. To overcome such limitations, techniques to identify FS and TO events were developed using portable tools such as inertial measurement units (IMUs), which are easy to use, low cost, and suitable for field measurements and very practical to use in a coaching environment (Camomilla et al., 2018).

Different techniques to identify gait events are available and depend on the placement of the IMU on the human body (Moe-Nilssen, 1998; Lee et al., 2010; Flaction et al., 2013; Giandolini et al., 2014; Norris et al., 2014; Giandolini et al., 2016; Gindre et al., 2016; Falbriard et al., 2018; Falbriard et al., 2020). Among them, when the IMU is positioned near the sacrum, that is, close to the center of mass, the vertical acceleration signal can be used to determine effective contact (t_{ce}) and flight (t_{fe}) times, instead of t_c and t_f (Flaction et al., 2013; Gindre et al., 2016). To delineate these effective timings, the vertical force is calculated based on Newton's second law using the body mass (m) of individuals and the vertical acceleration data. Then, these effective timings are based on effective FS (eFS) and effective TO (eTO) events. More precisely, eFS and eTO correspond to the instants of time where the vertical force increases above and decreases below body weight (mg), respectively (Cavagna et al., 1988). The authors (Flaction et al., 2013; Gindre et al., 2016) did not mention why a 20 N threshold was not used to determine FS and TO events from their IMU data, even though this is the reference when using force plates data for event detection (Smith et al., 2015). However, the vertical acceleration recorded by an IMU during t_f is usually negative (Gindre et al., 2016), while a force plate measure gives exactly zero. Therefore, it could be suspected that a 20 N threshold would not be reliable to obtain FS and TO events when dealing with IMU data, while the time at which the vertical force is equal to body weight would be equivalent between IMU and force plate data.

Using effective timings or t_c and t_f provide the same step duration, that is, it is given by either the sum of t_c and t_f or t_{ce} and t_{fe} . Thus, this temporal information is not lost. As for the effect of running speed, t_{ce} and t_c both decrease with increasing running speed, even though the decrease is much more important for t_c than t_{ce} (Cavagna et al., 2008; Da Rosa et al., 2019). Concerning t_{fe} and t_f , their trend with increasing running speed is not similar. Indeed, t_{fe} tends to slightly decrease, while t_f increases almost up to a plateau with increasing running speed (Cavagna et al., 2008; Da Rosa et al., 2019). In addition, t_{ce} and t_{fe} cannot directly be related to t_c and

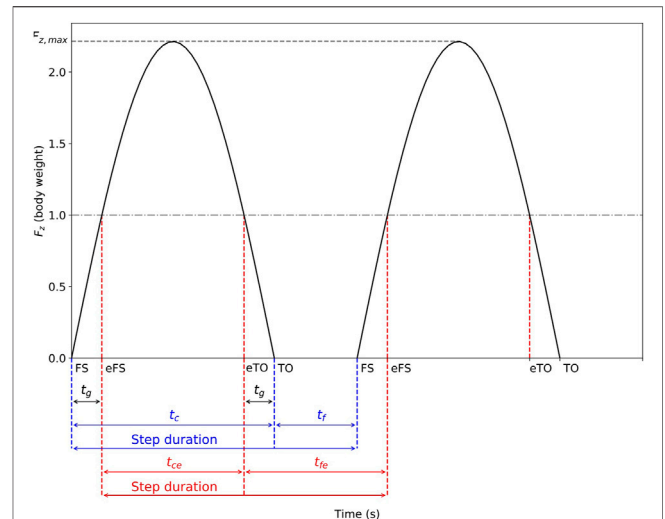


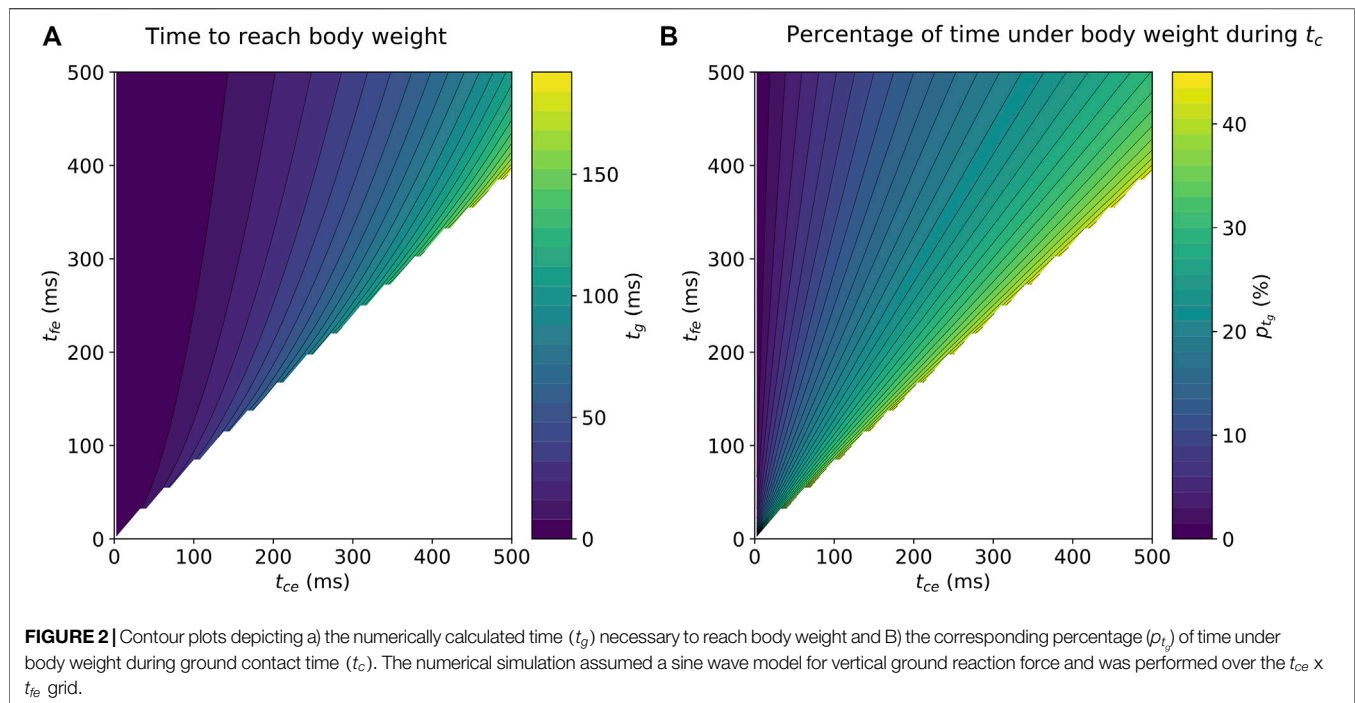
FIGURE 1 | Vertical ground reaction force (F_z) under the sine wave approximation, peak vertical force ($F_{z,max}$), foot-strike (FS) and toe-off (TO) events together with their corresponding effective events (eFS and eTO), as well as contact (t_c), flight (t_f), effective contact (t_{ce}), and effective flight (t_{fe}) times, and time to reach body weight (t_g), for a typical running stride. Noteworthy, step duration is the same when using effective or usual timings.

t_f , the reason being that the fraction of time spends below body weight during t_c depends on the shape of the vertical ground reaction force, which is not precisely known when using IMUs (see above). Thus, t_c and t_f , parameters that are directly related to them, for example, duty factor (Minetti, 1998; Folland et al., 2017), as well as parameters that can be estimated from them, for example, vertical oscillation and vertical stiffness (Morin et al., 2005), cannot be obtained. Hence, the assessment of running biomechanics is restricted when using t_{ce} and t_{fe} .

Nonetheless, the vertical ground reaction force can be approximated using a sine wave as $F_z(t) = F_{z,max} \sin(\pi t/t_c)$, where, based on momentum conservation law, $F_{z,max} = mg\pi(t_f/t_c + 1)/2$ (Alexander, 1989; Kram and Dawson, 1998; Dalleau et al., 2004; Morin et al., 2005). In such case, the vertical ground reaction force is symmetric around $t_c/2$, which means that the time duration between FS and eFS as well as between eTO and TO, called t_g in what follows, are the same. Thereby, under the sine wave assumption, t_c and t_f can be obtained from t_{ce} and t_{fe} using $t_c = t_{ce} + 2t_g$ and $t_f = t_{fe} - 2t_g$, if t_g is known. These timings and the sine wave vertical ground reaction force are depicted in **Figure 1** for a typical running stride. Recognizing that $F_z(t_g) = mg = F_{z,max} \sin(\frac{\pi t_g}{t_c})$, and using the definition of $F_{z,max}$ given before, the following equation is obtained:

$$\text{csc}\left(\frac{\pi t_g}{t_{ce} + 2t_g}\right) = \frac{\pi}{2} \left(\frac{t_{fe} - 2t_g}{t_{ce} + 2t_g} + 1\right), \quad (1)$$

which could not be solved analytically for t_g (transcendental equation; **Supplementary File**) using Mathematica v12.1 (Wolfram, Oxford, UK), that is, no closed-form solution exists. Therefore, a numerical solution is required for any pair of t_{ce} and t_{fe} . Ultimately, a mathematical modeling of t_g over the



numerical $t_{ce} \times t_{fe}$ grid could be performed, and its accuracy could be evaluated using advanced data analysis techniques like machine learning. Indeed, supervised machine learning models like linear regressions have been used to model relationships between biomechanical measures and clinical outcomes (Halilaj et al., 2018; Backes et al., 2020; Alcantara et al., 2021). However, to the best of our knowledge, no attempt to provide such a model equation for t_g has been made so far.

Hence, the purpose of this study was to obtain a mathematical modeling of t_g under the sine wave approximation of the vertical ground reaction force so that t_c and t_f can be reconstructed from t_{ce} and t_{fe} . As a direct experimental application, the proposed model was applied to experimentally measured t_{ce} values. Then, the reconstructed t_c values were compared to their corresponding experimental ground truth (gold standard).

MATERIALS AND METHODS

Numerical Analysis

Brent's method (also known as van Wijngaarden Dekker Brent method) (Brent, 1973; Press et al., 1992) was used to find the zeros of Eq. 1 for any pair of t_{ce} and t_{fe} . The zero of interest for a given t_{ce} and t_{fe} pair was considered to lie between 0 and the minimum of Eq. 1, which was minimized using the Broyden Fletcher Goldfarb Shanno method (Broyden, 1970; Fletcher, 1970; Goldfarb, 1970; Shanno, 1970). The numerical analysis was carried out using t_{ce} and t_{fe} values varying between 2.5 and 505 ms and using a grid spacing of 7.5 ms (4,624 grid points). The grid limits were chosen due to the fact that running requires 1) both a ground contact and a flight phase, that is, t_{ce} and t_{fe} cannot be 0 and 2) t_c belongs to the interval [100 ms, 400 ms] and t_f

belongs to the interval [0 ms, 250 ms] (Cavagna et al., 2008; Da Rosa et al., 2019; Lussiana et al., 2019), and to include any atypical t_{ce} and t_{fe} pair, that is, atypical runners. Noteworthy, the justification of the grid spacing is provided in Appendix. The grid spacing was dependent on the error threshold set to the mathematical modeling.

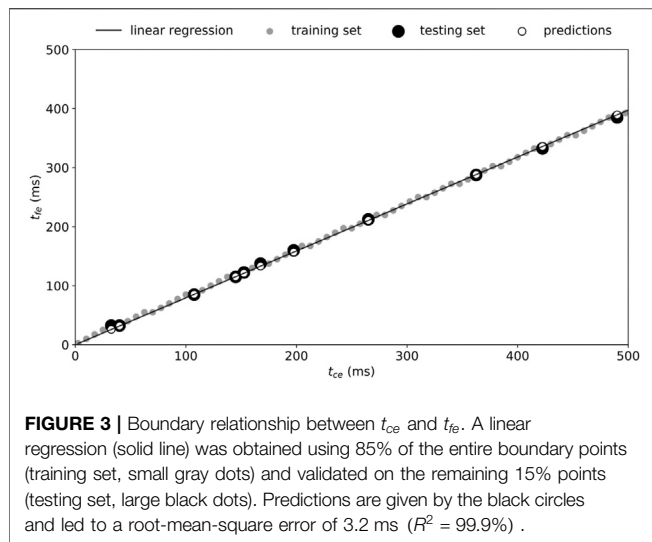
Mathematical Modeling

Boundary Relationship Between t_{ce} and t_{fe}

The numerical analysis showed that a linear boundary relationship is present between t_{ce} and t_{fe} (see Results Figure 2), that is, there is no solution for t_g if t_{fe} is higher than a certain percentage of t_{ce} . This boundary relationship was computed by extracting the boundary points, that is, the smallest existing t_{fe} values for every t_{ce} grid point (68 pair of points). Then, a linear regression using ordinary least square was performed on a training set consisting of 85% of the entire set of boundary points. The y -intercept of the fitted linear model was held fixed at 0, the reason being that a null t_{ce} necessarily ensures a null t_{fe} . The linear model was tested on the remaining 15% points (testing set) and evaluated using the coefficient of determination (R^2) and root-mean-square error (RMSE).

Modeling a t_g Surface as Function of t_{ce} and t_{fe}

The numerical analysis showed that t_g could be described by a smoothly increasing surface when increasing t_{ce} and t_{fe} (see Results Figure 2). Therefore, a multivariate polynomial regression using ordinary least square was performed on a training set consisting of t_g values corresponding to 85% of the points within the boundary limits (i.e., the non-discarded grid points). The regression was performed using polynomials of order 1 to 15 and including intercept and interaction terms.



RMSE on the remaining 15% points (testing set) was computed for each fitted polynomial.

Experimental Application

Participant Characteristics

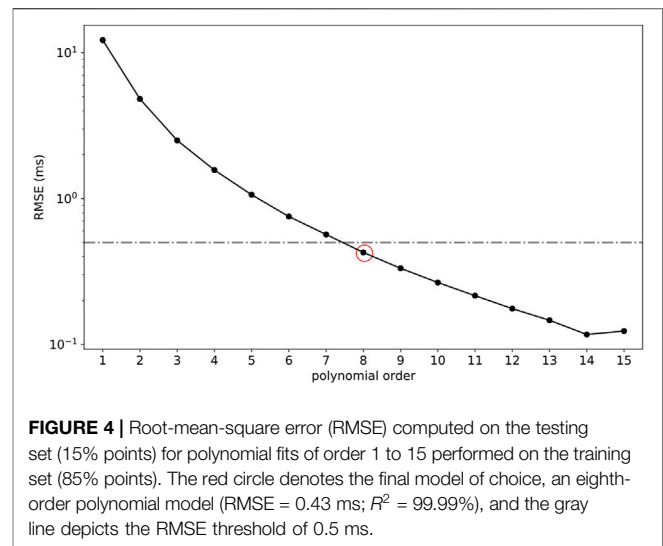
One hundred recreational runners (Honert et al., 2020), 75 males (age: 31 ± 8 years, height: 180 ± 6 cm, body mass: 70 ± 7 kg, and weekly running distance: 37 ± 24 km) and 25 females (age: 30 ± 7 years, height: 169 ± 5 cm, body mass: 61 ± 6 kg, and weekly running distance: 20 ± 14 km), voluntarily participated in the present study. For study inclusion, participants were required to be in good self-reported general health with no current or recent lower extremity injury (≤ 1 month), to run at least once a week, and to have an estimated maximal aerobic speed ≥ 14 km/h. The study protocol was approved by the Ethics Committee (CER-VD 2020-00334) and adhered to the latest Declaration of Helsinki of the World Medical Association.

Experimental Procedure

After providing written informed consent, each participant performed a 7-min warm-up run on an instrumented treadmill (Arsalis T150—FMT-MED, Louvain-la-Neuve, Belgium). Speed was set to 9 km/h for the first 3 min and was then increased by 0.5 km/h every 30 s. This was followed, after a short break (< 5 min), by three 1-min runs (9, 11, and 13 km/h) performed in a randomized order (1-min recovery between each run). 3D kinetic data were collected during the first 10 strides following the 30-s mark of running trials. All participants were familiar with running on a treadmill as part of their usual training program and wore their habitual running shoes.

Data Collection

3D kinetic data (1,000 Hz) were collected using the force plate embedded into the treadmill and using Vicon Nexus software



v2.9.3 (Vicon, Oxford, UK). The laboratory coordinate system was oriented such that x -, y -, and z -axes denoted mediolateral (pointing toward the right side of the body), posterioranterior, and inferiorsuperior axis, respectively. Ground reaction force (analog signal) was exported in .c3d format and processed in Visual3D Professional software v6.01.12 (C-Motion Inc, Germantown, MD, United States). 3D ground reaction force signal was low-pass-filtered at 20 Hz using a fourth-order Butterworth filter and down-sampled to 200 Hz to represent a sampling frequency corresponding to typical measurements recorded using a central inertial unit.

Data Analysis

For each running trial, eFS and eTO events were identified within Visual3D by applying a body weight threshold to the z -component of the ground reaction force (Cavagna et al., 1988). More explicitly, eFS was detected at the first data point greater or equal to mg within a running step, while eTO was detected at the last data point greater or equal to mg within the same running step. t_{ce} and t_{fe} were defined as the time from eFS to eTO of the same foot and from eTO of one foot to eFS of the contralateral foot, respectively.

In addition, FS and TO events were also identified within Visual3D. These events were detected by applying a 20 N threshold to the z -component of the ground reaction force (Smith et al., 2015). More explicitly, FS was detected at the first data point greater or equal to 20 N within a running step, while TO was detected at the last data point greater or equal to 20 N within the same running step. t_c and t_f were defined as the time from FS to TO of the same foot and from TO of one foot to FS of the contralateral foot, respectively.

The recorded vertical ground reaction force permitted to precisely measure t_c and t_f as well as t_{ce} and t_{fe} . Then, each t_{ce} and t_{fe} pair was fed to the best multivariate polynomial model to compute t_g , which ultimately allowed to obtain t_c . An instrumented treadmill was used to measure t_{ce} and t_{fe} (gold

standard), instead of an IMU to remove any potential measurement error that would come from the IMU itself. Hence, the error obtained when comparing the reconstructed t_c (obtained using the mathematical model and t_{ce} and t_{fe}) to its corresponding experimental ground truth (obtained from FS and TO events) could solely be coming from the sine wave assumption and the mathematical modeling but not from the measurement of t_{ce} and t_{fe} .

Statistical Analysis

All data are presented as mean \pm standard deviation. The reconstructed t_c values were compared to corresponding experimental ground truth t_c values using a BlandAltman plot (Bland and Altman, 1995; Atkinson and Nevill, 1998). Noteworthy, as step time is conserved, differences between measured and reconstructed t_f values depicted the opposite behavior compared with the differences between measured and reconstructed t_c values.

Systematic bias, lower and upper limit of agreements, and 95% confidence intervals (CI) were computed as well as RMSE. The difference between reconstructed and ground truth t_c values was quantified using Cohen's d effect size and interpreted as very small, small, moderate, and large when $|d|$ values were close to 0.01, 0.2, 0.5, and 0.8, respectively (Cohen, 1988). Statistical analysis was performed using Jamovi (v1.2, retrieved from <https://www.jamovi.org>), with the level of significance set at $p \leq 0.05$.

RESULTS

Numerical Analysis

The numerically calculated t_g values over the $t_{ce} \times t_{fe}$ grid are provided in **Figure 2A**, while **Figure 2B** depicts the corresponding percentage of time (p_{t_g}) spent under body weight during t_c , [$p_{t_g} = 100 * 2t_g / (t_{ce} + 2t_g)$].

Mathematical Modeling

Boundary Relationship Between t_{ce} and t_{fe}

The linear regression gave the model (Eq. 2):

$$t_{fe} = 0.795 t_{ce}. \quad (2)$$

Applying this model to the testing set led to an R^2 of = 99.9% and RMSE of 3.2 ms. The linear regression, training, and testing sets as well as predicted values are depicted in **Figure 3**.

Modeling a t_g Surface as Function of t_{ce} and t_{fe}

The grid points which did not satisfy the previously obtained boundary relationship (Eq. 2) were discarded (1814 discarded points). RMSE computed for each multivariate polynomial regression (order 1–15) is depicted in **Figure 4**. The polynomial which provided an RMSE smaller than 0.5 ms was kept as the final model of choice (RMSE = 0.43 ms; $R^2 = 99.99\%$) and corresponded to a polynomial model including up to eighth-order terms [$P_8(t_{ce}, t_{fe})$, Eq. 3]. The coefficients (α_{ij} ,

where $0 \leq i + j \leq 8$) of the multivariate polynomial model are given in **Table 1**.

$$P_8(t_{ce}, t_{fe}) = \sum_{i=0}^8 \sum_{j=0}^{8-i} \alpha_{i,j} t_{ce}^i t_{fe}^j \quad (3)$$

Noteworthy, the threshold on RMSE ensured an error smaller than 1 ms on the reconstructed t_c . The differences between t_g values computed numerically and using the eighth-order polynomial model for the testing set (15% points) are depicted in **Figure 5**.

Experimental Application

Reconstructed t_c values were compared to corresponding experimental ground truth t_c values using a BlandAltman plot, which is depicted in **Figure 6**. A systematic positive bias of 34.3 ms (95% CI [33.8 ms, 34.7 ms]) was obtained. The lower and upper limits of agreements were 0.0 ms (95% CI [-0.8 ms, 0.8 ms]) and 68.6 ms (95% CI [67.8 ms, 69.3 ms]), respectively. The RMSE between reconstructed and measured t_c was 38.5 ms (7.6%), and Cohen's d effect size was large ($d = 1.1$).

DISCUSSION

The proposed eighth-order multivariate polynomial model (Eq. 3) could be used to obtain t_c and t_f when an IMU is used to measure t_{ce} and t_{fe} . Thereby, important parameters to assess running biomechanics such as duty factor (Lussiana et al., 2019; Patoz et al., 2020), as well as vertical oscillation and vertical stiffness (Morin et al., 2005), could be calculated more precisely. Having these parameters would allow coaches and practitioners to better evaluate running performance outside the laboratory such as in a coaching environment and during an entire training or race, and to prevent running-related injuries.

In the case where an algorithm based on effective timings is running on the fly to provide live feedbacks, such as in sports watches, one could simply add the proposed model in the end of the algorithm chain, right before computing the biomechanical outcomes. However, many operations should be performed in a very small amount of time, where the number of operations is directly related to the order of the polynomial. Indeed, knowing that the number of terms in an n^{th} -order polynomial composed of two variables is given by C_2^{n+2} , then $C_2^{n+2} - 3$ calculations are required to compute the polynomial features, that is, t_{ce}^i and t_{fe}^i , where $2 \leq i \leq n$. In addition, $C_2^{n+2} - 1$ multiplications and $C_2^{n+2} - 1$ additions are necessary to calculate t_g . Therefore, such a large number of operations could be problematic for the small computing power available in sports watches. If this is really an issue, the order of the polynomial could be decreased. For instance, a third-order polynomial model gave an RMSE of 2.5 ms (**Figure 4**), which, depending on the application, might already be sufficient. In this case, the number of operations would be reduced from 130 (eighth order) to 25 (third order), leading to a 5 times speedup, assuming sequential calculations (no parallelization).

The multivariate polynomial model (Eq. 3) was applied to experimentally measured t_{ce} values. These results permitted us to

TABLE 1 | Coefficients (α_{ij} , where $0 \leq i + j \leq 8$) of the eighth-order multivariate polynomial model given by **Eq. 3**.

j (exponent of t_{fe})	j (exponent of t_{fe})									
	0	1	2	3	4	5	6	7	8	
0	-5.17E-5	-6.18E-2	2.73E0	-4.41E1	3.532	-1.55E3	3.783	-4.83E3	2.513	
1	2.84E-1	-1.41E1	2.64E2	-2.45E3	1.234	-3.38E4	4.834	-2.78E4		
2	1.17E1	-3.12E2	3.91E3	-2.49E4	8.434	-1.43E5	9.534			
3	8.26E1	-2.25E3	2.20E4	-1.01E5	2.155	-1.72E5				
4	5.13E2	-9.73E3	6.68E4	-1.90E5	1.865					
5	1.63E3	-2.32E4	9.82E4	-1.22E5						
6	3.41E3	-2.76E4	4.65E4							
7	3.15E3	-8.66E3								
8	4.62E2									

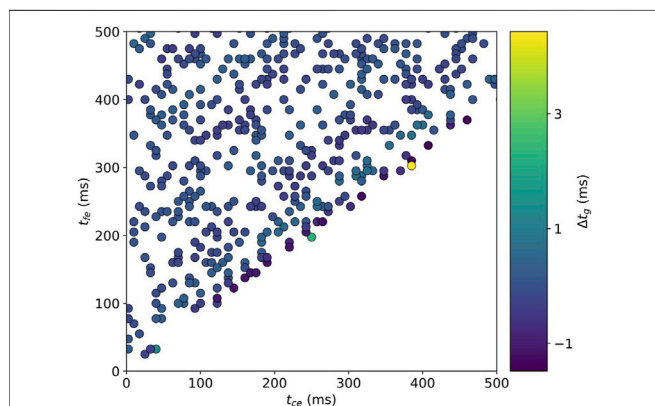


FIGURE 5 | Differences between t_g values (Δt_g) computed numerically (Section 2) and using the eighth-order polynomial model for the testing set (15% points). A difference larger than 2 ms was depicted for only two points (green and yellow circles) in the testing set, which were close to the boundary limit.

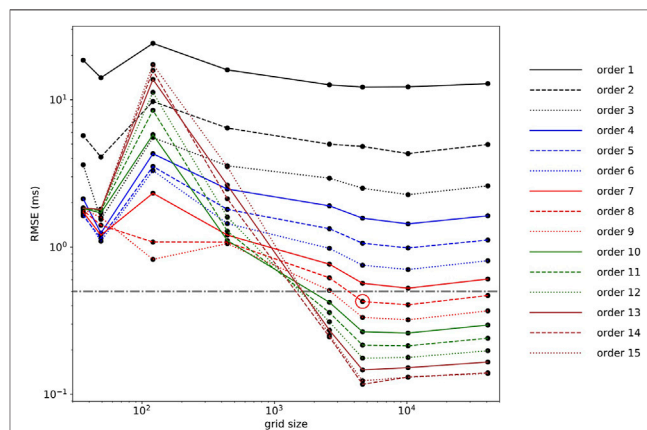


FIGURE 7 | Root-mean-square error as a function of grid size ranging from 36 to 40,804 total points and for each polynomial regression (1st to 15th order). The red circle denotes RMSE corresponding to a polynomial (eighth order) chosen in Section 3.2 (0.43 ms), and the gray line depicts an RMSE threshold of 0.5 ms.

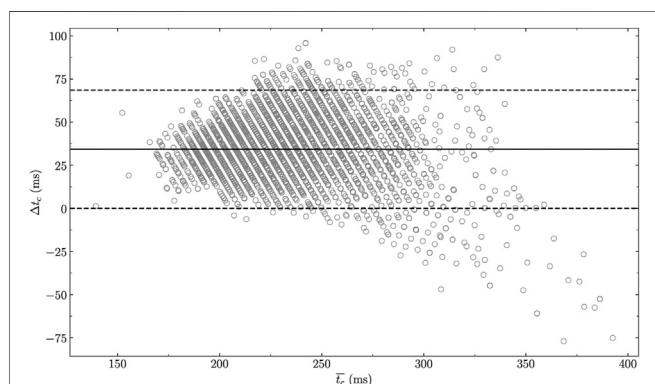


FIGURE 6 | BlandAltman plot comparing experimentally measured and reconstructed t_c using the multivariate polynomial model given by **Eq. 3**, which reports a systematic bias of 34.3 ms (95% confidence intervals [33.8 ms, 34.7 ms]). Δt_c : measured t_c - reconstructed t_c and \bar{t}_c : average of measured and reconstructed t_c .

show that the experimental ground truth t_c was, on average, 34.3 ms higher than the reconstructed one. Since the multivariate polynomial regression reported an RMSE of 0.43 ms, the large systematic bias obtained here was inherently due to the sine wave

approximation of the vertical ground reaction force. To further justify the previous statement, the polynomial depicting the smallest RMSE, that is, the 14th-order polynomial (RMSE = 0.12 ms; **Figure 7**), was used to compute t_c based on t_{ce} . Doing so, the following results were obtained: RMSE = 38.6 ms (7.6%), $d = 1.1$ (large effect size), and systematic bias = 34.2 ms [95% CI (33.7 ms, 34.6 ms)]. Therefore, to go beyond the scope of this study, future research should focus on defining a more accurate model of the vertical ground reaction force. Indeed, the sine wave approximation constituted the main limitation of the novel multivariate polynomial model proposed in this study.

CONCLUSION

To conclude, in the present study, an eighth-order multivariate polynomial model was constructed based on the numerical solution of the transcendental equation given by **Eq. 1**. The proposed model permitted to compute t_c and t_f from effective timings (t_{ce} and t_{fe}) using the sine wave approximation of the vertical ground reaction force. The model was chosen so that RMSE was smaller than 0.5 ms. Therefore, the error in the computation of t_c and t_f was coming

from the sine wave approximation, while the polynomial regression did not introduce further error.

DATA AVAILABILITY STATEMENT

The raw data supporting the conclusion of this article will be made available by the authors, without undue reservation.

ETHICS STATEMENT

The studies involving human participants were reviewed and approved by the Ethics Committee (CER-VD 2020–00334). The patients/participants provided their written informed consent to participate in this study.

AUTHOR CONTRIBUTIONS

Conceptualization, AP, TL, CG, and DM; methodology: AP, TL, CG, and DM; investigation: AP, TL, and BB; formal analysis: AP

REFERENCES

- Abendroth-Smith, J. (1996). Stride Adjustments during a Running Approach toward a Force Plate. *Res. Q. Exerc. Sport* 67, 97–101. doi:10.1080/02701367.1996.10607930
- Alcantara, R. S., Day, E. M., Hahn, M. E., and Grabowski, A. M. (2021). Sacral Acceleration Can Predict Whole-Body Kinetics and Stride Kinematics across Running Speeds. *PeerJ* 9, e11199. doi:10.7717/peerj.11199
- Alexander, R. M. (1989). On the Synchronization of Breathing with Running in Wallabies (Macropusspp.) and Horses (*Equus caballus*). *J. Zoolog.* 218, 69–85. doi:10.1111/j.1469-7998.1989.tb02526.x
- Ammann, R., Taube, W., and Wyss, T. (2016). Accuracy of PARTwear Inertial Sensor and Optojump Optical Measurement System for Measuring Ground Contact Time during Running. *J. Strength Conditioning Res.* 30, 2057–2063. doi:10.1519/jsc.0000000000001299
- Atkinson, G., and Nevill, A. M. (1998). Statistical Methods for Assessing Measurement Error (Reliability) in Variables Relevant to Sports Medicine. *Sports Med.* 26, 217–238. doi:10.2165/00007256-199826040-00002
- Backes, A., Skejo, S. D., Gette, P., Nielsen, R. Ø., Sørensen, H., Morio, C., et al. (2020). Predicting Cumulative Load during Running Using Field-based Measures. *Scand. J. Med. Sci. Sports* 30, 2399–2407. doi:10.1111/sms.13796
- Bland, J. M., and Altman, D. G. (1995). Comparing Methods of Measurement: Why Plotting Difference against Standard Method Is Misleading. *The Lancet* 346, 1085–1087. doi:10.1016/s0140-6736(95)91748-9
- Brent, R. P. (1973). *Algorithms for Minimization without Derivatives*. Englewood Cliffs, NJ: Prentice-Hall.
- Broyden, C. G. (1970). The Convergence of a Class of Double-Rank Minimization Algorithms 1. General Considerations. *IMA J. Appl. Math.* 6, 76–90. doi:10.1093/imamat/6.1.76
- Camomilla, V., Bergamini, E., Fantozzi, S., and Vannozzi, G. (2018). Trends Supporting the In-Field Use of Wearable Inertial Sensors for Sport Performance Evaluation: A Systematic Review. *Sensors* 18, 873. doi:10.3390/s18030873
- Cavagna, G. A., Franzetti, P., Heglund, N. C., and Willems, P. (1988). The Determinants of the Step Frequency in Running, Trotting and Hopping in Man and Other Vertebrates. *J. Physiol.* 399, 81–92. doi:10.1113/jphysiol.1988.sp017069
- Cavagna, G. A., Legramandi, M. A., and Peyré-Tartaruga, L. A. (2008). Old Men Running: Mechanical Work and Elastic Bounce. *Proc. R. Soc. B.* 275, 411–418. doi:10.1098/rspb.2007.1288

and BB; writing—original draft preparation: AP; writing—review and editing: AP, TL, BB, CG, and DM; supervision: AP, TL, CG, and DM

FUNDING

This study was supported by Innosuisse (grant no. 35793.1 IP-LS).

ACKNOWLEDGMENTS

The authors warmly thank the participants for their time and cooperation.

SUPPLEMENTARY MATERIAL

The Supplementary Material for this article can be found online at: <https://www.frontiersin.org/articles/10.3389/fbioe.2021.687951/full#supplementary-material>

- Cohen, J. (1988). *Statistical Power Analysis for the Behavioral Sciences*. Oxfordshire, England, UK: Routledge.
- Da Rosa, R. G., Oliveira, H. B., Gomeñuka, N. A., Masiero, M. P. B., Da Silva, E. S., Zanardi, A. P. J., et al. (2019). Landing-takeoff Asymmetries Applied to Running Mechanics: A New Perspective for Performance. *Front. Physiol.* 10, 415. doi:10.3389/fphys.2019.00415
- Dalleau, G., Belli, A., Viale, F., Lacour, J. R., and Bourdin, M. (2004). A Simple Method for Field Measurements of Leg Stiffness in Hopping. *Int. J. Sports Med.* 25, 170–176. doi:10.1055/s-2003-45252
- Debaere, S., Jonkers, I., and Delecluse, C. (2013). The Contribution of Step Characteristics to Sprint Running Performance in High-Level Male and Female Athletes. *J. Strength Conditioning Res.* 27, 116–124. doi:10.1519/jsc.0b013e31825183ef
- Falbriard, M., Meyer, F., Mariani, B., Millet, G. P., and Aminian, K. (2018). Accurate Estimation of Running Temporal Parameters Using Foot-Worn Inertial Sensors. *Front. Physiol.* 9, 610. doi:10.3389/fphys.2018.00610
- Falbriard, M., Meyer, F., Mariani, B., Millet, G. P., and Aminian, K. (2020). Drift-Free Foot Orientation Estimation in Running Using Wearable IMU. *Front. Bioeng. Biotechnol.* 8, 65. doi:10.3389/fbioe.2020.00065
- Flaction, P., Quievre, J., and Morin, J. B. (2013). *An Athletic Performance Monitoring Device*. Washington, DC: U.S. Patent and Trademark Office patent application.
- Fletcher, R. (1970). A New Approach to Variable Metric Algorithms. *Comp. J.* 13, 317–322. doi:10.1093/comjnl/13.3.317
- Folland, J. P., Allen, S. J., Black, M. I., Handsaker, J. C., and Forrester, S. E. (2017). Running Technique Is an Important Component of Running Economy and Performance. *Med. Sci. Sports Exerc.* 49, 1412–1423. doi:10.1249/mss.0000000000001245
- Giandolini, M., Horvais, N., Rossi, J., Millet, G. Y., Samozino, P., and Morin, J.-B. (2016). Foot Strike Pattern Differently Affects the Axial and Transverse Components of Shock Acceleration and Attenuation in Downhill Trail Running. *J. Biomech.* 49, 1765–1771. doi:10.1016/j.jbiomech.2016.04.001
- Giandolini, M., Poupard, T., Gimenez, P., Horvais, N., Millet, G. Y., Morin, J.-B., et al. (2014). A Simple Field Method to Identify Foot Strike Pattern during Running. *J. Biomech.* 47, 1588–1593. doi:10.1016/j.jbiomech.2014.03.002
- Gindre, C., Lussiana, T., Hebert-Losier, K., and Morin, J.-B. (2016). Reliability and Validity of the Myotest for Measuring Running Strike Kinematics. *J. Sports Sci.* 34, 664–670. doi:10.1080/02640414.2015.1068436

- Goldfarb, D. (1970). A Family of Variable-Metric Methods Derived by Variational Means. *Math. Comp.* 24, 23. doi:10.1090/s0025-5718-1970-0258249-6
- Halilaj, E., Rajagopal, A., Fiterau, M., Hicks, J. L., Hastie, T. J., and Delp, S. L. (2018). Machine Learning in Human Movement Biomechanics: Best Practices, Common Pitfalls, and New Opportunities. *J. Biomech.* 81, 1–11. doi:10.1016/j.jbiomech.2018.09.009
- Hébert-losier, K., Mourot, L., and Holmberg, H.-C. (2015). Elite and Amateur Orienteers' Running Biomechanics on Three Surfaces at Three Speeds. *Med. Sci. Sports Exerc.* 47, 381–389. doi:10.1249/mss.0000000000000413
- Honert, E. C., Mohr, M., Lam, W.-K., and Nigg, S. (2020). Shoe Feature Recommendations for Different Running Levels: A Delphi Study. *PLOS ONE* 15, e0236047. doi:10.1371/journal.pone.0236047
- Kram, R., and Dawson, T. J. (1998). Energetics and Biomechanics of Locomotion by Red Kangaroos (*Macropus rufus*). *Comp. Biochem. Physiol. B: Biochem. Mol. Biol.* 120, 41–49. doi:10.1016/s0305-0491(98)00022-4
- Lee, J. B., Mellifont, R. B., and Burkett, B. J. (2010). The Use of a Single Inertial Sensor to Identify Stride, Step, and Stance Durations of Running Gait. *J. Sci. Med. Sport* 13, 270–273. doi:10.1016/j.jsams.2009.01.005
- Lussiana, T., Patoz, A., Gindre, C., Mourot, L., and Hébert-Losier, K. (2019). The Implications of Time on the Ground on Running Economy: Less Is Not Always Better. *J. Exp. Biol.* 222, jeb192047. doi:10.1242/jeb.192047
- Lussiana, T., and Gindre, C. (2016). Feel Your Stride and Find Your Preferred Running Speed. *Biol. Open* 5, 45–48. doi:10.1242/bio.014886
- Maiwald, C., Sterzing, T., Mayer, T. A., and Milani, T. L. (2009). Detecting Foot-To-Ground Contact from Kinematic Data in Running. *Footwear Sci.* 1, 111–118. doi:10.1080/19424280903133938
- Minetti, A. E. (1998). A Model Equation for the Prediction of Mechanical Internal Work of Terrestrial Locomotion. *J. Biomech.* 31, 463–468. doi:10.1016/s0021-9290(98)00038-4
- Moe-Nilssen, R. (1998). A New Method for Evaluating Motor Control in Gait under Real-Life Environmental Conditions. Part 1: The Instrument. *Clin. Biomech.* 13, 320–327. doi:10.1016/s0268-0033(98)00089-8
- Moore, I. S., Ashford, K. J., Cross, C., Hope, J., Jones, H. S. R., and McCarthy-Ryan, M. (2019). Humans Optimize Ground Contact Time and Leg Stiffness to Minimize the Metabolic Cost of Running. *Front. Sports Act Living* 1, 53. doi:10.3389/fspor.2019.00053
- Morin, J.-B., Dalleau, G., Kyröläinen, H., Jeannin, T., and Belli, A. (2005). A Simple Method for Measuring Stiffness during Running. *J. Appl. Biomech.* 21, 167–180. doi:10.1123/jab.21.2.167
- Norris, M., Anderson, R., and Kenny, I. C. (2014). Method Analysis of Accelerometers and Gyroscopes in Running Gait: A Systematic Review. *Proc. Inst. Mech. Eng. P: J. Sports Eng. Tech.* 228, 3–15. doi:10.1177/1754337113502472
- Novacheck, T. F. (1998). The Biomechanics of Running. *Gait & Posture* 7, 77–95. doi:10.1016/s0966-6362(97)00038-6
- Patoz, A., Lussiana, T., Thouvenot, A., Mourot, L., and Gindre, C. (2020). Duty Factor Reflects Lower Limb Kinematics of Running. *Appl. Sci.* 10, 8818. doi:10.3390/app10248818
- Press, W. H., Teukolsky, S. A., and Vetterling, W. T. (1992). *Numerical Recipes in FORTRAN: The Art of Scientific Computing*. Cambridge, England: Cambridge University Press.
- Purcell, B., Channells, J., James, D., and Barrett, R. (2006). Use of Accelerometers for Detecting Foot-Ground Contact Time during Running. *Proc. SPIE - Int. Soc. Opt. Eng.* 6036, 292–299. doi:10.1117/12.638389
- Shanno, D. F. (1970). Conditioning of Quasi-Newton Methods for Function Minimization. *Math. Comp.* 24, 647. doi:10.1090/s0025-5718-1970-0274029-x
- Smith, L., Preece, S., Mason, D., and Bramah, C. (2015). A Comparison of Kinematic Algorithms to Estimate Gait Events during Overground Running. *Gait & Posture* 41, 39–43. doi:10.1016/j.gaitpost.2014.08.009

Conflict of Interest: The authors declare that the research was conducted in the absence of any commercial or financial relationships that could be construed as a potential conflict of interest.

Publisher's Note: All claims expressed in this article are solely those of the authors and do not necessarily represent those of their affiliated organizations, or those of the publisher, the editors, and the reviewers. Any product that may be evaluated in this article, or claim that may be made by its manufacturer, is not guaranteed or endorsed by the publisher.

Copyright © 2021 Patoz, Lussiana, Breine, Gindre and Malatesta. This is an open-access article distributed under the terms of the Creative Commons Attribution License (CC BY). The use, distribution or reproduction in other forums is permitted, provided the original author(s) and the copyright owner(s) are credited and that the original publication in this journal is cited, in accordance with accepted academic practice. No use, distribution or reproduction is permitted which does not comply with these terms.

APPENDIX: JUSTIFICATION OF THE CHOICE OF THE t_{ce} X t_{fe} GRID

To justify the grid choice, a similar numerical analysis was carried out but using different grid spacings (2.5, 5, 7.5, 10, 25, 50, 75, and 100 ms). t_{ce} and t_{fe} values were varied between 2.5 and 505 ms, which led to 6 to 202 points for both t_{ce} and t_{fe} and grid sizes ranging from 36 to 40,804 total grid points. The boundary relationship between t_{ce} and t_{fe} was computed on each grid. RMSE on the testing set (15% points) as a function of the number of points along t_{ce} is depicted in **Figure A1**. Noteworthy, as for grid spacings of 75 and 100 ms, using a 15% size for the testing set did not provide at least two points in such set. Therefore, two random points were forced to be attributed to the testing test (29 and 33% points in the testing set). As expected, RMSE decreased with decreasing grid spacing. Besides, it can be noticed that using a grid spacing of 10 ms did not seem to impact RMSE for the boundary relationship compared to the 7.5-ms grid spacing used before (RMSE \sim 3.5 ms). However, the polynomial regression should also be performed on these different grids to observe any additional features.

For this reason, a multivariate polynomial regression (polynomial order from 1 to 15) was performed on 85% of the points composing these different grids, after having discarded the points which were not within the corresponding boundary relationship. RMSE on the testing set (15% points) as a function of grid size is depicted for each polynomial order in **Figure A1**. It can be noticed that

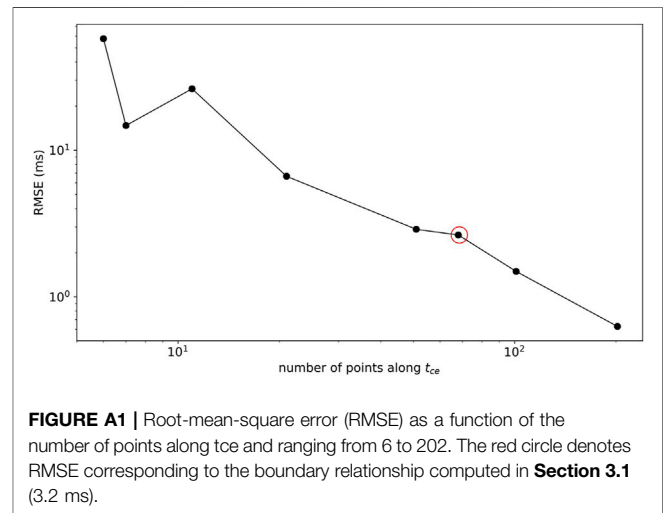


FIGURE A1 | Root-mean-square error (RMSE) as a function of the number of points along t_{ce} and ranging from 6 to 202. The red circle denotes RMSE corresponding to the boundary relationship computed in **Section 3.1** (3.2 ms).

the eighth-order polynomial is the lowest order polynomial, leading to an RMSE smaller than 0.5 ms on the testing set. In addition, the smallest grid to obtain such an RMSE threshold is given by a grid using a spacing of 7.5 ms, that is, 4,624 grid points. As for the grid spacing of 10 ms, it requires a polynomial of order 10 to achieve the requested RMSE threshold, which is less convenient as it requires 21 extra coefficients than the eighth-order polynomial. Therefore, these previous statements justify the grid choice used to construct the multivariate polynomial model (**Eq. 3**).

```
In[ ]:= Solve[Csc[( $\pi$  * tg) / (tce + 2 * tg)] ==  
             $\pi / 2 * ((tfe - 2 * tg) / (tce + 2 * tg) + 1), tg]$ 
```

... Solve: This system cannot be solved with the methods available to Solve.

```
Out[ ]:= Solve[Csc[ $\frac{\pi \text{tg}}{tce + 2 \text{tg}}$ ] ==  $\frac{1}{2} \pi \left(1 + \frac{tfe - 2 \text{tg}}{tce + 2 \text{tg}}\right), \text{tg}]$ 
```

9.5 There is no global running pattern more economic than another at endurance running speeds

Aurélien Patoz^{1,2,*}, Thibault Lussiana^{2,3,4}, Bastiaan Breine^{2,5}, Cyrille Gindre^{2,3}, Kim Hébert-Losier^{6,7}

¹ Institute of Sport Sciences, University of Lausanne, 1015 Lausanne, Switzerland

² Research and Development Department, Volodalen Swiss Sport Lab, 1860 Aigle, Switzerland

³ Research and Development Department, Volodalen, 39270 Chavéria, France

⁴ Research Unit EA3920 Prognostic Markers and Regulatory Factors of Cardiovascular Diseases and Exercise Performance, Health, Innovation platform, University of Bourgogne Franche-Comté, 2500 Besançon, France

⁵ Department of movement and Sports Sciences, Ghent University, 9000 Ghent, Belgium

⁶ Division of Health, Engineering, Computing and Science, Te Huataki Waiora School of Health, University of Waikato, Adams Centre for High Performance, 3116 Tauranga, New Zealand

⁷ Department of Sports Science, National Sports Institute of Malaysia, 57000 Kuala Lumpur, Malaysia

* Corresponding author

Published in **International Journal of Sports Physiology and Performance**

DOI: 10.1123/ijsp.2021-0345

There Is No Global Running Pattern More Economic Than Another at Endurance Running Speeds

Aurélien Patoz, Thibault Lussiana, Bastiaan Breine, Cyrille Gindre, and Kim Hébert-Losier

Purpose: The subjective Volodalen® score (V@score) and the objective duty factor metric can both assess global running patterns. The authors aimed to investigate the relation between running economy (RE) at endurance running speeds and the global running pattern quantified using both subjective and objective measures. **Methods:** RE and 3-dimensional whole-body kinematics were acquired by indirect calorimetry and an optoelectronic system, respectively, for 52 trained runners during treadmill runs at 10, 12, and 14 km/h. **Results:** Correlations between RE and V@score and RE and duty factor were *negligible* and nonsignificant across speeds tested ($P \geq .20$), except for a *low* and significant correlation between RE and V@score at 10 km/h. **Conclusions:** These findings suggest there is no global running pattern more economic than another at endurance running speeds. Therefore, there is no advantage of choosing, favoring, or prescribing one specific global running pattern along a continuum based on V@score or duty factor metrics, and coaches should not try to modify the spontaneous running pattern of runners at endurance running speed to improve RE.

Keywords: gait analysis, motion analysis, biomechanics, duty factor, Volodalen® score

As early as 1985, the running pattern was suggested to be multifactorial, and foot placement, arm swing, body angle, rear leg lift, and stride length should be considered together.¹ Following this concept, a subjective method allowing global definition of self-selected running patterns was created.² This method considers runners as global systems in which the change or alteration of one variable is likely to affect another. Runners are classified based on visual observations of 5 key elements where each element is scored on a 1 to 5 scale. The 5 individual scores are summed to provide a global score, the Volodalen® score (V@score), ranging from 5 to 25.² The resulting subjectively based score is used to classify runners in 2 groups: aerial (V@score > 15) and terrestrial (V@score ≤ 15).² The authors observed that runners in each group present similar running economy (RE) characteristics but employ different strategies to lower their energetic cost, with terrestrial runners relying more on forward propulsion strategies and aerial runners more on rebound strategies.²

Runners have also been categorized in 2 groups using the duty factor (DF),^{3,4} that is, an objective variable representing the ratio of ground contact time (t_c) to stride time [t_c + swing time (t_s)], with a higher DF reflecting a greater relative contribution of t_c to the running stride.⁵ DF was thought to be representative of a global biomechanical behavior, considering the duration of force

production (t_c) in relation to stride duration.^{3,4} Runners with a low DF exhibited a more symmetrical running step, anterior (midfoot and forefoot) strike pattern, and extended lower limb during t_c than runners with a high DF, whereas the latter runners exhibited greater lower limb flexion during t_c , more rearfoot strike pattern, and less work against gravity to generate forward propulsion.^{3,4} Therefore, runners with high and low DF values used different running strategies. Despite these kinematic differences, the 2 groups demonstrated similar RE values, indicating the 2 strategies are energetically equivalent at endurance running speeds.³

Given that the V@score and DF are continuous variables, the global running pattern of individuals could be defined along a continuum rather than categorized into 2 or more groups. However, the relation between RE and global running patterns along a continuum has, to the best of our knowledge, not been investigated so far. Hence, we aimed to investigate the relation between RE and global running pattern, assessed using either the subjective V@score or the objective DF metric. We hypothesized that RE would not be related to either V@score or DF.

Methods

Subjects

A total of 52 trained runners, 31 males (mean [SD]; age = 31 [8] y, height = 174 [7] cm, body mass = 66 [10] kg, 21.1 km recent running performance = 91 [9] min, running experience = 8 [6] y, weekly running distance = 55 [19] km) and 21 females (age = 32 [9] y, height = 162 [4] cm, body mass = 52 [5] kg, 21.1 km recent running performance = 102 [9] min, running experience = 7 [4] y, weekly running distance = 50 [21] km) participated in this study. Participants were required to be in good self-reported general health, with no current or recent (<3 mo) musculoskeletal injuries, and to have competed in a road race in the last year with finishing times of 10 km ≤ 50 min, 21.1 km ≤ 110 min, or 42.2 km ≤ 230 min. The ethical committee of the National Sports Institute of Malaysia

Patoz is with the Inst of Sport Sciences, University of Lausanne, Lausanne, Switzerland. Patoz, Lussiana, Breine, and Gindre are with the Research and Development Dept, Volodalen Swiss Sport Lab, Aigle, Switzerland. Lussiana and Gindre are with the Research and Development Dept, Volodalen, Chavéria, France. Lussiana is also with the Research Unit EA3920 Prognostic Markers and Regulatory Factors of Cardiovascular Diseases and Exercise Performance, Health, Innovation Platform, University of Bourgogne Franche-Comté, Besançon, France. Breine is also with the Dept of Movement and Sports Sciences, Ghent University, Ghent, Belgium. Hébert-Losier is with the Div of Health, Engineering, Computing and Science, Te Huataki Waiora School of Health, University of Waikato, Adams Centre for High Performance, Tauranga, New Zealand, and the Dept of Sports Science, National Sports Inst of Malaysia, Kuala Lumpur, Malaysia. Patoz (aurelien@volodalen.com) is corresponding author.

approved the study protocol (ISNRP: 26/2015), which adhered to the latest Declaration of Helsinki.

Design

Each participant completed one experimental laboratory session. After providing written informed consent, participants ran 5 minutes at 9 km/h on a treadmill (h/p/cosmos mercury®; h/p/cosmos sports & medical gmbh, Nussdorf-Traunstein, Germany) as warm-up. Participants then completed three 4-minute runs at 10, 12, and 14 km/h (with 2-min recovery between runs) on the treadmill, during which time RE was assessed (Appendix A). RE was expressed as the oxygen cost per mass to the power of 0.75 per kilometer (in milliliter per kilometer per kilogram^{0.75}) to minimize the influence of body mass per se on oxygen consumption during running.⁶ A higher RE value indicates a less economical runner.

Retroreflective markers were subsequently positioned on individuals to assess running kinematics (Appendix B). For each participant, a 1-second static calibration trial was recorded, which was followed by three 30-second runs at 10, 12, and 14 km/h (with 1-min recovery between runs) to collect 3-dimensional (3D) kinematic data in the last 10 seconds segment of these runs. RE and biomechanics were assessed separately given laboratory constraints and interference with data quality (eg, presence of testing equipment that occluded markers). All participants were familiar with running on a treadmill as part of their usual training programs and wore their habitual running shoes during testing (shoe mass = 223 [36] g, shoe stack height = 25 [3] mm, and shoe heel-to-toe drop = 8 [3] mm).

Methodology

The 5 elements of the V@score were objectively retrieved from 3D kinematic data (Appendix C). Each element was converted to a score from 1 to 5 using the 20th, 40th, 60th, 80th, and 100th percentiles. The V@score was subsequently obtained by summing these 5 objectively measured elements.

t_s and t_c were defined as the time from toe-off to foot strike and from foot strike to toe-off of the same foot, respectively, to calculate DF as⁵:

$$DF = \frac{t_c}{t_c + t_s}.$$

The biomechanical variables extracted from the 10-second data collection for each participant were averaged for subsequent statistical analyses.

Statistical Analysis

Descriptive statistics are presented using mean (SD). As all data were normality distributed based on Kolmogorov–Smirnov tests ($P \geq .08$), we extracted Pearson correlation coefficients (r) with 95% confidence intervals and corresponding P values to explore the relationship between RE and V@score and RE and DF at the 3 running speeds separately. Correlations were considered *very high*, *high*, *moderate*, *low*, and *negligible* when absolute r values were between .90 and 1.00, .70 and .89, .50 and .69, .30 and .49, and .00 and .29, respectively.⁹ Statistical analyses were performed using Jamovi (version 1.6.23; <https://www.jamovi.org>) with a level of significance set at $P \leq .05$.

Results

Correlations between RE and V@score and between RE and DF were *negligible* and nonsignificant at all tested speeds ($|r| \leq .18$; $P \geq .20$), except for a *low* and significant correlation between RE and V@score at 10 km/h ($r = .30$; $P = .03$; Figure 1).

Discussion

In line with our hypothesis, RE was not related to either V@score or DF, except at 10 km/h where a *low* correlation was observed between RE and V@score. This single *low* correlation suggests little clinical relevance and a potential spurious finding (Figure 1A). Similarly, no significant relation between RE and DF was detected (Figure 1B). This suggests that runners with a global running pattern at either ends of the subjective spectrum (most terrestrial, V@score = 5; vs most aerial, V@score = 25), or objective DF spectrum (highest vs lowest DF) exhibit similar RE at endurance running speeds. Therefore, there is no advantage of choosing, favoring, or prescribing one specific global running pattern along a continuum based on V@score or DF metrics. These results confirm previous findings of similar RE between runners categorized as terrestrial and aerial,² or as high and low DF runners.³

The subconscious fine-tuning of running biomechanics, known as self-optimization, was first introduced by Williams and Cavanagh¹⁰ and extended upon by Moore.¹¹ The concept of self-optimization might explain the null relationship found between RE and global running pattern. Indeed, RE was proposed to result from a weighted influence of several variables.¹⁰ Moreover, runners appear to naturally adopt a running biomechanics (eg, stride length, stride frequency, contact time, leg stiffness) that is energetically optimal, or at least near optimal.^{11,12} This altogether suggests that the relative importance of these underlying variables might differ along the spectrum of global running patterns as defined using the V@score or DF metric but that all these different global running patterns lead to a similar RE. Determining the global running pattern of a runner might nonetheless inform which variables are contributing the most to RE and not yet optimized for a given individual. Hence, slight alterations in suboptimal and interconnected variables might confer RE advantages at an individual level, notwithstanding that most biomechanical fine-tuning to improve RE may have already occurred in trained and experienced runners.¹¹

Practical Applications

There is no advantage of choosing, favoring, or prescribing one specific global running pattern along a continuum based on V@score or DF metrics. Therefore, coaches should not try to modify the spontaneous running pattern of runners at endurance running speed to improve RE.

Conclusions

The current study findings suggest there is no significant or meaningful relation between RE and global running pattern, assessed using either the V@score or the DF metric, meaning that any spontaneous self-selected running style might be energetically optimal. In other words, there is no global running pattern more economic than another at endurance running speeds.

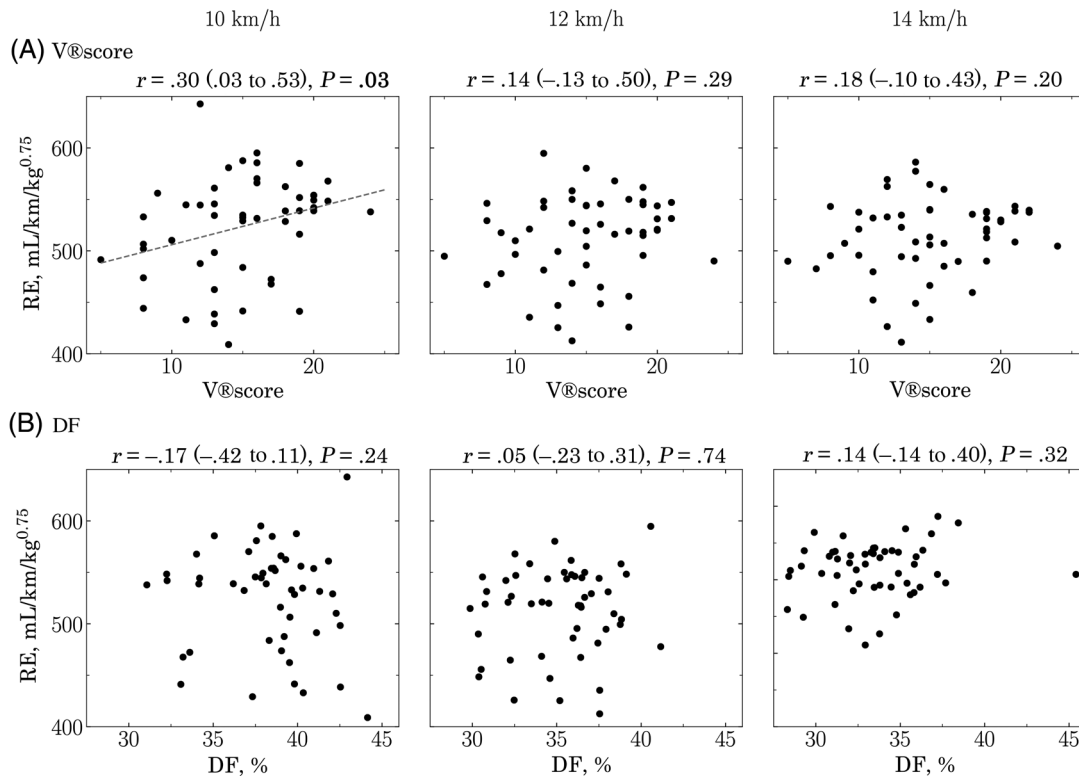


Figure 1 — RE as function of (A) V@score and (B) DF at 3 different running speeds for 52 participants. Statistical significance ($P \leq .05$) is indicated in bold. The gray dashed line between RE and V@score at 10 km/h represents a significant but low Pearson correlation. DF indicates duty factor; r , Pearson correlation coefficient together with its 95% CIs (lower and upper); RE, running economy; V@score, Volodalen® score.

Acknowledgments

The authors thank Mr. Chris Tee Chow Li for assistance during the data collection process. The authors also thank the participants for their time and participation. This study was financially supported by the University of Bourgogne Franche-Comté (France) and the National Sports Institute of Malaysia. C.G. is the originator of the Volodalen® scale. However, this paper does not constitute endorsement of the scale by the other authors and stems completely from a PhD research project undertaken at the Franche-Comté University by T.L. The data set supporting this article is available on request to the corresponding author. Conceptualization was done by T.L., C.G., and K.H.-L.; methodology by T.L., C.G., and K.H.-L.; investigation was by T.L. and K.H.-L.; formal analysis by T.L., A.P., B.B., and K.H.-L.; writing—original draft preparation—by A.P. and B.B.; writing—review and editing—by A.P., T.L., B.B., C.G., and K.H.-L.; supervision was by K.H.-L.; and funding acquisition was done by T.L. and K.H.-L.

References

- Subotnick SI. The biomechanics of running. Implications for the prevention of foot injuries. *Sports Med.* 1985;2(2):144–153. PubMed ID: [2860714](#) doi:[10.2165/00007256-198502020-00006](#)
- Lussiana T, Gindre C, Hébert-Losier K, Sagawa Y, Gimenez P, Mourot L. Similar Running economy with different running patterns along the aerial-terrestrial continuum. *Int J Sports Physiol Perform.* 2017;12(4):481. PubMed ID: [27617625](#) doi:[10.1123/ijspp.2016-0107](#)
- Lussiana T, Patoz A, Gindre C, Mourot L, Hébert-Losier K. The implications of time on the ground on running economy: less is not always better. *J Exp Biol.* 2019;222(6):jeb192047. doi:[10.1242/jeb.192047](#)
- Patoz A, Lussiana T, Thouvenot A, Mourot L, Gindre C. Duty factor reflects lower limb kinematics of running. *Appl Sci.* 2020;10(24):8818.
- Minetti AE. A model equation for the prediction of mechanical internal work of terrestrial locomotion. *J Biomech.* 1998;31(5):463–468. PubMed ID: [9727344](#) doi:[10.1016/S0021-9290\(98\)00038-4](#)
- Svedenhag J, Sjödin B. Body-mass-modified running economy and step length in elite male middle- and long-distance runners. *Int J Sports Med.* 1994;15(6):305–310. PubMed ID: [7822068](#) doi:[10.1055/s-2007-1021065](#)
- Altman AR, Davis IS. A kinematic method for footstrike pattern detection in barefoot and shod runners. *Gait Posture.* 2012;35(2):298–300. PubMed ID: [22075193](#) doi:[10.1016/j.gaitpost.2011.09.104](#)
- Lussiana T, Gindre C, Mourot L, Hébert-Losier K. Do subjective assessments of running patterns reflect objective parameters? *Eur J Sport Sci.* 2017;17(7):847–857. PubMed ID: [28488928](#) doi:[10.1080/17461391.2017.1325072](#)
- Hinkle DE, Wiersma W, Jurs SG. *Applied Statistics for the Behavioral Sciences.* 5th ed. Boston, MA: Houghton Mifflin; 2002.
- Williams KR, Cavanagh PR. Relationship between distance running mechanics, running economy, and performance. *J Appl Physiol.* 1987;63(3):1236–1245. PubMed ID: [3654469](#) doi:[10.1152/jappl.1987.63.3.1236](#)
- Moore IS. Is there an economical running technique? A review of modifiable biomechanical factors affecting running economy. *Sports Med.* 2016;46(6):793–807. PubMed ID: [26816209](#) doi:[10.1007/s40279-016-0474-4](#)

12. Moore IS, Ashford KJ, Cross C, Hope J, Jones HSR, McCarthy-Ryan M. Humans optimize ground contact time and leg stiffness to

minimize the metabolic cost of running. *Front Sports Act Living*. 2019;1:53. PubMed ID: [33344976](#) doi:[10.3389/fspor.2019.00053](#)

Appendix A: Gas Exchange Analysis

Gas exchange was measured using TrueOne 2400 (ParvoMedics, Inc, Sandy, UT) during the three 4-minute runs. Prior to the experiment, the gas analyzer was calibrated using ambient air (O₂: 20.93% and CO₂: 0.03%) and a gas mixture of known concentration (O₂: 16.00% and CO₂: 4.001%). Volume calibration was performed at different flow rates with a 3-L calibration syringe (5530 series; Hans Rudolph, Shawnee, KS). Oxygen consumption, carbon dioxide production, and respiratory

exchange ratio values were averaged over the last minute of each 4-minute run. Steady state was confirmed through visual inspection of the oxygen consumption and carbon dioxide production curves. Respiratory exchange ratio had to remain below unity during the trials for data to be included in the analysis; otherwise, the corresponding data were excluded as deemed to not represent a submaximal effort. No trial was excluded on this basis.

Appendix B: Kinematic Analysis

The 3D kinematic data were collected at 200 Hz using 7 infrared Oqus cameras (5 Oqus 300+, one Oqus 310+, and one Oqus 311+) and Qualisys Track Manager software (version 2.1.1) build 2902 together with the Project Automation Framework Running package (version 4.4; Qualisys AB, Göteborg, Sweden). A virtual laboratory coordinate system was generated such that the x - y - z axes denoted the mediolateral (pointing toward the right side of the body), posterior–anterior, and inferior–superior directions, respectively. A total of 35 retroreflective markers of 12 mm in diameter were used for static calibration and dynamic running trials and were affixed to the skin and shoes of individuals over anatomical landmarks using double-sided tape following standard guidelines from the Project Automation Framework Running package, as already reported elsewhere.³ The 3D marker data were exported in .c3d format and processed in Visual3D Professional software (version 5.02.25; C-Motion Inc, Germantown, MD). More explicitly, the 3D marker data were interpolated using a third-order polynomial least-square fit algorithm, allowing a maximum of 20 frames for gap filling, and subsequently low-pass filtered at 20 Hz using a fourth-order Butterworth filter.

From the marker set, a full-body biomechanical model with 6 degrees of freedom at each joint and 15 rigid segments was constructed. The model included the head, upper arms, lower arms, hands, thorax, pelvis, thighs, shanks, and feet. Segments were assigned inertial properties and center of mass (COM) locations based on their shape and relative mass. Kinematic parameters were calculated using rigid-body analysis and whole-body COM location was calculated from the parameters of all 15 segments.

Running events were derived from the trajectories of the 3D marker data using similar procedures to those previously reported elsewhere.³ More explicitly, a midfoot landmark was generated midway between the heel and toe markers. Foot-strike was defined as the instance when the midfoot landmark reached a local minimal vertical velocity prior to it reaching a peak vertical velocity reflecting the start of swing. Toe-off was defined as the instance when the toe marker attained a peak vertical acceleration before reaching a 7-cm vertical position. All events were verified to ensure correct identification and were manually adjusted when required.

Appendix C: Objective Measure of the 5 Elements of the V@score

The range of vertical displacement of the head COM, range of horizontal displacement of the elbow joint centers (ie, minimum to maximum horizontal position during each cycle), vertical position of the pelvis COM at foot strike, horizontal distance between the heel marker and pelvis COM at foot strike, and foot strike angle at ground contact were extracted. The first 4 elements were

normalized to participants' height. The foot strike angle was normalized to the foot-ground angle recording during the static trial following procedures described in Altman and Davis.⁷ These objective measures extracted from 3D data *largely* relate to their subjective Volodalen@ counterparts⁸ and were herein used to calculate the V@score.

9.6 Different plantar flexors neuromuscular and mechanical characteristics depending on the preferred running form

Sidney Grosprêtre^{1,*}, Philippe Gimenez¹, Adrien Thouvenot^{2,3}, Aurélien Patoz⁴, Thibault Lussiana^{2,3}, Laurent Mourot^{3,5}

¹ EA4660-C3S Laboratory - Culture, Sports, Health and Society, Univ. Bourgogne Franche-Comté, Besançon, France

² Research and Development Department, Volodalen, Chavéria, France

³ EA3920-Prognostic Markers and Regulatory Factors of Heart and Vascular Diseases, and Exercise Performance, Health, Innovation Platform, Univ. Bourgogne Franche-Comté, Besançon, France

⁴ Research and Development Department, Volodalen Swiss Sport Lab, Aigle, Switzerland

⁵ National Research Tomsk Polytechnic University, Tomsk, Russia

* Corresponding author

Published in **Journal of Electromyography and Kinesiology**

DOI: 10.1016/j.jelekin.2021.102568



Different plantar flexors neuromuscular and mechanical characteristics depending on the preferred running form

Sidney Grosprêtre^{a,*}, Philippe Gimenez^a, Adrien Thouvenot^{b,c}, Aurélien Patoz^d, Thibault Lussiana^{b,c}, Laurent Mourot^{c,e}

^a EA4660-C3S Laboratory - Culture, Sports, Health and Society, Univ. Bourgogne Franche-Comté, Besançon, France

^b Research and Development Department, Volodalen, Chavéria, France

^c EA3920-Prognostic Markers and Regulatory Factors of Heart and Vascular Diseases, and Exercise Performance, Health, Innovation Platform, Univ. Bourgogne Franche-Comté, Besançon, France

^d Research and Development Department, Volodalen Swiss Sport Lab, Aigle, Switzerland

^e National Research Tomsk Polytechnic University, Tomsk, Russia

ARTICLE INFO

Keywords:

Triceps surae
Electromyography
Rate of force development
Twitch
H-reflex
Running

ABSTRACT

Two main types of endurance runners have been identified: aerial runners (AER), who have a larger flight time, and terrestrial runners (TER), who have a longer ground contact time. The purpose of this study was to assess the neuromuscular characteristics of plantar flexors between AER and TER runners. Twenty-four well-trained runners participated in the experiment. They were classified either in a TER or AER group according to the Volodalen® scale. Plantar flexors' maximal rate of force development (RFD) and maximal voluntary contraction force (MVC) were assessed. Percutaneous electrical stimulation was delivered to the posterior tibial nerve to evoke maximal M-waves and H-reflexes of the triceps surae muscles. These responses, as well as voluntary activation, muscle potentiation, and V-waves, were recorded by superimposing stimulations to MVCs. RFD was significantly higher in AER than in TER, while MVC remained unchanged. This was accompanied by higher myoelectrical activity recorded in the soleus muscle. While M-waves and other parameters remained unchanged, maximal H-reflex was significantly higher in AER than in TER, still in soleus only. The present study raised the possibility of different plantar flexors' neuromuscular characteristics according to running profile. These differences seemed to be focused on the soleus rather than on the gastrocnemii.

1. Introduction

Sport practice has several long-term effects on the musculoskeletal system and neural network. When comparing athletes from untrained individuals, athletes showed greater force production capacity, as evidenced by higher rates of force development (RFD) (Tillin et al., 2010) and higher central activation (Ahtiainen and Häkkinen, 2009). Regarding some specific neural parameters, such as spinal excitability, the direction of the change depends upon the type of physical activity. Indeed, while power athletes usually exhibit lower values than untrained people, endurance athletes show greater spinal excitabilities

(Maffioletti et al., 2001).

In most of the previous literature, endurance athletes from various sports (e.g., cycling, running, triathlon, cross-country skiing) have been pooled together and compared to power athletes (mixing sprinters, jumpers, or throwers). However, it could be hypothesized that different neuromuscular profiles also exist when considering a narrower portion of the continuum between endurance- and power-type athletes, i.e. targeting inter-individual differences within the same activity. Specifically, endurance running appears to be an activity for which various running forms may exist among its practitioners, e.g., ranging from “Groucho” to “Pose” running styles (Arendse et al., 2004; McMahon

Abbreviations: AER, Group of aerial runners; TER, Group of terrestrial runners; MVC, Maximal Voluntary Contraction; V@score, Global Subjective Score; VAL, Voluntary Activation Level; SOL, Soleus muscle; GM, Gastrocnemius Medialis; GL, Gastrocnemius Lateralis; TA, Tibialis Anterior; VL, Vastus Lateralis; H_{MAX}, Maximal H-reflex at rest; H_{SUP}, Maximal superimposed H-reflex (evoked during the MVC); M_{atHmax}, M-wave accompanying H_{max}; M_{atHsup}, M-wave accompanying H_{sup}; M_{MAX}, Maximal M-wave at rest; M_{SUP}, Maximal superimposed M-wave (evoked during the MVC); RFD, Rate of Force Development; RMS, Root Mean Square of muscle electromyographic activity (EMG); EME, Electro-mechanical Efficiency; PT, Peak of the single twitch.

* Corresponding author at: EA4660-C3S “Culture, Sport, Health and Society”, UPFR Sport, 31, chemin de l'Épitaphe, 25000 Besançon, France.

E-mail address: sidney.grospretre@univ-fcomte.fr (S. Grosprêtre).

<https://doi.org/10.1016/j.jelekin.2021.102568>

Received 6 November 2020; Received in revised form 30 May 2021; Accepted 10 June 2021

Available online 16 June 2021

1050-6411/© 2021 Elsevier Ltd. All rights reserved.

et al., 1987).

Objective (Hoerzer et al., 2015; Lussiana et al., 2019; Phinyomark et al., 2015) and subjective (Lussiana et al., 2017b) kinematic and spatio-temporal differences between endurance runners have then been revealed. The terms Terrestrial (TER) and Aerial (AER) runners have been proposed to characterize these different running forms (Gindre et al., 2016). These TER and AER runners have been shown to have the same running economy (Lussiana et al., 2019, 2017a). To minimize the cost of movement, TER favour a long contact time associated with a rearfoot strike pattern, whereas AER favour a long flight time together with a forefoot strike pattern (Lussiana et al., 2019, 2017a). These observations were accompanied by an earlier activation of the gastrocnemius lateralis (GL) in preparation for landing in AER compared to TER (Lussiana et al., 2017a). Hence, the plantar flexor muscles group seems to be a key muscle group affected by the type of running pattern. Moreover, these muscles are one of the main investigated muscle groups in neuromuscular studies (Tucker et al., 2005). Early works using a similar approach at the ankle joint already identified links between kinematic variables and structural / neural properties of the plantar flexors of short and long-distance runners (Bach et al., 1983). The authors concluded that both neural and mechanical factors were key factors in determining the running pattern. Therefore, the purpose of the present study was to compare the neuromuscular and mechanical properties of the plantar flexors between AER and TER during a non-specific task. As AER have shorter ground contact time and forefoot strike pattern, we hypothesized that they would exhibit greater spinal excitability compared to TER that have longer ground contact time, possibly reflecting higher mechanical load on the plantar flexor muscles.

2. Material and methods

2.1. Participants

Twenty-four well-trained healthy participants (7 women and 17 men) gave written informed consent to participate in the present experiment (Table 1). None of them reported neurological, physical disorders, or previous lower-limb injury in the previous six months. All experimental procedures were performed in accordance with the latest version of the Declaration of Helsinki and approved by the Regional Ethics Committee (CPP Est I 2016-A00511-50).

2.2. Experimental design

The experiment was carried out in a single session (1 h 45 min), which included two parts performed randomly: an evaluation of the participant's running form (15 min) and a neuromuscular and mechanical evaluation (1 h 30 min). Both parts were performed in separate rooms with different operators, in a double-blind set-up : participants and operators were not informed of the results of the other experimental part (neuromuscular and runner's classification).

Table 1
Participant characteristics for Terrestrial (TER) and Aerial (AER) groups.
Note: Data are means \pm S.D. M: Male, F: Female, and NA: statistical test not applicable.

	TER	AER	P value
Age (y)	29.6 \pm 10.5	25.4 \pm 8.0	0.286
Height (m)	1.71 \pm 0.07	1.76 \pm 0.06	0.213
Mass (kg)	64.2 \pm 9.2	62.1 \pm 7.5	0.551
Training experience (y)	5.9 \pm 3.8	6.8 \pm 5.9	0.658
Running time (h/week)	4.9 \pm 1.9	7.1 \pm 3.6	0.072
Running distance (km/week)	42.5 \pm 12.1	51.7 \pm 16.5	0.136
Maximum aerobic speed (km/h)	17.2 \pm 1.3	18.4 \pm 1.8	0.084
V@score	11.7 \pm 1.9	20.2 \pm 2.2	NA
Sex	M = 6; F = 6	M = 11; F = 1	NA

2.3. Runner's classification

Participants performed a 5-min running warm-up at a self-selected speed, followed by a 10-min running trial at 12 km·h⁻¹ on a treadmill (Training Treadmill S1830, HEF Techmachine, Andrézieux-Bouthéon, France). Two running coaches with several years of experience using the Volodalen® scale focused on the overall movement form of participants as they ran. The coaches paid attention to five key elements: vertical oscillation of the head, antero-posterior motion of the elbows, pelvis position at ground contact, antero-posterior foot position at ground contact, and foot strike pattern (Gindre et al., 2016; Lussiana et al., 2017a). The intra- and inter-rater reliability of this method has been shown recently (Patoz et al., 2019). Each element was scored from one to five, leading to a global subjective score (V@score) that ultimately allows the classification of runners into TER (V@score \leq 15) or AER (V@score $>$ 15) group.

2.4. Force recordings

Participants seated in a comfortable experimental chair with hip, knee and ankle joints at 90°. The ankle was firmly strapped to a pedal equipped with a constraint gauge (PCE instruments, Soultz-Sous-Forêts France). They were instructed to keep their hands free and to maintain the trunk against chair's back. The recording of one antagonist (i.e., tibialis anterior, TA) and one knee extensor (i.e., vastus lateralis, VL) allowed to monitor the contribution of other muscle groups to the developed force.

Participants were first asked to warm-up by performing eight to ten sub-maximal isometric plantar flexions at a progressive force level. Then, they performed eight isometric plantar flexion maximal voluntary contractions (MVC) of about 4 s, separated by one-minute rest. During the plateau of each MVC, one nerve stimulation was triggered. The recording of RFD was assessed separately from MVC, as previously recommended (Maffioletti et al., 2016). Participants were asked to "push hard and fast" up to their maximal force, without maintaining it. A total of eight to ten trials was performed, with 30 s rest in-between. Trials with countermovement (dorsi-flexion preceding the start of the plantar flexion) were excluded.

The mechanical signals were digitized on-line (sampling frequency: 2 kHz) and simultaneously recorded with electromyography of the targeted muscles. Signals were stored for analysis in Labchart software (LabChart 8, ADInstruments, Sydney, Australia).

2.5. Electromyographic activity

Electromyographic activity (EMG) was recorded from four muscles of the right leg (soleus, SOL; gastrocnemius medialis, GM; gastrocnemius lateralis, GL; TA; VL). The skin was first shaved and dry-cleaned with alcohol to keep low impedance ($<$ 5 k Ω). EMG signals were recorded with Trigno sensors (Delsys, Natick, Massachusetts, USA), firmly strapped to the leg with a skin rubber. Sensors were placed according to SENIAM recommendations (Hermens et al., 2000). EMG signals were amplified with a bandwidth frequency ranging from 0.3 Hz to 2 kHz (gain: 1000) and digitized on-line (sampling frequency: 2 kHz) with Labchart software (LabChart 8, ADInstruments, Sydney, Australia).

2.6. Electrical nerve stimulation

The posterior tibial nerve was stimulated through single rectangular pulses (1-ms duration) delivered by a constant-current stimulator (Digitimer DS7A, Hertfordshire, UK). Stimulations were elicited with a self-adhesive cathode (8-mm diameter, Ag-AgCL) placed in the popliteal fossa and an anode (5 \times 10 cm, Medicomplex SA, Ecublens, Switzerland) placed over the patella. Once the optimal spot was determined, the stimulation electrode was firmly fixed to this site with straps. The intensity of the stimulation was then progressively increased from SOL,

GM and GL H-reflex threshold with 2 mA increment to maximal H-reflex (H_{MAX}) and then with 5 mA increment until M-wave of the three muscles no longer increased. This last stimulation-intensity was then increased by 20% to record maximal M-wave (M_{MAX}). Four stimulations were performed at each intensity.

2.7. Data analyses

All data were stored, synchronized and analyzed in LABCHART 8 software (LabChart 8, ADInstruments, Sydney, Australia).

2.8. Mechanical data

The RFD was analysed as the derivate of the mechanical signal (in $N \cdot sec^{-1}$) during the contraction ramp, i.e., from the baseline to the peak of force produced. The mean of the best three trials was analysed.

Maximal isometric force was taken as the peak of the mechanical signal obtained during the plateau of MVC prior to the stimulus artefact. Voluntary activation level (VAL) was determined using the twitch interpolation technique by using the following formula

$$VAL = 100 \left[1 - \left(\frac{PT_S}{PT_P} \right) \right],$$

where PT_S is the superimposed force amplitude induced by the stimulation at M_{MAX} intensity during the MVC. PT_P is the potentiated twitch force amplitude taken as the mechanical peak evoked at M_{MAX} following MVC.

Triceps surae potentiation was expressed as the change (%) between the amplitude of the resting twitch (PT_R) and PT_P

$$Potentiation = 100 \left[\frac{(PT_P - PT_R)}{PT_R} \right]$$

2.9. Electrophysiological data

The root mean square (RMS) value of SOL, GM and GL muscles EMG signals were determined with an integration time of 500 ms over the plateau during plantar flexion MVCs, prior to the stimulus artifacts. SOL and GM RMS were normalized by the corresponding M_{SUP} . During these RFDs, the contribution of each triceps surae muscle was calculated as the percentage of the sum of RMS/M_{SUP} of SOL, GM, and GL.

Peak-to-peak amplitudes of electromyographic responses at rest (H_{MAX} , M_{MAX}) and during MVC (H_{SUP} , M_{SUP} , V) were measured for quantitative analysis. It can be noticed that maximal H-reflex, reflecting spinal excitability, is generally associated with a small M-wave (noted M_{atHmax} at rest and M_{atHsup} during MVC), which was also measured. Contrary to rest, it can be noticed that M_{SUP} is followed by a reflexive response, called V-wave, which was used as an index of the supra-spinal descending neural drive (Grosprêtre and Martin, 2014). For each muscle, all responses were normalized to maximal M-wave evoked in the same condition. Thus, H_{MAX}/M_{MAX} , M_{atHmax}/M_{MAX} , H_{SUP}/M_{SUP} , M_{atHsup}/M_{SUP} , V/M_{SUP} , were considered as dependent variables and compared between TER and AER.

Finally, the total electro-mechanical efficiency (EME) was determined by the ratio of the peak twitch evoked at M_{max} (PT) over the sum of SOL and GM M-waves. EME reflects the excitation-contraction coupling efficiency.

2.10. Statistical analyses

All data are presented as the mean \pm standard deviation (S.D.). The normality of the data and the homogeneity of variances were confirmed through the Shapiro-Wilk and Levene's tests, respectively. Participant characteristics and dependent variables (mechanical and electrophysiological data) between AER and TER were analyzed through two-tailed

unpaired Student's t-tests. A separate analysis was performed for each muscle, except for the percentage of muscle contributions during the RFD, which were gathered for analysis, by means of a two-way ANOVA with factor *group* (AER vs. TER) and *muscle* (SOL vs. GM vs. GL). Main effects and interactions were followed-up by post hoc HSD Tukey's tests. Statistical analysis was performed using STATISTICA (8.0 version, Statsoft, Tulsa, Oklahoma, USA). The level of significance was set at $P < 0.05$.

3. Results

3.1. Characteristics of Aerial and Terrestrial runners

The participant characteristics for TER and AER are given in Table 1. All baseline characteristics were similar between both groups.

3.2. Mechanical data

There was no between-group difference observed in MVC ($P = 0.541$; Fig. 1A), mechanical twitches ($P = 0.454$; Fig. 1B) or activation levels ($P = 0.888$; Fig. 1C). However, muscle potentiation was significantly higher for TER than for AER ($P = 0.030$; Fig. 1D). No difference in EMG RMS recorded during MVC was found in any of the tested muscles between TER and AER (data not shown for the sake of clarity).

RFD was higher in AER than in TER ($P = 0.030$, Fig. 2A). This greater RFD in AER was accompanied by greater normalized EMG RMS observed in SOL muscle, while no differences were observed in gastrocnemii (Fig. 2B, C and D). When expressed as a percentage of the total activation (sum of all RMS/M_{SUP}), significant *group* \times *muscle* interaction has been found for the relative contributions of each muscle to the RFD ($P = 0.007$), AER showing a significantly greater SOL ($P = 0.010$) and a significantly lower GM ($P = 0.047$) muscles contribution to the RFD than TER (Fig. 2E).

3.3. Electrophysiological data

Firstly, no inter-group differences were found in muscle compound action potentials, for rest response (M_{MAX}) as for superimposed one (M_{SUP}), in any of the tested muscles. In addition, the submaximal M-waves that accompanied H-reflexes (M_{atHmax} and M_{atHsup}) did not differ between groups for all muscles.

Secondly, normalized maximal H-reflex at rest (H_{MAX}/M_{MAX}) was significantly higher in AER than TER for SOL muscle ($P = 0.040$; Fig. 3A), but not for GM ($P = 0.475$; Fig. 3B) and GL ($P = 0.804$, Fig. 3C). No significant differences were observed in superimposed H-reflexes (H_{SUP}/M_{SUP}) (SOL: $P = 0.346$; GM: $P = 0.170$; GL: $P = 0.711$, Fig. 3). Since V/M_{SUP} did not significantly differ between both groups for each tested muscle (SOL: $P = 0.573$; GM: $P = 0.509$; GL: $P = 0.533$, Fig. 3), no significant differences were found at the supraspinal level.

4. Discussion

The present study aimed to compare the neuromuscular and mechanical properties of the plantar flexors between two groups of endurance runners with different preferred running forms. AER exhibited higher RFD compared to TER despite a similar maximal peak force. This was accompanied by greater changes in SOL EMG activity and H-reflex for AER, whereas peripheral (M-waves) and supraspinal (V-waves) electrophysiological indexes were not different among groups. On the other hand, TER exhibited greater muscle potentiation, partly validating our hypothesis regarding this group.

4.1. Different muscle contributions

Leg muscles' contributions during running were different between AER and TER, as already shown during the running stance (Lussiana

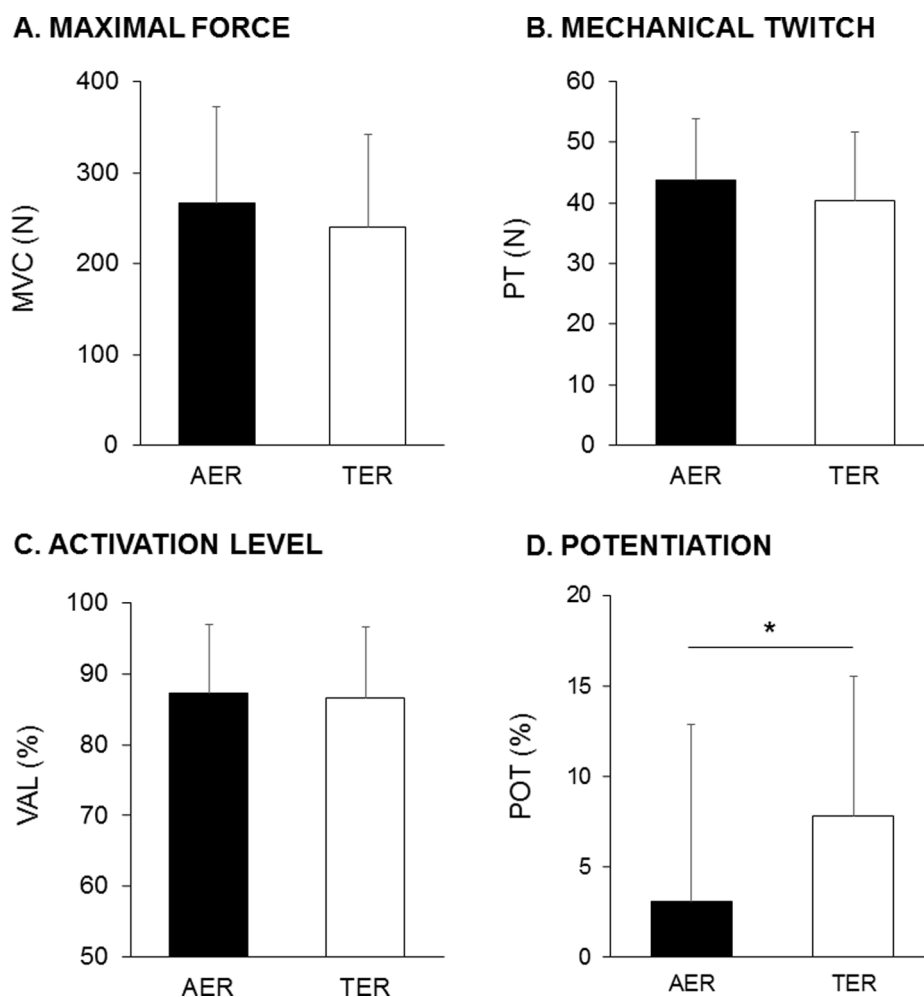


Fig. 1. Plantar flexors' mechanical data of Aerial (AER) and Terrestrial (TER) runners. Data are depicted as mean \pm SD. A. Maximal voluntary contraction (MVC) force. B. Peak-to-peak amplitude (PT) of the mechanical twitch associated with maximal M-wave. C. Voluntary activation level (VAL). D. Potentiation (POT) between the twitch evoked before the MVC and the twitch evoked after. *: significant inter-group difference at $P < 0.05$.

et al., 2017a). Concomitantly, it was shown that AER landed in a more plantar flexed position than TER. This suggests a greater contribution of the plantar flexor muscles in AER compared to TER, given its essential contribution at the ankle level. Accordingly, the results of the present study showed that AER exhibited a higher plantar flexor RFD compared to TER and the associated myoelectrical activities also argued in favor of a greater SOL contribution in such performance. AER is used to run with short contact time and large vertical oscillations. Therefore, for the same force production, AER could be able to support a greater RFD.

Given the fact that the tested performance was not running-specific, this result highlights a difference in general neural strategy. Our results showed that AER exhibited greater spinal excitability than TER in SOL muscle but not in gastrocnemii muscles. It has been shown that training of the plantar flexors can induce different adaptation in spinal excitabilities of SOL compared to GM (Duclay et al., 2008). These different adaptations can be attributed either to i) the different spinal network of SOL and gastrocnemii as a result of their different type of motor units, i. e. slow versus fast (Johnson et al., 1973) or ii) their difference in muscle spindles density, those which mediates the stretch reflex (Tucker et al., 2005). One interesting fact to notice is that one of the most effective modalities to induce such changes in spinal excitability and such discrepancy between muscles is eccentric training (Duclay et al., 2008). It was shown that SOL and gastrocnemii muscles exhibited different behavior in muscle fascicle stretch during plantar flexors eccentric actions but not always during concentric actions (Chino et al., 2008). These clues are in favor of greater eccentric load undertaken by AER.

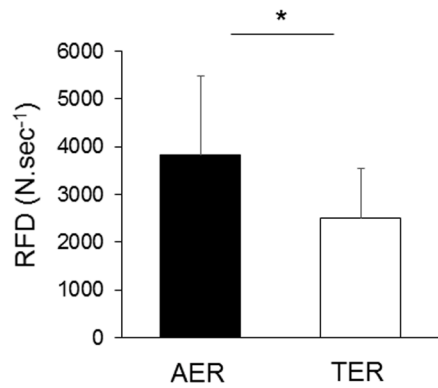
Indeed, plantar flexors being in eccentric modality during the first part of the stance, a larger aerial phase and vertical oscillation during the gait cycle leads to a higher load to support at landing, especially because AER favored a forefoot strike pattern (Lussiana et al., 2019, 2017a). Finally, although no significant inter-group difference in RMS/ M_{SUP} was observed for the gastrocnemii, it should be noted that the relative contributions of GM displayed a difference, while GL did not (Fig. 3). This result raises the fact that GM is the only muscle to compensate for a greater activation of SOL since GL exhibited a similar contribution between AER and TER.

4.2. Underlying mechanisms

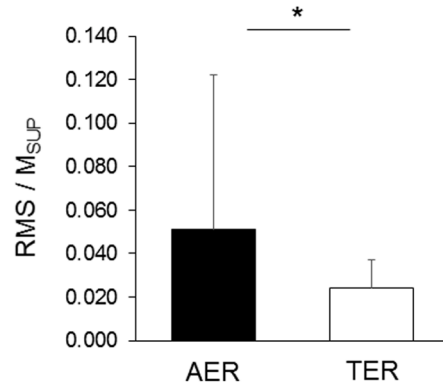
First of all, the lack of changes in MVC force, nor in VAL and V-wave amplitude, excludes a potential contribution of supraspinal levels to demonstrate the differences between the two groups. However, this does not preclude a more qualitative difference at a cortical level, such as different brain activations.

Regarding the RFD, a common opinion is to attribute a high performance to a high fast fibre proportion in the considered muscle group, being a marker of explosive muscle strength (Folland et al., 2014). Interestingly, although slightly superior in power athletes, the plantar flexors' RFD did not exhibit any differences between endurance- and power-type athletes. (Kyröläinen and Komi, 1994). These authors suggested that the global muscle mass or typology, could not be the unique factor to affect maximal RFD. For instance, despite conflicting results

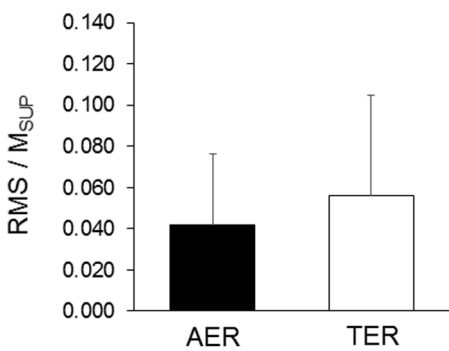
A. RATE OF FORCE DEVELOPMENT



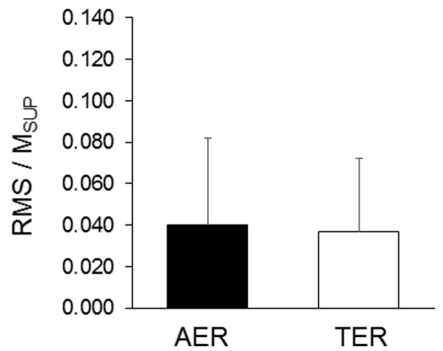
B. SOL



C. GM



D. GL



E. CONTRIBUTION OF EACH MUSCLE

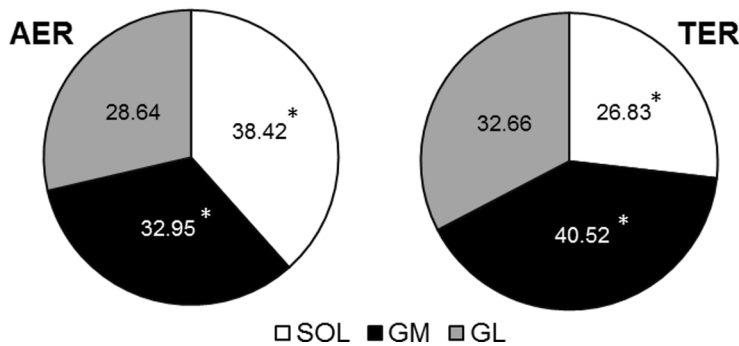


Fig. 2. Plantar flexors' rate of force development of Aerial (AER) and Terrestrial (TER) runners. Data are depicted as mean ± SD. A. Rate of force development (RFD) in plantar flexion. B, C and D, shows the associated peak in electromyographic activities, expressed as the root mean square of the activity (RMS) normalized by the maximal active M-wave (M_{SUP}), for the soleus muscle (SOL), gastrocnemius medialis (GM) and gastrocnemius lateralis (GL), respectively. Panel E depicts the relative contribution of each muscle to the RFD, in % of total muscle activity. *: significant intergroup difference at P < 0.05.

(Buckthorpe and Roi, 2018; Buckthorpe and Roi, 2018; Buckthorpe and Roi, 2018; Buckthorpe and Roi, 2018; Buckthorpe and Roi, 2018; Buckthorpe and Roi, 2018) a close link between plantar flexors RFD and musculo-tendinous stiffness has been observed (Driss et al., 2012). Hence, our previous observations of greater leg stiffness in AER as compared to TER (Gindre et al., 2016; Lussiana et al., 2017a) could partly explain this greater RFD in AER. But more importantly, several neural aspects, such as the synchronicity of motor unit recruitments and the efficiency of the neural drive, could also significantly impact RFD performance (Maffiuletti et al., 2016). In the present study, the difference observed in EMG activities recorded during RFD between AER and TER is the first clue that such plantar flexors' discrepancy also has a nervous origin. This is not surprising since a strong link is often established between an increase in RFD after training and an increase in the associated EMG activity of the considered muscle group (DelBalso and Cafarelli, 2007). Interestingly, a positive correlation between H-reflex and RFD increase has also been established after

plantar flexors training (Holtermann et al., 2007), raising the link between those neural factors and such performances. It was argued previously that the spinal efficiency was a primary factor in enhancing the discharge rate of the motor units needed to improve RFD performance (VanCutsem et al., 1998). In addition, early works of Capaday and Stein (Capaday and Stein, 1987) demonstrated that H-reflexes of the soleus muscles were lower during running than during walking, independently of the level of motor units activity. In other words, differences in H-reflexes can also occur between two different locomotor activities at a given similar EMG activity. Other central mechanisms such as presynaptic inhibition, closely related to muscle lengthening (Duchateau and Enoka, 2008), may be involved. This could also partly explain that the long-term use of different running patterns of AER and TER, and especially the fact that AER runners land in a more plantar flexed position than TER, would lead to long-term changes in spinal excitability. It is admitted that the type of training has a particular influence on medullary network plasticity (Grosprêtre et al., 2018), including interneuronal

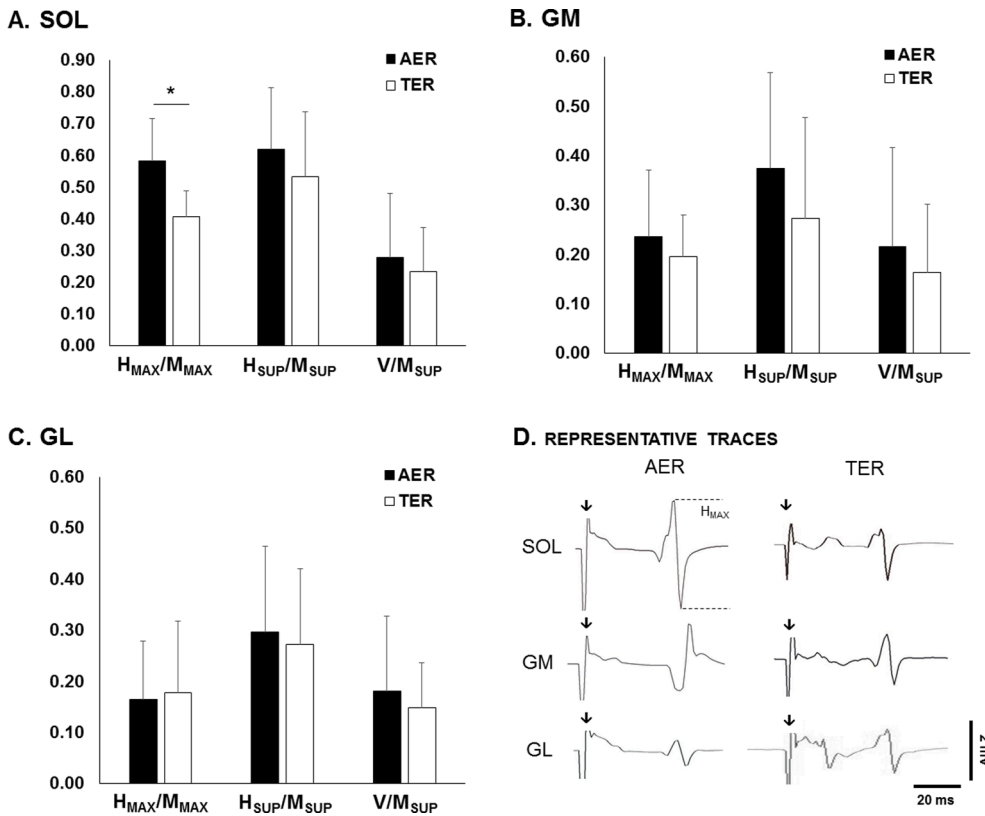


Fig. 3. Electrophysiological ratios of the triceps surae muscles of Aerial (AER) and Terrestrial (TER) runners. Data are depicted as mean \pm SD. Maximal rest H-reflex (H_{MAX}), maximal reflex evoked during maximal contraction (M_{SUP}) and voluntary wave (V) are normalized by their corresponding maximal M-wave (M_{MAX} or M_{SUP}). Results are depicted for the three muscles of the triceps surae: soleus (A, SOL), Gastrocnemius Medialis (B, GM) and Gastrocnemius Lateralis (C, GL). D shows the EMG traces of two representative participants. Signals are depicted for maximal H-reflex (H_{MAX}) of SOL, GM and GL. Vertical arrows represent the time of stimulation. *: significant inter-group difference at $P < 0.05$.

circuitry that controls and mediates the reflex pathway (Koceja et al., 2004). As a consequence, a greater SOL spinal excitability is usually observed in endurance- as compared to power athletes (Maffiuletti et al., 2001).

At muscle level, no electrophysiological differences have been observed, as evidenced by similar maximal muscle compound potentials (i.e. M-waves) between AER and TER. However, different muscle potentiations have been observed. Such twitch potentiation is attributed to intracellular muscle properties, such as the electrogenic Na^+-K^+ pumping efficiency (Cupido et al., 1996) or the intramuscular Ca^{2+} concentration (Klass, 2004). The fact that TER runners exhibit greater twitch potentiation than AER runners could indicate different intramuscular processes, although the twitch technique is not sufficiently accurate to discriminate one or the other cellular mechanisms.

4.3. Study limitations

Such a transversal study does not allow the genetic factor that could have led to recruit participants with particular profiles in the different trained groups to be distinguished. The constitution of groups, in terms of age, level of performance or anthropometric factors, is one of the primary key points of such inter-group comparison. Here, particular care was taken to keep both groups as homogenous as possible, particularly in terms of running experience. The lack of significant inter-group differences in participants' characteristics, limited the drawback of group constitutions. However, it should be noted that the different repartition of males and females between AER and TER could possibly interfere with the results. Some neuromuscular parameters were found to be higher in women than men, such as H_{MAX}/M_{MAX} ratio (Hoffman et al., 2018). However, the fact that more women were included in TER but greater H_{MAX}/M_{MAX} was observed in AER, highlights that gender difference did not affect the observed neuromuscular differences, or at worst should have minimized the differences. Overall, due to the lack of a significant global effect of sex on the several tested variables, we

suppose that the gender difference had a limited impact on the present results. It should be emphasized that most of the literature investigating sex differences in the previously mentioned performances and neuromuscular characteristics recruited untrained individuals.

Another consequence of such transversal study is the inability to decipher which parameter influences the other. In other terms, the question of whether neuromuscular characteristics determines the running profile or whether using a certain running profile during a long training period shapes the neuromuscular properties as part of a process of adaptation remains open. Previous studies using inter-group comparisons of several types of athletes involved also a control group of untrained participants, with similar characteristics (age, weight, etc) as a "baseline level" regarding neuromuscular parameters (Grosprêtre et al., 2018; Maffiuletti et al., 2001; Tillin et al., 2010). These previous studies tended to show that long term practice of one modality led to significant differences with the control group, in one direction or another. For instance, while triceps surae H-reflex is shown to be reduced in power athletes as compared to control, it is enhanced for endurance athletes (Maffiuletti et al., 2001). Finally, the best to understand the possible links between running profiles and neuromuscular parameters would be a longitudinal approach. Performing a long-term analysis of the neuromuscular parameters evolution with one or the other modality of running could help answering this key question.

5. Conclusion

Here, the differences observed between AER and TER runners raised a close link between running forms and neuromuscular and mechanical parameters. AER exhibited higher RFD accompanied by greater SOL EMG activity and H-reflex than TER. The mechanisms underlying different neuromuscular and mechanical profiles of AER and TER depicted a bottom-to-top gradient, significant effects being observed at muscle and spinal levels while no effect were found for any of the supraspinal indexes investigated. These differences seemed to be

muscle-specific, SOL being the most important muscle to differentiate AER and TER. Therefore, our results extended previous studies showing neuromuscular and mechanical properties differences in different sports by highlighting that neuromuscular and mechanical variability also exists within the same sport, in runners with the same level of expertise and performance that spontaneously chose different running forms. This could be of great importance for training and prophylactic purpose and open new areas of research.

Declaration of Competing Interest

The authors declare that they have no known competing financial interests or personal relationships that could have appeared to influence the work reported in this paper.

Acknowledgements

The authors would like to thank the subjects for their time and enthusiasm. We also thank Damien Young for editorial assistance. We confirm that we have read the Journal's position on issues involved in ethical publication and affirm that this report is consistent with those guidelines. None of the authors has any conflict of interest to disclose.

References

- Ahtiainen, J.P., Häkkinen, K., 2009. Strength Athletes Are Capable to Produce Greater Muscle Activation and Neural Fatigue During High-Intensity Resistance Exercise Than Nonathletes. *J. Strength Cond. Res.* 23, 1129–1134. <https://doi.org/10.1519/JSC.0b013e3181aa1b72>.
- Arendse, R.E., Noakes, T.D., Azevedo, L.B., Romanov, N., Schweltnus, M.P., Fletcher, G., 2004. Reduced eccentric loading of the knee with the pose running method. *Med. Sci. Sports Exerc.* 36, 272–277. <https://doi.org/10.1249/01.MSS.0000113684.61351.B0>.
- Bach, T.M., Chapman, A.E., Calvert, T.W., 1983. Mechanical resonance of the human body during voluntary oscillations about the ankle joint. *J. Biomech.* 16, 85–90. [https://doi.org/10.1016/0021-9290\(83\)90049-0](https://doi.org/10.1016/0021-9290(83)90049-0).
- Buckthorpe, M., Roi, G.S., 2018. The time has come to incorporate a greater focus on rate of force development training in the sports injury rehabilitation process. *Muscles. Ligaments Tendons J.* 7, 435–441. <https://doi.org/10.11138/mltj/2017.7.3.435>.
- Capaday, C., Stein, R.B., 1987. Difference in the amplitude of the human soleus H reflex during walking and running. *J. Physiol.* 392, 513–522. <https://doi.org/10.1113/jphysiol.1987.sp016794>.
- Chino, K., Oda, T., Kurihara, T., Nagayoshi, T., Yoshikawa, K., Kanehisa, H., Fukunaga, T., Fukushiro, S., Kawakami, Y., 2008. In vivo fascicle behavior of synergistic muscles in concentric and eccentric plantar flexions in humans. *J. Electromyogr. Kinesiol.* 18, 79–88. <https://doi.org/10.1016/j.jelekin.2006.08.009>.
- Cupido, C.M., Galea, V., McComas, A.J., 1996. Potentiation and depression of the M wave in human biceps brachii. *J. Physiol.* 541–550.
- DelBalso, C., Cafarelli, E., 2007. Adaptations in the activation of human skeletal muscle induced by short-term isometric resistance training. *J. Appl. Physiol.* 103, 402–411. <https://doi.org/10.1152/jappphysiol.00477.2006>.
- Driss, T., Lambert, D., Rouis, M., Vandewalle, H., 2012. Influence of musculo-tendinous stiffness of the plantar ankle flexor muscles upon maximal power output on a cycle ergometer. *Eur. J. Appl. Physiol.* 112, 3721–3728. <https://doi.org/10.1007/s00421-012-2353-5>.
- Duchateau, J., Enoka, R.M., 2008. Neural control of shortening and lengthening contractions: influence of task constraints. *J. Physiol.* 586, 5853–5864. <https://doi.org/10.1113/jphysiol.2008.160747>.
- Duclay, J., Martin, A., Robbe, A., Pousson, M., 2008. Spinal reflex plasticity during maximal dynamic contractions after eccentric training. *Med. Sci. Sports Exerc.* 40, 722–734. <https://doi.org/10.1249/MSS.0b013e31816184dc>.
- Folland, J.P., Buckthorpe, M.W., Hannah, R., 2014. Human capacity for explosive force production: Neural and contractile determinants. *Scand. J. Med. Sci. Sports* 24, 894–906. <https://doi.org/10.1111/sms.12131>.
- Gindre, C., Lussiana, T., Hébert-Losier, K., Mouro, L., 2016. Aerial and Terrestrial Patterns: A Novel Approach to Analyzing Human Running. *Int. J. Sports Med.* 37, 25–29. <https://doi.org/10.1055/s-0035-1555931>.
- Grosprêtre, S., Gimenez, P., Martin, A., 2018. Neuromuscular and electromechanical properties of ultra-power athletes: the traceurs. *Eur. J. Appl. Physiol.* 118, 1361–1371. <https://doi.org/10.1007/s00421-018-3868-1>.
- Grosprêtre, S., Martin, A., 2014. Conditioning effect of transcranial magnetic stimulation evoking motor-evoked potential on V-wave response. *Physiol. Rep.* 2 <https://doi.org/10.14814/phy2.12191>.
- Hermens, H.J., Freriks, B., Disselhorst-Klug, C., Rau, G., 2000. Development of recommendations for SEMG sensors and sensor placement procedures. *J. Electromyogr. Kinesiol.* 10, 361–374.
- Hoerzer, S., von Tscherner, V., Jacob, C., Nigg, B.M., 2015. Defining functional groups based on running kinematics using Self-Organizing Maps and Support Vector Machines. *J. Biomech.* 48, 2072–2079. <https://doi.org/10.1016/j.jbiomech.2015.03.017>.
- Hoffman, M., Norcross, M., Johnson, S., 2018. The Hoffmann reflex is different in men and women. *NeuroReport* 29, 314–316. <https://doi.org/10.1097/WNR.0000000000000961>.
- Holtermann, A., Roeleveld, K., Engström, M., Sand, T., 2007. Enhanced H-reflex with resistance training is related to increased rate of force development. *Eur. J. Appl. Physiol.* 101, 301–312. <https://doi.org/10.1007/s00421-007-0503-y>.
- Johnson, M.A., Polgar, J., Weightman, D., Appleton, D., 1973. Data on the distribution of fibre types in thirty-six human muscles. An autopsy study. *J. Neurol. Sci.* 18, 111–129.
- Klass, M., 2004. Limiting mechanisms of force production after repetitive dynamic contractions in human triceps surae. *J. Appl. Physiol.* 96, 1516–1521. <https://doi.org/10.1152/jappphysiol.01049.2003>.
- Koceja, D.M., Davison, E., Robertson, C.T., 2004. Neuromuscular Characteristics of Endurance- and Power-Trained Athletes. *Res. Q. Exerc. Sport* 75, 23–30. <https://doi.org/10.1080/02701367.2004.10609130>.
- Kyröläinen, H., Komi, P.V., 1994. Neuromuscular performance of lower limbs during voluntary and reflex activity in power- and endurance-trained athletes. *Eur. J. Appl. Physiol. Occup. Physiol.* 69, 233–239.
- Lussiana, T., Gindre, C., Hébert-Losier, K., Sagawa, Y., Gimenez, P., Mouro, L., 2017a. Similar running economy with different running patterns along the aerial-terrestrial continuum. *Int. J. Sports Physiol. Perform.* 12, 481–489. <https://doi.org/10.1123/ijsp.2016-0107>.
- Lussiana, T., Gindre, C., Mouro, L., Hébert-Losier, K., 2017b. Do subjective assessments of running patterns reflect objective parameters? *Eur. J. Sport Sci.* 17, 847–857. <https://doi.org/10.1080/17461391.2017.1325072>.
- Lussiana, T., Patoz, A., Gindre, C., Mouro, L., Hébert-Losier, K., 2019. The implications of time on the ground on running economy: less is not always better. *J. Exp. Biol.* 222, jeb192047. <https://doi.org/10.1242/jeb.192047>.
- Maffiuletti, Martin, A., Babault, N., Pensini, M., Lucas, B., Schieppati, M., 2001. Electrical and mechanical H(max)-to-M(max) ratio in power- and endurance-trained athletes. *J. Appl. Physiol.* 90, 3–9.
- Maffiuletti, N.A., Aagaard, P., Blazevich, A.J., Folland, J., Tillin, N., Duchateau, J., 2016. Rate of force development: physiological and methodological considerations. *Eur. J. Appl. Physiol.* 116, 1091–1116. <https://doi.org/10.1007/s00421-016-3346-6>.
- McMahon, T.A., Valiant, G., Frederick, E.C., 1987. Groucho running. *J. Appl. Physiol.* 62, 2326–2337. <https://doi.org/10.1152/jappphysiol.1987.62.6.2326>.
- Patoz, A., Gindre, C., Mouro, L., Lussiana, T., 2019. Intra and Inter-rater Reliability of the Volodalen © Scale to Assess Aerial and Terrestrial Running Forms. *J. Athl. Enhanc.* 8, 4–9.
- Phinyomark, A., Osis, S., Hettinga, B.A., Ferber, R., 2015. Kinematic gait patterns in healthy runners: A hierarchical cluster analysis. *J. Biomech.* 48, 3897–3904. <https://doi.org/10.1016/j.jbiomech.2015.09.025>.
- Tillin, N.A., Jimenez-Reyes, P., Pain, M.T.G., Folland, J.P., 2010. Neuromuscular Performance of Explosive Power Athletes versus Untrained Individuals. *Med. Sci. Sport. Exerc.* 42, 781–790. <https://doi.org/10.1249/MSS.0b013e3181be9c7e>.
- Tucker, K.J., Tuncer, M., Türker, K.S., 2005. A review of the H-reflex and M-wave in the human triceps surae. *Hum. Mov. Sci.* 24, 667–688. <https://doi.org/10.1016/j.humov.2005.09.010>.
- VanCutsem, M., Duchateau, J., Hainaut, K., 1998. Changes in single motor unit behaviour contribute to the increase in contraction speed after dynamic training in humans. *J. Physiol.* 295–305.

Sidney Grosprêtre received his PhD in Neurophysiology in 2013. He is now associate professor in the Laboratory C3S “Culture, Sport, Health and Society” (EA4660) in Besançon, France. He teaches neurosciences, physiology, and biomechanics. His main topic of research is about neuromuscular plasticity following acute interventions or training. More specifically, he works mainly on electro-stimulation and motor imagery's impact over the neuromuscular system. Part of his research is also dedicated to investigating the effects of plyometric and eccentric training. Since 2010, he is also founder and president of the French national parkour federation (FPK), a sport based on running and overcoming obstacles mainly in an urban landscape.

Dr. Philippe Gimenez is currently an Associate Professor at the University of Franche Comté, Besançon, France. He received his PhD in Exercise Physiology (2009) from the Faculty of Sports Sciences of the University of Saint-Etienne, France. He was then in a postdoctoral position in the University of Montreal, Montreal, Canada before joining the department Sports-Performance of the Laboratory Culture, Sport, Health and Society (C3S) of the University of Franche-Comté. His main topic of research concerns the physiological and biomechanical determinants of sports performance. More particularly, he is interested in energetic metabolism and associated control mechanisms. He currently works on the effects of combined environmental stressors to optimize training and recovery.

Adrien Thouvenot obtained a M.Sc. in Sport Science from University of Bourgogne-Franche Comté (in 2019). He is currently a PhD student within the Research and Development department of Volodalen, Chavéria, France, and the University Bourgogne-Franche Comté, Besançon, France, on an innovative project funded by a grant CIFRE (no. 2019/0586). His thesis is concerned with the prevention and rehabilitation of running-related injuries.

Dr. Aurélien Patoz graduated in Chemistry from Ecole Polytechnique Fédérale de Lausanne, Switzerland and obtained his Ph.D. in Computational Chemistry from the same school. He then obtained a M.Sc. in Sport Science from the University of Lausanne. He is now working as a research associate at the University of Lausanne on an innovative project funded by Innosuisse (grant no. 35793.1 IP-LS). His main research interests focus on running biomechanics. More specifically, his goal is to determine spontaneous running patterns using inertial sensors.

Dr. Thibault Lussiana graduated in Sport Science from University of Franche-Comté, France and obtained his Ph.D. in human movement analysis from the same University. He is now working as a scientist in the Volodalen company (Switzerland). His main research interests focus on the understanding of spontaneous running patterns of individuals.

Dr. Laurent Mourot received his Master degree dedicated to Movement and Health from the University of St Etienne (2000) and his PhD in Sports Sciences from University of Franche Comté (2004). He was a research engineer at the University Hospital of Besançon (Clinical Investigation Center in technological Innovation) before becoming Associate Professor (in 2011) in the Department of Sport Sciences at University of Franche Comté (France). His research interest include integrated physiology and the validation of methods and tools for training/health monitoring in healthy people and patients. He is especially interested in the use of physical activity as a therapeutic tool in cardiovascular disease, including running.

9.7 Does characterizing global running pattern help to prescribe individualized strength training in recreational runners?

Aurélien Patoz^{1,2,*}, Bastiaan Breine^{2,3}, Adrien Thouvenot^{4,5}, Laurent Mourot^{5,6}, Cyrille Gindre^{2,4}, Thibault Lussiana^{2,4,5}

¹ Institute of Sport Sciences, University of Lausanne, 1015 Lausanne, Switzerland

² Research and Development Department, Volodalen Swiss Sportlab, 1860 Aigle, Switzerland

³ Department of Movement and Sports Sciences, Ghent University, 9000 Ghent, Belgium

⁴ Research and Development Department, Volodalen, 39270 Chavéria, France

⁵ Research Unit EA3920 Prognostic Markers and Regulatory Factors of Cardiovascular Diseases and Exercise Performance, Health, Innovation platform, University of Bourgogne Franche-Comté, Besançon, France

⁶ Division for Physical Education, Tomsk Polytechnic University, 634040 Tomsk, Russia

* Corresponding author

Published in **Frontiers in Physiology**

DOI: 10.3389/fphys.2021.631637



Does Characterizing Global Running Pattern Help to Prescribe Individualized Strength Training in Recreational Runners?

Aurélien Patoz^{1,2*}, Bastiaan Breine^{2,3}, Adrien Thouvenot^{4,5}, Laurent Mourot^{5,6}, Cyrille Gindre^{2,4} and Thibault Lussiana^{2,4,5}

¹ Institute of Sport Sciences, University of Lausanne, Lausanne, Switzerland, ² Research and Development Department, Volodalen Swiss Sportlab, Aigle, Switzerland, ³ Department of Movement and Sports Sciences, Ghent University, Ghent, Belgium, ⁴ Research and Development Department, Volodalen, Chavéria, France, ⁵ Research Unit EA3920 Prognostic Markers and Regulatory Factors of Cardiovascular Diseases and Exercise Performance, Health, Innovation Platform, University of Bourgogne Franche-Comté, Besançon, France, ⁶ Division for Physical Education, Tomsk Polytechnic University, Tomsk, Russia

OPEN ACCESS

Edited by:

Vincent Pialoux,
Université Claude Bernard Lyon 1,
France

Reviewed by:

Fabien Andre Basset,
Memorial University of Newfoundland,
Canada
Caio Victor Sousa,
Northeastern University, United States

*Correspondence:

Aurélien Patoz
aurelien.patoz@unil.ch;
aurelien@volodalen.com

Specialty section:

This article was submitted to
Exercise Physiology,
a section of the journal
Frontiers in Physiology

Received: 20 November 2020

Accepted: 26 February 2021

Published: 17 March 2021

Citation:

Patoz A, Breine B, Thouvenot A, Mourot L, Gindre C and Lussiana T (2021) Does Characterizing Global Running Pattern Help to Prescribe Individualized Strength Training in Recreational Runners? *Front. Physiol.* 12:631637. doi: 10.3389/fphys.2021.631637

This study aimed to determine if concurrent endurance and strength training that matches the global running pattern would be more effective in increasing running economy (RE) than non-matched training. The global running pattern of 37 recreational runners was determined using the Volodalen® method as being aerial (AER) or terrestrial (TER). Strength training consisted of endurance running training and either plyometric (PLY) or dynamic weight training (DWT). Runners were randomly assigned to a matched ($n = 18$; DWT for TER, PLY for AER) or non-matched ($n = 19$; DWT for AER, PLY for TER) 8 weeks concurrent training program. RE, maximal oxygen uptake ($\dot{V}O_2\max$) and peak treadmill speed at $\dot{V}O_2\max$ (PTS) were measured before and after the training intervention. None of the tested performance related variables depicted a significant group effect or interaction effect between training and grouping ($p \geq 0.436$). However, a significant increase in RE, $\dot{V}O_2\max$, and PTS ($p \leq 0.003$) was found after the training intervention. No difference in number of responders between matched and non-matched groups was observed for any of the performance related variables ($p \geq 0.248$). In recreational runners, prescribing PLT or DWT according to the global running pattern of individuals, in addition to endurance training, did not lead to greater improvements in RE.

Keywords: running, plyometric training, dynamic weight training, concurrent training, sports biomechanics

INTRODUCTION

Running economy (RE), which refers to the steady-state of oxygen consumption at a given running speed, is a critical factor of running performance (Conley and Krahenbuhl, 1980). RE improves after years of endurance running training, and especially if high volume, high intensity interval, or uphill running training are undertaken (Barnes and Kilding, 2014). Beyond running, different

training strategies have been shown to potentially improve RE (Mikkola et al., 2007; Taipale et al., 2013; Barnes and Kilding, 2014). Among them, concurrent training, i.e., the use of strength training such as plyometric training (PLT) or dynamic weight training (DWT) in parallel with endurance running training, has been shown to further benefit RE (Barnes and Kilding, 2014). For instance, several studies that used this concurrent training method reported an improvement of RE ranging from 0 to 4.7% (Pellegrino et al., 2016; Meszler et al., 2019). However, the exact mechanisms leading to an improvement of RE after PLT or DWT remained unclear (Trowell et al., 2020).

PLT involves eccentric-concentric contraction cycles to allow the muscle-tendon unit to efficiently store and release elastic energy. During such cycle, there is a focus on a short ground contact time (t_c) and a high leg stiffness (k_{leg}) (Anderson, 1996). Common PLT exercises for runners are repeated rebound jumps or drop jumps. On the other hand, DWT involves a greater focus on concentric contractions aiming to produce a maximal power output, which is a compromise between speed and force generation (Kawamori and Haff, 2004). Common DWT exercises are, e.g., squats jumps and dynamic lunges. From a kinematic point of view, PLT implies shorter t_c than DWT, de facto theoretically more in line with the mechanical demands of running. Indeed, running is characterized by a short contact phase (dependent on the running speed but generally smaller than 400 ms) followed by a flight phase. Therefore, the running pattern is a succession of plyometric contractions showing a spring like behavior, as suggested by the spring mass model (Blickhan, 1989). However, all runners do not share a running pattern that equally resembles to a spring.

Indeed, some runners were shown to exhibit a more asymmetric contact phase (i.e., a longer duration of the propulsion phase than the braking phase) and less vertical oscillation of their center of mass during the flight time (t_f) than would be predicted by the spring-mass model (Lussiana et al., 2019). Thus, these running patterns are less accurately modeled by the spring-mass model. Following such ideas, it has been shown that individuals could be classified into two categories termed aerial (AER) and terrestrial (TER) using the subjective Volodalen® scale (Gindre et al., 2015). Shorter t_c and greater k_{leg} are exhibited in AER than TER, while greater leg compression during stance is observed in TER compared to AER (Gindre et al., 2015). These kinematic differences might indicate that theoretically certain training modalities such as PLT or DWT might better suit AER or TER, respectively.

It is well established that individual differences exist in response to training, where *high responders* show large responses whereas *low responders* show small responses or no responses at all (Mann et al., 2014). Interestingly, Hautala et al. (2006) reported that low responders to an endurance based training program could become high responders to a strength based training program. Unfortunately, this variability in training responsiveness is not well understood and might be attributable to various factors including the absence of definition for high and low responders in the scientific literature and a one size fits all approach to exercise prescription (Mann et al., 2014). It has been purported that a more “personalized approach”

to exercise prescription based on factors such as genotype, baseline phenotype, pre-training autonomic activity, individual homeostatic stress responses, recovery, and nutrition should improve training responsiveness (Mann et al., 2014). However, more research is still needed to clarify and quantify the role of these parameters. Also, for coaches, these factors are often hard to assess. In line with this view, Gindre et al. (2015) made the assumption that AER and TER could respond preferentially to different types of training interventions to improve RE. In other words, the knowledge of the global running pattern might provide useful indications for the prescription of training modalities toward an improvement in RE.

Hence, the purpose of the present study was to verify the effectiveness (i.e., mean increase in RE) and responsiveness (i.e., number of participants with a significant increase in RE) of two strength training modalities (i.e., PLT and DWT) on top of a standard endurance running training program to improve RE in runners with different global running patterns (i.e., AER and TER). We hypothesized that a training program that matches the underlying kinematics of the global running pattern (i.e., PLT for AER and DWT for TER) would be more efficient and thus would trigger a greater increase in RE and a lower rate of low-responders than a non-matched training program.

MATERIALS AND METHODS

Participants

The study has been conducted over a 3 months period, which permitted to test 37 recreational and regular runners among which there were 5 females (age: 29.0 ± 9.0 years, height: 168 ± 6 cm, body mass: 59.3 ± 3.0 kg, weekly training hours: 2.0 ± 1.2 h) and 32 males (age: 29.4 ± 9.3 years, height: 177 ± 8 cm, body mass: 73.4 ± 12.4 kg, weekly training hours: 2.6 ± 1.3 h). For study inclusion, voluntary participants were required to be in good self-reported general health with no current or recent (<3 months) musculoskeletal injuries, and to have not previously undertaken any structured PLT or DWT. Two groups of runners were set up. The matched group consisted of AER following PLT and TER following DWT ($n = 18$). The non-matched group consisted of AER following DWT and TER following PLT ($n = 19$). As assessed by two-tailed non-matched t -tests, there were no significant differences in age, height, body mass, and weekly training hours between both groups (Table 1).

TABLE 1 | Mean \pm SD of baseline participant characteristics for matched and non-matched groups.

	Matched (15 men, 3 women)	Non-matched (17 men, 2 women)	<i>p</i>
Age (y)	30.8 ± 8.4	28.0 ± 9.8	0.350
Height (cm)	177 ± 8	175 ± 8	0.499
Body mass (kg)	72.2 ± 10.7	70.8 ± 14.3	0.730
Weekly training hours (h-week ⁻¹)	2.50 ± 1.25	2.55 ± 1.31	0.901

No significant differences ($p \leq 0.05$) were reported between both groups.

Participants were informed of the benefits and risks of the investigation prior to signing an institutionally approved informed consent document to participate in the study. They were informed that the data and results were confidential, and that they could withdraw at any time during the study, that was approved by an Institutional Review Board of the University of Bourgogne, Franche-Comté (CPP: 2014-A00336-41) and adhered to the latest Declaration of Helsinki of the World Medical Association (World Medical Association, 2013).

Experimental Approach to the Problem

After providing written informed consent, participants performed an initial baseline experimental session including a series of tests. These tests consisted of the assessment of the global running pattern using the Volodalen® scale to classify a runner as AER or TER, jump tests to evaluate the explosive concentric capacity and plyometric characteristics of the lower limb, a submaximal running test to determine RE, and a maximal incremental running test to determine peak treadmill speed (PTS) and maximal oxygen uptake ($\dot{V}O_2\text{max}$) (Gindre et al., 2015). Tests were interspersed by a 5-min passive recovery in a seated position. After that, each participant was randomly assigned to one of two 8 week concurrent training modalities, i.e., a standard endurance running training program combined with either PLT or DWT. After this assignment, participants were regrouped for statistical analysis based on whether their running pattern (AER or TER) was matched or non-matched with their prescribed strength training (DWT or PLT).

Procedures

Global Running Pattern Assessment

During the warm-up of the initial baseline experimental session (5 min on a treadmill at $9 \text{ km}\cdot\text{h}^{-1}$), two running coaches with more than 3 years of experience using the Volodalen® method (CG and TL) paid attention to five key elements: vertical oscillation of the head, antero-posterior motion of the elbows, pelvis position at ground contact, foot position at ground contact, and foot strike pattern. Each element was scored from one to five, leading to a global subjective score (V° score) that represents the global running pattern of participants. This score ultimately allows the classification of runners into the two different categories (i.e., AER if V° score > 15 and TER otherwise). The Volodalen® method was fully described and studied elsewhere (Gindre et al., 2015) and was shown to be a reliable method to assess running pattern (Patoz et al., 2019). The two coaches disagreed in their assessment of 3 individuals (8.1%). In these cases, the two coaches adopted a consensus following a discussion.

Endurance Running Training

All participants followed a basic endurance running training in line with what they were used to do before the study. Noteworthy, participants were not following a proper periodization training before starting the given training, i.e., they were not in a specific phase of a global periodization training. Training

was divided into three different intensities based on their PTS: below 80%, between 80 and 95%, and between 95 and 105% of PTS. These percentages were chosen as to represent an aerobic, threshold and high intensity zone, respectively. The prescribed time in each of these three training zones during the 8 weeks training is described in **Table 2**. Main training volume (70–80%) was spent at running speeds below 80% of PTS.

Basic endurance sessions consisted of continuous running for 45–75 min, predominantly at a running speed below 80% of PTS with some unstructured bouts of faster running at 80–95% of PTS between 10 and 25 min per session. Interval sessions consisted of a 15 min easy warm-up at a running speed below 80% of PTS and involved repeated interval bouts ranging from 30 s to 2 min at 95–105% of PTS for an accumulated total of 6–12 min of fast running per session. In the beginning of the 8 weeks training plan, an example interval session consisted of 2 times 6 min of (30 s at 100% of PTS—30 s below 80% of PTS) with 2 min recovery between each 6 min block while at the end of the 8 weeks training plan, an example interval session consisted of 3 blocks of 2 repetitions of (2 min at 100% of PTS—1 min 30 s below 80% of PTS) with 5 min recovery between each block.

Plyometric or Dynamic Weight Training

Participants were asked to perform a predetermined circuit training composed of six exercises and designed as PLT or DWT (**Figure 1**). Details of the 8 weeks training are given in **Table 2**. Participants performed the same circuit training during the entire protocol but with progressive changes in the number of cycles and the exercise/rest ratio. Hence, despite different exercises, the total training load (total duration of effort and resting periods) was aimed to be equivalent between groups. Also, as the participants had no previous experience in resistance training, only body weight was used.

Jump Test

The squat jump test (SJ) was used to evaluate the explosive concentric capacity of the lower limbs (Bosco et al., 1983). Participants were required to jump vertically as high as possible from a static squat position and to start the landing with knees straight and ankles plantar-flexed. The depth of the squat was self-selected. Participants had to maintain the static squat position for two seconds prior to the jump. Squat jump height (SJ-h, in cm) was calculated from flight time (t_f) (Eq. 1) as measured by an optical measurement system (Optojump Next®, MicroGate Timing and Sport, Bolzano, Italy) sampling at 1,000 Hz.

$$\text{SJ} - h = \frac{g t_f^2}{2} \quad (1)$$

Following the SJ, a five-repetition rebound jump test (5RJ) was used to evaluate the plyometric characteristics of the participants' lower limbs (Bosco et al., 1983; Dalleau et al., 2004). Participants were required to jump vertically as high as possible while minimizing ground contact time (t_c) and maximizing flight time (t_f). Participants were also instructed to minimize knee actions (i.e., flexion and extension) during the test. t_f and t_c

TABLE 2 | Characteristics of the 8 weeks training program.

Weeks	1	2	3	4	5	6	7	8
Endurance training								
Volume (min)	130	135	145	150	160	165	170	175
Intensity < 80% PTS (min)	104 (80%)	106 (79%)	113 (78%)	114 (76%)	121 (76%)	121 (73%)	122 (72%)	123 (70%)
80% < Intensity < 95% PTS (min)	17 (13%)	19 (14%)	21 (14%)	24 (16%)	27 (17%)	30 (18%)	33 (19%)	35 (20%)
95% < Intensity < 105% PTS (min)	9 (7%)	10 (7%)	11 (8%)	12 (8%)	13 (7%)	14 (9%)	16 (9%)	17 (10%)
Strength training (PLT and DWT)								
Volume (min)	40	40	62	62	62	62	80	80
Session * cycle (per week)	1 * 4	1 * 4	1 * 4 + 1 * 2	2 * 4 + 1 * 2	3 * 4 + 1 * 2	4 * 4 + 1 * 2	2 * 4	2 * 4
Warm up (min)	7	7	7	7	7	7	7	7
Time per exercise (sec)	20	25	30	30	35	35	40	40
Rest between exercise (sec)	40	35	30	30	25	25	20	20
Rest between cycle (min)	3	3	3	3	3	3	3	3

PTS, Peak treadmill speed; PLT, plyometric training; DWT, dynamic weight training.

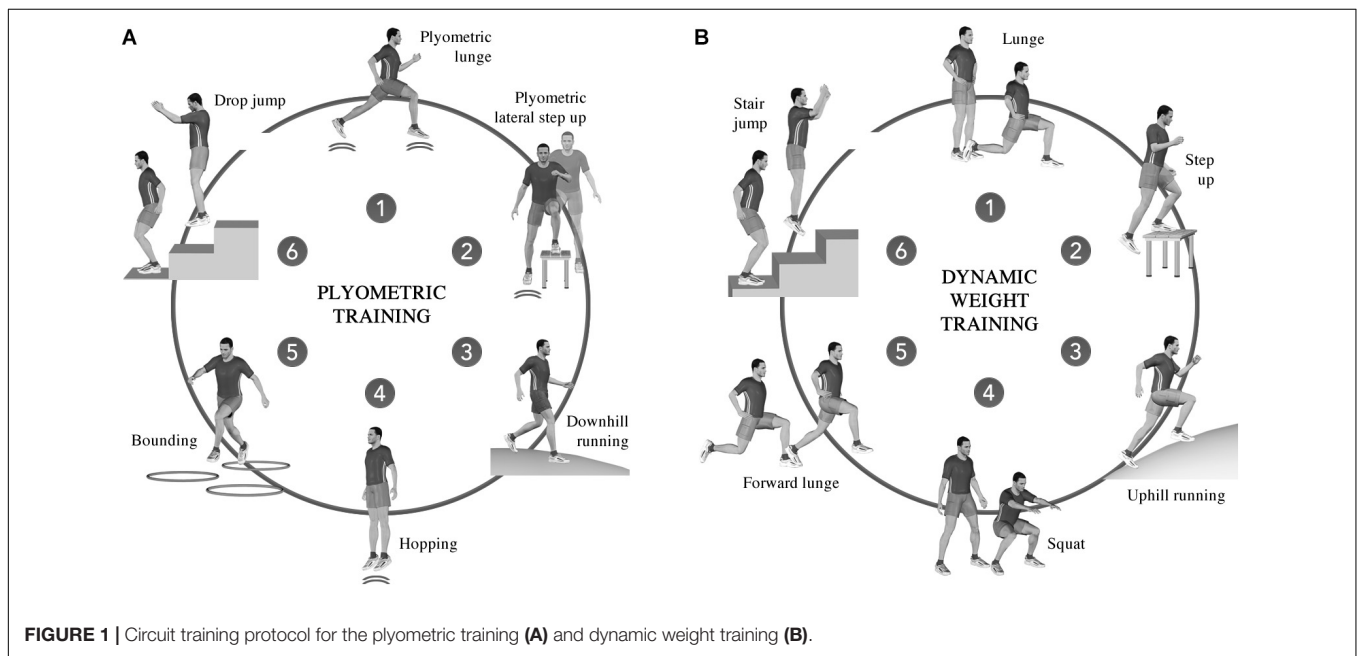


FIGURE 1 | Circuit training protocol for the plyometric training (A) and dynamic weight training (B).

were measured by the Optojump Next® system. The average mechanical power during the positive (concentric) work per body mass (5RJ-P, in $W \cdot kg^{-1}$) was then calculated on the basis of the methods described by Bosco et al. (1983) using the following formula (Eq. 2).

$$5RJ - P = \frac{g^2 t_f (t_c + t_f)}{4t_c} \quad (2)$$

All jumps were performed with hands placed on the hips and participants were wearing their habitual running shoes. After five practice trials of each jump, three repetitions of each jump test were performed with a 30 s rest between repetitions and a 2 min rest between the SJ and 5RJ tests. The best repetition of the SJ (based on the longest t_f) and 5RJ (based on the highest average mechanical power) was used for statistical analysis.

Submaximal Running Test

Participants ran for 5 min on a treadmill at $12 \text{ km} \cdot \text{h}^{-1}$. Gas exchange was measured breath-by-breath using a gas analyser (Cortex Metamax 3B, Cortex Biophysik, Leipzig, Germany) and subsequently averaged over 10 s intervals throughout the test. Before each test, the gas analyzer was calibrated following the manufacturer's recommendations using ambient air (O_2 : 20.93% and CO_2 : 0.03%) and a gas mixture of known composition (O_2 : 15.00% and CO_2 : 5.00%). The spirometer was calibrated using a 3 L syringe. Respiratory exchange ratio (RER), oxygen uptake ($\dot{V}O_2$), and carbon dioxide output ($\dot{V}CO_2$) were averaged over the last minute of the 5 min running trial. RER had to remain below 1.0 during the trials for the data to be included in the analysis, otherwise the corresponding data were excluded as deemed to not represent a submaximal effort. In such case, the selected submaximal speed was lowered iteratively by $1 \text{ km} \cdot \text{h}^{-1}$ until an RER below 1.0 was achieved. This resulted in submaximal testing

speeds of 9 ($n = 1$), 10 ($n = 6$), 11 ($n = 5$), and 12 $\text{km}\cdot\text{h}^{-1}$ ($n = 25$). These speeds were kept the same for the post testing. RE was calculated from the running velocity divided by net $\dot{V}O_2$ normalized to individual body mass ($\text{m}\cdot\text{ml}^{-1}\cdot\text{kg}^{-1}$) where net $\dot{V}O_2 = \dot{V}O_2 - \text{rest}\dot{V}O_2$, with rest $\dot{V}O_2$ given by the average over the last minute of a 5 min upright stance measure prior to the submaximal running test. This choice of units for RE have a conceptual advantage that numerical values are directly related to RE (i.e., the larger the numerical value, the better the RE) (Turner et al., 2003).

Maximal Incremental Test

Following the submaximal test, participants performed a maximal incremental running test on the treadmill. Starting at 8 $\text{km}\cdot\text{h}^{-1}$, the treadmill speed was increased by 0.5 $\text{km}\cdot\text{h}^{-1}$ every minute until volitional exhaustion. The participants received strong verbal encouragement to ensure attainment of maximal values during the test. $\dot{V}O_{2\text{max}}$, averaged over 30 s, was said attained when two or more of the following criteria were met: an increase in $\dot{V}O_2$ less than 2.1 $\text{ml}\cdot\text{kg}^{-1}\cdot\text{min}^{-1}$ between two consecutive stages, an RER greater than 1.1, and a heart rate (RS810, Polar Electro Oy, Kempele, Finland) of ± 10 beats per minute of the predicted maximal heart rate value (i.e., $220 - \text{age}$), as done by Howley et al. (1995). PTS is defined as the running speed of the last fully completed increment (MAS) plus the fraction of time spent in the following uncompleted increment (α) multiplied by the running speed increment ($\Delta s = 0.5 \text{ km}\cdot\text{h}^{-1}$) (Kuipers et al., 2003): $\text{PTS} = \text{MAS} + \alpha \Delta s$.

Statistical Analyses

Assuming a medium effect size [partial eta squared (η^2_p) = 0.06] in RE improvement between matched and non-matched training groups, an α error of 0.05, and a power of 0.8, sample size calculations resulted in the requirement of 34 participants (Faul et al., 2007). However, the 37 participants were kept to slightly increase statistical power. Test-retest reliability coefficients ranged from $r = 0.805$ to 0.954 ($p < 0.001$) indicating good to excellent reliability of measurements. Descriptive statistics are presented using mean \pm standard deviation. Effect sizes are reported as η^2_p values. The normality of the data and homogeneity of variances were verified using Shapiro-Wilk (p range: 0.163–0.943) and Levene's test (p range: 0.162–0.880), respectively. Unpaired two-sided Student's t -tests were used to compare participant characteristics between matched and non-matched groups at baseline. Statistical analysis was performed using Jamovi [version 1.0.8 (Computer Software), retrieved from <https://www.jamovi.org>] with a level of significance set at $p \leq 0.05$.

Effectiveness of the Training Interventions

A pre-post experimental design was used with two training groups (matched vs. non-matched). Effectiveness of the training protocol on performance parameters (primary criteria RE; secondary criteria $\dot{V}O_{2\text{max}}$, PTS, SJ-h, and 5RJ-P) was assessed by repeated measures ANOVA (RM-ANOVA) with pre vs. post testing as within-subject factor and matched vs. non-matched

grouping as between subject factor, and employing Bonferroni procedures for pair-wise *post-hoc* comparisons.

High Responders vs. Low Responders

Participants were all labeled as a responder or non-responder for the three performance variables that were significantly influenced (significant pre-post effect reported by the RM-ANOVA) by the protocol (i.e., RE, $\dot{V}O_{2\text{max}}$, and PTS) based on set % changes derived from the literature. A participant was determined as responder when RE increased by more than 2.6% (Barnes and Kilding, 2015), $\dot{V}O_{2\text{max}}$ by more than 5.9% (Dalleck et al., 2016), and PTS by more than 4% (arbitrary cut-off). Chi-squared analyses (χ^2) were performed on the number of responders and non-responders to assess if there was a difference of responsiveness for any of the three performance variables within matched and non-matched groups.

RESULTS

Effectiveness

No significant group effect or interaction effect were found between the training (pre-post) and grouping (matched vs. non-matched) for any of the tested performance related variables. These results indicate that the effect of the applied training intervention on the performance related variables did not significantly differ between the matched and non-matched groups ($p \geq 0.436$; **Table 3**). However, we found a significant increase in RE, PTS, and $\dot{V}O_{2\text{max}}$ after the training intervention ($p \leq 0.003$; **Table 3**). Noteworthy, *post-hoc* comparisons were not investigated as no interaction effect was reported.

Responsiveness to Training

No statistical difference in the responsiveness to training intervention were found between matched and non-matched groups for any of the performance related variables that were significantly influenced (significant pre-post effect reported by the RM-ANOVA; **Table 3**) by the protocol ($p \geq 0.248$; **Table 4**). Individual responses are shown in **Figure 2**.

DISCUSSION

This study aimed at determining the effectiveness and responsiveness to two strength training modalities (i.e., PLT and DWT) combined with standard endurance training to improve RE in recreational runners. Identifying the global running pattern (i.e., TER or AER) and matching it to a PLT or DWT type of strength training prescription resulted in similar RE improvements and response to training than if no matching had been performed. As such, the results of the present study could not support our hypotheses. The following discussion is elaborating on possible explanations for the rejection of our hypothesis and directions for future research.

When following a certain training intervention, some individuals show a large positive response while others a small

TABLE 3 | Mean \pm SD for running economy (RE), maximal oxygen uptake ($\dot{V}O_2$ max), peak treadmill speed (PTS), squat jump height (SJ-h), and average mechanical power during the positive (concentric) work per body mass of five repeated rebound jumps (5RJ-P) per training group, pre and post the training intervention as well as main effects (pre-post and group) and interaction effect (pre-post \times group) for these five performance related variables.

		Pre	Post
RE (m·ml ⁻¹ ·kg ⁻¹)	Matched	5.09 \pm 0.44	5.18 \pm 0.53
	Non-matched	5.18 \pm 0.35	5.32 \pm 0.39
	Main effect group	$\rho = 0.398$	$\eta^2_p = 0.020$
	Main effect pre-post	$\rho = 0.003$	$\eta^2_p = 0.223$
	Interaction pre-post \times group	$\rho = 0.565$	$\eta^2_p = 0.010$
$\dot{V}O_2$max (ml·min ⁻¹ ·kg ⁻¹)	Matched	53.4 \pm 8.27	55.6 \pm 7.35
	Non-matched	54.9 \pm 8.14	56.3 \pm 7.54
	Main effect group	$\rho = 0.663$	$\eta^2_p = 0.005$
	Main effect pre-post	$\rho = 0.002$	$\eta^2_p = 0.244$
	Interaction pre-post \times group	$\rho = 0.465$	$\eta^2_p = 0.015$
PTS (km·h ⁻¹)	Matched	15.1 \pm 1.83	15.8 \pm 1.67
	Non-matched	15.7 \pm 1.63	16.2 \pm 1.48
	Main effect group	$\rho = 0.353$	$\eta^2_p = 0.025$
	Main effect pre-post	$\rho < 0.001$	$\eta^2_p = 0.598$
	Interaction pre-post \times group	$\rho = 0.436$	$\eta^2_p = 0.017$
SJ-h (cm)	Matched	30.9 \pm 5.3	31.8 \pm 5.4
	Non-matched	31.0 \pm 5.6	31.7 \pm 5.1
	Main effect group	$\rho = 0.996$	$\eta^2_p = 0.000$
	Main effect pre-post	$\rho = 0.064$	$\eta^2_p = 0.095$
	Interaction pre-post \times group	$\rho = 0.888$	$\eta^2_p = 0.001$
5RJ-P (W)	Matched	35.7 \pm 6.6	36.0 \pm 7.6
	Non-matched	36.6 \pm 7.9	37.1 \pm 5.7
	Main effect group	$\rho = 0.647$	$\eta^2_p = 0.006$
	Main effect pre-post	$\rho = 0.606$	$\eta^2_p = 0.008$
	Interaction pre-post \times group	$\rho = 0.952$	$\eta^2_p = 0.000$

Significant effects ($p \leq 0.05$) are reported in bold font. Effect size is reported as partial eta squared (η^2_p) values.

TABLE 4 | Results of Chi-squared (χ^2) tests on the number of responders and non-responders for running economy (RE), maximal oxygen uptake ($\dot{V}O_2$ max), and peak treadmill speed (PTS) within the matched and non-matched training groups.

	Matched		Non-matched		χ^2	p
	Responder	Non-responder	Responder	Non-responder		
RE	7	11	9	10	0.271	0.603
$\dot{V}O_2$ max	8	10	5	14	1.33	0.248
PTS	8	10	9	10	0.032	0.858

No significant difference ($p \leq 0.05$) was observed.

or even no response (Mann et al., 2014). Moreover, individual responsiveness to training can vary by training mode (Hautala et al., 2006). Likewise, in the present study we aimed at improving RE and found a significant increase of 2.3% at groups level, but with individual effect ranging from a 4.8% decrease to a 13.8% increase. This was concomitant with an average PTS increase of 4.3% (ranging from a 3.8% decrease to a 12.5% increase) and a $\dot{V}O_2$ max increase of 3.8% (ranging from a 10.6% decrease to a 14.8% increase). This wide range

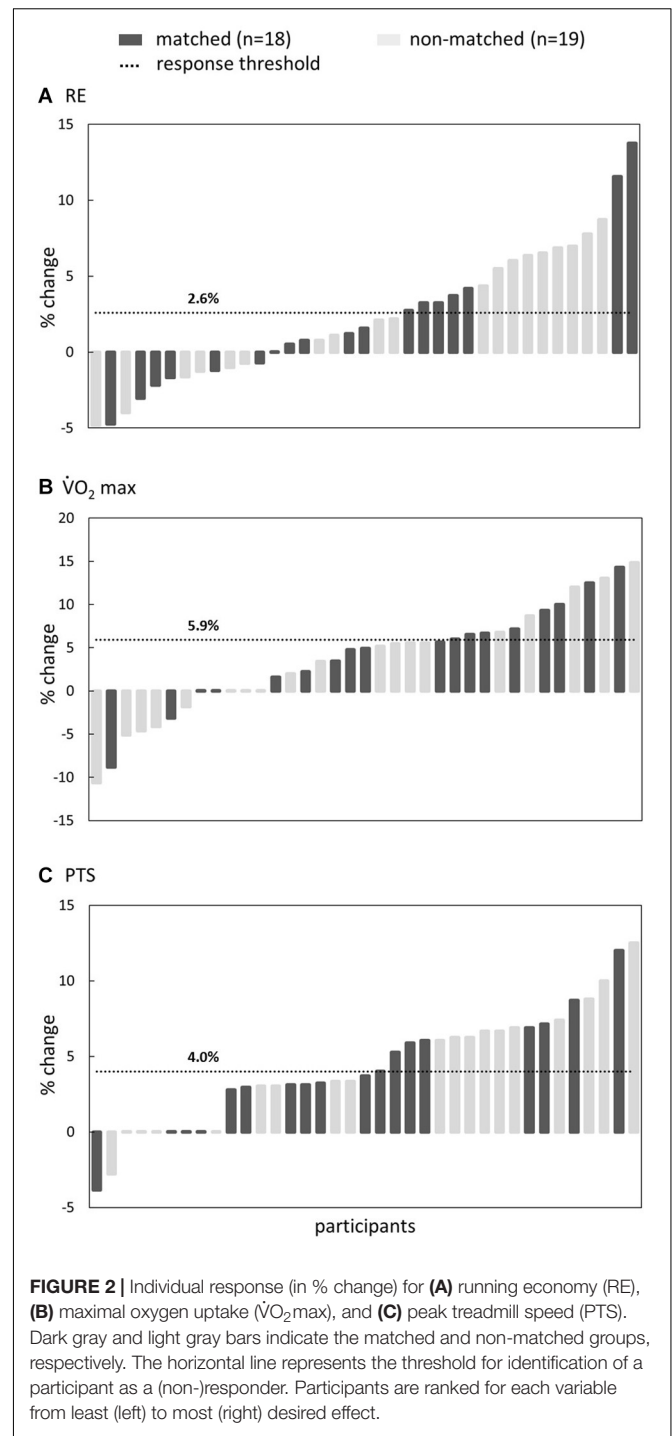


FIGURE 2 | Individual response (in % change) for (A) running economy (RE), (B) maximal oxygen uptake ($\dot{V}O_2$ max), and (C) peak treadmill speed (PTS). Dark gray and light gray bars indicate the matched and non-matched groups, respectively. The horizontal line represents the threshold for identification of a participant as a (non-)responder. Participants are ranked for each variable from least (left) to most (right) desired effect.

of individual responses highlights the importance of taking into account individual responses and not only the training effect on a group level (see Figure 2). It has been reported that average group level increases in RE ranged from 0 to 4.7% using heavy weight strength training (Johnston et al., 1997) and 0–4% using explosive training (Pellegrino et al., 2016; Meszler et al., 2019), which is in line with the current findings. Nevertheless, several studies reported no significant increase in

RE following concurrent endurance and strength training in recreational athletes despite improvements in muscle strength (Ferrauti et al., 2010; Mikkola et al., 2011; Taipale et al., 2013; Damasceno et al., 2015).

A possible explanation for the relatively small improvements in RE in our study can be found in the duration of the training period. A review by Denadai et al. (2017) highlighted that longer training periods (>8–21 weeks) are likely to result in greater RE improvements than shorter programs (6–8 weeks) due to the time-course of neuromuscular adaptations following concurrent training. A review on this topic by Rønnestad and Mujika (2014) stated that the possible mechanisms of how concurrent endurance and strength training can improve RE are related to a delayed activation of less efficient type II muscle fibers, an improved neuromuscular efficiency, the conversion of fast-twitch type IIX fibers into more fatigue resisted type IIA fibers, and an improved musculo-tendinous stiffness. During a short to medium term training period (up to 8 weeks), as was the case in the current study, the expected neuromuscular adaptations are an increased neural activation and a smaller relative proportion of type IIX than type IIA fibers, while an optimized musculo-tendinous stiffness is only achieved after longer training periods (>8–21 weeks). The absence of significant effects on any of the jumping performance parameters (SJ-h and 5RJ-P) in this study confirms a possible lack of musculo-tendinous adaptations after the 8 weeks training period. Therefore, when aiming at improving RE by strength training, longer training periods (>8–21 weeks) are advised.

Another possible explanation for unachieved RE improvement through concurrent training in some studies is that because the exact mechanisms behind RE improvement are still unknown, or the appropriate stimulus is not used. Some studies were able to induce neuromuscular adaptations (i.e., increase in maximal and explosive strength) through heavy weight training, while the intended effects on RE remained absent (Taipale et al., 2013; Vikmoen et al., 2016). A recent review on the effect of strength training on biomechanical and neuromuscular adaptations concluded that evidences that neuromuscular effects obtained by strength training transfer to running biomechanics are lacking (Trowell et al., 2020). In this study we tried to match the concurrent strength training to the global running pattern in order to obtain individualized neuromuscular adaptation in an attempt to maximize RE improvements. However, as we did not obtain better results, it seems that more insights are needed regarding the interaction between neuromuscular stimuli, its resulting adaptations, their transfer to the running pattern and their impact on RE.

A possible limitation to the current study might be that executed training sessions were unsupervised. Indeed, after an initial supervised strength training session, athletes were instructed to perform the training sessions on their own. Moreover, as runners were novice to strength training, the load of the training sessions was kept submaximal to avoid injuries. Higher training load might lead to greater RE improvements. Therefore, the adherence, intensity, order, and organization of

the training sessions was not strictly controlled and could partly explain the low mean training responses as well as the large inter-individual differences. On the other hand, it represents real-life conditions. In addition, even though runners were used to do interval trainings before starting the endurance training, the fact that they were now following a structured endurance training instead of their own “unstructured” one might partly explain the increase of $\dot{V}O_2\text{max}$, PTS, and RE. Finally, RE was assessed at a fixed running speed ($12 \text{ km}\cdot\text{h}^{-1}$), which was obviously not individualized for each participant. An alternative could have been to determine RE at different running speeds, as long as they fall below the respiratory compensation point and that a steady-state of oxygen consumption was reached within 3–15 min (Barnes and Kilding, 2015). These speeds could have been chosen to correspond to theoretical optimal running speeds to run 5, 10, 21, and 42 km races for each individual or to participants personal best on these distances. However, obtaining these speeds would have required to perform the maximal incremental running test before the submaximal one and to perform several submaximal tests, which would have increase the duration of the overall testing.

Future research should continue to focus on how neuromuscular adaptations, induced by individualized concurrent strength and endurance training, relate to changes in running biomechanics and improvement in performance (Trowell et al., 2020). Specific attention should go to the time-course of these adaptations to reveal if improvements are mainly made during the initial training period or if more long-term progress can be made, depending on the intervention. As well, a specific evaluation of the individually different responses to strength training, including PLY and DWT, should be done. Understanding these mechanisms should help predetermining which runner (i.e., global running pattern) needs which additional strength training to optimize performance. Such an individualized approach remains the ultimate goal for coaches and athletes.

As practical guidelines we can conclude that inter individual differences in training response to concurrent training are substantial (**Figure 2**). We encourage coaches and athletes to regularly evaluate the effectiveness of the prescribed training program and to keep looking for ways to individualize and optimize training responses. An initial assessment of the global running pattern as being rather AER or TER using the Volodalen method can be used as a way to identify the runners' preferences and be a guideline for training individualization.

CONCLUSION

As a conclusion, prescribing PLT or DWT strength training based on global running pattern, in addition to regular endurance training, did not lead to greater improvements in RE for recreational runners. In order to be able to optimize strength training prescription and its individualization in endurance runners, future research should aim to understand the exact mechanisms relating strength training to the resulting neuromuscular and biomechanical adaptations while running.

DATA AVAILABILITY STATEMENT

The raw data supporting the conclusions of this article will be made available by the authors, without undue reservation.

ETHICS STATEMENT

The studies involving human participants were reviewed and approved by Institutional Review Board of the University of Bourgogne, Franche-Comté (CPP: 2014-A00336-41). The patients/participants provided their written informed consent to participate in this study.

AUTHOR CONTRIBUTIONS

CG, LM, and TL: conceptualization, methodology, and supervision. AT and TL: investigation. AP, BB, and TL: formal

analysis and writing—original draft preparation. AP, BB, AT, LM, CG, and TL: writing—review and editing. All authors contributed to the article and approved the submitted version.

FUNDING

This study was supported by the University of Franche-Comté, Tomsk Polytechnic University CE Program, and Volodalen Swiss Sport Lab (CIFRE thesis 2013/0425).

ACKNOWLEDGMENTS

We thank the Compressport and Matsport companies for their loan of assessment devices. We also warmly thank the participants for their availability and their interest.

REFERENCES

- Anderson, T. (1996). Biomechanics and running economy. *Sports Med.* 22, 76–89. doi: 10.2165/00007256-199622020-00003
- Barnes, K. R., and Kilding, A. E. (2014). Strategies to improve running economy. *Sports Med.* 45, 37–56. doi: 10.1007/s40279-014-0246-y
- Barnes, K. R., and Kilding, A. E. (2015). Running economy: measurement, norms, and determining factors. *Sport Med. Open* 1, 1–15. doi: 10.1007/s00421-006-0147-3
- Blickhan, R. (1989). The spring-mass model for running and hopping. *J. Biomech.* 22, 1217–1227. doi: 10.1016/0021-9290(89)90224-8
- Bosco, C., Luhtanen, P., and Komi, P. V. (1983). A simple method for measurement of mechanical power in jumping. *Eur. J. Appl. Physiol. Occup. Physiol.* 50, 273–282. doi: 10.1007/bf00422166
- Conley, D. L., and Krahenbuhl, G. S. (1980). Running economy and distance running performance of highly trained athletes. *Med. Sci. Sport Exerc.* 12, 357–360. doi: 10.1249/00005768-198012050-00010
- Dalleau, G., Belli, A., Viale, F., Lacour, J. R., and Bourdin, M. (2004). A simple method for field measurements of leg stiffness in hopping. *Int. J. Sports Med.* 25, 170–176. doi: 10.1055/s-2003-45252
- Dalleck, L. C., Haney, D. E., Buchanan, C. A., and Weatherwax, R. M. (2016). Does a personalised exercise prescription enhance training efficacy and limit training unresponsiveness? A randomised controlled trial. *J. Fit. Res.* 5, 15–27.
- Damasco, M. V., Lima-Silva, A. E., Pasqua, L. A., Tricoli, V., Duarte, M., Bishop, D. J., et al. (2015). Effects of resistance training on neuromuscular characteristics and pacing during 10-km running time trial. *Eur. J. Appl. Physiol.* 115, 1513–1522. doi: 10.1007/s00421-015-3130-z
- Denadai, B. S., de Aguiar, R. A., de Lima, L. C. R., Greco, C. C., and Caputo, F. (2017). Explosive training and heavy weight training are effective for improving running economy in endurance athletes: a systematic review and meta-analysis. *Sports Med.* 47, 545–554. doi: 10.1007/s40279-016-0604-z
- Faul, F., Erdfelder, E., Lang, A.-G., and Buchner, A. G. (2007). Power 3: a flexible statistical power analysis program for the social, behavioral, and biomedical sciences. *Behav. Res. Methods* 39, 175–191. doi: 10.3758/bf03193146
- Ferrauti, A., Bergermann, M., and Fernandez-Fernandez, J. (2010). Effects of a concurrent strength and endurance training on running performance and running economy in recreational marathon runners. *J. Strength Cond. Res.* 24, 2770–2778. doi: 10.1519/jsc.0b013e3181d64e9c
- Gindre, C., Lussiana, T., Hebert-Losier, K., and Mourot, L. (2015). Aerial and terrestrial patterns: a novel approach to analyzing human running. *Int. J. Sports Med.* 37, 25–29. doi: 10.1055/s-0035-1555931
- Hautala, A. J., Kiviniemi, A. M., Mäkkikallio, T. H., Kinnunen, H., Nissilä, S., Huikuri, H. V., et al. (2006). Individual differences in the responses to endurance and resistance training. *Eur. J. Appl. Physiol.* 96, 535–542. doi: 10.1007/s00421-005-0116-2
- Howley, E. T., Bassett, D. R., and Welch, H. G. (1995). Criteria for maximal oxygen uptake. *Med. Sci. Sport Exerc.* 27, 1292–1301.
- Johnston, R. E., Quinn, T. J., Kertzer, R., and Vroman, N. B. (1997). Strength training in female distance runners: impact on running economy. *J. Strength Cond. Res.* 11, 224–229. doi: 10.1519/00124278-199711000-00004
- Kawamori, N., and Haff, G. G. (2004). The optimal training load for the development of muscular power. *J. Strength Cond. Res.* 18, 675–684. doi: 10.1519/00124278-200408000-00051
- Kuipers, H., Rietjens, G., Verstappen, F., Schoenmakers, H., and Hofman, G. (2003). Effects of stage duration in incremental running tests on physiological variables. *Int. J. Sports Med.* 24, 486–491. doi: 10.1055/s-2003-42020
- Lussiana, T., Patoz, A., Gindre, C., Mourot, L., and Hébert-Losier, K. (2019). The implications of time on the ground on running economy: less is not always better. *J. Exp. Biol.* 222(Pt 6):jeb192047. doi: 10.1242/jeb.192047
- Mann, T. N., Lamberts, R. P., and Lambert, M. I. (2014). High responders and low responders: factors associated with individual variation in response to standardized training. *Sports Med.* 44, 1113–1124. doi: 10.1007/s40279-014-0197-3
- Meszler, B., Atlasz, T., Misovics, B., Botka, B., Szabó, E., and Váci, M. (2019). Combined strength and plyometric exercise training improves running economy and muscle elastic energy storage and re-use in young untrained women. *Eur. J. Integr. Med.* 28, 86–91. doi: 10.1016/j.eujim.2019.05.004
- Mikkola, J., Rusko, H., Nummela, A., Pollari, T., and Häkkinen, K. (2007). Concurrent endurance and explosive type strength training improves neuromuscular and anaerobic characteristics in young distance runners. *Int. J. Sports Med.* 28, 602–611. doi: 10.1055/s-2007-964849
- Mikkola, J., Vesterinen, V., Taipale, R., Capostagno, B., Häkkinen, K., and Nummela, A. (2011). Effect of resistance training regimens on treadmill running and neuromuscular performance in recreational endurance runners. *J. Sports Sci.* 29, 1359–1371. doi: 10.1080/02640414.2011.589467
- Patoz, A., Gindre, C., Mourot, L., and Lussiana, T. (2019). Intra and inter-rater reliability of the Volodalen® scale to assess aerial and terrestrial running forms. *J. Athl. Enhanc.* 8, 4–9.
- Pellegrino, J., Ruby, B. C., and Dumke, C. L. (2016). Effect of plyometrics on the energy cost of running and MHC and titin isoforms. *Med. Sci. Sports Exerc.* 48, 49–56. doi: 10.1249/mss.0000000000000747
- Rønnestad, B. R., and Mujika, I. (2014). Optimizing strength training for running and cycling endurance performance: a review. *Scand. J. Med. Sci. Sport* 24, 603–612. doi: 10.1111/sms.12104
- Taipale, R. S., Mikkola, J., Vesterinen, V., Nummela, A., and Häkkinen, K. (2013). Neuromuscular adaptations during combined strength and endurance training

- in endurance runners: maximal versus explosive strength training or a mix of both. *Eur. J. Appl. Physiol.* 113, 325–335. doi: 10.1007/s00421-012-2440-7
- Trowell, D., Vicenzino, B., Saunders, N., Fox, A., and Bonacci, J. (2020). Effect of strength training on biomechanical and neuromuscular variables in distance runners: a systematic review and meta-analysis. *Sports Med.* 50, 133–150. doi: 10.1007/s40279-019-01184-9
- Turner, A. M., Owings, M., and Schwane, J. A. (2003). Improvement in running economy after 6 weeks of plyometric training. *J. Strength Cond. Res.* 17, 60–67. doi: 10.1519/00124278-200302000-00010
- Vikmoen, O., Raastad, T., Seynnes, O., Bergström, K., Ellefsen, S., and Rønnestad, B. R. (2016). Effects of heavy strength training on running performance and determinants of running performance in female endurance athletes. *PLoS One* 11:e0150799. doi: 10.1371/journal.pone.0150799
- World Medical Association (2013). World medical association declaration of helsinki ethical principles for medical research involving human subjects. *JAMA* 310, 2013–2016.
- Conflict of Interest:** CG was on the origin of the Volodalen® method. However, this paper does not constitute endorsement of the method by the authors and stems completely from a Ph.D. research project undertaken at the Bourgogne Franche-Comté University by TL.
- The remaining authors declare that the research was conducted in the absence of any commercial or financial relationships that could be construed as a potential conflict of interest.

Copyright © 2021 Patoz, Breine, Thouvenot, Mourot, Gindre and Lussiana. This is an open-access article distributed under the terms of the Creative Commons Attribution License (CC BY). The use, distribution or reproduction in other forums is permitted, provided the original author(s) and the copyright owner(s) are credited and that the original publication in this journal is cited, in accordance with accepted academic practice. No use, distribution or reproduction is permitted which does not comply with these terms.

9.8 PIMP Your Stride: Preferred Running Form to Guide Individualized Injury Rehabilitation

Cyrille Gindre¹, Bastiaan Breine^{1,2}, Aurélien Patoz^{1,3}, Kim Hébert-Losier^{4,5}, Adrien Thouvenot^{1,6}, Laurent Mouro^{6,7}, and Thibault Lussiana^{1,6,*}

¹ Research and Development Department, Volodalen Swiss Sportlab, Aigle, Switzerland,

² Department of Movement and Sports Sciences, Ghent University, Ghent, Belgium,

³ Institute of Sport Sciences, University of Lausanne, Lausanne, Switzerland,

⁴ Department of Sports Science, National Sports Institute of Malaysia, Kuala Lumpur, Malaysia,

⁵ Faculty of Health, Sport and Human Performance, University of Waikato, Adams Centre for High Performance, Tauranga, New Zealand,

⁶ Research Unit EA3920 Prognostic Markers and Regulatory Factors of Cardiovascular Diseases and Exercise Performance, Health, Innovation Platform, University of Bourgogne Franche-Comté, Besançon, France,

⁷ Division for Physical Education, Tomsk Polytechnic University, Tomsk, Russia

* Corresponding author

Published in **Frontiers in Rehabilitation Sciences**

DOI: 10.3389/fre.sc.2022.880483



PIMP Your Stride: Preferred Running Form to Guide Individualized Injury Rehabilitation

Cyrille Gindre¹, Bastiaan Breine^{1,2†}, Aurélien Patoz^{1,3†}, Kim Hébert-Losier^{4,5†},
Adrien Thouvenot^{1,6}, Laurent Mourot^{6,7†} and Thibault Lussiana^{1,6*†}

¹ Research and Development Department, Volodalen Swiss Sportlab, Aigle, Switzerland, ² Department of Movement and Sports Sciences, Ghent University, Ghent, Belgium, ³ Institute of Sport Sciences, University of Lausanne, Lausanne, Switzerland, ⁴ Department of Sports Science, National Sports Institute of Malaysia, Kuala Lumpur, Malaysia, ⁵ Faculty of Health, Sport and Human Performance, University of Waikato, Adams Centre for High Performance, Tauranga, New Zealand, ⁶ Research Unit EA3920 Prognostic Markers and Regulatory Factors of Cardiovascular Diseases and Exercise Performance, Health, Innovation Platform, University of Bourgogne Franche-Comté, Besançon, France, ⁷ Division for Physical Education, Tomsk Polytechnic University, Tomsk, Russia

OPEN ACCESS

Edited by:

Danièle Coraci,
University of Padua, Italy

Reviewed by:

Jannis Papatheanasiou,
Medical University - Sofia, Bulgaria
Aatik Arsh,
Khyber Medical University, Pakistan

*Correspondence:

Thibault Lussiana
lussiana.th@gmail.com

†ORCID:

Bastiaan Breine
orcid.org/0000-0002-7959-7721
Aurélien Patoz
orcid.org/0000-0002-6949-7989
Kim Hébert-Losier
orcid.org/0000-0003-1087-4986
Laurent Mourot
orcid.org/0000-0001-9486-3090
Thibault Lussiana
orcid.org/0000-0002-1782-401X

Specialty section:

This article was submitted to
Interventions for Rehabilitation,
a section of the journal
Frontiers in Rehabilitation Sciences

Received: 21 February 2022

Accepted: 13 May 2022

Published: 31 May 2022

Citation:

Gindre C, Breine B, Patoz A,
Hébert-Losier K, Thouvenot A,
Mourot L and Lussiana T (2022) PIMP
Your Stride: Preferred Running Form
to Guide Individualized Injury
Rehabilitation.
Front. Rehabil. Sci. 3:880483.
doi: 10.3389/fresc.2022.880483

Despite the wealth of research on injury prevention and biomechanical risk factors for running related injuries, their incidence remains high. It was suggested that injury prevention and reconditioning strategies should consider spontaneous running forms in a more holistic view and not only the injury location or specific biomechanical patterns. Therefore, we propose an approach using the preferred running form assessed through the Volodalen® method to guide injury prevention, rehabilitation, and retraining exercise prescription. This approach follows three steps encapsulated by the PIMP acronym. The first step (P) refers to the preferred running form assessment. The second step (I) is the identification of inefficiency in the vertical load management. The third step (MP) refers to the movement plan individualization. The answers to these three questions are guidelines to create individualized exercise pathways based on our clinical experience, biomechanical data, strength conditioning knowledge, and empirical findings in uninjured and injured runners. Nevertheless, we acknowledge that further scientific justifications with appropriate clinical trials and mechanistic research are required to substantiate the approach.

Keywords: rehabilitation, exercise, running, clinical evaluation, biomechanics

INTRODUCTION

Despite the wealth of research on injury prevention and biomechanical risk factors for running related injuries (RRI), their incidence remains high (1). Inconsistent associations between biomechanical factors and RRI have been observed, both in science and practice (2). As a result, injury prevention and strengthening, reconditioning, or rehabilitation programs in clinical management of runners can be challenging. Recently, Jauhiainen et al. (3) concluded that injury prevention and reconditioning strategies should consider spontaneous running forms in a more holistic view and not only the injury location or specific biomechanical patterns. Other authors suggested that the higher prevalence of soft tissue injuries and lacerations observed in cerebral palsy athletes compared to other disabled athletes could be explained by their moving and walking patterns (4). Herein, we suggest an approach using the preferred running form assessed through

the Volodalen[®] method (5) to guide injury prevention, rehabilitation, and retraining exercise prescription. The approach is based on biomechanical concepts from the scientific literature, as well as our clinical experiences, and evaluates potential discrepancies between spontaneously chosen running forms, biomechanical abnormalities, and the natural tendency for biological systems to self-optimize (6). In using this approach, clinicians need to answer three questions, following three steps, encapsulated by the **PIMP** acronym. The first step is **P**, which stands for Preferred running form assessment, with the question “Where is the runner on the terrestrial-aerial running form continuum?”. The second step is **I**, which stands for identification of Inefficiency in the vertical load management, with the question “Is the running stride too soft, too hard, or deems appropriate?”. The third step is **MP**, which stands for Movement Plan individualization, with the question “Would the runner benefits from extension- or flexion-based exercises?”. The answers to these three questions are guidelines to create individualized exercise pathways based on our clinical experience, acknowledging that clinical studies are required to support our approach.

THE FIRST STEP OF THE PIMP APPROACH

The first step in our approach is to determine the preferred running pattern. A wide range of running styles exists, with no unique style shown to be superior to another in terms of running endurance performance or injury risk (3, 6–8). Our research team has developed the Volodalen[®] method which allows placing a runner’s spontaneous running form along a continuum ranging from pronounced terrestrial to pronounced aerial. The Volodalen[®] method comes from field observation and the principle of self-optimized movements. The method evaluates and scores five items to obtain a global V[®]score: vertical head oscillation, anterior-posterior motion of the elbows, pelvis position at ground contact, foot position at ground contact, and foot strike pattern (5) (**Figure 1**). These five items are subjectively scored by an expert from 1 to 5 and summed to obtain a quantitative V[®]score. In other words, a pronounced terrestrial running form shows limited vertical oscillation, pronounced arm movement, a pelvis position close to the ground, a foot strike position in front of the center of mass, and a rearfoot strike pattern. A pronounced aerial running pattern is characterized by the opposite. Based on the V[®]score, four categories can be determined: pronounced terrestrial (V[®]score range: 5–10), terrestrial (V[®]score range: 11–15), aerial (V[®]score range: 16–20), and pronounced aerial (V[®]score range: 21–25). The validity of the Volodalen[®] method is supported by previous research (9, 10). Indeed, the visual observations of global running forms was shown to reflect quantifiable objective parameters (9). In addition, the method was shown to be a reliable tool to subjectively assess global running patterns, independently of the degree of expertise, whereas the subjective assessment of a single item of the V[®]score was rater-dependent (10). Alternatively, our research team showed that the duty factor (DF), the proportion of time spent in contact with the ground during a running

stride (11), can be used as a laboratory-based and objective alternative to the subjective V[®]score (12). To summarize, a pronounced aerial running form is characterized by a spring-like running pattern with pronounced vertical oscillations and a more anterior (midfoot and forefoot) strike pattern than a terrestrial running form. In contrast, a pronounced terrestrial running form shows small vertical oscillations, as well as longer contact times, and a more rearfoot strike pattern than an aerial running form. Although the categorization and dichotomization of running forms always involve simplification, this practice is useful from a clinical perspective. For the PIMP approach, we propose clustering individuals into four categories (**Figure 2**): pronounced terrestrial—terrestrial—aerial—pronounced aerial. This categorization can be obtained using either the subjective V[®]score or the objective DF (**Figure 1**).

The importance of determining the preferred running pattern can be demonstrated by its relationship with metabolic cost. When comparing a group of aerial and terrestrial runners, both groups showed similar metabolic costs despite distinct running kinetics and kinematics (7, 13), in accordance with findings of similar metabolic costs for different running styles, as summarized elsewhere (6). This supports the idea that self-selected running forms are often the most economical (6), and that humans tend to self-optimize movement patterns to reduce metabolic cost. Another factor that shows the importance of preferred running pattern is its relationship with vertical load management, which leads to step 2.

THE SECOND STEP OF THE PIMP APPROACH

The second step in our approach is to identify whether the runner or patient shows an inefficiency in the vertical load management. As running is a weight bearing activity, the way vertical load is handled is a key factor in RRI (2, 14). An efficient running stride comes from a compromise between compliance—the acceptance of joint deformation—and stiffness—the resistance against joint deformation. A terrestrial runner needs a certain degree of joint compliance to show a running pattern with less vertical oscillation and a smooth foot unroll. An efficient rearfoot strike needs sufficient ankle and knee range of motion to generate a smooth foot unroll during early stance (7, 14–16). On the contrary, an aerial runner needs a certain amount of leg stiffness to be able to perform a vertically oscillating stride. An efficient forefoot strike needs a sufficiently stiff ankle joint to be able to withstand the external ankle dorsiflexion moment during early stance (17, 18). However, both the aerial and terrestrial running pattern can become suboptimal in the vertical load management, which could lead to injury. Such inefficiencies can be categorized as either being “too soft”—an excessive compliance—or “too hard”—an excessive stiffness. Kinematic, kinetic, and spatiotemporal risk factors, as determined in a recent systematic review by Ceysens et al. (2) were categorized according to the inefficiency identified by the PIMP approach (**Table 1**). Almost each risk factor could be interpreted as a sign of a too soft or too hard running pattern. For more details about

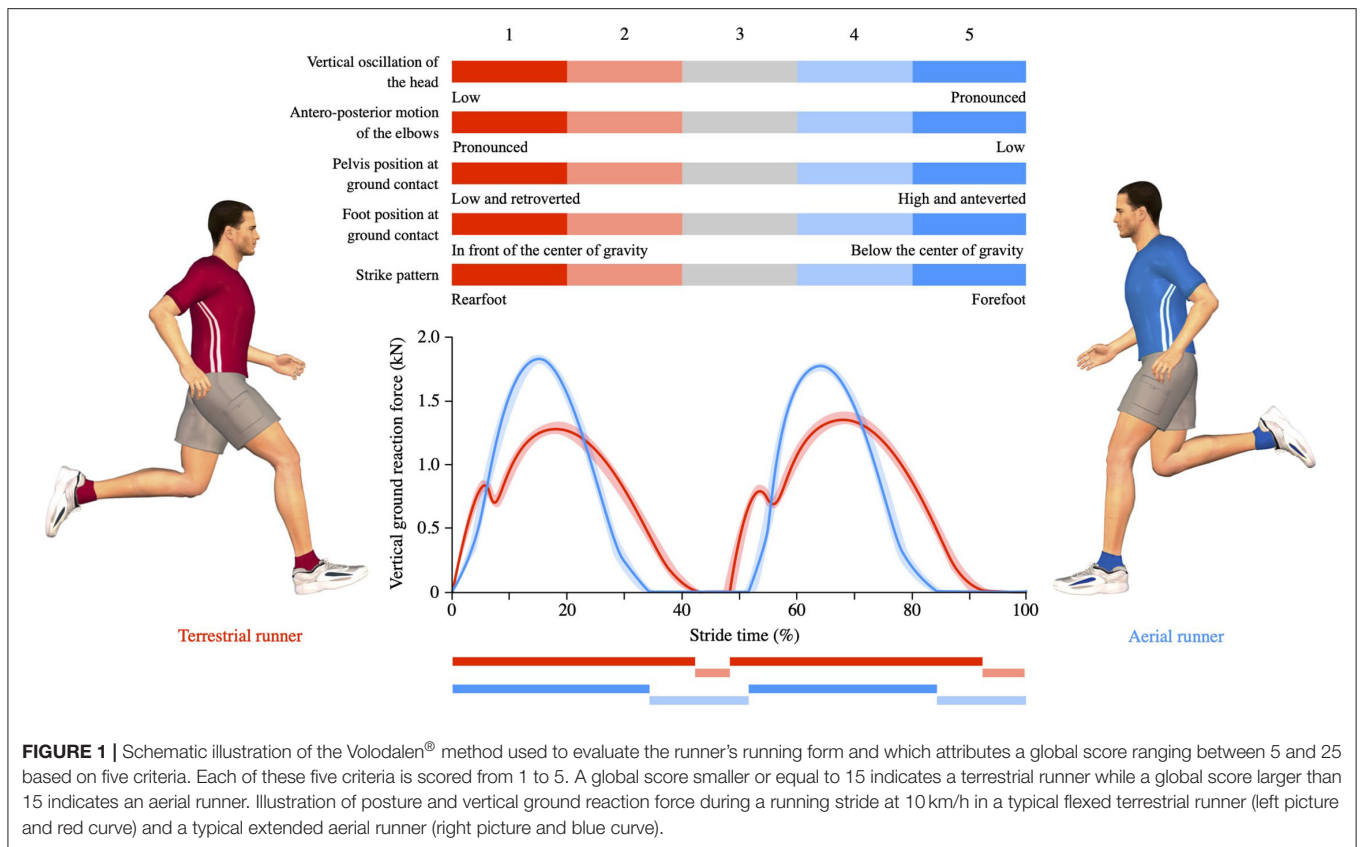


FIGURE 1 | Schematic illustration of the Volodalen® method used to evaluate the runner's running form and which attributes a global score ranging between 5 and 25 based on five criteria. Each of these five criteria is scored from 1 to 5. A global score smaller or equal to 15 indicates a terrestrial runner while a global score larger than 15 indicates an aerial runner. Illustration of posture and vertical ground reaction force during a running stride at 10 km/h in a typical flexed terrestrial runner (left picture and red curve) and a typical extended aerial runner (right picture and blue curve).

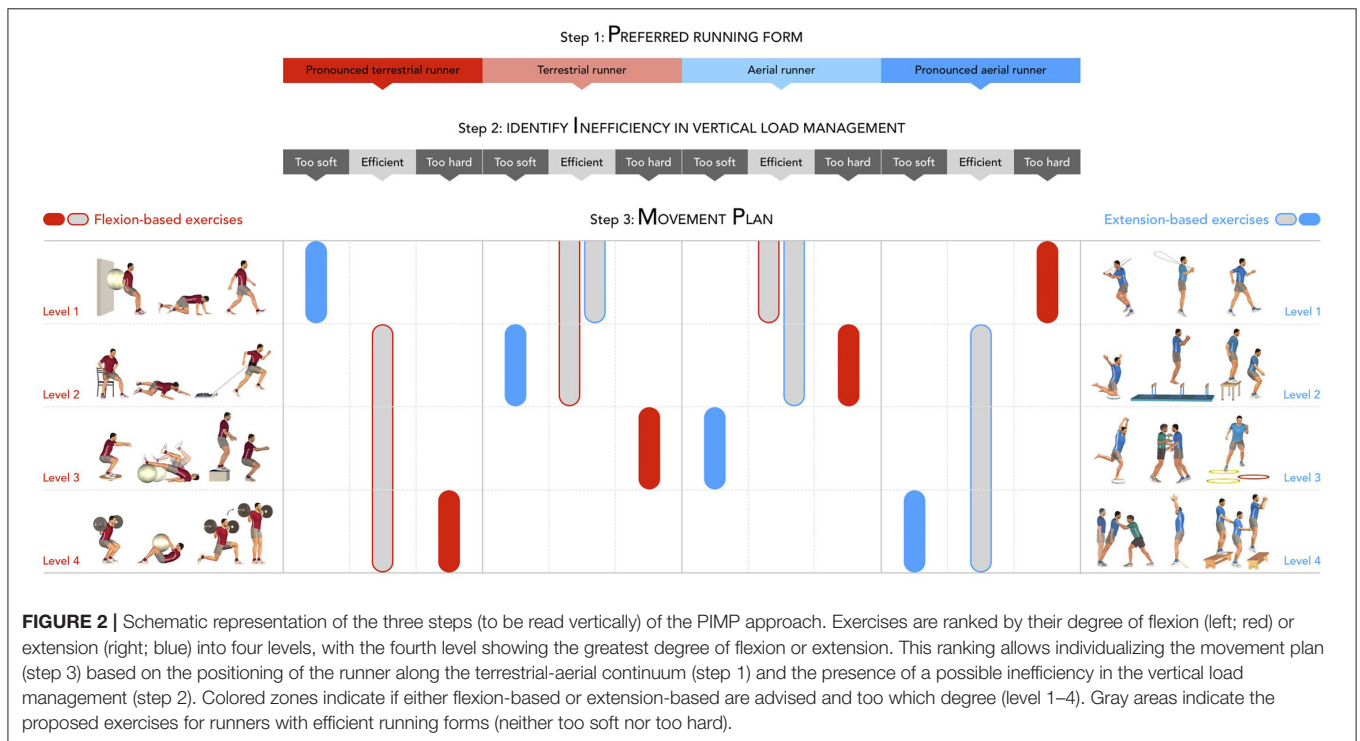


FIGURE 2 | Schematic representation of the three steps (to be read vertically) of the PIMP approach. Exercises are ranked by their degree of flexion (left; red) or extension (right; blue) into four levels, with the fourth level showing the greatest degree of flexion or extension. This ranking allows individualizing the movement plan (step 3) based on the positioning of the runner along the terrestrial-aerial continuum (step 1) and the presence of a possible inefficiency in the vertical load management (step 2). Colored zones indicate if either flexion-based or extension-based are advised and to which degree (level 1–4). Gray areas indicate the proposed exercises for runners with efficient running forms (neither too soft nor too hard).

TABLE 1 | Kinematic, kinetic, and spatiotemporal risk factors as determined by a systematic review by Ceysens et al. (2) and categorized according to the inefficiency identified by the PIMP approach.

Inefficiency	Risk factor	Injured runner	Non-injured runner	Sex
Too hard	↓ ankle eversion range of motion (°)	16.7 (2.5)	20.4 (3.7)	♀ / ♂
	↓ peak ankle eversion velocity (°/s)	326 (95)	479 (157)	♀ / ♂
	↑ knee joint stiffness (Nm/°)	6.89 (2.65)	6.72 (2.03)	♀ / ♂
	↑ vertical instantaneous loading rate (BW/s)	88.0 (13.9)	73.1 (15.9)	♀
		127 (40)	97 (31)	♂
	↑ vertical average loading rate (BW/s)	78.2 (11.1)	60.7 (12.8)	♀
	↑ vertical impact peak (BW)	1.72 (0.21)	1.51 (0.22)	♀
	↑ peak braking force (BW)	<-0.27	>-0.23	♀
	↓ step rate (over-striding) (steps/min)	<166	>178	♀ / ♂
	↓ ground contact time (s)	0.213 (0.040)	0.237 (0.026)	♂
Too soft	↑ peak hip adduction angle (°) (contralateral hip drop)	12.8 (2.8)	8.1 (4.5)	♀
	↑ internal knee abduction moment impulse (Nms)	9.2 (3.7)	4.7 (3.5)	♀ / ♂
	↑ peak external knee adduction moment (Nm/kg)	1.32 (1.08–1.56)	0.93 (0.78–1.08)	♀ / ♂
	↑ peak knee internal rotation angle	3.9 (3.7)	0.0 (4.6)	♀
	↑ peak ankle eversion velocity (°/s)	360 (271–449)	261 (212–310)	♀ / ♂
	↑ peak ankle eversion angle (°)	8.1 (3.0)	4.4 (4.2)	♀ / ♂
Other	↓ asymmetry in vertical impact peak (symmetry angle)	1.89 (1.88)	2.75 (2.48)	♀ / ♂
	↑ asymmetry in ground contact time (symmetry angle)	1.53 (1.04)	1.50 (2.06)	♀ / ♂

Each risk factor is categorized as “too hard”, “too soft”, or other according to the inefficiency identified by the PIMP approach. Presented risk factors were found to have at least limited evidence of being related to running related injuries. Variables with very limited or no statistical relation with injury were not included. For each variable, mean (standard deviation) or mean (95% confidence interval) for the injured and non-injured runners were presented where possible. If not, cut-off values for high- and low-risk groups were given. In the last column, a male (♂) or female (♀) symbol was used to indicate whether evidence exists for male, female, or both.

the experimental conditions in which these data were collected, we refer the readers to the review and associated original articles.

In running forms that are too hard, tissue vibrations or “noisy” strides linked to an excessive impact at ground contact are observed. For example, a runner that over-strides can be defined as having a too hard running pattern. Such a running pattern is characterized by a low step rate, an increased impact intensity, and large braking forces; all of which have been related to RRI (2). In contrast, inconsistencies in mobilities between transverse and coronal plane motion (especially at the feet, knees, and hips) and RRI conceptually underpin the too soft running form. In this case, the non-sagittal plane movements considerably contribute to impact attenuation. For instance, RRI such as the iliotibial band syndrome, can be associated with large ranges of non-sagittal motion, such as peak hip adduction (contralateral hip drop during stance) or knee internal rotation (19, 20). The excess of “softness” characteristics are more frequent in female runners, with a less clear association between non-sagittal plane biomechanics and RRI when considering both males and females (19).

These too soft and too hard characteristics can be observed in both aerial and terrestrial runners. The real challenge is to be able to observe these characteristics in a clinical setting. Most of these variables are only measurable in a laboratory setting, using equipment which most coaches, physiotherapists, or health clinicians do not have access too. However, it is possible to assess such motor inefficiency visually or by

using cheaper technologies such as wearable sensors or video analyses. It must be noted that there is no clear threshold to define what constitutes too much or too little for any given biomechanical parameter. Besides, the values associated with the risk factors presented in **Table 1** are speed, gender, method, and injury dependent. Hence, clinical judgment is essential in our proposed PIMP approach. Expertise in such clinical judgment can only be obtained through years of experience in assessing running gait parameters in uninjured and injured runners. The too soft or too hard concept should provide easy to interpret concepts for practitioners to develop such competence.

THE THIRD STEP OF THE PIMP APPROACH

The third step in our approach consists in designing an individualized movement plan (**Figure 2**). **Extension-based strengthening exercises** promote short ground contact times, pushing the center of mass forward and upward, stiffness, and body alignment, i.e., shoulder-hip-knee-ankle, and activation of the posterior muscular chains. Such exercises correspond with how aerial runners manage the vertical load during running. Therefore, these exercises are suggested for aerial runners or any runners presenting a too soft running pattern. In contrast, **flexion-based strengthening exercises** promote long ground contact times, pushing the center of mass backward and

TABLE 2 | Four examples of the application of the PIMP approach.

Complaint or injury	Step 1 Preferred running form	Step 2 Identify inefficiency	Step 3 Movement plan
Lower back pain	Pronounced terrestrial	Too hard: overstriding	Level 4 flexion-based exercises e.g.,: <i>core stability in flexed position</i>
Proximal hamstring pain	Terrestrial	Too soft: increased transversal and frontal plane pelvic rotation	Level 2 extension-based exercises e.g.,: <i>step downs with external hip rotation</i>
Iliotibial band syndrome	Aerial	Too soft: knee valgus	Level 3 extension-based exercises e.g.,: <i>skipping drills</i>
Achilles tendinopathy	Pronounced aerial	Too hard: pronounced forefoot strike and increased flight times	Level 1 flexion-based exercises e.g.,: <i>quarter-squats</i>

downward, large ranges of motion, and activation of the anterior muscular chains. Such exercises correspond with how terrestrial runners manage the vertical load during running. Therefore, these exercises are recommended for terrestrial runners or any runners presenting a too hard running pattern. In other words, the preferred running form, as classified along the terrestrial-aerial continuum, determines the starting point of strengthening exercises (from flexion-based to extension-based). With these individualized exercises, we aim to allow the runners to PIMP their running form toward becoming less hard or less soft. The approach can be clarified with four examples, as presented in **Table 2**.

Both a too soft or too hard running pattern have been linked independently with the same RRI (21). This highlights the importance of setting up a movement plan starting from the preferred running pattern and any inefficiency in the vertical load management, rather than only considering the type of injury. For instance, plantar fasciopathy has been related to both excessive pronation (too soft) and increased impact intensity (too hard) (21), warranting a different movement plan.

STRENGTHS AND LIMITATIONS

The PIMP approach presented herein proposed to understand and analyze the running form from both a global and local point of view to enhance the ability of practitioners to individualize prescription, rehabilitation, and retraining programs, with the goal of minimizing the recurrence of running-related injuries. Such multiscale (global and local movements reading) approach could allow a better understanding of clinical, scientific, and social issues linked to recurrent running-related injuries. Indeed, physical and rehabilitation medicine is a real challenge in the 21st century (22) but the ease of use of the subjective approach presented herein makes it replicable in resource limited settings.

Nonetheless, the scientific validation of the effectiveness of the proposed approach is still needed. Indeed, the method is based on our clinical experience, biomechanical data, strength and conditioning knowledge, and empirical observations in both injured and uninjured runners. We acknowledge that further scientific justifications with appropriate clinical trials and

mechanistic research are required to substantiate the approach and therefore constitute the main limitation of the method in its current form. Moreover, determining the preferred running pattern of injured runners might be a difficult task because of possible gait modifications due to pain. In that case, indirect information could be obtained, e.g., by looking at the wear patterns of the shoes, by assessing the antero-posterior position of the quiet standing center of pressure (23), or by asking how runners perceive their running form.

PERSPECTIVES

In addition to strengthening exercises, gait retraining, e.g., stride frequency or foot strike pattern manipulations, can be an important part of the rehabilitation program (24). The PIMP approach can also be used to guide gait retraining strategies and recommendations but elaborating on this PIMP application is beyond the scope of the current opinion and warrants a separate discussion. We believe the presented approach provides a general framework for practitioners to evaluate preferred running forms, identify inefficiency in vertical load management, and design an individualized movement plan.

DATA AVAILABILITY STATEMENT

The original contributions presented in the study are included in the article/supplementary material, further inquiries can be directed to the corresponding author/s.

AUTHOR CONTRIBUTIONS

CG was responsible for the conceptualization of the approach. All authors contributed to the article and approved the submitted version.

FUNDING

This work was supported by the Volodalen Company, the Université of Franche Comté and Tomsk Polytechnic University Development Program.

REFERENCES

- Dempster J, Dutheil F, Ugbohue UC. The prevalence of lower extremity injuries in running and associated risk factors: a systematic review. *Physical Act Health*. (2021) 5:133–45. doi: 10.5334/paah.109
- Ceyskens L, Vanelderden R, Barton C, Malliaras P, Dingenen B. Biomechanical risk factors associated with running-related injuries: a systematic review. *Sports Med*. (2019) 49:1095–115. doi: 10.1007/s40279-019-01110-z
- Jauhiainen S, Pohl AJ, Äyrämö S, Kauppi JP, Ferber R. A hierarchical cluster analysis to determine whether injured runners exhibit similar kinematic gait patterns. *Scand J Med Sci Sports*. (2020) 30:732–40. doi: 10.1111/sms.13624
- Patatoukas D, Farmakides A, Aggeli V, Fotaki S, Tsibidakis H, Mavrogenis AF, et al. Disability-related injuries in athletes with disabilities. *Folia Med*. (2011) 53:40–6. doi: 10.2478/v10153-010-0026-x
- Gindre C, Lussiana T, Hébert-Losier K, Mourot L. Aerial and terrestrial patterns: a novel approach to analyzing human running. *Int J Sports Med*. (2016) 37:25–9. doi: 10.1055/s-0035-1555931
- Moore IS. Is there an economical running technique? A review of modifiable biomechanical factors affecting running economy. *Sports Med*. (2016) 46:793–807. doi: 10.1007/s40279-016-0474-4
- Lussiana T, Gindre C, Hébert-Losier K, Sagawa Y, Gimenez P, Mourot L. Similar running economy with different running patterns along the aerial-terrestrial continuum. *Int J Sports Physiol Perform*. (2017) 12:481. doi: 10.1123/ijspp.2016-0107
- Hanley B, Bissas A, Merlino S, Gruber AH. Most marathon runners at the 2017 IAAF World Championships were rearfoot strikers, and most did not change footstrike pattern. *J Biomech*. (2019) 92:54–60. doi: 10.1016/j.jbiomech.2019.05.024
- Lussiana T, Gindre C, Mourot L, Hébert-Losier K. Do subjective assessments of running patterns reflect objective parameters? *Eur J Sport Sci*. (2017) 17:847–57. doi: 10.1080/17461391.2017.1325072
- Patoz A, Gindre C, Mourot L, Lussiana T. Intra and inter-rater reliability of the Volodalen® scale to assess aerial and terrestrial running forms. *J Athletic Enhancement*. (2019) 8:1–6.
- Minetti AE. A model equation for the prediction of mechanical internal work of terrestrial locomotion. *J Biomech*. (1998) 31:463–8. doi: 10.1016/S0021-9290(98)00038-4
- Patoz A, Gindre C, Thouvenot A, Mourot L, Hébert-Losier K, Lussiana T. Duty factor is a viable measure to classify spontaneous running forms. *Sports*. (2019) 7:233. doi: 10.3390/sports7110233
- Lussiana T, Patoz A, Gindre C, Mourot L, Hébert-Losier K. The implications of time on the ground on running economy: less is not always better. *J Exp Biol*. (2019) 222:jeb192047. doi: 10.1242/jeb.192047
- Breine B, Malcolm P, Van Caekenbergh I, Fiers P, Frederick EC, De Clercq D. Initial foot contact and related kinematics affect impact loading rate in running. *J Sports Sci*. (2017) 35:1556–64. doi: 10.1080/02640414.2016.1225970
- De Clercq D, Aerts P, Kunnen M. The mechanical characteristics of the human heel pad during foot strike in running: an *in vivo* cineradiographic study. *J Biomech*. (1994) 27:1213–22. doi: 10.1016/0021-9290(94)90275-5
- Gerritsen KGM, Van Den Bogert AJ, Nigg BM. Direct dynamics simulation of the impact phase in heel-toe running. *J Biomech*. (1995) 28:661–8. doi: 10.1016/0021-9290(94)00127-P
- Ahn AN, Brayton C, Bhatia T, Martin P. Muscle activity and kinematics of forefoot and rearfoot strike runners. *J Sport Health Sci*. (2014) 3:102–12. doi: 10.1016/j.jshs.2014.03.007
- Stearne SM, Alderson JA, Green BA, Donnelly CJ, Rubenson J. Joint kinetics in rearfoot versus forefoot running: implications of switching technique. *Med Sci Sports Exercise*. (2014) 46:1578–87. doi: 10.1249/MSS.0000000000000254
- Buist I, Bredeweg SW, Lemmink KPM, Van Mechelen W, Diercks RL. Predictors of running-related injuries in novice runners enrolled in a systematic training program: a prospective cohort study. *Am J Sports Med*. (2009) 38:273–80. doi: 10.1177/0363546509347985
- Ferber R, Noehren B, Hamill J, Davis I. Competitive female runners with a history of iliotibial band syndrome demonstrate atypical hip and knee kinematics. *J Orthopaedic Sports Physical Ther*. (2010) 40:52–8. doi: 10.2519/jospt.2010.3028
- Beeson P. Plantar fasciopathy: revisiting the risk factors. *Foot Ankle Surg*. (2014) 20:160–5. doi: 10.1016/j.fas.2014.03.003
- Troev T, Papathanasiou J. *Essentials of Physical and Rehabilitation Medicine for Undergraduate Medical Students*. Plovdiv: Lax Book (2016).
- Lussiana T, Potier C, Gindre C. Motor preferences in running and quiet standing. *Sci Sports*. (2018) 33:e249–52. doi: 10.1016/j.scispo.2018.04.006
- Davis IS, Tenforde AS, Neal BS, Roper JL, Willy RW. Gait retraining as an intervention for patellofemoral pain. *Curr Rev Musculoskelet Med*. (2020) 13:103–14. doi: 10.1007/s12178-020-09605-3

Conflict of Interest: CG is the originator of the Volodalen® method. CG, BB, and TL are employed by Volodalen. AT was employed by Volodalen at the time of writing the manuscript.

The remaining authors declare that the research was conducted in the absence of any commercial or financial relationships that could be construed as a potential conflict of interest.

Publisher's Note: All claims expressed in this article are solely those of the authors and do not necessarily represent those of their affiliated organizations, or those of the publisher, the editors and the reviewers. Any product that may be evaluated in this article, or claim that may be made by its manufacturer, is not guaranteed or endorsed by the publisher.

Copyright © 2022 Gindre, Breine, Patoz, Hébert-Losier, Thouvenot, Mourot and Lussiana. This is an open-access article distributed under the terms of the Creative Commons Attribution License (CC BY). The use, distribution or reproduction in other forums is permitted, provided the original author(s) and the copyright owner(s) are credited and that the original publication in this journal is cited, in accordance with accepted academic practice. No use, distribution or reproduction is permitted which does not comply with these terms.

9.9 Non-South East Asians have a better running economy and different anthropometrics and biomechanics than South East Asians.

Aurélien Patoz^{1,2,*}, Thibault Lussiana^{2,3,4}, Bastiaan Breine^{2,5}, Cyrille Gindre^{2,3}, Laurent Mourot^{4,6}, Kim Hébert-Losier^{7,8}

¹ Institute of Sport Sciences, University of Lausanne, 1015 Lausanne, Switzerland

² Research and Development Department, Volodalen Swiss Sport Lab, 1860 Aigle, Switzerland

³ Research and Development Department, Volodalen, 39270 Chavéria, France

⁴ Research Unit EA3920 Prognostic Markers and Regulatory Factors of Cardiovascular Diseases and Exercise Performance, Health, Innovation platform, University of Bourgogne Franche-Comté, 2500 Besançon, France

⁵ Department of movement and Sports Sciences, Ghent University, 9000 Ghent, Belgium

⁶ Division for Physical Education, Tomsk Polytechnic University, 634040 Tomsk, Russia

⁷ Division of Health, Engineering, Computing and Science, Te Huataki Waiora School of Health, University of Waikato, Adams Centre for High Performance, 3116 Tauranga, New Zealand

⁸ Department of Sports Science, National Sports Institute of Malaysia, 57000 Kuala Lumpur, Malaysia

* Corresponding author

Published in **Scientific Reports**

DOI: 10.1038/s41598-022-10030-4



OPEN

Non-South East Asians have a better running economy and different anthropometrics and biomechanics than South East Asians

Aurélien Patoz^{1,2✉}, Thibault Lussiana^{2,3,4}, Bastiaan Breine^{2,5}, Cyrille Gindre^{2,3}, Laurent Mourot⁴ & Kim Hébert-Losier^{6,7}

Running biomechanics and ethnicity can influence running economy (RE), which is a critical factor of running performance. Our aim was to compare RE of South East Asian (SEA) and non-South East Asian (non-SEA) runners at several endurance running speeds (10–14 km/h) matched for on-road racing performance and sex. Secondly, we explored anthropometric characteristics and relationships between RE and anthropometric and biomechanical variables. SEA were 6% less economical ($p = 0.04$) than non-SEA. SEA were lighter and shorter than non-SEA, and had lower body mass indexes and leg lengths ($p \leq 0.01$). In terms of biomechanics, a higher prevalence of forefoot strikers in SEA than non-SEA was seen at each speed tested ($p \leq 0.04$). Furthermore, SEA had a significantly higher step frequency ($p = 0.02$), shorter contact time ($p = 0.04$), smaller footstrike angle ($p < 0.001$), and less knee extension at toe-off ($p = 0.03$) than non-SEA. Amongst these variables, only mass was positively correlated to RE for both SEA (12 km/h) and non-SEA (all speeds); step frequency, negatively correlated to RE for both SEA (10 km/h) and non-SEA (12 km/h); and contact time, positively correlated to RE for SEA (12 km/h). Despite the observed anthropometric and biomechanical differences between cohorts, these data were limited in underpinning the observed RE differences at a group level. This exploratory study provides preliminary indications of potential differences between SEA and non-SEA runners warranting further consideration. Altogether, these findings suggest caution when generalizing from non-SEA running studies to SEA runners.

Running economy (RE), which refers to steady-state oxygen consumption at a given submaximal running speed, is a critical factor of running performance¹. RE has been shown to differ between ethnic groups^{2–5}. Indeed, Weston, et al.² noted greater RE in African than Caucasian distance runners though not elucidating the origin of these differences. Similarly, elite Kenyans were found more economical than their Caucasian counterparts^{3–5}. This difference was attributed to body dimensions, with longer legs (~5%), thinner and lighter calf musculature, as well as lower body mass and body mass index (BMI) in Kenyans than Caucasians, but not to differences in muscle fibre type^{3–6}. These findings may partially explain the success of African runners at the elite level. Indeed, the longer, slenderer legs of Kenyans could be advantageous when running as RE is correlated with leg mass⁶. However, the precise mechanisms underpinning anthropometric and economy relationships are not clear⁷.

¹Institute of Sport Sciences, University of Lausanne, 1015 Lausanne, Switzerland. ²Research and Development Department, Volodalen Swiss Sport Lab, 1860 Aigle, Switzerland. ³Research and Development Department, Volodalen, 39270 Chavéria, France. ⁴Research Unit EA3920 Prognostic Markers and Regulatory Factors of Cardiovascular Diseases and Exercise Performance, Health, Innovation Platform, University of Bourgogne Franche-Comté, 2500 Besançon, France. ⁵Department of Movement and Sports Sciences, Ghent University, 9000 Ghent, Belgium. ⁶Division of Health, Engineering, Computing and Science, Te Huataki Waiora School of Health, Adams Centre for High Performance, University of Waikato, Tauranga 3116, New Zealand. ⁷Department of Sports Science, National Sports Institute of Malaysia, 57000 Kuala Lumpur, Malaysia. ✉email: aurelien.patoz@unil.ch

Research into running and ethnic differences has mostly compared Caucasian and African runners^{2–5,8–13}. These studies highlight differences in physiological^{2–5,12}, anthropometrical^{9,14}, neuromuscular¹⁵, and running gait patterns^{8,10,11} between ethnicities. Altogether, these results indicate caution in the generalization of results from one ethnic group to another.

There exists only limited inclusion of Asian cohorts in running studies^{14–16} and, to the best of our knowledge, no study comparing their RE to another ethnic group. Nonetheless, road race participation continues to grow in Asia despite a decline in the number of participants since 2016 outside of Asia¹⁷. Therefore, the relative underrepresentation of Asian runners in research is of concern, especially when considering their unique anthropometric features^{18,19}, autonomic responses to exercise²⁰, muscle–tendon unit properties¹⁵, walking gait characteristics²¹, and footstrike patterns¹⁶ compared to other ethnic groups.

Although running biomechanics can influence RE¹, the relationships between select biomechanical variables and RE are unclear and even conflicting in the scientific literature. For instance, Gruber, et al.²² observed no difference in RE between rearfoot (RFS) and non-rearfoot (non-RFS) strike patterns, while both RFS²³ and non-RFS²⁴ patterns were suggested as more economical than the other. Similarly, superior RE has been linked with both long²⁵ and short²⁶ ground contact times (t_c), while Williams and Cavanagh²⁷ found no significant relation between RE and t_c . These divergent findings might be due to differences between the cohorts examined, including ethnic differences.

For these reasons, our primary aim was to explore whether South East Asian (SEA) and non-South East Asian (non-SEA) runners demonstrate similar RE at several endurance running speeds when matched for on-road running performance and sex. Secondly, we aimed to explore anthropometric differences between groups and potential relationships between RE and anthropometric and biomechanical variables in these groups.

Materials and methods

Participants. An existing database of 54 runners was explored to match SEA and non-SEA runners based on sex and on-road running performance on 21.1 km²⁸. The matching led to the inclusion of 34 trained runners, 20 males (variable: mean \pm standard deviation, age: 36 \pm 6 years, mass: 68 \pm 11 kg, height: 176 \pm 7 cm, leg length: 92 \pm 5 cm, BMI: 22 \pm 2 kg/m², running distance: 56 \pm 20 km/week, running experience: 9 \pm 7 y, and best half-marathon time: 93 \pm 9 min) and 14 females (age: 36 \pm 6 y, mass: 53 \pm 6 kg, height: 162 \pm 4 cm, leg length: 84 \pm 3 cm, BMI: 20 \pm 2 kg/m², running distance: 58 \pm 17 km/week, running experience: 7 \pm 5 years, and best half-marathon time: 100 \pm 9 min) in this study. For study inclusion, participants were required to be in good self-reported general health with no current or recent (<3 months) musculoskeletal injuries and to meet a certain level of running performance. More specifically, runners were required to have competed in a road race in the last year with finishing times of \leq 50 min for 10 km, \leq 1 h 50 min for 21.1 km or \leq 3 h 50 min for 42.2 km. The ethical committee of the National Sports Institute of Malaysia approved the study protocol prior to participant recruitment (ISNRP: 26/2015), which was conducted in accordance with international ethical standards²⁹ and adhered to the latest Declaration of Helsinki of the World Medical Association.

Runners were classified in two ethnic groups based on their nationality: SEA and non-SEA, which led to a total of 17 participants per group. SEA runners were from China ($n = 12$), Malaysia ($n = 14$), and Indonesia ($n = 1$); while non-SEA runners were from England ($n = 7$), Sweden ($n = 2$), Australia, Brazil, Canada, Denmark, France, Norway, Poland, and Scotland ($n = 1$ each). All non-SEA runners identified as “white”.

Experimental procedure. Each participant completed one experimental laboratory session. After providing written informed consent, the right leg length of participants was measured (from anterior superior iliac spine to medial malleolus in supine). Participants then ran 5 min at 9 km/h on a treadmill (h/p/cosmos mercury®, h/p/cosmos sports & medical gmbh, Nussdorf-Traunstein, Germany) as a warm-up. Participants then completed 3 \times 4-min runs at 10, 12, and 14 km/h (with 2-min recovery periods between runs) on the treadmill, during which time RE was assessed. Retro-reflective markers were subsequently positioned on individuals (described in *Data Collection* section) to assess running kinematics. For each participant, a 1-s static calibration trial was recorded, which was followed by 3 \times 30-s runs at 10, 12, and 14 km/h (with 1-min recovery periods between each runs) to collect three-dimensional (3D) kinematic data in the last 10-s segment of these runs (30 \pm 2 running steps), resulting in at least 25 steps being analysed³⁰. RE and biomechanics were assessed separately given laboratory constraints and interference with data quality (e.g., presence of testing equipment that occluded markers). All participants were familiar with running on a treadmill as part of their usual training programs and wore their habitual running shoes during testing.

Data collection. Gas exchange was measured using TrueOne 2400 (ParvoMedics, Sandy, UT, USA) during the 3 \times 4-min runs. Prior to the experiment, the gas analyzer was calibrated using ambient air (O₂: 20.93% and CO₂: 0.03%) and a gas mixture of known concentration (O₂: 16.00% and CO₂: 4.001%). Volume calibration was performed at different flow rates with a 3 L calibration syringe (5530 series, Hans Rudolph, Shawnee, KS, USA). Oxygen consumption ($\dot{V}O_2$), carbon dioxide production ($\dot{V}CO_2$), and respiratory exchange ratio (RER) values were averaged over the last minute of each 4-min run. Steady state was confirmed through visual inspection of the $\dot{V}O_2$ and $\dot{V}CO_2$ curves for all running trials. RER had to remain below unity during the trials for data to be included in the analysis, otherwise the corresponding data were excluded as deemed to not represent a submaximal effort. No trial was excluded on this basis. RE was expressed as the oxygen cost per mass to the power of 0.75 per kilometer (ml/kg^{0.75}/km) to minimize the influence of body mass per se on $\dot{V}O_2$ during running³¹. RE expressed in ml/kg/km was also computed for reference and is provided as supplementary materials. A higher RE value indicates a less economical runner.

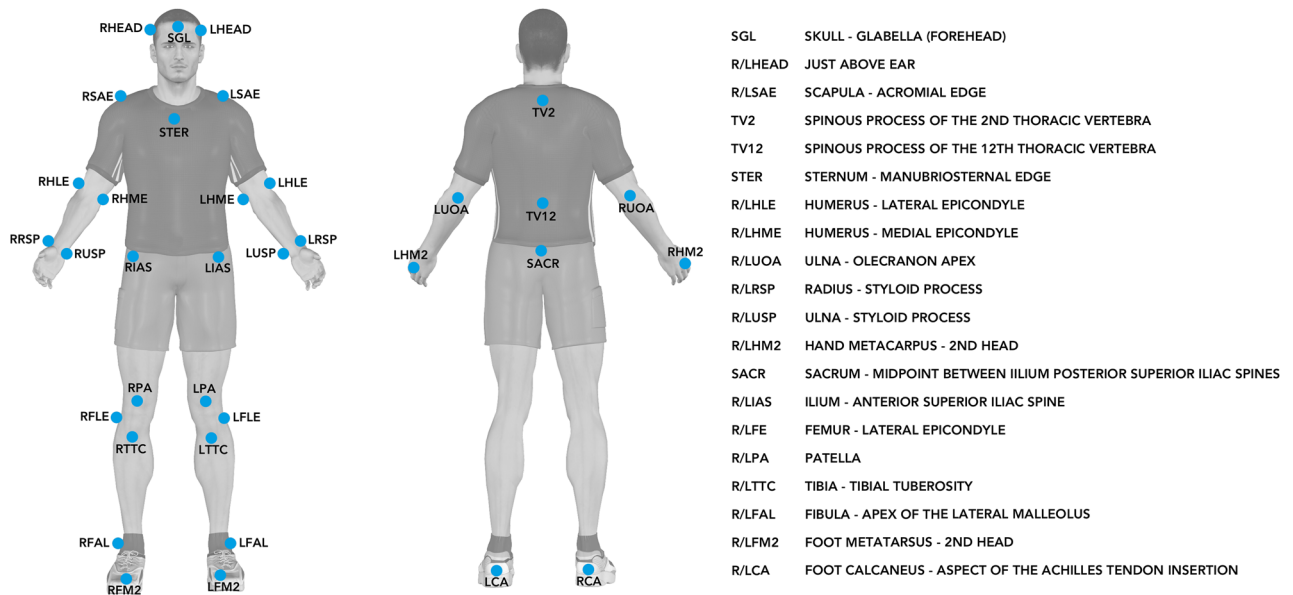


Figure 1. Retro-reflective markers ($N=35$) placed on anatomical landmarks of participants for biomechanical data collection. R and L at the start of the acronyms denote right and left, respectively.

3D kinematic data were collected at 200 Hz using seven infrared Oqus cameras (five Oqus 300+, one Oqus 310+, and one Oqus 311+) and Qualisys Track Manager software version 2.1.1 build 2902 together with the Project Automation Framework Running package version 4.4 (Qualisys AB, Göteborg, Sweden). A virtual laboratory coordinate system was generated such that the x - y - z axes denoted the medio-lateral (pointing towards the right side of the body), posterior-anterior, and inferior-superior directions, respectively. Thirty-five retro-reflective markers (Fig. 1) of 12 mm in diameter were used for static calibration and running trials, and were affixed to the skin and shoes of individuals over anatomical landmarks using double-sided tape following standard guidelines from the Project Automation Framework Running package³². The 3D marker data were exported in .c3d format and processed in Visual3D Professional software version 5.02.25 (C-Motion Inc., Germantown, MD, USA). More explicitly, the 3D marker data were interpolated using a third-order polynomial least-square fit algorithm, allowing a maximum of 20 frames for gap filling, and subsequently low-pass filtered at 20 Hz using a fourth-order Butterworth filter.

Biomechanical variables. From the marker set, a full-body biomechanical model with six degrees of freedom at each joint and 15 rigid segments was constructed. The model included the head, upper arms, lower arms, hands, thorax, pelvis, thighs, shanks, and feet. Segments were assigned inertial properties and centre of mass (COM) locations based on their shape³³ and attributed relative mass based on standard regression equations³⁴. Kinematic variables were calculated using rigid-body analysis and whole-body COM location was calculated from the parameters of all 15 segments. Ankle (θ_{ankle}) and knee (θ_{knee}) joint angles were defined as the orientation of the distal segment relative to the proximal one³⁵. Angles were computed using an x - y - z Cardan sequence^{36,37} equivalent to the joint coordinate system^{36,38}, leading to rotations with functional and anatomical meaning (flexion–extension, abduction–adduction, and internal–external rotation). Noteworthy, only the flexion–extension Cardan angle was considered for analysis due to possible errors linked with kinematic crosstalk^{39–41}. Joint angles were calculated at footstrike and toe-off events. Footstrike angle (FSA) was calculated following the procedure described in Altman and Davis⁴². FSA was normalized by taking the angle of the foot at footstrike and subtracting the angle of the foot during standing trial. The mean FSA was used to categorise footstrike patterns of runners in two categories: RFS when the FSA was greater than 8°, and non-RFS when 8° or less⁴². Among all running trials, 5% and 7% were borderline (within 1°) RFS and non-RFS, respectively. These borderline footstrike patterns were only present in SEA runners. Visual inspection confirmed the footstrike pattern classifications were correct.

Running events were derived from the trajectories of the 3D marker data using similar procedures to those previously reported^{43,44}. All events were verified to ensure correct identification and were manually adjusted when required.

Swing time (t_s) and t_e were defined as the time from toe-off to footstrike and from footstrike to toe-off of the same foot, respectively. Flight time (t_f) was defined as the time from toe-off to footstrike of the contralateral foot. Step frequency (SF) was calculated as $\text{SF} = \frac{1}{t_e + t_f}$, and step length (SL) as $\text{SL} = s/\text{SF}$, where s represents running speed. In addition to raw units, SL was expressed as a percentage of participant's leg length. The spring-mass characteristics of the lower limb were estimated using a sine-wave model following the procedure defined by Morin, et al.⁴⁵. More explicitly, leg stiffness (k_{leg}) was calculated as [Eq. (1)]

Characteristics	SEA	Non-SEA	<i>p</i>
Sex	M = 10; F = 7	M = 10; F = 7	NA
Age (y)	34 ± 4	38 ± 7	0.08
Mass (kg)	56 ± 9	68 ± 12	0.002
Height (cm)	167 ± 8	175 ± 9	0.01
Leg length (cm)	86 ± 4	91 ± 6	0.01
BMI (kg/m ²)	20 ± 2	22 ± 2	0.004
Leg length over height (%)	52 ± 1	52 ± 1	0.54
Running distance (km/week)	60 ± 19	54 ± 18	0.32
Running experience (y)	6 ± 3	11 ± 7	0.02
Running performance on 21.1 km (min)	96 ± 9	96 ± 10	0.81
Shoe mass (g)	231 ± 32	215 ± 39	0.22
Shoe stack height (mm)	25 ± 3	25 ± 3	0.83
Shoe heel-to-toe drop (mm)	8 ± 3	6 ± 3	0.01

Table 1. Participant and footwear characteristics for South East Asian (SEA) and non-South East Asian (non-SEA) runners. Significant differences ($p \leq 0.05$) identified by Student's or Welch's *t*-tests are reported in bold. *M* male, *F* female, *BMI* body mass index, and *NA* not applicable.

$$k_{\text{leg}} = \frac{F_{z,\text{max}}}{\Delta L} \quad (1)$$

where $F_{z,\text{max}}$ represents the maximal vertical force and was estimated using $F_{z,\text{max}} = mg \frac{\pi}{2} \left(\frac{t_f}{t_c} + 1 \right)$, ΔL is the maximal leg length deformation, i.e., the leg spring compression and given by $\Delta L = \sqrt{z_{\text{COM,FS}}^2 + s^2 t_b^2} - z_{\text{COM,MS}}$, where s defines running speed, t_b denotes the braking time, i.e., the time from footstrike to mid-stance, and $z_{\text{COM,FS}}$ and $z_{\text{COM,MS}}$ are the COM heights at footstrike and mid-stance, respectively. For all biomechanical measures, the values extracted from the 10-s data collection for each participant were averaged for subsequent statistical analyses.

Statistical analysis. Descriptive statistics are presented using mean ± standard deviation (SD). Data normality and homogeneity of variances were verified using Kolmogorov–Smirnov and Levene's test, respectively. Participant characteristics between SEA and non-SEA runners were compared using unpaired two-sided Welch's *t*-tests when homogeneity of variance assumptions were violated and unpaired two-sided Student's *t*-tests otherwise. The effect of group (SEA, non-SEA) and running speed on RE and biomechanical variables was evaluated using a linear mixed effects model fitted by restricted maximum likelihood. The within-subject nature was controlled for by including random effects for participants (individual differences in the intercept of the model). The fixed effects included group and running speed (both categorical variables). Cohen's *d* effect size was calculated when a significant group effect was observed⁴⁶, and classified as *small*, *moderate*, and *large* when *d* values were larger than 0.2, 0.5, and 0.8, respectively⁴⁶. Footstrike distribution between SEA and non-SEA runners were compared at all running speeds using Fisher exact tests given that some of the expected frequencies were less than five.

A correlation matrix between anthropometric characteristics (mass and height, leg length, BMI, and ratio of leg length over height) was generated to identify unrelated anthropometric characteristics. Pearson correlation coefficients (*r*) between RE and the identified independent anthropometric variables were computed using RE values at the three running speeds separately, as well as with and without subgrouping of participants based on ethnicity. Similarly, Pearson correlation coefficients (*r*) between RE and biomechanical variables were computed at the three running speeds separately, as well as with and without subgrouping of participants based on ethnicity. Correlations were considered *very high*, *high*, *moderate*, *low*, and *negligible* when absolute *r* values were between 0.90–1.00, 0.70–0.89, 0.50–0.69, 0.30–0.49, and 0.00–0.29, respectively⁴⁷. Given the number of correlations and exploratory nature of these analyses, only significant correlations reaching the *moderate* threshold were deemed meaningful. Statistical analyses were performed using Jamovi (version 1.2.17, Computer Software, retrieved from <https://www.jamovi.org>) and R (version 3.5.0, The R Foundation for Statistical Computing, Vienna, Austria) with a level of significance set at $p \leq 0.05$.

Results

Participant characteristics. Non-SEA runners were significantly heavier and taller, had a larger BMI and longer legs, had footwear with a larger heel-to-toe drop, and were more experienced than SEA runners ($p \leq 0.02$; Table 1). Otherwise, demographic and footwear characteristics of non-SEA and SEA runners were similar (see Table 1).

Running economy. SEA runners were significantly less economical (6%) than non-SEA runners (average across speeds: 522.6 ± 47.4 vs 492.4 ± 42.2 ml/kg^{0.75}/km), with a *moderate* main effect of group on RE ($p = 0.04$,

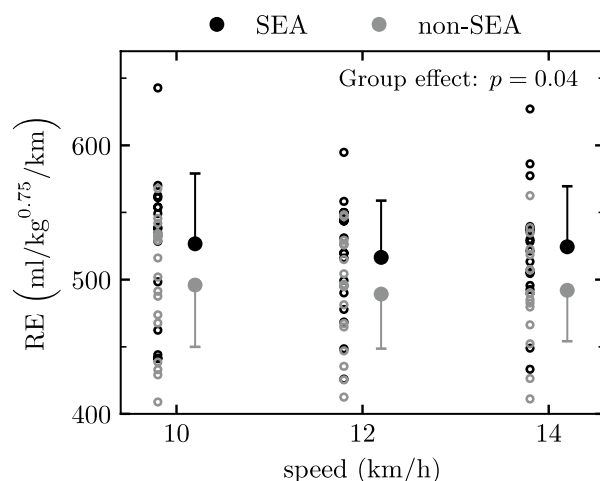


Figure 2. Running Economy (RE) of South East Asian (SEA) and non-South East Asian (non-SEA) runners at several endurance running speeds. Linear mixed effects modelling identified a significant group effect ($p \leq 0.05$).

Running speed (km/h)	Group	SF (steps/min)	SL (cm)	SL (%) ^a	t_c (ms)	t_f (ms)	k_{leg} (kN/m)
10	SEA	176 ± 9	95 ± 5	110 ± 7	268 ± 24	78 ± 21	12.3 ± 2.5
	Non-SEA	168 ± 9	100 ± 5	110 ± 6	287 ± 31	84 ± 23	13.5 ± 2.8
12	SEA	181 ± 10	111 ± 6	128 ± 8	237 ± 22	96 ± 21	12.3 ± 2.4
	Non-SEA	173 ± 10	116 ± 7	127 ± 6	253 ± 23	98 ± 25	13.5 ± 3.0
14	SEA	187 ± 11	125 ± 7	145 ± 9	215 ± 20	107 ± 19	12.0 ± 2.2
	Non-SEA	179 ± 11	131 ± 8	144 ± 7	231 ± 21	107 ± 23	12.8 ± 2.7
Group effect		0.02	0.03	0.78	0.04	0.67	0.23
Running speed effect		<0.001	<0.001	<0.001	<0.001	<0.001	0.009
Interaction effect		0.93	0.48	0.68	0.81	0.44	0.32

Table 2. Step frequency (SF), step length (SL), contact time (t_c), flight time (t_f), and spring-mass characteristics of the lower limb as given by leg stiffness (k_{leg}) for South East Asian (SEA) and non-South East Asian (non-SEA) runners at endurance running speeds. Significant differences ($p \leq 0.05$) identified by linear mixed effects modelling are indicated in bold. SL was expressed as a percentage of participant's leg length in addition to raw units. ^aStep length normalized to leg length.

$d = 0.67$; Fig. 2). There was no significant main effect of speed ($p = 0.27$) or group x speed interaction effect ($p = 0.89$) on RE. Larger differences were seen between SEA and non-SEA runners when expressing RE in ml/kg/km instead of ml/kg^{0.75}/km (see section S1 of supplementary materials).

Biomechanical characteristics. There was a significant main effect of group on SF, SL, and t_c ($p \leq 0.04$; Table 2), with SEA having a higher SF (*moderate* effect; $d = 0.75$), smaller SL (*small* effect; $d = 0.36$), and shorter t_c (*moderate* effect; $d = 0.67$) than non-SEA runners. There was no group effect on normalized SL, t_f and k_{leg} ($p \geq 0.23$; Table 2). A significant speed effect was observed for all temporal variables ($p \leq 0.01$; Table 2). SF, SL, and t_f increased with increasing speed, whereas t_c and k_{leg} decreased with increasing speed. None of these variables demonstrated a group x speed interaction ($p \geq 0.32$; Table 2).

There was a significant group effect on θ_{ankle} at footstrike and θ_{knee} at toe-off ($p \leq 0.03$; Table 3), with SEA having less ankle dorsiflexion than non-SEA at footstrike (*large* effect; $d = 1.20$) and less knee extension at toe-off (*moderate* effect; $d = 0.75$). A significant speed effect was observed for θ_{ankle} and θ_{knee} at toe-off ($p \leq 0.02$; Table 3), with greater flexion at footstrike and extension at toe-off with increasing speed. None of these variables showed a group x speed interaction except θ_{ankle} at footstrike ($p = 0.007$; Table 3), with SEA decreasing dorsiflexion with increasing speed while non-SEA increased dorsiflexion with increasing speed.

Footstrike angle and pattern. SEA had a significantly lower FSA than non-SEA runners (*large* effect; $d = 1.67$), as depicted by the group effect on FSA ($p < 0.001$; Table 4). A speed effect was observed on FSA ($p < 0.001$; Table 4), indicating an increase of FSA with increasing running speed, while no significant group x speed interaction effect was noted ($p = 0.13$; Table 4). Footstrike distribution between SEA and non-SEA runners differed significantly at all speeds, with non-SEA being more commonly RFS ($p \leq 0.04$; Table 4).

Running speed (km/h)	Group	$\theta_{\text{ankle}}(^{\circ})$		$\theta_{\text{knee}}(^{\circ})$	
		FS	TO	FS	TO
10	SEA	9 ± 5	-12 ± 8	17 ± 2	27 ± 4
	Non-SEA	14 ± 6	-9 ± 3	18 ± 3	24 ± 7
12	SEA	8 ± 5	-14 ± 8	17 ± 3	24 ± 4
	Non-SEA	15 ± 6	-11 ± 3	18 ± 4	21 ± 5
14	SEA	8 ± 6	-14 ± 9	18 ± 3	24 ± 4
	Non-SEA	15 ± 6	-11 ± 4	18 ± 4	20 ± 4
Group effect		0.001	0.18	0.57	0.03
Running speed effect		0.31	0.02	0.65	<0.001
Interaction effect		0.007	0.95	0.09	0.65

Table 3. Flexion–extension angle of the lower limb for South East Asian (SEA) and non-South East Asian (non-SEA) runners at endurance running speeds. Significant differences ($p \leq 0.05$) identified by linear mixed effects modelling are indicated in bold. θ_{ankle} : ankle joint angle, θ_{knee} : knee joint angle, FS: footstrike, and TO: toe-off.

Running speed (km/h)	Group	FSA ($^{\circ}$)	RFS—non-RFS	p
10	SEA	6 ± 4	4–13	<0.001
	Non-SEA	13 ± 5	16–1	
12	SEA	7 ± 4	6–11	<0.001
	Non-SEA	15 ± 5	16–1	
14	SEA	9 ± 4	10–7	0.04
	Non-SEA	17 ± 6	16–1	
Group effect		<0.001	NA	
Running speed effect		<0.001	NA	
Interaction effect		0.13	NA	

Table 4. Footstrike angle (FSA) and footstrike distribution [rearfoot strike (RFS) for FSA > 8° and non-rearfoot strike (non-RFS) otherwise⁴²] for South East Asian (SEA) and non-South East Asian (non-SEA) runners at endurance running speeds. Significant differences ($p \leq 0.05$) identified by linear mixed effects modelling and by Fisher exact tests are indicated in bold.

Group	SEA			non-SEA			ALL		
	10	12	14	10	12	14	10	12	14
Running speed (km/h)									
Mass (kg)	0.41	0.69	0.41	0.78	0.74	0.65	-0.41	0.42	0.23
	0.02	0.002	0.11	<0.001	<0.001	0.005	0.02	0.01	0.19
Leg length over height (%)	0.06	-0.21	-0.15	0.31	0.21	0.15	0.06	-0.04	-0.06
	0.72	0.42	0.56	0.23	0.42	0.57	0.73	0.81	0.74

Table 5. Pearson correlation coefficients between running economy and anthropometric characteristics (mass and ratio of leg length over height), together with their corresponding p -values underneath for South East Asian (SEA), non-South East Asian (non-SEA), as well as all runners pooled together (ALL). *Note.* Only the relationships between running economy and mass and ratio of leg length over height were considered because mass was highly and significantly correlated to height, leg length, and body mass index. Statistical significances ($p \leq 0.05$) gray shaded boxes denote correlation coefficients above an absolute value of 0.5 (moderate).

Relationship between RE and anthropometric characteristics. High positive correlations were identified between mass and height ($r \geq 0.83$; $p < 0.001$), mass and leg length ($r \geq 0.74$; $p < 0.001$), and mass and BMI ($r \geq 0.84$; $p < 0.001$), while the correlation between mass and ratio of leg length over height was negligible and not significant ($r \leq 0.17$; $p \geq 0.35$). Hence, relationships between RE and mass and ratio of leg length over height were further explored (Table 5). For SEA runners, a high positive correlation was observed between RE and mass at 12 km/h ($r = 0.69$, $p < 0.001$; Table 5), while high positive correlations were observed between RE and mass for non-SEA runners at all speeds ($r \geq 0.65$, $p \leq 0.005$; Table 5). For runners combined, the strongest correlations were low. Table 6 presents all correlations, including the low and negligible ones. Relationships between RE expressed in ml/kg/km and anthropometric characteristics are provided in section S1 of supplementary materials.

Group	SEA			non-SEA			ALL		
	10	12	14	10	12	14	10	12	14
Running speed (km/h)									
SF (steps/min)	-0.58 0.02	-0.49 0.04	-0.17 0.52	-0.44 0.08	-0.51 0.04	-0.47 0.05	-0.31 0.07	-0.31 0.07	-0.13 0.46
SL (cm)	0.56 0.02	0.48 0.05	0.16 0.55	0.46 0.06	0.51 0.04	0.46 0.06	0.32 0.06	0.31 0.07	0.14 0.44
SL (%) ^a	0.02 0.94	0.01 0.96	-0.13 0.62	-0.36 0.15	-0.21 0.43	-0.15 0.60	-0.13 0.46	-0.06 0.74	-0.11 0.55
t_c (ms)	0.36 0.16	0.79 <0.001	0.48 0.05	0.02 0.93	0.25 0.34	0.40 0.11	0.07 0.71	0.36 0.04	0.25 0.16
t_f (ms)	-0.12 0.64	-0.43 0.08	-0.38 0.14	0.32 0.21	0.21 0.42	0.12 0.66	0.05 0.78	-0.10 0.56	-0.12 0.48
k_{leg} (kN/m)	-0.04 0.88	-0.21 0.43	-0.21 0.42	0.64 0.005	0.49 0.05	0.36 0.16	0.21 0.23	0.09 0.63	0.02 0.93
FSA (°)	-0.40 0.11	-0.33 0.20	-0.14 0.60	0.24 0.35	0.22 0.39	0.11 0.67	-0.23 0.19	-0.22 0.21	-0.24 0.17
θ_{ankle} at FS (°)	-0.50 0.04	-0.48 0.05	-0.18 0.48	-0.01 0.96	0.10 0.71	0.06 0.83	-0.37 0.03	-0.31 0.08	-0.26 0.15
θ_{ankle} at TO (°)	-0.23 0.37	-0.46 0.06	-0.26 0.32	-0.04 0.89	0.04 0.86	-0.07 0.80	-0.24 0.18	-0.34 0.05	-0.25 0.15
θ_{knee} at FS (°)	0.09 0.72	0.10 0.71	0.04 0.89	0.22 0.40	-0.06 0.82	-0.03 0.90	-0.11 0.52	-0.03 0.87	-0.01 0.97
θ_{knee} at TO (°)	0.14 0.58	0.21 0.41	0.31 0.23	0.08 0.77	0.14 0.58	0.19 0.47	0.18 0.32	0.26 0.14	0.37 0.03

Table 6. Pearson correlation coefficients between running economy and biomechanical variables [step frequency (SF), step length (SL), contact time (t_c), flight time (t_f), spring-mass characteristics of the lower limb as given by leg stiffness (k_{leg}), footstrike angle (FSA), and flexion–extension ankle (θ_{ankle}) and knee (θ_{knee}) joint angle at footstrike (FS) and toe-off (TO)], together with their corresponding p -values underneath for South East Asian (SEA), non-South East Asian (non-SEA), as well as all runners pooled together (ALL). Statistical significances ($p \leq 0.05$) are indicated in bold. Gray shaded boxes denote correlation coefficients above an absolute value of 0.5 (moderate). SL was expressed as a percentage of participant's leg length in addition to raw units. ^aStep length normalized to leg length.

Relationships between RE and biomechanics. For SEA runners, a *high* positive correlation was seen between RE and t_c at 12 km/h ($|r| \geq 0.70$, $p \leq 0.002$; Table 6). SF and θ_{ankle} at footstrike at 10 km/h were *moderately* and negatively correlated to RE, whereas SL (10 km/h) was *moderately* and positively correlated to RE ($|r| \geq 0.50$, $p \leq 0.04$; Table 6).

For non-SEA runners, a *moderate* and negative correlation was observed between RE and SF at 12 km/h ($|r| \geq 0.51$, $p \leq 0.04$; Table 6). Besides, *moderate* positive correlations between RE and SL (12 km/h) and k_{leg} (10 km/h) were identified ($|r| \geq 0.51$, $p \leq 0.04$; Table 6).

For runners combined, the strongest correlations were *low*. Table 6 presents all correlations, including the *low* and *negligible* ones. Relationships between RE expressed in ml/kg/km and biomechanics are given in section S1 of supplementary materials.

Discussion

Differences in RE were observed between SEA and non-SEA runners despite being matched for recent (< 1 year) road running performance and sex. SEA runners were less economical than non-SEA runners at endurance running speeds. Anthropometric differences were observed between groups, depicting that SEA were lighter and shorter than non-SEA runners, and had a lower BMI and shorter legs. Differences in running biomechanics between cohorts were also observed, but correlations between anthropometric and biomechanical variables and RE measures at a group-level were of *small* magnitudes at best, and provided limited explanations of the underlying differences in RE.

Non-SEA were 6% more economical than SEA runners at endurance running speeds (Fig. 2). The lower RE in SEA than non-SEA runners could in part be due to anthropometric differences. We observed that SEA were lighter and shorter than non-SEA runners, and had a lower BMI and shorter legs (Table 1). Mass was significantly related to RE in both ethnic groups, with more economical runners having lower body mass. Mass was highly related to RE in SEA runners at 12 km/h and non-SEA at all speeds, but correlations became *low* or non-significant when pooling all runners together (Table 5). Previous studies showing that elite Caucasian runners were less economical than Kenyans attributed RE differences to longer legs (~ 5%), thinner and lighter calf musculature, and lower mass and BMI of Kenyan than Caucasian runners^{3–6}. Indeed, RE being correlated with leg mass, Kenyan runners could benefit from their long, slender legs⁶. In our case, the ratio of leg length over height was not related to RE (Table 5) and was similar between SEA and non-SEA, indicating similar lower limb proportions in these two groups (Table 1). In fact, due to both smaller mass and shorter legs (Table 1), SEA might have had a proportionally similar leg mass than non-SEA runners.

Participants wore their own running shoes during testing similar to previous research exploring differences in running mechanics between ethnic groups¹⁰. Given that differences in footwear characteristics can underpin differences in running biomechanics⁴⁸ and RE⁴⁹, using a standardised shoe might have led to different study outcomes. Noteworthy, however, is that there were no significant difference in shoe mass or stack height between groups, with the 2 mm difference in heel-to-toe drop between groups likely having limited biomechanical or performance implications⁵⁰. Recreational runners are more comfortable wearing their own shoes⁵¹, and show individual responses to novel footwear^{51,52} and cushioning properties⁵³. A recent meta-analysis indicates recreational runners demonstrate improved RE when wearing more comfortable shoes⁵⁴, supporting the appropriateness of participants wearing their own footwear for this investigation. Nevertheless, it is possible that other footwear characteristics not assessed as part of this study differed between groups, such as midsole cushioning and/or the longitudinal bending stiffness⁵⁰, and contributed to the biomechanical and RE differences observed.

Among all correlations between biomechanical variables and RE, only SF and SL were significantly related to RE in both ethnic groups. The SF and SL variables were moderately related to RE in SEA runners at 10 km/h and non-SEA at 12 km/h, but correlations became *low* and non-significant when all runners were pooled together (Table 6). Noteworthy, correlations between SL and RE were smaller and became non-significant when normalized to leg length. In addition, t_c was highly and positively related to RE for SEA runners at 12 km/h. The identified correlations between SF (and SL) and RE and between t_c and RE suggest that individuals with higher SF (and shorter SL) and smaller t_c (for SEA runners) are more economical. However, SEA had intrinsically higher SF (and shorter SL) and shorter t_c , but worse RE than non-SEA runners (Table 2); therefore, contradicting the observed correlations. Based on the cost-of-generating-force hypothesis, one requires less metabolic energy with increased t_c and longer leg lengths^{55–57}, both observed in non-SEA (Table 1). The longer t_c in non-SEA suggests that muscles had more time to shorten and produce the necessary forces to move the body than SEA runners. Based on the force–velocity relationship, if a muscle is shortening slower but only a given force is necessary (i.e., running on a treadmill), it could be speculated that the activation levels of the muscles were lower to reach the target force. These theories might partially explain the reduced metabolic cost in non-SEA than SEA runners, i.e., a longer t_c , lower SF, and longer leg lengths are more economical.

Nevertheless, studies indicate that increasing SF above self-selected ones in novice (156 ± 6 steps/min, 9.6 km/h) and trained (169 ± 11 steps/min, 12.6 km/h) runners acutely improves RE (+2%)⁵⁸, as does undertaking a 10-day training programme to increase SF (from 166 ± 4 to 180 ± 1 steps/min, 12.3 km/h)⁵⁹. At 12 km/h, mean SF values were 173 (range: 151 to 185) in non-SEA and 181 (range: 159 to 200) in SEA. Further increasing SF in runners with an intrinsically high SF might not be energetically optimal, but has yet to be examined. An extremely high SF might be suboptimal at endurance speeds given the greater mechanical power associated with increased frequency of reciprocal movements, which may require a greater reliance on less economical type II muscle fibers⁶⁰. Indeed, Kaneko et al.⁶⁰ suggested that SF and RE could be related through muscle fiber recruitment. Besides, given the shorter stature of our SEA vs non-SEA runners, their higher SF aligns with findings of moderate correlations between leg lengths and SF ($r = -0.53$, $p < 0.001$; 12 km/h), in agreement with previous literature ($r = -0.45$, $p < 0.001$)⁶¹, whereby individuals with shorter legs tend to adopt higher SF.

Alongside their higher SF and smaller SL, SEA had shorter t_c , smaller FSA (more forefoot strike pattern), and smaller θ_{ankle} at footstrike than non-SEA runners (Tables 2, 3, 4). Previous studies observed that running at a higher SF led to smaller t_c ⁶² and FSA⁶³, which is consistent with our findings. In addition, the prevalence of RFS was shown to be lower in Asian than North American recreational runners¹⁶, aligning with the findings of the present study. A smaller t_c might be associated with smaller braking and propulsion phases. Although short braking phases are considered important for economical running⁶⁴, SEA runners were less economical. Braking forces were not recorded herein due to unavailability of instrumented treadmills. Shorter braking times does not necessarily equate minimising braking forces, which is important in the context of RE⁶⁵. Moreover, it could be that the orientation of the ground reaction forces in SEA runners was suboptimal. Indeed, Moore, et al.⁶⁶ observed that a better alignment of the leg axis during propulsion and resultant ground reaction force improved RE, mainly via a more horizontal application of the ground reaction force. This idea is supported by our data, which show less extension of θ_{knee} at toe-off (Table 3), and thus potentially less horizontal propulsion for SEA than non-SEA runners. Nevertheless, θ_{knee} at toe-off was not correlated to RE (Table 6). Though SF, SL and t_c significantly differed between groups, no difference in k_{leg} was identified (Table 2), contradicting previous findings that k_{leg} relates to the aforementioned variables^{67–69}. These studies were all within-subject comparisons rather than between-subject ones; hence, at an individual level, the relationship might still hold within SEA and non-SEA participants. The lack of difference in k_{leg} between groups despite differences in SF, SL, and t_c potentially relates to the body mass difference between groups that is counterbalancing the spatiotemporal differences in the biomechanical variables [see Eq. (1)]. These biomechanical data were not clearly able to explain the variances in RE between groups, and support that RE improvements in various groups might need individualized training and considerations. A similar conclusion was made by Santos-Concejero, et al.¹⁰ when assessing RE differences between Eritrean and European runners. Moreover, these divergent findings overall suggest there is no unique or ideal running pattern that is the most economical amongst runners¹. The running pattern of an individual results from a complex interaction between several biomechanical factors⁷⁰ that are interconnected and interact in a global and dynamic manner⁷¹ to optimize RE.

A few limitations to the present study exist. Although the effect size was *moderate* ($d = 0.67$), the between-group difference in RE units was rather small (mean difference = 30.1 ml/kg^{0.75}/km; $p = 0.04$). In addition, the within-group variability in RE and biomechanical variables at a given running speed were relatively small. Therefore, observed correlations between RE and biomechanical variables might have been greater in more heterogeneous groups. Given the exploratory nature of this investigation, several variables were compared, leading to a high likelihood of finding a spurious difference or correlation. Nonetheless, our research provides preliminary indications of potential differences between SEA and non-SEA runners warranting further consideration. Moreover,

an underpinning factor to the differences in RE might be the running experience given that experienced runners self-optimize their running patterns better than novice runners¹. Non-SEA runners were more experienced (years running) than SEA runners (Table 1), but all runners trained regularly and had a minimum of 2 years running experience, indicating they were all "experienced" and not "novice" runners. Nonetheless, a gradual improvement in RE (+ 15%) over an 11-year time span has been reported for a former world record holder in the women's marathon⁷². Therefore, an effect due to running experience cannot be ruled out. Besides, several morphological factors which were not measured in this study might have partly explained differences in RE between SEA and non-SEA runners^{18,19,73–78} (more details are provided in section S2 of supplementary materials). Furthermore, although all SEA runners identified as "white", the numerous nationalities of the non-SEA group potentially increased the heterogeneity of our cohort and influenced our results. Lastly, RE and biomechanics were collected within the same experimental session, but the two were not collected simultaneously (as common in running research⁷⁹). Although possible that participants altered their runs, research indicates that metabolic equipment does not affect sagittal plane running kinematics and are comparable to running without metabolic testing⁸⁰.

Conclusion

SEA and non-SEA runners were different in terms of RE, with SEA runners being less economical than non-SEA runners at endurance running speeds. Differences in anthropometric characteristics and running biomechanics between cohorts were also observed, but explained differences in RE to a limited extent. Other factors, which could be related to ethnicity, might be underpinning such differences. Unfortunately, these factors were not measured in this study. Nonetheless, caution must be taken when generalizing from non-SEA running studies to SEA runners.

Data availability

The dataset supporting this article is available on request to the corresponding author.

Received: 8 August 2021; Accepted: 21 March 2022

Published online: 15 April 2022

References

- Moore, I. S. Is there an economical running technique? A review of modifiable biomechanical factors affecting running economy. *Sports Med.* **46**, 793–807. <https://doi.org/10.1007/s40279-016-0474-4> (2016).
- Weston, A. R., Mbambo, Z. & Myburgh, K. H. Running economy of African and Caucasian distance runners. *Med. Sci. Sports Exerc.* **32**, 1130–1134. <https://doi.org/10.1097/00005768-200006000-00015> (2000).
- Larsen, H. B. & Sheel, A. W. The Kenyan runners. *Scand. J. Med. Sci. Sports* **25**(Suppl 4), 110–118. <https://doi.org/10.1111/sms.12573> (2015).
- Larsen, H. B., Christensen, D. L., Nolan, T. & Søndergaard, H. Body dimensions, exercise capacity and physical activity level of adolescent Nandi boys in western Kenya. *Ann. Hum. Biol.* **31**, 159–173. <https://doi.org/10.1080/03014460410001663416> (2004).
- Saltin, B. *et al.* Aerobic exercise capacity at sea level and at altitude in Kenyan boys, junior and senior runners compared with Scandinavian runners. *Scand. J. Med. Sci. Sports* **5**, 209–221. <https://doi.org/10.1111/j.1600-0838.1995.tb00037.x> (1995).
- Larsen, H. B. Kenyan dominance in distance running. *Comp. Biochem. Physiol. A: Mol. Integr. Physiol.* **136**, 161–170. doi:[https://doi.org/10.1016/s1095-6433\(03\)00227-7](https://doi.org/10.1016/s1095-6433(03)00227-7) (2003).
- Lucia, A. *et al.* Physiological characteristics of the best Eritrean runners-exceptional running economy. *Appl. Physiol. Nutr. Metab.* **31**, 530–540. <https://doi.org/10.1139/h06-029> (2006).
- Lieberman, D. E. *et al.* Foot strike patterns and collision forces in habitually barefoot versus shod runners. *Nature* **463**, 531–535. <https://doi.org/10.1038/nature08723> (2010).
- Marino, F. E., Lambert, M. I. & Noakes, T. D. Superior performance of African runners in warm humid but not in cool environmental conditions. *J. Appl. Physiol.* **96**, 124–130. <https://doi.org/10.1152/jappphysiol.00582.2003> (2004).
- Santos-Concejero, J. *et al.* Gait-cycle characteristics and running economy in elite Eritrean and European runners. *Int. J. Sports Physiol. Perform.* **10**, 381–387. <https://doi.org/10.1123/ijsspp.2014-0179> (2015).
- Santos-Concejero, J. *et al.* Differences in ground contact time explain the less efficient running economy in north African runners. *Biol. Sport* **30**, 181–187. <https://doi.org/10.5604/20831862.1059170> (2013).
- Tam, E. *et al.* Energetics of running in top-level marathon runners from Kenya. *Eur. J. Appl. Physiol.* **112**, 3797–3806. <https://doi.org/10.1007/s00421-012-2357-1> (2012).
- Wishnizer, R. R., Inbar, O., Klinman, E. & Fink, G. Physiological differences between Ethiopian and Caucasian distance runners and their effects on 10 km running performance. *Adv Phys Educ* **3**, 9. <https://doi.org/10.4236/ape.2013.33023> (2013).
- Shu, Y. *et al.* Foot morphological difference between habitually shod and unshod runners. *PLoS ONE* **10**, e0131385. <https://doi.org/10.1371/journal.pone.0131385> (2015).
- Sano, K. *et al.* Can measures of muscle-tendon interaction improve our understanding of the superiority of Kenyan endurance runners?. *Eur. J. Appl. Physiol.* **115**, 849–859. <https://doi.org/10.1007/s00421-014-3067-7> (2015).
- Patoz, A., Lussiana, T., Gindre, C. & Hébert-Losier, K. Recognition of foot strike pattern in Asian recreational runners. *Sports* **7**, 147. <https://doi.org/10.3390/sports7060147> (2019).
- Andersen, J. J. & International Association of Athletics Federations. *The State of Running 2019*, (2020).
- Hawes, M. R. *et al.* Ethnic differences in forefoot shape and the determination of shoe comfort. *Ergonomics* **37**, 187–196. <https://doi.org/10.1080/00140139408963637> (1994).
- Zárate-Kalfópulos, B., Romero-Vargas, S., Otero-Cámara, E., Correa, V. C. & Reyes-Sánchez, A. Differences in pelvic parameters among Mexican, Caucasian, and Asian populations. *J. Neurosurg. Spine* **16**, 516–519. <https://doi.org/10.3171/2012.2.Spine.11755> (2012).
- Sun, P. *et al.* Autonomic recovery is delayed in Chinese compared with Caucasian following treadmill exercise. *PLoS ONE* **11**, e0147104. <https://doi.org/10.1371/journal.pone.0147104> (2016).
- Chen, W.-L., O'Connor, J. J. & Radin, E. L. A comparison of the gaits of Chinese and Caucasian women with particular reference to their heelstrike transients. *Clin. Biomech.* **18**, 207–213. [https://doi.org/10.1016/S0268-0033\(02\)00187-0](https://doi.org/10.1016/S0268-0033(02)00187-0) (2003).
- Gruber, A. H., Umberger, B. R., Braun, B. & Hamill, J. Economy and rate of carbohydrate oxidation during running with rearfoot and forefoot strike patterns. *J. Appl. Physiol.* **115**, 194–201. <https://doi.org/10.1152/jappphysiol.01437.2012> (2013).
- Ogueta-Alday, A. N. A., Rodríguez-Marroyo, J. A. & García-López, J. Rearfoot striking runners are more economical than midfoot strikers. *Med. Sci. Sports Exerc.* **46** (2014).

24. Di Michele, R. & Merni, F. The concurrent effects of strike pattern and ground-contact time on running economy. *J. Sci. Med. Sport* **17**, 414–418. <https://doi.org/10.1016/j.jsams.2013.05.012> (2014).
25. Støren, Ø., Helgerud, J. & Hoff, J. Running stride peak forces inversely determine running economy in elite runners. *J. Strength Cond. Res.* **25** (2011).
26. Paavolainen, L. M., Nummela, A. T. & Rusko, H. K. Neuromuscular characteristics and muscle power as determinants of 5-km running performance. *Med. Sci. Sports Exerc.* **31**, 124–130. <https://doi.org/10.1097/00005768-199901000-00020> (1999).
27. Williams, K. R. & Cavanagh, P. R. Relationship between distance running mechanics, running economy, and performance. *J. Appl. Physiol.* **63**, 1236–1245. <https://doi.org/10.1152/jappl.1987.63.3.1236> (1987).
28. Lussiana, T., Gindre, C., Mourot, L. & Hébert-Losier, K. Do subjective assessments of running patterns reflect objective parameters?. *Eur. J. Sport Sci.* **17**, 847–857. <https://doi.org/10.1080/17461391.2017.1325072> (2017).
29. Harriss, D. J., Macsween, A. & Atkinson, G. Standards for ethics in sport and exercise science research: 2018 update. *Int. J. Sports Med.* **38**, 1126–1131. <https://doi.org/10.1055/s-0043-124001> (2017).
30. Oliveira, A. S. & Pircoveanu, C. I. Implications of sample size and acquired number of steps to investigate running biomechanics. *Sci. Rep.* **11**, 3083. <https://doi.org/10.1038/s41598-021-82876-z> (2021).
31. Svedenhag, J. & Sjödin, B. Body-mass-modified running economy and step length in elite male middle- and long-distance runners. *Int. J. Sports Med.* **15**, 305–310. <https://doi.org/10.1055/s-2007-1021065> (1994).
32. Tranberg, R., Saari, T., Zügner, R. & Kärrholm, J. Simultaneous measurements of knee motion using an optical tracking system and radiostereometric analysis (RSA). *Acta Orthop.* **82**, 171–176. <https://doi.org/10.3109/17453674.2011.570675> (2011).
33. Hanavan, E. A mathematical model of the human body. *AMRL-TR. Aerospace Med Res Lab* **1**, 1–149 (1964).
34. Dempster, W. T. *Space requirements of the seated operator: geometrical, kinematic, and mechanical aspects of the body with special reference to the limbs.* (Wright Air Development Center, 1955).
35. Woltring, H. Representation and calculation of 3-D joint movement. *Hum. Mov. Sci.* **10**, 603–616. [https://doi.org/10.1016/0167-9457\(91\)90048-3](https://doi.org/10.1016/0167-9457(91)90048-3) (1991).
36. Cole, G. K., Nigg, B. M., Ronsky, J. L. & Yeadon, M. R. Application of the joint coordinate system to three-dimensional joint attitude and movement representation: a standardization proposal. *J. Biomech. Eng.* **115**, 344–349. <https://doi.org/10.1115/1.2895496> (1993).
37. Davis, R. B., Öunpuu, S., Tyburski, D. & Gage, J. R. A gait analysis data collection and reduction technique. *Hum. Mov. Sci.* **10**, 575–587. [https://doi.org/10.1016/0167-9457\(91\)90046-Z](https://doi.org/10.1016/0167-9457(91)90046-Z) (1991).
38. Grood, E. S. & Suntay, W. J. A joint coordinate system for the clinical description of three-dimensional motions: application to the knee. *J. Biomech. Eng.* **105**, 136–144. <https://doi.org/10.1115/1.3138397> (1983).
39. Blankevoort, L., Huiskes, R. & de Lange, A. The envelope of passive knee joint motion. *J. Biomech.* **21**, 705–720. [https://doi.org/10.1016/0021-9290\(88\)90280-1](https://doi.org/10.1016/0021-9290(88)90280-1) (1988).
40. Kadaba, M. P., Ramakrishnan, H. K. & Wootten, M. E. Measurement of lower extremity kinematics during level walking. *J. Orthop. Res.* **8**, 383–392. <https://doi.org/10.1002/jor.1100080310> (1990).
41. Piazza, S. J. & Cavanagh, P. R. Measurement of the screw-home motion of the knee is sensitive to errors in axis alignment. *J. Biomech.* **33**, 1029–1034. [https://doi.org/10.1016/s0021-9290\(00\)00056-7](https://doi.org/10.1016/s0021-9290(00)00056-7) (2000).
42. Altman, A. R. & Davis, I. S. A kinematic method for footstrike pattern detection in barefoot and shod runners. *Gait Posture* **35**, 298–300. <https://doi.org/10.1016/j.gaitpost.2011.09.104> (2012).
43. Lussiana, T., Patoz, A., Gindre, C., Mourot, L. & Hébert-Losier, K. The implications of time on the ground on running economy: less is not always better. *J. Exp. Biol.* **222**, jeb192047, doi:<https://doi.org/10.1242/jeb.192047> (2019).
44. Maiwald, C., Sterzing, T., Mayer, T. A. & Milani, T. L. Detecting foot-to-ground contact from kinematic data in running. *Footwear Sci.* **1**, 111–118. <https://doi.org/10.1080/19424280903133938> (2009).
45. Morin, J.-B., Dalleau, G., Kyröläinen, H., Jeannin, T. & Belli, A. A simple method for measuring stiffness during running. *J. Appl. Biomech.* **21**, 167–180. <https://doi.org/10.1123/jab.21.2.167> (2005).
46. Cohen, J. *Statistical Power Analysis for the Behavioral Sciences.* (Routledge, 1988).
47. Hinkle, D. E., Wiersma, W. & Jurs, S. G. *Applied Statistics for the Behavioral Sciences.* 768 (Houghton Mifflin (p. 109), 2002).
48. Sinclair, J., Fau-Goodwin, J., Richards, J. & Shore, H. The influence of minimalist and maximalist footwear on the kinetics and kinematics of running. *Footwear Sci.* **8**, 33–39. <https://doi.org/10.1080/19424280.2016.1142003> (2016).
49. Fuller, J. T., Bellenger, C. R., Thewlis, D., Tsiros, M. D. & Buckley, J. D. The effect of footwear on running performance and running economy in distance runners. *Sports Med.* **45**, 411–422. <https://doi.org/10.1007/s40279-014-0283-6> (2015).
50. Sun, X., Lam, W.-K., Zhang, X., Wang, J. & Fu, W. Systematic review of the role of footwear constructions in running biomechanics: implications for running-related injury and performance. *J. Sports Sci. Med.* **19**, 20–37 (2020).
51. Hébert-Losier, K. *et al.* Metabolic and performance responses of male runners wearing 3 types of footwear: Nike Vaporfly 4%, Saucony Endorphin racing flats, and their own shoes. *J. Sport Health Sci.* <https://doi.org/10.1016/j.jshs.2020.11.012> (2020).
52. Tam, N., Tucker, R. & Astephen Wilson, J. L. Individual Responses to a barefoot running program: insight into risk of injury. *Am. J. Sports Med.* **44**, 777–784, doi:<https://doi.org/10.1177/0363546515620584> (2016).
53. Tung, K. D., Franz, J. R. & Kram, R. A test of the metabolic cost of cushioning hypothesis during unshod and shod running. *Med. Sci. Sports Exerc.* **46**, 324–329. <https://doi.org/10.1249/MSS.0b013e3182a63b81> (2014).
54. Van Alsenoy, K., van der Linden, M. L., Girard, O. & Santos, D. Increased footwear comfort is associated with improved running economy - a systematic review and meta-analysis. *Eur. J. Sport Sci.*, 1–13, doi:<https://doi.org/10.1080/17461391.2021.1998642> (2021).
55. Roberts, T. J., Kram, R., Weyand, P. G. & Taylor, C. R. Energetics of bipedal running. I. Metabolic cost of generating force. *J. Exp. Biol.* **201**, 2745–2751, doi:<https://doi.org/10.1242/jeb.201.19.2745> (1998).
56. Roberts, T. J., Chen, M. S. & Taylor, C. R. Energetics of bipedal running. II. Limb design and running mechanics. *J. Exp. Biol.* **201**, 2753–2762, doi:<https://doi.org/10.1242/jeb.201.19.2753> (1998).
57. Kram, R. & Taylor, C. R. Energetics of running: a new perspective. *Nature* **346**, 265–267. <https://doi.org/10.1038/346265a0> (1990).
58. de Ruiter, C. J., Verdijk, P. W. L., Werker, W., Zuidema, M. J. & de Haan, A. Stride frequency in relation to oxygen consumption in experienced and novice runners. *Eur. J. Sport Sci.* **14**, 251–258. <https://doi.org/10.1080/17461391.2013.783627> (2014).
59. Quinn, T. J., Dempsey, S. L., LaRoche, D. P., Mackenzie, A. M. & Cook, S. B. Step frequency training improves running economy in well-trained female runners. *J. Strength Cond. Res.* <https://doi.org/10.1519/jsc.0000000000003206> (2019).
60. Kaneko, M., Matsumoto, M., Ito, A. & Fuchimoto, T. *Optimum step frequency in constant speed running.* (Human Kinetics, 1987).
61. Tenforde, A. S., Borgstrom, H. E., Outerleys, J. & Davis, I. S. Is cadence related to leg length and load rate?. *J. Orthop. Sports Phys. Ther.* **49**, 280–283. <https://doi.org/10.2519/jospt.2019.8420> (2019).
62. Adams, D., Pozzi, F., Willy, R. W., Carrol, A. & Zeni, J. Altering cadence or vertical oscillation during running: effects on running related injury factors. *Int. J. Sports Phys. Ther.* **13**, 633–642 (2018).
63. Allen, D. J., Heisler, H., Mooney, J. & Kring, R. The effect of step rate manipulation on foot strike pattern of long distance runners. *Int. J. Sports Phys. Ther.* **11**, 54–63 (2016).
64. Nummela, A., Keränen, T. & Mikkelsson, L. Factors related to top running speed and economy. *Int. J. Sports Med.* **28**, 655–661 (2007).

65. Lieberman, D. E., Warrener, A. G., Wang, J. & Castillo, E. R. Effects of stride frequency and foot position at landing on braking force, hip torque, impact peak force and the metabolic cost of running in humans. *J. Exp. Biol.* **218**, 3406–3414. <https://doi.org/10.1242/jeb.125500> (2015).
66. Moore, I. S., Jones, A. M. & Dixon, S. J. Reduced oxygen cost of running is related to alignment of the resultant GRF and leg axis vector: a pilot study. *Scand. J. Med. Sci. Sports* **26**, 809–815. <https://doi.org/10.1111/sms.12514> (2016).
67. Farley, C. T. & González, O. Leg stiffness and stride frequency in human running. *J. Biomech.* **29**, 181–186. [https://doi.org/10.1016/0021-9290\(95\)00029-1](https://doi.org/10.1016/0021-9290(95)00029-1) (1996).
68. Morin, J. B., Samozino, P., Zameziati, K. & Belli, A. Effects of altered stride frequency and contact time on leg-spring behavior in human running. *J. Biomech.* **40**, 3341–3348. <https://doi.org/10.1016/j.jbiomech.2007.05.001> (2007).
69. Monte, A., Muollo, V., Nardello, F. & Zamparo, P. Sprint running: how changes in step frequency affect running mechanics and leg spring behaviour at maximal speed. *J. Sports Sci.* **35**, 339–345. <https://doi.org/10.1080/02640414.2016.1164336> (2017).
70. Saunders, P. U., Pyne, D. B., Telford, R. D. & Hawley, J. A. Factors affecting running economy in trained distance runners. *Sports Med.* **34**, 465–485. <https://doi.org/10.2165/00007256-200434070-00005> (2004).
71. Dickinson, M. H. *et al.* How animals move: an integrative view. *Science* **288**, 100. <https://doi.org/10.1126/science.288.5463.100> (2000).
72. Jones, A. M. The physiology of the world record holder for the women's marathon. *Int. J. Sports Sci. Coach.* **1**, 101–116. <https://doi.org/10.1260/174795406777641258> (2006).
73. Yue, B. *et al.* Differences of knee anthropometry between Chinese and white men and women. *J. Arthroplasty* **26**, 124–130. <https://doi.org/10.1016/j.arth.2009.11.020> (2011).
74. Scholz, M. N., Bobbert, M. F., van Soest, A. J., Clark, J. R. & van Heerden, J. Running biomechanics: shorter heels, better economy. *J. Exp. Biol.* **211**, 3266. <https://doi.org/10.1242/jeb.018812> (2008).
75. Hunter, G. R. *et al.* Tendon length and joint flexibility are related to running economy. *Med. Sci. Sports Exerc.* **43**, 1492–1499. <https://doi.org/10.1249/MSS.0b013e318210464a> (2011).
76. Ueno, H. *et al.* Relationship between Achilles tendon length and running performance in well-trained male endurance runners. *Scand. J. Med. Sci. Sports* **28**, 446–451. <https://doi.org/10.1111/sms.12940> (2018).
77. Kunimasa, Y. *et al.* Specific muscle-tendon architecture in elite Kenyan distance runners. *Scand. J. Med. Sci. Sports* **24**, e269–274. <https://doi.org/10.1111/sms.12161> (2014).
78. Mooses, M. *et al.* Dissociation between running economy and running performance in elite Kenyan distance runners. *J. Sports Sci.* **33**, 136–144. <https://doi.org/10.1080/02640414.2014.926384> (2015).
79. Hunter, I. *et al.* Running economy, mechanics, and marathon racing shoes. *J. Sports Sci.* **37**, 2367–2373. <https://doi.org/10.1080/02640414.2019.1633837> (2019).
80. Sloan, R. S., Wight, J. T., Hooper, D. R., Garman, J. E. J. & Pujalte, G. G. A. Metabolic testing does not alter distance running lower body sagittal kinematics. *Gait Posture* **76**, 403–408. <https://doi.org/10.1016/j.gaitpost.2020.01.001> (2020).

Acknowledgements

The authors thank Mr. Chris Tee Chow Li for assistance during the data collection process. The authors also thank the participants for their time and participation.

Author contributions

Conceptualization: T.L., C.G., and K.H.-L.; Methodology: T.L., L.M., C.G., and K.H.-L.; Investigation: T.L. and K.H.-L.; Formal analysis: T.L., A.P., K.H.-L., and B.B.; Writing—original draft preparation: A.P. and B.B.; Writing—review and editing: A.P., B.B., T.L., L.M., C.G., and K.H.-L.; Supervision: L.M. and K.H.-L.; Project administration: L.M.; Funding acquisition: T.L., L.M., and K.H.-L.

Funding

This study was financially supported by the University of Bourgogne Franche-Comté (France) and the National Sports Institute of Malaysia.

Competing interests

The authors declare no competing interests.

Additional information

Supplementary Information The online version contains supplementary material available at <https://doi.org/10.1038/s41598-022-10030-4>.

Correspondence and requests for materials should be addressed to A.P.

Reprints and permissions information is available at www.nature.com/reprints.

Publisher's note Springer Nature remains neutral with regard to jurisdictional claims in published maps and institutional affiliations.



Open Access This article is licensed under a Creative Commons Attribution 4.0 International License, which permits use, sharing, adaptation, distribution and reproduction in any medium or format, as long as you give appropriate credit to the original author(s) and the source, provide a link to the Creative Commons licence, and indicate if changes were made. The images or other third party material in this article are included in the article's Creative Commons licence, unless indicated otherwise in a credit line to the material. If material is not included in the article's Creative Commons licence and your intended use is not permitted by statutory regulation or exceeds the permitted use, you will need to obtain permission directly from the copyright holder. To view a copy of this licence, visit <http://creativecommons.org/licenses/by/4.0/>.

© The Author(s) 2022

Supplementary Materials for:

Non-South East Asians have a better running economy and different anthropometrics and biomechanics than South East Asians.

S1. Running economy between South East Asians and non-South East Asians expressed in ml/kg/km

Expressing running economy (RE) in ml/kg/km resulted in larger differences between South East Asians (SEA) and non-SEA runners than in the main manuscript. SEA runners were significantly less economical (10%) than non-SEA runners (average across speeds: 191.7 ± 14.9 vs 171.9 ± 10.8 ml/kg/km), with a *large* main effect of group on RE ($p < 0.001$, *large* effect size: $d = 1.52$; Figure S1). There were no significant main effect of speed ($p = 0.28$) and group x speed interaction effect ($p = 0.89$) on RE.

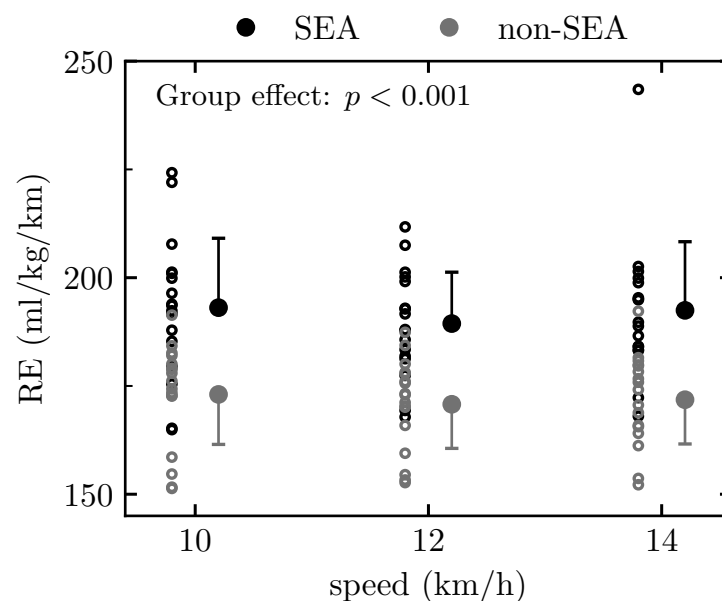


Figure S1. Running Economy (RE; in ml/kg/km) of South East Asian (SEA) and non-South East Asian (non-SEA) runners at several endurance running speeds. Linear mixed effects modelling identified a significant group effect ($p \leq 0.05$).

Relationships between RE and anthropometric characteristics unrelated to other anthropometric characteristics (mass and ratio of leg length over height) were computed and reported in Table S1. All correlations were *negligible* or *low*, and non-significant.

Table S1. Pearson correlation coefficients between running economy (in ml/kg/km) and anthropometric characteristics (mass and ratio of leg length over height), together with their corresponding p -values underneath for South East Asian (SEA), non-South East Asian (non-SEA), as well as all runners pooled together (ALL). Statistical significances ($p \leq 0.05$) are indicated in bold.

Group	SEA			non-SEA			ALL		
Running speed (km/h)	10	12	14	10	12	14	10	12	14
Mass (kg)	0.26	0.27	-0.06	0.47	0.35	0.16	-0.06	-0.13	-0.29
	0.32	0.29	0.82	0.06	0.17	0.54	0.74	0.46	0.10
Leg length over height (%)	0.01	-0.17	-0.07	0.20	0.05	-0.04	0.00	-0.13	-0.12
	0.98	0.53	0.80	0.44	0.86	0.87	0.99	0.46	0.50

Note. Only the relationships between running economy and mass and ratio of leg length over height were considered because mass was highly and significantly correlated to height, leg length, and body mass index.

For SEA runners, a *high* positive correlation was seen between RE and contact time (t_c) at 12 km/h ($|r| \geq 0.76$, $p \leq 0.001$; Table S1). Step frequency (SF) and ankle angle (θ_{ankle}) at footstrike at 10 km/h were *moderately* and negatively correlated to RE, whereas step length (SL) was *moderately* and positively correlated to RE at 10 km/h ($|r| \geq 0.54$, $p \leq 0.02$; Table S1). At 12 km/h, SF, k_{leg} , and θ_{ankle} at footstrike and toe-off were *moderately* and negatively correlated to RE, whereas SL was *moderately* and positively correlated to RE ($|r| \geq 0.54$, $p \leq 0.03$; Table S1).

For non-SEA runners, there was no *moderate* or *high* correlations between RE and any biomechanical variables.

For runners combined, footstrike angle (FSA) and θ_{ankle} at footstrike were *moderately* and negatively correlated to RE at 10 and 12 km/h ($|r| \geq 0.50$, $p \leq 0.003$; Table S1). Table S1 presents all correlations, including the *low*, *negligible*, and non-significant ones.

Table S2. Pearson correlation coefficients between running economy (in ml/kg/km) and biomechanical variables [step frequency (SF), step length (SL), contact time (t_c), flight time (t_f), spring-mass characteristics of the lower limb as given by leg stiffness (k_{leg}), footstrike angle (FSA), and flexion-extension ankle (θ_{ankle}) and knee (θ_{knee}) joint angle at footstrike (FS) and toe-off (TO)], together with their corresponding p -values underneath for South East Asian (SEA), non-South East Asian (non-SEA), as well as all runners pooled together (ALL). Statistical significances ($p \leq 0.05$) are indicated in bold. Gray shaded boxes denote correlation coefficients above an absolute value of 0.5 (*moderate*). SL was expressed as a percentage of participant's leg length in addition to raw units.

Group	SEA			non-SEA			ALL		
	10	12	14	10	12	14	10	12	14
Running speed (km/h)									
SF (steps/min)	-0.68 0.003	-0.66 0.004	-0.11 0.67	-0.20 0.43	-0.22 0.40	-0.12 0.65	-0.10 0.57	-0.07 0.70	0.14 0.42
SL (cm)	0.69 0.002	0.67 0.003	0.13 0.63	0.23 0.38	0.21 0.41	0.10 0.69	0.10 0.56	0.07 0.70	-0.13 0.46
SL (%) ^a	0.29 0.26	0.38 0.14	0.09 0.72	-0.35 0.17	-0.17 0.50	-0.11 0.67	0.05 0.76	0.15 0.39	0.06 0.74
t_c (ms)	0.25 0.34	0.78 <0.001	0.29 0.27	-0.06 0.82	0.28 0.28	0.41 0.10	-0.11 0.52	0.18 0.32	0.01 0.94
t_f (ms)	0.10 0.72	-0.25 0.33	-0.21 0.43	0.26 0.32	-0.02 0.95	-0.18 0.48	0.05 0.77	-0.14 0.43	-0.16 0.36
k_{leg} (kN/m)	-0.26 0.31	-0.54 0.03	-0.38 0.13	0.38 0.14	0.11 0.69	-0.07 0.78	-0.12 0.51	-0.30 0.09	-0.28 0.11
FSA (°)	-0.42 0.10	-0.38 0.13	-0.06 0.81	0.05 0.85	0.02 0.94	-0.11 0.66	-0.50 0.003	-0.52 0.001	-0.45 0.007
θ_{ankle} at FS (°)	-0.54 0.02	-0.55 0.02	-0.07 0.78	-0.12 0.66	0.00 1.00	-0.09 0.74	-0.54 <0.001	-0.51 0.002	-0.38 0.03
θ_{ankle} at TO (°)	-0.30 0.25	-0.62 0.008	-0.24 0.35	0.00 0.99	-0.07 0.78	-0.31 0.23	-0.33 0.06	-0.48 0.004	-0.32 0.06
θ_{knee} at FS (°)	0.01 0.98	0.04 0.89	0.00 1.00	-0.08 0.76	0.08 0.77	0.13 0.63	-0.12 0.48	-0.03 0.84	0.03 0.87
θ_{knee} at TO (°)	-0.01 0.97	0.03 0.90	0.18 0.50	0.16 0.53	0.30 0.25	0.31 0.23	0.23 0.20	0.35 0.04	0.43 0.01

^a Step length normalized to leg length.

S2. Morphological factors potentially explaining differences in running economy between South East Asians and non-South East Asians

Asian and non-Asian individuals have been shown to differ morphologically¹⁻³. For instance, the shape of the forefoot of Japanese and Korean males differs from North American males¹; Chinese knees (mediolateral and anteroposterior size of the femur) are generally smaller than Caucasian ones²; and pelvic parameters (e.g., pelvic tilt and incidence) also differ between Asian, Mexican, and Caucasian individuals³. These specific parameters were not examined and, although most likely not associated with RE directly, can potentially play a role in the biomechanical and physiological differences we observed.

Achilles tendon moment arms and foot-lever ratios are two additional parameters that relate to RE. Indeed, a previous study found a strong correlation between the moment arm of the Achilles tendon and RE, where smaller muscle moment arms correlated with lower rates of metabolic energy consumption⁴. Hunter et al.⁵ also observed that longer lower limb tendons (especially Achilles tendon) and less flexible lower limb joints were linked with improved RE. Recently, Ueno et al.⁶ proposed that longer Achilles tendons may be advantageous to achieve superior running endurance performance associated with better RE, in support of previous findings. In addition, longer moment arms and shorter feet (smaller foot-lever ratio) of elite Kenyan than Japanese runners were associated with better RE⁷. However, discrepancies exist in the scientific literature, as smaller moment arms have been associated with greater RE in high-level Kenyan distance runners⁸. Clearly, more research is needed on this subject as these parameters were not measured in this study, but could have partly explained differences in RE between SEA and non-SEA runners.

References

- 1 Hawes, M. R. *et al.* Ethnic differences in forefoot shape and the determination of shoe comfort. *Ergonomics* **37**, 187-196, doi:10.1080/00140139408963637 (1994).
- 2 Yue, B. *et al.* Differences of knee anthropometry between Chinese and white men and women. *J. Arthroplasty* **26**, 124-130, doi:10.1016/j.arth.2009.11.020 (2011).
- 3 Zárate-Kalfópulos, B., Romero-Vargas, S., Otero-Cámara, E., Correa, V. C. & Reyes-Sánchez, A. Differences in pelvic parameters among Mexican, Caucasian, and Asian populations. *J. Neurosurg. Spine* **16**, 516-519, doi:10.3171/2012.2.Spine11755 (2012).
- 4 Scholz, M. N., Bobbert, M. F., van Soest, A. J., Clark, J. R. & van Heerden, J. Running biomechanics: shorter heels, better economy. *J. Exp. Biol.* **211**, 3266, doi:10.1242/jeb.018812 (2008).
- 5 Hunter, G. R. *et al.* Tendon length and joint flexibility are related to running economy. *Med. Sci. Sports Exerc.* **43**, 1492-1499, doi:10.1249/MSS.0b013e318210464a (2011).
- 6 Ueno, H. *et al.* Relationship between Achilles tendon length and running performance in well-trained male endurance runners. *Scand. J. Med. Sci. Sports* **28**, 446-451, doi:10.1111/sms.12940 (2018).
- 7 Kunimasa, Y. *et al.* Specific muscle-tendon architecture in elite Kenyan distance runners. *Scand. J. Med. Sci. Sports* **24**, e269-274, doi:10.1111/sms.12161 (2014).
- 8 Mooses, M. *et al.* Dissociation between running economy and running performance in elite Kenyan distance runners. *J. Sports Sci.* **33**, 136-144, doi:10.1080/02640414.2014.926384 (2015).

9.10 The Nike Vaporfly 4%: a game changer to improve performance without biomechanical explanation yet

Aurélien Patoz^{1,2,*}, Thibault Lussiana^{2,3,4}, Bastiaan Breine^{2,5}, Cyrille Gindre^{2,3}

¹ Institute of Sport Sciences, University of Lausanne, 1015 Lausanne, Switzerland

² Research and Development Department, Volodalen Swiss Sport Lab, 1860 Aigle, Switzerland

³ Research and Development Department, Volodalen, 39270 Chavéria, France

⁴ Research Unit EA3920 Prognostic Markers and Regulatory Factors of Cardiovascular Diseases and Exercise Performance, Health, Innovation platform, University of Franche-Comté, Besançon, France

⁵ Department of Movement and Sports Sciences, Ghent University, 9000 Ghent, Belgium

* Corresponding author

Published in **Footwear Science**

DOI: 10.1080/19424280.2022.2077844

The Nike Vaporfly 4%: a game changer to improve performance without biomechanical explanation yet

Aurélien Patoz^{a,b} , Thibault Lussiana^{b,c,d} , Bastiaan Breine^{b,e}  and Cyrille Gindre^{b,c}

^aInstitute of Sport Sciences, University of Lausanne, Lausanne, Switzerland; ^bResearch and Development Department, Volodalen Swiss Sport Lab, Aigle, Switzerland; ^cResearch and Development Department, Volodalen, Chavéria, France; ^dResearch Unit EA3920 Prognostic Markers and Regulatory Factors of Cardiovascular Diseases and Exercise Performance, Health, Innovation platform, University of Franche-Comté, France Besançon; ^eDepartment of Movement and Sports Sciences, Ghent University, Ghent, Belgium

ABSTRACT

In a recent article published in *Footwear Science*, the *teeter-totter effect* was indirectly observed with the Nike Vaporfly 4% (VP4) running shoe. This mechanism was attributed to the presence of a curved carbon-fibre (stiff) plate, and potentially causes runners to propel forward during push-off. It was suggested that such mechanism should explain the 4% improvement of performance of the VP4 compared to regular shoes. However, there was, to the best of the authors' knowledge, no attempt to associate this VP4-specific mechanism to the change in running economy and personal best time yet. Furthermore, a recent article published in the *Journal of Sport and Health Science* observed that the stiffening effect of the curved carbon-fibre plate plays a limited role in the energy savings, which therefore questions the presence of the teeter-totter effect in the VP4 shoe. In our view, the better running economy and personal best time obtained with the VP4 shoe cannot be currently explained from a biomechanical standpoint. With this letter, we would like to (1) summarise the specificities of the VP4 shoe, (2) report the observed improvements in running economy and personal best time, and (3) point out the absence of any biomechanical explanation to the better performance yet.

ARTICLE HISTORY

Received 3 February 2022
Accepted 10 May 2022

KEYWORDS

Running economy;
footwear; running;
biomechanics; physiology

1. The specificities of the Nike Vaporfly 4% shoe

The VP4 shoe is lighter than comparable marathon racing shoes (Hoogkamer et al., 2018; Nigg et al., 2020). This shoe has a curved carbon-fibre plate, which increases the longitudinal bending stiffness (Burns & Tam, 2020; Hoogkamer et al., 2018; Nigg et al., 2020), embedded in a thick foam midsole made in polyether block amide (Pebax; Nike ZoomX, Nike Inc., Beaverton, OR), which is less dense, lighter, and more resilient than traditional foams (Burns & Tam, 2020; Hoogkamer et al., 2018). The low-density foam allows for more highly resilient material without adding mass and thus allows for a higher heel thickness (shoe-heel height = 31 mm) than habitual marathon shoes, which also provides an increased cushioning and a rocking effect (Burns & Tam, 2020). It was first thought that the midsole thickness should be regulated to have a *fair* competitive footwear (Burns & Tam,

2020). However, Frederick (2020) and Hoogkamer (2020) suggested that there was insufficient scientific evidence to support a proposal to regulate the stack height of marathon racing shoes. Hence, the VP4 shoe was considered as a valid shoe for competition by the International Association of Athletics Federations for road races (International Association of Athletics Federations. Book of Rules. Available: <https://www.worldathletics.org/about-iaaf/documents/book-of-rules>).

2. The improvements in running economy and personal best time

According to recent research, the VP4 shoe is a viable mechanical ergogenic aid that improves running economy in elite (Barnes & Kilding, 2019; Hoogkamer et al., 2018; Hunter et al., 2019) and recreational (Hébert-Losier et al., 2020) runners by up to 4.4% compared with established track spikes (Barnes & Kilding, 2019), marathon racing

(Hoogkamer et al., 2018; Hunter et al., 2019), and habitual running shoes (Hébert-Losier et al., 2020). Additionally, by wearing the VP4 shoe instead of their habitual running shoes, recreational runners improve their 3-km time-trial by 2.4% (Hébert-Losier et al., 2020) and elite runners improve their marathon racing time by 0.7% (Rodrigo-Carranza et al., 2021). Hence, the VP4 shoe provides advantageous technological assistance, especially because it does not involve any increase in the training load, which is a risk factor for overuse injury (van Poppel et al., 2021). Nonetheless, large interindividual variations were reported (Barnes & Kilding, 2019; Hébert-Losier et al., 2020). For instance, changes in running economy and 3-km time-trial in recreational runners ranged from -8.6% to

13.3% and -3.8% to 8.2% , respectively, when wearing the VP4 shoe instead of their habitual running shoes (Hébert-Losier et al., 2020). In addition, non-rearfoot strikers respond less favourably to the VP4 shoe than rearfoot strikers (Hébert-Losier et al., 2020; Hoogkamer et al., 2019). These observations might partly be explained by the fact that each runner adopts a spontaneous running style (Gindre et al., 2016; van Oeveren et al., 2021) and hence responds differently to footwear, but this warrant further investigation.

3. The absence of any biomechanical explanation yet

Running with the VP4 shoe led to several conflicting evidence in terms of kinetic-kinematic running



Figure 1. Infographic summarising the specificities of the Nike Vaporfly 4% running shoe, reporting the observed improvements in running economy and personal best time, and pointing out the absence of any biomechanical explanation to the better performance yet.

adaptations, which were, if any, small (Barnes & Kilding, 2019; Hoogkamer et al., 2018; 2019; Hunter et al., 2019). Ground contact time, flight time, and step frequency decreased, increased, or did not change (Barnes & Kilding, 2019; Hoogkamer et al., 2018; 2019; Hunter et al., 2019) when using the VP4 shoe compared to other marathon shoes while the peak vertical force either increased or did not change (Hoogkamer et al., 2018; 2019; Hunter et al., 2019). All these variables could not explain the better performance (Barnes & Kilding, 2019; Hoogkamer et al., 2018).

Hoogkamer et al. (2019) observed that the dorsiflexion and work rate at the ankle and metatarsophalangeal (MTP) joint were reduced in the VP4 shoe compared to other marathon shoes. Similarly, Healey and Hoogkamer (2021) reported biomechanical differences in the MTP joint with decreased MTP dorsiflexion angle, angular velocity, and negative power in the VP4 compared to cut (six medio-lateral cuts through the carbon-fibre plate in the forefoot to reduce its stiffness) VP4 shoe. Additionally, using a curved-carbon fibre plate reduced the MTP joint work without increasing the mechanical demand at the ankle (Farina et al., 2019). However, none of these studies attempted to associate these VP4-specific biomechanical adaptations to the better observed performance.

The teeter-totter effect, which should result in a force acting on the heel during push-off that acts at the right location and time and with the right frequency (2–4 Hz), and which could potentially explain the 4% improvement of performance (Nigg et al., 2020, 2021), was explored and indirectly observed in the VP4 shoe (Subramaniam & Nigg, 2021). This effect was attributed to the presence of a curved carbon-fibre (stiff) plate in the VP4 shoe (Nigg et al., 2020, 2021). Further, the thickness of the heel seems important because a thicker heel allows the stiff plate to be more curved, hence permitting to increase the teeter-totter effect (Nigg et al., 2020, 2021). However, Subramaniam and Nigg (2021) did not report any relation between the presence of the teeter-totter effect and the improvement of performance, most likely because the results were obtained from a pilot study conducted on only two participants (the authors fairly mentioned that a larger study involving ~20 participants will be conducted). Nevertheless, as the

stiffening effect of the curved carbon-fibre plate was shown to play a limited role in the energy savings of the VP4 shoe (Healey & Hoogkamer, 2021), the presence of a teeter-totter effect in the VP4 shoe could be questioned.

Altogether, as no VP4-specific biomechanical adaptations were associated to the better running economy and personal best time obtained with the VP4 shoe, the better performance cannot be currently explained from a biomechanical standpoint (Figure 1).

4. Conclusion

The VP4 shoe is a game changer to improve running economy and personal best time. The energy savings of the VP4 shoe are likely from the combination and interaction of the highly compliant and resilient midsole, curved carbon-fibre plate, and shoe geometry (Healey & Hoogkamer, 2021; Ortega et al., 2021). However, there is a lack of understanding of this footwear as there is no biomechanical explanation to the better performance yet. Future studies should try to associate the VP4-specific biomechanical adaptations to the improvement in running economy and personal best time to decipher why the VP4 shoe is such a game changer. Keeping in mind that the running pattern is a dynamic system with several interconnected variables (Novacheck, 1998), the energy savings might be due to the combination of many but small biomechanical adaptations. Moreover, as large interindividual variations were reported in terms of running economy in response to the VP4 shoe (Barnes & Kilding, 2019; Hébert-Losier et al., 2020), pooling all runners together might mask an effect that would be observed when only considering high responders, e.g., runners with an improvement in running economy greater than 2.6% (Barnes & Kilding, 2015), or subgroups of runners determined using their spontaneous running style (Gindre et al., 2016; van Oeveren et al., 2021). Hence, we suggest that the relation between the VP4-specific biomechanical adaptations and improvement in running economy should be multifactorial, consider only high responders, and take into account the running style.

Disclosure statement

No potential conflict of interest was reported by the author(s).

ORCID

Aurélien Patoz  <http://orcid.org/0000-0002-6949-7989>
 Thibault Lussiana  <http://orcid.org/0000-0002-1782-401X>
 Bastiaan Breine  <http://orcid.org/0000-0002-7959-7721>

References

- Barnes, K. R., & Kilding, A. E. (2015). Running economy: Measurement, norms, and determining factors. *Sports Medicine - Open*, 1(1), 8. <https://doi.org/10.1186/s40798-015-0007-y>
- Barnes, K. R., & Kilding, A. E. (2019). A randomized crossover study investigating the running economy of highly-trained male and female distance runners in marathon racing shoes versus track spikes. *Sports Medicine (Auckland, N.Z.)*, 49(2), 331–342. <https://doi.org/10.1007/s40279-018-1012-3>
- Burns, G. T., & Tam, N. (2020). Is it the shoes? A simple proposal for regulating footwear in road running. *British Journal of Sports Medicine*, 54(8), 439–440. <https://doi.org/10.1136/bjsports-2018-100480>
- Farina, E. M., Haight, D., & Luo, G. (2019). Creating footwear for performance running. *Footwear Science*, 11(sup1), S134–S135. <https://doi.org/10.1080/19424280.2019.1606119>
- Frederick, E. C. (2020). No evidence of a performance advantage attributable to midsole thickness. *Footwear Science*, 12(1), 1–2. <https://doi.org/10.1080/19424280.2019.1690327>
- Gindre, C., Lussiana, T., Hébert-Losier, K., & Mourot, L. (2016). Aerial and terrestrial patterns: A novel approach to analyzing human running. *International Journal of Sports Medicine*, 37(1), 25–29. <https://doi.org/10.1055/s-0035-1555931>
- Healey, L. A., & Hoogkamer, W. (2021). Longitudinal bending stiffness does not affect running economy in Nike Vaporfly Shoes. *Journal of Sport and Health Science*, 1–8. <https://doi.org/10.1016/j.jshs.2021.07.002>
- Hébert-Losier, K., Finlayson, S. J., Driller, M. W., Dubois, B., Esculier, J. F., & Beaven, C. M. (2020). Metabolic and performance responses of male runners wearing 3 types of footwear: Nike Vaporfly 4%, Saucony Endorphin racing flats, and their own shoes. *Journal of Sport and Health Science*, 1–10. <https://doi.org/10.1016/j.jshs.2020.11.012>
- Hoogkamer, W. (2020). More isn't always better. *Footwear Science*, 12(2), 75–77. <https://doi.org/10.1080/19424280.2019.1710579>
- Hoogkamer, W., Kipp, S., Frank, J. H., Farina, E. M., Luo, G., & Kram, R. (2018). A comparison of the energetic cost of running in marathon racing shoes. *Sports Medicine*, 48(4), 1009–1019. <https://doi.org/10.1007/s40279-017-0811-2>
- Hoogkamer, W., Kipp, S., & Kram, R. (2019). The biomechanics of competitive male runners in three marathon racing shoes: A randomized crossover study. *Sports Medicine (Auckland, N.Z.)*, 49(1), 133–143. <https://doi.org/10.1007/s40279-018-1024-z>
- Hunter, I., McLeod, A., Valentine, D., Low, T., Ward, J., & Hager, R. (2019). Running economy, mechanics, and marathon racing shoes. *Journal of Sports Sciences*, 37(20), 2367–2373. <https://doi.org/10.1080/02640414.2019.1633837>
- International Association of Athletics Federations. (2021). *Book of rules*. Retrieved December 21, from <https://www.worldathletics.org/about-iaaf/documents/book-of-rules>
- Nigg, B. M., Cigoja, S., & Nigg, S. R. (2020). Effects of running shoe construction on performance in long distance running. *Footwear Science*, 12(3), 133–138. <https://doi.org/10.1080/19424280.2020.1778799>
- Nigg, B. M., Cigoja, S., & Nigg, S. R. (2021). Teeter-totter effect: A new mechanism to understand shoe-related improvements in long-distance running. *British Journal of Sports Medicine*, 55(9), 462–463. <https://doi.org/10.1136/bjsports-2020-102550>
- Novacheck, T. F. (1998). The biomechanics of running. *Gait & Posture*, 7(1), 77–95. [https://doi.org/10.1016/S0966-6362\(97\)00038-6](https://doi.org/10.1016/S0966-6362(97)00038-6)
- Ortega, J. A., Healey, L. A., Swinnen, W., & Hoogkamer, W. (2021). Energetics and biomechanics of running footwear with increased longitudinal bending stiffness: A narrative review. *Sports Medicine (Auckland, N.Z.)*, 51(5), 873–894. <https://doi.org/10.1007/s40279-020-01406-5>
- Rodrigo-Carranza, V., González-Mohíno, F., Santos del Cerro, J., Santos-Concejero, J., & González-Ravé, J. M. (2021). Influence of advanced shoe technology on the top 100 annual performances in men's marathon from 2015 to 2019. *Scientific Reports*, 11(1), 22458. <https://doi.org/10.1038/s41598-021-01807-0>
- Subramaniam, A., & Nigg, B. (2021). Exploring the teeter-totter effect in shoes with curved carbon fibre plates. *Footwear Science*, 13(sup1), S74–S75. <https://doi.org/10.1080/19424280.2021.1917689>
- van Oeveren, B. T., de Ruiter, C. J., Beek, P. J., & van Dieën, J. H. (2021). The biomechanics of running and running styles: A synthesis. *Sports Biomechanics*, 1–39. <https://doi.org/10.1080/14763141.2021.1873411>
- van Poppel, D., van der Worp, M., Slabbekoorn, A., van den Heuvel, S. S. P., van Middelkoop, M., Koes, B. W., Verhagen, A. P., & Scholten-Peeters, G. G. M. (2021). Risk factors for overuse injuries in short- and long-distance running: A systematic review. *Journal of Sport and Health Science*, 10(1), 14–28. <https://doi.org/10.1016/j.jshs.2020.06.006>

9.11 Accurate estimation of peak vertical ground reaction force using the duty factor in level treadmill running

Aurélien Patoz^{1,2,*}, Thibault Lussiana^{2,3,4}, Bastiaan Breine^{2,5}, Cyrille Gindre^{2,3}, Davide Malatesta¹

¹ Institute of Sport Sciences, University of Lausanne, 1015 Lausanne, Switzerland

² Research and Development Department, Volodalen Swiss Sport Lab, 1860 Aigle, Switzerland

³ Research and Development Department, Volodalen, 39270 Chavéria, France

⁴ Research Unit EA3920 Prognostic Markers and Regulatory Factors of Cardiovascular Diseases and Exercise Performance, Health, Innovation platform, University of Franche-Comté, Besançon, France

⁵ Department of Movement and Sports Sciences, Ghent University, 9000 Ghent, Belgium

* Corresponding author

Published in **Scandinavian Journal of Medicine & Science in Sports**

DOI: 10.1111/sms.14252

Accurate estimation of peak vertical ground reaction force using the duty factor in level treadmill running

Aurélien Patoz^{1,2}  | Thibault Lussiana^{2,3,4}  | Bastiaan Breine^{2,5}  |
Cyrille Gindre^{2,3} | Davide Malatesta¹ 

¹Institute of Sport Sciences, University of Lausanne, Lausanne, Switzerland

²Research and Development Department, Volodalen Swiss Sport Lab, Aigle, Switzerland

³Research and Development Department, Volodalen, Chavéria, France

⁴Research Unit EA3920 Prognostic Markers and Regulatory Factors of Cardiovascular Diseases and Exercise Performance, Health, Innovation Platform, University of Franche-Comté, Besançon, France

⁵Department of Movement and Sports Sciences, Ghent University, Ghent, Belgium

Correspondence

Aurélien Patoz, Institute of Sport Sciences, University of Lausanne, 1015 Lausanne, Switzerland.

Email: aurelien.patoz@unil.ch

Funding information

Innosuisse - Schweizerische Agentur für Innovationsförderung, Grant/Award Number: 35793.1 IP-LS

This study aimed to (1) construct a statistical model (SMM) based on the duty factor (DF) to estimate the peak vertical ground reaction force ($F_{v,max}$) and (2) to compare the estimated $F_{v,max}$ to force plate gold standard (GSM). One hundred and fifteen runners ran at 9, 11, and 13 km/h. Force (1000 Hz) and kinematic (200 Hz) data were acquired with an instrumented treadmill and an optoelectronic system, respectively, to assess force-plate and kinematic based DFs. SMM linearly relates $F_{v,max}$ to the inverse of DF because DF was analytically associated with the inverse of the average vertical force during ground contact time and the latter was *very highly* correlated to $F_{v,max}$. No systematic bias and a 4% root mean square error (RMSE) were reported between GSM and SMM using force-plate based DF values when considering all running speeds together. Using kinematic based DF values, SMM reported a systematic but small bias (0.05BW) and a 5% RMSE when considering all running speeds together. These findings support the use of SMM to estimate $F_{v,max}$ during level treadmill runs at endurance speeds if underlying DF values are accurately measured.

KEYWORDS

biomechanics, curve fitting, gait analysis, linear regression, statistical model

1 | INTRODUCTION

Running offers many health benefits. However, between 19% and 79% of recreational runners are expected to contract a running related injury each year.^{1,2} Therefore, the incidence of these injuries is high. The magnitude of the peak of the vertical ground reaction force ($F_{v,max}$; active peak force)^{3,4} is related to an increased risk for various running musculoskeletal injuries.⁵⁻⁷ In addition, the peak axial tibial compressive force was shown to be moderately

correlated with $F_{v,max}$.⁸ Hence, Sasimontokul et al.⁴ suggest that the risk of tibial stress fracture is most closely associated with the forces acting during midstance, and that adopting a running technique to reduce $F_{v,max}$ may reduce the risk of tibial stress fracture. These observations make $F_{v,max}$ to be a biomechanical variable of major interest that needs to be accurately measured.

To measure $F_{v,max}$, the gold standard method (GSM) is to use a force plate, which could unfortunately not always be affordable or at hand.^{9,10} In such case, a first alternative

would be to use a sacral-mounted inertial measurement unit (IMU),^{11–13} which is low-cost and practical to use in a coaching environment.¹⁴ For instance, Alcantara et al.¹² predicted $F_{v,max}$ using machine learning and reported a root mean square error (RMSE) of 0.15 body weight (BW). Moreover, weak to moderate correlations were obtained between $F_{v,max}$ measured using GSM and estimated using IMU data.¹¹ These authors observed an effect of the low-pass cutoff frequency used for the IMU data, where a better correlation was depicted for a 10 Hz than a 5 or 30 Hz cutoff frequency. A second alternative would be to assume a sine-wave model for the vertical ground reaction force.^{15–17} Doing so, $F_{v,max}$ (expressed in BW units) could be estimated based on contact (t_c) and flight (t_f) times.¹⁷ This method reported a 7% bias compared to GSM for treadmill running.¹⁷ A third alternative would be to construct a statistical model relating $F_{v,max}$ to the duty factor (DF),^{18,19} that is, the ratio of t_c to stride duration (Equation 3). Ultimately, this model (statistical model method: SMM) could estimate $F_{v,max}$ only using a temporal parameter, that is, DF. Such SMM model would prove to be useful if the measurement system provides an accurate estimation of DF (or t_c and t_f , that is, its subcomponents) but does not provide an estimation of $F_{v,max}$, as it is often the case for foot-worn²⁰ or ankle-worn²¹ inertial sensors. However, SMM has, to the best of our knowledge, never been constructed so far.

Hence, the first purpose of this study was to construct a statistical model relating $F_{v,max}$ to DF, where both variables were obtained from force plate data, and to compare $F_{v,max}$ estimated by this model to GSM. Then, as a practical application, the second purpose of this study was to use SMM with kinematic based DF values to estimate $F_{v,max}$ and to compare these estimations to GSM. We hypothesized that (1) $F_{v,max}$ estimated by SMM using force-plate based DF values should report a similar RMSE than in Alcantara et al.,¹² that is, ~ 0.15 BW and (2) $F_{v,max}$ estimated by SMM using kinematic based DF values should also report an RMSE of ~ 0.15 BW.

2 | MATERIALS AND METHODS

2.1 | Participant characteristics

An existing database of 115 recreational runners, 87 males (age: 30 ± 8 years, height: 180 ± 6 cm, body mass: 70 ± 7 kg, and weekly running distance: 38 ± 24 km) and 28 females (age: 30 ± 7 years, height: 169 ± 5 cm, body mass: 61 ± 6 kg, and weekly running distance: 22 ± 16 km), was used in the present study.²² For study inclusion, participants were required to not have current or recent lower-extremity injury (≤ 1 month), to run at least once a week, and to have

an estimated maximal aerobic speed ≥ 14 km/h. The study protocol was approved by the local Ethics Committee (CER-VD 2020-00334).

2.2 | Statistical model method

First, in what follows, DF is shown to be analytically proportional to the inverse of the mean vertical ground reaction force during t_c ($F_{v,mean}$), that is, the integral of the vertical ground reaction force during t_c divided by t_c ($F_{v,mean} = \int_{FS}^{TO} F_v(t) dt / t_c$, where FS, TO, and $F_v(t)$ represent foot-strike, toe-off, and vertical ground reaction force signal, respectively). Starting from vertical momentum conservation law during a running step, which states that the vertical momentum at FS is the same than the one at contralateral FS, or, in other words, that the integral of the vertical external forces during a running step is null, one can easily obtain that:

$$\int_{FS}^{TO} (F_v(t) - mg) dt - mgt_f = 0 \quad (1)$$

where mg represents BW. Solving Equation 1 for t_f leads to

$$t_f = \frac{\int_{FS}^{TO} F_v(t) dt}{mg} - t_c = t_c \frac{F_{v,mean}}{mg} - t_c \quad (2)$$

where the definition of $F_{v,mean}$ was used in the last step. Ultimately, by expressing DF as (the stride duration is assumed to be equal to two times $t_c + t_f$):

$$DF = \frac{t_c}{2(t_c + t_f)} \quad (3)$$

one can get that:

$$DF = \frac{mg}{2F_{v,mean}} \quad (4)$$

which proves that when DF is computed using Equation 3, DF is analytically proportional to the inverse of $F_{v,mean}$.

Then, assuming that $F_{v,mean}$ is linearly related to $F_{v,max}$ (linearity assumption), as it is analytically the case when using a sine-wave model for the vertical ground reaction force,¹⁷ DF should be linearly related to the inverse of $F_{v,max}$. Therefore, rearranging for $F_{v,max}$ should lead to a statistical model relating $F_{v,max}$ to DF (see Equation 5 in the Results section), for which the accuracy should depend on the validity of the linearity assumption.

SMM could then be used to estimate $F_{v,max}$ but using DF values obtained from any measurement systems (IMU, motion capture system, light-based optical technology, etc.), which is a direct practical application of SMM.

Indeed, using SMM with force-plate based DF values to estimate $F_{v,max}$ does not prove to be useful because, in this case, a force-plate based $F_{v,max}$ (gold standard) is directly provided, but this was required to construct SMM. However, using SMM with DF values obtained, for instance, from a motion capture system (kinematic data) allows estimating $F_{v,max}$ when no force plate is available.

2.3 | Experimental procedure, data collection, and data processing

The experimental procedure, data collection, and data processing have been described in more detail elsewhere.²² Briefly, after providing written informed consent, 43 retroreflective markers of 12.5 mm diameter were affixed to skin and shoes of individuals over anatomical landmarks using double-sided tape following standard guidelines.²³ Then, a 7-min warm-up run (9–13 km/h) was performed on an instrumented treadmill (Arsalis T150 – FMT-MED). This was followed, after a short break (<5 min), by a 1-s static trial on the same treadmill for calibration. Then, four retroreflective markers were removed (medial epicondyle of femur and apex of medial malleolus), and three 1-min runs (9, 11, and 13 km/h) were performed in a randomized order (1-min recovery between each run). Three-dimensional (3D) kinematic and kinetic data were collected during the last 30 s following the 30-s mark of running trials (40 ± 9 running steps), resulting in at least 25 steps being analyzed.²⁴ All participants wore their habitual running shoes and were familiar with running on a treadmill as part of their usual training program.

Motion capture (eight cameras, Vicon) and Vicon Nexus software v2.9.3 (Vicon) were used to collect whole-body 3D kinematic data at 200 Hz. The force plate embedded into the treadmill was used to collect synchronized kinetic data (1000 Hz). 3D marker and ground reaction force (analog signal) were exported in .c3d format and processed in Visual3D Professional software v6.01.12 (C-Motion Inc.). Ground reaction force data were down sampled to 200 Hz to match the sampling frequency of marker data. Then, 3D marker and ground reaction force data were low-pass filtered at 20 Hz using a fourth-order Butterworth filter.²⁵

2.4 | Biomechanical variables obtained from force plate data

For each running trial, force-plate based t_c and t_f were obtained from FS and TO events identified using the vertical ground reaction force and implemented within Visual3D. These events were detected by applying a 20 N threshold to the vertical component of the ground reaction force.²⁶

t_c was defined as the time from FS to TO of the same foot while t_f was given by the time from TO of one foot to FS of the contralateral foot. Then, force-plate based DF was given by Equation 3.

Force-plate based $F_{v,max}$ and $F_{v,mean}$ were given by the maximum vertical ground reaction force between FS and TO events and by the integral of the vertical ground reaction force between FS and TO events divided by t_c . The integration was carried out numerically using a second-order method known as trapezoidal rule. $F_{v,max}$ and $F_{v,mean}$ were expressed in BW while DF was given in percent.

2.5 | Biomechanical variables obtained from kinematic data

t_c , t_f , and DF were calculated from FS and TO events identified using kinematic data. The kinematic algorithm which permitted to obtain FS and TO events has been implemented within Visual3D and was based only on the foot markers. This algorithm has been described elsewhere and reported systematic biases and root mean square errors (RMSE) ≤ 12 ms compared to gold standard events at running speeds ranging from 9 to 13 km/h.²⁷ The kinematic based DF could then be inserted into SMM to estimate $F_{v,max}$ when no force plate is available. Systematic biases of 6 ms, –6 ms, and 0.9% were reported for t_c , t_f , and DF when considering all running speeds together (see Section S1 of Appendix S1).

All force-plate and kinematic based biomechanical variables extracted from the 10 analyzed strides were averaged for each participant for subsequent analyses.

2.6 | Data analysis

The error of SMM based on both force plate and kinematic based DF to estimate $F_{v,max}$ was calculated using RMSE (in absolute and relative units, that is, normalized by the corresponding mean value over all participants and obtained using GSM) considering each running speed separately and all running speeds together. Data analysis was performed using Python (v3.7.4, <http://www.python.org>).

2.7 | Statistical analysis

All data are presented as mean \pm standard deviation. Since all data were normally distributed based on Kolmogorov–Smirnov tests ($p \geq 0.13$), Pearson correlation coefficients (r) between DF and $F_{v,mean}^{-1}$, $F_{v,mean}$ and $F_{v,max}$, and $F_{v,max}^{-1}$ and DF as well as corresponding p -values were extracted considering each running speed separately and all running

speeds together. Correlations were considered *very high*, *high*, *moderate*, *low*, and *negligible* when absolute r values were between 0.90–1.00, 0.70–0.89, 0.50–0.69, 0.30–0.49, and 0.00–0.29, respectively.²⁸ Coefficient of determination (R^2) was given by the square of r .

Bland–Altman plots were constructed to examine the presence of systematic bias on $F_{v,\max}$ between GSM and SMM.²⁹ Corresponding lower and upper limit of agreements and 95% confidence intervals (CI) were calculated. Systematic biases have a direction, that is, positive values indicate overestimations of SMM while negative values indicate underestimations. Then, after having inspected residual plots and having observed no obvious deviations from homoscedasticity or normality, Student's t -tests were used to compare GSM and SMM. Differences between GSM and SMM were quantified using Cohen's d effect size and interpreted as *very small*, *small*, *moderate*, and *large* when $|d|$ values were close to 0.01, 0.2, 0.5, and 0.8, respectively.³⁰ The analyses comparing SMM to GSM were performed considering each running speed separately and all running speeds together and two times (1) using force-plate based and (2) using kinematic based DF values. Statistical analysis was performed using Jamovi (v1.6, <https://www.jamovi.org>) with a level of significance set at $p \leq 0.05$.

3 | RESULTS

Considering all running speeds together, DF was *very highly* correlated to $F_{v,\text{mean}}^{-1}$ ($r = 1.00$, $p < 0.001$, **Figure 1A**), $F_{v,\text{mean}}$ was *very highly* correlated to $F_{v,\text{max}}$ ($r = 0.90$, $p < 0.001$, **Figure 1B**), and $F_{v,\text{max}}^{-1}$ was *very highly* correlated

to DF ($r = 0.91$, $p < 0.001$, **Figure 1C**), which led to the following SMM (obtained using a linear least-squares regression; **Equation 5**):

$$F_{v,\text{max}} = \frac{1}{0.0097 \text{ DF} + 0.0635} \quad (5)$$

Considering each running speed separately, DF was *very highly* correlated to $F_{v,\text{mean}}^{-1}$ ($r = 1.00$, $p < 0.001$), $F_{v,\text{mean}}$ was *highly* correlated to $F_{v,\text{max}}$ ($r \geq 0.88$, $p < 0.001$), and $F_{v,\text{max}}^{-1}$ was *highly* correlated to DF ($r \geq 0.88$, $p < 0.001$).

Using force-plate based DF to estimate $F_{v,\text{max}}$, RMSEs of 4% and up to *small* effect sizes (**Table 1**) were reported between GSM and SMM when considering each running speed separately and all running speeds together. No systematic biases were obtained at 11 km/h and when considering all running speeds together while small but systematic biases were reported at 9 and 13 km/h (**Figure 2A** and **Table 1**). $F_{v,\text{max}}$ estimated using SMM based on force-plate DF values was significantly different than $F_{v,\text{max}}$ obtained using GSM at 9 and 13 km/h ($P \leq 0.03$; **Table 2**).

Using kinematic based DF to estimate $F_{v,\text{max}}$, systematic biases were obtained between GSM and SMM at each speed employed (though very small at 13 km/h) as well as when considering all running speeds together (**Figure 2B** and **Table 1**). RMSEs were up to 6% and effect sizes up to *moderate* (**Table 1**) when considering each running speed separately and all running speeds together. $F_{v,\text{max}}$ estimated using SMM based on kinematic DF values was significantly different than $F_{v,\text{max}}$ obtained using GSM at 9 and 11 km/h as well as when considering all running speeds together ($p < 0.001$; **Table 2**).

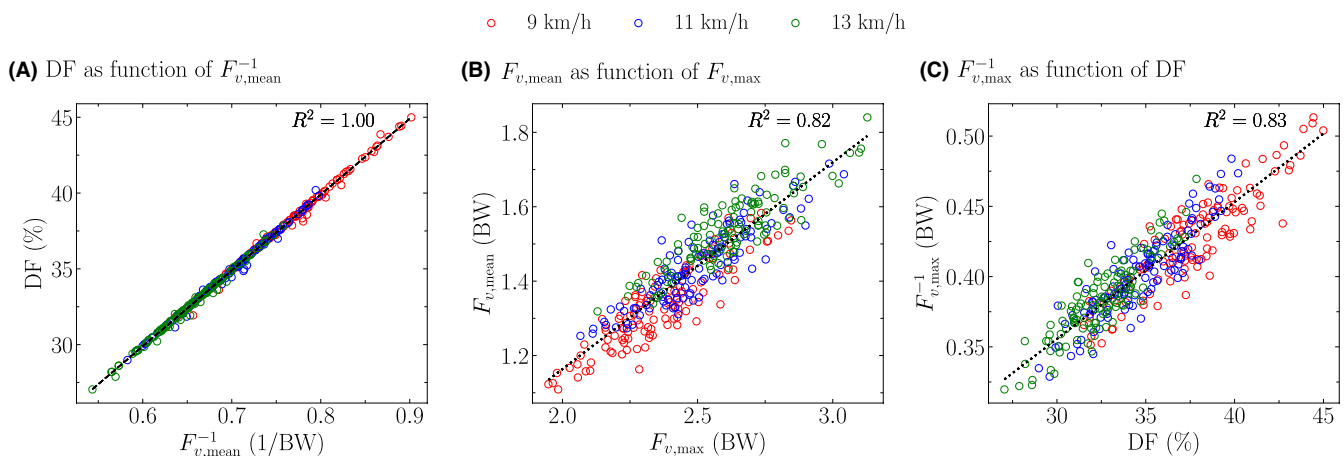


FIGURE 1 Linear relation obtained using Pearson correlation between (A) duty factor (DF) and the inverse of the mean vertical ground reaction force during contact time ($F_{v,\text{mean}}^{-1}$), (B) $F_{v,\text{mean}}$ and peak vertical ground reaction force ($F_{v,\text{max}}$), and (C) the inverse of $F_{v,\text{max}}$ and DF, together with their corresponding coefficient of determination (R^2), and considering all running speeds together (9, 11, and 13 km/h). Ground reaction force variables were expressed in body weight (BW). Each dot represents the average over the 10 analyzed strides for one subject at a particular running speed.

TABLE 1 Systematic bias, lower limit of agreement (lloa), upper limit of agreement (uloa), root mean square error [RMSE; both in absolute (body weight; BW) and relative (%) units], and Cohen's *d* effect size between peak vertical ground reaction force ($F_{v,max}$) obtained using statistical model (SMM) and gold standard (GSM) method, considering each running speed separately (9, 11, and 13 km/h) and all running speeds together.

	Running speed	Systematic bias (BW)	Lloa (BW)	Uloa (BW)	RMSE (BW)	<i>d</i> (-)
GSM vs. force-plate based SMM	9 km/h	-0.03 [-0.04, -0.01]	-0.20 [-0.22, -0.17]	0.14 [0.11, 0.17]	0.09 (4%)	0.15
	11 km/h	0.00 [-0.02, 0.01]	-0.18 [-0.21, -0.15]	0.17 [0.15, 0.20]	0.09 (4%)	0.02
	13 km/h	0.02 [0.00, 0.04]	-0.16 [-0.19, -0.13]	0.20 [0.17, 0.23]	0.09 (4%)	-0.11
	All together	0.00 [-0.01, 0.01]	-0.18 [-0.20, -0.17]	0.18 [0.16, 0.19]	0.09 (4%)	0.02
GSM vs. kinematic based SMM	9 km/h	-0.09 [-0.11, -0.07]	-0.07 [-0.29, -0.33]	0.11 [0.08, 0.15]	0.14 (6%)	0.50
	11 km/h	-0.05 [-0.07, -0.03]	-0.26 [-0.29, -0.23]	0.16 [0.13, 0.19]	0.12 (5%)	0.27
	13 km/h	-0.01 [-0.03, 0.01]	-0.22 [-0.25, -0.18]	0.20 [0.16, 0.23]	0.11 (4%)	0.06
	All together	-0.05 [-0.06, -0.04]	-0.27 [-0.29, -0.25]	0.17 [0.15, 0.19]	0.12 (5%)	0.23

Note: 95% confidence intervals are given in square brackets. SMM based on both force plate and kinematic data were used to estimate $F_{v,max}$. For systematic bias, positive and negative values indicate that SMM overestimated and underestimated $F_{v,max}$, respectively.

4 | DISCUSSION

In line with our first and second hypotheses, RMSEs of 0.09 and 0.12BW (4% and 5%) were obtained for SMM based on force plate and kinematic data, respectively. Conventional statistical approaches demonstrated no systematic bias of $F_{v,max}$ between GSM and SMM based on force plate data when considering all running speeds together while systematic but small bias (-0.05BW) was obtained between GSM and SMM based on kinematic data. These results suggest SMM to be a valid method to estimate $F_{v,max}$ if underlying DF values are accurately measured.

The linear relation between DF and the inverse of $F_{v,mean}$, which has been analytically derived (Equation 4) when DF is computed using Equation 3, was confirmed by the very high correlation reported in this study ($R^2 = 1.00$; Figure 1A). Nonetheless, several points did not exactly fall on the regression line (Figure 1A). This might be explained by several reasons. First, the integration of the vertical ground reaction force encompasses errors due to its numerical nature (second-order trapezoidal rule). Second, even though the raw vertical ground reaction force signal was filtered (fourth-order Butterworth low-pass filter at 20 Hz), it still contains some noise, thus affecting the outcome of its numerical integration. Third, the calibration of the force plate may be not 100% accurate, thus affecting the values of the force signal. It is also worth mentioning that similar results would have been obtained when using the exact definition of DF, that is, the ratio of t_c over stride time.^{18,19} Indeed, RMSE $\leq 0.12\%$ were obtained when comparing DF calculated using Equation 3 to its exact definition (see Section S2 of Appendix S1). This result corroborates the small symmetry indices $\leq 4\%$ previously reported for the step time of competitive, recreational, and novice runners at running speeds ranging from 8 to

12 km/h.³¹ The authors reported similar symmetry indices for DF ($\leq 4\%$), the reason being that the stride time was close to perfectly symmetric ($\leq 1\%$), reflecting that the symmetry of DF was mostly affected by the symmetry of t_c ($\sim 3\%$).³¹

SMM reported no systematic bias and an RMSE of 4% when using force plate DF values and considering all running speeds together (Figure 2A and Tables 1 and 2), which permitted to validate the proposed statistical model (Equation 5). However, using SMM with force-plate based DF values to estimate $F_{v,max}$ does not prove to be useful because, in this case, a gold standard $F_{v,max}$ is directly provided. Therefore, as a direct practical application, SMM was used with DF values obtained from kinematic data to estimate $F_{v,max}$. A systematic bias of -0.05BW and an RMSE of 5% were reported when considering all running speeds together (Figure 2B and Tables 1 and 2). $F_{v,max}$ estimated using sacral-mounted IMUs reported similar differences¹¹ [≤ 20 N (≤ 0.03 BW for a 70 kg person) at 14–19 km/h] and RMSE¹² (0.15 BW at 13.5–19.5 km/h) with respect to GSM than SMM used in the present study. In addition, a 6% error on $F_{v,max}$ (6–21 km/h) was reported using an IMU placed on the leg along the tibial axis³² while a 3% error (10–14 km/h) was achieved using three IMUs (two on lower legs and one on pelvis) and two artificial neural networks.³³ Thus, estimated $F_{v,max}$ depicted similar error ($\sim 5\%$) than previous estimations which used IMUs.

$F_{v,max}$ was estimated using SMM, a statistical model solely based on DF (Equation 5) and reported a 5% RMSE (Table 1). The only requirement to obtain an accurate estimation of $F_{v,max}$ is that DF, or the two variables defining it, that is, t_c and t_f , should be accurately measured (see Section S1 of Appendix S1). Therefore, SMM could be combined with any measurement system accurately

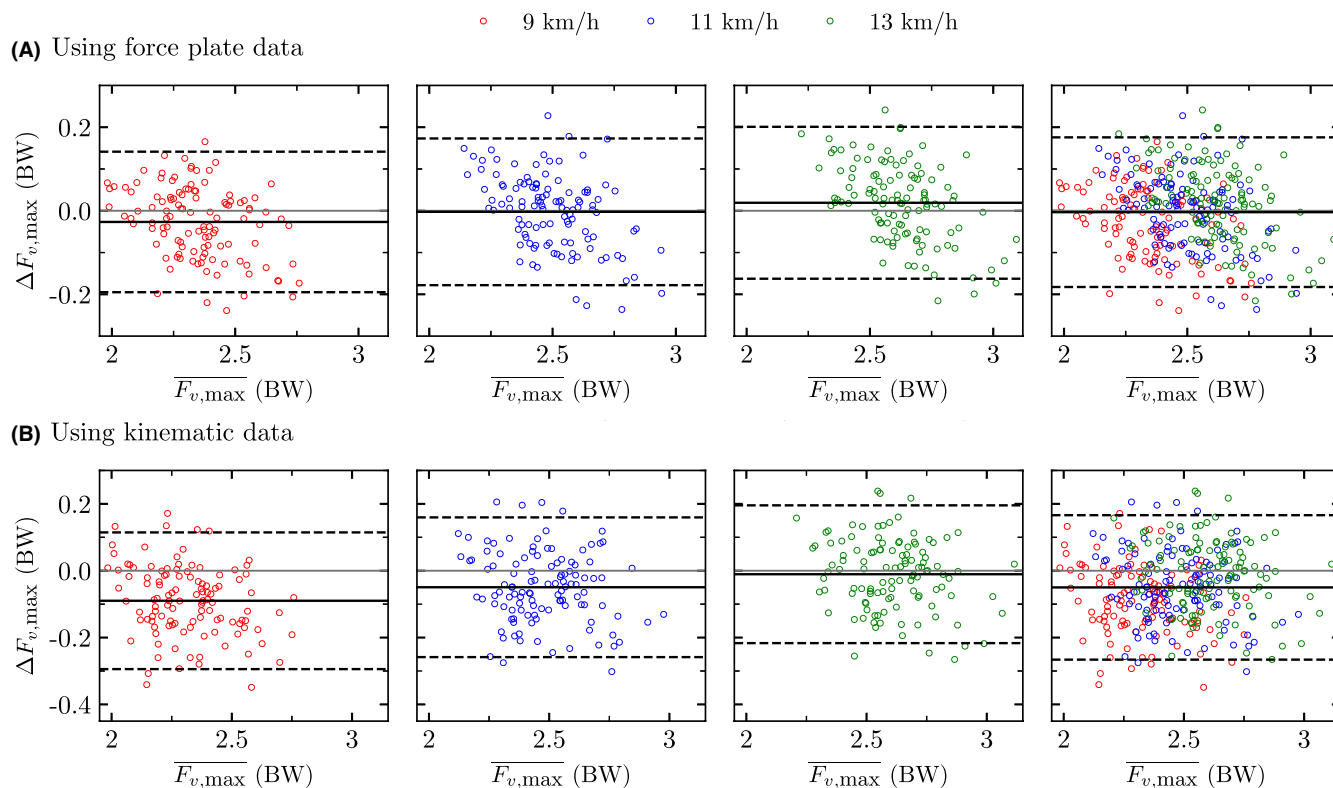


FIGURE 2 Comparison of peak vertical ground reaction force [$F_{v,\max}$; in body weight (BW)] obtained using gold standard method and statistical model method (SMM) [differences (Δ) as function of mean values together with systematic bias (black solid line) as well as lower and upper limit of agreements (black dashed lines), that is, Bland–Altman plots] considering each running speed separately (9, 11, and 13 km/h) and all running speeds together. The estimation of $F_{v,\max}$ using SMM was based on (A) force plate data and (B) kinematic data. Positive and negative Δ values indicate an overestimation and underestimation of $F_{v,\max}$ by SMM. Each dot represents the average over the 10 analyzed strides for one subject at a particular running speed.

TABLE 2 Peak vertical ground reaction force [$F_{v,\max}$; in body weight (BW)] obtained using gold standard (GSM) and statistical model (SMM) methods, considering each running speed separately (9, 11, and 13 km/h) and all running speeds together.

Running speed	9 km/h	11 km/h	13 km/h	All together
$F_{v,\max}$ using GSM	2.36 ± 0.19	2.50 ± 0.19	2.61 ± 0.19	2.49 ± 0.22
$F_{v,\max}$ using force-plate based SMM	2.34 ± 0.16	2.50 ± 0.15	2.63 ± 0.15	2.49 ± 0.20
p	0.001	0.76	0.03	0.49
$F_{v,\max}$ using kinematic based SMM	2.27 ± 0.17	2.45 ± 0.17	2.60 ± 0.17	2.44 ± 0.22
p	<0.001	<0.001	0.29	<0.001

Note: SMM based on both force plate and kinematic data were used to estimate $F_{v,\max}$. Significant differences ($p \leq 0.05$) between $F_{v,\max}$ obtained using GSM and SMM as determined by Student's t -tests are depicted in bold.

providing DF or its underlying variables, such as an IMU,^{11,12} a motion capture system,^{27,34,35} or a light-based optical technology.³⁶ Day et al.¹¹ reported that a 5 Hz low-pass filtering of the vertical acceleration recorded using a sacral-mounted IMU was resulting in the best correlation between t_c obtained from GSM and their method while a 10 Hz low-pass filter produced the best estimated $F_{v,\max}$. These results demonstrated that different cutoff frequencies were required for different biomechanical parameters, agreeing with previous observations that the low-pass cutoff frequency affected biomechanical outcomes.^{37,38}

However, using two different filters is not very practical. In this case, SMM could be advantageous as it could avoid using the second filter, which is computationally more expensive than using SMM, without losing accuracy. Indeed, SMM could be applied using estimated t_c and t_f from the IMU to directly obtain $F_{v,\max}$.

A few limitations to this study exist. SMM was constructed using running trials between 9 and 13 km/h and using treadmill runs. Therefore, this study could not conclude that SMM would correctly estimate $F_{v,\max}$ at faster running speeds and overground. Hence, further studies

should record running trials at faster running speeds and overground to obtain the accuracy of SMM in these conditions. However, although controversial,³⁹ SMM might perform well overground, at least at similar running speeds than the ones used to construct the statistical model (9–13 km/h), because spatiotemporal parameters between treadmill and overground running are largely comparable.⁴⁰ Moreover, SMM tries to estimate $F_{v,max}$ as if it was obtained using the vertical ground reaction force signal recorded by the specific instrumented treadmill used in the present study. Though the choice of filter and frequency used to filter the vertical ground reaction force (20 Hz and fourth-order Butterworth filter herein) should be chosen to remove as much noise as possible without altering the force signal, that is, everyone should have a similar force signal independently of the underlying force plate, there might still be small discrepancies in the force signals recorded by different instrumented treadmills. Hence, using another instrumented treadmill might affect the integration of the vertical ground reaction force signal and the determination of FS and TO events, and thus the coefficients of the statistical model (Equation 5). Therefore, further studies investigating if the choice of the other instrumented treadmill affects the coefficients of the statistical model are needed and would allow generalizing to a statistical model that estimates $F_{v,max}$ independently of the instrumented treadmill employed.

4.1 | Perspective

A simple statistical model solely based on DF was constructed to estimate $F_{v,max}$ (Equation 5). This model was shown to provide an accurate estimation of $F_{v,max}$ if underlying DF values or its subcomponents (t_c and t_f ; Equation 3) are accurately measured. Hence, this model could be implemented in any measurement system that accurately provides DF values (e.g., a smartwatch and/or smartphone). This would allow to monitor $F_{v,max}$ and loading in real time and could therefore help for preventing running related injuries.

5 | CONCLUSION

To conclude, this study proposed to construct a statistical model only using the DF to estimate $F_{v,max}$, because DF is analytically related to $F_{v,mean}$ and the latter is very highly correlated to $F_{v,max}$. Considering all running speeds together and using force-plate based DF values for SMM, no systematic bias and a 4% RMSE were reported between GSM and SMM. Using kinematic based DF values, SMM

reported a systematic but small bias ($-0.05BW$) and a 5% RMSE when considering all running speeds together. Therefore, the findings of this study support the use of SMM to estimate $F_{v,max}$ during level treadmill runs at endurance speeds if underlying DF values are accurately measured.

AUTHOR CONTRIBUTIONS

Conceptualization, A.P., T.L., C.G., and D.M.; methodology, A.P., T.L., C.G., and D.M.; investigation, A.P., T.L., and B.B.; formal analysis, A.P. and B.B.; writing—original draft preparation, A.P.; writing—review and editing, A.P., T.L., B.B., C.G., and D.M.; supervision, A.P., T.L., C.G., and D.M.

ACKNOWLEDGEMENTS

The authors warmly thank the participants for their time and cooperation.

FUNDING INFORMATION

This study was supported by the Innosuisse grant no. 35793.1 IP-LS.





CONFLICT OF INTEREST

No potential competing interest was reported by the authors.

DATA AVAILABILITY STATEMENT

The data that support the findings of this study are available from the corresponding author upon reasonable request.

ORCID

Aurélien Patoz  <https://orcid.org/0000-0002-6949-7989>
 Thibault Lussiana  <https://orcid.org/0000-0002-1782-401X>
 Bastiaan Breine  <https://orcid.org/0000-0002-7959-7721>
 Davide Malatesta  <https://orcid.org/0000-0003-3905-5642>

REFERENCES

- van der Worp MP, ten Haaf DSM, van Cingel R, de Wijer A, Nijhuis-van der Sanden MWG, Staal JB. Injuries in runners; a systematic review on risk factors and sex differences. *PLoS ONE*. 2015;10(2):e0114937.
- van Gent RN, Siem D, van Middelkoop M, van Os AG, Bierma-Zeinstra SM, Koes BW. Incidence and determinants of lower extremity running injuries in long distance runners: a systematic review. *Br J Sports Med*. 2007;41(8):469-480.
- Scott SH, Winter DA. Internal forces of chronic running injury sites. *Med Sci Sports Exerc*. 1990;22(3):357-369.
- Sasimontokul S, Bay BK, Pavol MJ. Bone contact forces on the distal tibia during the stance phase of running. *J Biomech*. 2007;40(15):3503-3509.

5. Popp KL, McDermott W, Hughes JM, Baxter SA, Stovitz SD, Petit MA. Bone strength estimates relative to vertical ground reaction force discriminates women runners with stress fracture history. *Bone*. 2017;94:22-28.
6. Bigouette J, Simon J, Liu K, Docherty CL. Altered vertical ground reaction forces in participants with chronic ankle instability while running. *J Athl Train*. 2016;51(9):682-687.
7. Milner CE, Ferber R, Pollard CD, Hamill J, Davis IS. Biomechanical factors associated with tibial stress fracture in female runners. *Med Sci Sports Exerc*. 2006;38(2):323-328.
8. Matijevich ES, Branscombe LM, Scott LR, Zelik KE. Ground reaction force metrics are not strongly correlated with tibial bone load when running across speeds and slopes: implications for science, sport and wearable tech. *PLoS ONE*. 2019;14(1):e0210000.
9. Maiwald C, Sterzing T, Mayer TA, Milani TL. Detecting foot-to-ground contact from kinematic data in running. *Footwear Sci*. 2009;1(2):111-118.
10. Abendroth-Smith J. Stride adjustments during a running approach toward a force plate. *Res Q Exerc Sport*. 1996;67(1):97-101.
11. Day EM, Alcantara RS, McGeehan MA, Grabowski AM, Hahn ME. Low-pass filter cutoff frequency affects sacral-mounted inertial measurement unit estimations of peak vertical ground reaction force and contact time during treadmill running. *J Biomech*. 2021;119:110323.
12. Alcantara RS, Day EM, Hahn ME, Grabowski AM. Sacral acceleration can predict whole-body kinetics and stride kinematics across running speeds. *PeerJ*. 2021;9:e11199.
13. Ancillao A, Tedesco S, Barton J, O'Flynn B. Indirect measurement of ground reaction forces and moments by means of wearable inertial sensors: a systematic review. *Sensors (Basel)*. 2018;18(8):2564.
14. Camomilla V, Bergamini E, Fantozzi S, Vannozzi G. Trends supporting the In-field use of wearable inertial sensors for sport performance evaluation: a systematic review. *Sensors (Basel)*. 2018;18(3):873.
15. Blickhan R. The spring-mass model for running and hopping. *J Biomech*. 1989;22(11):1217-1227.
16. Dalleau G, Belli A, Bourdin M, Lacour JR. The spring-mass model and the energy cost of treadmill running. *Eur J Appl Physiol Occup Physiol*. 1998;77(3):257-263.
17. Morin J-B, Dalleau G, Kyröläinen H, Jeannin T, Belli A. A simple method for measuring stiffness during running. *J Appl Biomech*. 2005;21(2):167-180.
18. Minetti AE. A model equation for the prediction of mechanical internal work of terrestrial locomotion. *J Biomech*. 1998;31(5):463-468.
19. Folland JP, Allen SJ, Black MI, Handsaker JC, Forrester SE. Running technique is an important component of running economy and performance. *Med Sci Sports Exerc*. 2017;49(7):1412-1423.
20. Falbriard M, Meyer F, Mariani B, Millet GP, Aminian K. Accurate estimation of running temporal parameters using foot-worn inertial sensors. *Front Physiol*. 2018;9:610.
21. Yang Y, Wang L, Su S, Watsford M, Wood LM, Duffield R. Inertial sensor estimation of initial and terminal contact during In-field running. *Sensors (Basel)*. 2022;22(13):4812.
22. Patoz A, Lussiana T, Breine B, Gindre C, Malatesta D. Both a single sacral marker and the whole-body center of mass accurately estimate peak vertical ground reaction force in running. *Gait Posture*. 2021;89:186-192.
23. Tranberg R, Saari T, Zügner R, Kärrholm J. Simultaneous measurements of knee motion using an optical tracking system and radiostereometric analysis (RSA). *Acta Orthop*. 2011;82(2):171-176.
24. Oliveira AS, Pircscoveanu CI. Implications of sample size and acquired number of steps to investigate running biomechanics. *Sci Rep*. 2021;11(1):3083.
25. Swinnen W, Mylle I, Hoogkamer W, De Groote F, Vanwanseele B. Changing stride frequency alters average joint power and power distributions during ground contact and leg swing in running. *Med Sci Sports Exerc*. 2021;53(10):2111-2118.
26. Smith L, Preece S, Mason D, Bramah C. A comparison of kinematic algorithms to estimate gait events during overground running. *Gait Posture*. 2015;41(1):39-43.
27. Patoz A, Lussiana T, Gindre C, Malatesta D. A novel kinematic detection of foot-strike and toe-off events during noninstrumented treadmill running to estimate contact time. *J Biomech*. 2021;128:110737.
28. Hinkle DE, Wiersma W, Jurs SG. *Applied Statistics for the Behavioral Sciences*. Houghton Mifflin; 2002.
29. Bland JM, Altman DG. Comparing methods of measurement: why plotting difference against standard method is misleading. *Lancet*. 1995;346(8982):1085-1087.
30. Cohen J. *Statistical Power Analysis for the Behavioral Sciences*. Routledge; 1988.
31. Mo S, Lau FOY, Lok AKY, et al. Bilateral asymmetry of running gait in competitive, recreational and novice runners at different speeds. *Hum Mov Sci*. 2020;71:102600.
32. Charry E, Hu W, Umer M, Ronchi A, Taylor S. Study on estimation of peak Ground Reaction Forces using tibial accelerations in running. Paper presented at: 2013 IEEE Eighth International Conference on Intelligent Sensors, Sensor Networks and Information Processing; 2-5 April 2013, 2013.
33. Wouda FJ, Giuberti M, Bellusci G, et al. Estimation of vertical ground reaction forces and sagittal knee kinematics during running using three inertial sensors. *Front Physiol*. 2018;9:218.
34. Lussiana T, Patoz A, Gindre C, Mourot L, Hébert-Losier K. The implications of time on the ground on running economy: less is not always better. *J Exp Biol*. 2019;222(6):jeb192047.
35. Patoz A, Lussiana T, Thouvenot A, Mourot L, Gindre C. Duty factor reflects lower limb kinematics of running. *Appl Sci*. 2020;10(24):8818.
36. Debaere S, Jonkers I, Delecluse C. The contribution of step characteristics to Sprint running performance in high-level male and female athletes. *J Strength Cond Res*. 2013;27(1):116-124.
37. Mai P, Willwacher S. Effects of low-pass filter combinations on lower extremity joint moments in distance running. *J Biomech*. 2019;95:109311.
38. Kiernan D, Miller RH, Baum BS, Kwon HJ, Shim JK. Amputee locomotion: frequency content of prosthetic vs. intact limb vertical ground reaction forces during running and the effects of filter cut-off frequency. *J Biomech*. 2017;60:248-252.
39. Bailey JP, Mata T, Mercer JD. Is the relationship between stride length, frequency, and velocity influenced by running on a treadmill or overground? *Int J Exerc Sci*. 2017;10(7):1067-1075.

40. Van Hooren B, Fuller JT, Buckley JD, et al. Is motorized treadmill running biomechanically comparable to Overground running? A systematic review and meta-analysis of cross-over studies. *Sports Med.* 2020;50(4):785-813.

SUPPORTING INFORMATION

Additional supporting information can be found online in the Supporting Information section at the end of this article.

How to cite this article: Patoz A, Lussiana T, Breine B, Gindre C, Malatesta D. Accurate estimation of peak vertical ground reaction force using the duty factor in level treadmill running. *Scand J Med Sci Sports.* 2022;00:1-9. doi: [10.1111/sms.14252](https://doi.org/10.1111/sms.14252)

